UC Berkeley
UC Berkeley Electronic Theses and Dissertations

Title

Hydroamination and C–C Activation Methods for the Expedient Synthesis of Lycopodium Alkaloids and Phomactin Natural Products

Permalink
https://escholarship.org/uc/item/9dw4s8f7

Author

Leger, Paul Robert

Publication Date

2016

Peer reviewed|Thesis/dissertation

eScholarship.org
Powered by the California Digital Library
University of California

Hydroamination and C–C Activation Methods for the Expedient Synthesis of *Lycopodium* Alkaloids and Phomactin Natural Products

By

Paul Robert Leger

A dissertation submitted in partial satisfaction of the

requirements for the degree of

Doctor of Philosophy

in

Chemistry

in the

Graduate Division

of the

University of California, Berkeley

Committee in charge:

Professor Richmond Sarpong, Chair
Professor Thomas Maimone
Professor Polina Lishko

Fall 2016

Abstract

Hydroamination and C–C Activation Methods for the Expedient Synthesis of *Lycopodium* Alkaloids and Phomactin Natural Products

by

Paul Robert Leger

Doctor of Philosophy in Chemistry

University of California, Berkeley

Professor Richmond Sarpong, Chair

This dissertation describes our efforts toward the total synthesis of complex natural products in the *Lycopodium* alkaloid and phomactin terpenoid families. The first chapter focuses on our strategy to construct fawcettimine-type *Lycopodium* alkaloids (such as palhinine A) that contain unique bridging ring systems. The synthesis of a model substrate to examine an atom-transfer radical cyclization is described, as well as the synthesis of a 6-5-9 tricycle that could serve as a common intermediate to access many fawcettimine-type natural products.

After observing an unprecedented hydroamination while working toward the synthesis of *Lycopodium* alkaloids, we explored the possibility that trimethylsilyl iodide (TMSI) could be a novel effector of this transformation. The second chapter describes our optimization studies of this hydroamination reaction on simple sulfonamides. We show that catalytic amounts of TMSI and water are unique in their ability to effect hydroamination and hydroetherification of unactivated olefins at room temperature. We found that the iodide anion is crucial to obtain high reactivity at low temperatures.

The third chapter of this dissertation provides background and initial strategies toward the synthesis of phomactin natural products. Biological activity and previous syntheses are described. Our general strategy for accessing the phomactin terpenoids by utilizing strategic C–C activation of a cyclobutanol-derived substrate is illustrated as well as initial strategies and model studies. These include investigating C(sp^3)–H functionalization reactions with a ketone-derived directing group and assessing the ability to accomplish a hydrazine/aldehyde “traceless” bond construction.

The fourth chapter describes the development of our synthetic route to access several phomactin-like compounds. This has been accomplished through exploiting the unique properties of cyclobutanol-containing compounds. Both π-allyl cross-coupling and aldehyde addition reactions are efficient means of appending the linear fragment to the [3.1.1]bicycle. Templated macrocyclization was achieved in excellent yield, aided by the scaffolding ability of the rigid [3.1.1]bicycle. The cyclobutanol was selectively cleaved open through the action of rhodium catalysis. We’ve shown mechanistically that the products of this process are dependent on subtle changes to the substrate as well as the solvent. Final functionalizations include a reductive sulfone removal in the presence of an enone moiety via the intermediacy of an in situ generated cyclopropanol “protecting group”.

Table of Contents

Acknowledgements iv

Chapter 1: Synthetic Studies Toward Palhinine A, an Architecturally Unique Lycopodium Alkaloid

1.1 Overview 1
1.2 Heathcock-Inspired Strategies toward the Fawcettimine-type Alkaloids 3
1.3 Approaches to the Palhinine Core 4
1.4 Retrosynthetic Analysis for Architecturally Unique Alkaloids 6
1.5 Synthesis of Cyclization Model System 7
1.6 Cyclization Attempts 11
1.7 Synthesis of Advanced 6-5-9 Tricycle 14
1.8 Transannular Hydroamination 15
1.9 Conclusion and Outlook 17
1.10 Experimental Contributors 18
1.11 Experimental Methods 18
1.12 References and Notes 33
Appendix 1: Spectra Relevant to Chapter 1 35

Chapter 2: Hydrogen Iodide-Catalyzed Hydroamination and Hydroetherification of Unactivated Olefins

2.1 Hydroamination Overview 69
2.2 Initial Studies of TMSI-Mediated Hydroamination 70
2.3 Optimization of Reaction Conditions 72
2.4 Additive Effects – The Importance of Iodide Anion 74
2.5 Substrate Scope 77
2.6 Comparative Robustness Screen 79
2.7 Conclusion and Outlook 80
2.8 Experimental Contributors 80
2.9 Experimental Methods 81
2.10 References and Notes 97
Appendix 2: Spectra Relevant to Chapter 2 99

Chapter 3: Initial Strategies for the Synthesis of Phomactin Natural Products

3.1 Structural Overview of the Phomactin Terpenoids 113
3.2 Platelet Activating Factor 114
3.3 Previous Phomactin Total Syntheses 116
3.4 Cyclobutanol C–C Activation 121
3.5 Initial Strategy: Ketone-Directed C–H Functionalization 123
3.6 Initial Strategy: “Traceless” Bond Construction 130
3.7 Conclusion 132
3.8 Experimental Contributors 132
3.9 Experimental Methods 133
3.10 References and Notes 144
Appendix 3: Spectra Relevant to Chapter 3 146

Chapter 4: Exploiting Cyclobutanol Reactivity Toward the Total Synthesis of Phomactin Natural Products

4.1 Macrocyclization Considerations 159
4.2 Revised Strategy Exploiting the Properties Inherent in Cyclobutanols 161
4.3 Attempts at Utilizing C–H Silylation for Fragment Coupling 163
4.4 The π-allyl Stille Reaction for Fragment Coupling and Macrocyclization Findings 166
4.5 Divergent Reactivity in the Rhodium-Catalyzed C–C Activation 171
4.6 Revised Fragment Coupling – Aldehyde Addition 177
4.7 Late-stage Functionalization and Challenges 181
4.8 Conclusion and Outlook 185
4.9 Experimental Contributors 185
4.10 Experimental Methods 186
4.11 References and Notes 206
Appendix 4: Spectra Relevant to Chapter 4 208

Acknowledgements

First, I am grateful for the support that Professor Richmond Sarpong has given me. Richmond has been a great advisor during my graduate studies and has always been supportive and helpful. Richmond truly cares about cultivating a lab environment where learning and mentorship are in the forefront, and these things were crucial to my success. I've grown a tremendous amount in the four and a half years since I started grad school, and I credit that to Richmond and to the entire group of wonderful chemists that are dedicated to learning as well as conducting research. Additionally, I appreciate how invested Richmond is in his students' success and future careers after grad school. Because of this, I will be moving on to an exciting job where I can really put all my chemistry knowledge to work.

I'm also extremely thankful that I got a chance to work with Rebecca Murphy during my first year and a half of graduate school. She served as my mentor during this time and I learned so much from her expertise and positive attitude. Rebecca was, without fail, always enthusiastic to lend her help or provide valuable insights about chemistry. I was also extremely fortunate to be joined by two talented postdocs during my final years of grad school, Dr. Stanley Chang and Dr. Yusuke Kuroda. They have both been fantastic to work with. Not only did they lend their chemistry expertise to the project, but they were also very supportive and enjoyable to work with. Additionally, I'd like to thank Diana Wang and Katie Blackford for being awesome undergrads to work with during my graduate research.

I'd like to thank the entire group of people who where a part of the Sarpong lab while I was there. This group was always so supportive, I always felt like I had the power of all my coworkers whenever I was up against a daunting task. In particular, I'd like to call out Chris Marth and Raul Leal as being amazing labmates for the majority of my time in Latimer 847. They certainly provided a constant source of entertainment during long hours in the lab.

I'm also extremely thankful for my good friend, Zach Hallberg. One of my favorite rituals during grad school was my Monday, Wednesday, Friday bubble tea outings with Zach. From first year problem solving sessions to daily doses of conversation and boba, he never failed to find excitement in everything. His passion for science is unmatched and he has made me a better all-around scientist (and person) because of it.

Finally, I owe a huge thank you to my family and to my girlfriend, Grace. They have provided never-ending support and encouragement throughout this entire process. I truly couldn't have done this without them.

Chapter 1: Synthetic Studies Toward Palhinine A, an Architecturally Unique *Lycopodium* Alkaloid

1.1 Overview

The *Lycopodium* alkaloids are a diverse family of over 250 natural products, primarily isolated from the *Lycopodium* genus of club mosses.[1] Many compounds from the *Lycopodium* alkaloid family have demonstrated the ability to reversibly bind to the active site of acetylcholinesterase (AChE), thus inhibiting its activity and slowing the degradation of the neurotransmitter acetylcholine.[2] This activity is the basis for many current therapeutics for the treatment of the symptoms of Alzheimer's disease, including huperzine A (**1.1**, Figure 1) which is a lycodine-type *Lycopodium* alkaloid.[3] Huperzine A is sold as a dietary supplement in the US, but in China it has undergone clinical trials and is currently used by patients with Alzheimer's disease. Additionally, complanadine A (**1.2**) and other members of the *Lycopodium* alkaloid family have demonstrated the ability to increase the levels of nerve growth factor (NGF), a protein that is crucial for neurons to grow and avoid degradation.[4] An imbalance of NGF is suspected to accelerate the onset of various psychiatric disorders including many types of dementia.[5] This activity could provide another interesting avenue for treating neurodegeneration.

Figure 1: Bioactive *Lycopodium* alkaloids

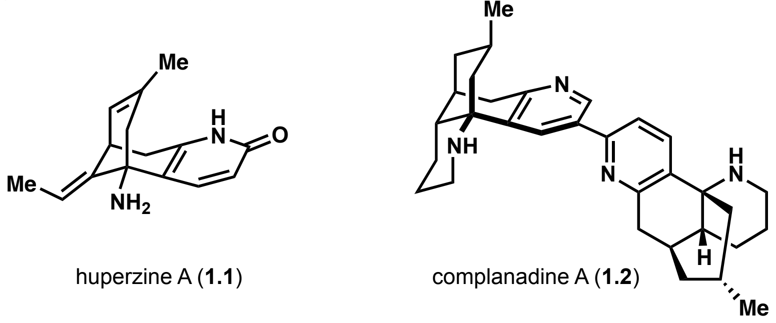

huperzine A (**1.1**)

complanadine A (**1.2**)

Although the *Lycopodium* alkaloid family possesses a wide range of structural diversity, the natural products are broadly classified into four categories based on their structural similarities (Figure 2). Three of the categories are named after their archetypal parent compounds – lycodine, lycopodine, and fawcettimine, while the fourth category serves as a miscellaneous class. This chapter will focus on compounds from the fawcettimine class of natural products. The structures of these natural products are characterized by a fused 6-5 bicycle framework as well as an azanonane ring.

Figure 2: *Lycopodium* alkaloid structural classification

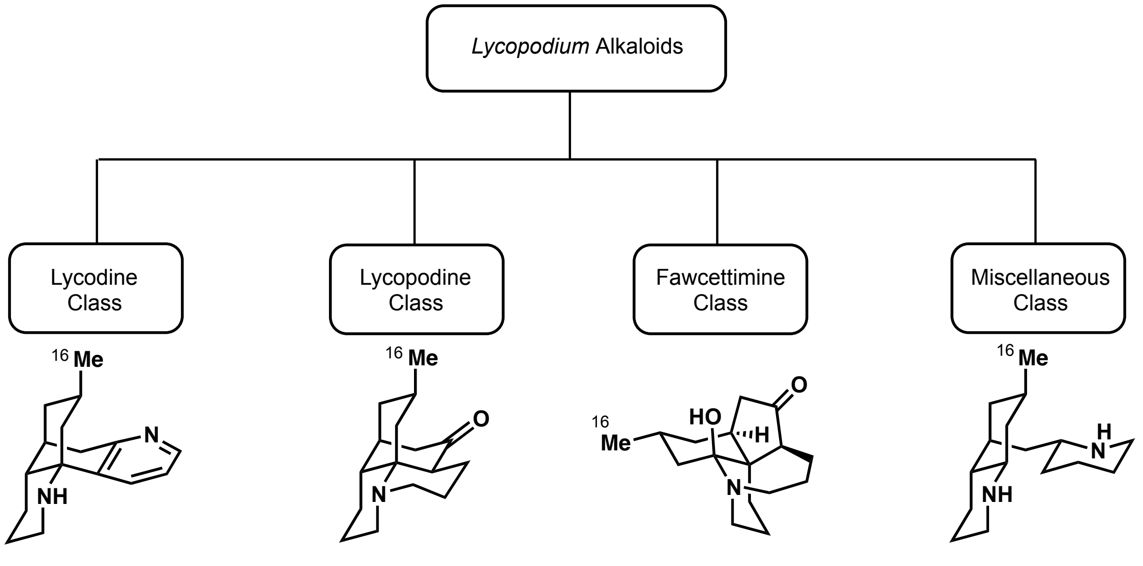

lycodine lycopodine fawcettimine phlegmarine

A structural feature present in all classes of *Lycopodium* alkaloids is the C16 methyl group (see Figure 2). Only a small sub-set of natural products are functionalized at this position, usually bearing oxygenation in the form of an alcohol or ester moiety. There are even fewer natural products where this C16 position is actually incorporated into a new ring system (Figure 3). These complex compounds are of particular interest because this rare structural feature presents an intriguing challenge to the synthetic chemistry community. Specifically, palhinine A (**1.3**)[6] and lycopladine D (**1.4**)[7] are two fawcettimine-type *Lycopodium* alkaloids that are particularly interesting. Palhinine A contains an additional C–C bond between C16 and C4, resulting in a caged and congested skeleton. In lycopladine D, the C16 position has been oxidized and participates in a bridging lactone ring.

Figure 3: Architecturally unique *Lycopodium* alkaloids

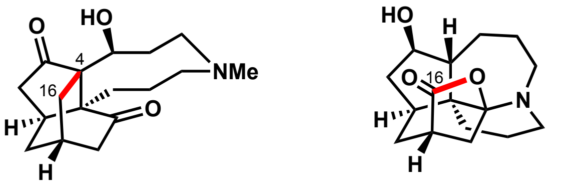

palhinine A (**1.3**) lycopladine D (**1.4**)

Although these features give rise to unique natural product architectures, we hoped to exploit the innate characteristics of the fawcettimine class – the fused 6-5 bicycle and the azanonane ring system – to build a common 6-5-9 tricycle that would allow access to both palhinine A and lycopladine D through a divergent synthetic route (see Section 1.4). This strategy was largely inspired by Heathcock's pioneering synthetic studies of fawcettimine in the 1980's.

1.2 Heathcock-Inspired Strategies toward the Fawcettimine-type Alkaloids

When fawcettimine was first isolated in 1959, its exact structure was unknown.[8] The stereochemistry at C4 was uncertain, and several plausible hemiaminal structures were proposed (**1.5** or **1.7**) along with the tricyclic structure **1.6** (Scheme 1).

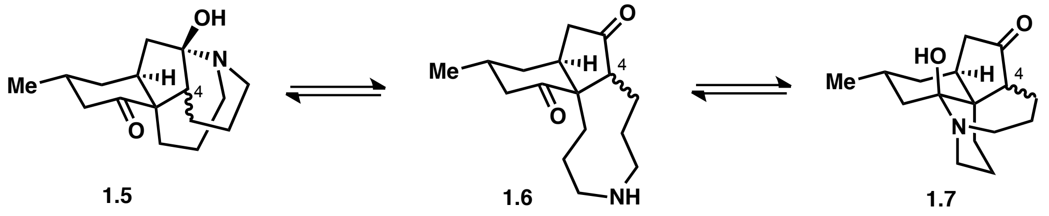

Scheme 1: Possible tautomeric structures of fawcettimine

The first total synthesis of fawcettimine was accomplished in 1979 by the group of Inubushi (Scheme 2).[9] However, this synthetic effort was not sufficient for complete structural elucidation. The penultimate step in their synthesis was a hydrogenation of 6-5-9 tricycle **1.8**, but since this transformation was not diastereoselective, both epimers at C4 were formed (see **1.9)**. Upon treatment with potassium hydroxide, the trifluoroacetamide was hydrolyzed and afforded the natural product. But since the C4 stereocenter could also epimerize under these conditions, the stereochemistry at C4 was still unknown after this 26-step synthesis.

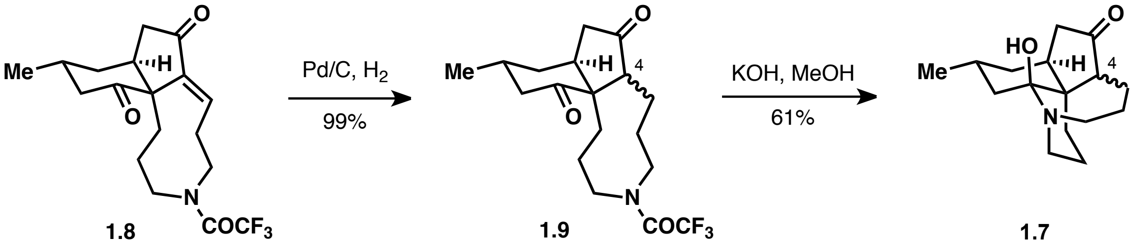

Scheme 2: Inubushi's synthesis of fawcettimine

In 1986, Heathcock and coworkers published pioneering conformational studies of the fawcettimine framework.[10] They accessed 6-5-9 tricycle **1.6a** as a single diastereomer, arising from cyclization of tosylamide **1.10** (Scheme 3). Since Heathcock was able to access a single diastereomer of tricycle **1.6a**, he showed that tricycle **1.6a** preferred to sit as the tricycle, with limited equilibration to hemiaminal **1.5a** and no sign of hemiaminal **1.7a**. Upon treatment of tricycle **1.6a** with base to epimerize the C4 stereocenter, complete conversion to hemiaminal **1.7b** was observed, corresponding to the structure of the natural product. This 13-step synthesis provided complete structural assignment for fawcettimine and set a strong precedent for an efficient strategy to construct fawcettimine and related molecules.

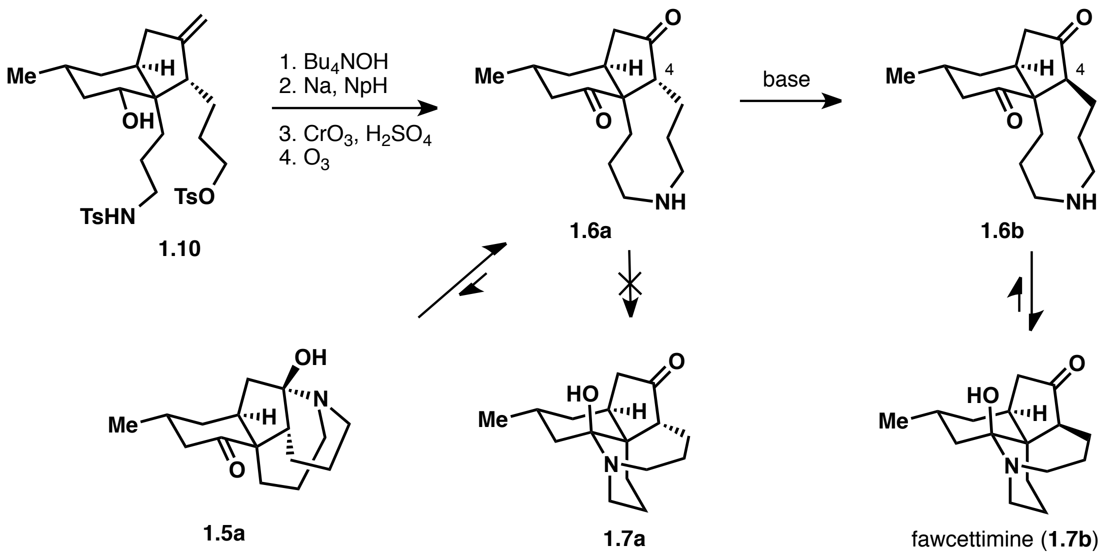

Scheme 3: Heathcock's synthesis of fawcettimine

Even 30 years after these initial reports, analogs of the 6-5-9 tricycle prepared by Inubushi and Heathcock are still investigated and are often considered as integral to the best strategy for accessing fawcettimine-type *Lycopodium* alkaloids. A review of these "Heathcock-inspired strategies" has recently been published, so the many contributions to this area will not be detailed here.[11] It's worth noting that since palhinine A and lycopladine D contain unique bridging ring systems, the choice to pursue a Heathcock-inspired strategy is non-obvious. In fact, none of the reported approaches to palhinine A make use of a 6-5-9 tricyclic intermediate (see Section 1.3). We hope that by employing this strategy, it will render our synthesis amenable to diversification and enable a collective synthesis of several fawcettimine-type *Lycopodium* alkaloids.

1.3 Approaches to the Palhinine Core

To date, there have been no published syntheses of palhinine A. However, several routes aimed at accessing the caged 6-6-5 core of palhinine A have been published, almost exclusively based on an intramolecular Diels-Alder (IMDA) approach. In 2012, She and coworkers demonstrated the use of a temporary ether linkage combined with an oxidative dearomatization to initiate the IMDA (Scheme 4A).[12] This directly afforded the desired [2.2.2] bicycle present in the natural product. In 6 more steps, the 5-membered ring was forged, but an inability to install the azanonane ring resulted in an incomplete synthesis. Due to this complication of late-stage azanonane formation, She and coworkers recently published a second-generation route focused on early nitrogen installation and a transannular IMDA (Scheme 4B).[13] With this approach, the azanonane ring and [2.2.2] bicycle are furnished in a single complexity-building step. However, transforming the resultant product into palhinine A does not appear to be a straightforward endeavor.

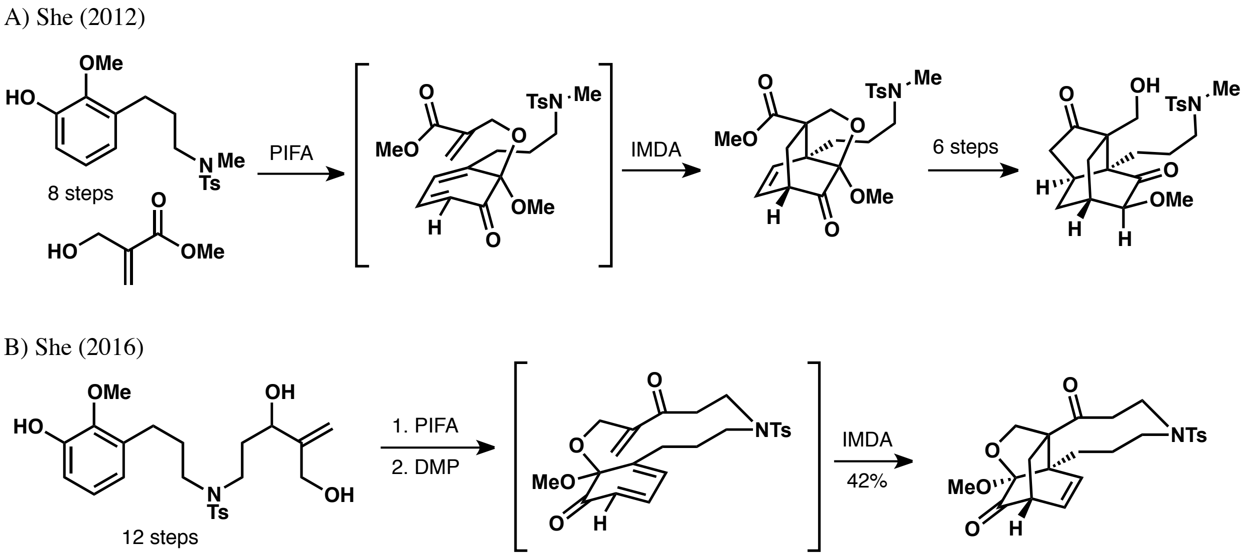
A) She (2012)
OMe
HO
N Me
Ts
8 steps
HO
OMe
PIFA
MeO
TsN
Me
H
OMe
IMDA
MeO
6 steps
OH
H
B) She (2016)
OH
N
Ts
12 steps
1. PIFA
2. DMP
NTs
MeO
IMDA
42%

Scheme 4: She's oxidative dearomatization/IMDA approach to the palhinine core

Shortly after the initial report by She and coworkers, Fan and coworkers reported the synthesis of the palhinine A core through an IMDA originating from enolization of an appropriate enone (Scheme 5A).[14] This elegant transformation allows rapid construction of the caged system and both quaternary centers in a single step. Similarly, in 2014, Rychnovsky and coworkers reported an IMDA on a system very similar to that of Fan and coworkers, again highlighting the utility of a silyl dienol ether / IMDA approach to rapidly build bridged ring systems (Scheme 5B).[15] However, in all cases, the authors have yet to report the transformation of the resultant Diels-Alder adduct to the natural product, highlighting the challenge of forming the azanonane ring.

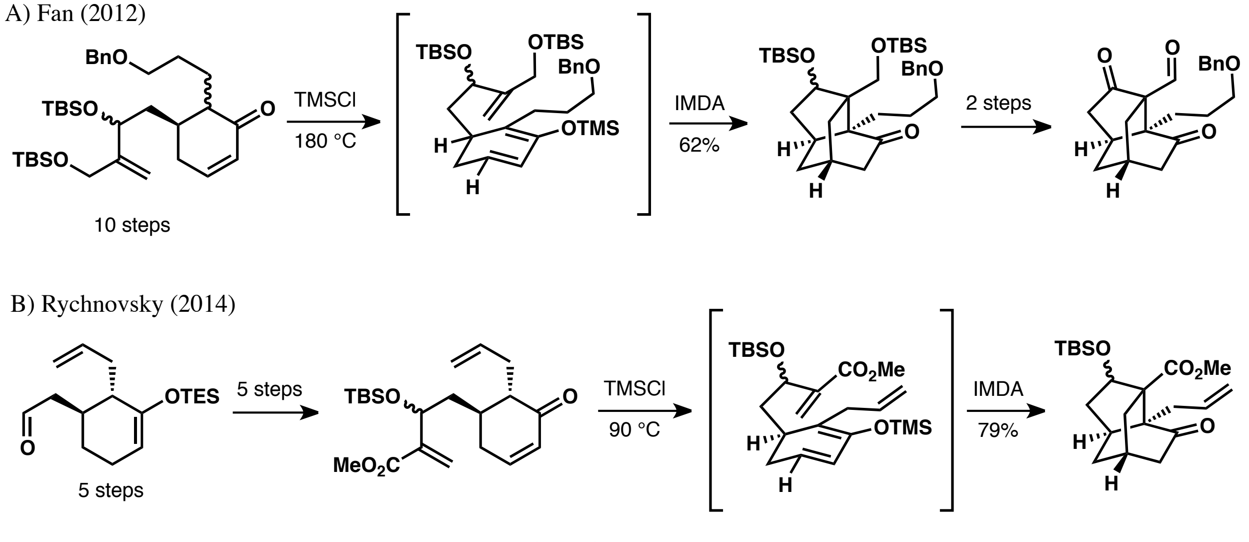
A) Fan (2012)
BnO
TBSO
TBSO
10 steps
TMSCl
180 °C
OTBS
OTMS
IMDA
62%
2 steps
B) Rychnovsky (2014)
OTES
5 steps
5 steps
MeO_2C
TMSCl
90 °C
CO_2Me
IMDA
79%

Scheme 5: Fan's and Rychnovsky's silyl dienol ether/IMDA approaches to the palhinine core

1.4 Retrosynthetic Analysis for Architecturally Unique Alkaloids

In our strategy for the total synthesis of palhinine A, we sought to bring together lessons learned from previous *Lycopodium* alkaloid syntheses. To avoid the apparent difficulties of forming the azanonane ring after establishing the caged 6-6-5 tricycle, we imagined fashioning the fused 6-5-9 tricycle prior to establishing the caged structure. By doing so, we could take advantage of the pioneering studies by Heathcock and many others (see Section 1.2) to establish chemistry for this tricycle. Additionally, by delaying the construction of the unique C16–C4 bond present in palhinine A until the end of the synthesis, we could utilize this route to gain access to additional *Lycopodium* alkaloids that have functionalization at C16 such as lycopladine D. Thus, we envisioned both palhinine A and lycopladine D arising from the same 6-5-9 tricyclic intermediate **1.11** (Scheme 6). The key synthetic challenge in accessing palhinine A would lie in late-stage construction of the tetracyclic caged structure. We envisioned accomplishing this through an atom-transfer radical cyclization (ATRC) of a primary alkyl iodide such as **1.12**.[16] For lycopladine D, we hypothesized that the key bonds could be formed by a nucleophilic ring-forming cascade, initiated by cleavage of the nitrogen protecting group of **1.13**.

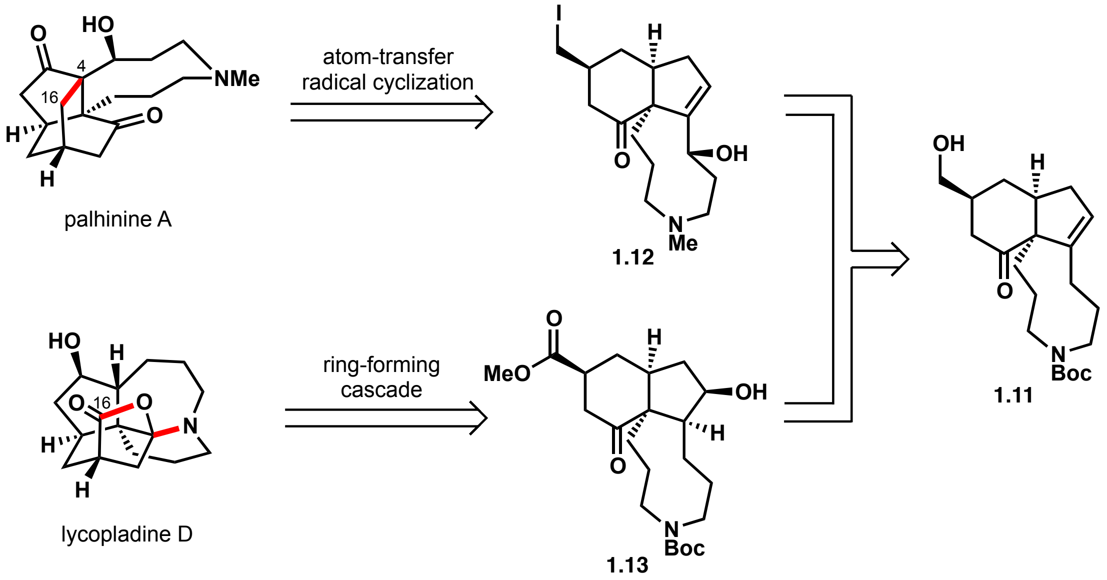

Scheme 6: Retrosynthetic analysis of palhinine A and lycopladine D from tricycle **1.11**

Tricyclic intermediate **1.11** could originate from directed hydrogenation of tricycle **1.14** where the azanonane ring could arise from reduction of α,β-unsaturated ester **1.15** followed by ring closure (Scheme 7). Boc-protected amine **1.15** could be accessed from coupling of an appropriate alkyl nucleophile with vinyl triflate **1.16**. Triflate **1.16** could be synthesized through a Diels-Alder cycloaddition between diene **1.17** and dienophile **1.18** followed by vinyl triflate formation.

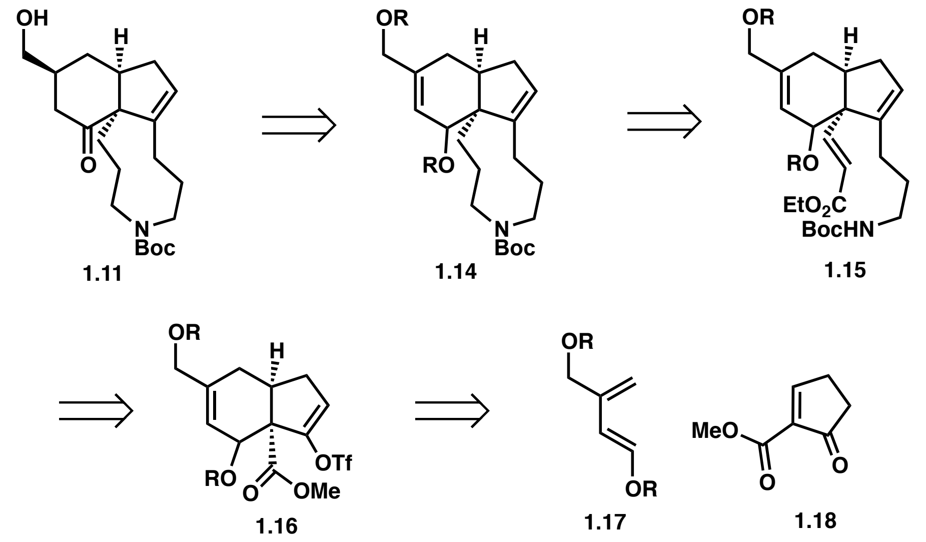
OH
H
O
N
Boc
1.11
OR
H
RO
N
Boc
1.14
OR
H
RO
EtO2C
BocHN
1.15
OR
H
RO
O
OMe
OTf
1.16
OR
OR
1.17
MeO
O
O
1.18

Scheme 7: Retrosynthetic analysis of common tricycle **1.11**

1.5 Synthesis of Cyclization Model System

While designing this synthetic route, we recognized that an ATRC to furnish the caged core of palhinine A would be an ambitious key step, especially knowing it would need to be investigated during the final stages of the synthesis. Because of this, we thought it prudent to investigate this proposed transformation on a simplified model substrate (**1.19** to **1.20,** Scheme 8). This model system would contain the requisite reactive partners (primary alkyl iodide and trisubstituted olefin) that would be positioned appropriately by the presence of a 6-5 bicycle. Only the azanonane ring would be lacking, but we rationalized that this should have relatively little consequence on the outcome of the transformation.

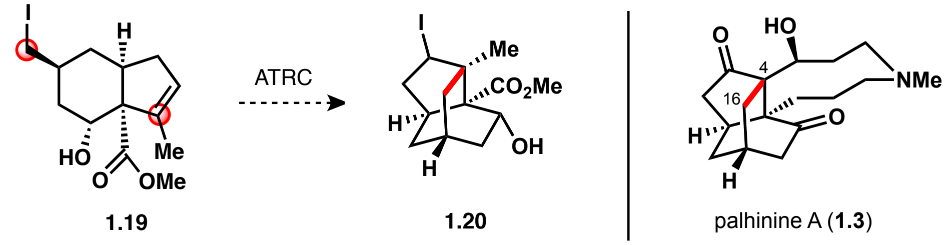
I
H
HO
O
OMe
Me
1.19
ATRC
I
Me
CO2Me
H
H
OH
1.20
O
HO
4
16
NMe
O
H
H
palhinine A (1.3)

Scheme 8: Model system for assessing cyclization toward the palhinine core

In order to gain access to model substrate **1.19**, it was first necessary to devise a route to diene **1.24** (Scheme 9). A short and chromatography-free route to diene precursor, enal **1.23,** was realized through protection of ethyl-3-methyl-4-oxocrotonate (**1.21**) as the dioxolane followed by a reduction of the ester group of **1.22** with diisobutylaluminium hydride and oxidation to the enal with manganese dioxide.

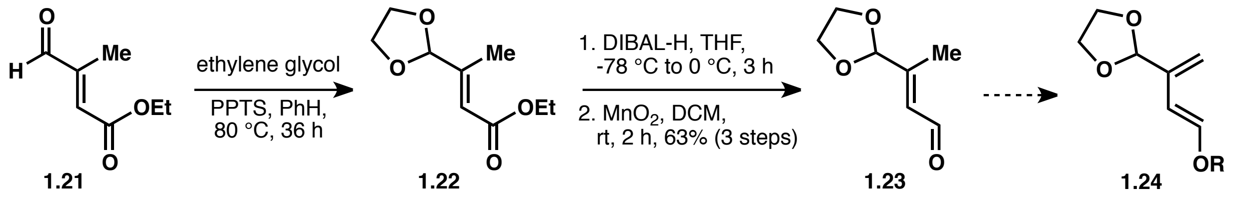

Scheme 9: Syntheis of diene precursor **1.23**

From enal **1.23**, many hard and soft enolization conditions were attempted in hopes of trapping the dienol with chloromethyl methyl ether (MOMCl) to form the desired dienol ether (**1.25**, Table 1). Soft enolization conditions utilizing triethylamine, ZnCl$_2$, and MOMCl failed to give any dienol ether products (entry 1).[17] Turning to conditions that applied kinetic deprotonation followed by an excess of MOMCl primarily generated undesired dienol ether **1.26** (entries 3,4). When lithium bis(trimethylsilyl)amide (LiHMDS) was utilized in the presence of hexamethylphosphoramide (HMPA) as a cosolvent, small amounts of **1.25** were isolated, but inconsistent results and competing formation of the undesired regioisomer (i.e., **1.26**) plagued this transformation (entries 5-8).

Table 1: Enolization attempts to form diene **1.25**

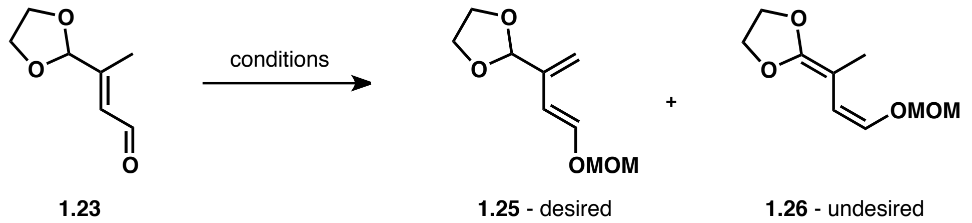

entry	base (equiv)	MOMCl equiv	solvent	result (yield)
1	Et$_3$N (1.5), ZnCl$_2$	1.1	DCM	No rxn
2	KHMDS (1.2)	1.1	THF	No rxn
3	KHMDS (1.2)	5	THF	**1.26** (10%)
4	NaHMDS (1.2)	5	THF	**1.26** (8%)
5	LiHMDS (1.2)	5	THF:HMPA (3:2)	**1.25** (16%) **1.26** (9%)
6	LiHMDS (1.2)	5	THF:HMPA (2:1)	Trace **1.25**
7	LiHMDS (1.2)	5	THF:HMPA (10:1)	Trace **1.26**
8	LiHMDS (1.2)	5	THF:HMPA (1:1)	Trace **1.26**

Alternatively, soft enolization conditions utilizing triethylamine, ZnCl$_2$, and *tert*-butyldimethylsilyl trifluoromethanesulfonate (TBSOTf) were moderately successful at forming silyl dienol ether **1.27** (Scheme 10). Although low yielding, this transformation proved to be more reliable and provided access to desired diene **1.27** after purification by column chromatography. With this diene in hand, a Diels-Alder cycloaddition with dienophile **1.18** afforded bicycle **1.28** as a 1:1 mixture of diastereomers. At this stage, we hoped to achieve a diastereoselective hydrogenation of trisubstituted olefin **1.28**. If hydrogen was delivered from the convex face of the bicycle, then the key stereocenter of compound **1.29** would be set. However, many standard hydrogenation catalysts failed to show reactivity and the small amount of product that formed with PtO$_2$ as a catalyst resulted in a mixture of diastereomers.

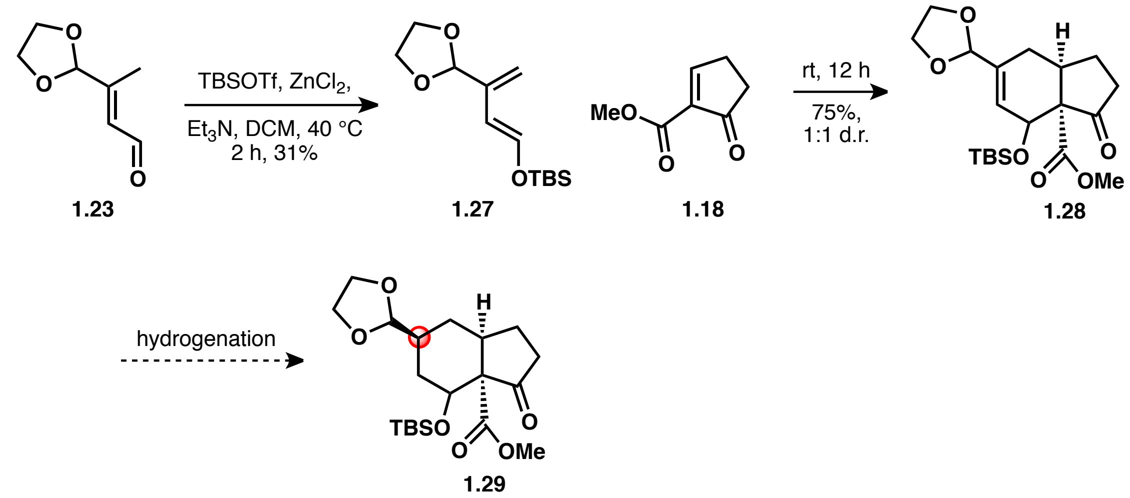

Scheme 10: Diels-Alder reaction to forge 6-5 bicycle **1.28**

To obtain a diastereoselective hydrogenation, we sought to unmask the secondary allylic alcohol moiety to achieve a directed hydrogenation, although this would require utilizing only the α-epimer of TBS ether **1.28** (Scheme 11). At this stage, the diastereomers were not readily separable, so both epimers were subjected to potassium bis(trimethylsilyl)amide (KHMDS) with subsequent enolate trapping to afford a vinyl triflate handle for cross-coupling. Although a longer nitrogen-containing fragment would ideally be used for the natural product synthesis, we chose to append a simple methyl group for this model system. Utilizing various types of alkyl metal species resulted in no reaction (trimethylboroxine) or decomposition (trimethylaluminum, dimethylzinc, ethylmagnesium bromide), but switching to tetramethyltin resulted in a clean reaction to access trisubstituted olefin **1.29**. At this stage, the two diastereomers were readily separable and desired α-OTBS compound **1.29a** was isolated. Cleavage of the TBS group occurred smoothly upon exposure to TBAF, unveiling the free hydroxyl group to serve in the directed hydrogenation. Elevated pressures of hydrogen (500 psi) were necessary to achieve full conversion when catalytic amounts of Crabtree's catalyst were used. Although hydrogenated compound **1.30** was obtained in moderate yield (resulting from competing reduction of the more distal trisubstituted olefin), the transformation was completely diastereoselective.

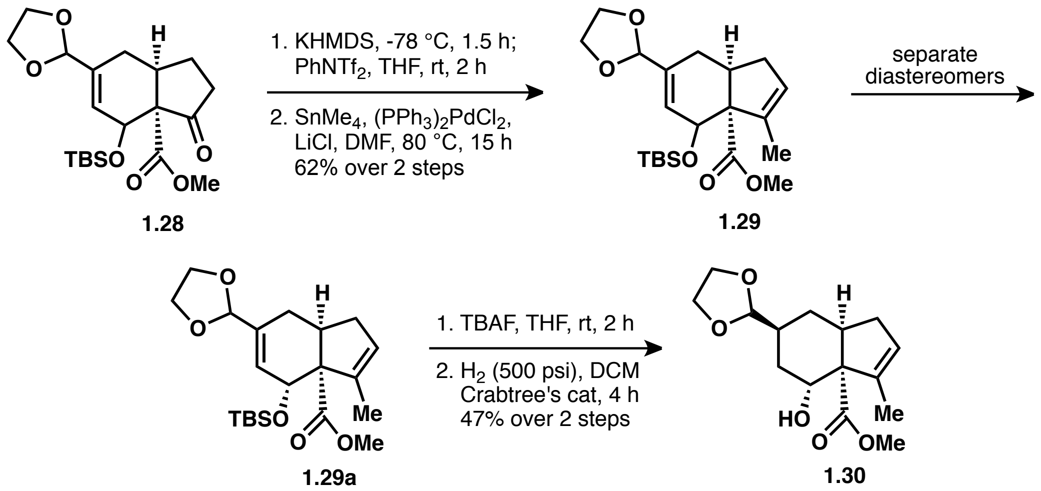
1. KHMDS, -78 °C, 1.5 h; PhNTf2, THF, rt, 2 h
2. SnMe4, (PPh3)2PdCl2, LiCl, DMF, 80 °C, 15 h
62% over 2 steps
separate diastereomers
1. TBAF, THF, rt, 2 h
2. H2 (500 psi), DCM Crabtree's cat, 4 h
47% over 2 steps
TBSO
HO
H
Me
OMe
O
1.28
1.29
1.29a
1.30

Scheme 11: Directed hydrogenation to access the desired diastereomer of **1.30**

While utilizing a directed hydrogenation was critical for setting the correct relative stereochemistry, it was unfortunate to have to discard half the material from the unwanted diastereomer of the Diels-Alder adduct. Fortuitously, we recognized that upon subjecting TBS ether **1.29a** to TBAF, the desired alcohol **1.31a** was obtained along with 5-10% of the corresponding β-epimer (Scheme 12). This epimerization presumably occurs through a retro-aldol ring opening followed by re-closure onto the intermediate aldehyde. After observing epimerization at this position, we rationalized that the undesired diastereomer **1.29b** could be subjected to TBAF for an extended amount of time in order to equilibrate between the two diastereomers. Although this process was not extensively optimized, initial results indicated a 2:1 ratio of diastereomers forming in favor of the desired α-epimer. This could provide an effective method for funneling the material to the desired stereoisomer.

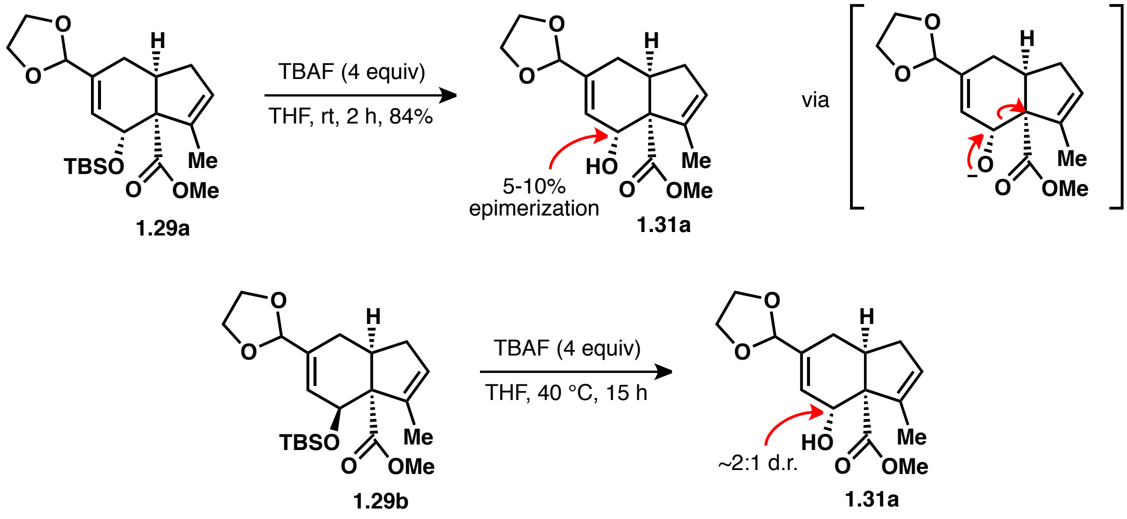
TBAF (4 equiv)
THF, rt, 2 h, 84%
5-10% epimerization
via
TBAF (4 equiv)
THF, 40 °C, 15 h
~2:1 d.r.
TBSO
HO
H
Me
OMe
O
1.29a
1.31a
1.29b
1.31a

Scheme 12: Epimerization studies

To complete the synthesis of the model system, dioxolane **1.30** was hydrolyzed with water and pyridinium *p*-toluenesulfonate (PPTS), then reduced to alcohol **1.32** with sodium borohydride (Scheme 13). Utilizing standard Appel conditions (I_2, PPh_3, imidazole) to iodinate the hydroxyl group of **1.32** only resulted in exo-methylene **1.33**, presumably due to facile elimination of the alkyl iodide product under basic conditions. Therefore, less basic protocols were examined, specifically, a modified Mitsunobu procedure that utilizes iodomethane as the iodide source. This protocol succeeded at delivering alkyl iodide **1.34** without any elimination products.

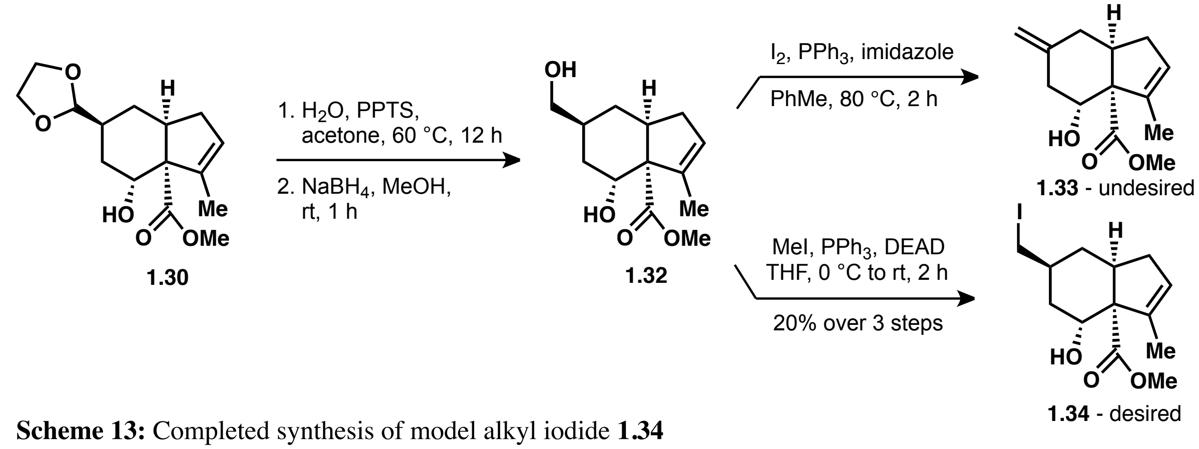

Scheme 13: Completed synthesis of model alkyl iodide **1.34**

1.6 Cyclization Attempts

With alkyl iodide **1.34** in hand, we set out to test the feasibility of an ATRC on this model substrate. Simply subjecting the material to UV irradiation (310 nm) only returned starting material while changing the irradiation to 254 nm light resulted in a complex mixture of compounds (Table 2, entries 1,2). These products contained new alkene peaks as seen in the ^{1}H NMR, indicating a non-productive reaction. Switching to a Ru^{2+} catalyst known to promote ATRC only resulted in decomposition (entry 3).[18] We next sought to utilize some tin chemistry as popularized by Dennis Curran for complex molecule total synthesis. Unfortunately, decomposition resulted with $(Bu_3Sn)_2$ and sunlamp irradiation, while only reduction compound **1.36** was obtained with Bu_3SnH and azobisisobutyronitrile (AIBN) (entries 4-6). This indicated that the primary alkyl radical could be formed under these conditions but the subsequent cyclization was slow and unfavorable.

Table 2: Investigation of conditions for ATRC of model alkyl iodide **1.34**

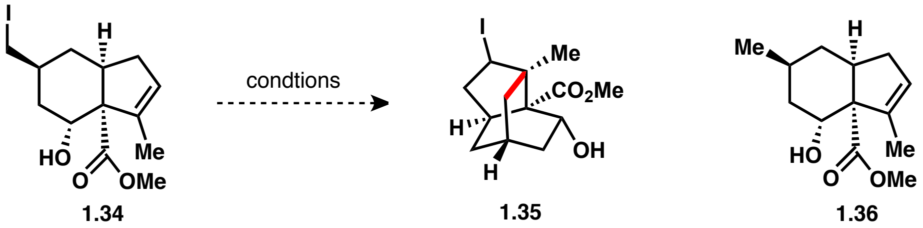

entry	conditions	result
1	hν (310 nm), PhH, rt	No rxn
2	hν (254 nm), PhH, rt	Many unknown pdts
3	$RuCl_2(PPh_3)_2$, PhH, 150 °C	Decomposition
4	$(Bu_3Sn)_2$, sunlamp, PhH, 80 °C	Decomposition
5	Bu_3SnH (2 equiv), AIBN	**1.36** (complex mixture)
6	Bu_3SnH (20 equiv), AIBN	**1.36** (clean)

In addition to the ATRC conditions, a few attempts were made at initiating an alkyl-Heck reaction. Alkyl-Heck reactions have historically been quite challenging due to the low reactivity of alkyl halides to oxidative addition and the propensity for the organo-palladium intermediate to undergo β-hydride elimination, but recent advances by several labs including those of Alexanian[19] and Fu[20] indicated that the desired cyclization could be possible. However, upon surveying both palladium and nickel catalysts, only starting material was obtained and this strategy was abandoned (Scheme 14).

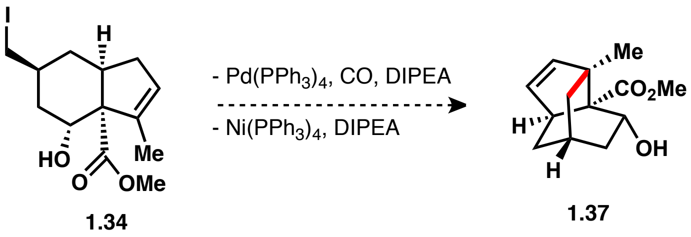

Scheme 14: Survey of alkyl-Heck reaction

Having had no success in achieving any type of cyclization, we turned to computational methods to investigate the conformational bias inherent in these substrates (Figure 4). By using Monte Carlo conformational searches, it quickly became clear that this 6-5 bicyclic system preferred to sit in a way that placed the reactive methyl radical in a pseudo-equatorial position and thus very far away from the olefin functionality (see **1.38**).[21] We were interested to see if modifying the substituents around the 6-membered ring could have an effect on the conformational preference of this system. Interestingly, simply by oxidizing the secondary alcohol group of **1.38** to the corresponding ketone **1.39**, another conformation became preferable that placed the methyl radical in a pseudo-axial position and thus in a more favorable position for productive cyclization.

Figure 4: Conformational analysis of 6-5 bicycles

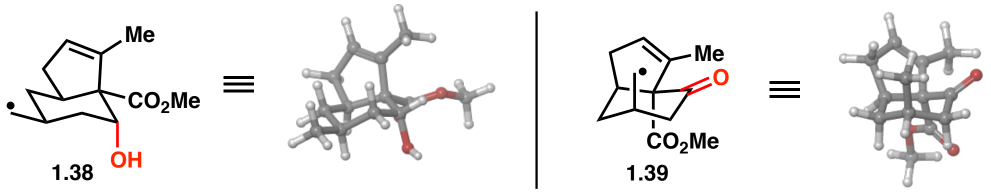

1.38

1.39

Putting this idea into practice, oxidation of alcohol **1.34** with Dess-Martin periodinane (DMP) proceeded to give ketone **1.40** (Scheme 15). However this substrate failed to give any productive cyclization products under ATRC conditions. Even though this substrate had a better conformational preference, a high-energy boat conformation is most likely required to promote this cyclization.

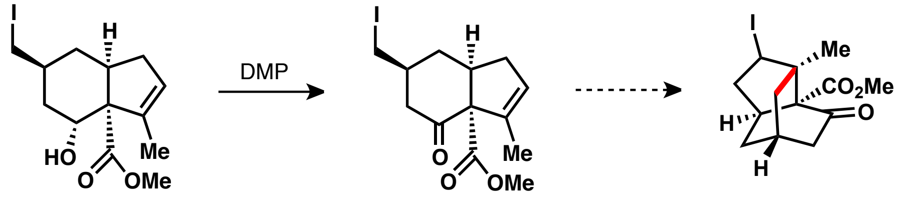

1.34

1.40

1.41

Scheme 15: Attempted cyclization of ketone **1.40**

Although we were never able to effect the desired ATRC, several potential strategies for constructing the key C–C bond still remain. The most promising strategy involves an enolate alkylation that would take advantage of the electrophilic alkyl iodide. The only necessary modification would be a hydroboration/oxidation sequence to yield ketone **1.42** (Scheme 16). An intermediate enolate should be less reactive and more persistent than a primary alkyl radical, thus allowing access to higher-energy conformations necessary for cyclization.

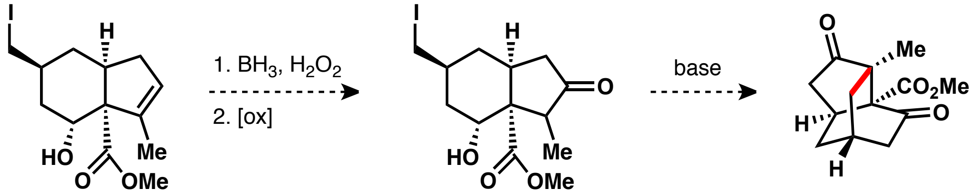

1.34

1.42

1.43

Scheme 16: Proposed enolate alkylation strategy for constructing caged system

1.7 Synthesis of Advanced 6-5-9 Tricycle

Concurrent with my investigation of the cyclization model system, a fellow graduate student, Rebecca Murphy, developed a 12-step sequence to access tricycle **1.54** (see Scheme 18). This compound is reminiscent of the proposed common intermediate (see **1.11,** Scheme 6) necessary to access our natural product targets. I was able to carry out this synthetic sequence on large scale to explore further reactivity of this key intermediate. This synthesis commenced with the enyne metathesis of TBS protected propargyl alcohol and ethyl vinyl ether to yield diene **1.44** as a 7:3 ratio of *E/Z* isomers (Scheme 17).[22] Upon heating diene **1.44** with dienophile **1.18**, Diels-Alder adduct **1.45** formed as a separable mixture of diastereomers (*d.r.* = 3:2). Although ultimately inconsequential, the major diastereomer could be isolated and carried forward. Treatment of this bicycle with KHMDS and subsequent enolate trapping using phenyl triflimide afforded vinyl triflate **1.46**, providing a functional handle for cross coupling later in the sequence. Reduction of the ester group with excess diisobutylaluminium hydride and oxidation with Dess-Martin periodinane yielded aldehyde **1.47** in 53% yield over 3 steps. Heating this aldehyde with phosphorous ylide **1.48** smoothly afforded unsaturated ester **1.49** in 94% yield.

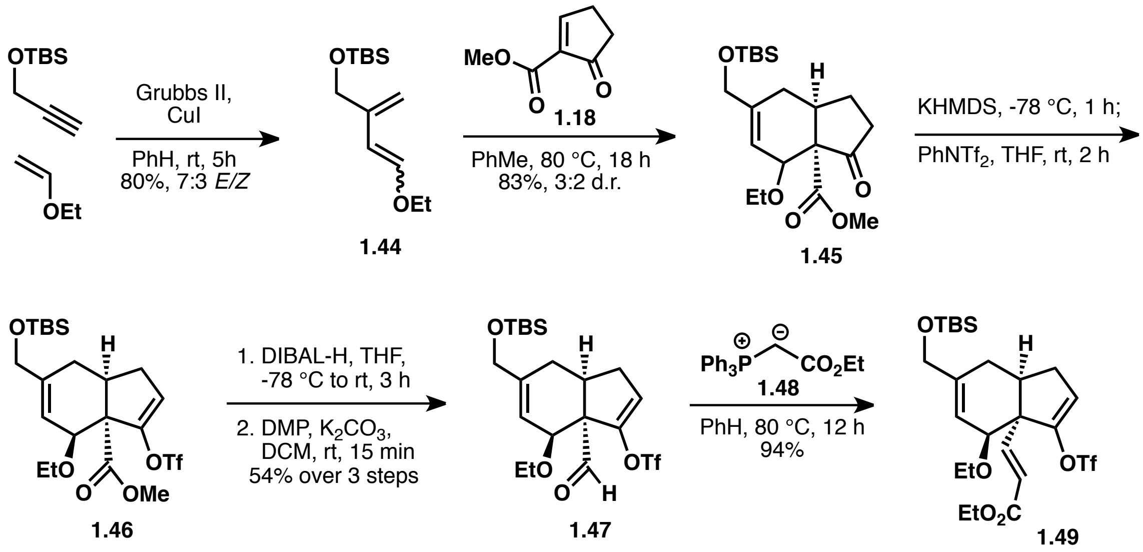
OTBS
OEt
Grubbs II, CuI
PhH, rt, 5h
80%, 7:3 E/Z
OTBS
OEt
1.44
MeO
O
O
1.18
PhMe, 80 °C, 18 h
83%, 3:2 d.r.
OTBS
H
EtO
O
O
OMe
1.45
KHMDS, -78 °C, 1 h;
PhNTf2, THF, rt, 2 h
OTBS
H
EtO
OTf
O
OMe
1.46
1. DIBAL-H, THF, -78 °C to rt, 3 h
2. DMP, K2CO3, DCM, rt, 15 min
54% over 3 steps
OTBS
H
EtO
OTf
O
H
1.47
Ph3P
CO2Et
1.48
PhH, 80 °C, 12 h
94%
OTBS
H
EtO
OTf
EtO2C
1.49

Scheme 17: Synthesis of alternative 6-5 bicycle **1.45** and further elaboration

The functionalized vinyl triflate **1.49** underwent a Suzuki cross-coupling with freshly prepared trialkylborane **1.50** to give product **1.51** in 90% yield (Scheme 18).[23] At this stage, all the carbons necessary for the natural product had been installed. Ester reduction with diisobutylaluminium hydride followed by a directed hydrogenation with Wilkinson's catalyst afforded primary alcohol **1.52** in 67% yield over 2 steps. Finally, closure of the azanonane ring was achieved through a three-step sequence. First, tosylation followed by iodination yielded primary alkyl iodide **1.53**. Displacement of the iodide was achieved by treatment with potassium hydride to afford tricycle **1.54**, although elimination of the alkyl iodide was always a competing pathway.

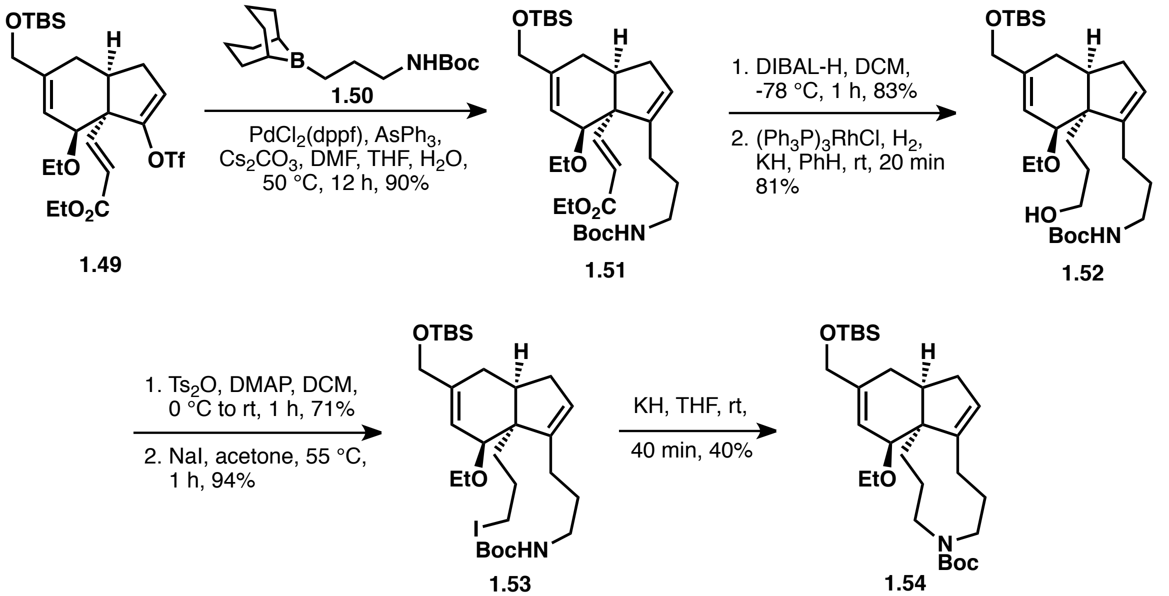
OTBS
H
OTf
EtO
EtO2C
1.49
B
NHBoc
1.50
PdCl2(dppf), AsPh3,
Cs2CO3, DMF, THF, H2O,
50 °C, 12 h, 90%
1.51
BocHN
1. DIBAL-H, DCM,
-78 °C, 1 h, 83%
2. (Ph3P)3RhCl, H2,
KH, PhH, rt, 20 min
81%
HO
1.52
1. Ts2O, DMAP, DCM,
0 °C to rt, 1 h, 71%
2. NaI, acetone, 55 °C,
1 h, 94%
I
1.53
KH, THF, rt,
40 min, 40%
N
Boc
1.54

Scheme 18: Completion of 6-5-7 tricycle **1.54**

At this stage, we were interested in exploring the feasibility of installing the C5 oxygenation that is present in palhinine A. We found that although reactivity of the tricycle **1.54** was low, selenium dioxide could chemo- and regioselectively oxidize the desired allylic position of bicycle **1.53** to yield enone **1.55**, albeit in low yield (Scheme 19). Under the reaction conditions, deprotection of the allylic alcohol group (possibly mediated by trace selenous acid) and oxidation to the aldehyde was also observed. Although this proved selenium dioxide oxidation to be a viable strategy, other oxidation methods could be explored. Of particular interest, acetoxylated compound **1.57** could be accessed from **1.56** using the late-stage C–H oxidation chemistry developed by the Sanford group.[24]

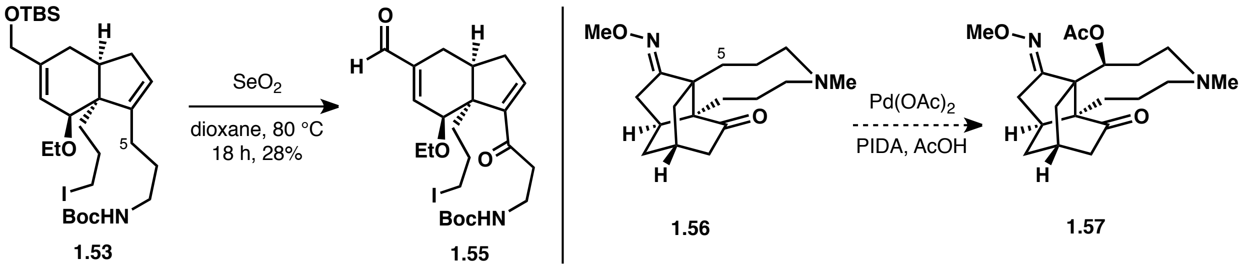
OTBS
H
EtO
5
I
BocHN
1.53
SeO2
dioxane, 80 °C
18 h, 28%
O
H
O
1.55
MeO
N
5
NMe
O
H
1.56
Pd(OAc)2
PIDA, AcOH
AcO
1.57

Scheme 19: Possible methods for installing C5 oxygenation

1.8 Transannular Hydroamination

With 6-5-9 tricycle **1.54** in hand, we recognized that cleavage of the ethyl ether moiety to give alcohol **1.58** was necessary to continue with the synthesis and begin modification of the cyclohexyl ring (Scheme 20). Unfortunately, the majority of conditions typically employed for alkyl ether cleavage are Brønsted or Lewis acidic and our substrate was quite acid-sensitive.

Therefore, in situ generated trimethylsilyl iodide (TMSI) was investigated as a promising set of conditions. Interestingly, upon subjecting tricycle **1.54** to these conditions, enal **1.59** was obtained. This product presumably arises from TMSI-promoted elimination of ethanol to give dienol ether **1.60**. Hydrolysis of the TBS enol ether affords unconjugated enal **1.61** that can isomerize to give the thermodynamically more favored enal **1.59**. It is also possible that this transformation could be promoted by small amounts of hydrogen iodide generated under these reaction conditions.

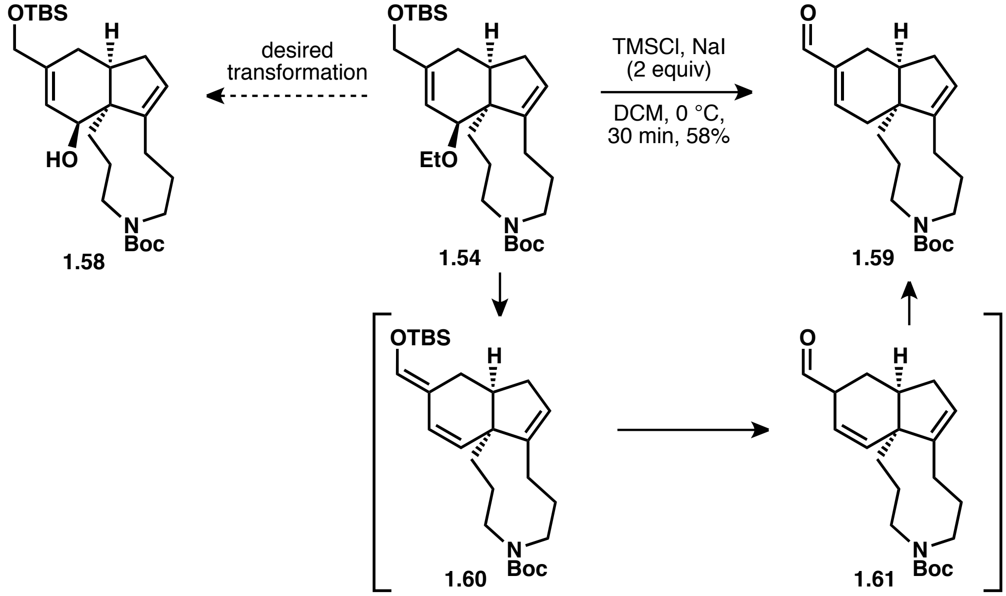

Scheme 20: Transformation from tricycle **1.54** to enal **1.59**

To our surprise, increasing the amount of TMSI from 2 to 10 equivalents promoted the transformation of **1.54** to tetracycle **1.62** in 50% yield (Scheme 21). This 6-5-6-5 tetracycle maps onto the tetracyclic core of the natural products serratine (**1.63**) and 8-deoxyserratine (**1.64**). The structure of **1.62** was confirmed by single crystal X-ray crystallographic analysis. In the remarkable conversion of **1.54** to **1.62**, not only was the allylic ether moiety on the six-membered ring converted to the enal motif (see Scheme 20), but also, the Boc-protecting group was cleaved and the resulting amine underwent transannular hydroamination with the carbon-carbon double bond in the five-membered ring to form a new C–N bond to the C4 position. Cleavage of Boc protecting groups is known to be mediated by TMSI as well as strong acids, so it is unsurprising that the secondary amine of **1.54** would be deprotected under these conditions. What was unanticipated is the efficient hydroamination under such mild conditions given the general difficulty of effecting these transformations. In this case, it is likely that the proximity of the secondary amine to the alkene group plays a role in facilitating this reaction. Our hypothesis is that the azonane ring resides underneath the 6-5 bicycle in **1.54**, positioning the amine group very close to the carbon-carbon double bond.

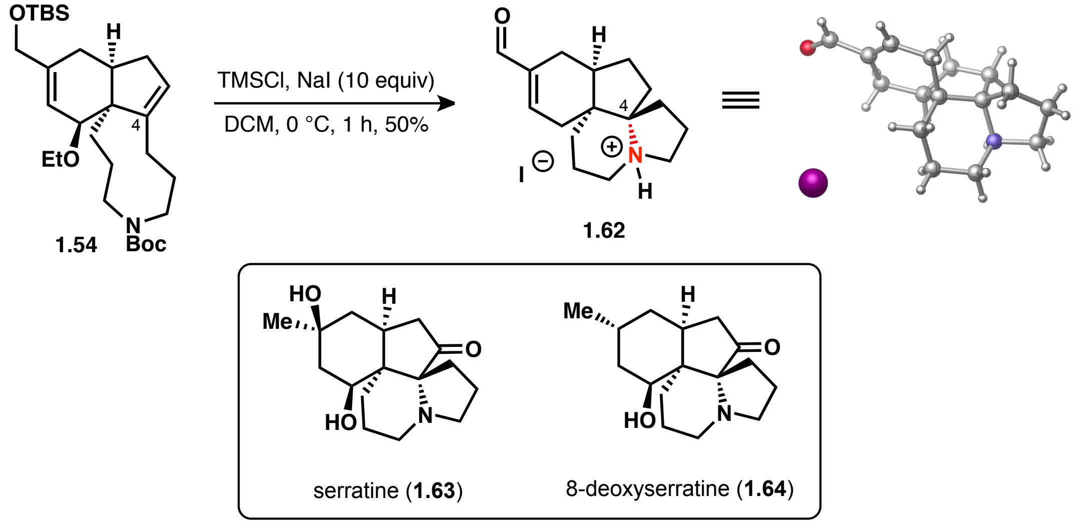
OTBS
H
4
EtO
1.54
N
Boc
TMSCl, NaI (10 equiv)
DCM, 0 °C, 1 h, 50%
O
H
4
I ⊖
⊕ N
H
1.62
HO
Me
H
O
HO
N
serratine (**1.63**)
Me
H
O
HO
N
8-deoxyserratine (**1.64**)

Scheme 21: Unexpected transannular hydroamination mediated by TMSI to give tetracycle **1.62**

1.9 Conclusion and Outlook

While we were working on this project, the Zhao group published a synthesis of lycopladine D that utilized a similar end-game strategy to the one we had proposed.[25] They were able to access functionalized tricycle **1.66** from bicycle **1.65**, and exposure of the tricycle to trifluoroacetic acid initiated the nucleophilic ring-forming cascade to give the natural product (Scheme 22).

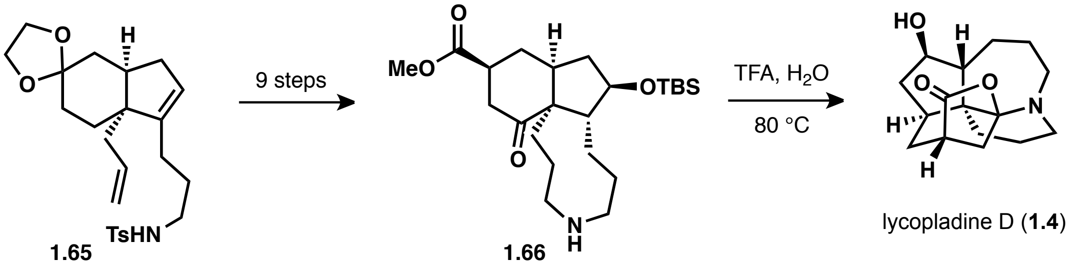
O
O
H
TsHN
1.65
9 steps
O
MeO
H
OTBS
O
N
H
1.66
TFA, H2O
80 °C
HO
H
O
O
H
N
H
lycopladine D (**1.4**)

Scheme 22: Zhao's synthesis of lycopladine D via nucleophilic ring-forming cascade

Because the Zhao group reported this transformation to access lycopladine D and due to our lack of success at building the core of palhinine A, we decided to stop pursuing the total synthesis of these *Lycopodium* alkaloids. Nonetheless, during the course of this project, we were able to construct an advanced 6-5-9 tricycle that could be amenable to the synthesis of several architecturally unique *Lycopodium* alkaloids. We've shown on a model system how the cyclohexyl ring can be modified to give a precursor for cyclization necessary to construct the caged system of palhinine A. Finally, while investigating transformations on the advanced tricycle, an unexpected TMSI-mediated hydroamination occurred. This interesting discovery paved the way for studies that are outlined in Chapter 2 of this dissertation.

1.10 Experimental Contributors

Rebecca Murphy (graduate student, Sarpong lab) developed and carried out all the original chemistry for the synthesis of 6-5-9 tricycle **1.54** (Schemes 17 and 18), but all the reported yields were obtained from my own experiments. She also was the first to show the synthesis of TBS-dienol ether **1.27** (Scheme 10). Additionally, Rebecca was the first to discover the unexpected reactivity of tricycle **1.54** when exposed to in situ generated TMSI (Schemes 20 and 21). She obtained the crystal structure for tetracycle **1.62**. The remainder of the work presented in this chapter was conducted by Paul R. Leger.

1.11 Experimental Methods

All reactions were performed in flame-dried glassware fitted with a Teflon stir bar and rubber septa under a nitrogen atmosphere unless otherwise specified. Liquid reagents and solvents were transferred via syringe under nitrogen. Tetrahydrofuran (THF), diethyl ether (Et_2O), benzene, toluene, and triethylamine were dried over alumina under a nitrogen atmosphere in a GlassContour solvent system. Dichloromethane (DCM) was distilled over calcium hydride. All other solvents and reagents were used as received unless otherwise noted. Reaction temperatures above 23 °C were controlled by an IKA® temperature modulator. Reactions were monitored by thin layer chromatography (TLC) using SiliCycle silica gel 60 F254 precoated plates (0.25 mm) which were visualized using UV light and *p*-anisaldehyde stain. Sorbent silica gel (particle size 40-63 µm) was used for flash chromatography. ^{1}H and ^{13}C NMR were recorded on Bruker AVB-400, AV-500, DRX-500 or AV-600 MHz spectrometers with ^{13}C operating frequencies of 100, 125, 125, and 150 MHz, respectively, in $CDCl_3$ at 23 °C. Chemical shifts (δ) are reported in ppm relative to the residual solvent signal ($CDCl_3$ $\delta = 7.26$ for ^{1}H NMR and $\delta = 77.16$ for ^{13}C NMR). IR spectra were recorded on a Nicolet MAGNA-IR 850 spectrometer. Mass spectral data were obtained from the Mass Spectral Facility at the University of California, Berkeley. Melting points were taken in duplicate using a Mel-Temp II instrument from Laboratory Devices, USA.

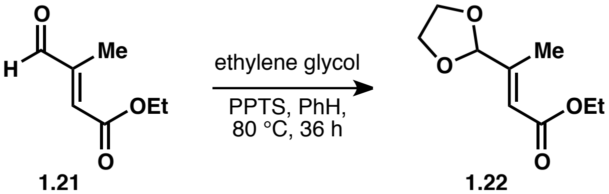

Dioxolane **1.22**

To a solution of ethyl-3-methyl-4-oxocrotonate (30.0 mL, 220 mmol) in benzene (400 mL), ethylene glycol (123 mL, 2.20 mol) and pyridinium *p*-toluenesulfonate (61.0 g, 162 mmol) were added. The resulting solution was heated to reflux and stirred for 36 h. After cooling back to room temperature, the mixture was diluted with EtOAc (300 mL) and washed with water (2 x 400 mL), sodium bicarbonate (2 x 400 mL), and brine (1 x 400 mL). The organic layer was dried, filtered, and concentrated to yield the crude dioxolane **1.22** which was carried on without purification.

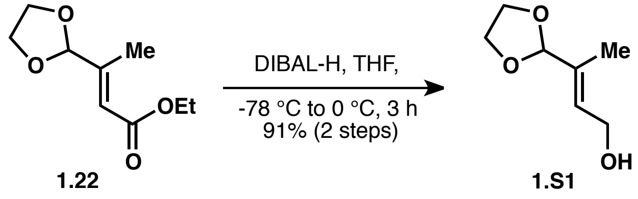

Allylic alcohol **1.S1**

Crude dioxolane **1.22** (39.5 g, 212 mmol) in THF (1 L) was cooled to -78 °C. Diisobutylaluminum hydride (95 mL, 530 mmol) was added slowly and this resultant mixture was stirred for 30 min, after which the solution was allowed to warm to 0 °C and stir for another 2 h. At this point, saturated Rochelle's salt solution (800 mL) was added slowly while keeping the mixture at 0 °C. This mixture was then extracted with EtOAc (3 x 800 mL), letting each addition stir 30 min before separation. The combined organic layers were dried over magnesium sulfate, filtered, and concentrated to yield allylic alcohol **1.S1** (28.9 g, 91%) as a colorless oil. The spectral data were identical to those that were previously reported.[26]

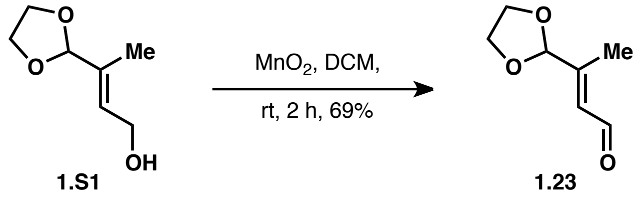

Enal **1.23**

To a solution of allylic alcohol **1.S1** (28.9 g, 200 mmol) in DCM (1.1 L) was added activated manganese dioxide (174 g, 2.00 mol) and the resulting heterogeneous black mixture was stirred at room temperature for 2 h. This mixture was then filtered through a plug of silica and washed with DCM to yield enal **1.23** (19.5 g, 69%) as a colorless oil. ^{1}H NMR (600 MHz, CDCl$_3$): δ 10.09 (d, *J* = 8 Hz, 1H), 6.16 (d, *J* = 8 Hz, 1H), 5.28 (s, 1H), 3.96-4.04 (m, 4H), 2.15 (s, 3H); ^{13}C NMR (100 MHz, CDCl$_3$): δ 191.5, 156.1, 127.8, 104.8, 65.7, 12.2; IR (thin film) υ_{max} cm^{-1} 2890, 1680, 1443, 1371, 1131, 1027, 941; HRMS (ESI) calculated for $[C_7H_{10}O_3Na]^+$ $[M+Na]^+$: *m/z* 165.0522, found 165.0520.

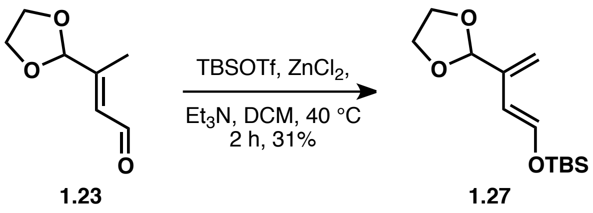

Silyl dienol ether **1.27**

A heterogeneous mixture of zinc (II) chloride (1.87 g, 13.7 mmol) and DCM was cooled to 0 °C. Enal **1.23** (19.5 g, 137 mmol) was then added to the stirring mixture followed by triethylamine (29.0 mL, 206 mmol) and trifluoromethanesulfonic acid *tert*-butyldimethylsilyl ester (35.0 mL, 151 mmol). The mixture was then warmed to 40 °C and stirred at this temperature for 2 h. Then, the reaction was washed with sodium bicarbonate (3 x 500 mL). The organic layer was dried over magnesium sulfate, filtered, concentrated, and purified by column chromatography (SiO_2, 10% EtOAc/ hexane) to yield silyl dienol ether **1.27** (10.8 g, 31%) as a pale yellow oil. ^{1}H NMR (500 MHz, $CDCl_3$): δ 6.83 (d, *J* = 12 Hz, 1H) 5.67 (d, *J* = 12 Hz, 1H), 5.36 (s, 1H), 5.14 (s, 1H), 5.03 (s, 1H), 3.89-4.07 (m, 4H), 0.91 (s, 9H), 0.10 (s, 6H); ^{13}C NMR (100 MHz, $CDCl_3$): δ 143.7, 140.7, 112.0, 110.2, 103.5, 65.1, 25.7, 18.4, -5.1; IR (thin film) υ_{max} cm^{-1} 2956, 2930, 2886, 2859, 1647, 1472, 1256, 1172, 1109; HRMS (ESI) calculated for $[C_{13}H_{25}O_3Si]^+$ $[M+H]^+$: *m/z* 257.1567, found 257.1565.

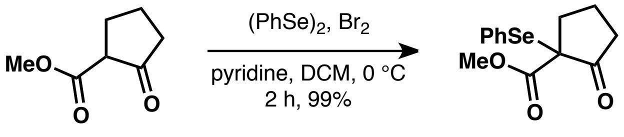

1.S2 **1.S3**

α-Seleno-β-ketoester **1.S3**

A 500 mL flask was charged with diphenyl diselenide (7.50 g, 24.2 mmol) and DCM (170 mL). Bromine (1.20 mL, 23.8 mmol) was added and the solution was stirred for 25 min at which time it was cooled to 0 °C. Pyridine (4.9 mL, 60 mmol) and methyl 2-oxo-cyclopentane-1-carboxylate (5.00 mL, 40.3 mmol) were added sequentially and stirring was continued for 90 min. The solution was diluted with DCM (250 mL) and washed with hydrochloric acid (1 M, 2 x 300 mL) and then sodium bicarbonate (2 x 300 mL). The organic layer was dried over magnesium sulfate, filtered, and concentrated to yield α-seleno-β-ketoester **1.S3** (12.1 g, 99%) as a yellow oil. The spectral data were identical to that which were previously reported.[27]

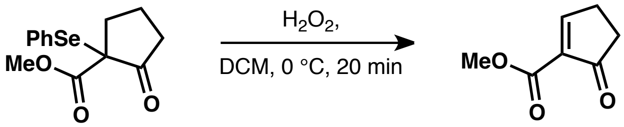

1.S3 **1.18**

Dienophile **1.18**

A 250 mL flask was charged with α-seleno-β-ketoester **1.S3** (5.50 g, 18.4 mmol) and DCM (100 mL) and cooled to 0 °C. Hydrogen peroxide (30% aq. solution, 4.0 mL) was added dropwise and the reaction mixture was stirred vigorously for 20 min. The reaction mixture was then diluted with DCM (100 mL) and water (120 mL). The aqueous phase was extracted with DCM (3 x 100 mL). The combined organic layers were dried over magnesium sulfate, filtered, and concentrated to yield dienophile **1.18** as a pale yellow oil. This compound was not stable for extended periods of time and was carried on unpurified.

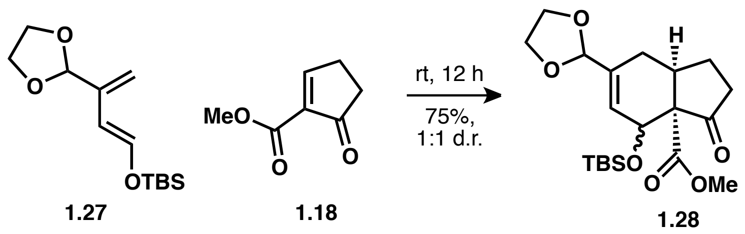

Bicycle **1.28**

Silyl dienol ether **1.27** (1.43 g, 5.58 mmol) and dienophile **1.18** (1.17 g, 8.37 mmol) were combined and stirred at room temperature for 12 h. The resulting yellow solid was purified by column chromatography (SiO_2, 10% EtOAc/ hexane) to yield bicycle **1.28** (1.66 g, 75%, *d.r.* = 1:1) as a white solid. ^{1}H NMR (600 MHz, $CDCl_3$): δ 5.99 (d, *J* = 5 Hz, 1H x 50/100), 5.96 (d, *J* = 5 Hz, 1H x 50/100), 5.19 (s, 1H x 50/100), 5.12 (s, 1H x 50/100), 4.95 (s, 1H x 50/100), 4.78 (s, 1H x 50/100), 3.88-4.00 (m, 8H x 50/100), 3.71 (s, 1H x 50/100), 3.70 (s, 1H x 50/100), 3.24 (q, *J* = 7 Hz, 1H x 50/100), 3.06 (dt, *J* = 7, 14 Hz, 1H x 50/100), 2.54 (dd, *J* = 8, 18 Hz, 1H x 50/100), 2.25-2.37 (m, 4 x 50/100), 2.15-2.23 (m, 3 x 50/100), 2.07 (dd, *J* = 10, 20 Hz, 1H x 50/100), 1.98 (q, *J* = 9 Hz, 1H x 50/100), 1.77 (dd, *J* = 6, 17 Hz, 1H x 50/100), 1.69 (t, *J* = 12 Hz, 1H x 50/100), 0.82 (s, 9H), 0.05 (s, 6H); ^{13}C NMR (125 MHz, $CDCl_3$): δ 212.3, 211.0, 170.8, 167.9, 138.1, 135.1, 127.3, 126.1, 105.1, 104.6, 67.6, 66.2, 65.3, 65.2, 63.2, 52.6, 52.5, 39.1, 37.3, 35.2, 33.1, 27.3, 26.3, 25.7, 25.6, 25.3, 23.0, 17.8, 17.8, -3.9, -4.4, -5.0, -5.2; IR (thin film) υ_{max} cm^{-1} 2954, 2887, 2857, 1756, 1735, 1472, 1434, 1255, 1079, 1030; HRMS (ESI) calculated for $[C_{20}H_{32}O_6NaSi]^+$ $[M+Na]^+$: *m/z* 419.1860, found 419.1859; Melting point: 69.2 – 70.1 °C.

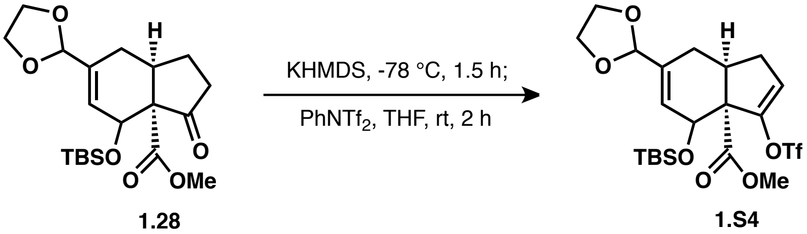

Vinyl triflate **1.S4**

A solution of bicycle **1.28** (433 mg, 1.09 mmol) in THF (2.8 mL) was cooled to -78 °C under a nitrogen atmosphere. Potassium bis(trimethylsilyl)amide (0.5 M in toluene, 2.84 mL, 1.42 mmol) was slowly added and the mixture was stirred for 1.5 h. Then, phenyltriflimide (547 mg, 1.53 mmol) was added and the solution was allowed to warm to room temperature with stirring for an additional 2 h. The solution was diluted with diethyl ether (3 mL) and washed with sodium bicarbonate (3 x 5 mL). The organic layer was dried over magnesium sulfate, filtered, concentrated, and purified by column chromatography (SiO_2, 2.5% Et_2O/ hexane, then 10% EtOAc/ hexane) to yield vinyl triflate **1.S4** (391 mg, 67%, *d.r.* = 1:1) as a colorless oil. ^{1}H NMR (500 MHz, $CDCl_3$): δ 6.09 (d, *J* = 5 Hz, 1H x 50/100), 6.08 (d, *J* = 5 Hz, 1H x 50/100), 5.77 (t, *J* = 3 Hz, 1H x 50/100), 5.72 (t, *J* = 3 Hz, 1H x 50/100), 5.19 (s, 1H x 50/100), 5.18 (s, 1H x 50/100), 4.84 (d, *J* = 4 Hz, 1H x 50/100), 4.59 (d, *J* = 5 Hz, 1H x 50/100), 3.90-4.02 (m, 8 x 50/100), 3.75 (s, 3H x 50/100), 3.74 (dq, *J* = 4, 9 Hz, 1H x 50/100), 3.73 (s, 3H x 50/100), 3.37 (dq, *J* = 3, 9 Hz, 1H x 50/100), 2.96 (dq, *J* = 5, 9 Hz, 1H x 50/100), 2.68 (dd, *J* = 9, 16 Hz, 1H x

50/100), 2.53-2.63 (m, 2H x 50/100), 2.20 (d, *J* = 5 Hz, 2H x 50/100), 2.11 (dd, *J* = 6, 17 Hz, 1H x 50/100), 1.99 (dt, *J* = 4, 17 Hz, 1H x 50/100), 1.94 (dd, *J* = 4, 15 Hz, 1H x 50/100), 0.86 (s, 9H x 50/100), 0.82 (s, 9H x 50/100), 0.05 (s, 6H x 50/100), 0.03 (s, 6H x 50/100); ^{13}C NMR (125 MHz, $CDCl_3$): δ 173.5, 171.0, 146.1, 145.6, 140.2, 136.6, 133.2, 129.8, 129.7, 123.8, 121.2, 121.1, 104.3, 103.9, 70.4, 67.0, 65.5, 65.4, 65.2, 64.6, 52.7, 52.4, 40.2, 35.9, 34.3, 34.2, 27.4, 26.7, 25.7, 25.7, 18.1, 17.9, -3.9, -4.6, -5.2, -5.3; IR (thin film) υ_{max} cm^{-1} 2955, 2931, 2889, 2859, 1741, 1422, 1214; HRMS (ESI) calculated for $[C_{21}H_{31}O_8F_3NaSSi]^+$ $[M+Na]^+$: *m/z* 551.1353, found 551.1364.

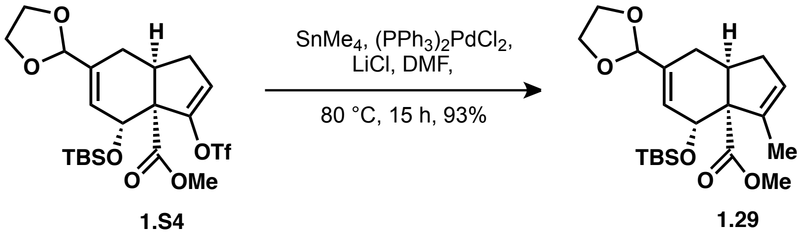

1.S4 **1.29**

Trisubstituted olefin **1.29**

To a solution of vinyl triflate **1.S4** (599 mg, 1.13 mmol, single diastereomer) in DMF (10 mL) was added LiCl (240 mg, 5.67 mmol) and $(PPh_3)_2PdCl_2$ (80 mg, 0.113 mmol). Then tetramethyltin (0.31 mL, 2.27 mmol) was added, the vessel was filled with an inert nitrogen atmosphere, sealed, and heated to 80 °C for 15 h. Upon cooling, water (30 mL) was added to the solution. The phases were separated and the aqueous phase was extracted with diethyl ether (3 x 50 mL). The organic layer was then washed with water (2 x 50 mL), dried over magnesium sulfate, filtered over a short Celite plug and concentrated to yield trisubstituted olefin **1.29** (415 mg, 93%) as a colorless oil. Purification by column chromatography (SiO_2, 10% to 20% EtOAc/ hexane) was necessary to achieve the highest level of purity, but this material was typically carried forward without purification. ^{1}H NMR (500 MHz, $CDCl_3$) δ 6.02 (d, *J* = 4.7 Hz, 1H), 5.43 (d, *J* = 2.5 Hz, 1H), 5.18 (s, 1H), 4.52 (d, *J* = 4.8 Hz, 1H), 4.02-3.86 (m, 4H), 3.66 (s, 3H), 3.13 (tdd, *J* = 7.7, 4.9, 2.7 Hz, 1H), 2.65 (ddt, *J* = 16.5, 8.2, 2.5 Hz, 1H), 2.50 (ddd, *J* = 15.7, 7.2, 1.8 Hz, 1H), 1.88 (dq, *J* = 16.6, 2.4 Hz, 1H), 1.81 (dd, *J* = 15.7, 5.0 Hz, 1H), 1.72 (d, *J* = 2.3 Hz, 3H), 0.83 (s, 9H), 0.04 (d, *J* = 5.1 Hz, 6H). ^{13}C NMR (126 MHz, $CDCl_3$) δ 173.99, 139.75, 138.71, 129.48, 129.04, 104.75, 68.26, 67.90, 65.41, 65.30, 51.63, 39.51, 37.83, 28.41, 25.79, 18.03, 14.82, -3.54, -4.96.

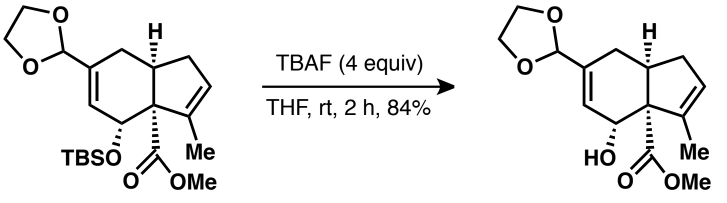

1.29a **1.31a**

Allylic alcohol **1.31a**

A solution of trisubstituted olefin **1.29a** (207 mg, 0.525 mmol) in THF (5 mL) was cooled to 0 °C. A solution of tetrabutylammonium fluoride (2.10 mL, 1 M THF, 2.10 mmol) was added over the course of 1 min, then the reaction mixture was allowed to warm to room temperature. After stirring for 4 h, the reaction was diluted with DCM (25 mL) and washed with brine (3 x 20 mL). The organic layer dried over magnesium sulfate, filtered, concentrated, and purified by column chromatography (SiO_2, 1% Et_3N/ DCM) to yield allylic alcohol **1.31a** (124 mg, 84%) as a colorless oil. ^{1}H NMR (500 MHz, $CDCl_3$) δ 6.12 (t, *J* = 2.6 Hz, 1H), 5.54 (q, *J* = 2.0 Hz, 1H), 5.19 (s, 1H), 4.18 (d, *J* = 6.8 Hz, 1H), 4.03-3.87 (m, 4H), 3.71 (s, 3H), 3.46 (d, *J* = 10.7 Hz, 1H), 2.88 (tt, *J* = 8.0, 6.2 Hz, 1H), 2.60 (ddt, *J* = 16.0, 8.5, 2.5 Hz, 1H), 2.41 (dd, *J* = 16.8, 7.5 Hz, 1H), 2.02 (ddq, *J* = 16.1, 6.6, 2.4 Hz, 1H), 1.86 (ddt, *J* = 16.9, 6.0, 1.9 Hz, 1H), 1.82 (q, *J* = 2.0 Hz, 3H). ^{13}C NMR (126 MHz, $CDCl_3$) δ 175.83, 142.22, 135.98, 132.87, 127.99, 104.54, 71.27, 65.43, 65.34, 52.30, 42.43, 38.36, 26.01, 25.78, 15.26.

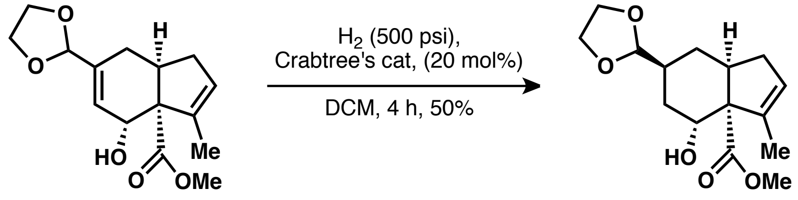

1.31a **1.30**

Hydrogenated compound **1.30**

A solution of allylic alcohol **1.31a** (123 mg, 0.439 mmol) in DCM (5 mL) was transferred into a vial containing Crabtree's catalyst (71 mg, 0.0878 mmol) and a stir bar. This vial was then placed in a bomb hydrogenator which was then sealed and pressurized with hydrogen gas (500 psi). The reaction was allowed to stir for 4 h before the pressure was released. The reaction mixture was concentrated and purified by column chromatography (SiO_2, 50% EtOAc/ hexane + 1% Et_3N) to yield hydrogenated compound **1.30** (61.3 mg, 50%) as a colorless oil. ^{1}H NMR (600 MHz, $CDCl_3$) δ 5.51 (s, 1H), 4.63 (d, *J* = 4.4 Hz, 1H), 4.47 (s, 1H), 3.98-3.81 (m, 4H), 3.68 (s, 3H), 2.88 (dt, *J* = 12.0, 6.0 Hz, 1H), 2.66 (dp, *J* = 15.8, 2.6 Hz, 1H), 2.03 (tdd, *J* = 12.0, 8.4, 4.1 Hz, 1H), 1.97-1.84 (m, 2H), 1.79-1.75 (m, 2H), 1.75 (s, 3H), 1.31-1.23 (m, 1H), 0.99 (q, *J* = 12.7 Hz, 1H).

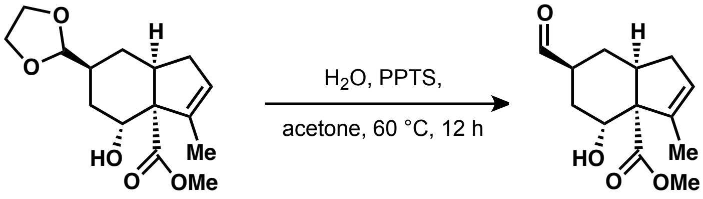

1.30 **1.S5**

Aldehyde **1.S5**

To a solution of hydrogenated compound **1.30** (53 mg, 0.19 mmol) in acetone (1.9 mL) was added pyridinium *p*-toluenesulfonate (47 mg, 0.19 mmol) and water (0.04 mL, 19 mmol). The vessel was sealed and heated to 60 °C for 12 hours. Upon cooling, water (10 mL) was added and this solution was extracted with EtOAc (3 x 10 mL). The organic layers were dried over magnesium sulfate, filtered, and concentrated to yield aldehyde **1.S5** (47 mg, crude) which was carried on to the next step without purification.

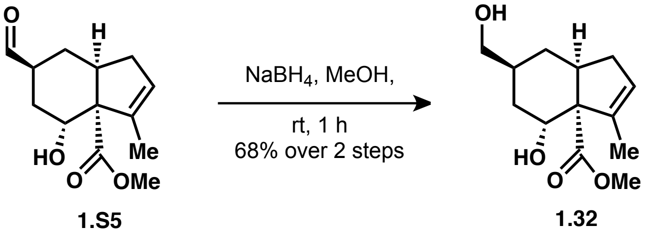

Primary alcohol **1.32**

To a solution of aldehyde **1.S5** (45 mg, 0.19 mmol) in methanol (1.9 mL) was added sodium borohydride (14 mg, 0.38 mmol). After stirring for 1 h, the reaction was quenched by the addition of water (5 mL) followed by extraction with 50:50 EtOAc/Et_2O (3 x 10 mL). The organic layers were dried over magnesium sulfate, filtered, concentrated, and purified by column chromatography (SiO_2, 1% Et_3N/ DCM to 1% Et_3N, 5% MeOH/ DCM) to yield primary alcohol **1.32** (31 mg, 68%) as a colorless oil. ^{1}H NMR (500 MHz, $CDCl_3$) δ 5.52 (t, *J* = 1.4 Hz, 1H), 4.45 (t, *J* = 3.3 Hz, 1H), 3.68 (s, 3H), 3.44 (d, *J* = 6.1 Hz, 2H), 2.89 (dt, *J* = 11.9, 6.0 Hz, 1H), 2.67 (ddt, *J* = 16.0, 5.2, 2.6 Hz, 1H), 2.07 (s, 1H), 2.00-1.80 (m, 3H), 1.81-1.72 (m, 4H), 1.14 (td, *J* = 12.8, 11.6, 2.2 Hz, 1H), 0.84 (q, *J* = 12.5 Hz, 1H). ^{13}C NMR (126 MHz, $CDCl_3$) δ 174.39, 137.50, 129.57, 68.17, 67.90, 64.54, 51.92, 38.67, 38.06, 33.19, 33.08, 31.27, 14.04.

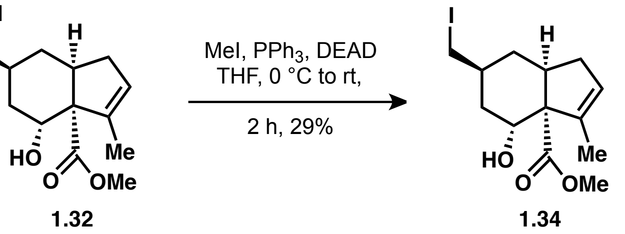

Primary alkyl iodide **1.34**

A solution of primary alcohol **1.32** (16 mg, 0.067 mmol) and triphenyl phosphine (35 mg, 0.133 mmol) in THF (1 mL) was cooled to 0 °C. Then diethyl azodicarboxylate (0.021 mL, 0.133 mmol) and methyliodide (0.008 mL, 0.113 mmol) were added sequentially. After warming to room temperature and stirring for 1.5 h, the reaction was quenched by the addition of aqueous sodium bicarbonate. Following extraction with diethyl ether (3 x 2 mL), the organic layers were dried over magnesium sulfate, filtered, concentrated and purified by column chromatography (SiO_2, 20% EtOAc/ hexane) to yield primary alkyl iodide **1.34** (6.7 mg, 29%) as a colorless oil. ^{1}H NMR (500 MHz, $CDCl_3$) δ 5.53 (s, 1H), 4.44 (s, 1H), 3.68 (s, 3H), 3.07 (d, *J* = 6.0 Hz, 2H), 2.92 (dt, *J* = 11.6, 5.9 Hz, 1H), 2.67 (ddt, *J* = 17.8, 5.1, 2.6 Hz, 1H), 1.96-1.80 (m, 3H), 1.80-1.74 (m, 2H), 1.75 (s, 3H), 1.11 (td, *J* = 12.6, 11.8, 2.6 Hz, 1H), 0.83 (q, *J* = 12.5 Hz, 1H).

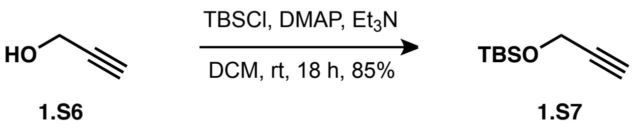

TBS propargyl alcohol **1.S7**

A solution of propargyl alcohol (5.0 mL, 85 mmol) and triethylamine (35.0 mL, 254 mmol) in DCM (180 mL) was stirred for 30 min in a dry 500 mL flask. Dimethylaminopyridine (0.62 g, 5.1 mmol) and *tert*-butyldimethylsilyl chloride (15.3 g, 102 mmol) were sequentially added and the solution was stirred for 18 h, at which point water (50 mL) was added. The organic layer was washed with hydrochloric acid (2 M, 3 x 50 mL) and brine (1 x 50 mL), dried over magnesium sulfate, filtered, and concentrated. The resulting oil was filtered through a plug of silica, washed with diethyl ether, and concentrated to yield TBS propargyl alcohol **1.S7** (12 g, 85%) as a pale yellow oil. The spectral data were identical to those that were previously reported.[28]

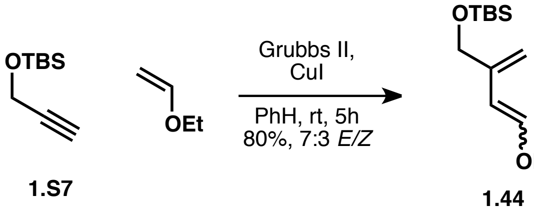

Diene **1.44**

A dry 2 L round-bottomed flask was charged with TBS propargyl alcohol **1.S7** (6.45 g, 37.9 mmol, 1 equiv), Grubbs II (0.64 g, 0.76 mmol, 2 mol%), copper (I) iodide (0.22 g, 1.14 mmol, 3 mol%) and diethyl ether (380 mL). Ethyl vinyl ether (91 mL, 0.95 mol, 25 equiv) was added immediately and the reaction mixture was allowed to stir at room temperature. After 18 h, the crude reaction mixture was concentrated and purified by column chromatography (SiO_2, 3% to 10% EtOAc/ hexane) to give diene **1.44** (7.3 g, 80%) as a 7:3 mixture of *E*/*Z* isomers. ^{1}H NMR (400 MHz, $CDCl_3$): δ 6.64 (d, *J* = 13 Hz, 1H x 70/100), 5.99 (d, *J* = 7 Hz, 1H x 30/100), 5.54 (d, *J* = 13 Hz, 1H x 70/100), 5.20-5.23 (m, 2H x 30/100), 4.97 (s, 1H x 70/100), 4.86 (s, 1H x 70/100), 4.82 (d, *J* = 7 Hz, 1H x 30/100), 4.34 (s, 2H x 30/100), 4.24 (s, 2H x 70/100), 3.85 (q, *J* = 7 Hz, 2H x 30/100), 3.80 (q, *J* = 7 Hz, 2H x 70/100), 1.29 (t, *J* = 7 Hz, 3H x 70/100), 1.28 (t, *J* = 7 Hz, 3H x 30/100), 0.93 (s, 9H x 30/100), 0.92 (s, 9H x 70/100), 0.08 (s, 6H); ^{13}C NMR (100 MHz, $CDCl_3$): δ 147.5, 146.3, 143.4, 143.1, 110.3, 109.7, 106.2, 104.2, 68.8, 65.4, 64.0, 26.1, 18.5, 15.4, 15.0, -5.2; IR (thin film) υ_{max} cm^{-1} 2956, 2930, 2885, 2857, 1651, 1472, 1254, 1183, 1109, 776; HRMS (ESI) calculated for $[C_{13}H_{27}O_2Si]^+$ $[M+H]^+$: *m/z* 243.1775, not found.

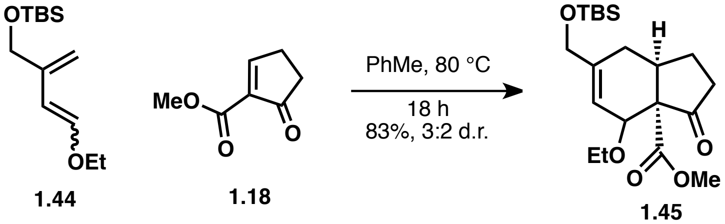

Bicycle **1.45**

A 100 mL Schlenk flask was charged with unpurified dienophile **1.18** (2.56 g, 18.4 mmol), diene **1.44** (6.70 g, 27.7 mmol), and toluene (12 mL). The mixture was heated to 80 °C and stirred for 18 h in the sealed flask. The solution was then concentrated and purified by column chromatography (SiO_2, 5% EtOAc/ hexane, then 10 % EtOAc/ hexane) to yield bicycle

1.45 as a separable mixture of diastereomers (5.83 g, 83%, *d.r.* = 1.5:1). ^{1}H NMR (600 MHz, CDCl$_3$): δ 5.94 (s, 1H), 4.53 (s, 1H), 4.07 (s, 2H), 3.72 (s, 3H), 3.58 (dq, *J* = 7.2, 7.2 Hz, 1H), 3.44 (dq, *J* = 7.2, 7.2 Hz, 1H), 3.04 (dt, *J* = 7.2, 6.0 Hz, 1H), 2.40 (dd, *J* = 8.4, 18.6 Hz, 1H), 2.28 (m, 2H), 2.07 (m, 2H), 1.97 (dt, *J* = 7.8, 10.8 Hz, 1H), 1.08 (d, *J* = 6.6 Hz, 3H), 0.92 (s, 9H), 0.07 (s, 6H); ^{13}C NMR (150 MHz, CDCl$_3$): δ 212.7, 171.0, 138.3, 118.1, 72.3, 66.6, 66.2, 63.1, 52,8, 39.1, 37.2, 26.4, 26.1, 26.0, 18.5, 15.5, -5.2; IR (thin film) υ_{max} cm^{-1} 2954, 2929, 2857, 1756, 1729, 1472, 1254, 1073; HRMS (ESI) calculated for $[C_{20}H_{34}O_5NaSi]^+$ $[M+Na]^+$: *m/z* 405.2068, found 405.2073.

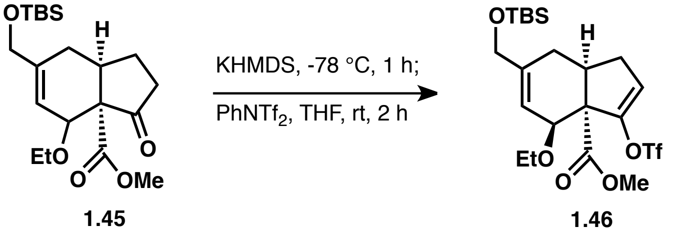

Ester vinyl triflate **1.46**

A solution of bicycle **1.45** (4.73 g, 12.4 mmol) in THF (28 mL) was cooled to -78 °C under a nitrogen atmosphere. Potassium bis(trimethylsilyl)amide (0.5 M in toluene, 27.2 mL, 13.6 mmol) was slowly added and the resulting deep red solution was stirred for 1 h. Then, phenyltriflimide (5.31 g, 14.9 mmol) was added and the solution was allowed to warm to room temperature and stirred for an additional 2 h. The solution was washed with sodium bicarbonate (3 x 60 mL). The organic layer was dried over magnesium sulfate, filtered, and concentrated to yield ester vinyl triflate **1.46** as a pale yellow oil that was carried on unpurified.

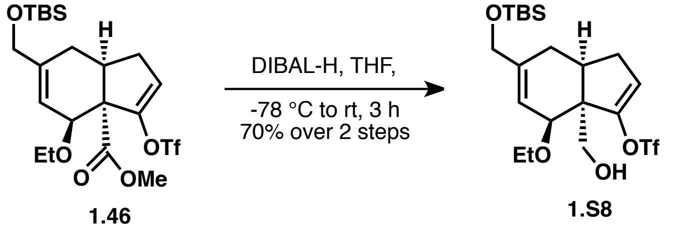

Alcohol vinyl triflate **1.S8**

A solution of ester vinyl triflate **1.46** (6.44 g, 12.4 mmol) in THF (140 mL) was cooled to -78 °C under a nitrogen atmosphere. Diisobutylaluminum hydride (11 mL, 62 mmol) was slowly added and the resulting solution was stirred for 1 h. The solution was then warmed to 0 °C and stirred for another 2 h. EtOAc (140 mL) and a saturated solution of Rochelle's salt (280 mL) was then added and the mixture was stirred for another hour. The layers were separated and the aqueous layer was extracted with EtOAc (2 x 200 mL). The combined organic layers were dried over magnesium sulfate, filtered, concentrated, and purified by column chromatography (SiO$_2$, 10% EtOAc/ hexane) to yield alcohol vinyl triflate **1.S8** (4.20 g, 70% over 2 steps) as a colorless oil. ^{1}H NMR (400 MHz, CDCl$_3$): δ 5.95 (b, 1H), 5.72 (s, 1H), 4.07 (s, 2H), 3.82 (dd, *J* = 10.8, 2.8 Hz, 1H), 3.73 (d, *J* = 3.6 Hz, 1H), 3.62 (dq, *J* = 9.2, 7.2 Hz, 1H), 3.47 (dd, *J* = 10.8, 8.0 Hz, 1H), 3.36 (dq, J = 9.2, 7.2 Hz, 1H), 2.51-2.64 (m, 2H), 2.08 (dd, J = 8.0, 6.4 Hz, 1H), 1.94 (b, 1H), 1.16 (t, J = 6.8, 3H), 0.90 (s, 9H), 0.06 (s, 6H); ^{13}C NMR (100 MHz, $CDCl_3$): δ 147.0, 140.7, 121.8, 118.9, 74.2, 65.1, 65.0, 64.3, 58.0, 35.5, 33.1, 28.6, 25.0, 17.5, 14.3, -6.2; IR (thin film) υ_{max} cm^{-1} 3443, 2955, 2930, 2885, 2858, 1665, 1473, 1464, 1422, 1209, 1145; HRMS (ESI) calculated for $[C_{20}H_{33}O_6F_3NaSSi]^+$ $[M+Na]^+$: *m/z* 509.1611, found 509.1636.

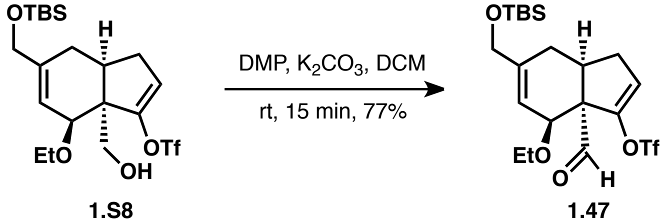

Aldehyde vinyl triflate **1.47**

To a solution of alcohol vinyl triflate **1.S8** (4.20 g, 8.64 mmol) in DCM (170 mL), potassium carbonate (7.16 g, 51.8 mmol) was added, then Dess-Martin periodinane (7.33 g, 17.3 mmol) and the mixture was stirred for 15 min. Saturated solutions of sodium bicarbonate (170 mL) and sodium sulfite (170 mL) were then added to quench the reaction. The layers were separated and the aqueous layer was extracted with EtOAc (3 x 200 mL). The combined organic layers were then dried over magnesium sulfate, filtered, concentrated, and purified by column chromatography (SiO_2, 10% EtOAc/ hexane) to yield aldehyde vinyl triflate **1.47** (3.20 g, 77%) as a colorless oil. ^{1}H NMR (400 MHz, $CDCl_3$): δ 9.61 (s, 1H), 5.98 (s, 1H), 5.86 (s, 1H), 4.40 (s, 1H), 4.06 (s, 2H), 3.60 (dq, J = 9.0, 7.0 Hz, 1H), 3.43 (dq, J = 9.0, 7.0 Hz, 1H), 2.86 (dq, J = 9.0, 6.0 Hz, 1H) 2.63 (dq, J = 9.0, 2.5 Hz, 1H) 2.08-2.19 (m, 3H), 1.16 (t, J = 6.8 Hz, 3H), 0.90 (s, 9H), 0.05 (s, 6H); ^{13}C NMR (100 MHz, $CDCl_3$): δ 199.2, 145.3, 141.9, 122.7, 121.3, 72.4, 68.4, 65.8, 65.4, 36.8, 34.3, 29.0, 26.0, 18.5, 15.3, -5.2; IR (thin film) υ_{max} cm^{-1} 2956, 2930, 2857, 1731, 1662, 1473, 1424, 1211, 1143; HRMS (ESI) calculated for $[C_{20}H_{31}O_6F_3NaSSi]^+$ $[M+Na]^+$: *m/z* 507.1455, not found.

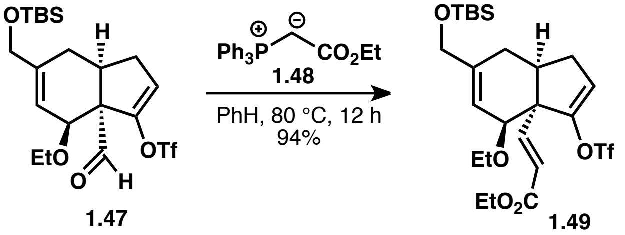

Ester vinyl triflate **1.49**

To a solution of aldehyde vinyl triflate **1.47** (1.88 g, 3.88 mmol) in benzene (31 mL), ethyl-(triphenylphosphoranylidene)acetate (2.99 g, 7.77 mmol) was added and the mixture was heated to 80 °C and stirred at this temperature in a sealed 100 mL Schlenk flask for 18 h. The reaction mixture was then concentrated and purified by column chromatography (SiO_2, 10% EtOAc/ hexane) to yield ester vinyl triflate **1.49** (2.01 g, 94%) as a yellow oil. ^{1}H NMR (400 MHz, $CDCl_3$): δ 6.89 (d, J = 16.0 Hz, 1H), 6.02 (d, J = 4.0 Hz, 1H), 5.82 (d, J = 16.4 Hz, 1H), 5.73 (t, *J* = 2.4 Hz, 1H) 4.19 (q, *J* = 7.2 Hz, 2H), 4.10 (s, 2H), 3.92 (d, *J* = 4.4 Hz, 1H), 3.56 (dq, *J* = 9.2, 7.2 Hz, 1H), 3.38 (dq, *J* = 9.2, 7.2 Hz, 1H), 2.60 (dq, *J* = 9.2, 2.8 Hz, 1H), 2.49 (dq, 6.8, 4.8 Hz, 1H), 2.05-2.22 (m, 3H), 1.29 (t, 6.8 Hz, 3H), 1.14 (t, 7.2 Hz, 3H), 0.91 (s, 9H), 0.07 (s, 6H); ^{13}C NMR (100 MHz, CDCl$_3$): δ 166.5, 150.6, 147.7, 143.3, 121.1, 117.4, 74.9, 65.9, 64.9, 60.7, 58.8, 41.8, 34.3, 29.7, 26.0, 18.5, 15.3, 14.4, -5.2; IR (thin film) υ_{max} cm^{-1} 2957, 2930, 2857, 1725, 1649, 1425, 1250, 1211; HRMS (ESI) calculated for $[C_{24}H_{37}O_7F_3NaSSi]^+$ $[M+Na]^+$: *m/z* 577.1874, not found.

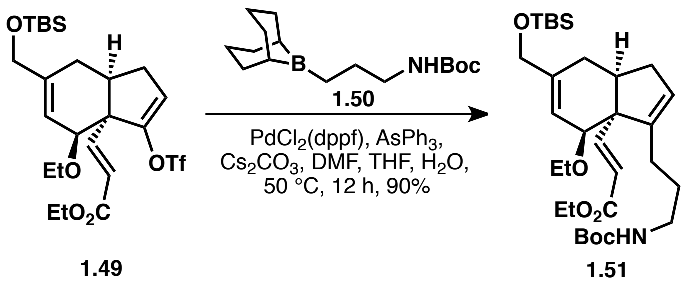

Suzuki coupled product **1.51**

A dry 250 mL flask was charged with Boc-protected allyl amine (1.41 g, 8.99 mmol), 9-borabicyclo[3.3.1]nonane (0.5 M in THF, 24.0 mL, 12.0 mmol), and THF (50 mL) and stirred for 4 h. This reaction was then quenched by the addition of water (2.5 mL) and the resulting biphasic solution was immediately transferred to a 100 mL Schlenk flask containing ester vinyl triflate **1.49** (3.32 g, 5.99 mmol), 1,1'-bis(diphenylphosphino)ferrocene-palladium(II)dichloride (0.438 g, 0.599 mmol), triphenylarsine (0.183 g, 0.599 mmol), cesium carbonate (3.71 g, 11.4 mmol), and DMF (25 mL). This mixture was stirred in the sealed Schlenk flask at 50 °C for 12 h. The mixture was then diluted with EtOAc (50 mL) and washed with NaOH (1 M, 3 x 50 mL) and brine (1 x 50 mL). The organic layer was dried over magnesium sulfate, filtered, concentrated, and purified by column chromatography (SiO$_2$, 10% EtOAc/ hexane) to yield the desired Suzuki coupled product **1.51** (3.05 g, 90%) as a colorless oil. ^{1}H NMR (400 MHz, CDCl$_3$): δ 6.97 (d, *J* = 16.2 Hz, 1H), 5.91 (s, 1H), 5.67 (d, *J* = 16.2 Hz, 1H), 5.50 (s, 1H), 4.66 (b, 1H), 4.17 (q, *J* = 6.6 Hz, 2H), 4.06 (s, 2H), 3.96 (d, *J* = 2.4 Hz, 1H), 3.59 (dq, *J* = 9.0, 7.2 Hz, 1H), 3.35 (dq, *J* = 9.0, 7.2 Hz, 1H), 3.13 (b, 1H), 2.53 (dd, *J* = 13.6, 10.0 Hz, 1H), 2.41 (dd, 6.6, 5.8 Hz, 1H), 1.93-2.10 (m, 4H), 1.85 (quin, *J* = 7.2 Hz, 1H), 1.65 (m, 2H), 1.43 (s, 9H), 1.29 (t, *J* = 7.2 Hz, 3H), 1.13 (t, *J* = 7.2 Hz, 3H), 0.90 (s, 9H), 0.06 (s, 6H); ^{13}C NMR (100 MHz, CDCl$_3$): δ 167.3, 156.1, 155.5, 144.0, 142.7, 126.7, 122.2, 119.4, 77.6, 77.4, 66.1, 64.8, 62.4, 60.4, 43.7, 40.6, 39.2, 30.5, 28.6, 26.1, 26.0, 18.6, 15.6, 14.4, 1.2, -5.2; IR (thin film) υ_{max} cm^{-1} 3368, 2979, 2929, 2856, 1717, 1644, 1518, 1451, 1252, 1174; HRMS (ESI) calculated for $[C_{31}H_{53}NO_6Si]^+$ $[M+H]^+$: *m/z* 564.3642, found 564.3744.

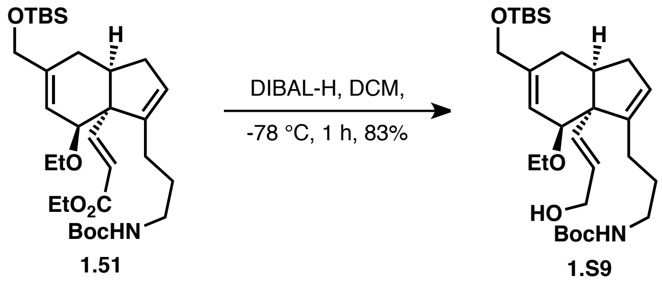

Allylic alcohol **1.S9**

A solution of Suzuki coupled product **1.51** (1.49 g, 2.64 mmol) in DCM (38 mL) was cooled to -78 °C. Diisobutylaluminum hydride (1.20 mL, 6.61 mmol) was slowly added and the mixture was stirred for 1 h. EtOAc (40 mL) and a saturated solution of Rochelle's salt (80 mL) was then added and stirring was continued for at least 1 additional h. The layers were separated and the aqueous layer was then extracted with EtOAc (2 x 40 mL). The combined organic layers were dried over magnesium sulfate, filtered, concentrated, and purified by column chromatography (SiO_2, 20% EtOAc/ hexane) to yield allylic alcohol **1.S9** (1.14 g, 83%) as a colorless oil. ^1H NMR (400 MHz, $CDCl_3$): δ 5.89 (d, *J* = 3.5 Hz, 1H), 5.71 (d, *J* = 15.5 Hz, 1H), 5.52 (dt, *J* = 15.5, 6.0 Hz, 1H), 5.42 (s, 1H), 4.71 (b, 1H), 4.10 (d, *J* = 6.0 Hz, 2H), 4.06 (s, 2H), 3.88 (d, *J* = 4.0 Hz, 1H), 3.57 (dq, *J* = 9.5, 7.0 Hz, 1H), 3.33 (dq, *J* = 9.5, 7.0 Hz, 1H), 3.11 (q, *J* = 6.0 Hz, 2H), 2.49 (dd, *J* = 14.0, 9.0 Hz, 1H), 2.39 (dq, *J* = 7.5, 5.5 Hz, 1H), 1.99-2.09 (m, 3H), 1.92 (d, *J* = 15.5 Hz, 1H), 1.61-1.74 (m, 2H), 1.43 (s, 9H), 1.25 (t, *J* = 7.5 Hz, 1H), 1.12 (t, *J* = 7.0 Hz, 3H), 0.90 (s, 9H), 0.05 (s, 6H); ^{13}C NMR (150 MHz, $CDCl_3$): δ 156.1, 150.4, 139.7, 135.5, 128.2, 123.5, 122.7, 80.4, 77.4, 66.3, 65.2, 64.4, 58.5, 44.0, 37.7, 29.0, 28.6, 28.4, 26.1, 18.6, 15.7, 8.1, 1.2, -5.1; IR (thin film) υ_{max} cm^{-1} 3359, 2954, 2929, 2856, 1692, 1518, 1252, 1172; HRMS (ESI) calculated for $[C_{29}H_{51}O_5NNaSi]^+$ $[M+Na]^+$: *m/z* 544.3429, found 544.3451.

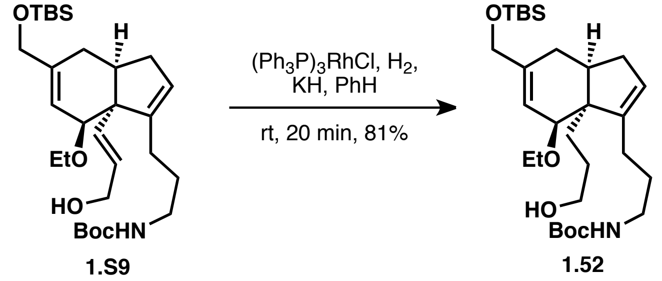

Primary alcohol **1.52**

A 250 mL flask was charged with allylic alcohol **1.S9** (1.12 g, 2.15 mmol) and benzene (55 mL). The flask was flushed with hydrogen (1 atm) then potassium hydride (0.17 g, 4.3 mmol) and Wilkinson's catalyst (1.99 g, 2.15 mmol) were added sequentially. The reaction mixture was stirred vigorously for 30 min and then quenched with methanol (40 mL). This mixture was concentrated and purified by column chromatography (SiO_2, 20% EtOAc/ hexane) to yield primary alcohol **1.52** (0.91 g, 81%) as a pale yellow oil. ^1H NMR (500 MHz, $CDCl_3$): δ 5.86 (d, *J* = 3.5 Hz, 1H), 5.32 (s, 1H), 4.82 (b, 1H), 4.06 (s, 2H), 3.64 (d, *J* = 3.5 Hz, 1H), 3.53-3.59 (m, 3H), 3.29 (dq, *J* = 9.5, 7.0 Hz, 1H), 3.12 (q, *J* = 6.5 Hz, 2H), 2.42 (dd, *J* = 14.0, 9.5, 1H) 2.22 (dq, *J* = 7.5, 5.5 Hz, 1H), 1.95-2.12 (m, 3H), 1.80-1.85 (m, 3H), 1.60-1.74 (m, 3H), 1.42 (s, 9H), 1.30 (d, *J* = 10.0 Hz, 2H), 1.12 (t, *J* = 7.0 Hz, 3H), 0.89 (s, 9H), 0.04 (s, 6H); ^{13}C NMR (125 MHz, $CDCl_3$): δ 156.2, 144.9, 141.9, 124.8, 123.7, 79.9, 77.4, 66.2, 64.8, 63.6, 59.9, 40.5, 40.3, 39.3, 33.6, 30.9, 28.6, 28.1, 27.7, 26.0, 25.0, 18.6, 15.6, -5.2; IR (thin film) υ_{max} cm^{-1} 3351, 2953, 2929, 2855, 1694, 1520, 1252, 1172; HRMS (ESI) calculated for $[C_{29}H_{53}O_5NNaSi]^+$ $[M+Na]^+$: *m/z* 546.3585, found 546.3600.

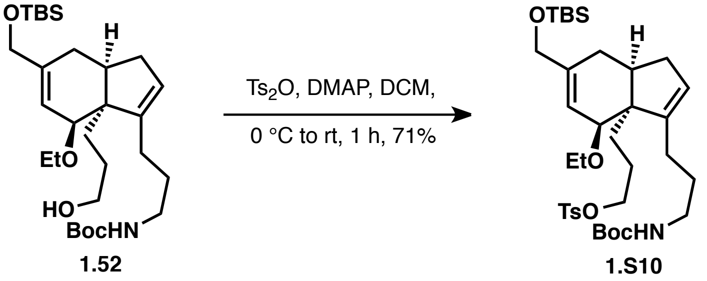

Alkyl tosylate **1.S10**

A solution of 4-methylbenzenesulfonic anhydride (1.23 g, 3.78 mmol) in DCM (50 mL) was cooled to 0 °C. Dimethylaminopyridine (0.924 g, 7.56 mmol) was added and the solution was warmed to room temperature and stirred for 30 min. Primary alcohol **1.52** (0.99 g, 1.9 mmol) was added and the mixture was stirred for an additional 45 min, then the mixture was concentrated and purified by column chromatography (SiO_2, 20% EtOAc/ hexanes) to yield alkyl tosylate **1.S10** (0.904 g, 71%) as a colorless oil. ^{1}H NMR (500 MHz, $CDCl_3$): δ 7.78 (d, *J* = 8.0 Hz, 2H), 7.34 (d, *J* = 8.0 Hz, 2H), 5.83 (d, *J* = 3.5 Hz, 1H), 5.30 (s, 1H), 4.76 (s, 1H), 4.05 (s, 2H), 3.98 (dt, *J* = 6.5, 4.0 Hz, 2H), 3.57 (d, *J* = 4.0 Hz, 1H), 3.55 (dq, *J* = 9.5, 7.0 Hz, 1H), 3.27 (dq, *J* = 9.5, 7.0 Hz, 1H), 3.11 (q, *J* = 6.5 Hz, 1H), 2.45 (s, 3H), 2.36 (dd, *J* = 17.0, 9.5 Hz, 1H), 2.09 (dd, *J* = 6.0, 5.0 Hz, 1H), 1.97-2.05 (m, 2H), 1.94 (dd, *J* = 15.0, 7.0 Hz, 1H), 1.80 (d, *J* = 16.0 Hz, 1H), 1.74 (d, *J* = 16.0 Hz, 1H), 1.67 (quin, *J* = 6.5 Hz, 1H), 1.54-1.61 (m, 2H), 1.43 (s, 9H), 1.40 (dd, *J* = 6.0, 5.0 Hz, 1H), 1.26 (d, *J* = 6.0 Hz, 2H), 1.12 (t, *J* = 7.0 Hz, 3H), 0.90 (s, 9H), 0.05 (s, 6H); ^{13}C NMR (150 MHz, $CDCl_3$): δ 156.1, 144.7, 144.5, 141.9, 133.4, 129.9, 128.0, 125.2, 123.6, 79.9, 78.9, 71.5, 66.1, 64.8, 59.8, 40.5, 40.2, 39.3, 33.1, 30.9, 28.6, 28.2, 26.0, 25.1, 24.2, 21.7, 18.5, 15.6, -5.2; IR (thin film) υ_{max} cm^{-1} 3373, 2973, 2928, 1692, 1366, 1176; HRMS (ESI) calculated for $[C_{36}H_{59}O_7NNaSSi]^+$ $[M+Na]^+$: *m/z* 700.3674, found 700.3693.

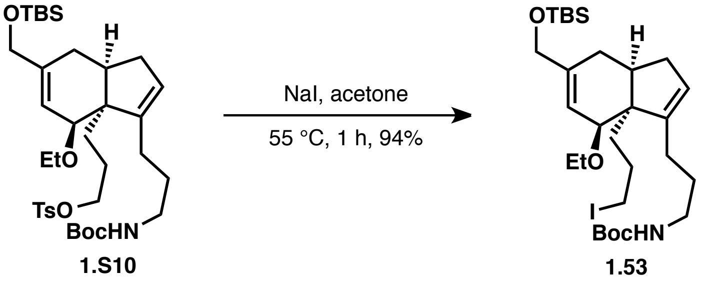

Alkyl iodide **1.53**

A 10 mL flask was charged with alkyl tosylate **1.S10** (82.9 mg, 0.122 mmol), sodium iodide (91.7 mg, 0.612 mmol) and acetone (3.7 mL) and heated to 55 °C. After stirring at this temperature for 1 h, water (5 mL) was added and the mixture was extracted with EtOAc (3 x 5 mL). The combined organic layers were dried over magnesium sulfate, filtered, concentrated, and purified by column chromatography (SiO_2, 20% EtOAc/ hexanes) to yield alkyl iodide **1.53** (72.5 mg, 94%) as a colorless oil. ^{1}H NMR (600 MHz, $CDCl_3$): δ 5.87 (s, 1H), 5.33 (s, 1H), 4.76 (b, 1H), 4.07 (s, 2H), 3.64 (s, 1H), 3.57 (dq, *J* = 9, 7 Hz, 1H), 3.30 (dq, *J* = 9, 7 Hz, 1H), 3.14 (b, 4H), 2.42 (dd, *J* = 15, 11 Hz, 1H), 2.20 (b, 1H), 1.96-2.13 (m, 3H), 1.81-1.89 (m, 2H), 1.66-1.75 (m, 3H), 1.53-1.66 (m, 2H), 1.43 (s, 9H), 1.36 (t, *J* = 11 Hz, 1H), 1.14 (t, *J* = 6 Hz, 3H), 0.90 (s, 9H), 0.06 (s, 6H); ^{13}C NMR (150 MHz, $CDCl_3$): δ 156.1, 144.9, 142.0, 125.0, 123.6, 79.8, 78.9, 66.2, 64.8, 59.8, 40.6, 40.5, 39.3, 38.5, 30.9, 28.8, 28.6, 28.2, 26.1, 25.1, 18.6, 15.7, 8.2, -5.1; IR (thin film) υ_{max} cm^{-1} 3361, 2928, 2855, 1716, 1510, 1251, 1172; HRMS (ESI) calculated for $[C_{29}H_{52}O_4NINaSi]^+$ $[M+Na]^+$: *m/z* 656.2603, found 656.2619.

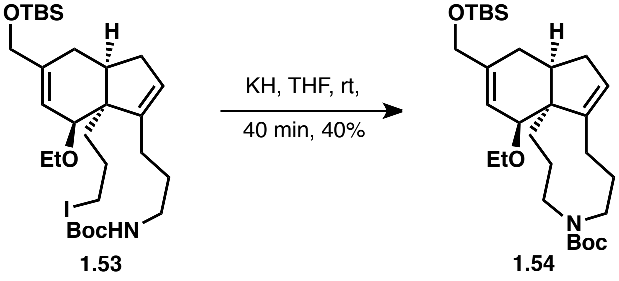

1.53 **1.54**

Azanonane **1.54**

To a solution of alkyl iodide **1.53** (72 mg, 0.11 mmol) in THF (1.3 mL), potassium hydride (18 mg, 0.46 mmol) was added. This solution was stirred for 45 min before being quenched with methanol (1 mL) and concentrated. This crude product was then purified by column chromatography (SiO_2, 10% EtOAc/ hexanes) to yield azanonane **1.54** (34 mg, 60%) as a colorless oil. ^{1}H NMR (500 MHz, $CDCl_3$): δ 5.87 (t, *J* = 4, 1H), 5.33-5.43-5.49 (rotamers, 1H), 4.07 (s, 2H), 3.50-3.60 (m, 2H), 3.29 (ddd, *J* = 16, 8, 6 Hz, 1H), 3.12 (td, *J* = 11, 5 Hz, 1H), 2.46 (q, *J* = 11, 1H), 2.36 (dd, *J* = 14, 6 Hz, 1H) 2.04-2.19 (m, 4H), 1.95-2.04 (m, 2H), 1.84 (t, *J* = 14 Hz, 1H), 1.68 (ddd, *J* = 16, 11, 6 Hz, 2H), 1.62 (s, 2H), 1.52 (t, *J* = 8 Hz, 2H), 1.45 (d, *J* = 14 Hz, 9H), 1.25 (b, 1H), 1.11 (t, *J* = 7Hz, 3H), 0.90 (s, 9H), 0.05 (s, 6H); ^{13}C NMR (100 MHz, $CDCl_3$): δ 157.2, 145.2, 141.9, 126.3, 124.1, 80.4, 79.1, 66.3, 64.8, 61.6, 48.8, 41.3, 40.4, 39.8, 30.8, 28.7, 28.6, 27.3, 26.5, 26.1, 23.1, 21.0, 18.6, 15.6, -5.1; IR (thin film) υ_{max} cm^{-1} 2928, 2856, 1696, 1170; HRMS (ESI) calculated for $[C_{29}H_{51}O_4NNaSi]^+$ $[M+Na]^+$: *m/z* 528.3480, found 528.3499.

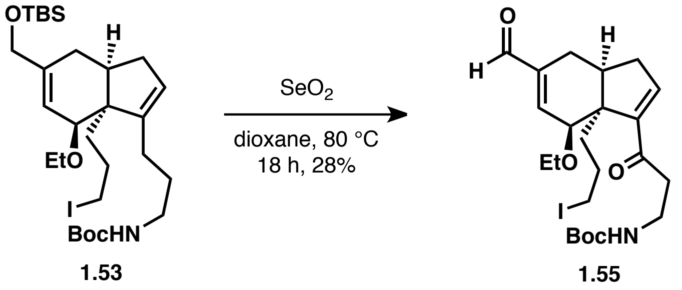

1.53 **1.55**

Ketoaldehyde **1.55**

To a solution of alkyl iodide **1.53** (7.3 mg, 0.012 mmol) in 1,4-dioxane (0.2 mL), selenium dioxide (2.7 mg, 0.024 mmol) was added. The yellow solution was heated to 80 °C and stirred at this temperature for 18 h before the solvent was removed under reduced pressure. The resultant yellow oil was diluted with diethyl ether (1 mL) and washed with H_2O (2 x 1 mL) and brine (1 x 1 mL). The combined organic layers were dried over magnesium sulfate, filtered, concentrated, and purified by column chromatography (SiO_2, 25% EtOAc/ hexanes) to yield ketoaldehyde **1.55** (1.7 mg, 28%) as a pale yellow oil. ^1H NMR (500 MHz, $CDCl_3$): δ 9.55 (s, 1H), 7.08 (d, *J* = 5 Hz, 1H), 6.63 (t, *J* = 7 Hz, 1H), 5.08 (b, 1H), 4.16 (d, *J* = 5 Hz, 1H), 3.48 (dq, *J* = 9, 7 Hz, 1H), 3.39 (dd, *J* = 15, 6 Hz, 2H), 3.33 (dq, *J* = 9, 7 Hz, 1H), 3.14 (dt, *J* = 10, 7 Hz, 1H), 3.07 (dt, *J* = 10, 7 Hz, 1H), 2.86 (q, *J* = 5 Hz, 2H), 2.67 (ddd, *J* = 18, 8, 3 Hz, 1H), 2.56 (d, *J* = 8 Hz, 1H), 2.18-2.26 (m, 2H), 2.04-2.15 (m, 2H), 1.63 (tt, *J* = 8, 6 Hz, 1H), 1.42 (s, 9H), 1.24 (d, *J* = 3 Hz, 2H), 1.03 (t, *J* = 7 Hz, 3H); ^{13}C NMR (125 MHz, $CDCl_3$): δ 199.1, 192.3, 156.0, 151.2, 145.2, 144.3, 144.1, 79.3, 78.1, 66.0, 60.0, 40.5, 40.0, 39.3, 39.1, 29.9, 29.2, 28.6, 24.7, 15.7, 6.9; IR (thin film) υ_{max} cm^{-1} 3369, 2974, 2927, 2853, 1713, 1693, 1505, 1170; HRMS (ESI) calculated for $[C_{23}H_{34}O_5NNaI]^+$ $[M+Na]^+$: *m/z* 554.1374, found 554.1372.

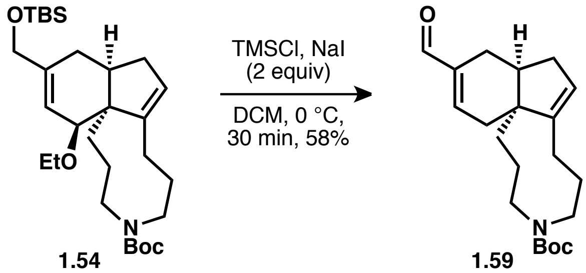

Enal **1.59**

A solution of tricycle **1.54** (34 mg, 0.067 mmol) in DCM (0.7 mL) was cooled to 0 °C. Chlorotrimethylsilane (17 µL, 0.13 mmol) and dry sodium iodide (20 mg, 0.13 mmol) were added and the translucent yellow solution was stirred for 30 min at 0 °C. A solution of saturated sodium bicarbonate was then added and the biphasic mixture was extracted with DCM (3 x 2 mL). The combined organic layer was dried over magnesium sulfate, filtered, and concentrated. The resulting oil was purified by column chromatography (10-25% ethyl acetate in hexane) to give enal **1.59** (14 mg, 58%) as a mixture of Boc-rotomers. ^1H NMR (500 MHz, $CDCl_3$): δ 9.45 (s, 1H), 6.95 (dt, *J* = 5.1, 1.3 Hz, 1H), 5.41-5.37 (m, 1H), 3.53-3.27 (m, 1H), 3.23-2.94 (m, 3H), 2.51 (dt, *J* = 8.6, 1.3 Hz, 1H), 2.35-2.19 (m, 5H), 2.14-2.02 (m, 3H), 1.97-1.83 (m, 1H), 1.78-1.68 (m, 2H), 1.65-1.59 (m, 3H), 1.47-1.44 (d, 9H); ^{13}C NMR (125 MHz, $CDCl_3$): δ 192.4, 157.0, 152.7, 146.4, 143.3, 126.1, 79.3, 56.7, 48.8, 47.0, 44.8, 40.0, 39.3, 35.9, 28.7, 27.2, 25.4, 22.8, 21.5; IR (film) 2973, 2921, 2847, 1685, 1413, 1167 cm^{-1}; HRMS (ESI) calculated for $[C_{21}H_{31}O_3NNa]^+$ $[M+Na]^+$: *m/z* 368.2196, not found.

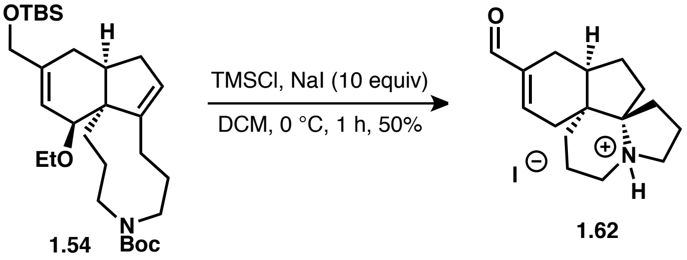

1.54

1.62

Tetracycle **1.62**

A solution of tricycle **1.54** (22 mg, 0.043 mmol) in DCM (0.8 mL) was cooled to 0 °C. Chlorotrimethylsilane (55 µL, 0.43 mmol) and sodium iodide (65 mg, 0.43 mmol) were added and the solution was allowed to stir at 0 °C for 1 h, at which point it was diluted with DCM (10 mL) and washed with a saturated solution of sodium bicarbonate (3 x 3 mL) and brine (3 mL). The organic layer was dried over magnesium sulfate, filtered and concentrated to cleanly provide tetracycle **1.62**. ^{1}H NMR (600 MHz, $CDCl_3$): δ 10.52-10.47 (bs, 1H), 9.47-9.45 (m, 1H), 6.69 (dt, J = 1.5, 0.7 Hz, 1H), 3.91-3.85 (m, 1H), 3.47-3.40 (m, 1H), 3.09-2.99 (m, 2H), 2.71-2.64 (m, 1H), 2.45-2.39 (m, 2H), 2.34-2.27 (m, 2H), 2.20-2.17 (m, 4H), 2.08-1.88 (m, 4H), 1.80-1.76 (m, 1H), 1.71-1.67 (m, 1H); ^{13}C NMR (150 MHz, $CDCl_3$): δ 193.7, 145.1, 138.4, 80.4, 53.0, 51.7, 43.7, 35.8, 33.8, 33.0, 29.0, 28.6, 26.8, 26.0, 20.5, 18.3, 18.1; IR (film) 2961, 2926, 1681, 1462, 1413 cm^{-1}; HRMS (EI) calculated for $[C_{16}H_{24}NO]^+$ $[M]^+$: *m/z* 246.1852, found 246.1855.

1.12 References and Notes

[1] Ma, X.; Gang, D. R. *Nat. Prod. Rep.* **2004,** *21,* 752-772.

[2] Bei, D. L.; Tang, X. C.; He, X. C. *Curr. Med. Chem.* **2000**, *7,* 355-374.

[3] Wang, B-S.; Wang, H.; Wei, Z-H.; Song, Y-Y.; Zhang, L.; Chen, H-Z. *J. Neural Transm.* **2009,** *116*, 457-465.

[4] Ishiuchi, K.; Kubota, T.; Hoshino, T.; Obara, Y.; Nakahata, N.; Kobayashi, J. *Bioorg. Med. Chem.* **2006,** *14*, 5995-6000.

[5] Counts, S. E.; Mufson, E. J. *J. Neuropathol. Exp. Neurol.* **2005**, *64*, 263-272.

[6] Zhao, F.-W.; Sun, Q.-Y.; Yang, F.-M.; Hu, G.-W.; Luo, J.-F.; Tang, G.-H.; Wang, Y.-H.; Long, C.-L. *Org. Lett.* **2010,** *12*, 3922-3925.

[7] Ishiuchi, K.; Kubota, T.; Hoshino, T.; Obara, Y.; Nakahatab, N.; Kobayashi, J. *Bioorg. Med. Chem.* **2006,** *14,* 5995-6000.

[8] Burnell, R. H. *J. Chem. Soc.* **1959**, 3091-3093.

[9] Harayama, T.; Takatani, M.; Inubushi, Y. *Tetrahedron Lett.* **1979**, *20*, 4307-4310.

[10] [a] Heathcock, C. H.; Smith, K. M.; Blumenkopf, T. A. *J. Am. Chem. Soc.* **1986**, *108*, 5022-5024. [b] Heathcock, C. H.; Blumenkopf, T. A.; Smith, K. M. *J. Org. Chem.* **1989**, *54*, 1548-1562.

[11] Murphy, R. A.; Sarpong, R. *Chem. Eur. J.* **2014**, *20*, 42–56.

[12] Zhao, C.; Zheng, H.; Jing, P.; Fang, B.; Xie, X.; She, X. *Org. Lett.* **2012,** *14,* 2293-2295.

[13] Duan, S.; Long, D.; Zhao, C.; Zhao, G.; Yuan, Z.; Xie, X.; Fang, J.; She, X. *Org. Chem. Front.* **2016**, *3*, 1137-1143.

[14] Zhang, G.-B.; Wang, F.-X.; Du, J.-Y.; Qu, H.; Ma, X.-Y.; Wei, M.-X.; Wang, C.-T.; Fan, C.-A. *Org. Lett.* **2012,** *14,* 3696-3699.

[15] Sizemore, N.; Rychnovsky, S. D. *Org. Lett.* **2014**, *16*, 688-691.

[16] Jasperse, C. P.; Curran, D. P.; Fevig, T. L. *Chem. Rev*. **1991**, *91*, 1237-1286.

[17] O'Connor, P. D.; Kim, U. B.; Brimble, M. A. *Eur. J. Org. Chem.* **2009**, *26*, 4405- 4411.

[18] Severin, K. *Chimia*. **2012**, *66*, 386-388.

[19] Bloome, K. S.; McMahen, R. L.; Alexanian, E. J. *J. Am. Chem. Soc.* **2011,** *133,* 20146-20148.

[20] Firmansjah, L.; Fu, G. C. *J. Am. Chem. Soc.* **2007**, *129*, 11340-11341.

[21] Monte Carlo conformational searches (OPLS_2005).

[22] Giessert, A. J.; Snyder, L.; Markham, J.; Diver, S. T. *Org. Lett.* **2003**, *5*, 1793-1796.

[23] Linghu, X.; Kennedy-Smith, J. J.; Toste, F. D. *Angew. Chem. Int. Ed.* **2007**, *46*, 7671-7673.

[24] Desai, L. V.; Hull, K. L.; Sanford, M. S. *J. Am. Chem. Soc.* **2004,** *126,* 9542-9543.

[25] Zeng, C.; Zheng, C.; Zhao, J.; Zhao, G. *Org. Lett.* **2013**, *15*, 5846-5849.

[26] Torrado, A.; Iglesias, B.; Lopez, S.; Lera, A. R.; *Tetrahedron,* **1995,** *51,* 2435-2454.

[27] Ley, S. V.; Murray, P. J.; Palmer, B. D. *Tetrahedron,* **1985,** *41,* 4765-4770.

[28] Perreault, S.; Spino, C. *Org. Lett*. **2006**, *8*, 4385-4388.

Appendix 1: Spectra Relevant to Chapter 1

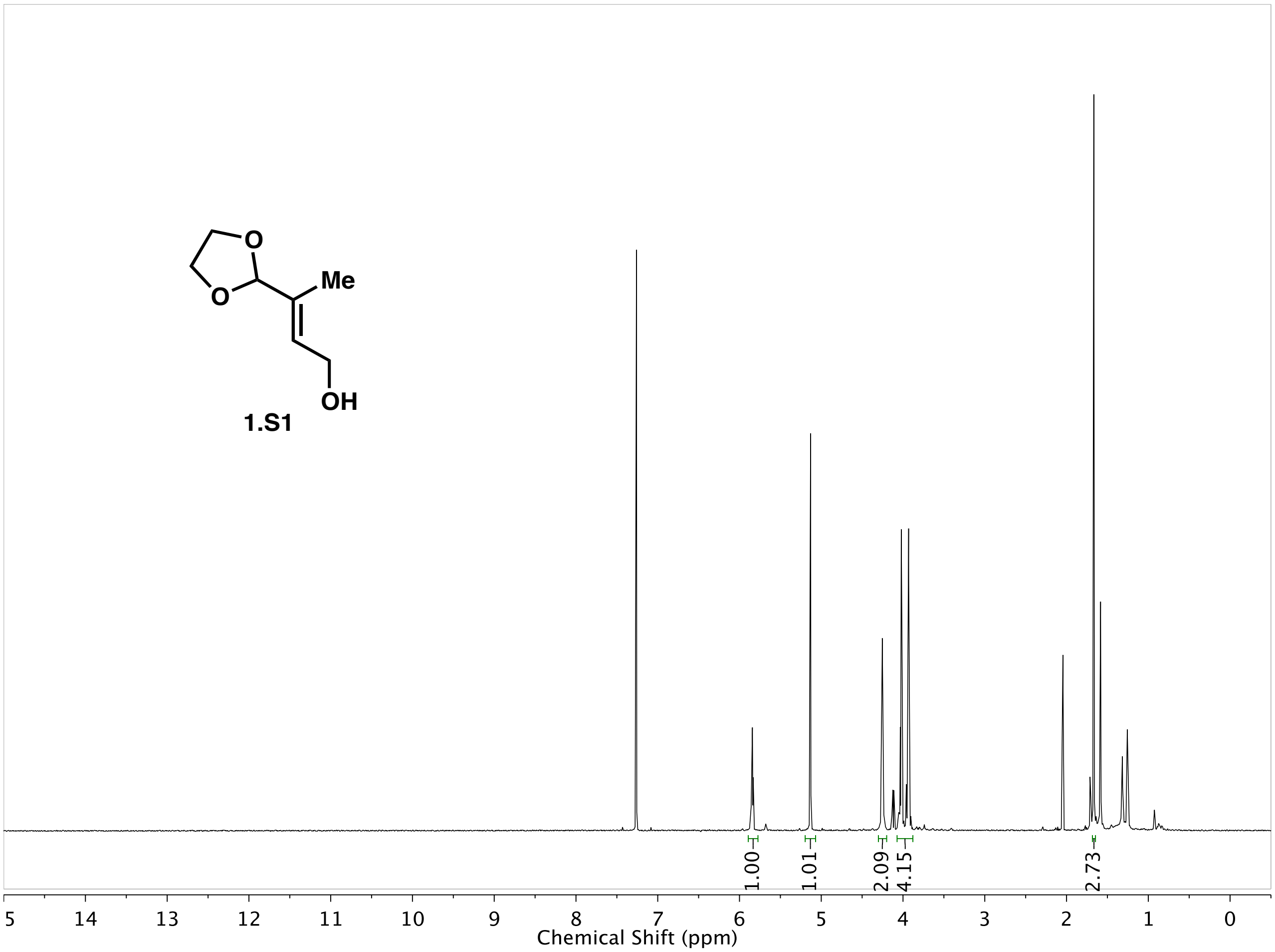

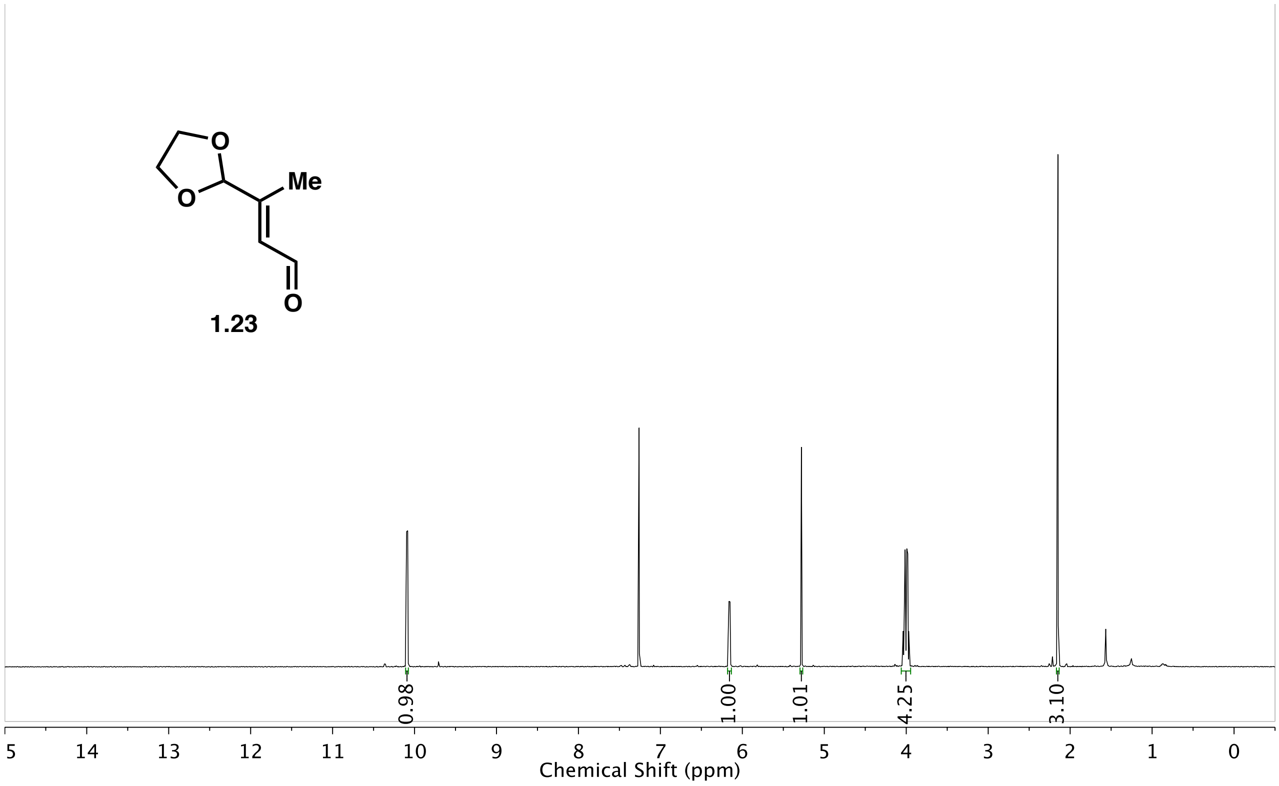
O
O
Me
O
1.23
0.98
1.00
1.01
4.25
3.10
5 14 13 12 11 10 9 8 7 6 5 4 3 2 1 0
Chemical Shift (ppm)

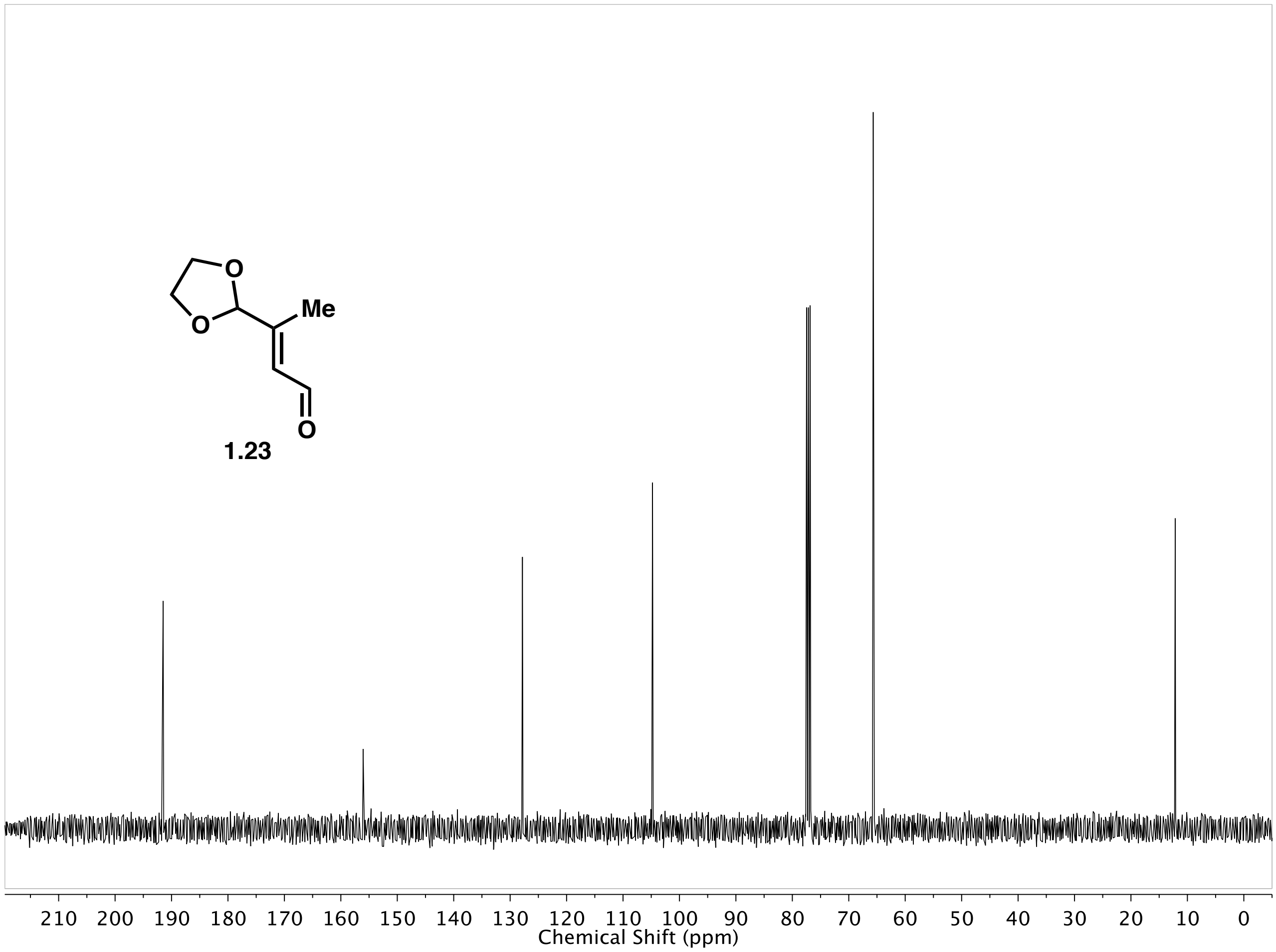
O
O
Me
O
1.23
210 200 190 180 170 160 150 140 130 120 110 100 90 80 70 60 50 40 30 20 10 0
Chemical Shift (ppm)

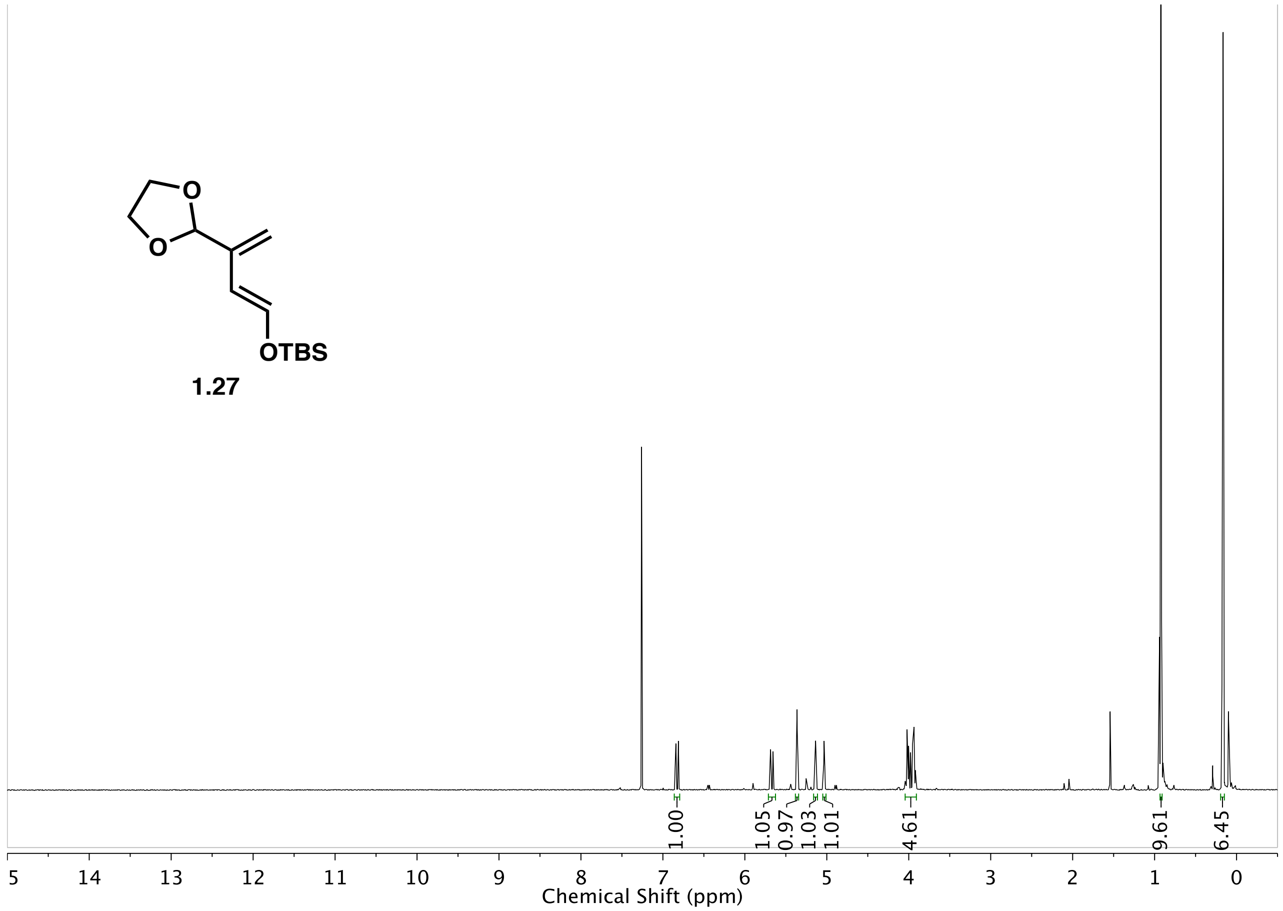
1.27

O
O
OTBS
1.00
1.05
0.97
1.03
1.01
4.61
9.61
6.45
5
14
13
12
11
10
9
8
7
6
5
4
3
2
1
0
Chemical Shift (ppm)

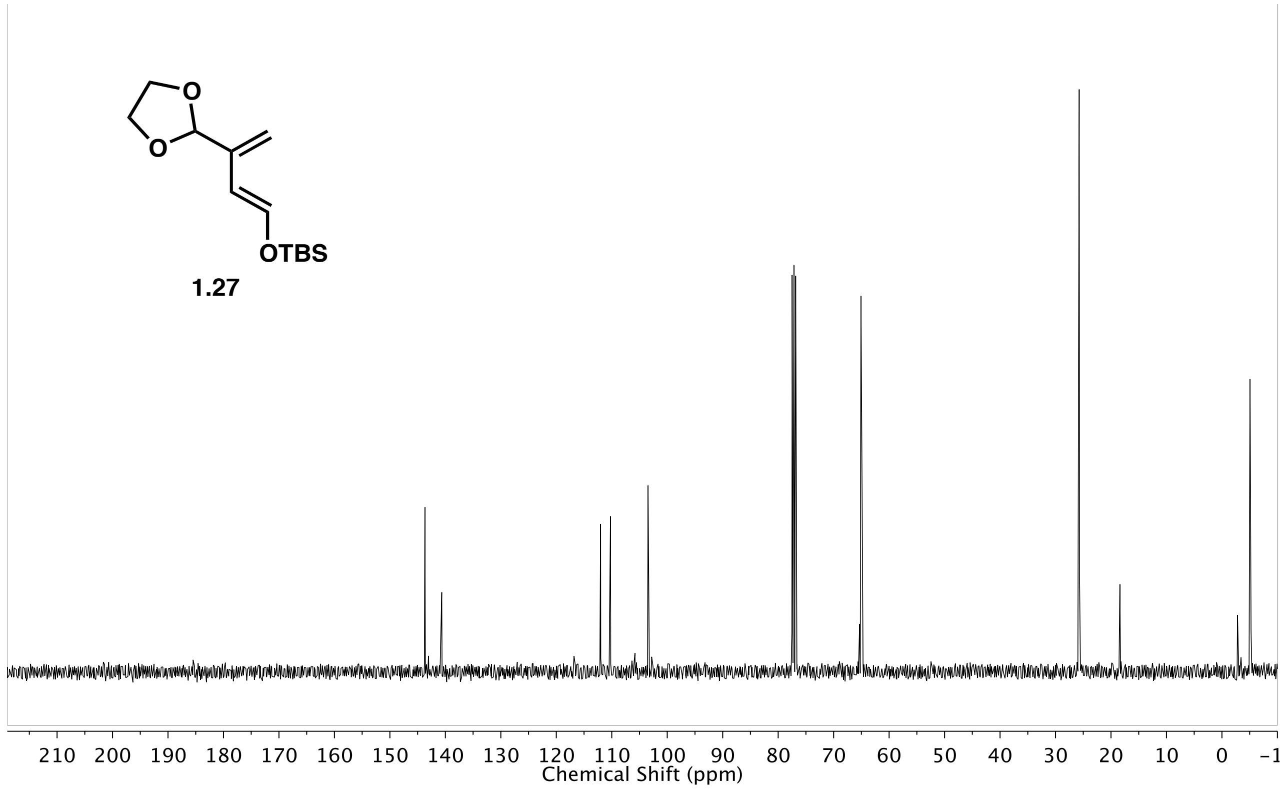
1.27

O
O
OTBS
210
200
190
180
170
160
150
140
130
120
110
100
90
80
70
60
50
40
30
20
10
0
–1
Chemical Shift (ppm)

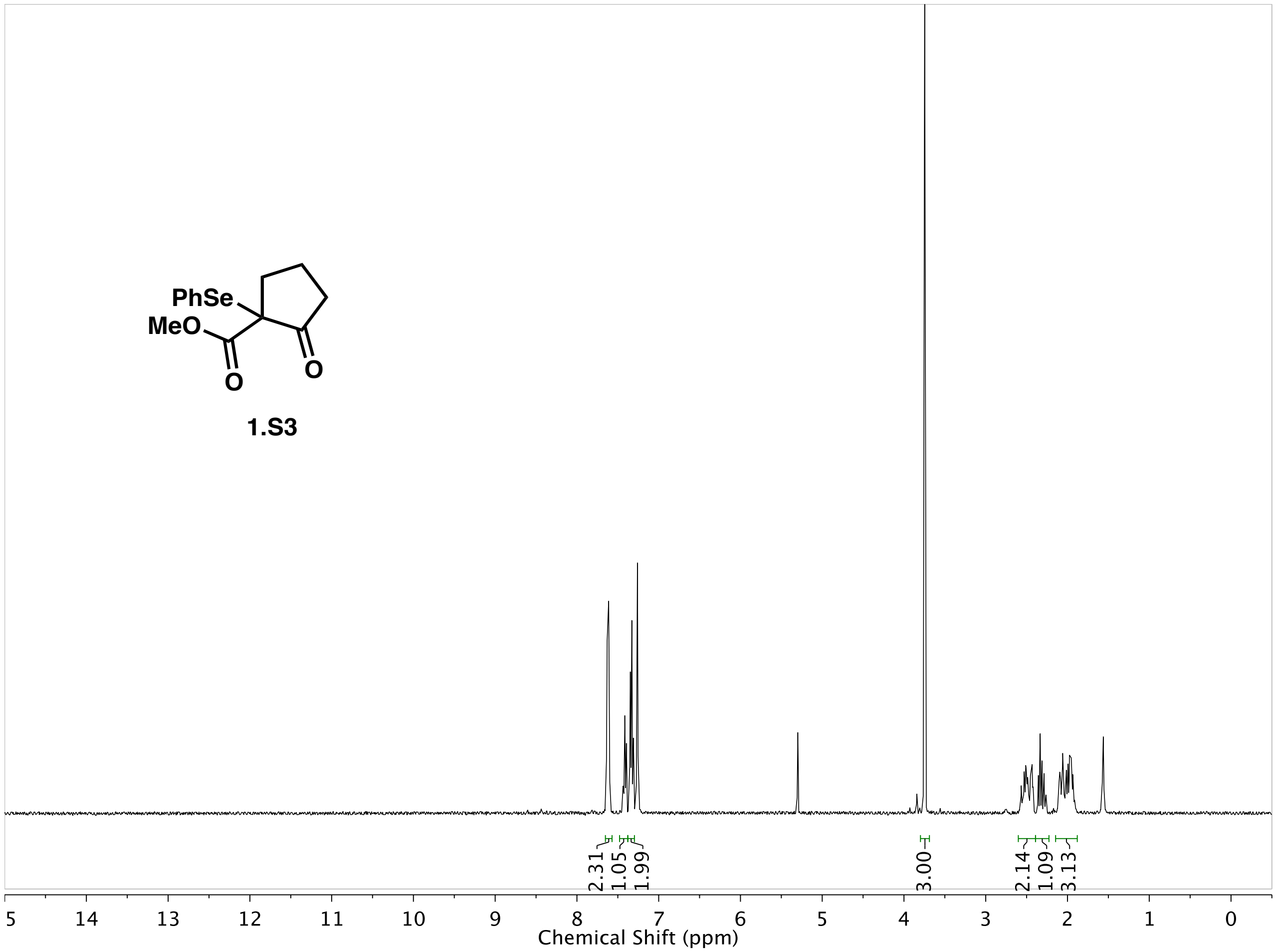
PhSe
MeO
O
O
2.31
1.05
1.99
3.00
2.14
1.09
3.13
5
14
13
12
11
10
9
8
7
6
5
4
3
2
1
0
Chemical Shift (ppm)

1.S3

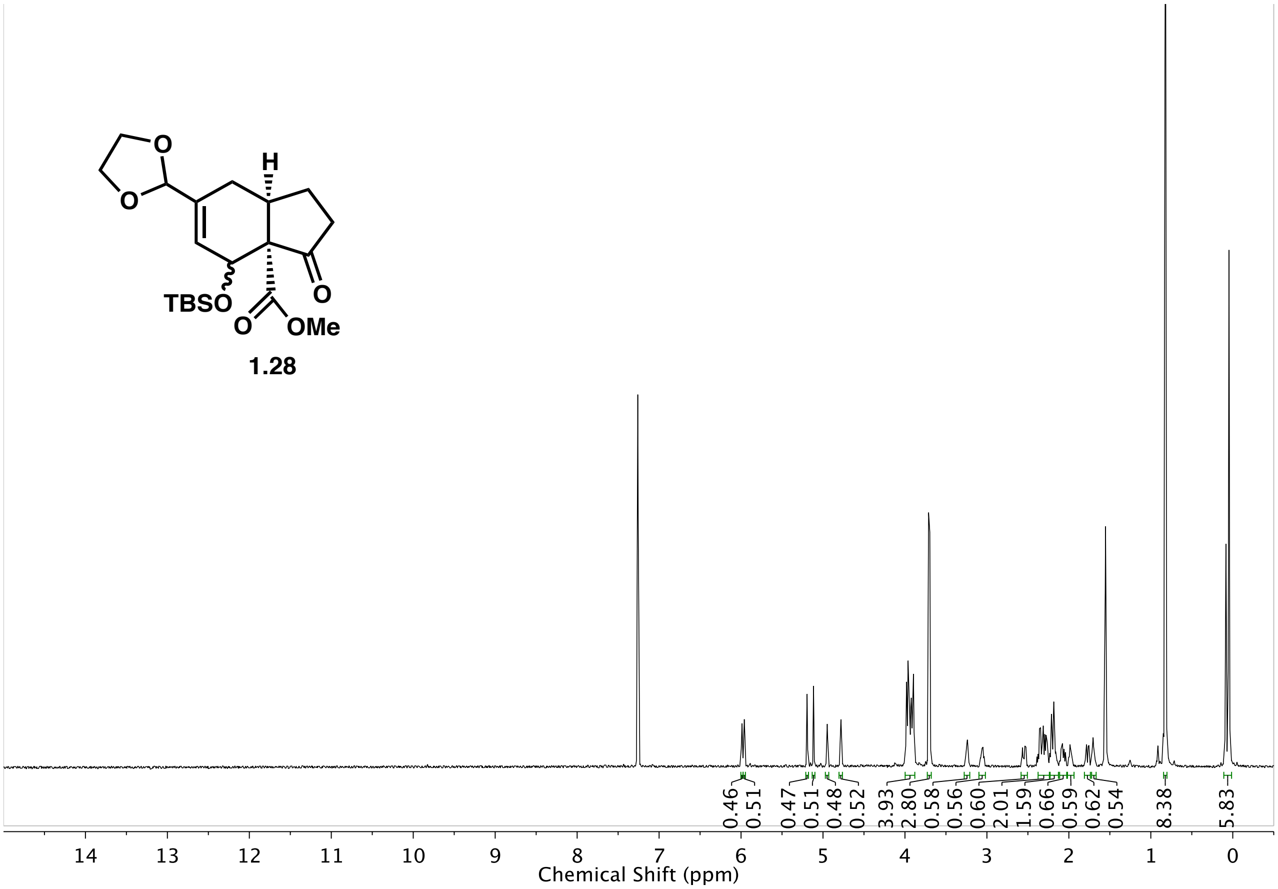
O
O
H
TBSO
O
O
OMe
1.28
0.46
0.51
0.47
0.51
0.48
0.52
3.93
2.80
0.58
0.56
0.60
2.01
1.59
0.66
0.59
0.62
0.54
8.38
5.83
14
13
12
11
10
9
8
7
6
5
4
3
2
1
0
Chemical Shift (ppm)

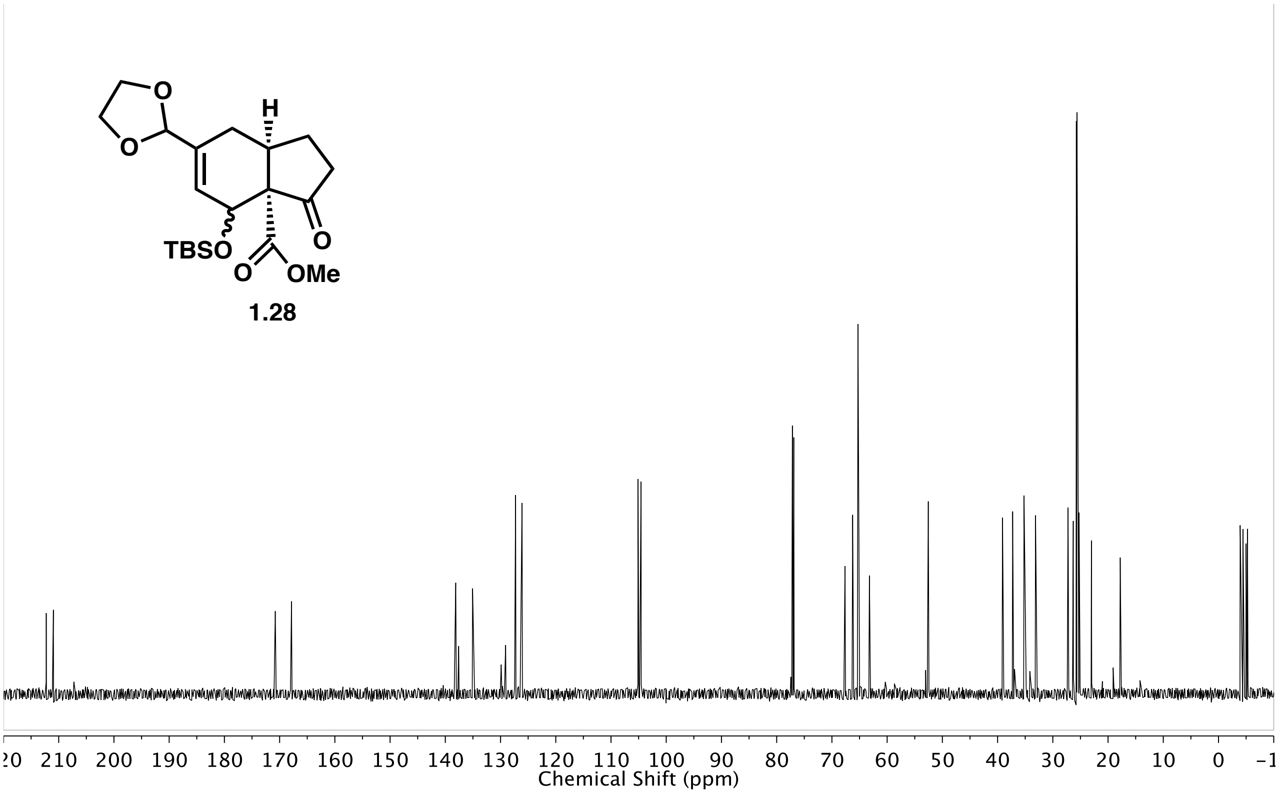
O
O
H
TBSO
O
O
OMe
1.28
20
210
200
190
180
170
160
150
140
130
120
110
100
90
80
70
60
50
40
30
20
10
0
−1
Chemical Shift (ppm)

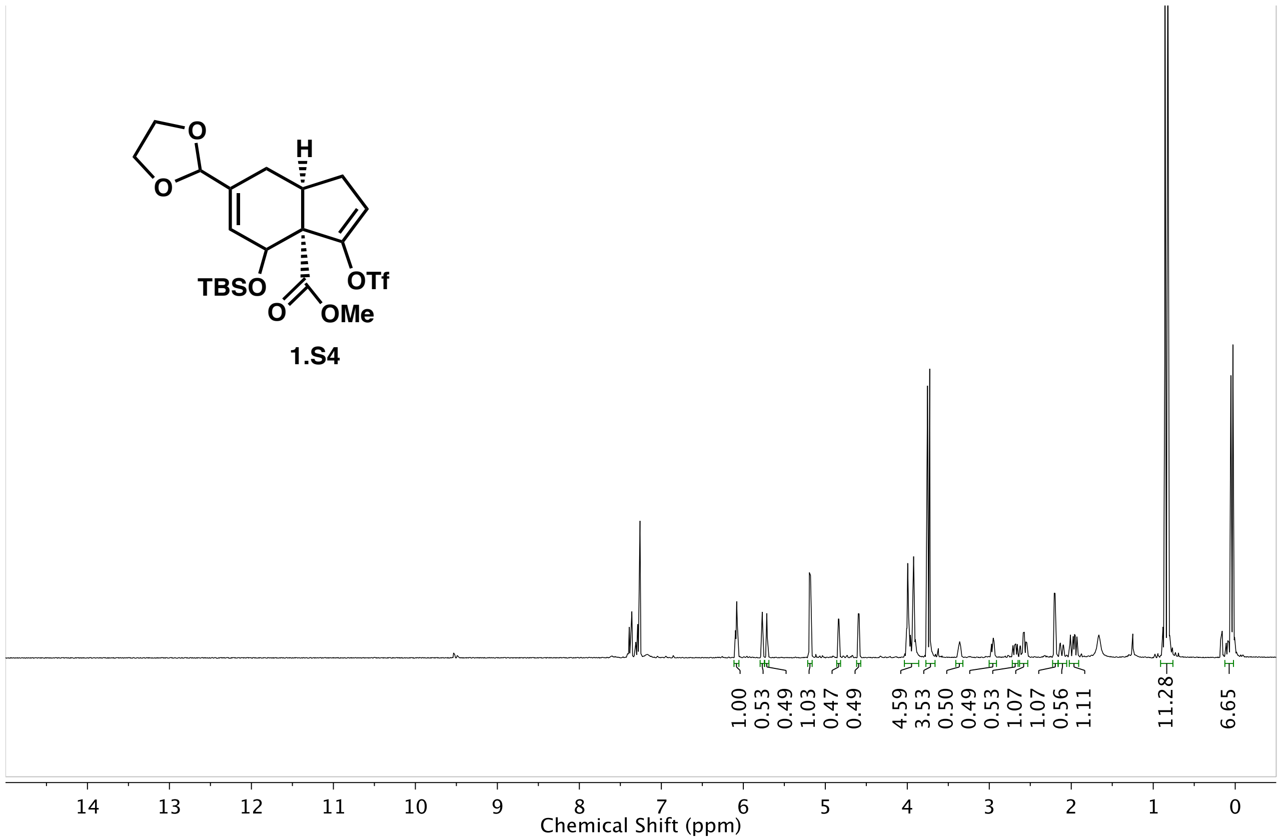

O
O
H
TBSO
OTf
O
OMe
1.S4
1.00
0.53
0.49
1.03
0.47
0.49
4.59
3.53
0.50
0.49
0.53
1.07
1.07
0.56
1.11
11.28
6.65
14
13
12
11
10
9
8
7
6
5
4
3
2
1
0
Chemical Shift (ppm)

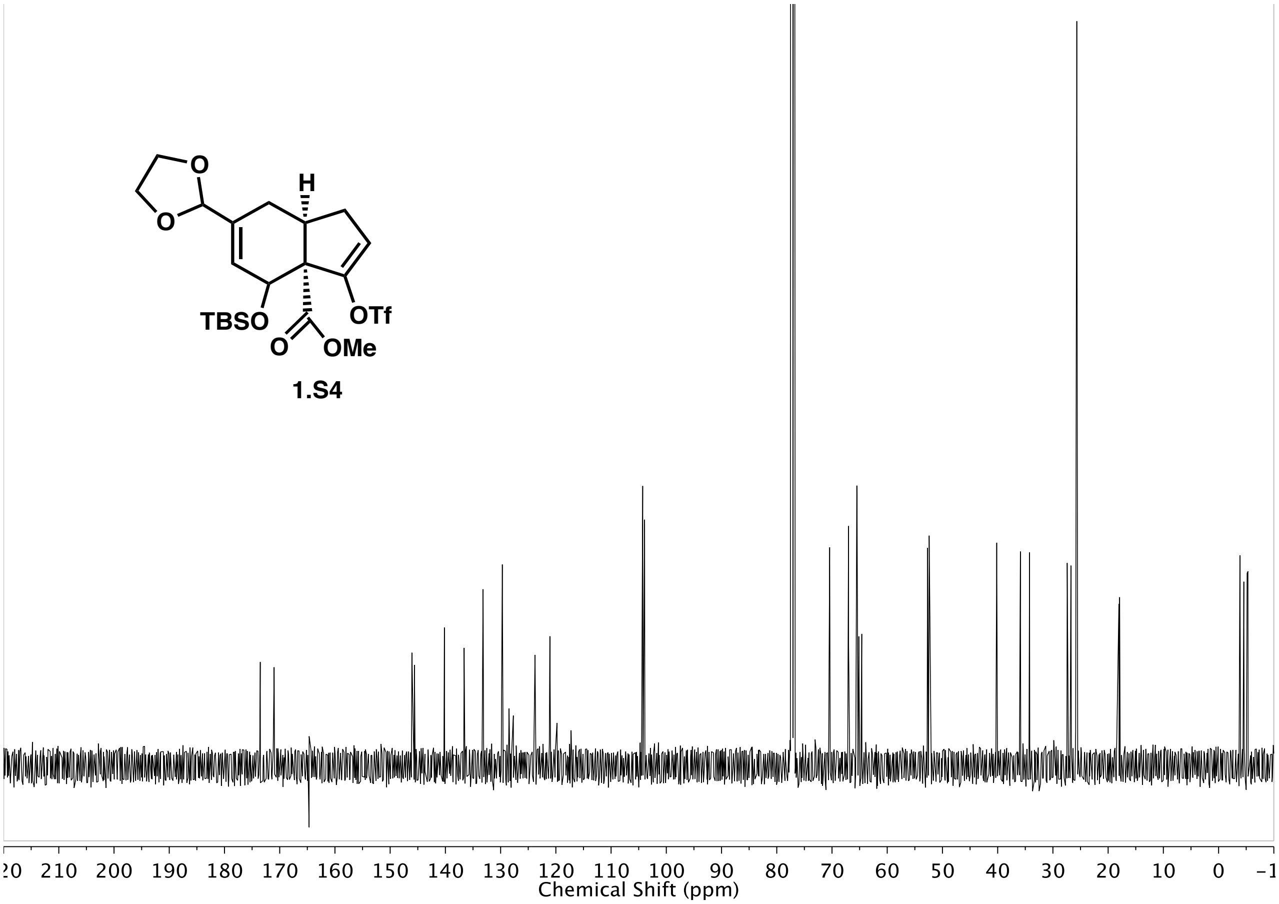

O
O
H
TBSO
OTf
O
OMe
1.S4
20
210
200
190
180
170
160
150
140
130
120
110
100
90
80
70
60
50
40
30
20
10
0
–1
Chemical Shift (ppm)

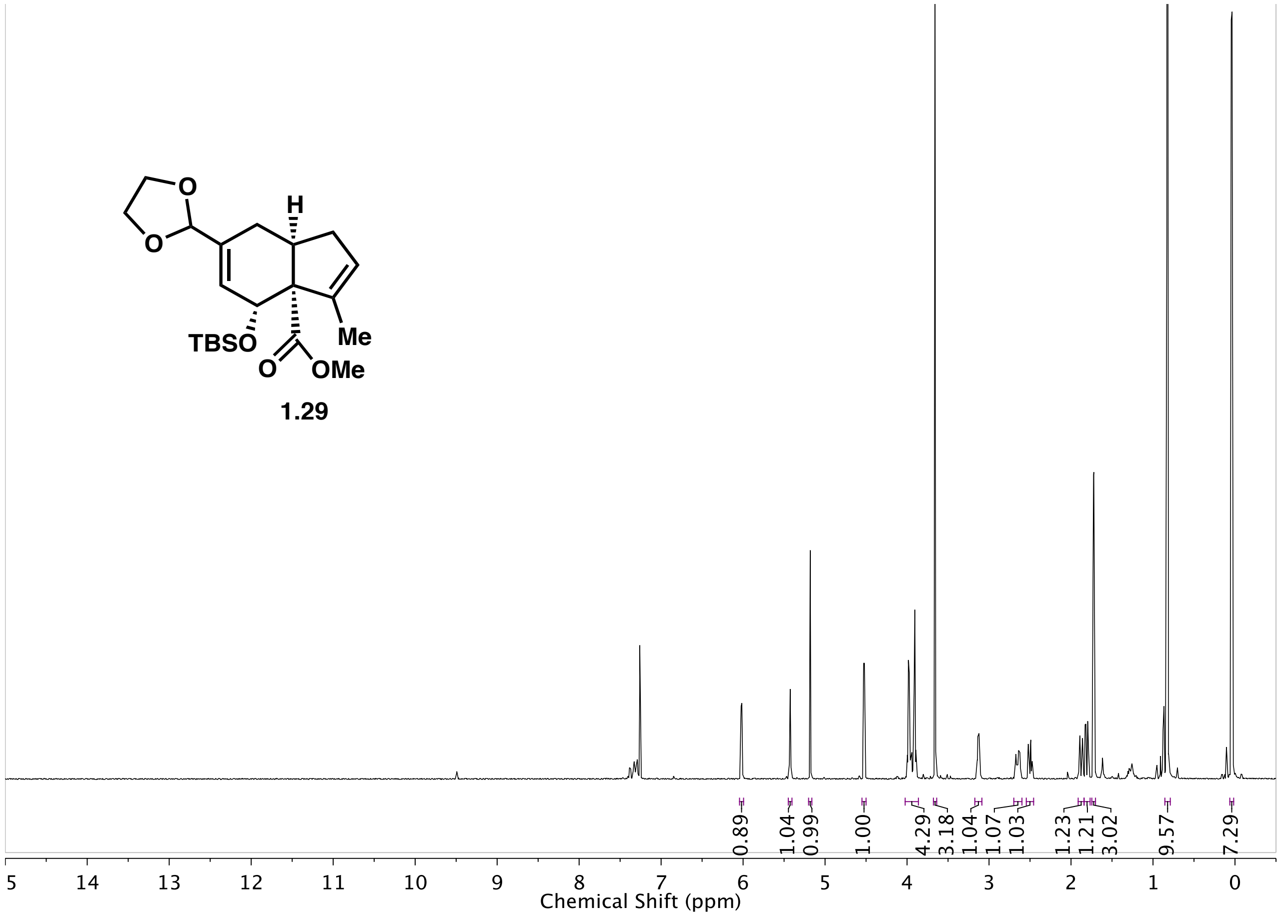
1.29

0.89
1.04
0.99
1.00
4.29
3.18
1.04
1.07
1.03
1.23
1.21
3.02
9.57
7.29
5 14 13 12 11 10 9 8 7 6 5 4 3 2 1 0
Chemical Shift (ppm)
TBSO
O
OMe
Me
H

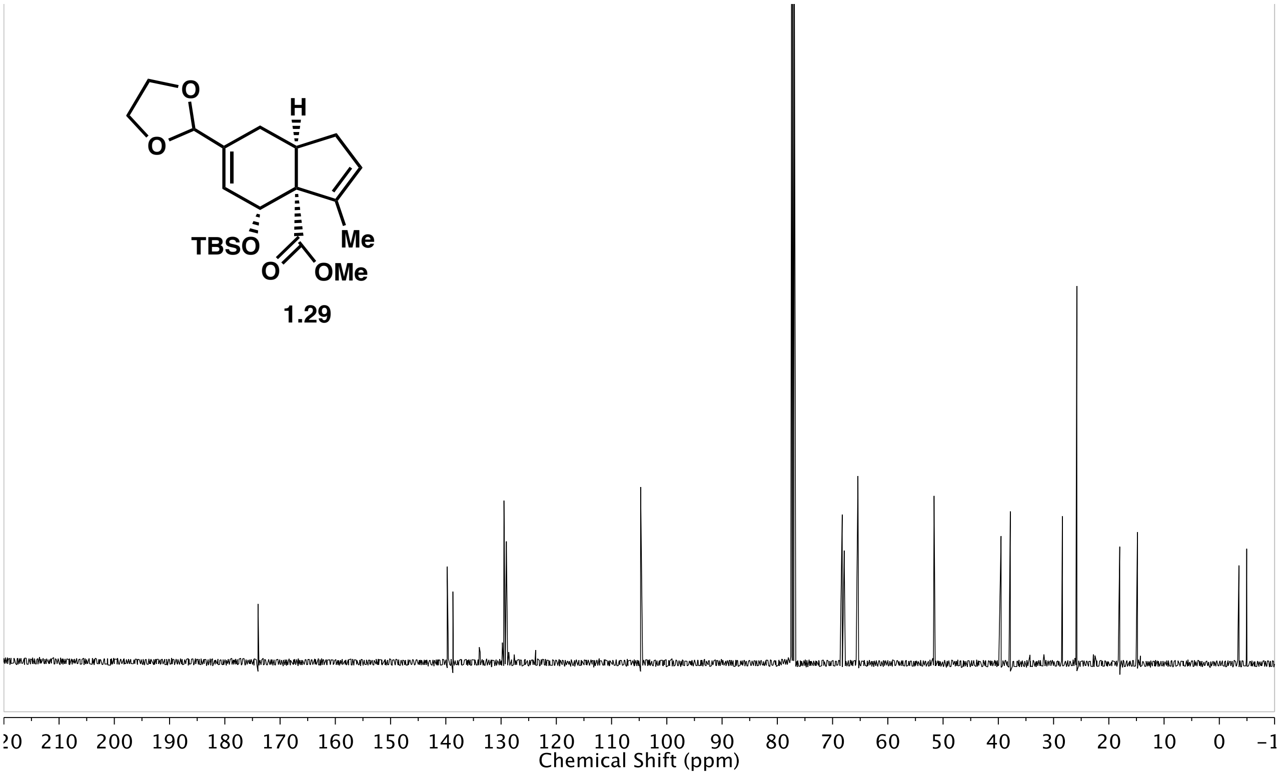
1.29

20 210 200 190 180 170 160 150 140 130 120 110 100 90 80 70 60 50 40 30 20 10 0 −1
Chemical Shift (ppm)
TBSO
O
OMe
Me
H

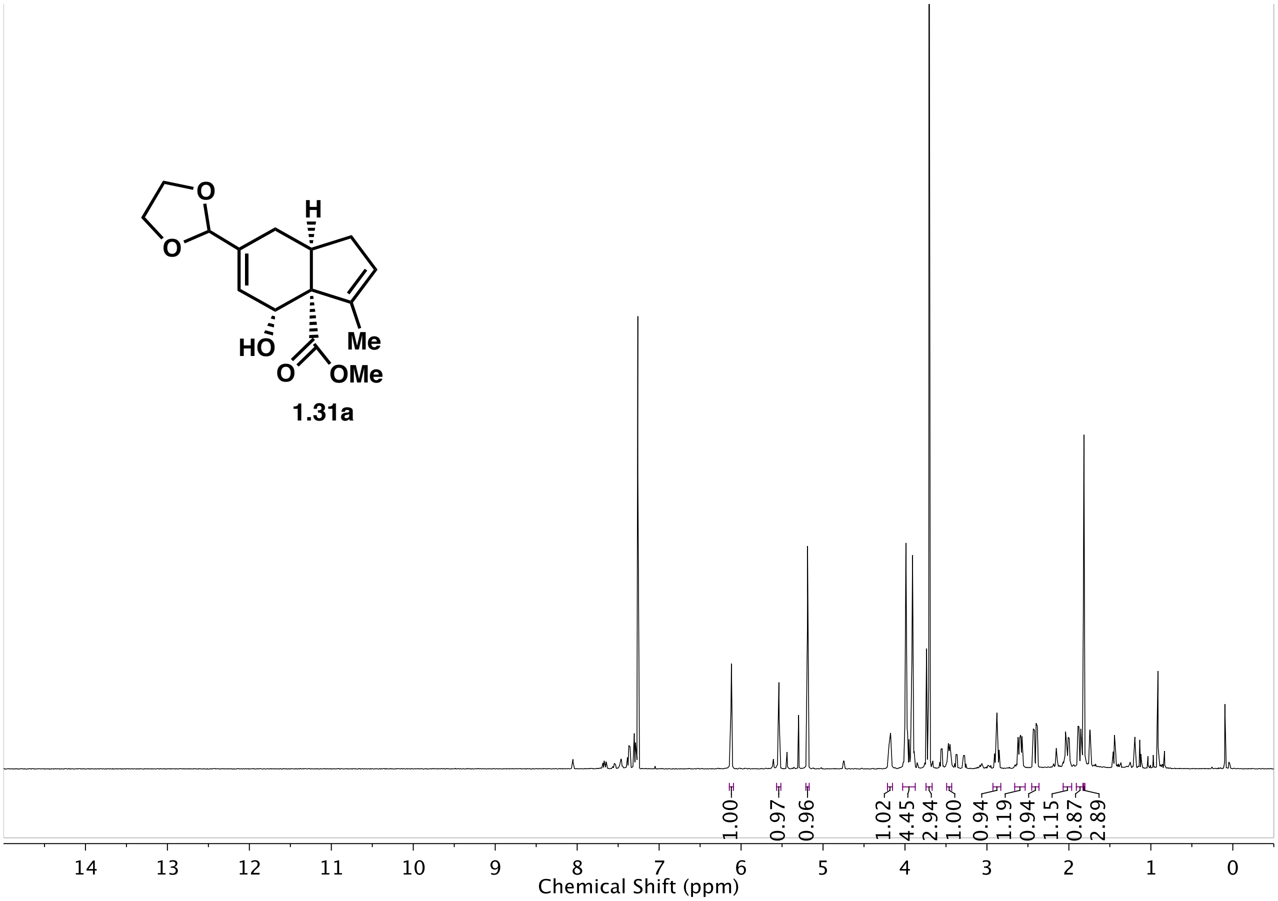
O
O
H
HO
O
OMe
Me
1.00
0.97
0.96
1.02
4.45
2.94
1.00
0.94
1.19
0.94
1.15
0.87
2.89
14
13
12
11
10
9
8
7
6
5
4
3
2
1
0
Chemical Shift (ppm)

1.31a

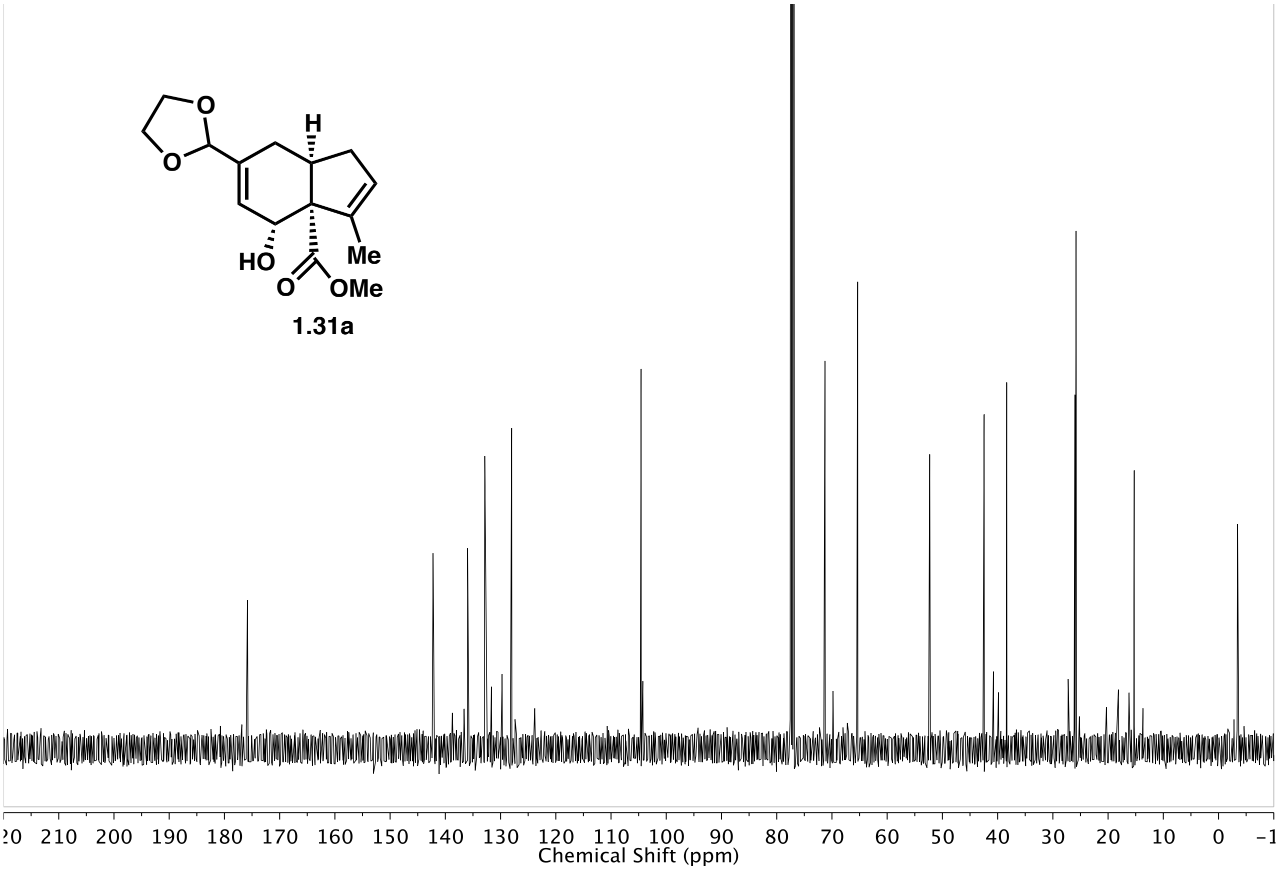
O
O
H
HO
O
OMe
Me
210
200
190
180
170
160
150
140
130
120
110
100
90
80
70
60
50
40
30
20
10
0
Chemical Shift (ppm)

1.31a

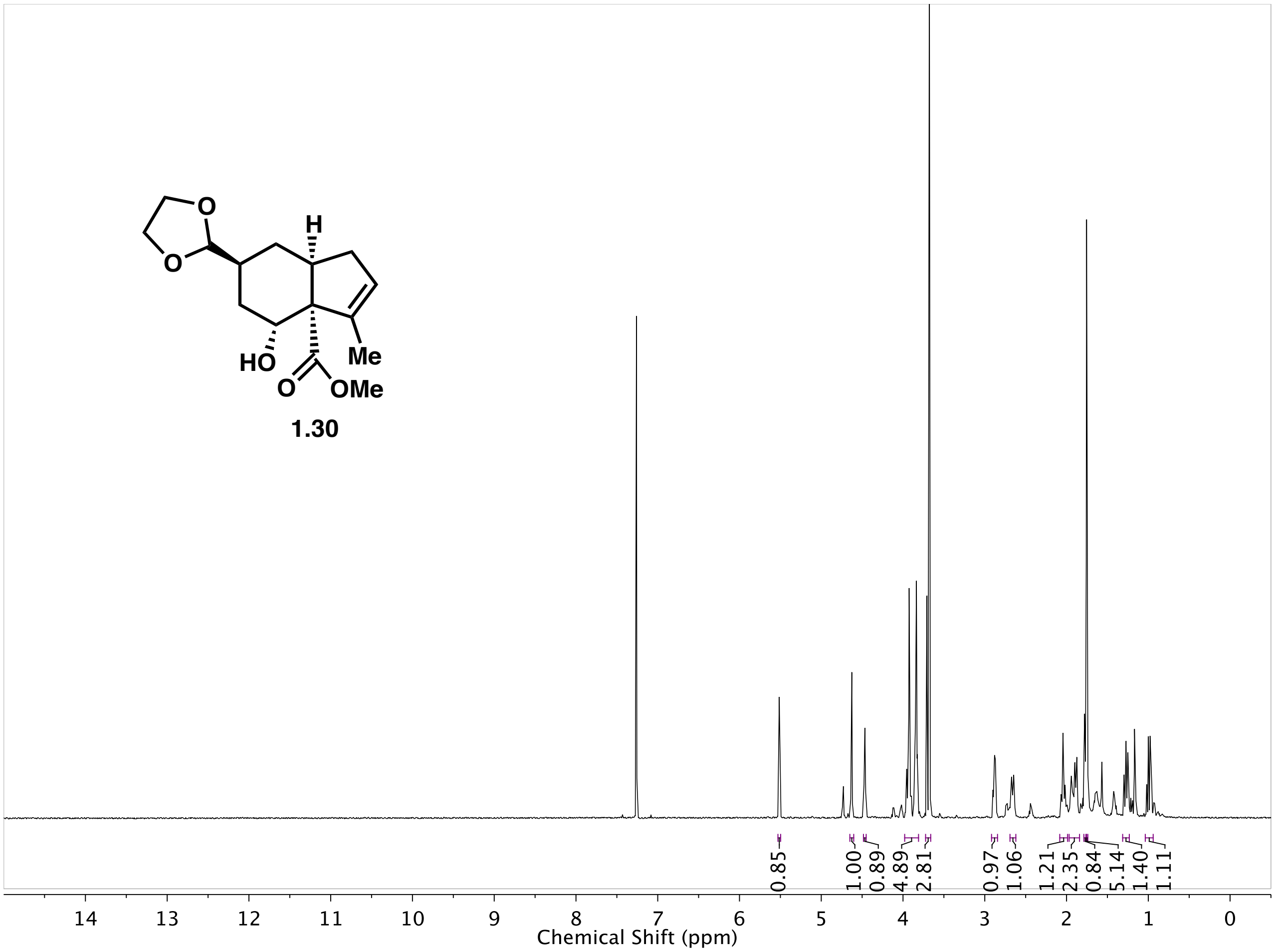

1.30

O
O
H
HO
Me
O
OMe
0.85
1.00
0.89
4.89
2.81
0.97
1.06
1.21
2.35
0.84
5.14
1.40
1.11
14
13
12
11
10
9
8
7
6
5
4
3
2
1
0
Chemical Shift (ppm)

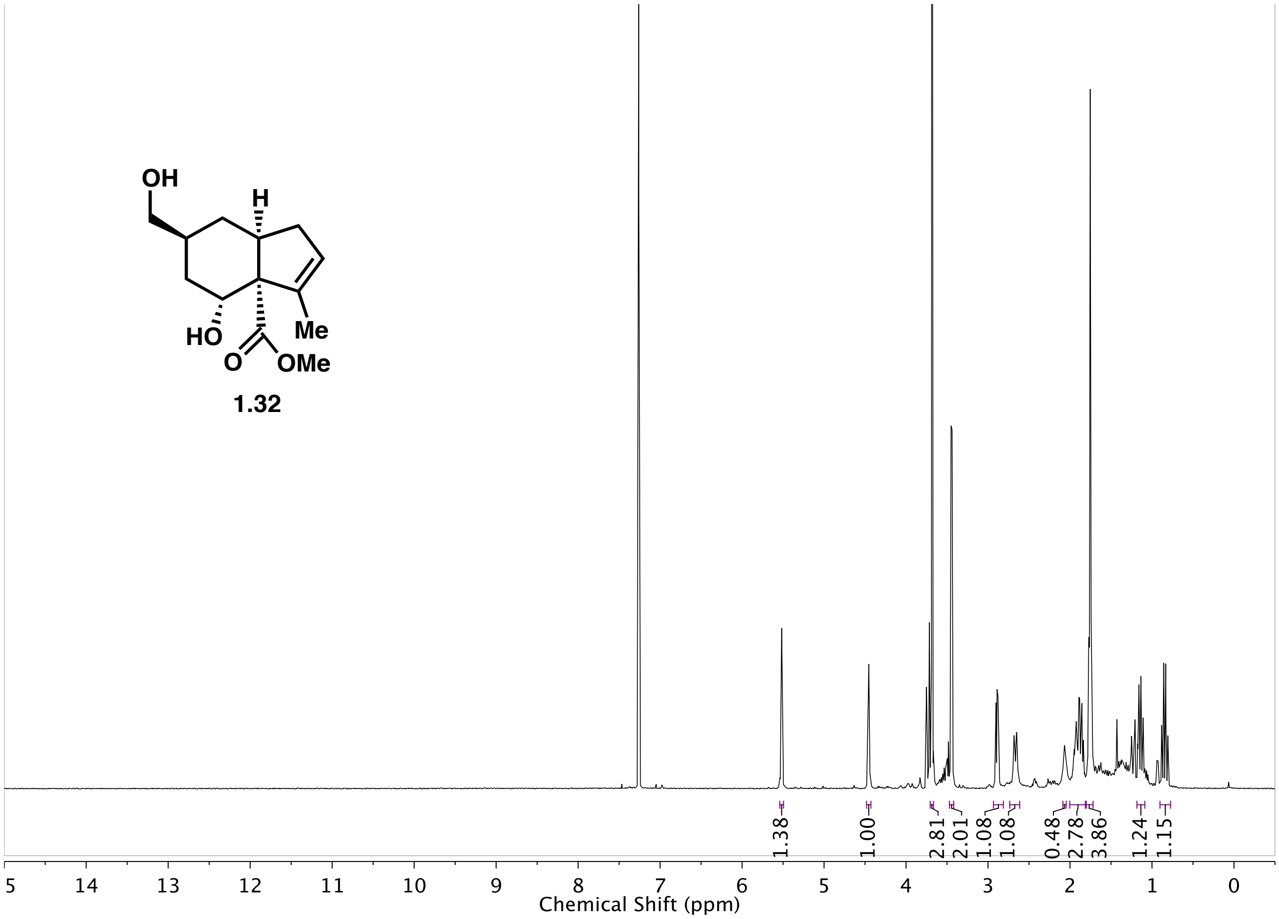
OH
H
HO
Me
O
OMe
1.32
1.38
1.00
2.81
2.01
1.08
1.08
0.48
2.78
3.86
1.24
1.15
5
14
13
12
11
10
9
8
7
6
5
4
3
2
1
0
Chemical Shift (ppm)

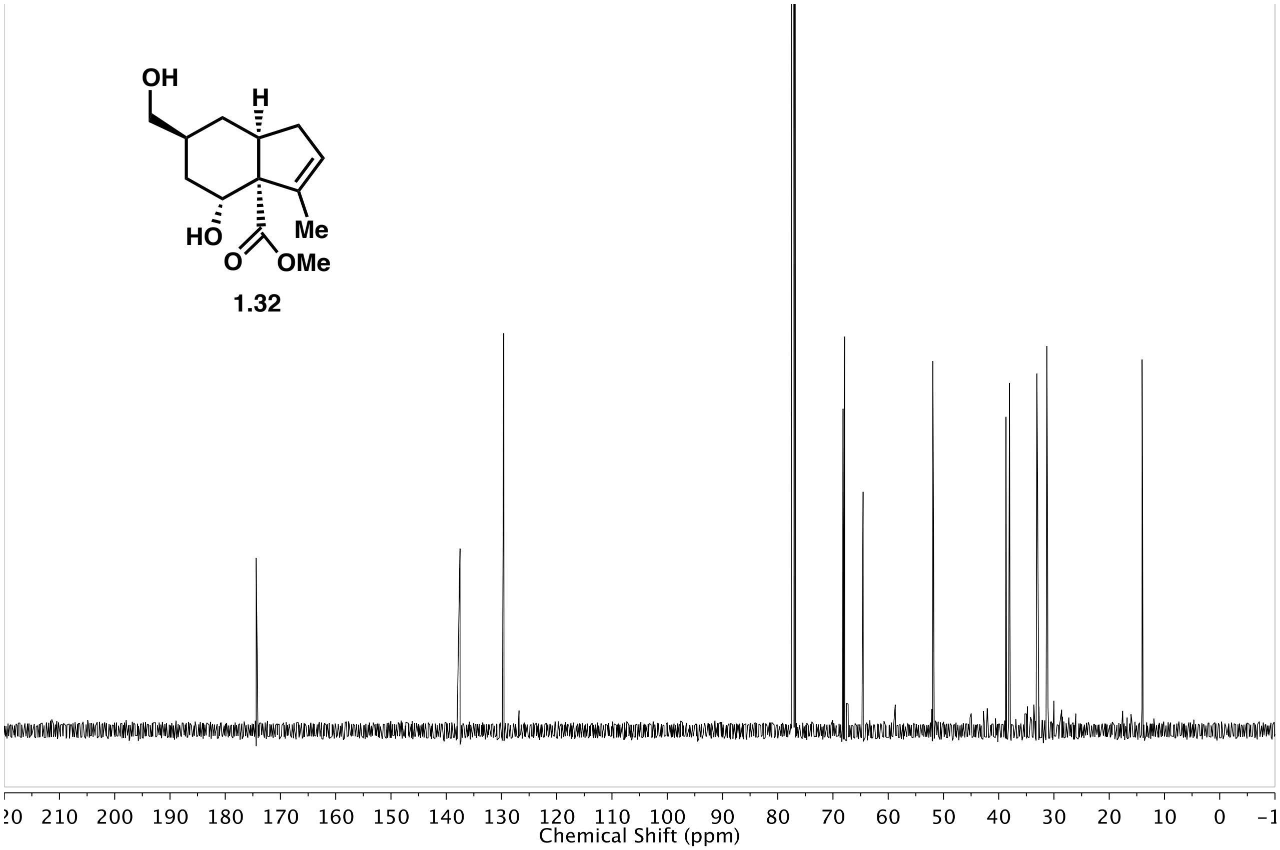
OH
H
HO
Me
O
OMe
1.32
20
210
200
190
180
170
160
150
140
130
120
110
100
90
80
70
60
50
40
30
20
10
0
–1
Chemical Shift (ppm)

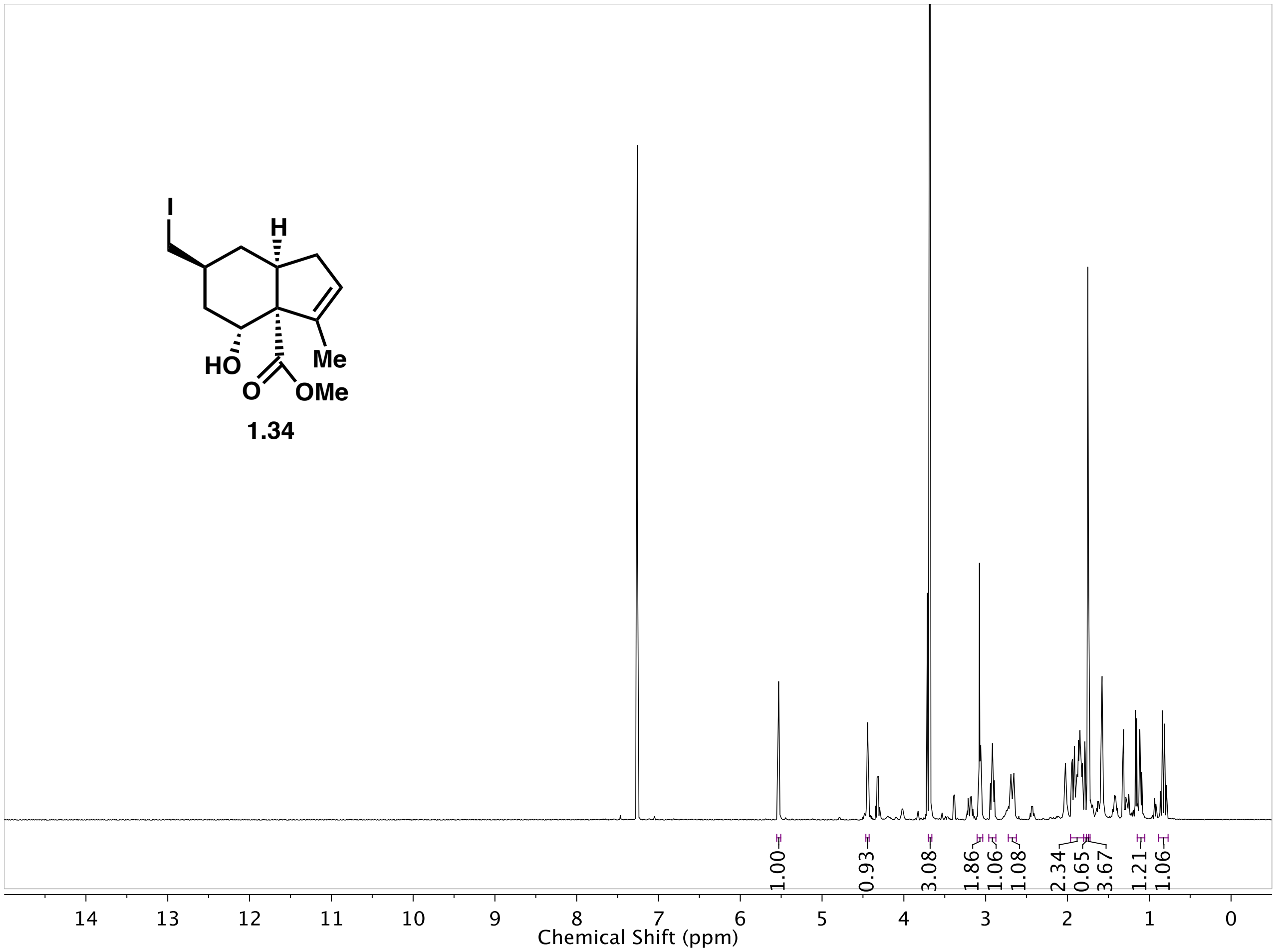
I
H
Me
HO
O
OMe
1.34
1.00
0.93
3.08
1.86
1.06
1.08
2.34
0.65
3.67
1.21
1.06
14
13
12
11
10
9
8
7
6
5
4
3
2
1
0
Chemical Shift (ppm)

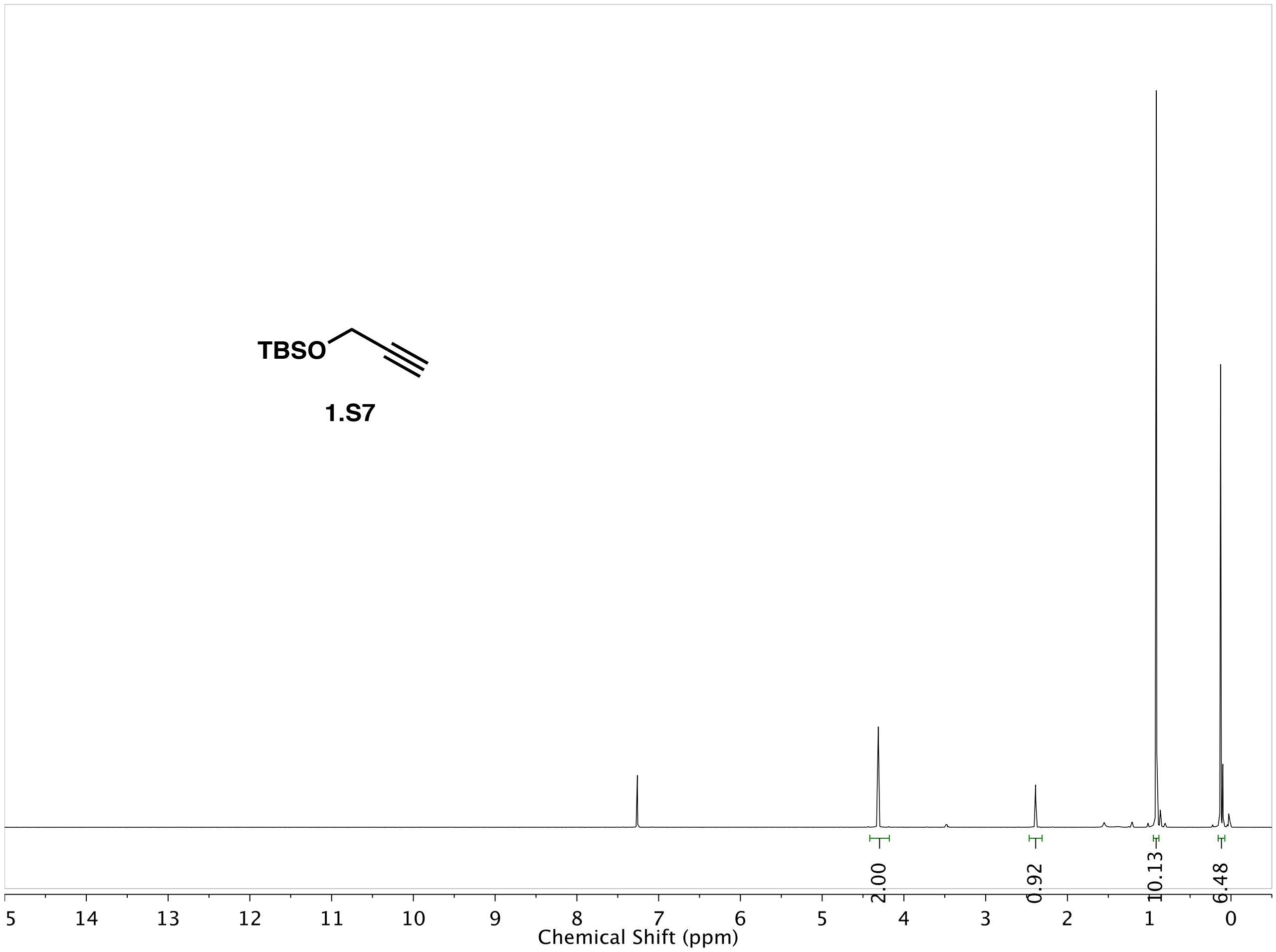
TBSO
1.S7
2.00
0.92
10.13
6.48
5
14
13
12
11
10
9
8
7
6
5
4
3
2
1
0
Chemical Shift (ppm)

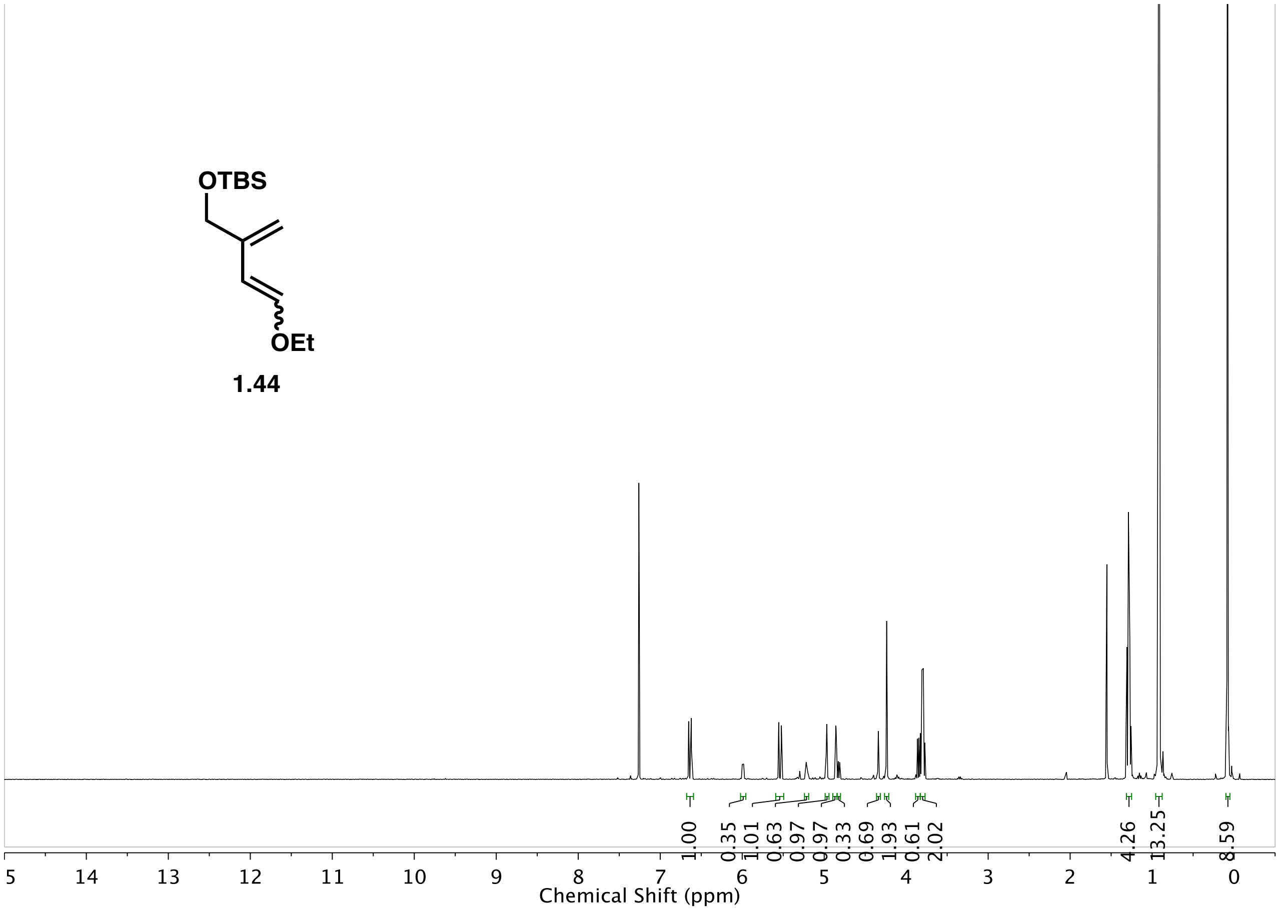
OTBS
OEt
1.44
1.00
0.35
1.01
0.63
0.97
0.97
0.33
0.69
1.93
0.61
2.02
4.26
13.25
8.59
5
14
13
12
11
10
9
8
7
6
5
4
3
2
1
0
Chemical Shift (ppm)

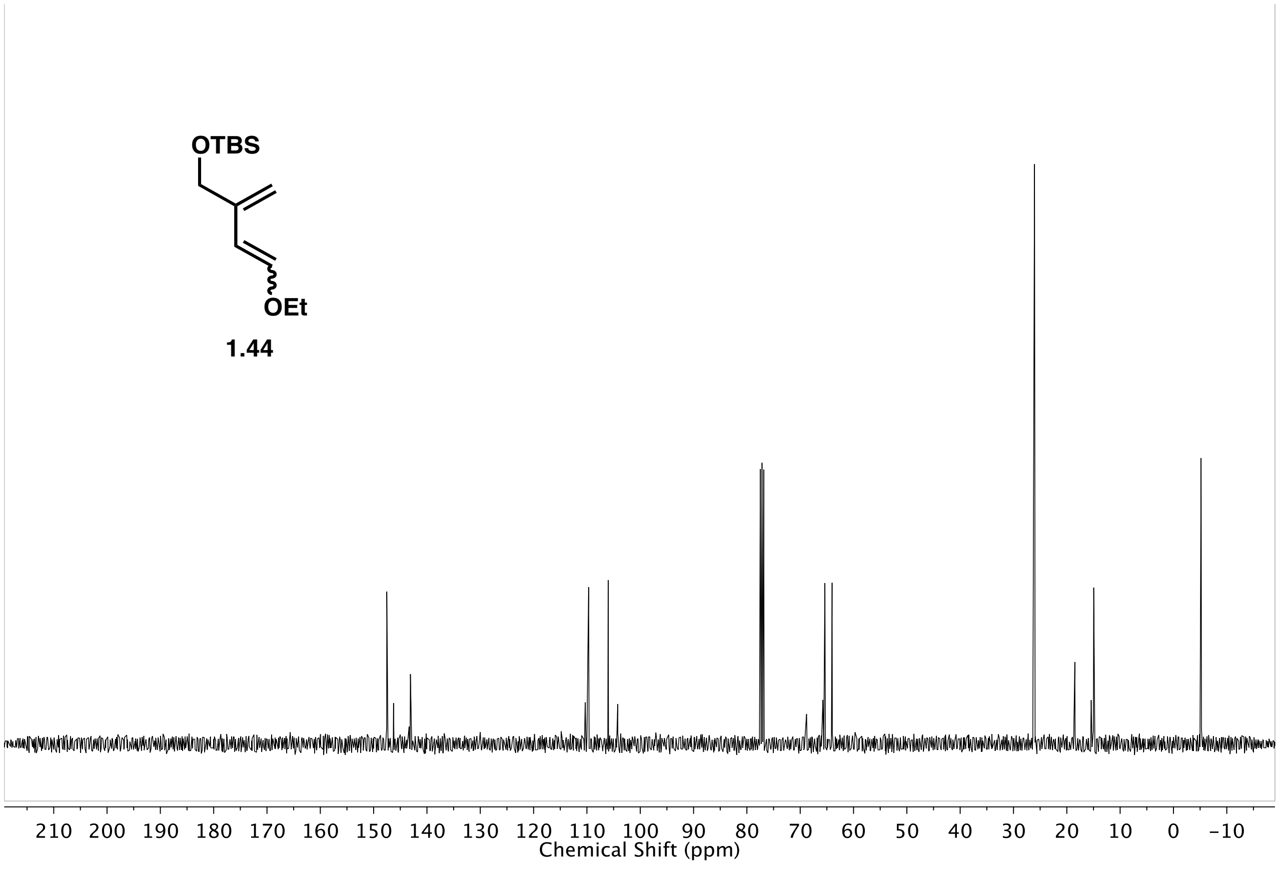
OTBS
OEt
1.44
210
200
190
180
170
160
150
140
130
120
110
100
90
80
70
60
50
40
30
20
10
0
−10
Chemical Shift (ppm)

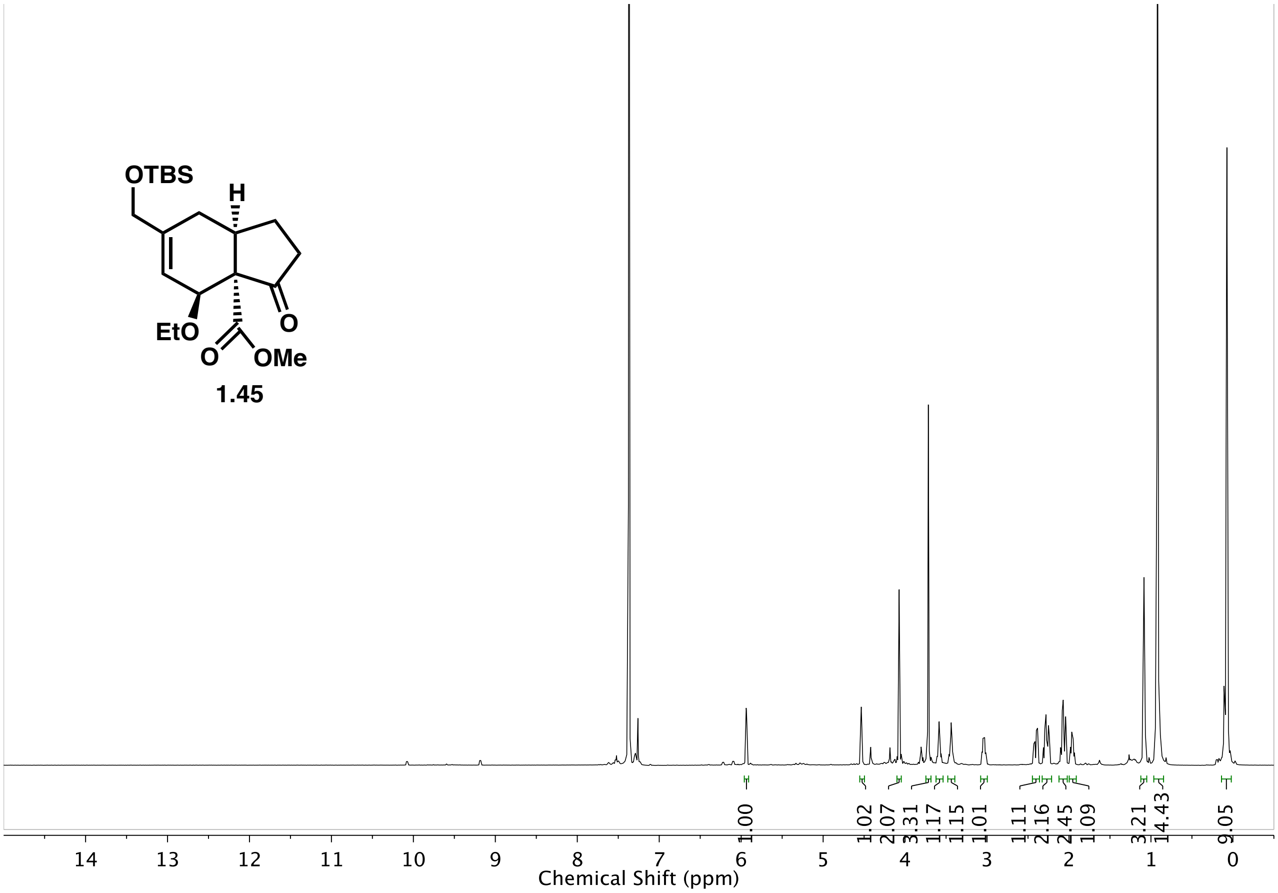
OTBS
H
O
EtO
O
OMe
1.45
1.00
1.02
2.07
3.31
1.17
1.15
1.01
1.11
2.16
2.45
1.09
3.21
14.43
9.05
14
13
12
11
10
9
8
7
6
5
4
3
2
1
0
Chemical Shift (ppm)

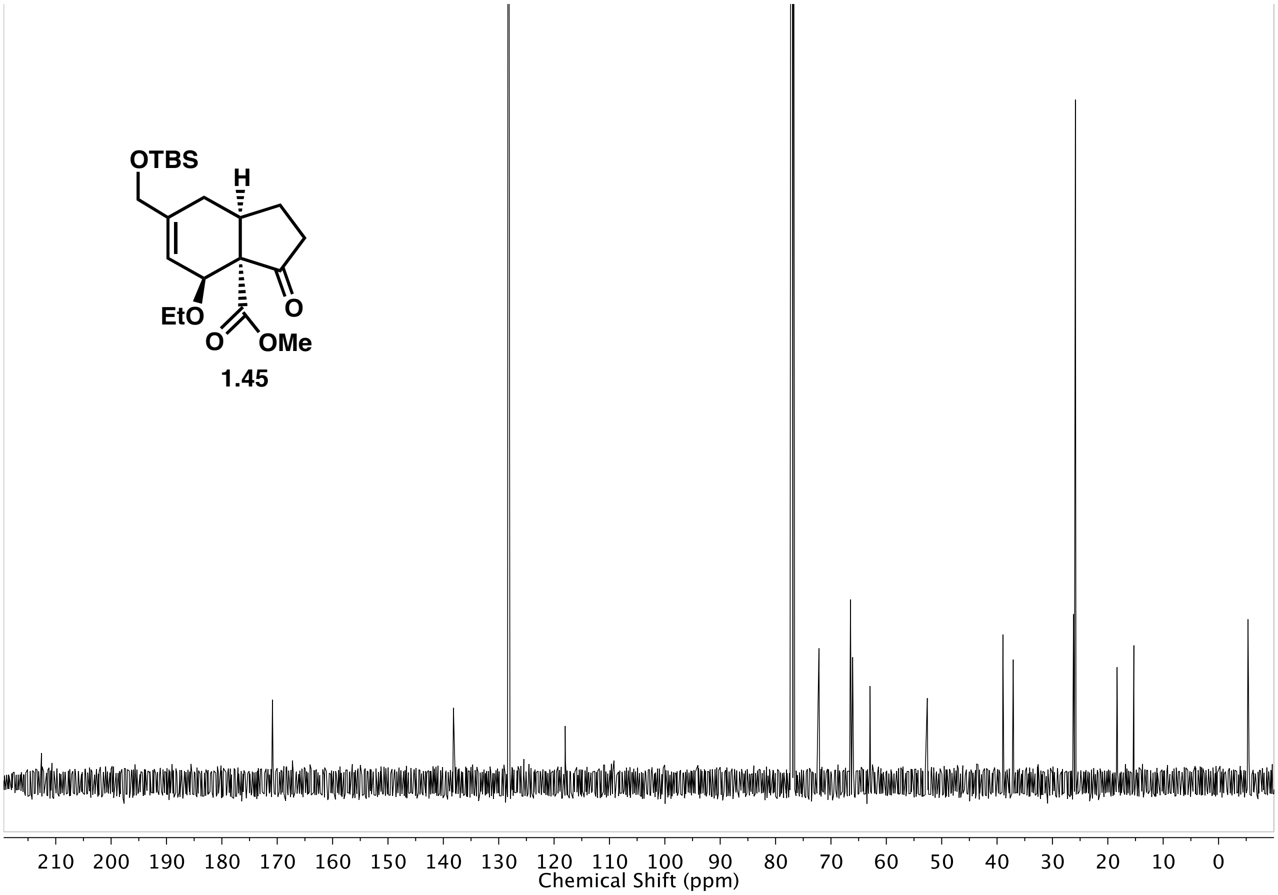
OTBS
H
O
EtO
O
OMe
1.45
210
200
190
180
170
160
150
140
130
120
110
100
90
80
70
60
50
40
30
20
10
0
Chemical Shift (ppm)

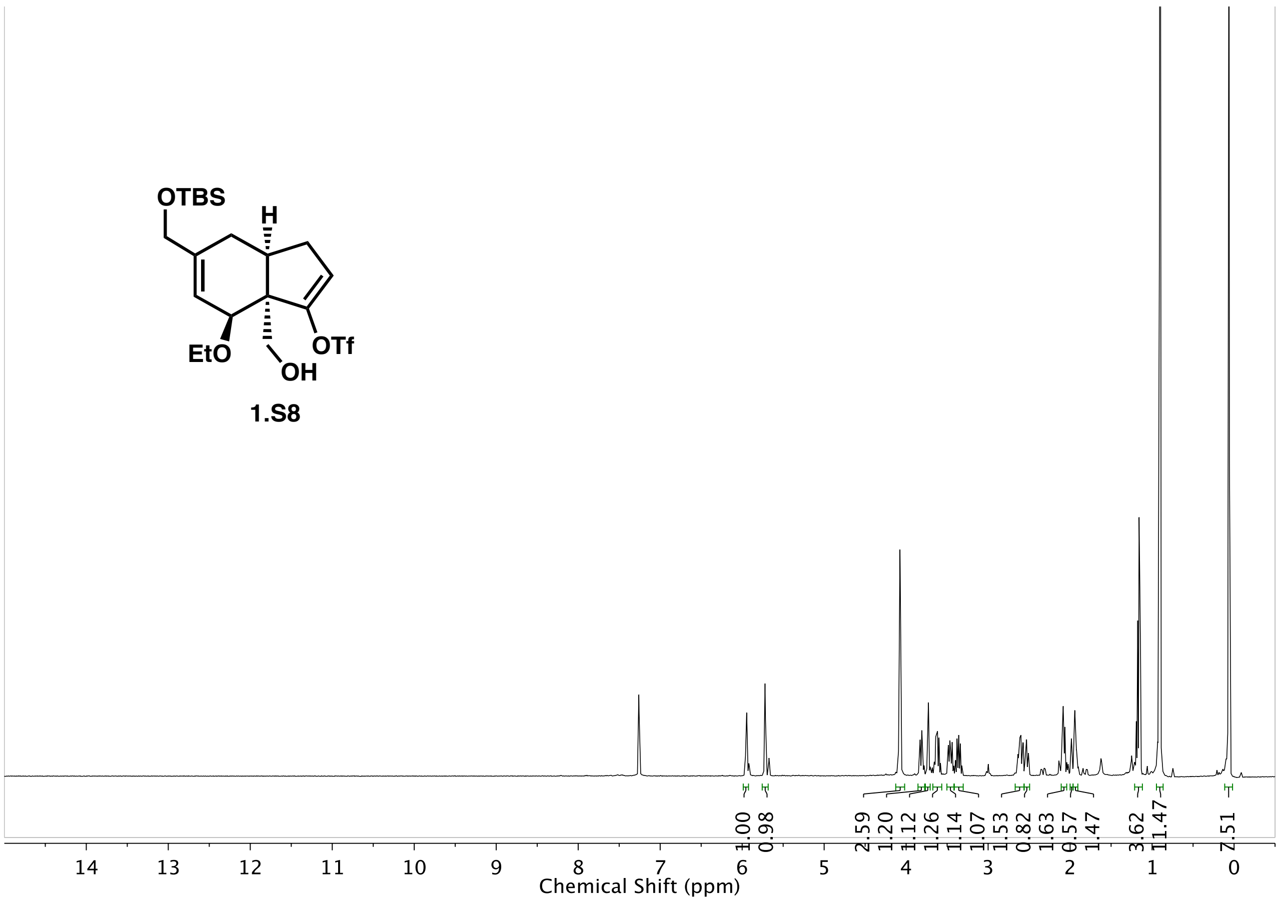
OTBS
H
OTf
EtO
OH
1.S8
1.00
0.98
2.59
1.20
1.12
1.26
1.14
1.07
1.53
0.82
1.63
0.57
1.47
3.62
11.47
7.51
14 13 12 11 10 9 8 7 6 5 4 3 2 1 0
Chemical Shift (ppm)

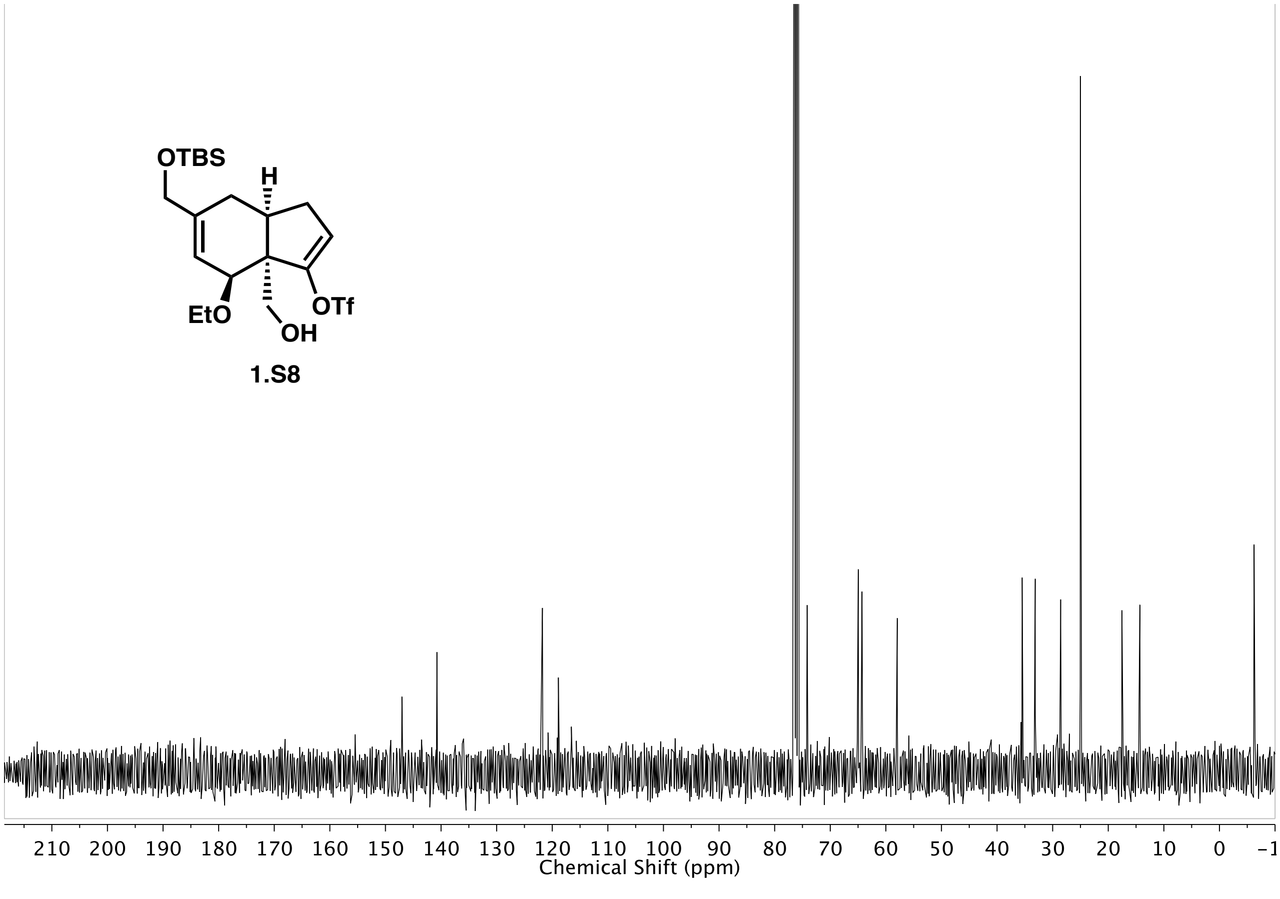
OTBS
H
OTf
EtO
OH
1.S8
210 200 190 180 170 160 150 140 130 120 110 100 90 80 70 60 50 40 30 20 10 0 −1
Chemical Shift (ppm)

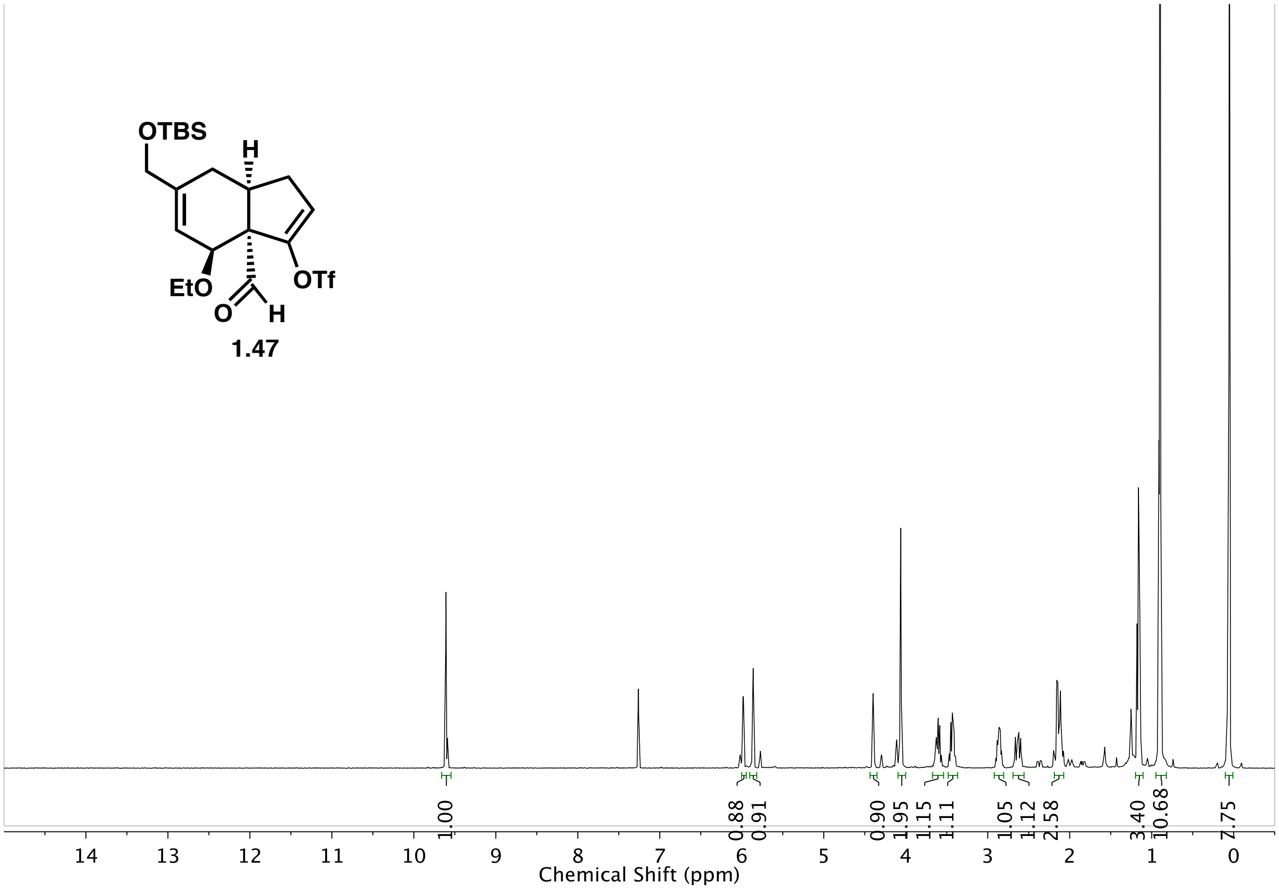
1.47

OTBS
H
EtO
O
H
OTf
1.00
0.88
0.91
0.90
1.95
1.15
1.11
1.05
1.12
2.58
3.40
10.68
7.75
14 13 12 11 10 9 8 7 6 5 4 3 2 1 0
Chemical Shift (ppm)

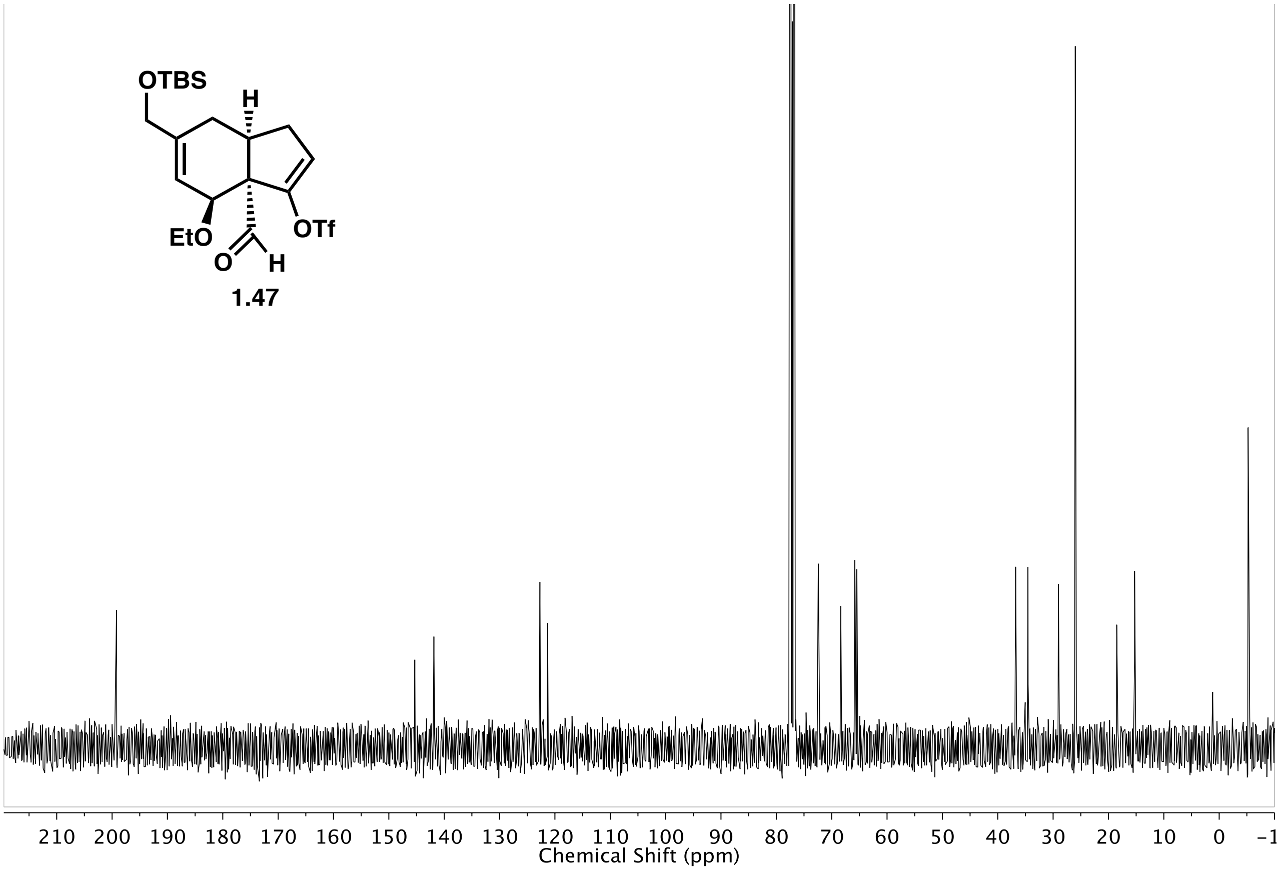
1.47

OTBS
H
EtO
O
H
OTf
210 200 190 180 170 160 150 140 130 120 110 100 90 80 70 60 50 40 30 20 10 0 −1
Chemical Shift (ppm)

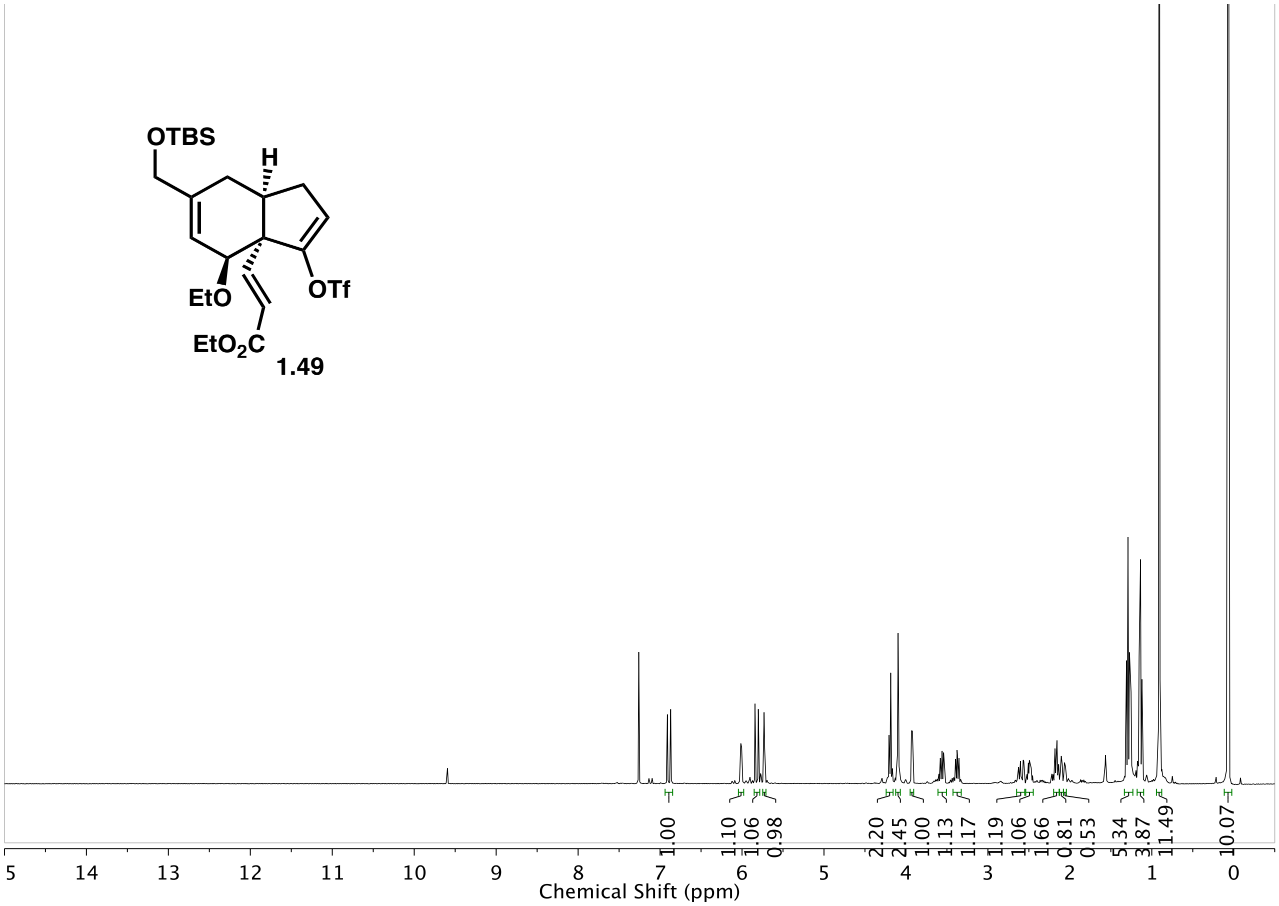

OTBS
H
OTf
EtO
EtO2C
1.49
1.00
1.10
1.06
0.98
2.20
2.45
1.00
1.13
1.17
1.19
1.06
1.66
0.81
0.53
5.34
3.87
11.49
10.07
5
14
13
12
11
10
9
8
7
6
5
4
3
2
1
0
Chemical Shift (ppm)

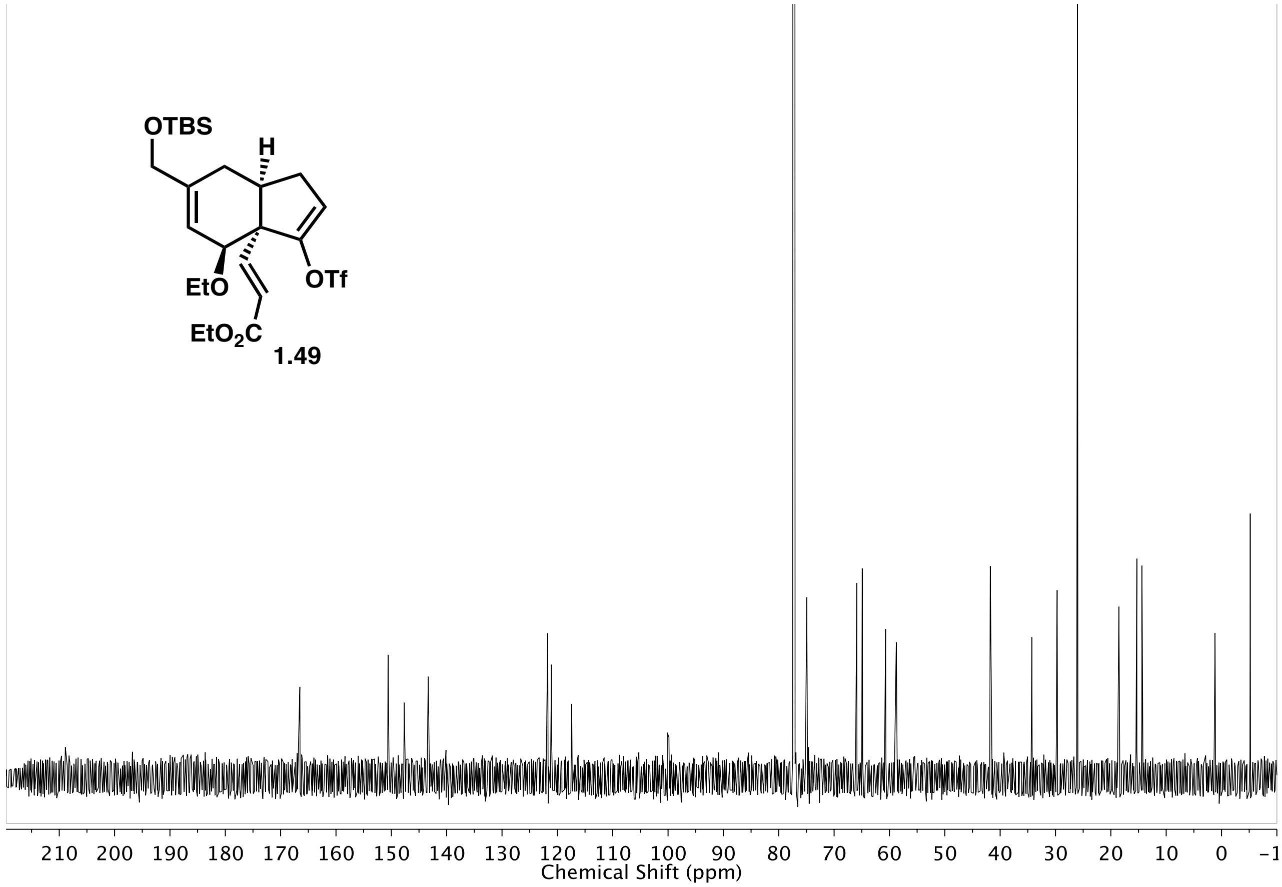

OTBS
H
OTf
EtO
EtO2C
1.49
210
200
190
180
170
160
150
140
130
120
110
100
90
80
70
60
50
40
30
20
10
0
−1
Chemical Shift (ppm)

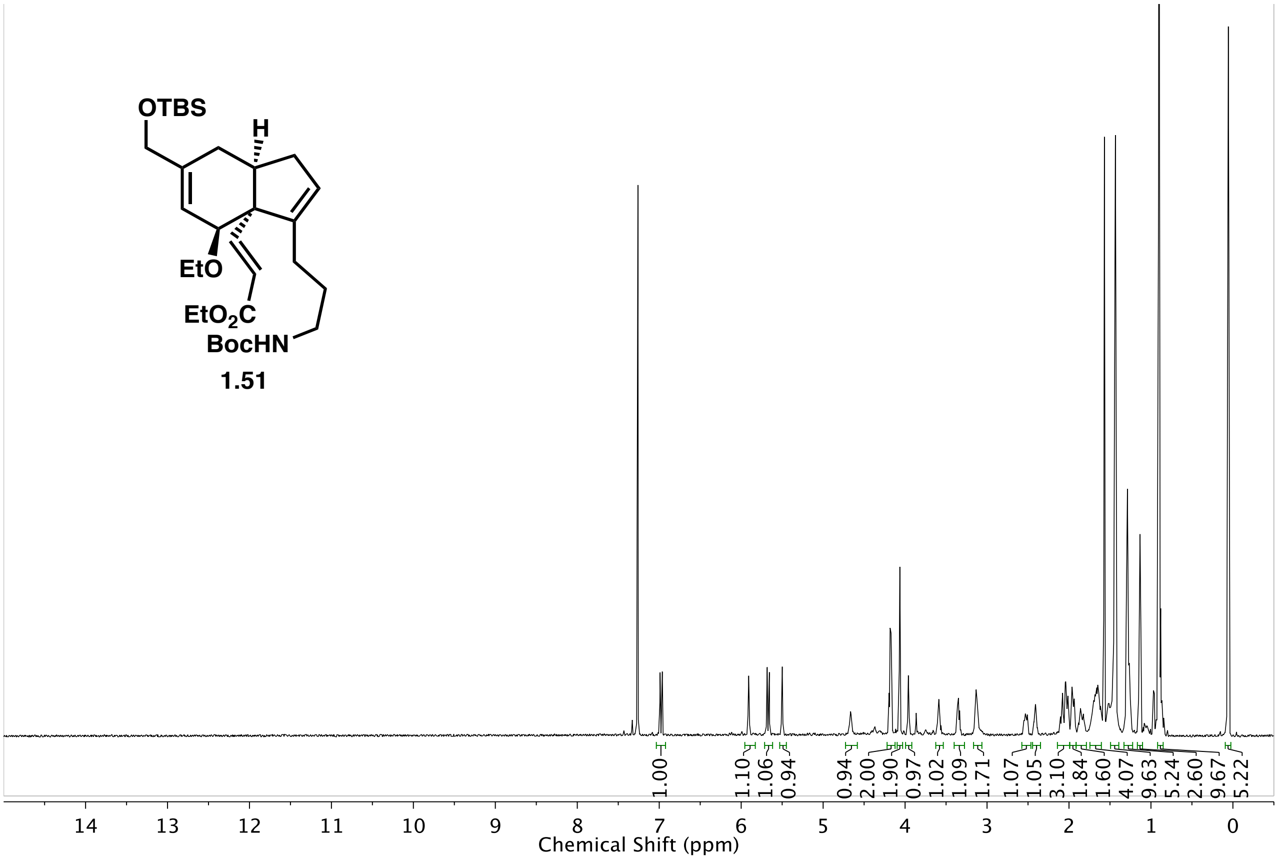
OTBS
H
EtO
EtO$_2$C
BocHN
1.51
1.00
1.10
1.06
0.94
0.94
2.00
1.90
0.97
1.02
1.09
1.71
1.07
1.05
3.10
1.84
1.60
4.07
9.63
5.24
2.60
9.67
5.22
14
13
12
11
10
9
8
7
6
5
4
3
2
1
0
Chemical Shift (ppm)

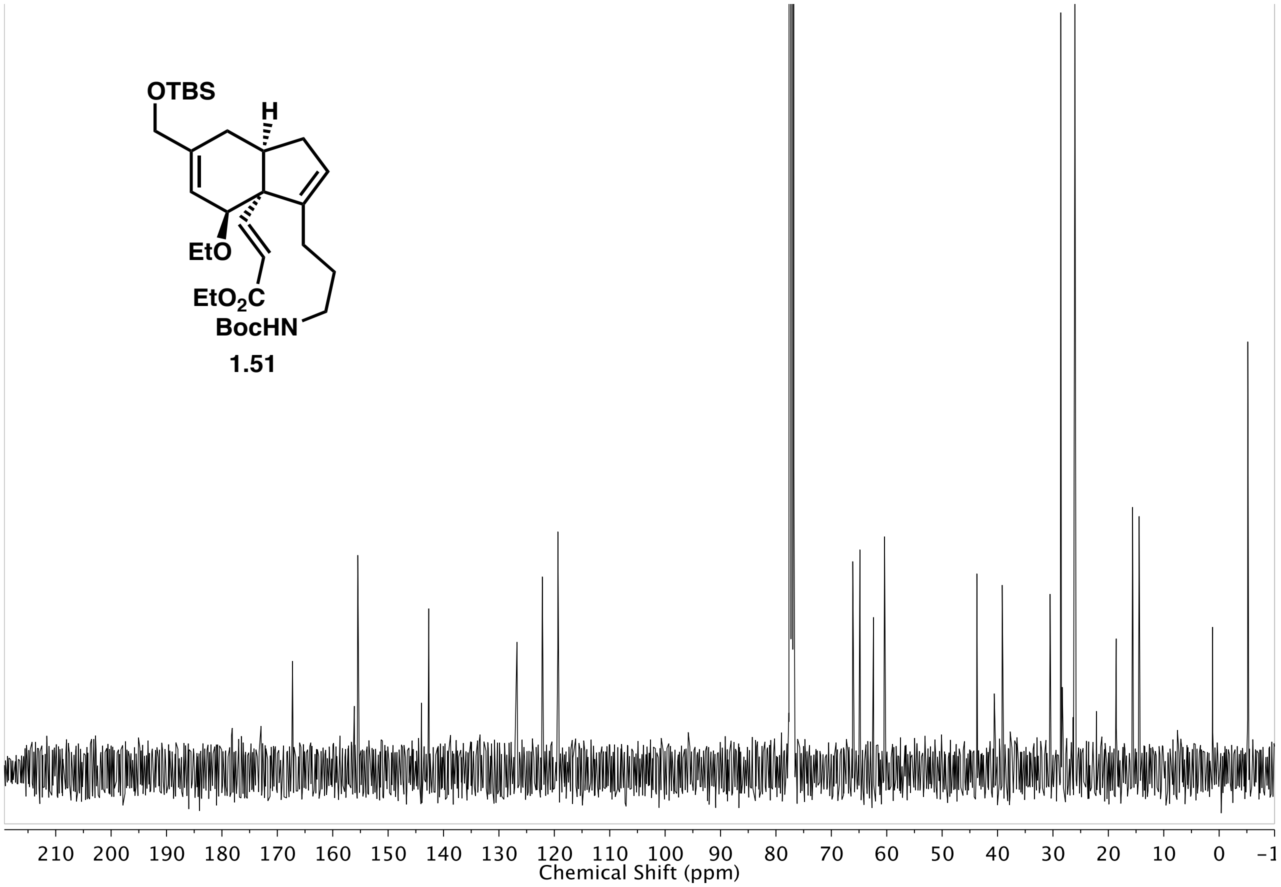
OTBS
H
EtO
EtO$_2$C
BocHN
1.51
210
200
190
180
170
160
150
140
130
120
110
100
90
80
70
60
50
40
30
20
10
0
−1
Chemical Shift (ppm)

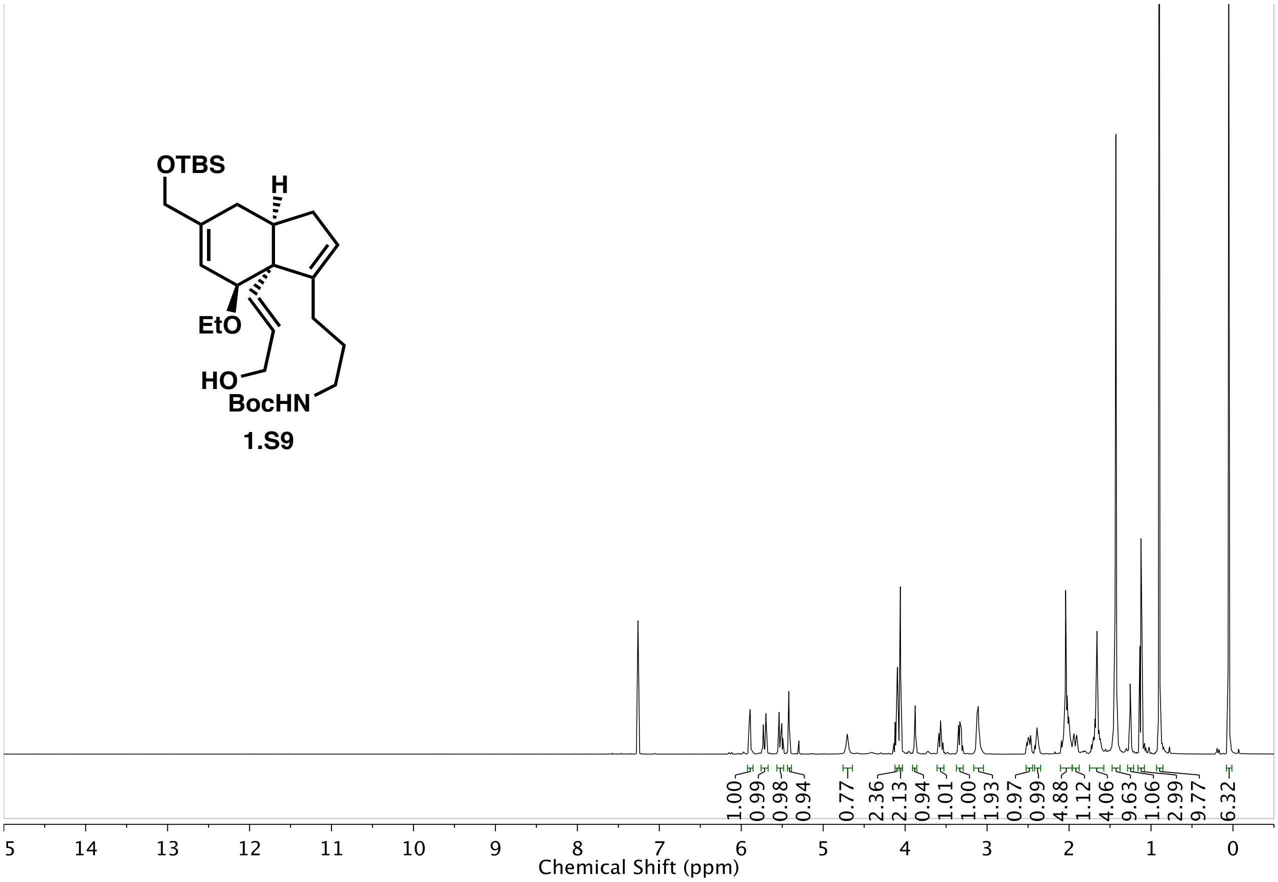
OTBS
H
EtO
HO
BocHN
1.S9
1.00
0.99
0.98
0.94
0.77
2.36
2.13
0.94
1.01
1.00
1.93
0.97
0.99
4.88
1.12
4.06
9.63
1.06
2.99
9.77
6.32
5
14
13
12
11
10
9
8
7
6
5
4
3
2
1
0
Chemical Shift (ppm)

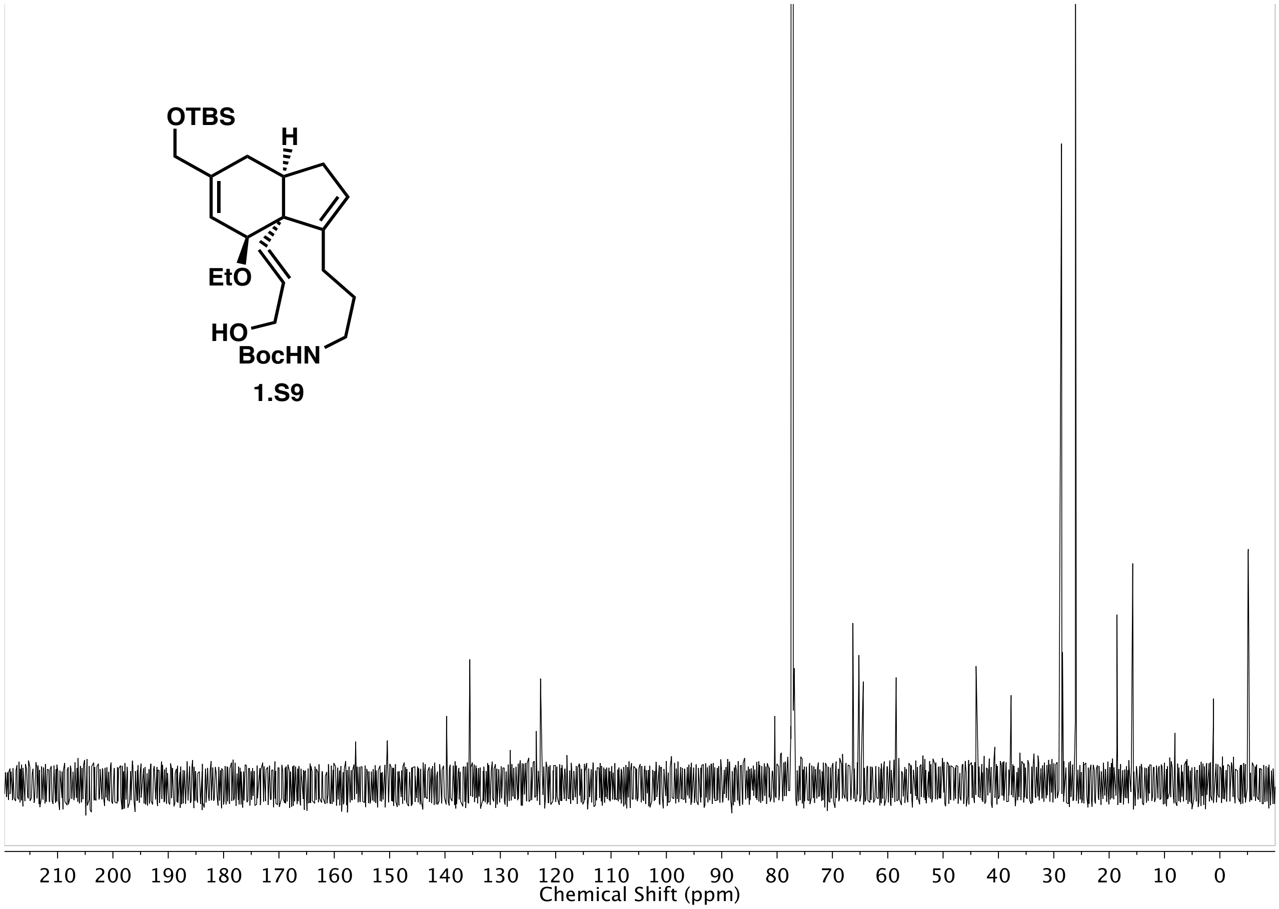
OTBS
H
EtO
HO
BocHN
1.S9
210
200
190
180
170
160
150
140
130
120
110
100
90
80
70
60
50
40
30
20
10
0
Chemical Shift (ppm)

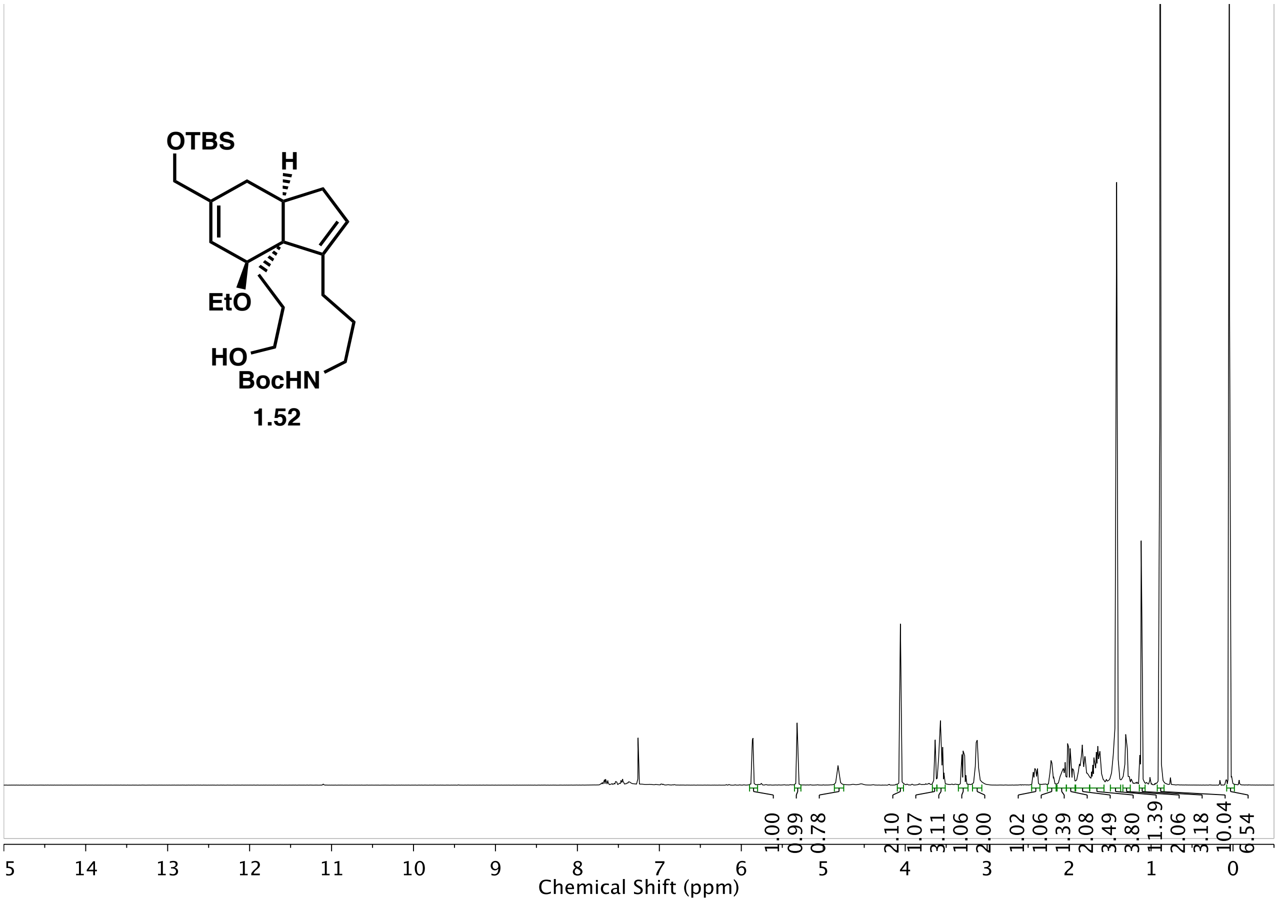
OTBS
H
EtO
HO
BocHN
1.52
1.00
0.99
0.78
2.10
1.07
3.11
1.06
2.00
1.02
1.06
1.39
2.08
3.49
3.80
11.39
2.06
2.06
3.18
10.04
6.54
5
14
13
12
11
10
9
8
7
6
5
4
3
2
1
0
Chemical Shift (ppm)

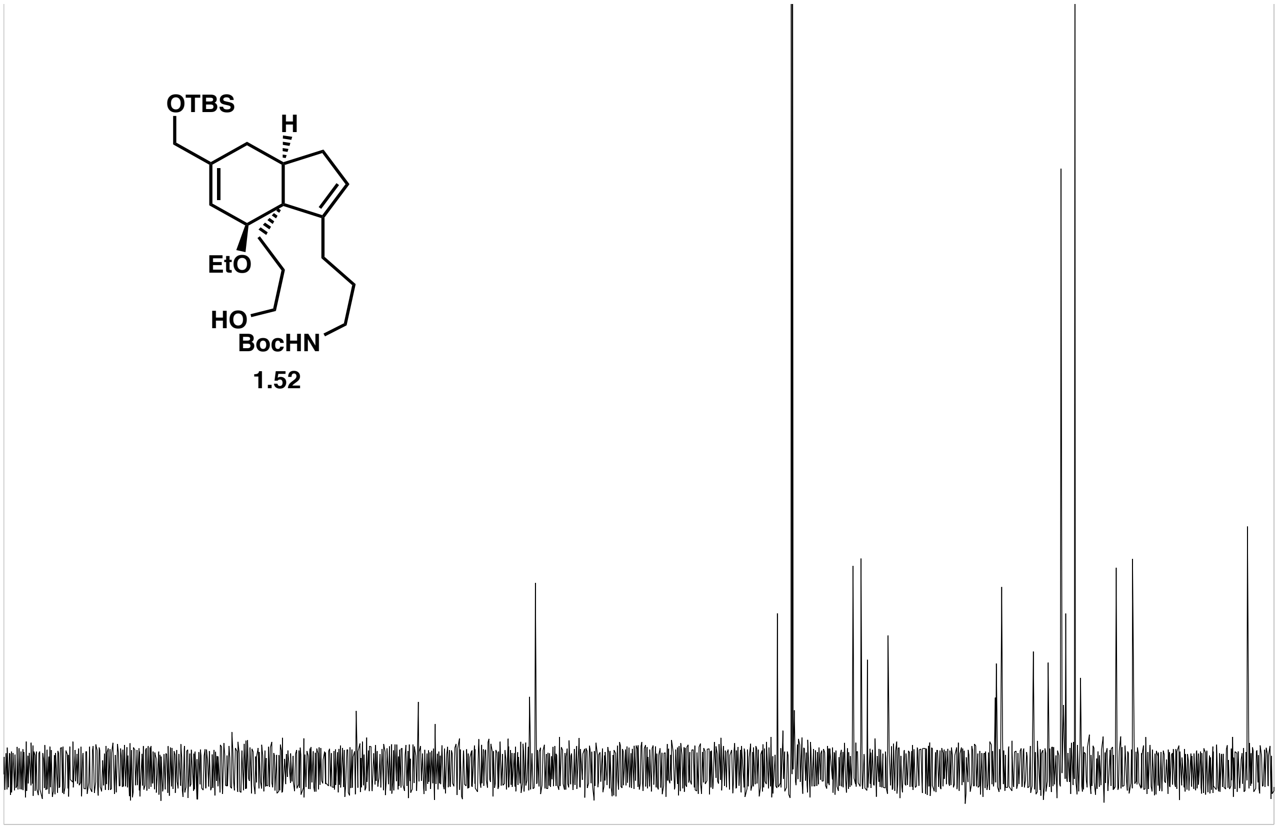
OTBS
H
EtO
HO
BocHN
1.52
20
210
200
190
180
170
160
150
140
130
120
110
100
90
80
70
60
50
40
30
20
10
0
–1
Chemical Shift (ppm)

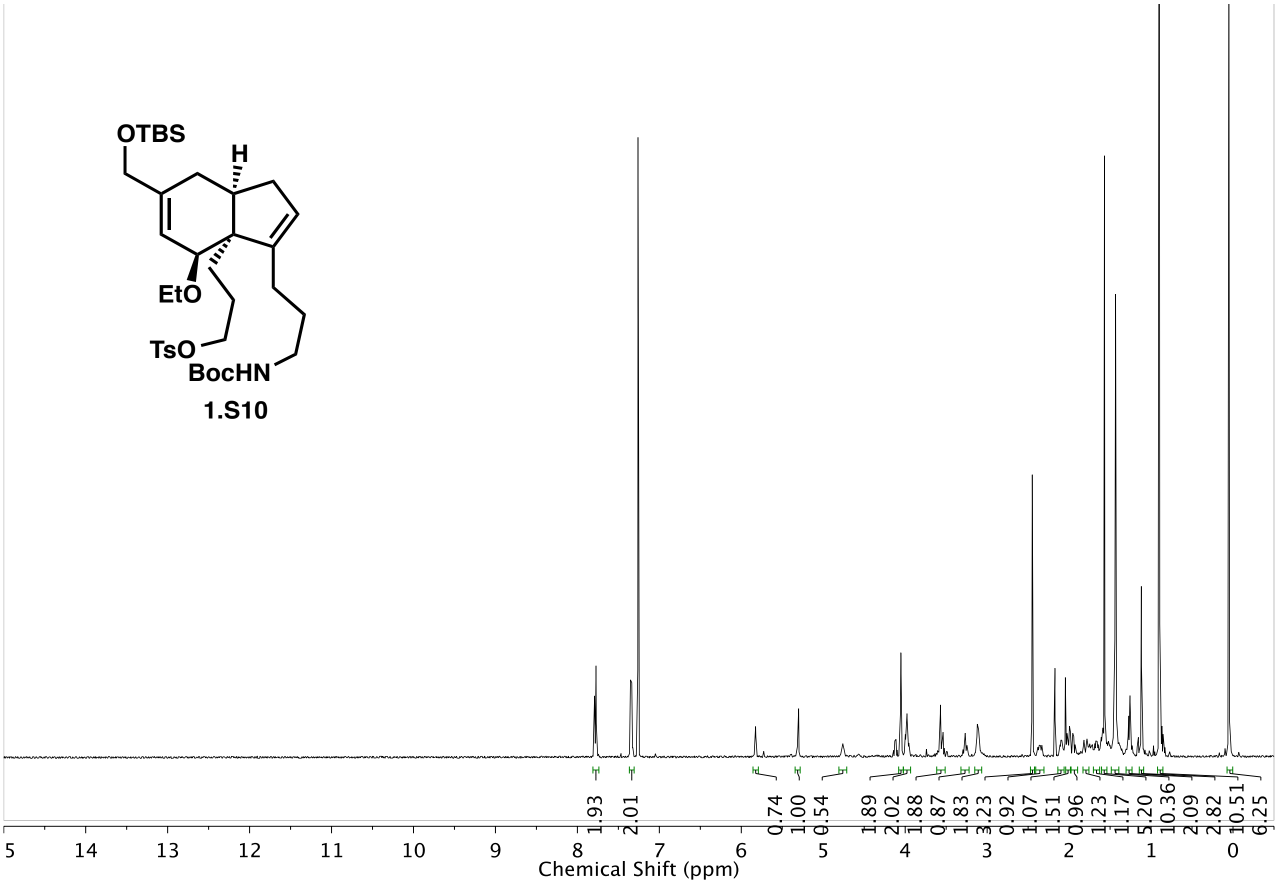
OTBS
H
EtO
TsO
BocHN
1.S10
1.93
2.01
0.74
1.00
0.54
1.89
2.02
1.88
0.87
1.83
3.23
0.92
1.07
1.51
0.96
1.23
1.17
5.20
10.36
2.09
2.82
10.51
6.25
5
14
13
12
11
10
9
8
7
6
5
4
3
2
1
0
Chemical Shift (ppm)

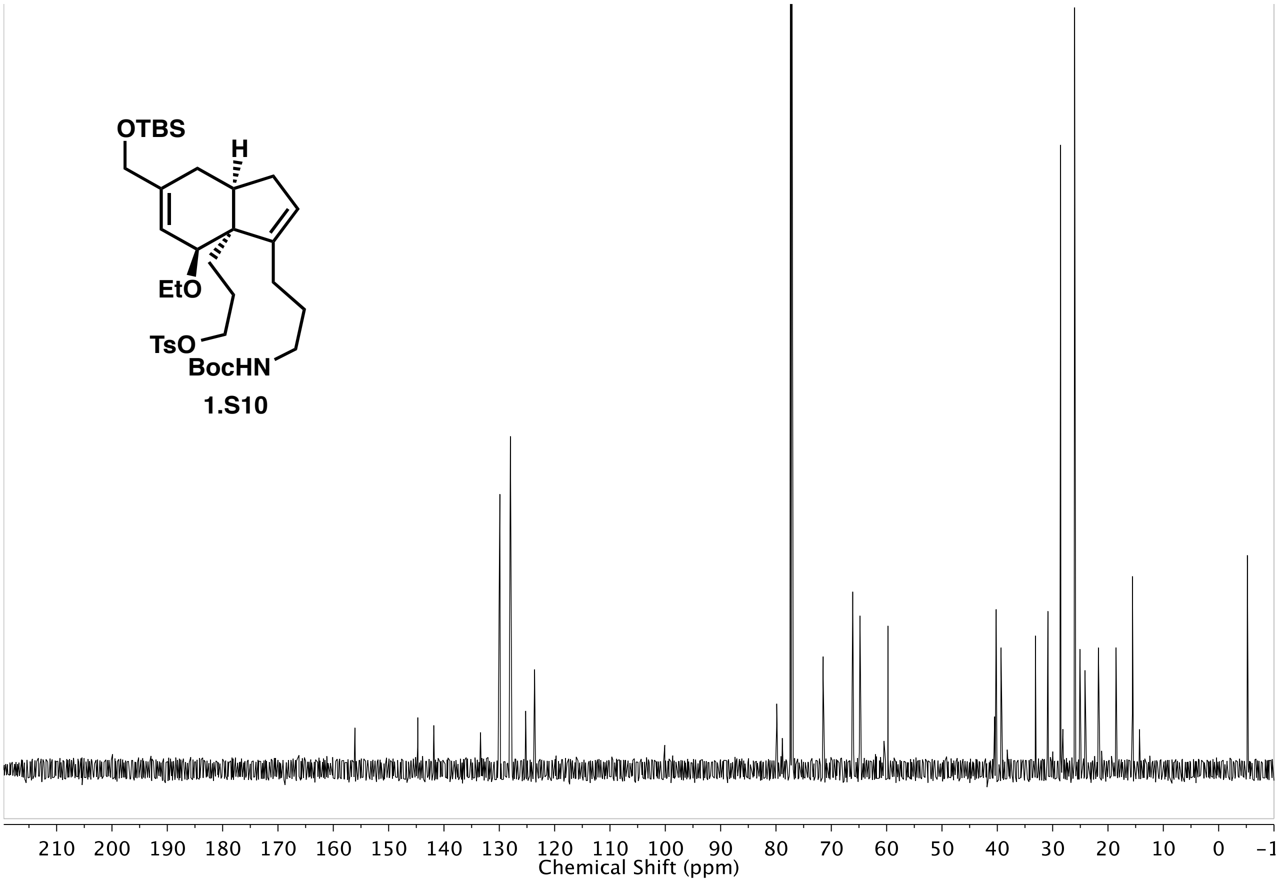
OTBS
H
EtO
TsO
BocHN
1.S10
210
200
190
180
170
160
150
140
130
120
110
100
90
80
70
60
50
40
30
20
10
0
−1
Chemical Shift (ppm)

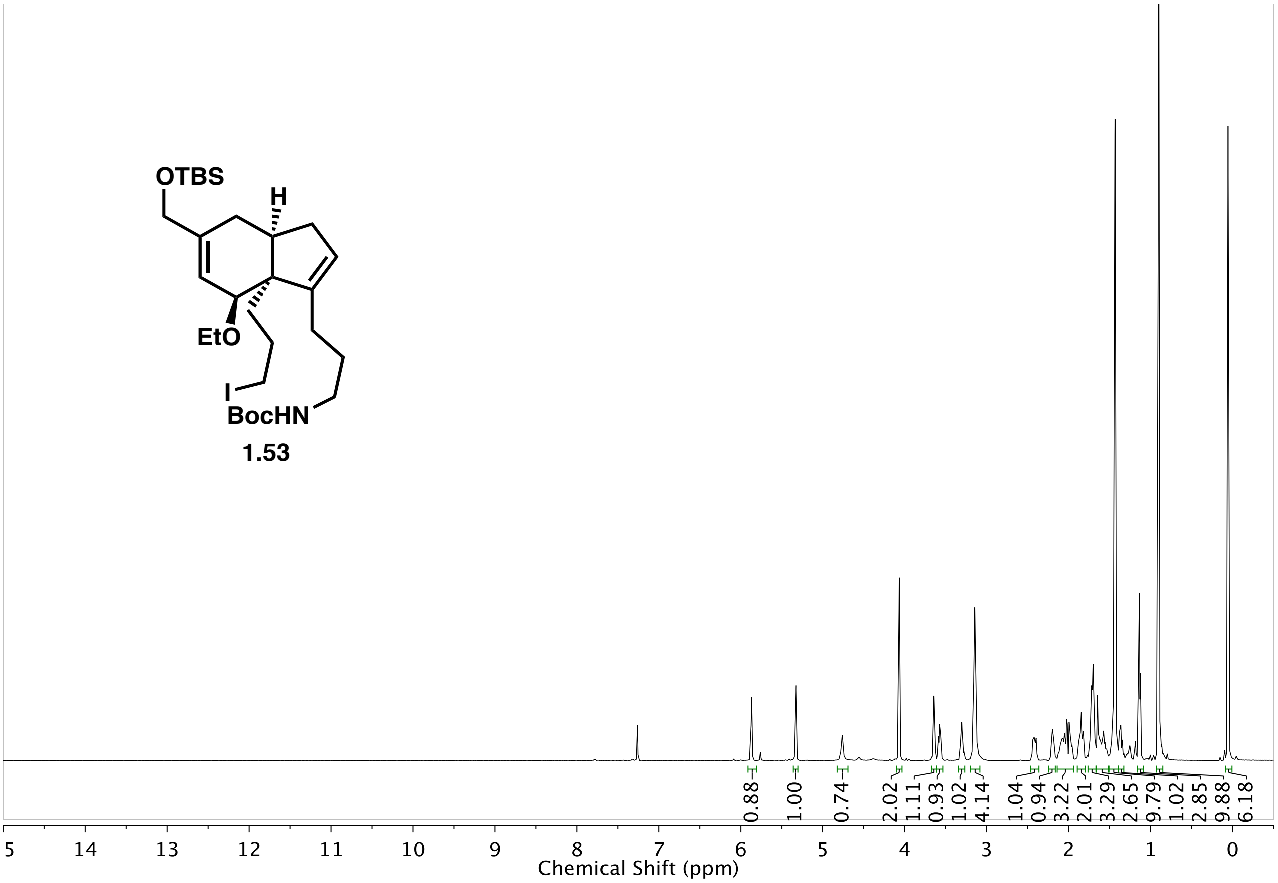
OTBS
H
EtO
I
BocHN
1.53
0.88
1.00
0.74
2.02
1.11
0.93
1.02
4.14
1.04
0.94
3.22
2.01
3.29
2.65
9.79
1.02
2.85
9.88
6.18
5
14
13
12
11
10
9
8
7
6
5
4
3
2
1
0
Chemical Shift (ppm)

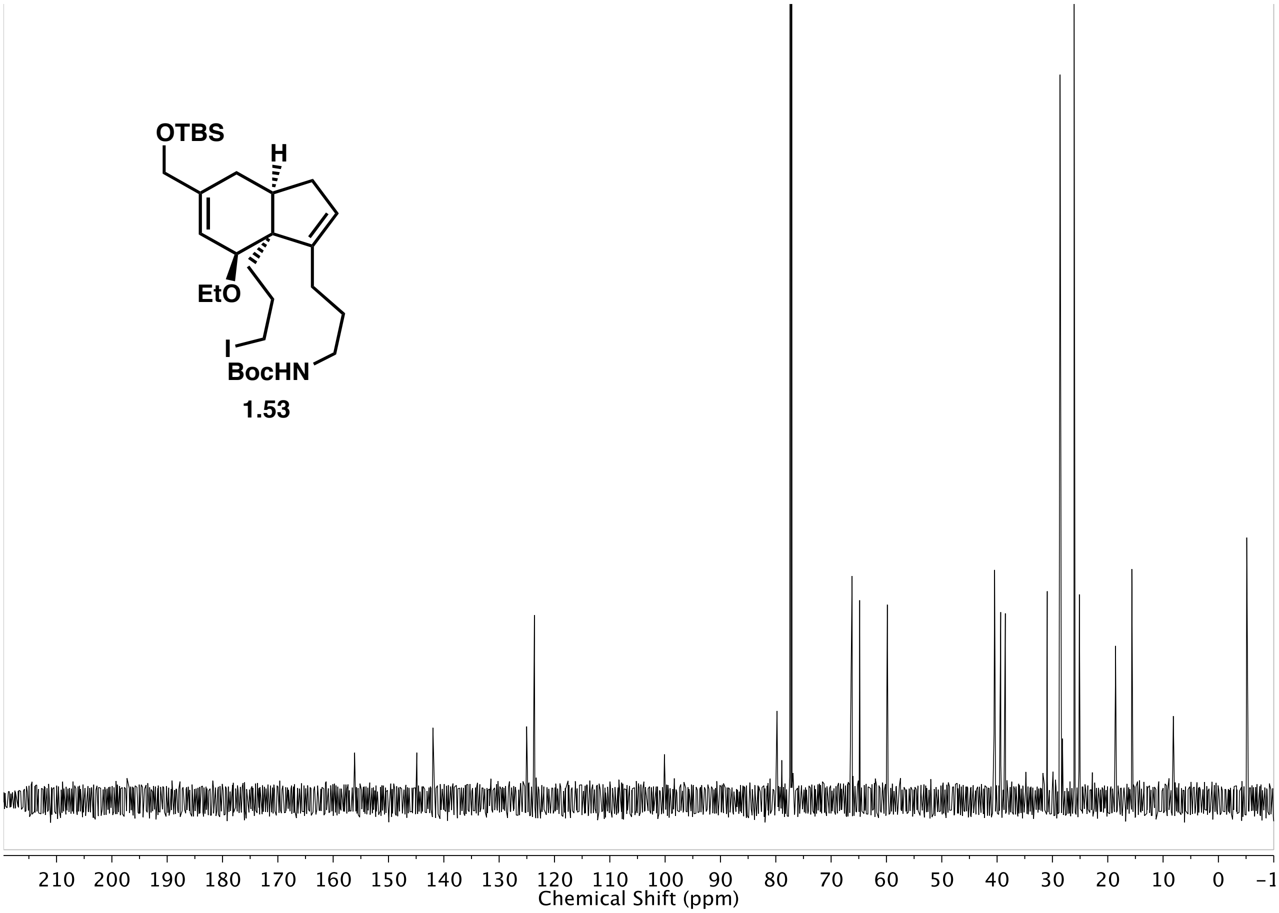
OTBS
H
EtO
I
BocHN
1.53
210
200
190
180
170
160
150
140
130
120
110
100
90
80
70
60
50
40
30
20
10
0
−1
Chemical Shift (ppm)

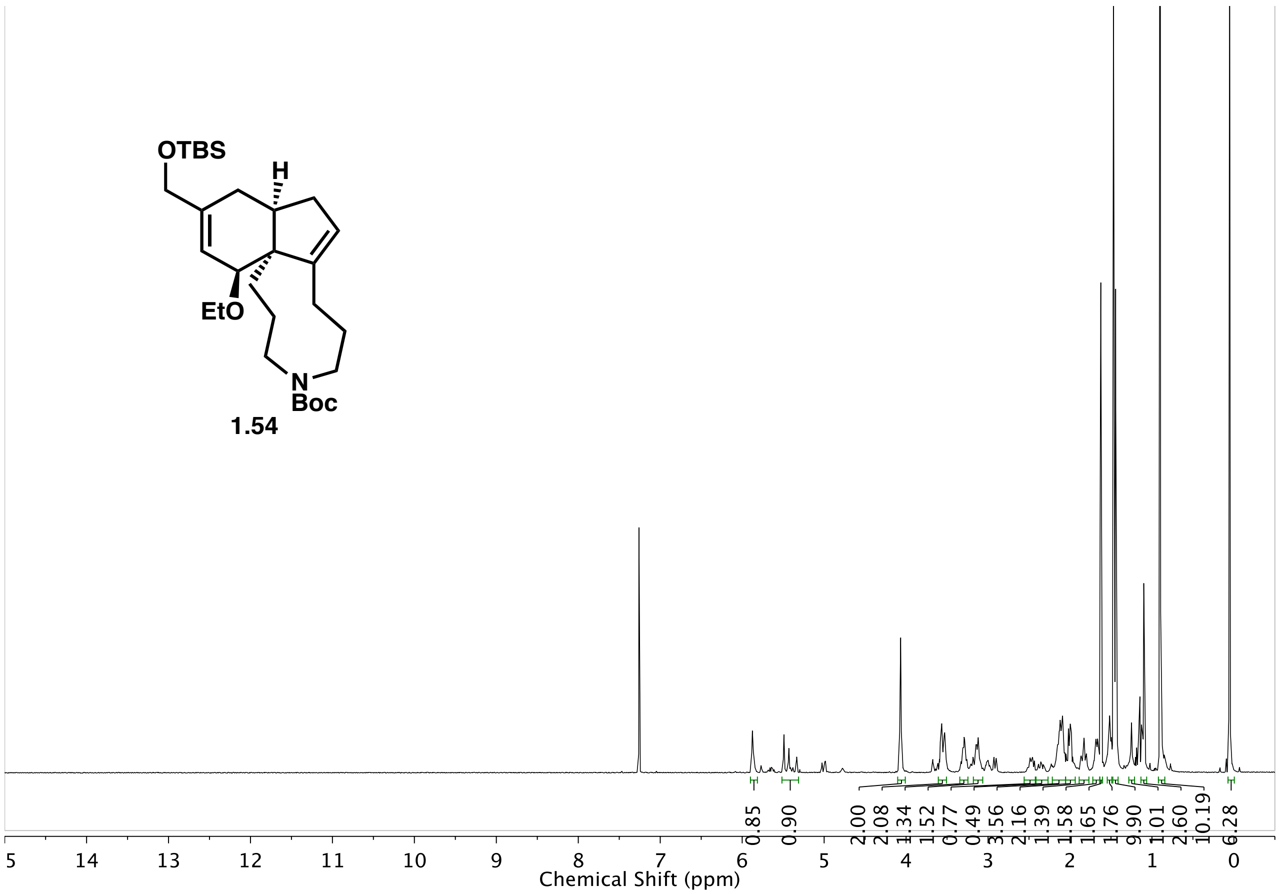
OTBS
H
EtO
N
Boc
1.54
0.85
0.90
2.00
2.08
1.34
1.52
0.77
0.49
3.56
2.16
1.39
1.58
1.65
1.76
9.90
1.01
2.60
10.19
6.28
5
14
13
12
11
10
9
8
7
6
5
4
3
2
1
0
Chemical Shift (ppm)

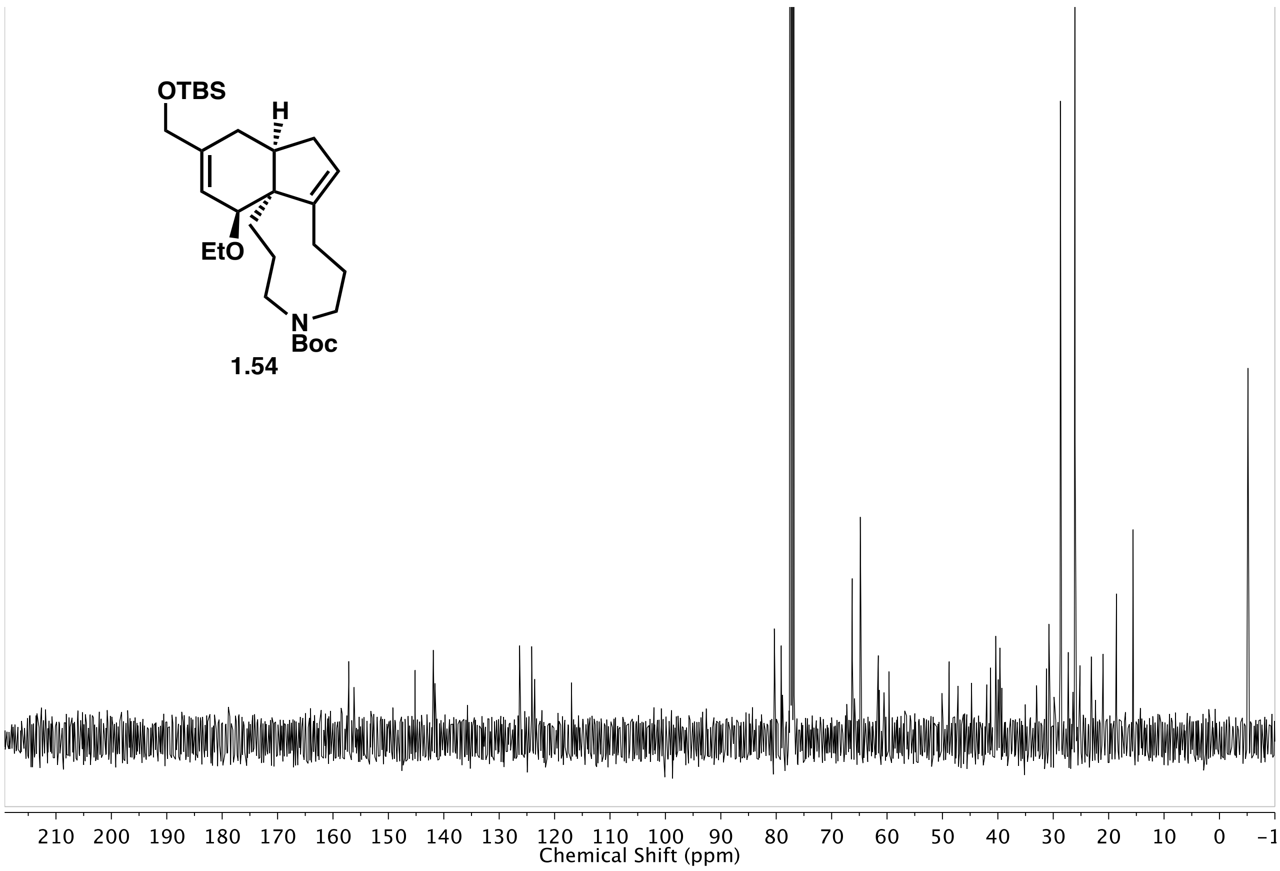
OTBS
H
EtO
N
Boc
1.54
210
200
190
180
170
160
150
140
130
120
110
100
90
80
70
60
50
40
30
20
10
0
–1
Chemical Shift (ppm)

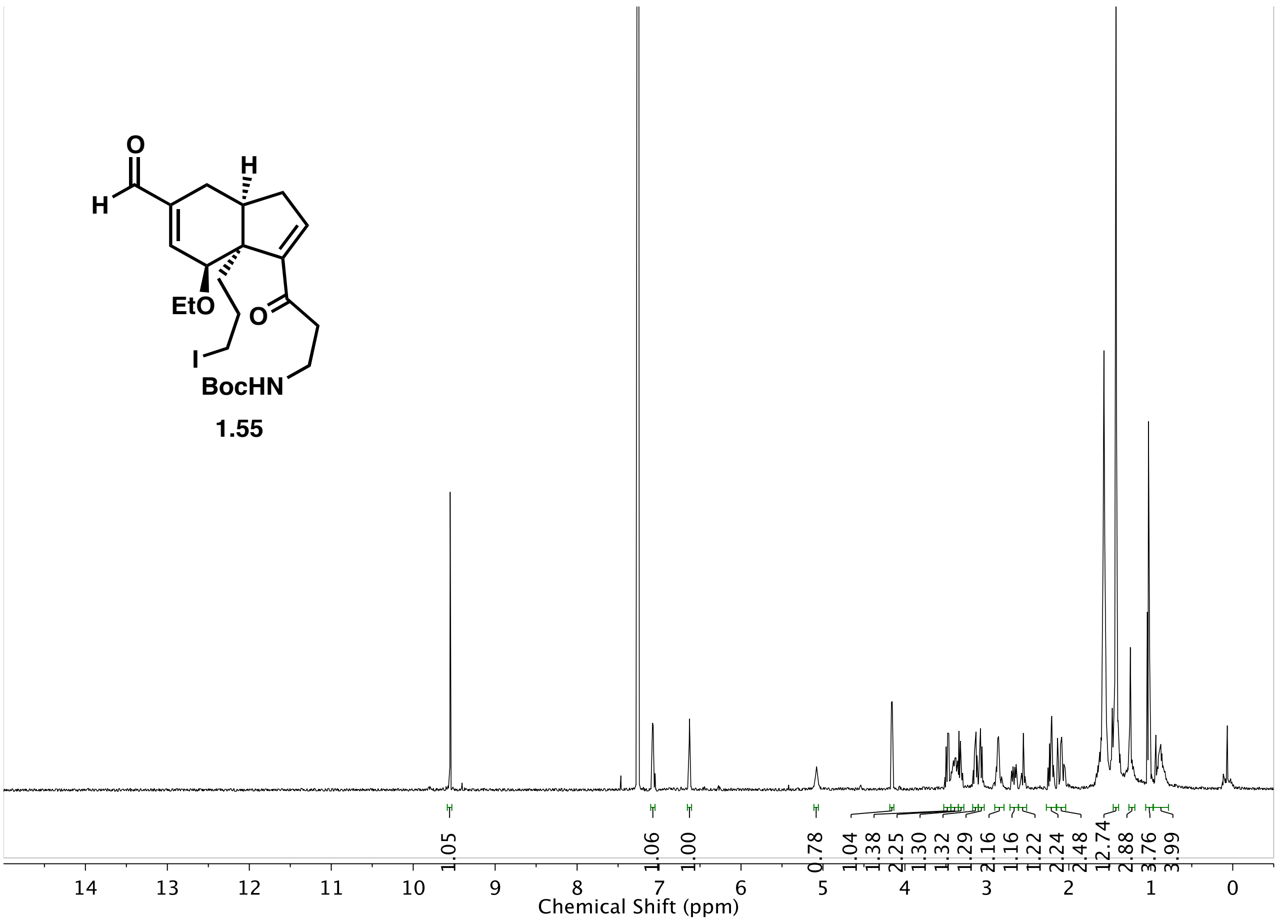
O
H
H
EtO
O
I
BocHN
1.55
1.05
1.06
1.00
0.78
1.04
1.38
2.25
1.30
1.32
1.29
2.16
1.16
1.22
2.24
2.48
12.74
2.88
3.76
3.99
14
13
12
11
10
9
8
7
6
5
4
3
2
1
0
Chemical Shift (ppm)

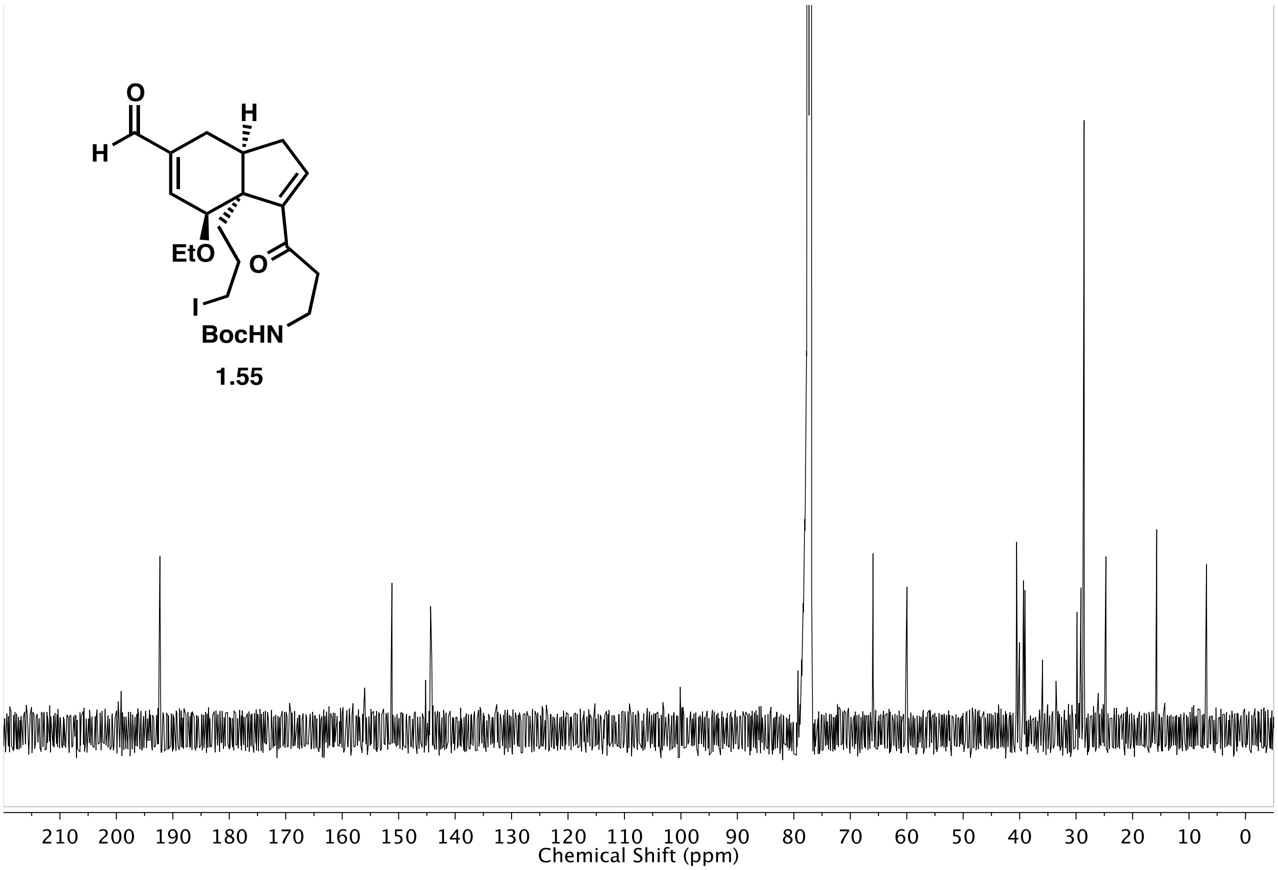
O
H
H
EtO
O
I
BocHN
1.55
210
200
190
180
170
160
150
140
130
120
110
100
90
80
70
60
50
40
30
20
10
0
Chemical Shift (ppm)

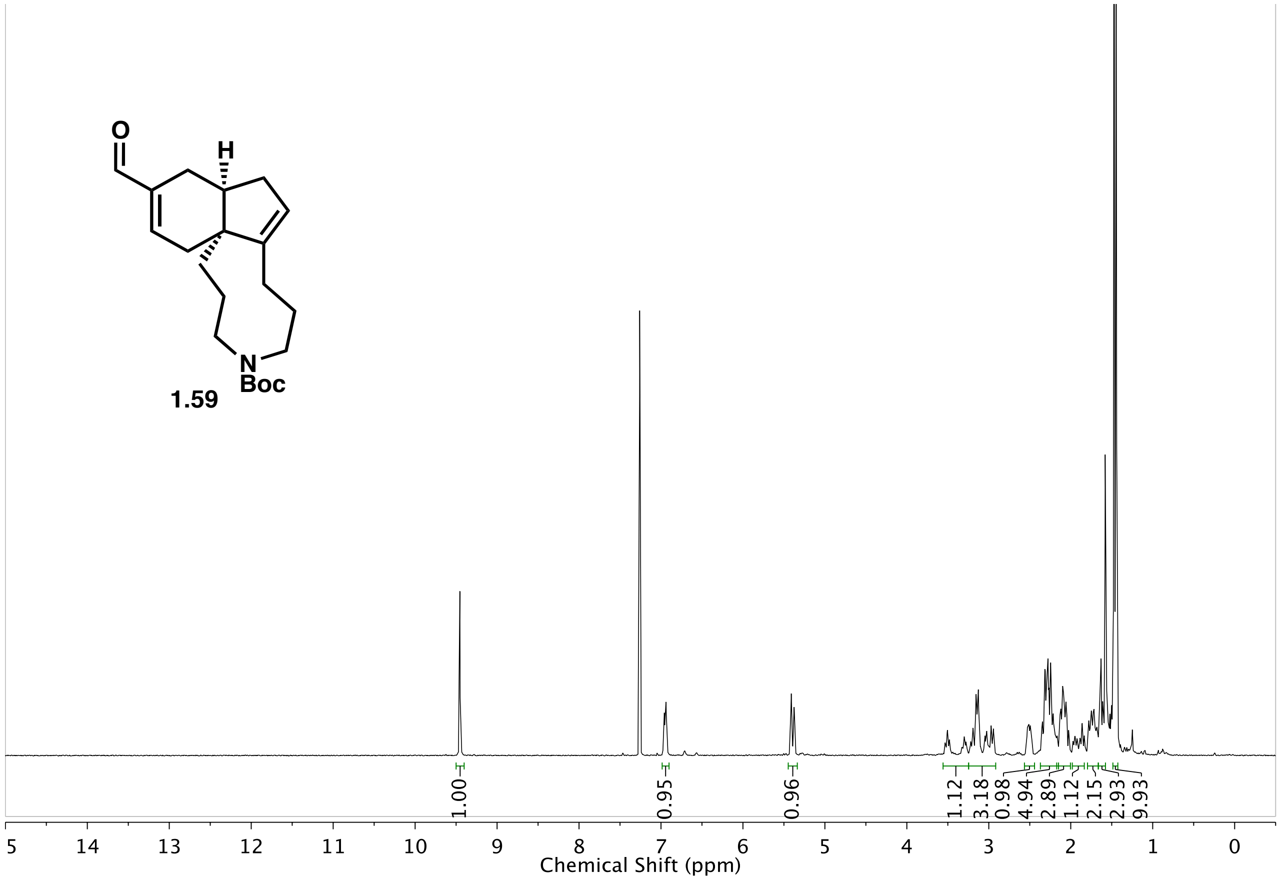
O
H
N
Boc
1.59
1.00
0.95
0.96
1.12
3.18
0.98
4.94
2.89
1.12
2.15
2.93
9.93
5
14
13
12
11
10
9
8
7
6
5
4
3
2
1
0
Chemical Shift (ppm)

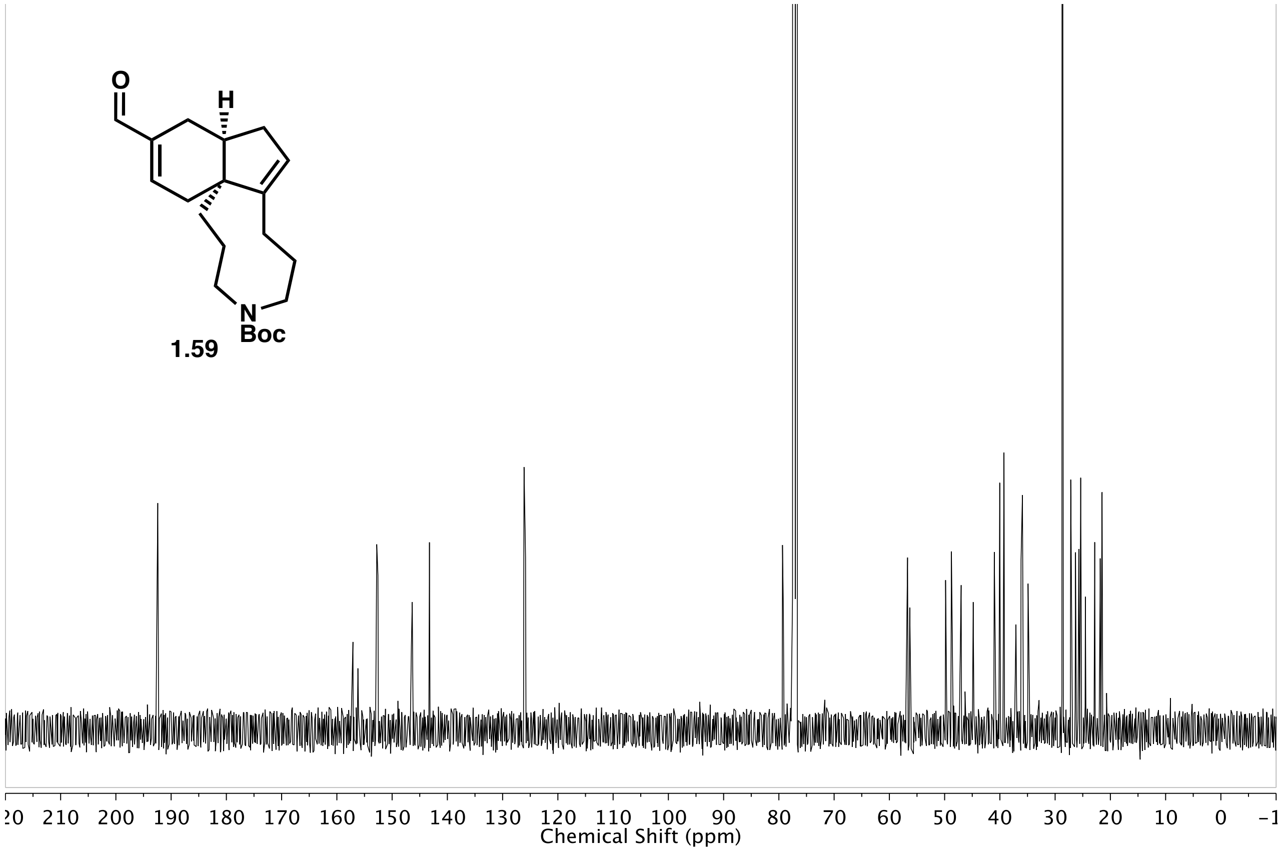
O
H
N
Boc
1.59
20
210
200
190
180
170
160
150
140
130
120
110
100
90
80
70
60
50
40
30
20
10
0
–1
Chemical Shift (ppm)

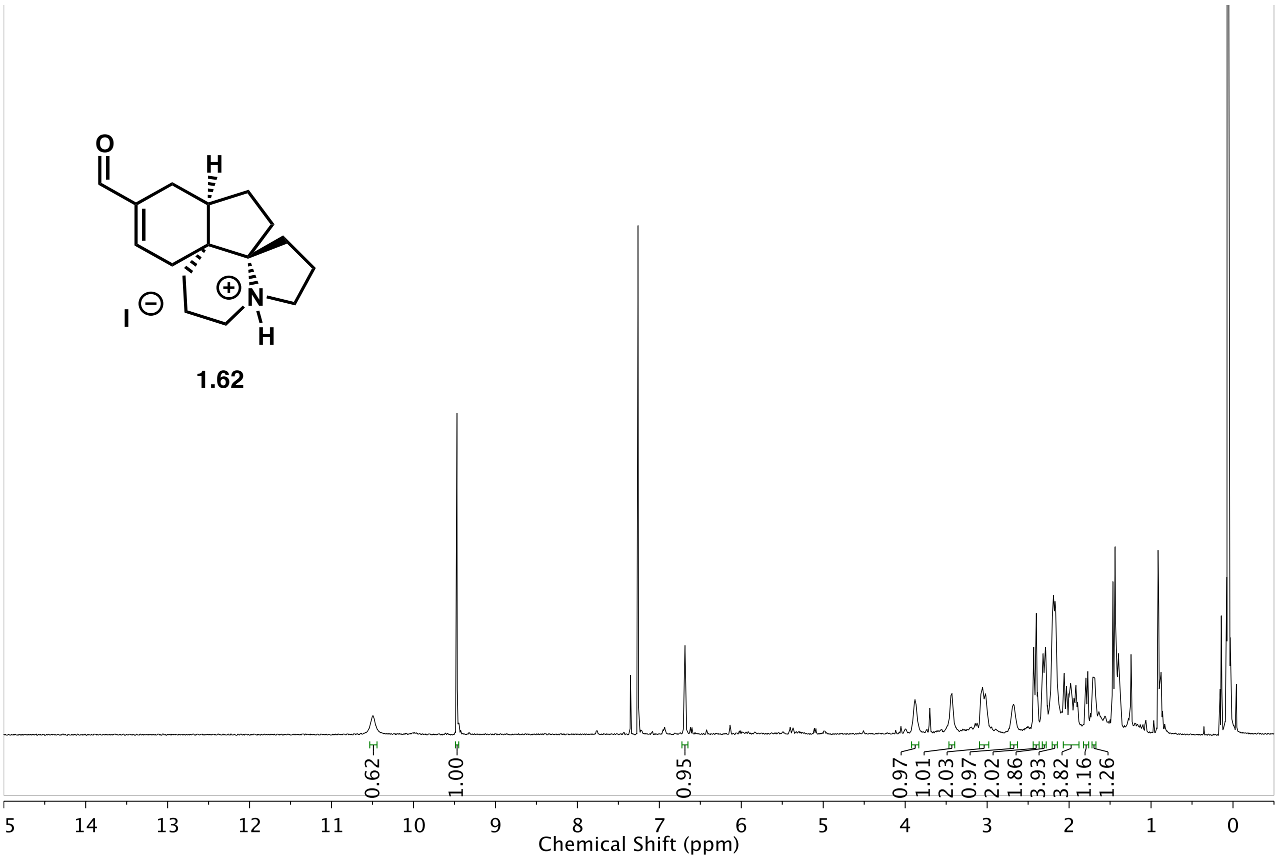
O
H
I ⊖
⊕ N
H
1.62
0.62
1.00
0.95
0.97
1.01
2.03
0.97
2.02
1.86
3.93
3.82
1.16
1.26
5
14
13
12
11
10
9
8
7
6
5
4
3
2
1
0
Chemical Shift (ppm)

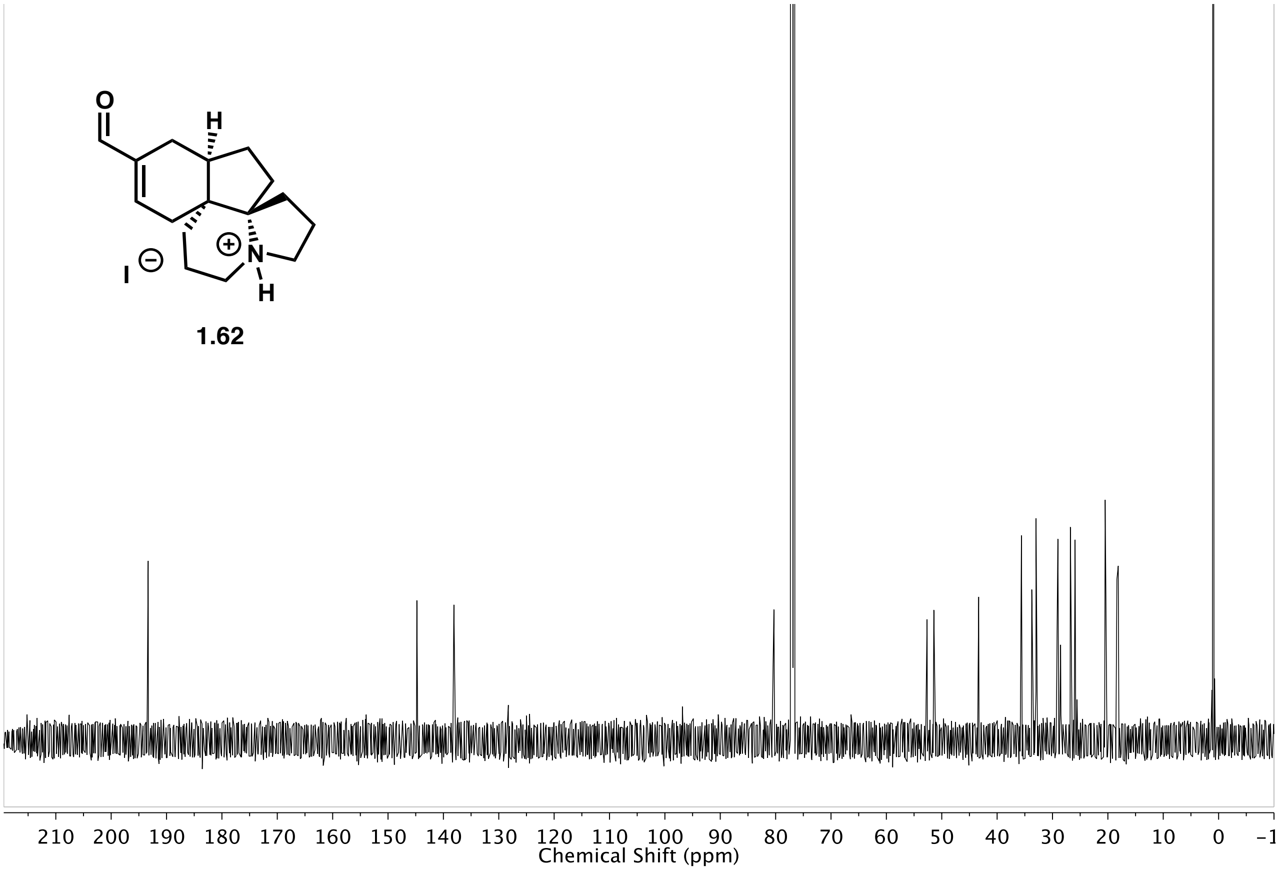
O
H
I ⊖
⊕ N
H
1.62
210
200
190
180
170
160
150
140
130
120
110
100
90
80
70
60
50
40
30
20
10
0
–1
Chemical Shift (ppm)

X-ray Crystallographic Analysis of Tetracycle 1.62

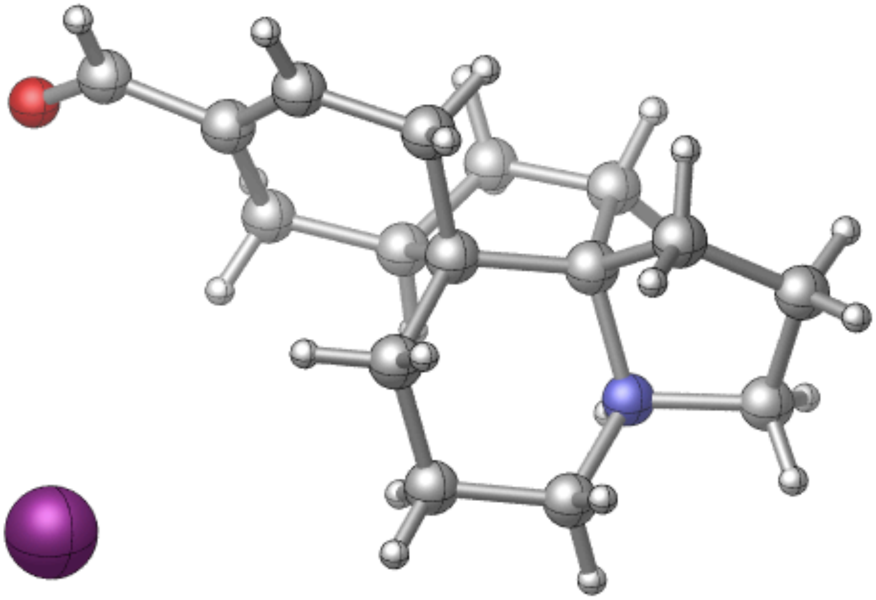

Crystal data and Structure Refinement for tetracycle 1.62

A colorless prism 0.030 x 0.020 x 0.020 mm in size was mounted on a Cryoloop with Paratone oil. Data were collected in a nitrogen gas stream at 100(2) K using phi and omega scans. Crystal-to-detector distance was 40 mm and exposure time was 10 seconds per frame using a scan width of 0.5°. Data collection was 99.9% complete to 25.000° in q. A total of 12675 reflections were collected covering the indices, -8<=*h*<=8, -16<=*k*<=16, -9<=*l*<=9. 2796 reflections were found to be symmetry independent, with an R_{int} of 0.0229. Indexing and unit cell refinement indicated a primitive, monoclinic lattice. The space group was found to be P 21 (No. 4). The data were integrated using the Bruker SAINT software program and scaled using the SADABS software program. Solution by iterative methods (DIRDIF-2008) produced a complete heavy-atom phasing model consistent with the proposed structure All non-hydrogen atoms were refined anisotropically by full-matrix least-squares (SHELXL-2013). All hydrogen atoms were placed using a riding model. Their positions were constrained relative to their parent atom using the appropriate HFIX command in SHELXL-2013. Absolute stereochemistry was unambiguously determined to be *R* at N1, C8, and C11, and *S* at C1, respectively.

Table 1. Crystal data and structure refinement for **1.62**.

X-ray ID	sarpong72	
Sample/notebook ID	RMXIV-009	
Empirical formula	C16 H24 I N O	
Formula weight	373.26	
Temperature	100(2) K	
Wavelength	0.71073 Å	
Crystal system	Monoclinic	
Space group	P 21	
Unit cell dimensions	a = 7.4235(4) Å	a= 90°.
	b = 13.9192(8) Å	b= 97.699(2)°.
	c = 7.6105(5) Å	g = 90°.
Volume	779.30(8) $Å^3$	
Z	2	
Density (calculated)	1.591 Mg/m^3	
Absorption coefficient	2.048 mm^{-1}	
F(000)	376	
Crystal size	0.030 x 0.020 x 0.020 mm^3	
Crystal color/habit	colorless prism	
Theta range for data collection	2.701 to 25.371°.	
Index ranges	-8<=h<=8, -16<=k<=16, -9<=l<=9	
Reflections collected	12675	
Independent reflections	2796 [R(int) = 0.0229]	
Completeness to theta = 25.000°	99.9 %	
Absorption correction	Semi-empirical from equivalents	
Max. and min. transmission	0.929 and 0.873	
Refinement method	Full-matrix least-squares on F^2	
Data / restraints / parameters	2796 / 1 / 172	
Goodness-of-fit on F^2	1.119	
Final R indices [I>2sigma(I)]	R1 = 0.0179, wR2 = 0.0443	
R indices (all data)	R1 = 0.0183, wR2 = 0.0445	
Absolute structure parameter	-0.021(10)	
Extinction coefficient	n/a	
Largest diff. peak and hole	0.663 and -0.444 e.$Å^{-3}$	

Table 2. Atomic coordinates (x 10^4) and equivalent isotropic displacement parameters ($Å^2$x 10^3) for **20**. U(eq) is defined as one third of the trace of the orthogonalized U^{ij} tensor.

	x	y	z	U(eq)
C(1)	2233(6)	5124(3)	2245(6)	8(1)
C(2)	3818(6)	4644(3)	3405(6)	11(1)
C(3)	3423(6)	4490(3)	5305(6)	14(1)
C(4)	1730(6)	3882(3)	5293(6)	14(1)
C(5)	-1482(6)	3641(3)	3978(7)	15(1)
C(6)	-1684(6)	3303(4)	2043(7)	19(1)
C(7)	-8(6)	3691(3)	1314(6)	14(1)
C(8)	375(6)	4635(3)	2298(5)	10(1)
C(9)	-1024(6)	5435(3)	1696(6)	11(1)
C(10)	12(7)	6392(3)	1808(6)	12(1)
C(11)	1873(5)	6166(6)	2833(5)	9(1)
C(12)	3414(7)	6867(3)	2598(6)	12(1)
C(13)	4315(6)	6657(3)	973(6)	10(1)
C(14)	3954(5)	5877(3)	-38(6)	9(1)
C(15)	2600(6)	5133(3)	294(5)	10(1)
C(16)	5667(6)	7337(3)	488(6)	13(1)
N(1)	118(5)	4334(2)	4199(5)	10(1)
O(1)	6107(4)	8068(2)	1291(4)	18(1)
I(1)	8199(1)	6079(1)	6534(1)	18(1)

Table 3. Bond lengths [Å] and angles [°] for **1.62**.

C(1)-C(2)	1.527(6)
C(1)-C(8)	1.544(6)
C(1)-C(15)	1.545(6)
C(1)-C(11)	1.552(9)
C(2)-C(3)	1.528(6)
C(2)-H(2A)	0.9900
C(2)-H(2B)	0.9900
C(3)-C(4)	1.515(6)
C(3)-H(3A)	0.9900
C(3)-H(3B)	0.9900
C(4)-N(1)	1.502(5)
C(4)-H(4A)	0.9900
C(4)-H(4B)	0.9900
C(5)-N(1)	1.522(6)
C(5)-C(6)	1.534(7)
C(5)-H(5A)	0.9900
C(5)-H(5B)	0.9900
C(6)-C(7)	1.528(6)
C(6)-H(6A)	0.9900
C(6)-H(6B)	0.9900
C(7)-C(8)	1.519(6)
C(7)-H(7A)	0.9900
C(7)-H(7B)	0.9900
C(8)-N(1)	1.542(5)
C(8)-C(9)	1.550(6)
C(9)-C(10)	1.536(6)
C(9)-H(9A)	0.9900
C(9)-H(9B)	0.9900
C(10)-C(11)	1.525(6)
C(10)-H(10A)	0.9900
C(10)-H(10B)	0.9900
C(11)-C(12)	1.532(8)
C(11)-H(11)	1.0000
C(12)-C(13)	1.511(6)
C(12)-H(12A)	0.9900
C(12)-H(12B)	0.9900
C(13)-C(14)	1.337(6)
C(13)-C(16)	1.462(6)
C(14)-C(15)	1.489(6)
C(14)-H(14)	0.9500
C(15)-H(15A)	0.9900
C(15)-H(15B)	0.9900
C(16)-O(1)	1.210(5)
C(16)-H(16)	0.9500
N(1)-H(1)	1.0000

C(2)-C(1)-C(8)	114.4(3)
C(2)-C(1)-C(15)	109.7(3)
C(8)-C(1)-C(15)	107.6(3)
C(2)-C(1)-C(11)	113.1(4)
C(8)-C(1)-C(11)	102.5(3)
C(15)-C(1)-C(11)	109.2(3)
C(1)-C(2)-C(3)	112.2(3)
C(1)-C(2)-H(2A)	109.2
C(3)-C(2)-H(2A)	109.2
C(1)-C(2)-H(2B)	109.2
C(3)-C(2)-H(2B)	109.2
H(2A)-C(2)-H(2B)	107.9
C(4)-C(3)-C(2)	109.7(4)
C(4)-C(3)-H(3A)	109.7
C(2)-C(3)-H(3A)	109.7
C(4)-C(3)-H(3B)	109.7
C(2)-C(3)-H(3B)	109.7
H(3A)-C(3)-H(3B)	108.2
N(1)-C(4)-C(3)	111.6(4)
N(1)-C(4)-H(4A)	109.3

C(3)-C(4)-H(4A)	109.3
N(1)-C(4)-H(4B)	109.3
C(3)-C(4)-H(4B)	109.3
H(4A)-C(4)-H(4B)	108.0
N(1)-C(5)-C(6)	106.0(4)
N(1)-C(5)-H(5A)	110.5
C(6)-C(5)-H(5A)	110.5
N(1)-C(5)-H(5B)	110.5
C(6)-C(5)-H(5B)	110.5
H(5A)-C(5)-H(5B)	108.7
C(7)-C(6)-C(5)	105.1(4)
C(7)-C(6)-H(6A)	110.7
C(5)-C(6)-H(6A)	110.7
C(7)-C(6)-H(6B)	110.7
C(5)-C(6)-H(6B)	110.7
H(6A)-C(6)-H(6B)	108.8
C(8)-C(7)-C(6)	103.6(4)
C(8)-C(7)-H(7A)	111.0
C(6)-C(7)-H(7A)	111.0
C(8)-C(7)-H(7B)	111.0
C(6)-C(7)-H(7B)	111.0
H(7A)-C(7)-H(7B)	109.0
C(7)-C(8)-N(1)	100.9(3)
C(7)-C(8)-C(1)	118.5(4)
N(1)-C(8)-C(1)	111.6(3)
C(7)-C(8)-C(9)	113.7(4)
N(1)-C(8)-C(9)	108.0(3)
C(1)-C(8)-C(9)	103.9(3)
C(10)-C(9)-C(8)	107.2(3)
C(10)-C(9)-H(9A)	110.3
C(8)-C(9)-H(9A)	110.3
C(10)-C(9)-H(9B)	110.3
C(8)-C(9)-H(9B)	110.3
H(9A)-C(9)-H(9B)	108.5
C(11)-C(10)-C(9)	105.2(4)
C(11)-C(10)-H(10A)	110.7
C(9)-C(10)-H(10A)	110.7
C(11)-C(10)-H(10B)	110.7
C(9)-C(10)-H(10B)	110.7
H(10A)-C(10)-H(10B)	108.8
C(10)-C(11)-C(12)	116.6(5)
C(10)-C(11)-C(1)	103.0(4)
C(12)-C(11)-C(1)	113.6(4)
C(10)-C(11)-H(11)	107.7
C(12)-C(11)-H(11)	107.7
C(1)-C(11)-H(11)	107.7
C(13)-C(12)-C(11)	113.1(4)
C(13)-C(12)-H(12A)	109.0
C(11)-C(12)-H(12A)	109.0
C(13)-C(12)-H(12B)	109.0
C(11)-C(12)-H(12B)	109.0
H(12A)-C(12)-H(12B)	107.8
C(14)-C(13)-C(16)	118.1(4)
C(14)-C(13)-C(12)	123.4(4)
C(16)-C(13)-C(12)	118.4(4)
C(13)-C(14)-C(15)	123.7(4)
C(13)-C(14)-H(14)	118.1
C(15)-C(14)-H(14)	118.1
C(14)-C(15)-C(1)	112.3(3)
C(14)-C(15)-H(15A)	109.2
C(1)-C(15)-H(15A)	109.2
C(14)-C(15)-H(15B)	109.2
C(1)-C(15)-H(15B)	109.2
H(15A)-C(15)-H(15B)	107.9
O(1)-C(16)-C(13)	124.4(4)
O(1)-C(16)-H(16)	117.8
C(13)-C(16)-H(16)	117.8
C(4)-N(1)-C(5)	110.3(3)
C(4)-N(1)-C(8)	116.4(3)
C(5)-N(1)-C(8)	105.1(3)
C(4)-N(1)-H(1)	108.2
C(5)-N(1)-H(1)	108.2
C(8)-N(1)-H(1)	108.2

Table 4. Anisotropic displacement parameters ($Å^2$x 10^3) for **1.62**. The anisotropic displacement factor exponent takes the form: -2p^2[h^2 a*^{2}U^{11} + ... + 2 h k a* b* U^{12}]

	U^{11}	U^{22}	U^{33}	U^{23}	U^{13}	U^{12}
C(1)	4(2)	9(2)	10(2)	0(2)	-2(2)	1(2)
C(2)	5(2)	13(2)	16(2)	3(2)	0(2)	1(2)
C(3)	8(2)	18(2)	14(2)	7(2)	-6(2)	1(2)
C(4)	11(2)	13(2)	15(3)	7(2)	-4(2)	1(2)
C(5)	8(2)	13(2)	23(3)	5(2)	-4(2)	-4(2)
C(6)	12(2)	17(2)	27(3)	-1(2)	-1(2)	-8(2)
C(7)	12(2)	15(2)	16(2)	-3(2)	0(2)	-3(2)
C(8)	8(2)	12(2)	7(2)	1(2)	0(2)	0(2)
C(9)	9(2)	15(2)	10(2)	2(2)	1(2)	2(2)
C(10)	13(2)	11(2)	12(2)	0(2)	4(2)	3(2)
C(11)	12(2)	7(3)	7(2)	-3(2)	1(1)	4(2)
C(12)	15(2)	12(2)	10(2)	-2(2)	3(2)	-4(2)
C(13)	5(2)	12(2)	12(2)	4(2)	-1(2)	1(2)
C(14)	6(2)	10(4)	10(2)	1(2)	0(2)	6(2)
C(15)	13(2)	9(2)	10(2)	-3(2)	1(2)	2(2)
C(16)	9(2)	17(2)	11(2)	5(2)	0(2)	2(2)
N(1)	6(2)	10(2)	13(2)	3(1)	-1(1)	-2(1)
O(1)	20(2)	15(2)	19(2)	0(1)	2(1)	-7(1)
I(1)	22(1)	18(1)	14(1)	-4(1)	5(1)	0(1)

Table 5. Hydrogen coordinates (x 10^4) and isotropic displacement parameters (Å^{2}x 10 ^{3}) for **1.62**.

	x	y	z	U(eq)
H(2A)	4917	5048	3423	13
H(2B)	4072	4015	2882	13
H(3A)	4468	4166	6006	17
H(3B)	3244	5119	5865	17
H(4A)	1948	3238	4808	16
H(4B)	1465	3797	6525	16
H(5A)	-2603	3968	4230	18
H(5B)	-1242	3089	4795	18
H(6A)	-1723	2593	1977	23
H(6B)	-2811	3563	1367	23
H(7A)	1031	3244	1565	17
H(7B)	-262	3798	19	17
H(9A)	-1599	5316	465	14
H(9B)	-1988	5449	2478	14
H(10A)	135	6636	608	14
H(10B)	-628	6881	2441	14
H(11)	1738	6149	4123	11
H(12A)	2921	7529	2511	14
H(12B)	4340	6836	3661	14
H(14)	4599	5793	-1024	11
H(15A)	3051	4494	-12	13
H(15B)	1445	5256	-486	13
H(16)	6239	7194	-526	15
H(1)	-240	4916	4840	12

Chapter 2: Hydrogen Iodide-Catalyzed Hydroamination and Hydroetherification of Unactivated Olefins

2.1: Hydroamination Overview

Hydroamination, the formation of a new C–N bond by the addition of an amine across an unsaturated C–C bond, has been a topic of great scientific interest. Notably, within the last 20 years, research into hydroamination has greatly intensified as shown by a dramatic increase in publications related to the topic.[1] Hydroamination has proved to be an efficient and atom-economical method for building nitrogen-containing heterocycles – compounds that are of great importance in pharmaceuticals as well as bulk and specialty chemicals.

This utility has spurred considerable research into hydroamination methodologies, but research has also been stimulated by the challenges that are inherent to these reactions. Hydroaminations are often thermoneutral or only slightly exothermic, usually have negative reaction entropies, and almost always have high activation barriers.[2] The latter observation arises from the interaction of an amine's lone pair of electrons with the electron-rich pi system of the olefin.[3] Additionally, a [2+2] cycloaddition between the sigma N–H bond and the pi C=C system is forbidden. Therefore, designing catalysts for hydroamination has become critically important, with fine-tuning of the thermodynamics of each step essential to achieving efficient reactivity. Furthermore, high reaction temperatures must be avoided; otherwise the negative reaction entropy can disfavor the reaction equilibrium.

In addition to these thermodynamic challenges, the control of regiochemistry is of critical importance. With the addition of an amine across an unsymmetrical olefin, both Markovnikov and anti-Markovnikov products are possible (Scheme 1).[4] Therefore, when designing a catalytic system, emphasis must be placed not only on efficiency, but also on achieving high selectivity for one of the constitutional isomers over the other.

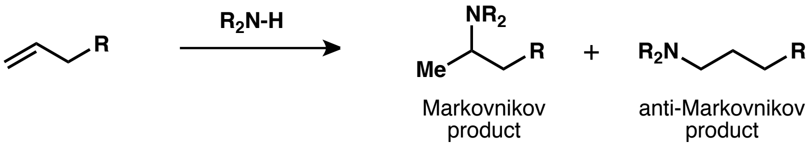

Scheme 1: Regioselectivity in hydroaminations

In spite of these challenges, many different types of catalysts have been developed to facilitate hydroamination: transition metals (early and late), rare-earth metals, Brønsted acids, Brønsted bases, and even main group metals (such as lithium, calcium, and aluminum).[1,5] While transition metal and rare-earth metal catalysts have been the most extensively studied, they present some drawbacks. These catalysts are often quite expensive and usually require stabilizing ligands that may require multi-step synthesis. Additionally, modest selectivity, sluggish rates, and limited functional group tolerance indicate that advances can still be made in this field. We were especially drawn to the benefits of avoiding metal catalysts in favor of Brønsted acids since they are less expensive and are known for giving exclusively Markovnikov selectivity by proceeding through carbocation intermediates.

While acid-mediated hydration and hydroetherification of unactivated alkenes has been known for over a century,[6] the analogous acid-mediated reaction with nitrogen nucleophiles has been much more elusive. Acid catalysis of hydroamination has the associated hurdle in that acidic conditions will protonate the amine, rendering it non-nucleophilic. It wasn't until 2002 that Hartwig and coworkers disclosed the first acid-catalyzed hydroamination of unactivated olefins in which they utilized triflic acid (TfOH) at elevated temperatures (100 °C) to effectively catalyze a C–N bond-forming process (Scheme 2).[7] The nitrogen basicity problem was overcome in this case by employing tosylamides (**2.1a**) as nucleophiles. Tosylamides are basic enough to be protonated by triflic acid, yet the resulting tosylamidium ion is acidic enough to transfer its proton to the alkene group, thus allowing for productive C–N bond formation to yield the pyrrolidine products (**2.1b**).

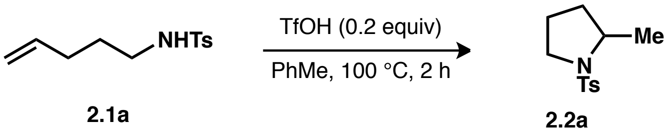

Scheme 2: Triflic acid catalyzed hydroamination with tosylamides

A few other examples of acid-catalyzed hydroaminations have been reported since Hartwig's seminal report; however, most protocols require elevated temperatures to achieve good conversion.[8] We sought to build upon this previous work and our serendipitous hydroamination observation (en route to the synthesis of *Lycopodium* alkaloids, see Section 1.8) by exploring the role of TMSI in hydroamination reactions. The results of this investigation are detailed below and have been published in a peer-reviewed journal.[9]

2.2: Initial Studies of TMSI-Mediated Hydroamination

When we initially observed the transannular hydroamination of tricycle **2.3**, we were curious to know whether this transformation was being mediated by trimethylsilyl iodide (TMSI) or trace in situ generated hydrogen iodide (HI). As shown in Section 1.8, exposure of tricycle **2.3** to in situ generated TMSI (using equal amounts TMSCl and NaI) yielded enal **2.4** quite rapidly (Table 1, entry 1) while extended reaction times resulted in the hydroamination product **2.5** (entry 2). When exposed to commercially available TMSI, the same hydroamination took place (entry 3). Interestingly, when 1 equivalent of water was added, the hydroamination was successful (entry 4), indicating that HI could be essential. Conversely, when aqueous HI was utilized instead of TMSI, the hydroamination was sluggish (entry 5). Finally, addition of a base such as triethylamine shut down the reaction (entry 6). These results were inconclusive and made it hard to deduce anything about the mechanism or active catalyst in this transformation. This was compounded by the fact that several steps need to take place in order to furnish tetracycle **2.5** from tricycle **2.3** and these individual steps could be mediated by different species.

Table 1: Initial hydroamination studies with tricycle **2.3**

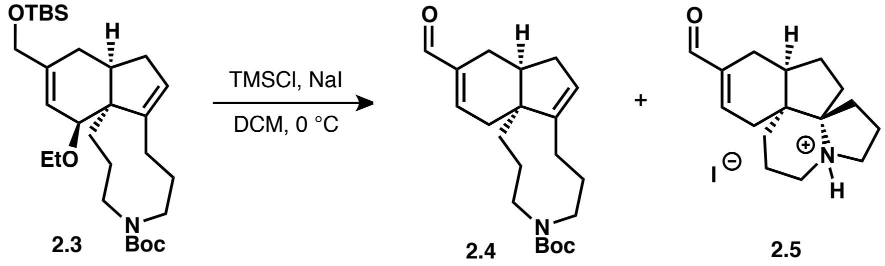

entry	TMSCl/NaI equiv	additive	rxn time	major product
1	2	-	30 min	**2.4**
2	2	-	1 h	**2.5**
3	0	TMSI (2 equiv)	1 h	**2.5**
4	2	H_2O (1 equiv)	1 h	**2.5**
5	0	HI (57% aq)	1 h	**2.4**:**2.5** (2:1)
6	2	Et_3N (4 equiv)	1 h	No rxn

In order to gain insight into the reaction mechanism, we sought to test this reaction on a simpler substrate – one that only contained a nitrogen nucleophile and a pendant olefin (such as **2.1**, Table 2). This served to provide us access to substantial quantities of material as well as eliminate the unnecessary variables inherent in the relatively complex system (i.e. **2.3**). We commenced these studies by investigating the necessity of a nitrogen protecting group. Even though we suspected the hydroamination of tricycle **2.3** occurred from the free secondary amine, it quickly became clear that simple amines would not be amenable to this type of reactivity (entry 1). This supports our hypothesis that tricycle **2.3** was predisposed to hydroamination with the azanonane ring sitting directly under the carbon-carbon double bond. Subjecting *t*-butyloxycarbonyl (Boc) protected amines to TMSI only resulted in cleavage of the Boc group (entry 2). This was not surprising, as both TMSI and HI are known reagents for the cleavage of Boc protecting groups. More robust carbamate protected amines such as carboxybenzyl (Cbz) amines resulted in complex reaction mixtures with no observable hydroamination (entry 3). When alkenyl acetamides were screened for reactivity, compound **2.6** was observed resulting from formal HI addition across the double bond (entry 4). Much to our delight, tosylamides were competent nucleophiles in this intramolecular hydroamination, delivering pyrolidine **2.2** cleanly (entry 5). Other sulfonamides showed promising reactivity, however the less nucleophilic nosyl-protected amine resulted in competing olefin hydroiodination (i.e. **2.6,** entry 6). Therefore, tosylamide **2.1a** was chosen to continue optimization and mechanistic studies.

Table 2: Role of nitrogen protecting group in hydroamination

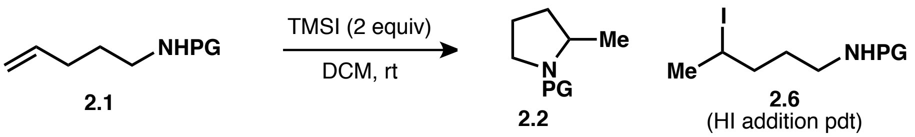

entry	PG identity	result
1	H	No rxn
2	Boc	Boc cleavage, no hydroamination
3	Cbz	Unknown pdts, no hydroamination
4	Ac	HI addition across alkene (**2.6**)
5	Ts	Hydroamination (**2.2**), 100% conversion
6	Ns	Hydroamination and HI addition (1:1)

2.3: Optimization of Reaction Conditions

After demonstrating that tosylamides were competent nitrogen nucleophiles, we next turned our attention to assessing the reaction conditions. Using the same reagents (TMSCl/NaI) that had been employed in the conversion of tricycle **2.3** to **2.5**, alkenyl tosylamide **2.1a** was fully converted to afford pyrrolidine **2.2a** (Table 3, entry 1). In the absence of NaI (i.e., with TMSCl alone), the starting material was recovered and none of the hydroamination product was observed (entry 2). When a stronger silylating reagent (TMSOTf) was employed, 47% conversion to the hydroamination product was achieved after 2 hours at room temperature (entry 3). Using commercially available TMSI gave complete conversion to the hydroamination product after only 1 hour (entry 4). Furthermore, a catalytic amount of TMSI (0.2 equiv) could be used, which led to 97% conversion to **2.2a** in 4 hours (entry 5). In contrast, TMSOTf and TMSBr were non-optimal when sub-stoichiometric amounts of these reagents were employed, leading only to 21% and 30% conversion, respectively, after 4 hours (entries 6 and 7).

Table 3: Effect of various activating reagents

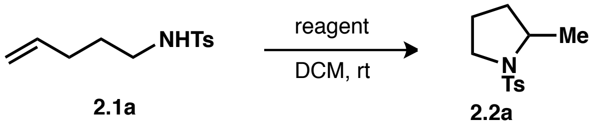

entry	reagent (equiv)	time	conversion
1	TMSCl/NaI (2)	1 h	100%
2	TMSCl (2)	20 h	0%
3	TMSOTf (2)	2 h	47%
4	TMSI (2)	1 h	100%
5	TMSI (0.2)	4 h	97%
6	TMSOTf (0.2)	4 h	21%
7	TMSBr (0.2)	4 h	30%
8	57% HI (2)	20 h	33%

With the initially established conditions for the hydroamination of **2.1a** in hand, we next turned to investigate the mechanism of this transformation. The addition of base either shut down the reaction (with 0.2 equivalents triethylamine) or severely retarded the rate (15% conversion after 20 hours with 0.2 equivalents 2,6-di-*tert*-butylpyridine). This suggested that the generation of acid was vital to the success of this reaction. However, when HI (57% solution in water) was used instead of TMSI, the reaction proceeded at a sluggish rate, indicating that *in situ* generation of HI might not be the sole accelerating factor (see Table 3, entry 8). From these observations, we hypothesized that a silylated amine intermediate could be responsible for the milder reaction temperatures required for the TMSI-promoted hydroamination relative to the triflic acid-mediated conditions identified by Hartwig.[7] TMSI could silylate tosylamide **2.1**, thus generating an active ion pair **2.7** that could participate in a facile protonation of the alkene group followed by cyclization (Scheme 3A). However, we did not observe any silylated intermediates in the reaction mixture when the reaction was conducted in CD_2Cl_2 and monitored by ^1H NMR. Additionally, we observed that for a mixture of *N*-methyl tosylamide and TMSI, the equilibrium lies strongly toward the free tosylamide and TMSI as opposed to the silylated tosylamide, and only upon addition of a base (2,6-lutidine) did we observe any silylation of the tosylamide (Scheme 3B). Although this certainly does not disprove the silylation hypothesis, it indicated that silylation of the tosylamide with TMSI is not nearly as favorable as protonation with HI.[10]

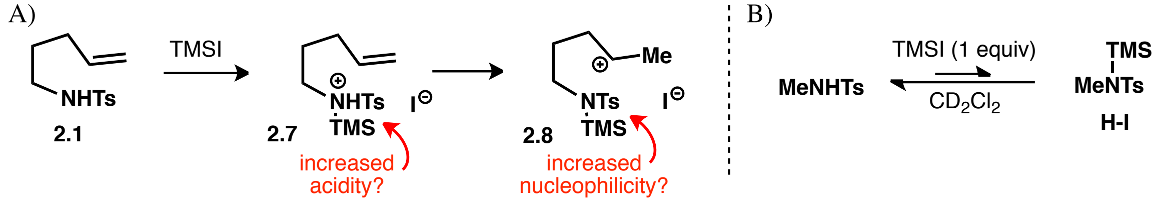

Scheme 3: Possible silylated tosylamide intermediate

A key observation came when we tried conducting the TMSI-promoted conversion of **2.1a** to **2.2a** on gram scale. This reaction proceeded in a modest 76% conversion after 4 hours, indicating that the reaction conditions did not scale appropriately (Table 4, entry 1). This decreased reaction rate upon scale-up suggested that adventitious water could be playing an important role. To test this hypothesis, a series of large-scale experiments were carried out where varying amounts of water were introduced. The results are summarized in Table 4 and show that the addition of 0.05 equivalents of water (entry 2) is optimal. It therefore seems unlikely that TMSI is the active catalyst in this reaction; rather, TMSI may serve as a precursor to generate HI and hexamethyldisiloxane in the presence of trace water. We believe that larger quantities of water retard the reaction rate due to the Lewis basicity of the water oxygen atom (see Section 2.6 for more discussion). This also explains why HI as a 57% aqueous solution gave very low conversion. Thus, TMSI in the presence of small amounts of water most likely serves as a source of 'anhydrous' HI. In order to take advantage of this adventitious water effect, it was necessary to measure 0.05 equivalents of water for reactions run on any scale. We found that the most reproducible method for doing this was to utilize the known solubility of water in dichloromethane (2.0 mg/L at 20 °C).[11] By using a certain amount of dry dichloromethane with an added amount of 'wet' dichloromethane (solvent that had been pre-saturated with water), small quantities of water could be accurately added to any scale reaction.

Table 4: Effect of added water on hydroamination conversion

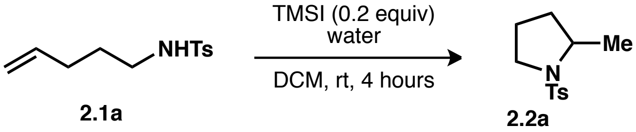

entry	water (equiv)	conversion
1	0	76%
2	0.05	96%
3	0.10	88%
4	0.25	89%
5	0.50	78%

As a means of comparison, we wanted to see if alternative methods for generating anhydrous HI could also efficiently catalyze this hydroamination reaction. One of the methods investigated was reported by Koreeda and coworkers. They demonstrated that a combination of iodine and thioacetic acid react to produce HI and a disulfide as the byproduct.[12] However, when these reaction conditions were utilized with alkenyl tosylamide **2.1a**, clean hydroamination was not observed (Scheme 4). Some amount of the desired cyclized product was observed, but the conversion was low and it was observed along with an unknown side product, possibly resulting from deleterious reactivity with the disulfide that is formed.

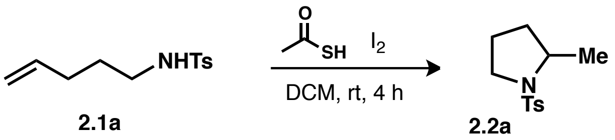

product : SM : unknown
(0.33 : 1 : 0.21)

Scheme 4: Alternative method of generating anhydrous HI

2.4: Additive Effects – The Importance of Iodide Anion

All evidence up to this stage pointed toward a Brønsted acid-catalyzed hydroamination, but we were intrigued by the fact that ‘anhydrous’ HI could catalyze this reaction under milder conditions as compared to triflic acid. This difference is not explained by relative acid strength since triflic acid (pKa = –12) is more acidic as compared to HI (pKa = –10). Moreover, both triflic acid and HI are strong enough to fully protonate the tosylamide (pKa of an alkyl tosylamidium ~ –6).[13] This leveling effect should render both acid-catalyzed reactions identical in rate since the active acid in both cases is the tosylamidium. However, this is not what was observed.

To further elucidate the differences between the triflic acid and HI-mediated hydroaminations, we compared conversion at room temperature in the presence of various additives. As shown in Table 5, the conversion after 4 h was the same whether triflic acid or TMSOTf (in the presence of water; to generate TfOH in situ) were used (entries 1 and 2). Similar observations were made for the reaction conducted in the presence of triflic acid and hexamethyldisiloxane ($(TMS)_2O$, 0.05 equiv, entry 3). These comparisons indicated that hexamethyldisiloxane did not play a significant role in the hydroamination. Due to the difficult nature of dispensing exact amounts of pure, anhydrous HI, we were unable to conduct the analogous experiment with TMSI and HI. However, the introduction of exogenous hexamethyldisiloxane to the TMSI-promoted hydroamination did not lead to an appreciable increase in rate. Alternatively, it is possible that small quantities of iodine are being generated and that iodination serves to acidify the tosylamidium species. However, addition of exogenous iodine to various reaction conditions failed to accelerate the reaction rate. Attempts to sequester any in situ formed iodine were met with inconclusive results as the basicity of the sequestering additives could often account for the variations in conversion.

Table 5: Additive effects

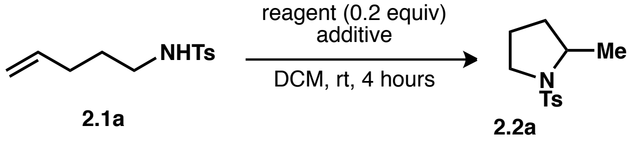

entry	reagent	additive (equiv)	conversion
1	TfOH	--	20%
2	TMSOTf[a]	--	21%
3	TfOH	$(TMS)_2O$ (0.2)	19%
4	TMSI[a]	--	97%
5	TMSCl[a]	NaI (0.2)	94%
6	TMSI[a]	NaOTf (0.2)	97%
7	TMSOTf[a]	--	21%
8	TMSOTf[a]	NaI (0.2)	76%
9	TfOH	NaI (0.2)	83%
10	TfOH	$NaBF_4$ (0.2)	22%
11	TfOH	$NaBAr^F_4$ (0.2)	13%

[a] Water (0.05 equiv) was also added to these reactions

We next sought to ascertain the effect of the counter-anion on the rate of the hydroamination reaction. The importance of counter-anions is well documented in transition metal-catalyzed hydroaminations, with less coordinating anions (e.g., $^{-}$OTf, $^{-}$OTs, and $^{-}BAr^F_4$) generally increasing the catalytic activity of the metal.[14] However, the role of the counter-anion in Brønsted acid-catalyzed hydroaminations is not as well studied.[15] To explore the role of the counter-anion for the HI-mediated hydroamination, we tested the effect of several salt additives (Table 5, entries 4-11). As noted previously, the use of in situ generated TMSI (from TMSCl/NaI) results in 94% conversion (entry 5). This conversion was retained when NaOTf was added to the standard conditions (entry 6). Interestingly, the addition of NaI to TMSOTf (entry 8) or to triflic acid (entry 9) increased the reaction conversion substantially to 76% and 83%, respectively, as compared to ~20% without added NaI (compare to entries 1 and 2). These results indicated that the iodide anion is essential to the success of the Brønsted acid-catalyzed hydroamination at room temperature. Several other non-coordinating anions such as BF_4^- and $BAr^F{}_4^-$ (entries 10 and 11) were investigated with triflic acid; however, iodide was the only anion that substantially accelerated the reaction rate. The basis for this unique effect of iodide is still unclear but we hypothesize that the iodide anion likely forms a loose ion pair with the tosylamidium (**2.9**, Scheme 5), which leads to an increase in acidity relative to the tosylamidium triflate ion pair. It is well known that ion pair acidities can differ substantially from standard ionic acidity and thus can vary based on the counter anion.[16] This acidification would serve to accelerate intramolecular olefin protonation (**2.9** to **2.10**), which has been well established as the rate-determining step in Brønsted acid-catalyzed hydroamination reactions.[7] To finish the catalytic cycle, intramolecular attack on the carbocation furnishes pyrrolidinium **2.11,** which serves to liberate HI or directly protonate another molecule of the starting tosylamide.

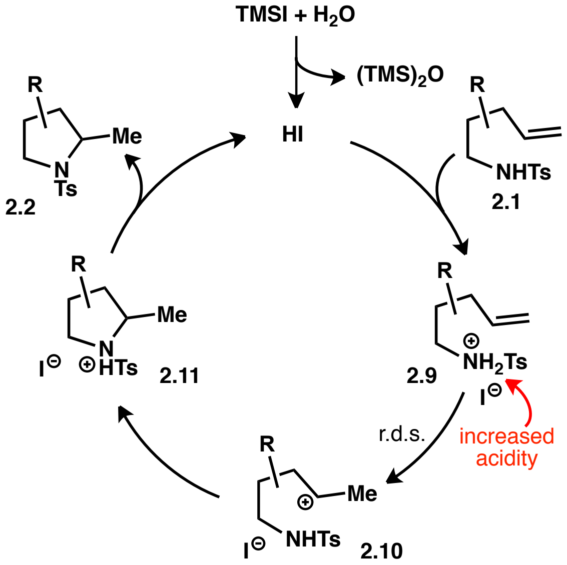

Scheme 5: Proposed mechanism of HI catalysis

Further evidence to support our proposed mechanism stemmed from attempts to construct a 6-membered piperidine ring (Scheme 6). When hexenyl tosylamide **2.12** was subjected to the hydroamination conditions, a mixture of products was observed. Reaction pathways resulting from a discrete carbocation (e.g., hydride shift followed by cyclization to form **2.1g** or iodide addition to form **2.14**) compete with the direct cyclization pathway (to form **2.13**) since cyclization to the 6-membered ring is slower than for the corresponding 5-membered ring. This shows direct evidence for the formation of a discrete carbocation and rules out the possibility of a more concerted addition across the double bond, at least when forming 6-membered rings.

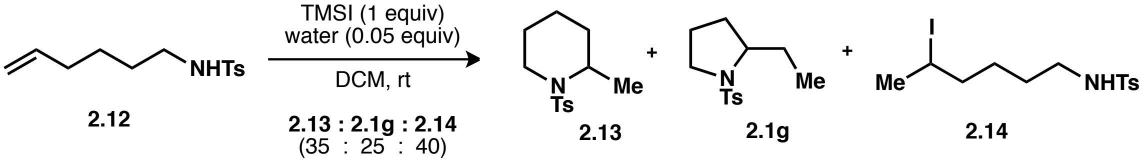

Scheme 6: Reaction of hexenyl tosylamide **2.12** shows evidence for a discrete carbocation

Another mechanistic hypothesis that we quickly dismissed was the possibility that an alkyl iodide served as an intermediate in these reactions. Displacement by the pendant tosylamide could then yield the observed hydroamination products. However, when alkyl iodide **2.14** was isolated and exposed to the reaction conditions, no further reactivity was observed. The same is true when we isolated and re-subjected the alkyl iodide resulting from HI addition across **2.1a**. These alkyl iodides did not cyclize to give the formal hydroamination product.

2.5: Substrate Scope

Following our optimization of reaction conditions and investigation of the roles of each reagent and additive, we sought to examine the scope of the reaction (Table 6). We found that primary and secondary alkyl tosylamides **2.1a-c** are efficient substrates. Styrenyl compounds **2.1d-e** also undergo facile hydroamination. Notably, this substrate list includes the *p*-anisole derivative **2.1e**, which is known to be sensitive to other, harsher, Brønsted acid-mediated hydroamination conditions.[7] Various substitution patterns on the olefin component are also tolerated (**2.1f-g**), although notably, internal olefins require slightly longer reaction times. Diene **2.1h** also readily undergoes HI-catalyzed hydroamination to afford the corresponding allylic tosylamide (**2.2h**).

Table 6: Cyclizations of tosylamides with anhydrous HI

reactant	product	yield[a]
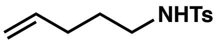 **2.1a**	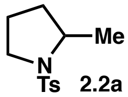 **2.2a**	95%
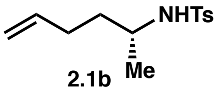 **2.1b**	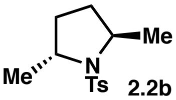 **2.2b**	90% d.r.: 55:45
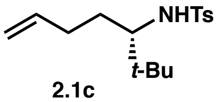 **2.1c**	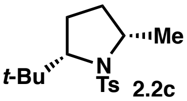 **2.2c**	66% d.r.: 60:40
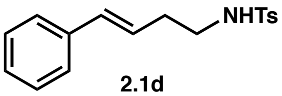 **2.1d**	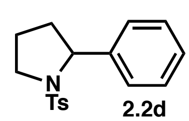 **2.2d**	84%[b]
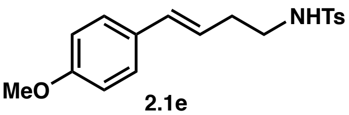 **2.1e**	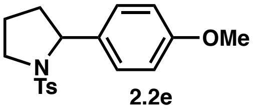 **2.2e**	87%
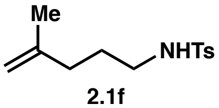 **2.1f**	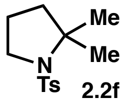 **2.2f**	78%
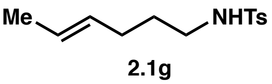 **2.1g**	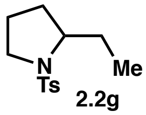 **2.2g**	47%[b,c]
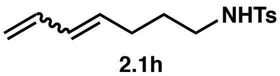 **2.1h** *E*:*Z* = 56:44	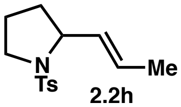 **2.2h**	86% *E*:*Z* = 91:9

[a] Isolated yield. Reactions conducted using standard conditions: TMSI (0.2 equiv), water (0.05 equiv), DCM (0.2 M), room temperature, 4 hours
[b] 2 x 0.2 equiv TMSI used over a reaction time of 12 hours
[c] Isolated an additional 14% unreacted starting material after 12 hours

Gratifyingly, this hydroamination methodology can be extended to the hydroetherification of alkenyl alcohols to provide a range of cyclic ethers (Table 7). Primary and secondary alcohols (**2.15a-c**) readily undergo cyclization to the corresponding 2- and 2,5-functionalized tetrahydrofurans (**2.16a-c)**. Additionally, carboxylic acid **2.15d** serves as a suitable oxygen nucleophile to provide lactone **2.16d**, albeit at a slower reaction rate. In an effort to estimate the relative cyclization rates of alcohols and tosylamides, alkenyl hydroxyl tosylamide **2.15e** was subjected to the standard set of cyclization conditions. The pyrrolidine product (**2.1i**) was obtained in 31% yield and the tetrahydrofuran product (**2.16e**) was obtained in 56% yield, indicating that hydroetherification occurs slightly faster than hydroamination.

Table 7: Cyclizations of oxygen nucleophiles

reactant	product	yield[a]
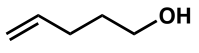 **2.15a**	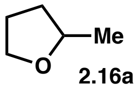 **2.16a**	84%[b,c]
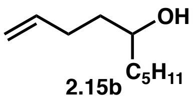 **2.15b**	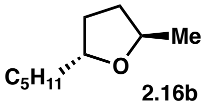 **2.16b**	61% d.r.: 85:15
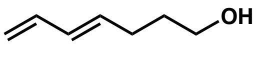 **2.15c**	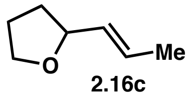 **2.16c**	98%[b] *E*:*Z* = 91:9
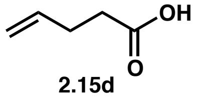 **2.15d**	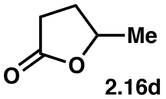 **2.16d**	58%[b,d]
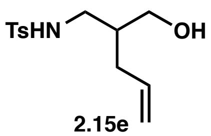 **2.15e**	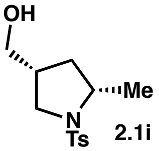 **2.1i** 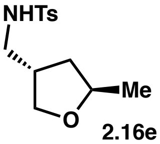 **2.16e**	**2.1i** = 31% d.r.: 75:25 **2.16e** = 56% d.r.: 66:33

[a] Isolated yield. Reactions conducted using standard conditions: TMSI (0.2 equiv), water (0.05 equiv), DCM (0.2 M), room temperature, 4 hours

[b] NMR yield, DCM-d_2, mesitylene as internal standard

[c] Contained 13% unreacted starting material after 4 hours

[d] Contained 30% unreacted starting material after 24 hours, 2 x 0.2 equiv TMSI used

Although there were many types of substrates that were successful in this reaction, there were several substrates that gave poor reactivity (Scheme 7). When pi systems other than alkenes and dienes were utilized as substrates, complex mixtures of products were observed. Allene **2.17** failed to deliver any detectable product when subjected to the standard reaction conditions (0.2 equivalents TMSI). When more TMSI was added, allene **2.17** reacted to produce some of the desired product, however, this reaction was low yielding and unclean. Alkyne **2.18** gave a complex reaction mixture; a small amount of HI addition across the alkyne group was observed, but no detectable cyclized product. We also observed that alkyl tosylamides were unique in their productive reactivity; upon slight variation of the nitrogen nucleophile, the reaction was unsuccessful. The lowered nucleophilicity of tosyl-protected aniline **2.19** can account for alkene iodination outcompeting cyclization. HI addition is quite deleterious in these reactions because it consumes the active catalyst and thus shuts down the desired hydroamination. In the case of sulfinamide **2.20**, the weaker electron-withdrawing group is unable to suitably lower the pKa of the protonated form. Thus, protonation of the sulfinamide results in an inactive species, incapable of effecting an intramolecular olefin protonation.

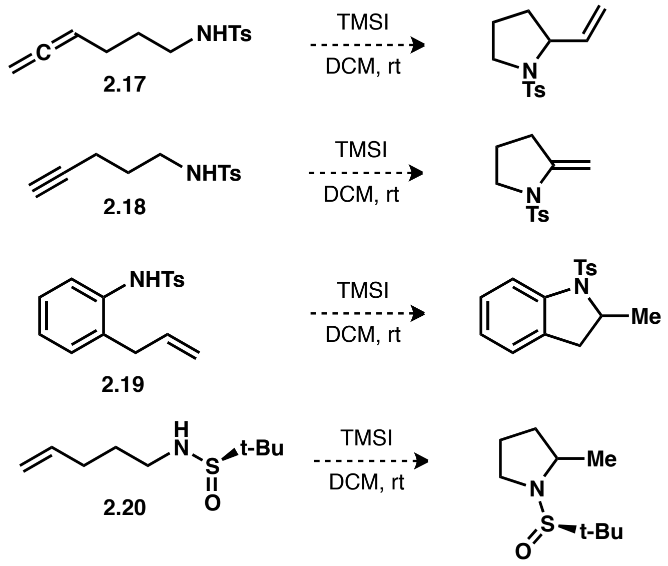

- no rxn w/ 0.2 equiv TMSI
- low yielding (unclean) reaction w/ 2 equiv TMSI

- complex mixture, some HI addition product

- mostly SM, some HI addition product

- no reaction

Scheme 7: Substrates with poor reactivity toward TMSI hydroamination

2.6: Comparative Robustness Screen

Many of the previously reported Brønsted acid-catalyzed hydroaminations require temperatures at or above 100 °C.[7] Since our newly developed conditions did not require elevated temperatures, we postulated that these conditions could provide better functional group tolerance, especially pertaining to acid-sensitive groups. To test this hypothesis, we compared our conditions to the standard triflic acid-mediated hydroamination conditions (at 100 °C) in a "robustness screen" as recently popularized by Glorius and coworkers.[17] We began by testing a range of acid-sensitive additives including silyl ethers, silyl enol ethers, benzyl ethers, and acetals (Figure 1A). We found that our HI-mediated hydroamination conditions produced moderate product conversions and moderate additive recovery, though the additive recovery varied depending on the inherent stability of the additive (see Section 2.9). In contrast, the triflic acid hydroamination conditions usually produced excellent product yields but significantly lower recoveries of the acid-sensitive additives. The room temperature HI-mediated hydroamination conditions proved to be milder towards acid-sensitive functional groups; however, these functional groups also stalled the progress of the reaction. Thus, the functional group robustness screen demonstrated the complementary nature of HI and triflic acid in mediating hydroamination reactions.

Figure 1: Robustness screen additives

A) Acid-sensitive additives

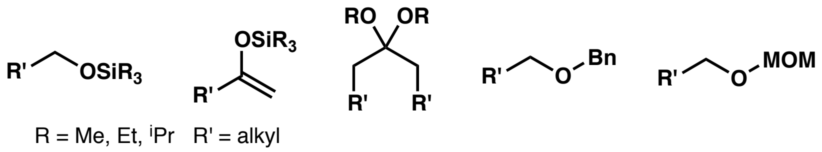

B) Lewis basic additives

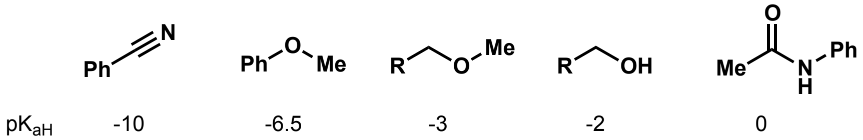

The inhibition of hydroamination by these additives is likely due to their mild Lewis basic character relative to the tosylamide. To test this hypothesis, we conducted another screen of additives, choosing additives that had conjugate acids with pKas ranging from –10 to 0 (Figure 1B). We found that indeed, additives with conjugate acids possessing pKas above –5 completely hindered the HI-mediated reaction, whereas less basic additives were tolerated without any drop in product yield (see Section 2.9). Comparing these observations to the triflic acid-mediated conditions at 100 °C, we found that more basic functional groups are tolerated under the latter set of conditions. Only additives possessing conjugate acids with pKa above –1 completely inhibited the reaction. These conditions likely work in the presence of more basic additives due to the elevated temperature at which these reactions are run. Overall, while the HI-mediated reactions occur at a milder temperature, they do not necessarily result in improved reaction yields over the triflic acid-mediated hydroamination reaction conditions. The HI-promoted conditions do, however, provide a complementary approach to hydroamination.

2.7: Conclusion and Outlook

A fortuitously observed hydroamination in the context of complex molecule total synthesis has led to further investigation of its limitations and scope. Through these studies, we have demonstrated the critical importance of the iodide anion in promoting this Brønsted acid-catalyzed transformation. Due to the synthetic ease of generating 'anhydrous' HI from TMSI as well as the effectiveness of this hydroamination method, we believe it will find broad utility in the future development of acid-catalyzed carbon-heteroatom bond-forming reactions.

2.8: Experimental Contributors

The initial discovery that tricycle **2.3** could undergo a hydroamination to give tetracycle **2.6** was observed by Rebecca Murphy (graduate student, Sarpong group). The remainder of the work presented in this chapter was conducted by Paul R. Leger.

2.9 Experimental Methods

All reactions were run in flame-dried round-bottom flasks or vials under a nitrogen atmosphere. Reactions were monitored by thin layer chromatography (TLC) on Silicycle Siliaplate^{TM} glass backed TLC plates (250 µm thickness, 60 Å porosity, F- 254 indicator) and visualized using UV irradiation and *para*-anisaldehyde stain. For heated reactions, the temperature was monitored using an IKA® temperature control. Trimethylsilyl iodide (TMSI) was obtained from Sigma Aldrich, stored in a glove box, and removed directly prior to use. Dry acetonitrile, diethyl ether, tetrahydrofuran (THF), triethylamine (TEA), benzene, and methanol were obtained by passing these previously degassed solvents through activated alumina columns. Dichloromethane (DCM) was distilled over calcium hydride before use. Volatile solvents were removed under reduced pressure on a rotary evaporator. All flash chromatography was conducted using Sorbent Technologies 60 Å, 230x400 mesh silica gel (40-63 µm). ^{1}H NMR and ^{13}C NMR spectra were acquired using Bruker 300, 400, 500, and 600 MHz (75, 100, 125, and 150 MHz for ^{13}C NMR) spectrometers in $CDCl_3$. Chemical shifts are measured relative to the shift of the residual solvent (^{1}H NMR - $CDCl_3$ $\delta = 7.26$, MeOD $\delta = 3.31$, CD_2Cl_2 $\delta = 5.32$; ^{13}C NMR $CDCl_3$ $\delta = 77.16$, MeOD $\delta = 49.00$). NMR data are reported as follows: chemical shift (multiplicity, coupling constant, integration). Splitting is reported with the following symbols: s = singlet, bs = broad singlet, d = doublet, t = triplet, q = quartet, m = multiplet. IR spectra were acquired on a Nicolet 380 spectrometer as thin films on NaCl plates unless otherwise specified. Spectra are reported in frequency of absorption in cm^{-1}. Only selected resonances are reported. High-resolution mass spectra (HRMS) were performed by the mass spectral facility at the University of California, Berkeley.

*General procedure for the synthesis of alkenyl tosylamides **2.1** by Mitsunobu reaction (Procedure A)*

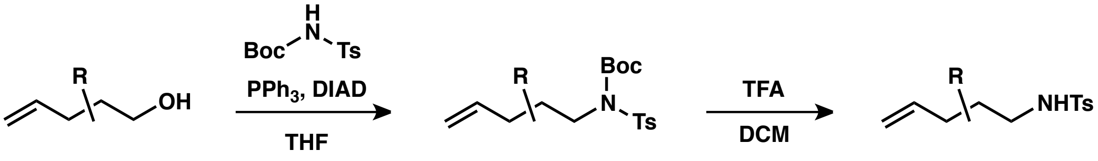

The alkenyl alcohol (57.9 mmol, 1 equiv), *N*-(*tert*-butoxycarbonyl)-*p*-toluenesulfonamide (15.7 g, 57.9 mmol, 1 equiv), and triphenylphosphine (15.2 g, 57.9 mmol, 1 equiv) were dissolved in THF (100 mL) and cooled to 0 °C. Diisopropyl azodicarboxylate (11.4 mL, 57.9 mmol, 1 equiv) was added dropwise over a period of 5 minutes. The solution was allowed to stir for 3 hours at room temperature at which point the solution was concentrated and loaded directly onto silica and purified by column chromatography (10% ethyl acetate in hexane). This oil was dissolved in DCM (300 mL), then trifluoroacetic acid (30 mL) was added and the mixture was allowed to stir at room temperature overnight. This mixture was quenched by addition of aqueous potassium carbonate, washed with brine (3 x 100 mL), dried over magnesium sulfate, filtered, and concentrated to yield pure alkenyl tosylamide **2.1**.

General procedure for the synthesis of alkenyl tosylamides ***2.1*** *using Wittig olefination, phthalimide cleavage, and tosylation (Procedure B)*

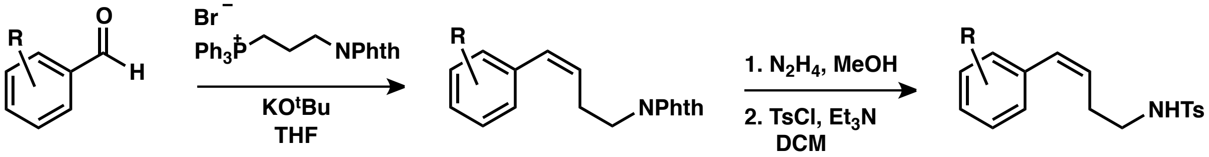

A benzaldehyde derivative (3.29 mmol, 1 equiv) and triphenyl(3-phthalimido-propyl)phosphonium bromide (1.74 g, 3.29 mmol, 1 equiv) were dissolved in THF (15 mL), cooled to 0 °C, and allowed to stir for 15 minutes. Then potassium *tert*-butoxide (3.29 mL, 1M THF, 1 equiv) was added and the mixture was stirred for another 15 minutes, warmed to room temperature, stirred for 1 hour, then heated at reflux for 2 days. Upon cooling, the reaction mixture was filtered to remove solids and concentrated, then loaded onto silica and purified by column chromatography (20% ethyl acetate in hexane). The resulting solid (1.94 mmol, 1 equiv) was dissolved in methanol (7 mL), then hydrazine hydrate (0.33 mL, 5.83 mmol, 3 equiv) was added and the mixture was refluxed for 3 hours. Upon cooling to room temperature, concentrated hydrochloric acid (1 mL) was added and the mixture was heated at reflux for another hour. Upon cooling, the solids were filtered, and the filtrate was concentrated and redissolved in ethanol (10 mL). The solids were again filtered and the filtrate was concentrated. The resulting material was diluted with sodium hydroxide (4 N, 10 mL) and extracted with diethyl ether (3 x 10 mL). The combined organic layers were dried with magnesium sulfate, filtered, and concentrated. The resulting oil (0.78 mmol, 1 equiv) was dissolved in DCM (8 mL) and cooled to 0 °C. Triethylamine (0.17 mL, 1.18 mmol, 1.5 equiv) and 4-toluenesulfonyl chloride (150 mg, 0.78 mmol, 1 equiv) were added. The solution was allowed to stir overnight, at which point the solution was washed with HCl (1 M, 1 x 5 mL), NaOH (1 N, 1 x 5 mL), and brine (1 x 5 mL). The organic layer was dried with magnesium sulfate, filtered, concentrated and purified by column chromatography (20% ethyl acetate in hexane) to yield pure alkenyl tosylamide **2.1**.

General procedure for the synthesis of alkenyl tosylamides ***2.1*** *using Wittig olefination (Procedure C)*

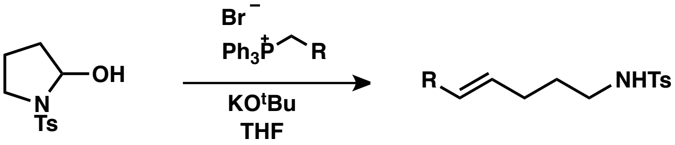

A dry 15 mL round-bottomed flask was charged with the requisite phosphonium salt (1.24 mmol, 1.5 equiv) and THF (3 mL), then potassium *tert*-butoxide (1M in THF, 1.33 mL, 1.33 mmol, 1.6 equiv) was added dropwise and cooled to 0 °C. Then a solution of 1-tosylpyrrolidin-2-ol (200 mg, 0.83 mmol, 1 equiv) in THF (1 mL) was added dropwise and the reaction mixture was allowed to warm to room temperature and stir overnight. Upon quenching with HCl (2N, 3 mL) and extracting with ethyl acetate (3 x 3 mL), the combined organic layers were dried with magnesium sulfate, filtered, concentrated, and purified by column chromatography (20% ethyl acetate in hexane) to yield pure alkenyl tosylamide **2.1**.

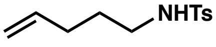

2.1a

4-methyl-*N*-(pent-4-en-1-yl)benzenesulfonamide (**2.1a**)

Starting from 4-penten-1-ol and following Procedure A, **2.1a** was obtained as a colorless oil in 87% overall yield. The spectral data are consistent with those previously reported in the literature.[18] ^{1}H NMR (500 MHz, $CDCl_3$): δ 7.74 (d, *J* = 8.1 Hz, 2H), 7.31 (d, *J* = 8.0 Hz, 2H), 5.71 (ddt, *J* = 17.0, 10.2, 6.7 Hz, 1H), 5.01-4.93 (m, 2H), 4.31 (t, *J* = 6.3 Hz, 1H), 2.95 (q, *J* = 6.8 Hz, 2H), 2.43 (s, 3H), 2.05 (q, *J* = 7.0 Hz, 2H), 1.57 (p, *J* = 7.0 Hz, 2H).

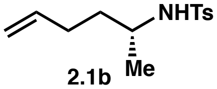

2.1b

(*R*)-*N*-(hex-5-en-2-yl)-4-methylbenzenesulfonamide (**2.1b**)

Starting from (*S*)-5-hexen-2-ol and following Procedure A, **2.1b** was obtained as a white solid in 17% overall yield. The spectral data are consistent with those previously reported in the literature.[19] ^{1}H NMR (600 MHz, $CDCl_3$): δ 7.75 (d, *J* = 8.0 Hz, 2H), 7.30 (d, *J* = 7.9 Hz, 2H), 5.68 (ddt, *J* = 17.0, 10.3, 6.6 Hz, 1H), 4.95-4.89 (m, 2H), 4.14 (d, *J* = 8.0 Hz, 1H), 3.34 (dq, *J* = 13.0, 6.5 Hz, 1H), 2.43 (s, 3H), 2.00 (ddd, *J* = 32.8, 14.5, 7.3 Hz, 2H), 1.45 (ddd, *J* = 12.3, 6.1, 3.5 Hz, 2H), 1.03 (d, *J* = 6.5 Hz, 3H).

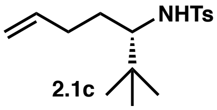

2.1c

(*S*)-*N*-(2,2-dimethylhept-6-en-3-yl)-4-methylbenzenesulfonamide (**2.1c**)

Starting from (*S*)-*tert*-leucinol and following a literature procedure, **2.1c** was obtained as a white solid in 50% overall yield. The spectral data are consistent with those previously reported in the literature.[19] ^{1}H NMR (400 MHz, $CDCl_3$): δ 7.74 (d, *J* = 8.0 Hz, 2H), 7.28 (d, *J* = 7.7 Hz, 2H), 5.68 (ddt, *J* = 16.9, 10.5, 6.6 Hz, 1H), 4.94-4.84 (m, 2H), 4.08 (d, *J* = 8.4 Hz, 1H), 3.08 (td, *J* = 9.7, 2.7 Hz, 1H), 2.41 (s, 3H), 1.98-1.79 (m, 2H), 1.71-1.61 (m, 1H), 1.20 (dt, *J* = 14.5, 4.7 Hz, 1H), 0.80 (s, 9H).

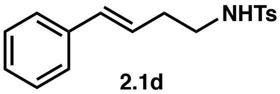

2.1d

(*E*)-4-methyl-*N*-(4-phenylbut-3-en-1-yl)benzenesulfonamide (**2.1d**)

Starting from benzaldehyde and following Procedure B, **2.1d** was obtained as a yellow oil in 31% overall yield. The spectral data are consistent with those previously reported in the literature.[7] ^{1}H NMR (500 MHz, $CDCl_3$): δ 7.69 (d, *J* = 8.0 Hz, 2H), 7.32-7.25 (m, 5H), 7.18 (d, *J*

= 7.5 Hz, 2H), 6.53 (d, J = 11.6 Hz, 1H), 5.48 (dt, J = 11.6, 7.2 Hz, 1H), 4.38 (t, J = 5.5 Hz, 1H), 3.06 (q, J = 6.7 Hz, 2H), 2.47 (qd, J = 7.8, 1.7 Hz, 2H), 2.41 (s, 3H).

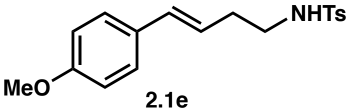

2.1e

(*E*)-*N*-(4-(4-methoxyphenyl)but-3-en-1-yl)-4-methylbenzenesulfonamide (**2.1e**)

Starting from 4-anisaldehyde and following Procedure B, **2.1e** was obtained as a yellow oil in 23% overall yield. The spectral data are consistent with those previously reported in the literature.[20] ^{1}H NMR (500 MHz, CDCl$_3$): δ 7.69 (d, J = 8.4 Hz, 2H), 7.26 (d, J = 8.2 Hz, 2H), 7.13 (d, J = 8.4 Hz, 2H), 6.85 (d, J = 8.7 Hz, 2H), 6.46 (dt, J = 11.5, 1.9 Hz, 1H), 5.37 (dt, J = 11.6, 7.2 Hz, 1H), 4.32 (t, J = 6.1 Hz, 1H), 3.82 (s, 3H), 3.06 (q, J = 6.6 Hz, 2H), 2.47 (qd, J = 6.9, 1.8 Hz, 2H), 2.41 (s, 3H).

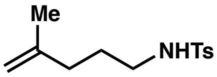

2.1f

4-methyl-*N*-(4-methylpent-4-en-1-yl)benzenesulfonamide (**2.1f**)

Starting from 4-methylpent-4-en-1-ol and following Procedure A, **2.1f** was obtained as a yellow oil in 24% overall yield. The spectral data are consistent with those previously reported in the literature.[20] ^{1}H NMR (500 MHz, CDCl$_3$): δ 7.74 (d, J = 8.1 Hz, 2H), 7.31 (d, J = 7.9 Hz, 2H), 4.70 (s, 1H), 4.61 (s, 1H), 4.30 (t, J = 6.0 Hz, 1H), 2.95 (q, J = 6.8 Hz, 2H), 2.43 (s, 3H), 1.99 (t, J = 7.5 Hz, 2H), 1.66 (s, 3H), 1.60 (d, J = 6.9 Hz, 2H).

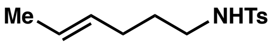

2.1g

(*E*)-*N*-(hex-4-en-1-yl)-4-methylbenzenesulfonamide (**2.1g**)

Starting from ethyl phosphonium bromide and following Procedure C, **2.1g** was obtained as a colorless oil in 31% overall yield. The spectral data are consistent with those previously reported in the literature.[21] ^{1}H NMR (400 MHz CDCl$_3$): δ 7.74 (d, J = 8.0 Hz, 2H), 7.31 (d, J = 8.0 Hz, 2H), 5.46 (dq, J = 13.4, 7.1 Hz, 1H), 5.27 (q, J = 8.5 Hz, 1H), 4.27 (t, J = 6.3 Hz, 1H), 2.95 (q, J = 6.8 Hz, 2H), 2.43 (s, 3H), 2.03 (q, J = 7.4 Hz, 2H), 1.52 (m, J = 7.2 Hz, 5H).

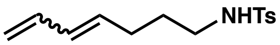

2.1h

N-(hepta-4,6-dien-1-yl)-4-methylbenzenesulfonamide (**2.1h**)

Starting from allyl phosphonium bromide and following Procedure C, **2.1h** was obtained as a colorless oil as a 56:44 of trans/cis isomers in 13% yield. The spectral data are consistent with those previously reported in the literature.[22]

Trans isomer: ^{1}H NMR (400 MHz, CDCl$_3$): δ 7.74 (d, *J* = 8.0 Hz, 2H), 7.30 (d, *J* = 8.0 Hz, 2H), 6.25 (dt, *J* = 17.0, 10.3 Hz, 1H), 5.98 (dd, *J* = 16.1, 10.3 Hz, 1H), 5.56 (dt, *J* = 14.7, 7.0 Hz, 1H), 5.13-5.03 (m, 1H), 4.97 (d, *J* = 10.0 Hz, 1H), 4.59 (s, 1H), 2.94 (qd, *J* = 6.8, 3.1 Hz, 2H), 2.42 (s, 3H), 2.07 (q, *J* = 7.2 Hz, 2H), 1.57 (p, *J* = 7.2 Hz, 2H).

Cis isomer: 7.74 (d, *J* = 8.0 Hz, 2H), 7.30 (d, *J* = 8.0 Hz, 2H), 6.53 (dt, *J* = 16.8, 10.6 Hz, 1H), 5.98 (dd, *J* = 16.1, 10.3 Hz, 1H), 5.32 (dt, *J* = 10.6, 7.7 Hz, 1H), 5.18 (dd, *J* = 16.9, 1.9 Hz, 1H), 5.13-5.03 (m, 1H), 4.59 (s, 1H), 2.94 (qd, *J* = 6.8, 3.1 Hz, 2H), 2.42 (s, 3H), 2.17 (q, *J* = 7.5 Hz, 2H), 1.57 (p, *J* = 7.2 Hz, 2H).

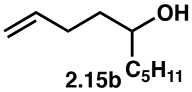

2.15b

dec-1-en-5-ol (**2.15b**)

Starting from 2-(but-3-enyl)oxirane and *n*-BuLi, **2.15b** was prepared according to literature precedent and the spectral data are consistent with those previously reported in the literature.[23] ^{1}H NMR (400 MHz, CDCl$_3$): δ 5.85 (ddt, *J* = 16.9, 10.2, 6.6 Hz, 1H), 5.05 (dq, *J* = 17.2, 1.7 Hz, 1H), 4.97 (dq, *J* = 10.1, 1.4 Hz, 1H), 3.61 (q, *J* = 7.5, 6.4 Hz, 1H), 2.16 (dq, *J* = 31.4, 10.2, 7.6 Hz, 2H), 1.62-1.48 (m, 2H), 1.44 (t, *J* = 4.9 Hz, 2H), 1.37-1.24 (m, 6H), 0.90 (t, *J* = 7.2 Hz, 3H).

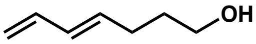

2.15c

(*E*)-hepta-4,6-dien-1-ol (**2.15c**)

Starting from 1,4-pentadien-3-ol and triethylorthoacetate, **2.15c** was prepared according to literature precedent and the spectral data are consistent with those previously reported in the literature.[24] ^{1}H NMR (500 MHz, CDCl$_3$): δ 6.31 (dt, *J* = 17.0, 10.3 Hz, 1H), 6.09 (dd, *J* = 15.3, 10.4 Hz, 1H), 5.72 (dt, *J* = 14.7, 7.0 Hz, 1H), 5.11 (dd, *J* = 16.9, 1.7 Hz, 1H), 4.98 (dd, *J* = 10.2, 1.7 Hz, 1H), 3.67 (q, *J* = 6.1 Hz, 2H), 2.19 (q, *J* = 7.3 Hz, 2H), 1.68 (p, *J* = 7.1 Hz, 2H).

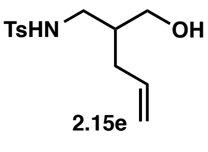

2.15e

N-(2-(hydroxymethyl)pent-4-en-1-yl)-4-methylbenzenesulfonamide (**2.15e**)

A dry 10 mL round-bottomed flask was charged with 2-(aminomethyl)pent-4-en-1-ol[25] (120 mg, 1.04 mmol, 1 equiv), triethylamine (0.31 mL, 2.19 mmol, 2.1 equiv), and DCM (2 mL) and cooled to 0 °C. In a separate vial, 4-toluenesulfonyl chloride (209 mg, 1.09 mmol, 1.05

equiv) was dissolved in DCM (1 mL) and subsequently added to the round-bottom flask dropwise over a period of about 1 hour. After stirring at 0 °C for 5 hours, the solution was washed with water (3 x 5 mL), dried with magnesium sulfate, filtered, concentrated, and purified by column chromatography (50% ethyl acetate in hexane) to yield pure **2.15e** as a colorless oil in 72% yield. ^{1}H NMR (500 MHz, $CDCl_3$): δ 7.73 (d, *J* = 8.3 Hz, 2H), 7.30 (d, *J* = 8.0 Hz, 2H), 5.67 (ddt, *J* = 17.3, 10.3, 7.1 Hz, 1H), 5.44 (t, *J* = 6.5 Hz, 1H), 5.01 (dd, *J* = 8.2, 1.6 Hz, 1H), 4.99 (t, *J* = 0.8 Hz, 1H), 3.69 (dt, *J* = 11.1, 4.4 Hz, 1H), 3.53 (dt, *J* = 11.5, 5.8 Hz, 1H), 3.03 (ddd, *J* = 13.1, 7.0, 4.3 Hz, 1H), 2.89 (dt, *J* = 13.0, 7.1, 6.0 Hz, 1H), 2.45 (t, *J* = 5.5 Hz, 1H), 2.42 (s, 3H), 2.07-1.91 (m, 2H), 1.75 (ddt, *J* = 10.4, 7.1, 3.6 Hz, 1H); ^{13}C NMR (126 MHz, $CDCl_3$) δ 143.6, 136.8, 135.7, 129.9, 127.1, 117.2, 63.8, 44.6, 40.0, 33.4, 21.6; IR (film) 3510, 3277, 2925, 1153 cm^{-1}; HRMS (ESI) calculated for $[C_{13}H_{18}NO_3S]^-$ $[M-H]^-$: *m/z* 268.1013, found 268.1013.

*General procedure for the synthesis of pyrrolidines **2.2** (or tetrahydrofurans **2.16**) from alkenyl tosylamides **2.1** (or alkenyl alcohols **2.15**) (Procedure D)*

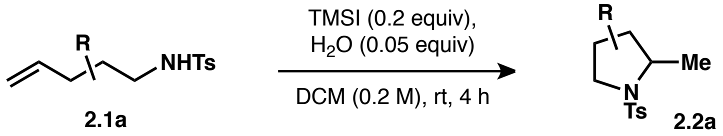

Tosylamide **2.1** (0.84 mmol, 1 equiv) was dissolved in dry DCM (3.8 mL). DCM pre-saturated with water (0.38 mL wet DCM, 0.042 mmol water, 0.05 equiv) was then added, followed by TMSI (24 μL, 0.17 mmol, 0.2 equiv). The reaction mixture was allowed to stir at room temperature. After 4 hours, the mixture was quenched with saturated sodium bicarbonate (2 mL) and saturated sodium sulfite (1 mL) and extracted with DCM (3 x 3 mL). The combined organic layers were dried over magnesium sulfate, concentrated, and purified by column chromatography (20% ethyl acetate in hexane) to yield pure pyrrolidine **2.2**.

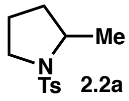

2.2a

2-methyl-1-tosylpyrrolidine (**2.2a**)

Utilizing **2.1a** and following Procedure D, **2.2a** was obtained as a white solid in 95% yield. The spectral data are consistent with those previously reported in the literature.[26] ^{1}H NMR (600 MHz, $CDCl_3$): δ 7.72 (d, *J* = 7.9 Hz, 2H), 7.30 (d, *J* = 7.9 Hz, 2H), 3.71 (qt, *J* = 6.3, 4.7, 4.2, 2.3, 2.2 Hz, 1H), 3.44 (dt, *J* = 10.8, 5.9 Hz, 1H), 3.14 (dt, *J* = 10.2, 7.4 Hz, 1H), 2.43 (s, 3H), 1.82 (dq, *J* = 12.9, 6.7, 6.1 Hz, 1H), 1.69 (p, *J* = 7.7, 6.5, 6.5, 5.4 Hz, 1H), 1.50 (ddd, *J* = 22.4, 11.6, 5.9 Hz, 2H), 1.31 (d, *J* = 6.3 Hz, 3H).

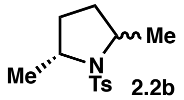

2.2b

(2*R*)-2,5-dimethyl-1-tosylpyrrolidine (**2.2b**)

Utilizing **2.1b** and following Procedure D, **2.2b** was obtained as a white solid in 90% yield as a 55:45 mixture of *trans*/*cis* diastereomers. The spectral data are consistent with those previously reported in the literature.[27] *Trans* isomer: ^{1}H NMR (500 MHz, CDCl$_3$): δ 7.71 (d, *J* = 8.6 Hz, 2H), 7.26 (d, *J* = 8.2 Hz, 2H), 4.02 (p, *J* = 6.4 Hz, 2H), 2.41 (s, 3H), 2.16-2.06 (m, 2H), 1.61-1.46 (m, 2H), 1.19 (d, *J* = 6.4 Hz, 6H). *Cis* isomer: ^{1}H NMR (500 MHz, CDCl$_3$): δ 7.74 (d, *J* = 8.5 Hz, 2H), 7.29 (d, *J* = 7.9 Hz, 2H), 3.67 (h, *J* = 6.3 Hz, 2H), 2.42 (s, 3H), 1.61-1.46 (m, 4H), 1.34 (d, *J* = 6.4 Hz, 6H).

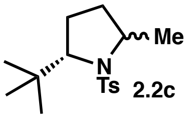

2.2c

(5*R*)-2-(*tert*-butyl)-5-methyl-1-tosylpyrrolidine (**2.2c**)

Utilizing **2.1c** and following Procedure D, **2.2c** was obtained as a white solid in 66% yield as a 60:40 mixture of *cis*/*trans* diastereomers. The spectral data are consistent with those previously reported in the literature.[19] *Cis* isomer: ^{1}H NMR (600 MHz, CDCl$_3$): δ 7.73 (d, *J* = 7.9 Hz, 2H), 7.30 (d, *J* = 7.9 Hz, 2H), 3.58-3.64 (m, *J* = 9.1 Hz, 2H), 2.43 (s, 3H), 1.73-1.65 (m, 4H), 1.37 (d, *J* = 6.4 Hz, 3H), 0.99 (s, 9H). *Trans* isomer: ^{1}H NMR (600 MHz, CDCl$_3$): δ 7.76 (d, *J* = 8.0 Hz, 2H), 7.26 (d, *J* = 8.7 Hz, 2H), 4.22 (dd, *J* = 9.5, 5.0 Hz, 1H), 3.43 (p, *J* = 6.0, 5.4, 4.3 Hz, 1H), 2.41 (s, 3H), 1.92-1.85 (m, 1H), 1.49 (tt, *J* = 12.6, 7.8 Hz, 1H), 1.27 (d, *J* = 7.0 Hz, 3H), 1.24-1.08 (m, 2H), 1.00 (s, 9H).

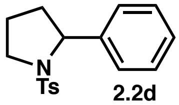

2.2d

2-phenyl-1-tosylpyrrolidine (**2.2d**)

Utilizing **2.1d** and following a modification of Procedure D, where TMSI (0.4 equiv) was added in 2 portions (at 0 and 6 hours) and stirred over a 12-hour period, **2.2d** was obtained as a white solid in 84% yield. The spectral data are consistent with those previously reported in the literature.[20] ^{1}H NMR (600 MHz, CDCl$_3$): δ 7.67 (d, *J* = 7.9 Hz, 2H), 7.30 (d, *J* = 4.3 Hz, 4H), 7.28 (d, *J* = 7.9 Hz, 2H), 7.23 (p, *J* = 4.2 Hz, 1H), 4.79 (dd, *J* = 8.1, 3.7 Hz, 1H), 3.62 (ddd, *J* = 10.9, 7.1, 4.7 Hz, 1H), 3.43 (dt, *J* = 10.3, 7.4 Hz, 1H), 2.43 (s, 3H), 2.02-1.94 (m, 1H), 1.89-1.78 (m, 2H), 1.66 (ddd, *J* = 12.7, 8.7, 3.9 Hz, 1H).

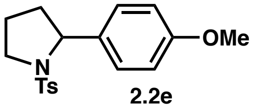

2.2e

2-(4-methoxyphenyl)-1-tosylpyrrolidine (**2.2e**)

Utilizing **2.1e** and following Procedure D, **2.2e** was obtained as a yellow solid in 87% yield. The spectral data are consistent with those previously reported in the literature. ^{1}H NMR (500 MHz, $CDCl_3$): δ 7.66 (d, *J* = 8.1 Hz, 2H), 7.28 (d, *J* = 8.0 Hz, 2H), 7.22 (d, *J* = 8.5 Hz, 2H), 6.83 (d, *J* = 8.6 Hz, 2H), 4.72 (dd, *J* = 7.9, 3.9 Hz, 1H), 3.79 (s, 3H), 3.60 (ddd, *J* = 10.1, 7.1, 4.8 Hz, 1H), 3.40 (dt, *J* = 10.1, 7.2 Hz, 1H), 2.42 (s, 3H), 1.95 (qd, *J* = 9.0, 7.3, 6.9, 4.1 Hz, 1H), 1.90-1.75 (m, 2H), 1.65 (dtd, *J* = 12.2, 4.9, 4.9, 2.1 Hz, 1H).

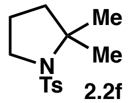
2.2f

2,2-dimethyl-1-tosylpyrrolidine (**2.2f**)

Utilizing **2.1f** and following Procedure D, **2.2f** was obtained as a white solid in 78% yield. The spectral data are consistent with those previously reported in the literature.[28] ^{1}H NMR (500 MHz, $CDCl_3$): δ 7.73 (d, *J* = 8.0 Hz, 2H), 7.27 (d, *J* = 6.6 Hz, 2H), 3.38 (t, *J* = 6.5 Hz, 2H), 2.41 (s, 3H), 1.86-1.72 (m, 4H), 1.44 (s, 6H).

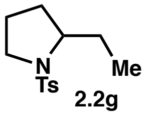
2.2g

2-ethyl-1-tosylpyrrolidine (**2.2g**)

Utilizing **2.1g** and following a modification of Procedure D, where TMSI (0.4 equiv) was added in 2 portions (at 0 and 6 hours) and stirred over a 12-hour period, **2.2g** was obtained as a white solid in 47% yield (with an additional 14% of recovered starting material **2.1g**). The spectral data are consistent with those previously reported in the literature.[29] ^{1}H NMR (600 MHz $CDCl_3$): δ 7.71 (d, *J* = 7.9 Hz, 2H), 7.30 (d, *J* = 7.9 Hz, 2H), 3.54 (dq, *J* = 10.4, 5.4 Hz, 1H), 3.37 (dt, *J* = 11.0, 6.1 Hz, 1H), 3.18 (dt, *J* = 10.5, 7.3 Hz, 1H), 2.42 (s, 3H), 1.85 (dt, *J* = 11.6, 7.9, 5.1 Hz, 1H), 1.76 (dtd, *J* = 14.8, 7.7, 7.1, 4.8 Hz, 1H), 1.56 (q, *J* = 6.5 Hz, 2H), 1.48 (ddq, *J* = 18.3, 12.3, 6.9, 6.2 Hz, 2H), 0.90 (t, *J* = 7.4 Hz, 3H).

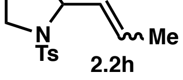
2.2h

(*E*)-2-(prop-1-en-1-yl)-1-tosylpyrrolidine (**2.2h**)

Utilizing **2.1h** and following Procedure D, **2.2h** was obtained as a yellow solid in 86% yield as a 91:9 mixture of *E/Z* isomers. The spectral data are consistent with those previously reported in the literature.[30] E isomer: ^{1}H NMR (600 MHz, $CDCl_3$): δ 7.71 (d, *J* = 8.1 Hz, 2H), 7.29 (d, *J* = 7.8 Hz, 2H), 5.66 (ddd, *J* = 15.2, 6.6, 1.2 Hz, 1H), 5.36 (ddq, *J* = 15.0, 6.7, 1.7 Hz, 1H), 4.10 (td, *J* = 7.4, 3.7 Hz, 1H), 3.41 (ddd, *J* = 10.2, 7.4, 5.0 Hz, 1H), 3.25 (dt, *J* = 10.1, 7.3

Hz, 1H), 2.42 (s, 3H), 1.80 (dddd, *J* = 14.2, 12.9, 6.5, 4.2 Hz, 1H), 1.73-1.68 (m, 1H), 1.66 (dq, *J* = 6.6, 1.6 Hz, 3H), 1.64-1.58 (m, 2H).
Z isomer: ^{1}H NMR (600 MHz, $CDCl_3$): δ 7.71 (d, *J* = 8.1 Hz, 2H), 7.29 (d, *J* = 7.8 Hz, 2H), 5.49 (dd, *J* = 11.2, 6.9 Hz, 1H), 5.41 (ddd, *J* = 10.8, 8.9, 1.7 Hz, 1H), 4.37 (q, *J* = 7.4 Hz, 1H), 3.41 (ddd, *J* = 10.2, 7.4, 5.0 Hz, 1H), 3.32 (td, *J* = 6.7, 3.1 Hz, 1H), 2.42 (s, 3H), 1.86 (ddt, *J* = 12.2, 6.9, 2.2 Hz, 1H), 1.73-1.68 (m, 4H), 1.64-1.58 (m, 2H).

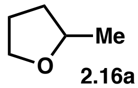

2.16a

2-methyltetrahydrofuran (**2.16a**)

Starting from 4-penten-1-ol (15.5 µL, 0.15 mmol, 1 equiv) and following a modification of Procedure D (reaction was conducted in an NMR tube with DCM-d_2 as solvent and mesitylene (20.9 µL, 0.15 mmol, 1 equiv) as an internal standard), **2.16a** was obtained in 84% NMR yield (yield calculated by comparison of the integration of key resonances to that of mesitylene; an additional 13% of unreacted 4-penten-1-ol was also observed). The spectral data are consistent with those previously reported in the literature.[31] ^{1}H NMR (500 MHz, CD_2Cl_2) δ 3.91 (dt, *J* = 7.8, 6.1 Hz, 1H), 3.84 (dt, *J* = 7.9, 6.0 Hz, 1H), 3.66 (dt, *J* = 8.0, 6.6 Hz, 1H), 2.03-1.80 (m, 3H), 1.39 (dq, *J* = 11.8, 7.9 Hz, 1H), 1.19 (d, *J* = 6.1 Hz, 3H).

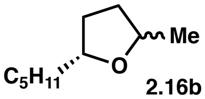

2.16b

2-methyl-5-pentyltetrahydrofuran (**2.16b**)

Utilizing **2.15b** and following Procedure D, **2.16b** was obtained as a colorless oil in 66% yield as a 85:15 mixture of *trans*/*cis* diastereomers. The spectral data are consistent with those previously reported in the literature.[32] *Trans* isomer: ^{1}H NMR (600 MHz, $CDCl_3$): δ 4.08 (dt, *J* = 7.9, 5.8 Hz, 1H), 3.96 (p, *J* = 6.6 Hz, 1H), 2.02 (qp, *J* = 8.6, 4.4 Hz, 2H), 1.53-1.40 (m, 2H), 1.38 (tt, *J* = 10.1, 4.8 Hz, 2H), 1.34-1.25 (m, 6H), 1.21 (d, *J* = 6.1 Hz, 3H), 0.88 (t, *J* = 6.8 Hz, 3H). *Cis* isomer: ^{1}H NMR (600 MHz, $CDCl_3$): δ 3.92 (dt, *J* = 12.7, 6.3 Hz, 1H), 3.77 (dt, *J* = 13.2, 6.5 Hz, 1H), 1.94 (q, *J* = 5.6, 4.9 Hz, 2H), 1.64-1.54 (m, 2H), 1.38 (tt, *J* = 10.1, 4.8 Hz, 2H), 1.34-1.25 (m, 6H), 1.23 (d, *J* = 6.1 Hz, 3H), 0.88 (t, *J* = 6.8 Hz, 3H).

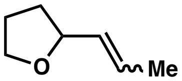

2.16c

2-(prop-1-en-1-yl)tetrahydrofuran (**2.16c**)

Starting from **2.15c** (16.8 mg, 0.15 mmol, 1 equiv) and following a modification of Procedure D (reaction was conducted in an NMR tube with DCM-d_2 as solvent and mesitylene (20.9 µL, 0.15 mmol, 1 equiv) as an internal standard), **2.16c** was obtained in 98% NMR yield (yield calculated by comparison of the integration of key resonances to those of mesitylene) as a

91:9 mixture of *trans*/*cis* diastereomers. The spectral data are consistent with those previously reported in the literature.[33] ^{1}H NMR (500 MHz, CD_2Cl_2) δ 5.67 (dq, *J* = 14.9, 6.0 Hz, 1H), 5.47 (ddd, *J* = 15.3, 7.3, 1.7 Hz, 1H), 4.19 (q, *J* = 7.2 Hz, 1H), 3.84 (q, *J* = 7.3 Hz, 1H), 3.72 (td, *J* = 7.9, 5.9 Hz, 1H), 2.08-1.82 (m, 3H), 1.69 (dd, *J* = 6.4, 1.2 Hz, 3H), 1.56 (dq, *J* = 12.0, 8.0 Hz, 1H).

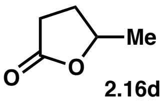

2.16d

5-methyldihydrofuran-2(3*H*)-one (**2.16d**)

Starting from 4-pentenoic acid (15.3 μL, 0.15 mmol, 1 equiv) and following a modification of Procedure D (reaction was conducted in an NMR tube with DCM-d_2 as solvent and mesitylene (20.9 μL, 0.15 mmol, 1 equiv) as an internal standard, TMSI (0.4 equiv) was added in two portions over a 24 hour period), **2.16d** was obtained in a 58% NMR yield (yield calculated by comparison of the integration of key resonances to that of mesitylene; an additional 30% of unreacted 4-pentenoic acid was also observed). The spectral data are consistent with those previously reported in the literature.[34] ^{1}H NMR (600 MHz, CD_2Cl_2) δ 4.64 (h, *J* = 6.7 Hz, 1H), 2.54 (dd, *J* = 9.2, 7.2 Hz, 2H), 2.36 (ddt, *J* = 27.3, 14.3, 7.4 Hz, 1H), 1.82 (dq, *J* = 12.8, 9.0 Hz, 1H), 1.40 (d, *J* = 6.1 Hz, 3H).

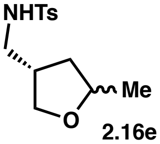

2.16e

4-methyl-*N*-((5-methyltetrahydrofuran-3-yl)methyl)benzenesulfonamide (**2.16e**)

Utilizing **2.15e** and following Procedure D, **2.16e** was obtained as a colorless oil in 56% yield (along with 31% of **2.2i,** see below) as a 66:33 mixture of *trans*/*cis* diastereomers.

Trans isomer: ^{1}H NMR (600 MHz, $CDCl_3$): δ 7.74 (d, *J* = 7.9 Hz, 2H), 7.31 (d, *J* = 7.9 Hz, 2H), 4.92 (q, *J* = 5.8 Hz, 1H), 3.86 (dt, *J* = 9.1, 6.0 Hz, 1H), 3.70 (t, *J* = 8.5 Hz, 1H), 3.55 (dd, *J* = 9.0, 4.9 Hz, 1H), 2.98-2.85 (m, 2H), 2.42 (s, 3H), 2.11 (ddd, *J* = 13.5, 8.1, 6.1 Hz, 1H), 1.72 (dt, *J* = 13.4, 6.7, 4.7 Hz, 1H), 1.21 (d, *J* = 6.0 Hz, 3H), 1.05 (dt, *J* = 12.5, 8.3 Hz, 1H).

Cis isomer: ^{1}H NMR (600 MHz, $CDCl_3$): δ 7.74 (d, *J* = 7.9 Hz, 2H), 7.31 (d, *J* = 7.9 Hz, 2H), 4.92 (q, *J* = 5.8 Hz, 1H), 3.99 (h, *J* = 6.5 Hz, 1H), 3.92 (t, *J* = 9.3, 6.9 Hz, 1H), 3.35 (dd, *J* = 9.0, 5.9 Hz, 1H), 2.98-2.85 (m, 2H), 2.42 (s, 3H), 2.40 (q, *J* = 6.3 Hz, 2H), 1.55 (dt, *J* = 12.7, 8.1 Hz, 1H), 1.16 (d, *J* = 6.1 Hz, 3H).

^{13}C NMR (151 MHz, $CDCl_3$) δ 143.7, 143.6, 136.9, 136.9, 129.9, 129.9, 127.2, 127.1, 74.7, 70.9, 70.8, 47.0, 46.1, 39.9, 39.5, 37.8, 37.1, 21.7, 21.1, 20.8, 20.8; IR (film) 3277, 2928, 1157 cm^{-1}; HRMS (ESI) calculated for $[C_{13}H_{19}NO_3SNa]^+$ $[M+Na]^+$: *m/z* 292.0978, found 292.0976.

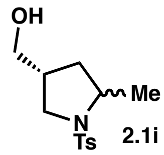

2.1i

(5-methyl-1-tosylpyrrolidin-3-yl)methanol (**2.2i**)

Utilizing **2.15e** and following Procedure D, **2.2i** was obtained as a colorless oil in 31% yield (along with 56% of **2.16e,** see above) as a 75:25 mixture of *cis*/*trans* diastereomers.

Cis isomer: ^{1}H NMR (500 MHz, CDCl$_3$): δ 7.71 (dd, *J* = 8.3, 2.4 Hz, 2H), 7.31 (d, *J* = 8.0 Hz, 2H), 3.61-3.45 (m, 4H), 3.19 (dd, *J* = 11.2, 8.7 Hz, 1H), 2.43 (s, 3H), 2.05 (dt, *J* = 13.4, 7.1 Hz, 1H), 1.86 (ddd, *J* = 15.7, 8.7, 6.7 Hz, 1H), 1.59 (ddd, *J* = 10.3, 6.6, 3.4 Hz, 1H), 1.40 (d, *J* = 6.2 Hz, 3H).

Trans isomer: ^{1}H NMR (500 MHz, CDCl$_3$): δ 7.71 (dd, *J* = 8.3, 2.4 Hz, 2H), 7.31 (d, *J* = 8.0 Hz, 2H), 3.78 (td, *J* = 7.0, 3.5 Hz, 1H), 3.61-3.45 (m, 1H), 3.38 (dd, *J* = 10.6, 6.1 Hz, 1H), 3.27 (dd, *J* = 10.7, 7.2 Hz, 1H), 2.94 (dd, *J* = 10.0, 7.8 Hz, 1H), 2.48 (dd, *J* = 15.0, 7.4 Hz, 1H), 2.43 (s, 3H), 1.50 (dt, *J* = 12.5, 8.4 Hz, 1H), 1.31 (d, *J* = 6.2 Hz, 3H), 1.28 (dd, *J* = 9.2, 3.2 Hz, 1H).

^{13}C NMR (126 MHz, CDCl$_3$) δ 143.5, 143.4, 134.8, 134.7, 129.8, 129.7, 127.7, 127.6, 64.3, 63.9, 56.7, 55.8, 52.2, 51.3, 40.0, 39.5, 37.5, 36.1, 23.2, 23.0, 21.7, 21.7; IR (film) 3519, 2930, 1159 cm^{-1}; HRMS (ESI) calculated for [C$_{13}$H$_{19}$NO$_3$SNa]$^+$ [M+Na]$^+$: *m/z* 292.0978, found 292.0977.

Robustness Screen

A simplified robustness screen as recently reported by Glorius and coworkers has been conducted to evaluate the stability of acid-sensitive functional groups to our newly developed reaction conditions as well as compare the stability of these acid-sensitive functional groups to triflic acid-mediated reaction conditions previously reported by Hartwig and coworkers. This screen involves conducting a standard reaction in the presence of one molar equivalent of a given additive. Then, after a pre-determined reaction time, the yield of the product, the starting material remaining, and the remaining additive is determined by gas chromatography (GC) analysis. The calibration of the additives, starting material, and the product was undertaken using the single point calibration technique. The tables below show the effect of a given additive on the standard reaction. For the product (**2.2a**) yield and the additive recovery, the % yields are color coded for ready assessment: green (above 66%), yellow (34-66%), red (below 34%).

TMSI sample procedure:

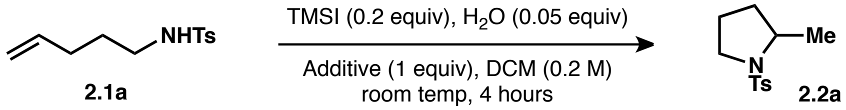
NHTs
2.1a
TMSI (0.2 equiv), H2O (0.05 equiv)
Additive (1 equiv), DCM (0.2 M)
room temp, 4 hours
Me
N
Ts
2.2a

A stock solution of tosylamide **2.1a** (1.196 g, 5.00 mmol) and pre-saturated water in DCM (2.25 mL wet DCM, 0.25 mmol water) was prepared and diluted with dry DCM (0.2 M, total volume of 25 mL) in a volumetric flask. Each additive (0.20 mmol) was added to its own flame-dried vial equipped with a stir bar and Teflon septum. To each nitrogen-flushed vial was then added a portion of the stock solution (1.0 mL, 0.20 mmol **2.1a**), followed by TMSI (5.7 µL, 0.04 mmol). The reaction mixtures were then allowed to stir at room temperature. After 4 hours, mesitylene (28 µL, 0.20 mmol) was added and the mixture was quenched with saturated sodium bicarbonate (2 mL) and sodium sulfite (1 mL). An aliquot of the DCM solution was then taken for GC analysis.

Triflic acid sample procedure:

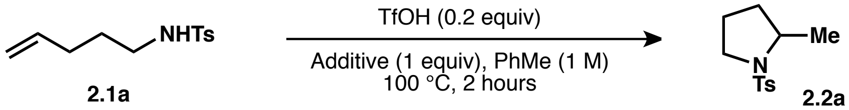

A stock solution of tosylamide **2.1a** (5.98 g, 25.0 mmol) was prepared and diluted with dry toluene (1 M, total volume of 25 mL) in a volumetric flask. Each additive (0.40 mmol) was added to its own flame-dried vial equipped with a stir bar and Teflon septum. To each nitrogen-flushed vial was then added a portion of the stock solution (0.4 mL, 0.40 mmol **2.1a**), followed by triflic acid (7.1 µL, 0.08 mmol). The vial was then tightly capped and heated to 100 °C and held at this temperature for 2 hours. Once cooled, mesitylene (56 µL, 0.40 mmol) was added and the mixture was quenched with saturated sodium bicarbonate (2 mL) and sodium sulfite (1 mL). An aliquot of the toluene solution was then taken for GC analysis.

Group A: Acid Sensitive Functional Groups - TMSI Conditions

Entry	Additive	Amount (0.20 mmol)	% Yield of 2.2a	% Additive Remaining	Starting Material (2.1a) Remaining
A1	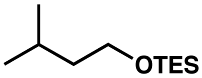	40.5 mg	X 31	X 25	74
A2	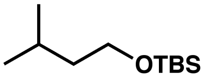	40.5 mg	- 58	✓ 67	41
A3	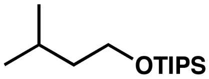	48.9 mg	X 15	- 63	86
A4	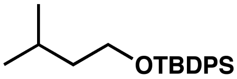	65.3 mg	✓ 84	✓ 78	15
A5	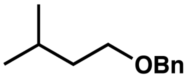	35.7 mg	X 21	✓ 86	84
A6	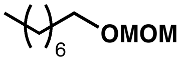	34.9 mg	X 0	X 28	75
A7	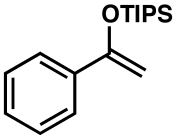	55.3 mg	X 0	X 0	> 95
A8	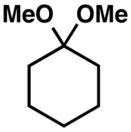	28.8 mg	X 1	- 63	> 95
A9	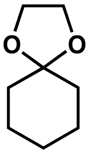	28.4 mg	✓ 87	✓ 68	13
A10	none	-	✓ 92	-	6

Group B: Lewis Basic Functional Groups - TMSI Conditions

Entry	Additive	Amount (0.20 mmol)	% Yield of 2.2a	% Additive Remaining	Starting Material (2.1a) Remaining
B1	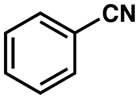	20.6 μL	✓ 92	✓ > 95	5
B2	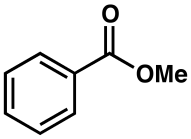	23.0 μL	✓ 93	✓ > 95	4
B3	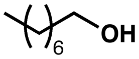	31.6 μL	✗ 8	✓ 94	95
B4	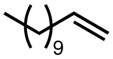	45.6 μL	✗ 30	✓ > 95	74
B5	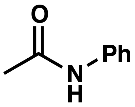	29.8 mg	✗ 1	✓ > 95	> 95
B6	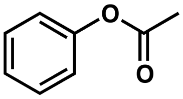	25.4 μL	✓ 93	✓ > 95	5
B7	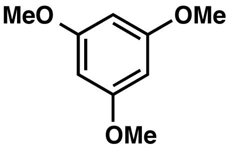	42.0 mg	✓ 90	✓ > 95	8
B8	none	-	✓ 95	-	2

Group A: Acid Sensitive Functional Groups - TfOH Conditions

Entry	Additive	Amount (0.20 mmol)	% Yield of 2.2a	% Additive Remaining	Starting Material (2.1a) Remaining
A1	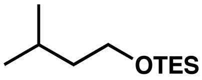	40.5 mg	✓ 91	X 21	3
A2	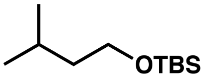	40.5 mg	✓ 93	- 59	3
A3	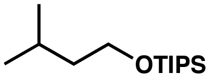	48.9 mg	✓ 87	✓ 84	6
A4	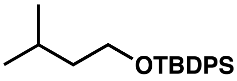	65.3 mg	- 49	✓ 69	50
A5	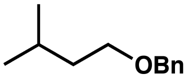	35.7 mg	✓ 91	X 25	1
A6	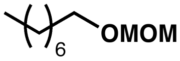	34.9 mg	X 3	X 0	0
A7	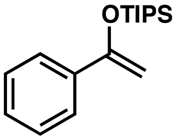	55.3 mg	X 1	X 3	> 95
A8	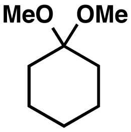	28.8 mg	✓ 86	X 0	2
A9	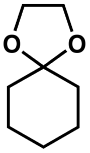	28.4 mg	✓ 94	X 0	2
A10	none	-	✓ 96	-	0

Group B: Lewis Basic Functional Groups - TfOH Conditions

Entry	Additive	Amount (0.20 mmol)	% Yield of 2.2a	% Additive Remaining	Starting Material (2.1a) Remaining
B1	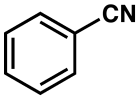	20.6 µL	✓ > 95	✓ 94	0
B2	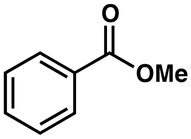	23.0 µL	✓ > 95	✓ > 95	0
B3	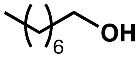	31.6 µL	✓ 75	✓ 93	21
B4	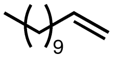	45.6 µL	✓ 93	X 33	1
B5	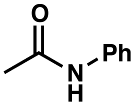	29.8 mg	X 4	✓ > 95	> 95
B6	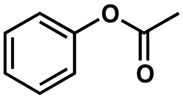	25.4 µL	✓ > 95	✓ 92	1
B7	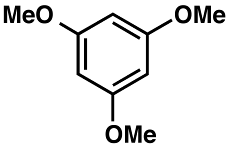	42.0 mg	✓ > 95	✓ > 95	0
B8	none	-	✓ > 95	-	0

2.10 References and Notes

[1] For a general review on hydroamination, see: Muller, T. E.; Hultzsch, K. C.; Yus, M.; Foubelo, F.; Tada, M. *Chem. Rev.* **2008,** *108,* 3795-3892.

[2] Johns, A. M.; Sakai, N.; Ridder, A.; Hartwig, J. F. *J. Am. Chem. Soc.* **2006**, *128*, 9306-9307.

[3] Steinborn, D.; Taube, R. *Z. Chem.* **1986**, *26*, 349-359.

[4] Beller, M.; Seayad, J.; Tillack, A.; Jioa, H. *Angew, Chem., Int. Ed.* **2004,** *43,* 3368-3398.

[5] Huang, L,; Arndt, M.; Gooßen, K; Heydt, H.; Gooßen, L. J. *Chem. Rev.* **2015** *115*, 2596-2697.

[6] Markovnikov, V. V. *Ann. Chem. Pharm.* **1870**, *153*, 228-259.

[7] Schlummer, B.; Hartwig, J. F. *Org. Lett.* **2002,** *4,* 1471-1474.

[8] For Brønsted acid-catalyzed hydroaminations, see: a) Schlummer, B.; Hartwig, J. F. *Org. Lett.* **2002,** *4,* 1471-1474; b) Haskins, C. M.; Knight, D. W. *Chem. Commun.* **2002**, *22,* 2724-2725; c) Anderson, L. L.; Arnold, J.; Bergman, R. G. *J. Am. Chem. Soc.* **2005,** *127,* 14542-14543; d) Yin, Y.; Zhao, G. *Heterocycles* **2006**, *68*, 23-31; e) Marcsekova, K.; Doye, S. *Synthesis* **2007,** *1,* 145-154; f) Ackermann, L.; Kaspar, L. T.; Althammer, A. *Org. Biomol. Chem.* **2007**, *5*, 1975-1978.

[9] Leger, P. R.; Murphy, R. A.; Pushkarskaya, E.; Sarpong, R. *Chem. Eur. J.* **2015**, *21,* 4377-4383.

[10] Shortly after the publication of our findings, a report by Shibuya and coworkers came out detailing new conditions for intramolecular hydroetherification of unactivated olefins. In their system, a combination of iodine (10 mol%) and phenylsilane (20 mol%) is used in order to generate $PhSiH_2I$, the proposed active catalyst in the transformation. In contrast to our conclusions, they propose that silylation of the hydroxyl group is responsible for the increased reaction rate under these conditions, in a similar manner to our initial proposal. Fujita, S.; Abe, M.; Shibuya, M.; Yamamoto, Y. *Org. Lett.* **2015***, 17*, 3822-3825.

[11] National Institute of Standards and Technology Solubility Database. https://srdata.nist.gov/solubility/sol_detail.aspx?goBack=Y&sysID=60_242 (accessed Oct 18, 2016).

[12] Chervin, S. M.; Abada, P.; Koreeda, M. *Org. Lett.* **2000**, *2*, 369-372.

[13] a) Laughlin, R. G. *J. Am. Chem. Soc.* **1967,** *89,* 4268-4271; b) Shainyan, B. A.; Chipanina, N. N.; Oznobikhina, L. P. *J. Phys. Org. Chem.* **2012,** *25,* 738-747.

[14] a) Kawatsura, M.; Hartwig, J. F. *J. Am. Chem. Soc.* **2000,** *122,* 9546-9547; b) Muller, T. E.; Grosche, M.; Herdtweck, E.; Pleier, A.-K.; Walter, E.; Yan, Y.-K. *Organometallics* **2000,** *19,* 170-183; c) Burling, S.; Field, L. D.; Messerle, B. A.; Turner, P. *Organometallics* **2004,** *23,* 1714-1721; d) Brunet, J.-J.; Chu, N.-C.; Rodriguez-Zubiri, M. *Eur. J. Inorg. Chem.* **2007,** *30,* 4711-4722.

[15] a) Anderson, L. L.; Arnold, J.; Bergman, R. G. *J. Am. Chem. Soc.* **2005,** *127,* 14542-14543; b) Ackermann, L.; Kaspar, L. T.; Althammer, A. *Org. Biomol. Chem.* **2007**, *5*, 1975-1978.

[16] Streitwieser, A.; Kim, Y.-J. *J. Am. Chem. Soc.* **2000,** *122,* 11783-11786.

[17] a) Collins, K. D.; Glorius, F. *Nat. Chem.* **2013**, *5*, 597-601; b) Collins, K. D.; Rühling, A.; Glorius, F. *Nat. Protoc.* **2014**, *9*, 1348-1353; c) Collins, K. D.; Rühling, A.; Lied, F.; Glorius, F. *Chem. Eur. J.* **2014**, *20*, 3800-3805.

[18] Zhang, G.; Cui, L.; Wang, Y.; Zhang, L. *J. Am. Chem. Soc.* **2010,** *132,* 1474-1475.

[19] Sherman, E. S.; Fuller, P. H.; Kasi, D.; Chemler, S. R. *J. Org. Chem.* **2007**, *72*, 3896-3905.

[20] Larock, Y.; Weinreb, H. *J. Org. Chem.* **1994**, *59*, 4172-4178.

[21] Cernak, T. A.; Lambert, T. H. *J. Am. Chem. Soc.* **2009**, *131*, 3124-3125.

[22] [a] Pierson, J. M.; Ingalls, E. L.; Vo, R. D.; Michael, F. E. *Angew. Chem. Int. Ed.,* **2013,** *52*, 13311-13313. [b] Yamamoto, H.; Sasaki, I.; Shiomi, S.; Yamasaki, N.; Imagawa, H. *Org. Lett.* **2012**, *14*, 2266-2269.

[23] Moretti, J. D.; Wang, X.; Curran, D. P. *J. Am. Chem. Soc.* **2012**, *134*, 7963–7970.

[24] Willems, L. I.; Verdoes, M.; Florea, B. I.; van der Marel, G. A.; Overkleeft, H. S. *Chem. Bio. Chem.* **2010,** *11*, 1769-1781.

[25] Terao, K.; Toshimitsu, A.; Uemura, S. *J. Chem. Soc., Perkin Trans. 1* **1986**, 1837-1844.

[26] Andrés, J. M.; Herráiz-Sierra, I.; Pedrosa, R.; Pérez-Encabo, A. *Eur. J. Org. Chem.* **2000**, 1719-1726.

[27] Baeckvall, J.-E.; Schink, H. E.; Renko, Z. D. *J. Org. Chem.* **1990**, *55*, 826-831.

[28] Henry-Riyad, H.; Kobayashi, S.; Tidwell, T. T. *Arkivoc*, **2005**, *6*, 266-276.

[29] Shi, W.; Bai, C.-M.; Zhu, K.; Cui, D.-M.; Zhang, C. *Tetrahedron*, **2014**, *70*, 434-438.

[30] Cochet, T.; Bellosta, V.; Roche, D.; Ortholand, J.-Y.; Greiner, A.; Cossy, J. *Chem. Commun.* **2012**, *48*, 10745-10747.

[31] Gellert, B. A.; Kahlcke, N.; Feurer, M.; Roth, S. *Chem. Eur. J.* **2011**, 12203-12209.

[32] Mihailovic, M. L.; Cekovic, Z.; Maksimovic, Z.; Jeremic, D.; Lorenc, L.; Mamuzic, R. I. *Tetrahedron,* **1965,** *21,* 2799-2812.

[33] Yamamoto, H.; Shiomi, S.; Odate, D.; Sasaki, I.; Namba, K.; Imagawa, H.; Nishizawa, M. *Chem. Lett.* **2010,** *39*, 830-831.

[34] Jhulki, S.; Seth, S.; Mondal, M.; Moorthy, J. N. *Tetrahedron*, **2014,** *70*, 2286-2293.

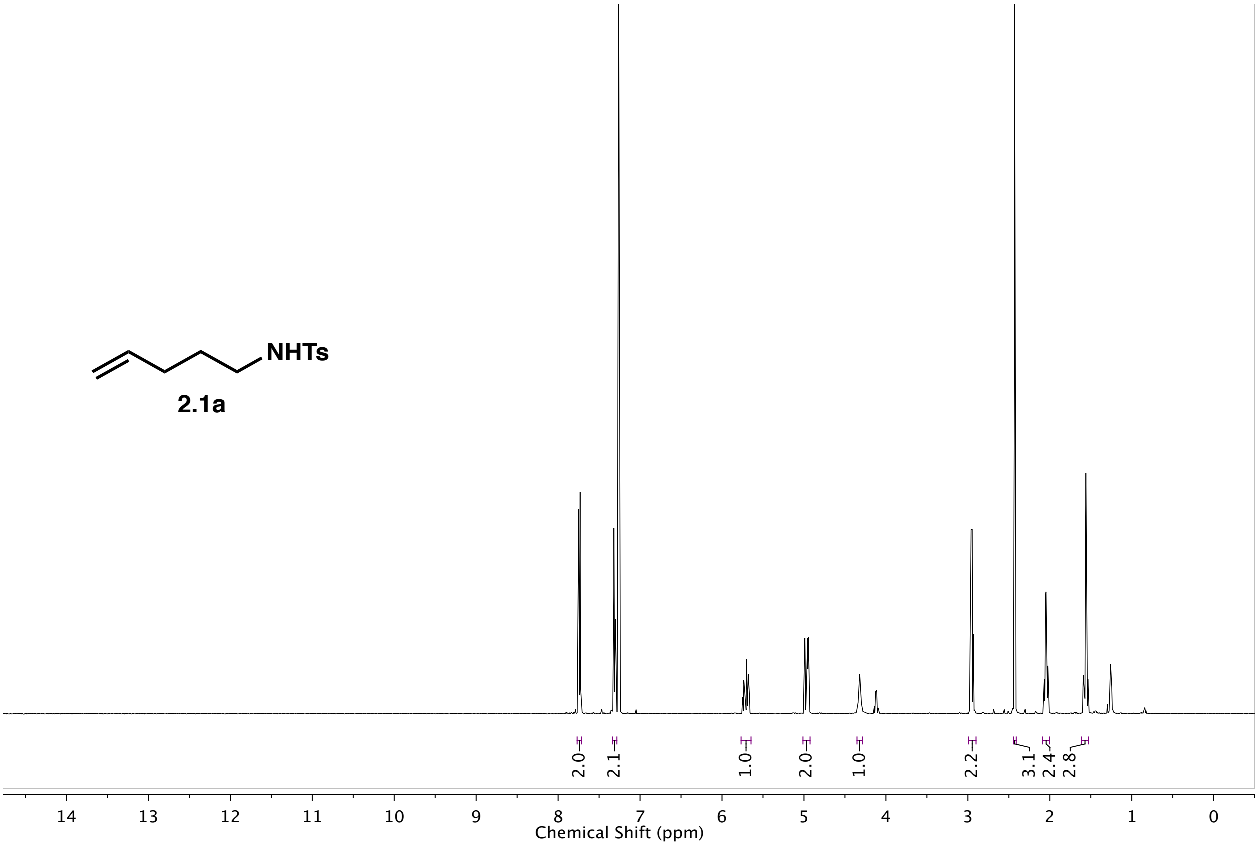
NHTs
2.1a
2.0
2.1
1.0
2.0
1.0
2.2
3.1
2.4
2.8
14
13
12
11
10
9
8
7
6
5
4
3
2
1
0
Chemical Shift (ppm)

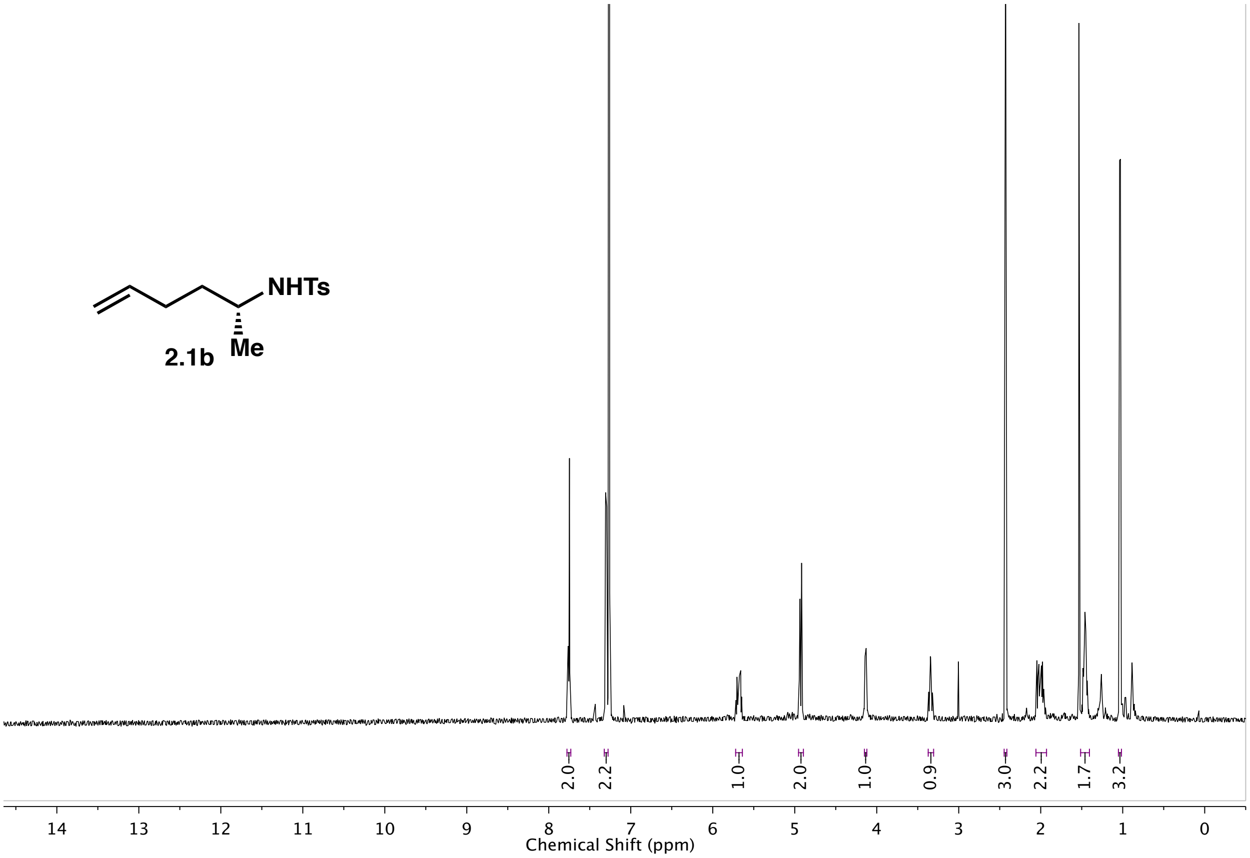
NHTs
Me
2.1b
2.0
2.2
1.0
2.0
1.0
0.9
3.0
2.2
1.7
3.2
14
13
12
11
10
9
8
7
6
5
4
3
2
1
0
Chemical Shift (ppm)

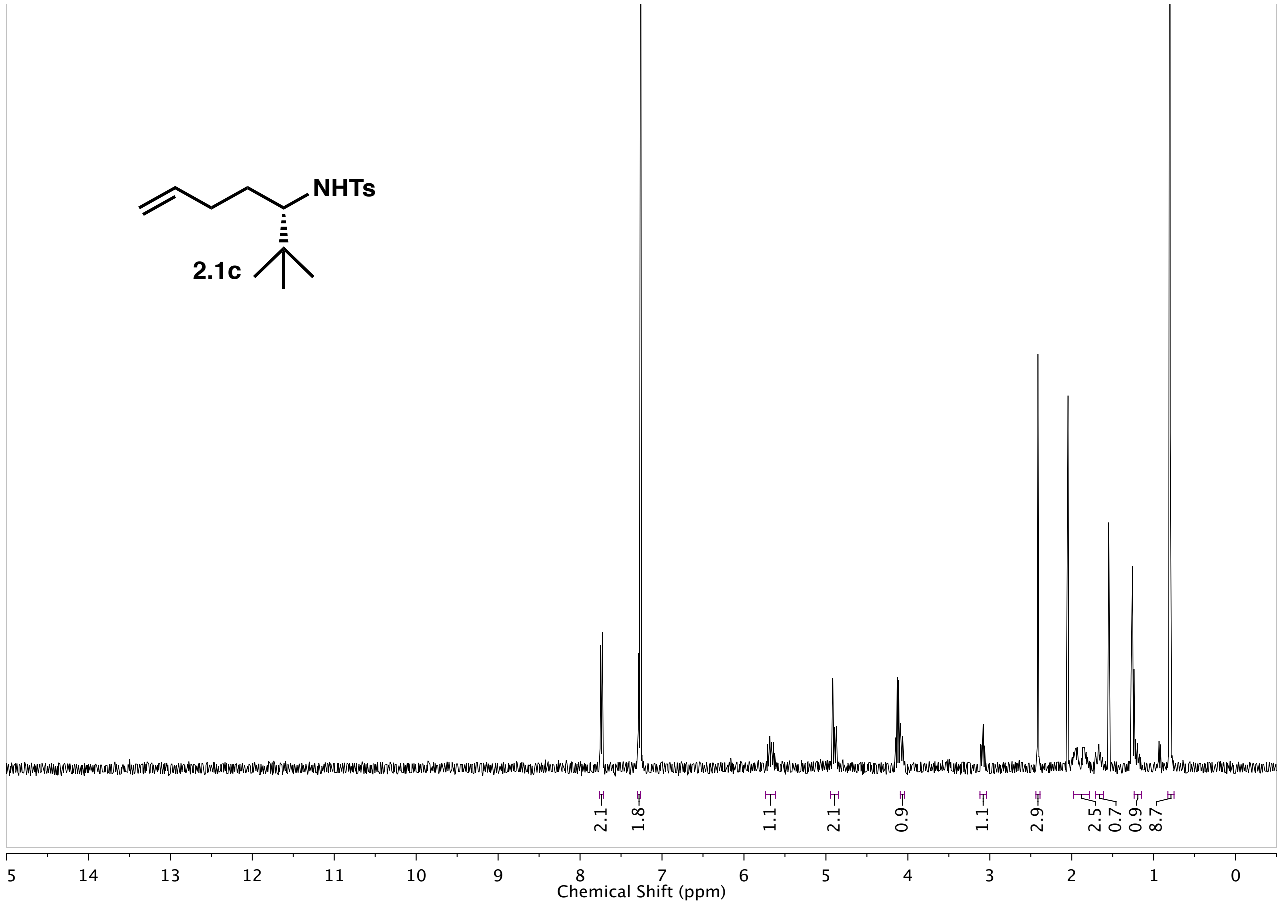
NHTs
2.1c
2.1
1.8
1.1
2.1
0.9
1.1
2.9
2.5
0.7
0.9
8.7
5
14
13
12
11
10
9
8
7
6
5
4
3
2
1
0
Chemical Shift (ppm)

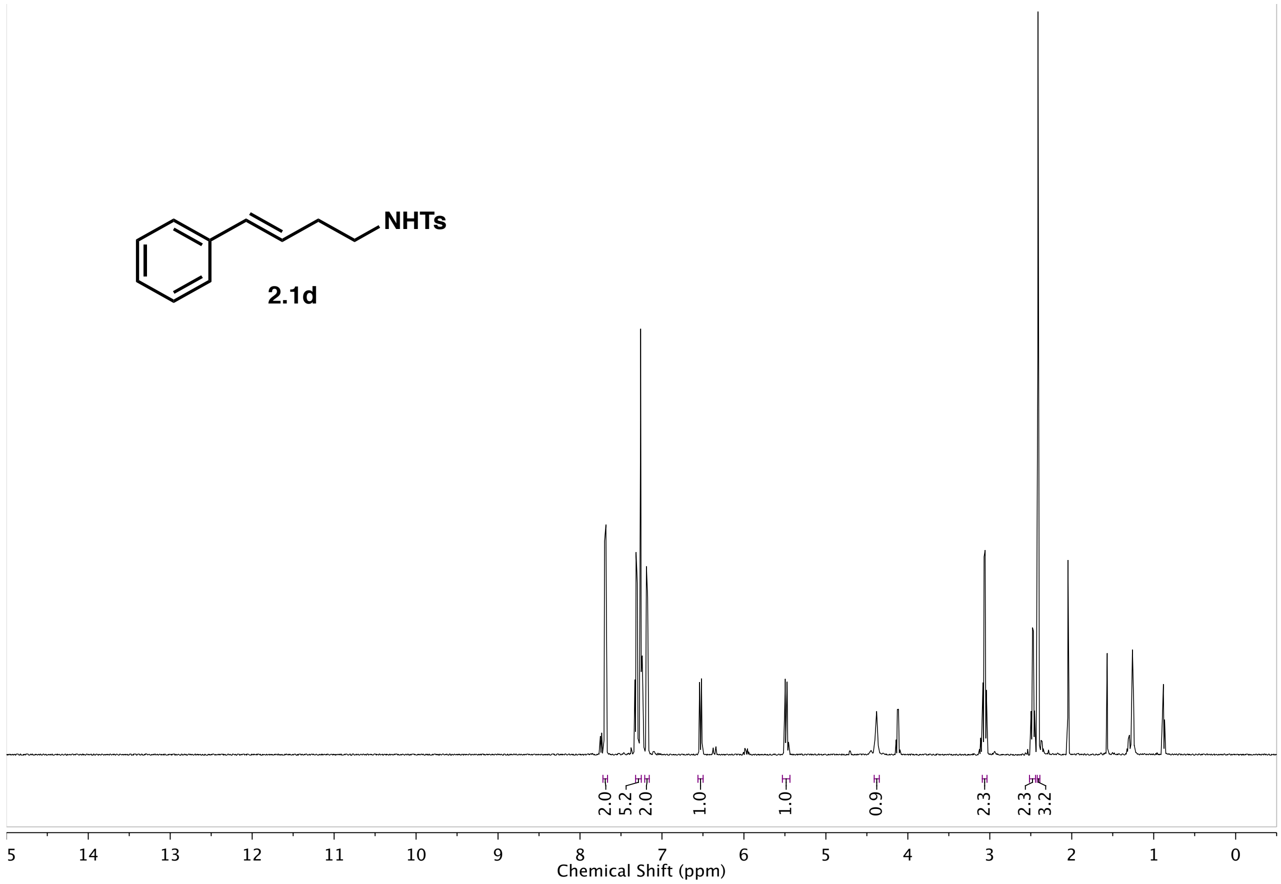
NHTs
2.1d
2.0
5.2
2.0
1.0
1.0
0.9
2.3
2.3
3.2
5
14
13
12
11
10
9
8
7
6
5
4
3
2
1
0
Chemical Shift (ppm)

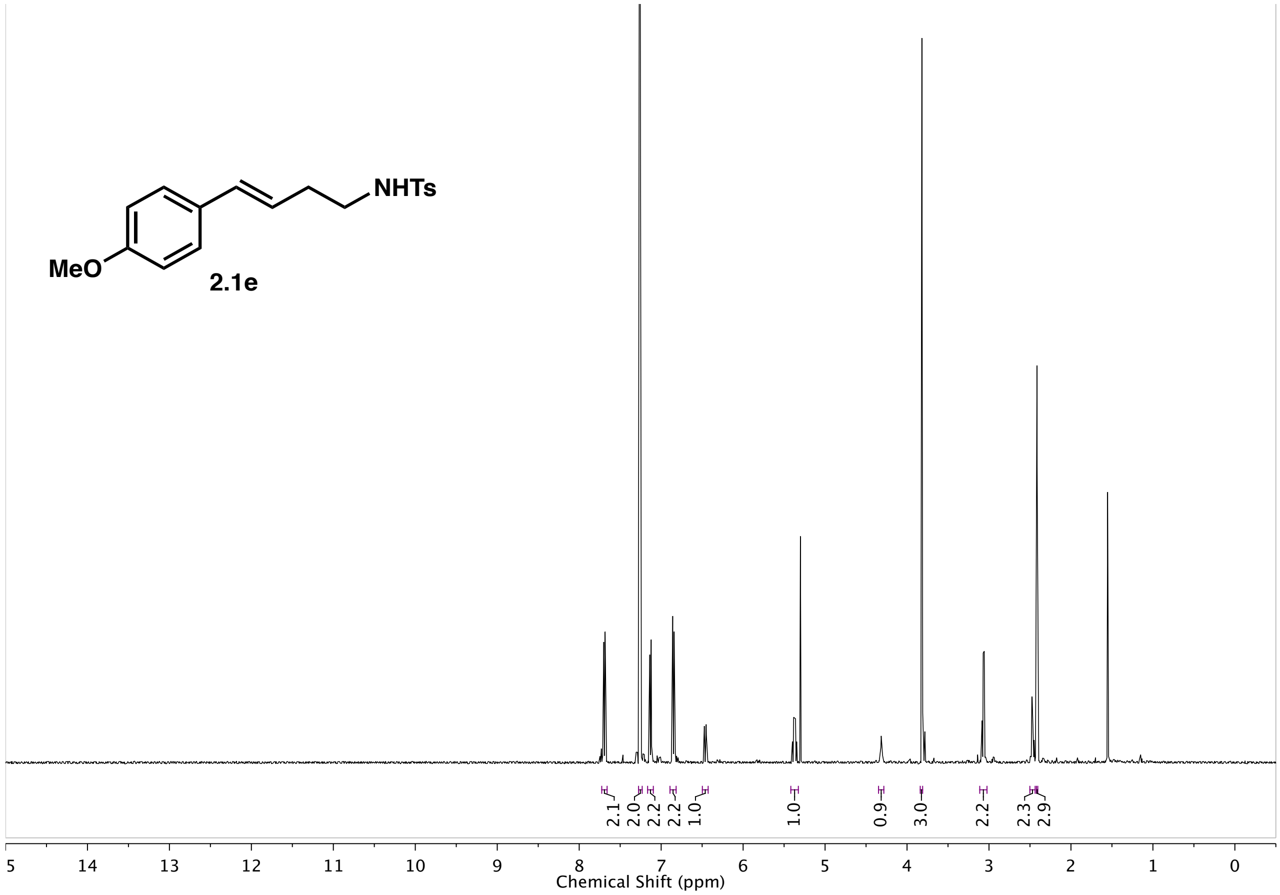
2.1e
MeO
NHTs
2.1
2.0
2.2
2.2
1.0
1.0
0.9
3.0
2.2
2.3
2.9
5
14
13
12
11
10
9
8
7
6
5
4
3
2
1
0
Chemical Shift (ppm)

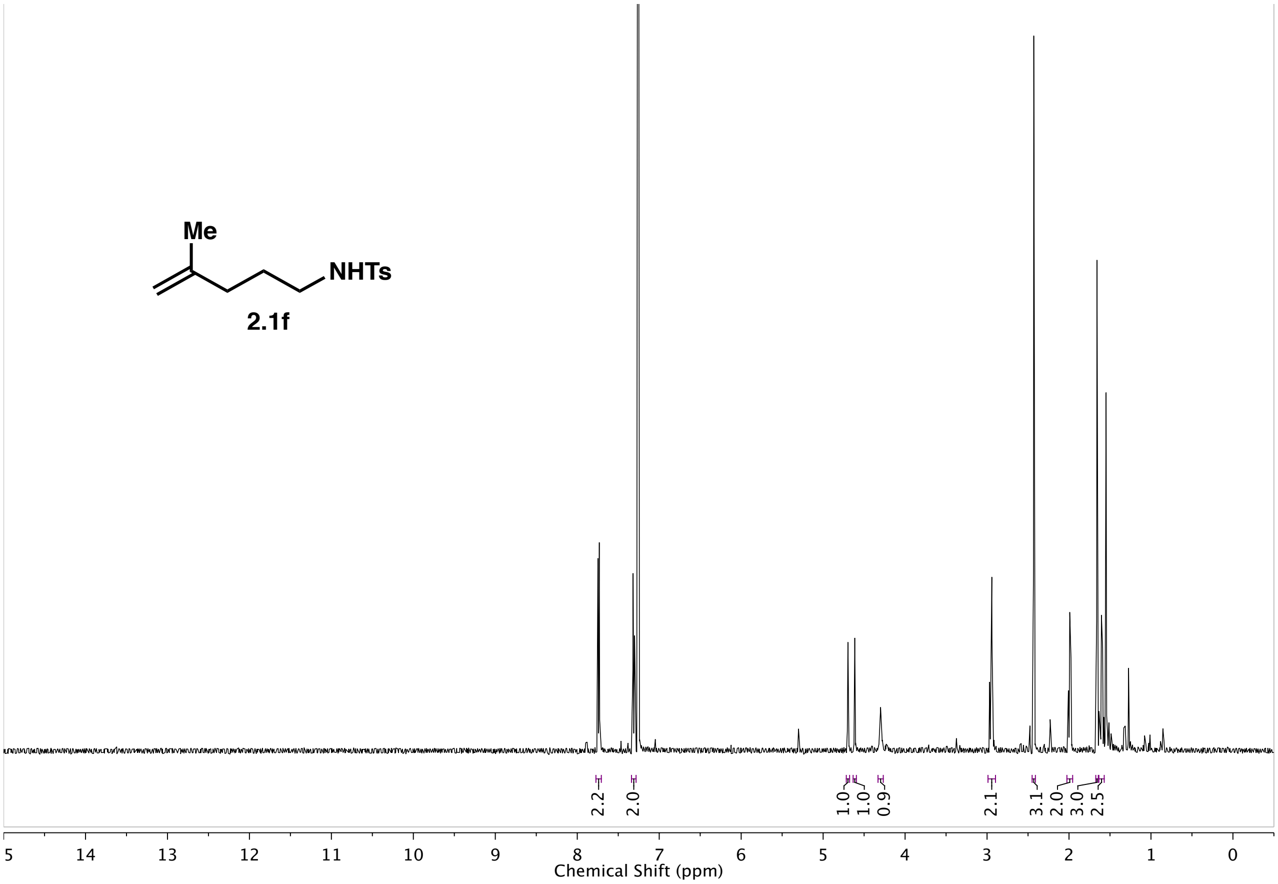
2.1f
Me
NHTs
2.2
2.0
1.0
1.0
0.9
2.1
3.1
2.0
3.0
2.5
5
14
13
12
11
10
9
8
7
6
5
4
3
2
1
0
Chemical Shift (ppm)

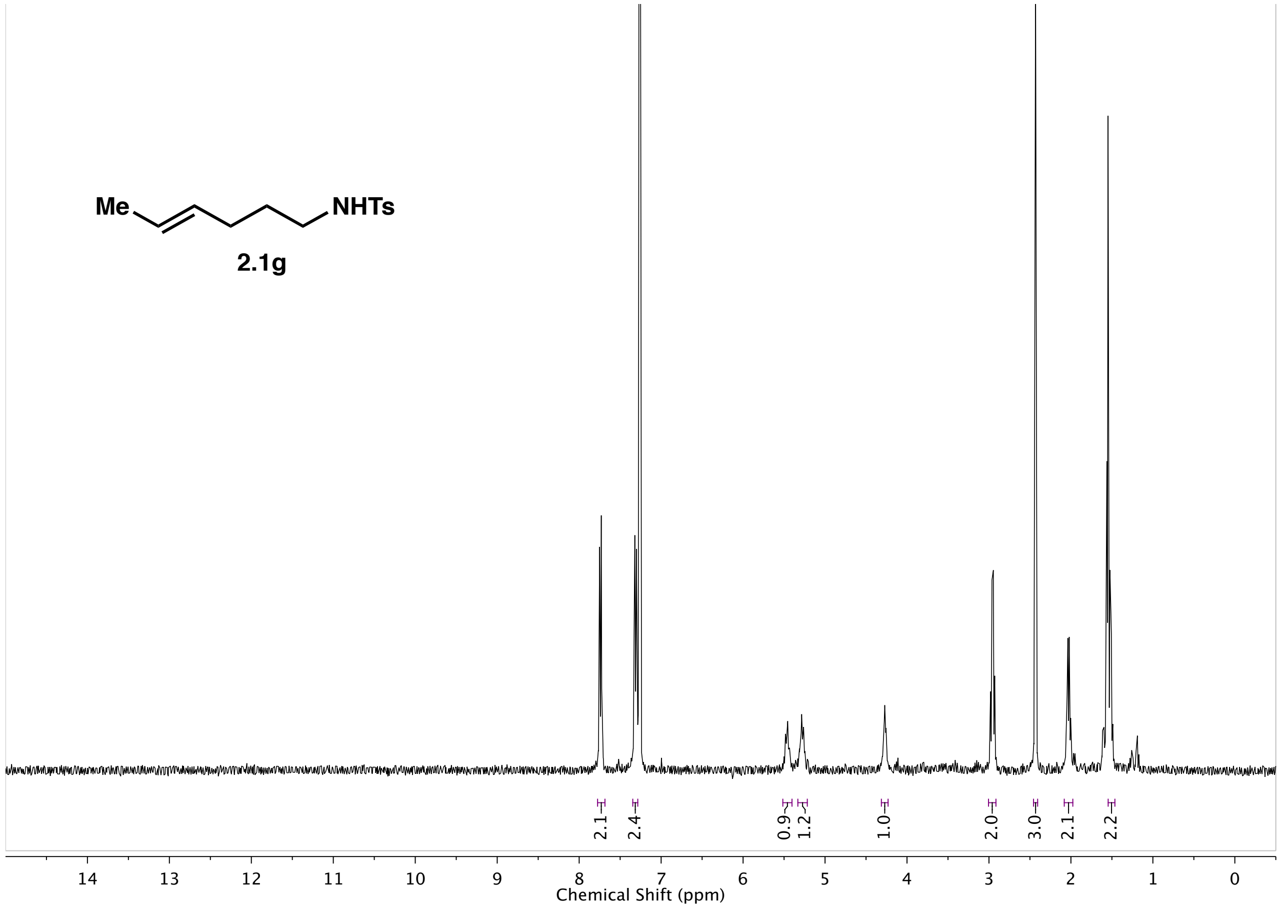
Me
NHTs
2.1g
2.1
2.4
0.9
1.2
1.0
2.0
3.0
2.1
2.2
14
13
12
11
10
9
8
7
6
5
4
3
2
1
0
Chemical Shift (ppm)

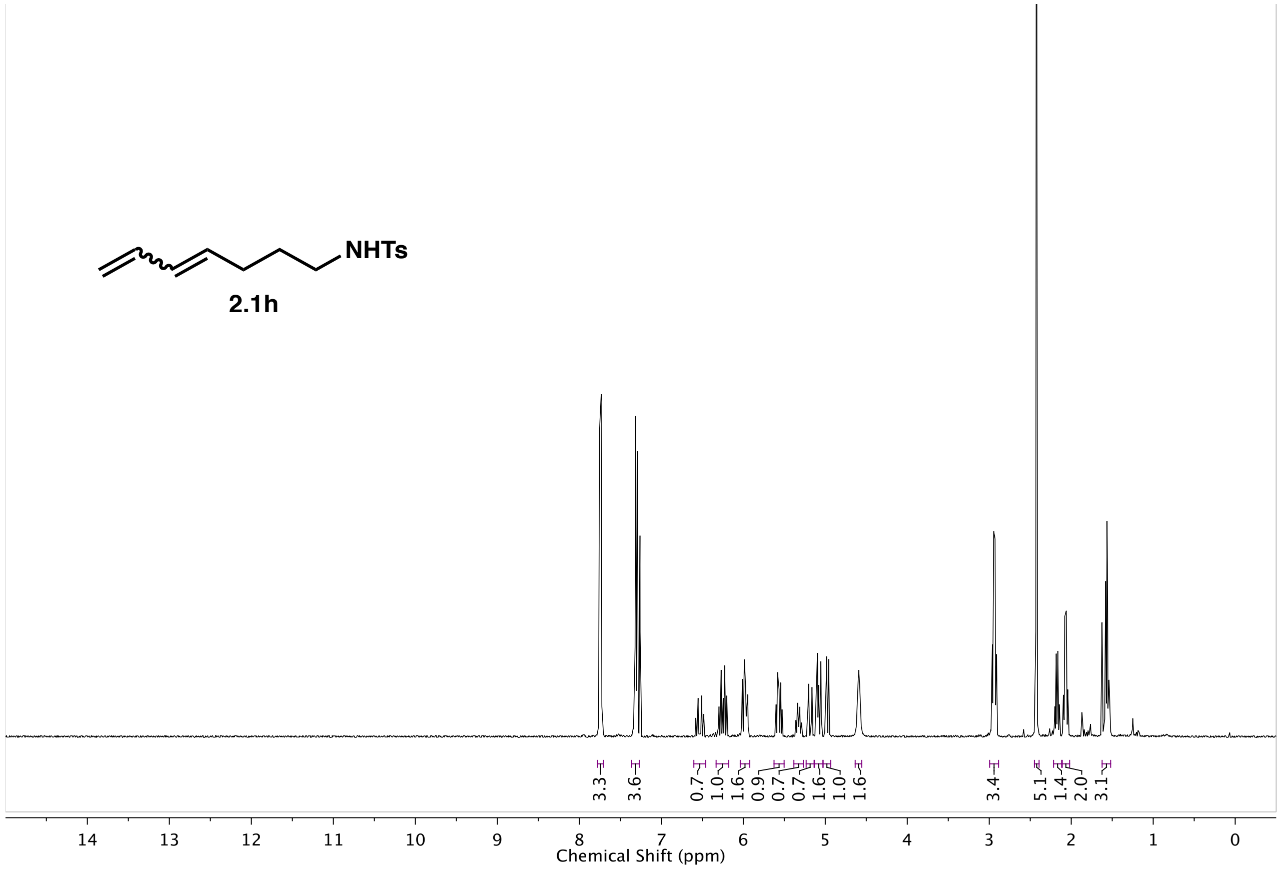
NHTs
2.1h
3.3
3.6
0.7
1.0
1.6
0.9
0.7
0.7
1.6
1.0
1.6
3.4
5.1
1.4
2.0
3.1
14
13
12
11
10
9
8
7
6
5
4
3
2
1
0
Chemical Shift (ppm)

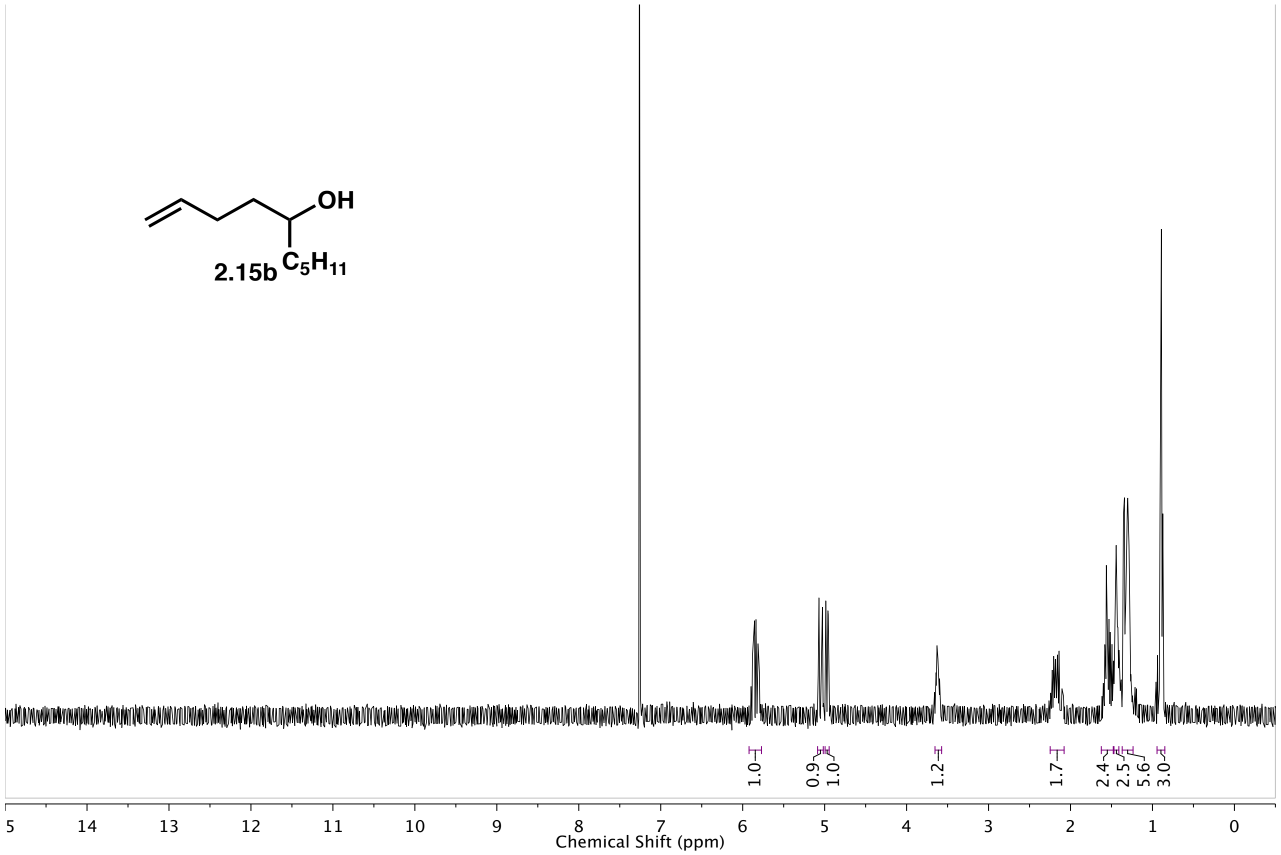
OH
C_5H_{11}
2.15b
1.0
0.9
1.0
1.2
1.7
2.4
2.5
5.6
3.0
5
14
13
12
11
10
9
8
7
6
5
4
3
2
1
0
Chemical Shift (ppm)

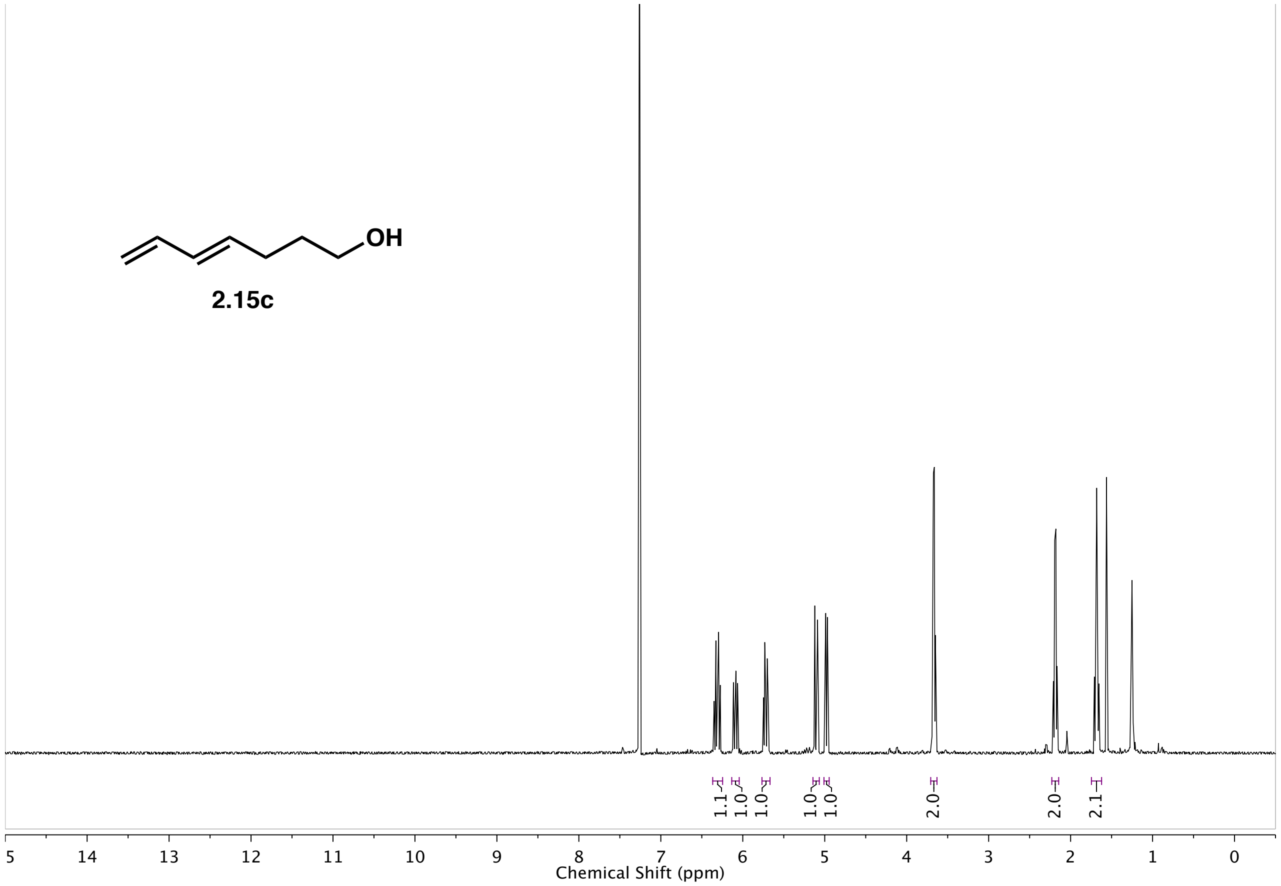
OH
2.15c
1.1
1.0
1.0
1.0
1.0
2.0
2.0
2.1
5
14
13
12
11
10
9
8
7
6
5
4
3
2
1
0
Chemical Shift (ppm)

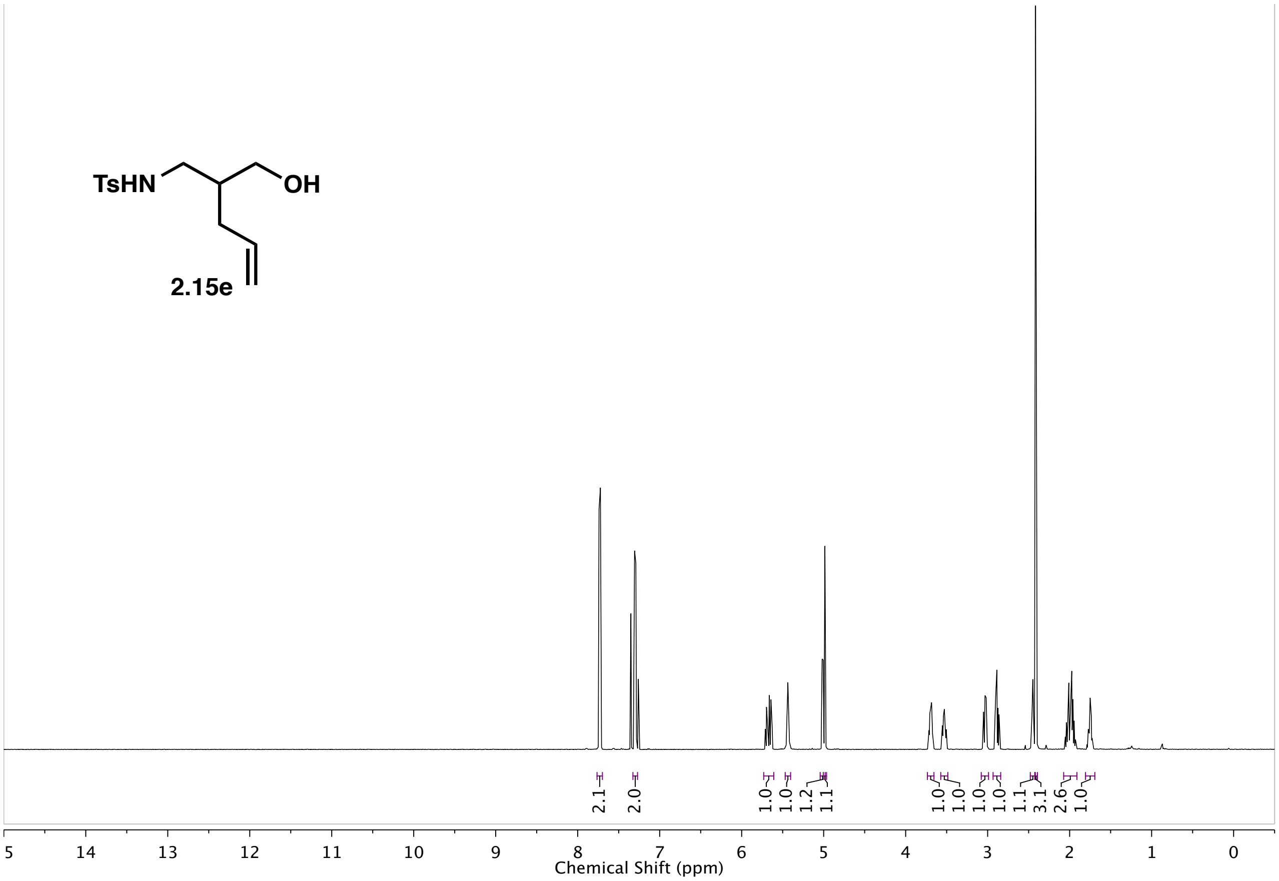
TsHN
OH
2.15e
2.1
2.0
1.0
1.0
1.2
1.1
1.0
1.0
1.0
1.0
1.1
3.1
2.6
1.0
5
14
13
12
11
10
9
8
7
6
5
4
3
2
1
0
Chemical Shift (ppm)

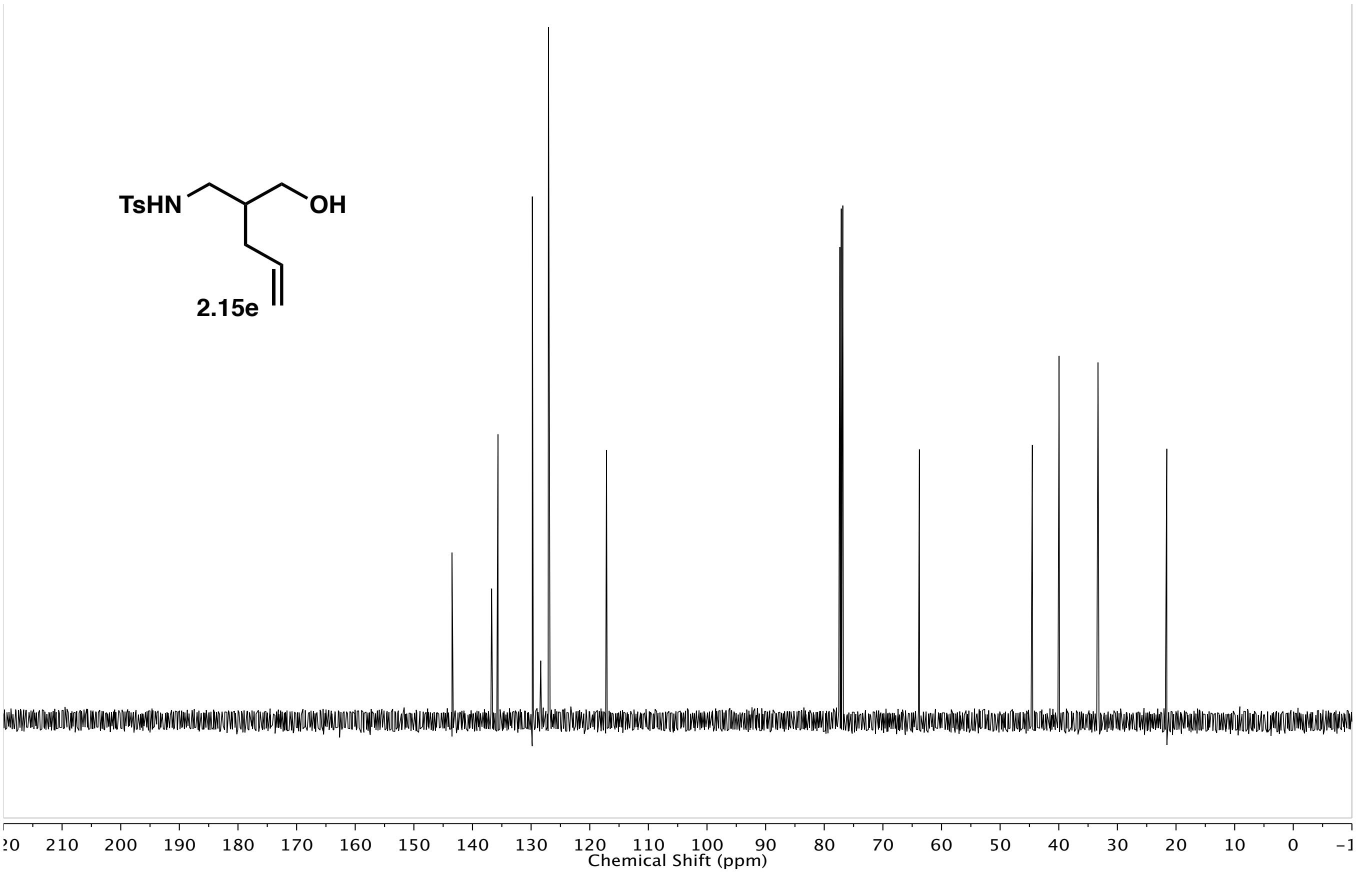
TsHN
OH
2.15e
20
210
200
190
180
170
160
150
140
130
120
110
100
90
80
70
60
50
40
30
20
10
0
-1
Chemical Shift (ppm)

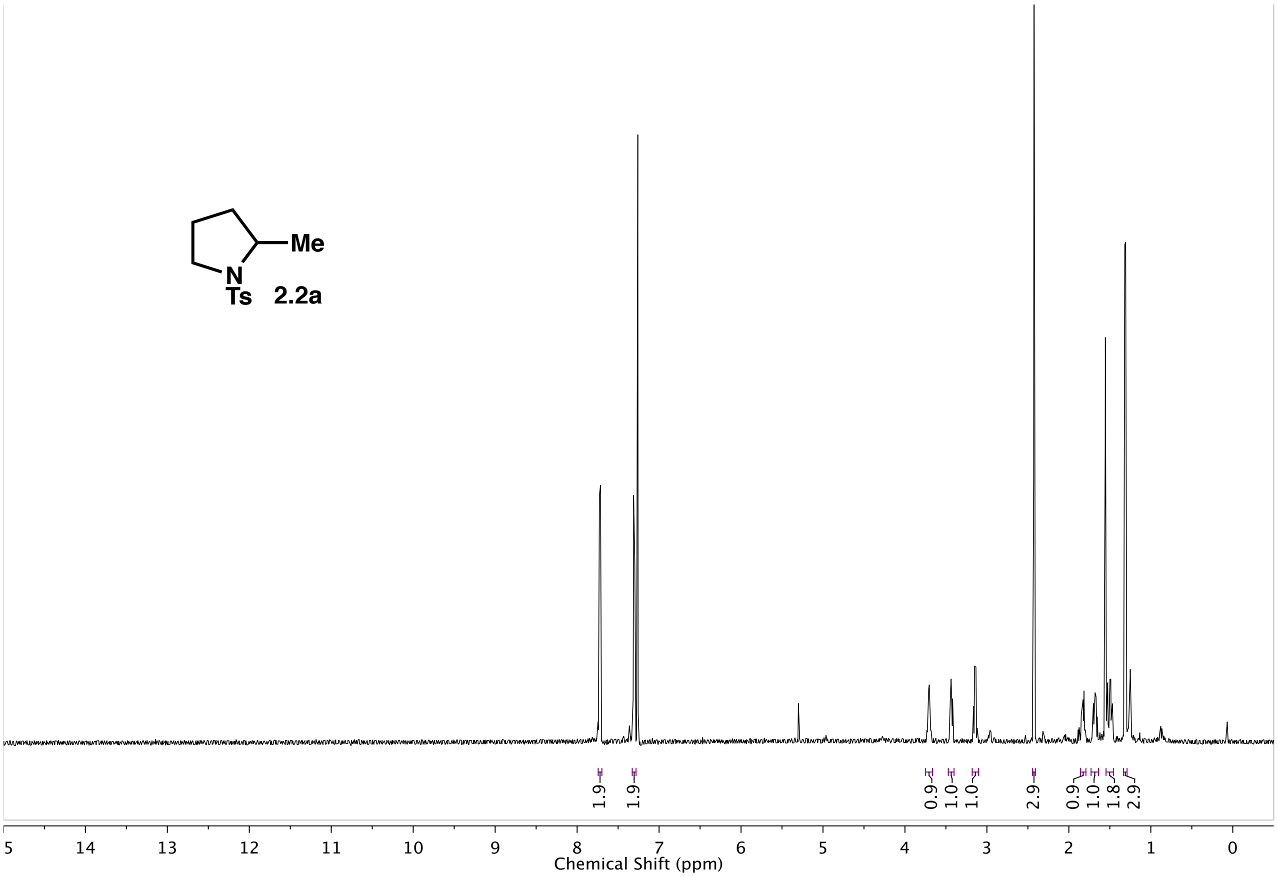
2.2a

Me
N
Ts
1.9
1.9
0.9
1.0
1.0
2.9
0.9
1.0
1.8
2.9
5
14
13
12
11
10
9
8
7
6
5
4
3
2
1
0
Chemical Shift (ppm)

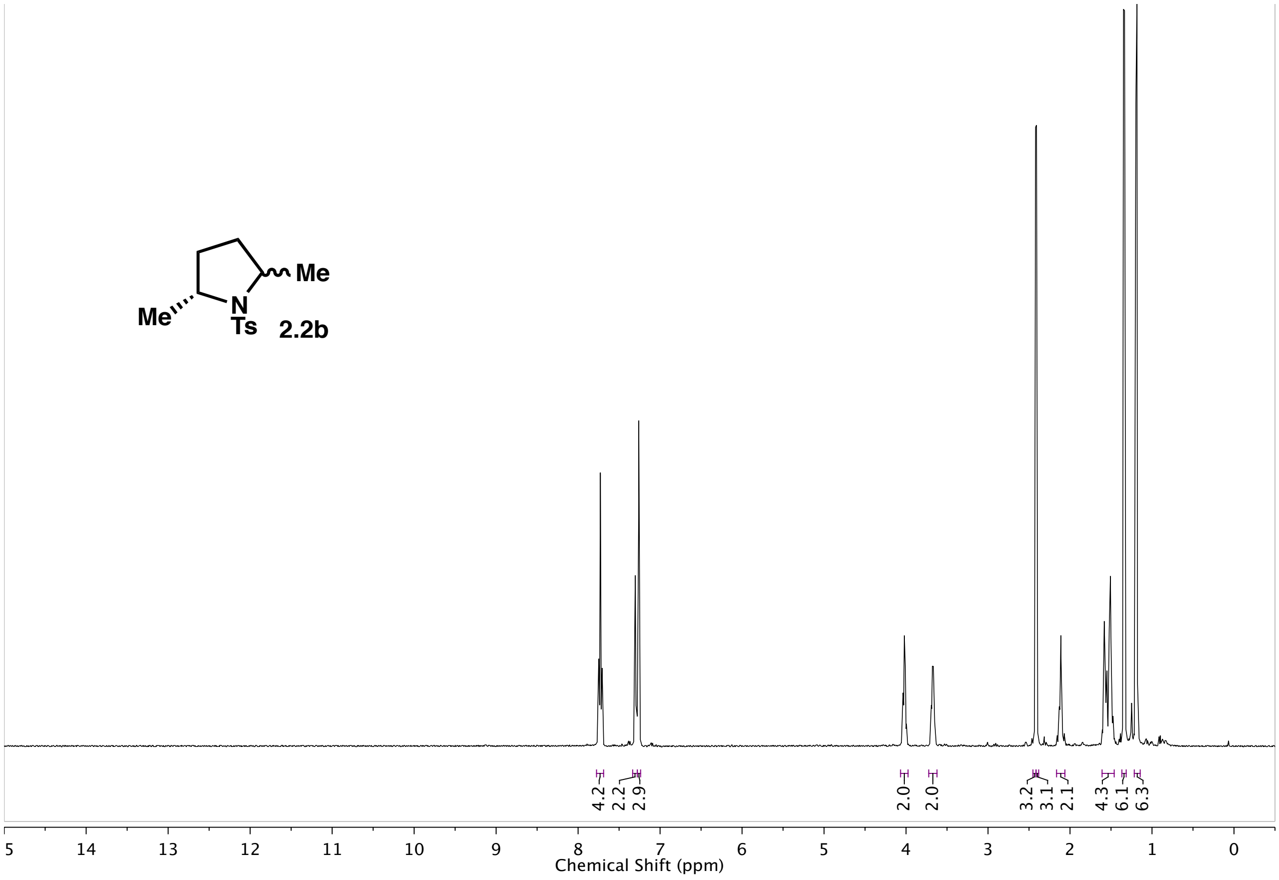
2.2b

Me
Me
N
Ts
4.2
2.2
2.9
2.0
2.0
3.2
3.1
2.1
4.3
6.1
6.3
5
14
13
12
11
10
9
8
7
6
5
4
3
2
1
0
Chemical Shift (ppm)

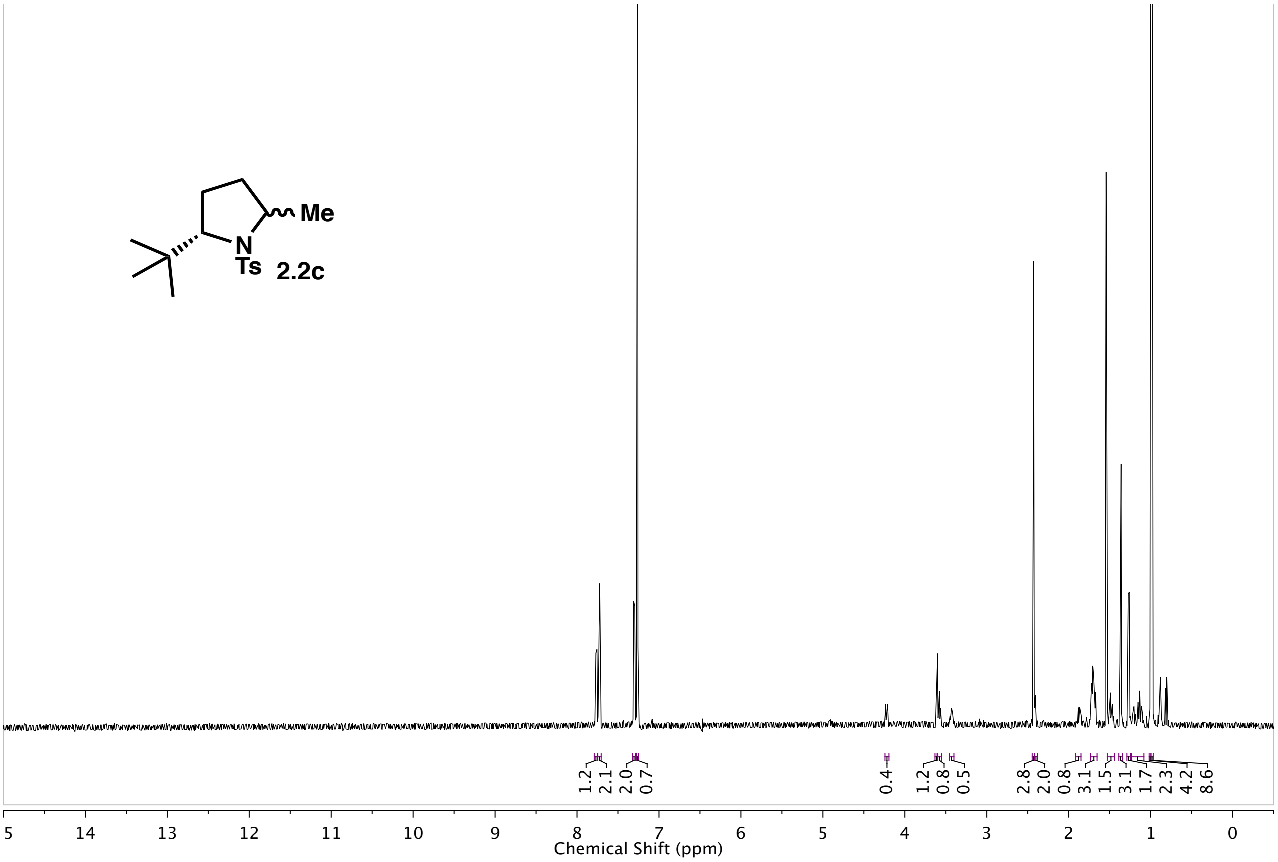
Me
N
Ts
2.2c
1.2
2.1
2.0
0.7
0.4
1.2
0.8
0.5
2.8
2.0
0.8
3.1
1.5
3.1
1.7
2.3
4.2
8.6
5
14
13
12
11
10
9
8
7
6
5
4
3
2
1
0
Chemical Shift (ppm)

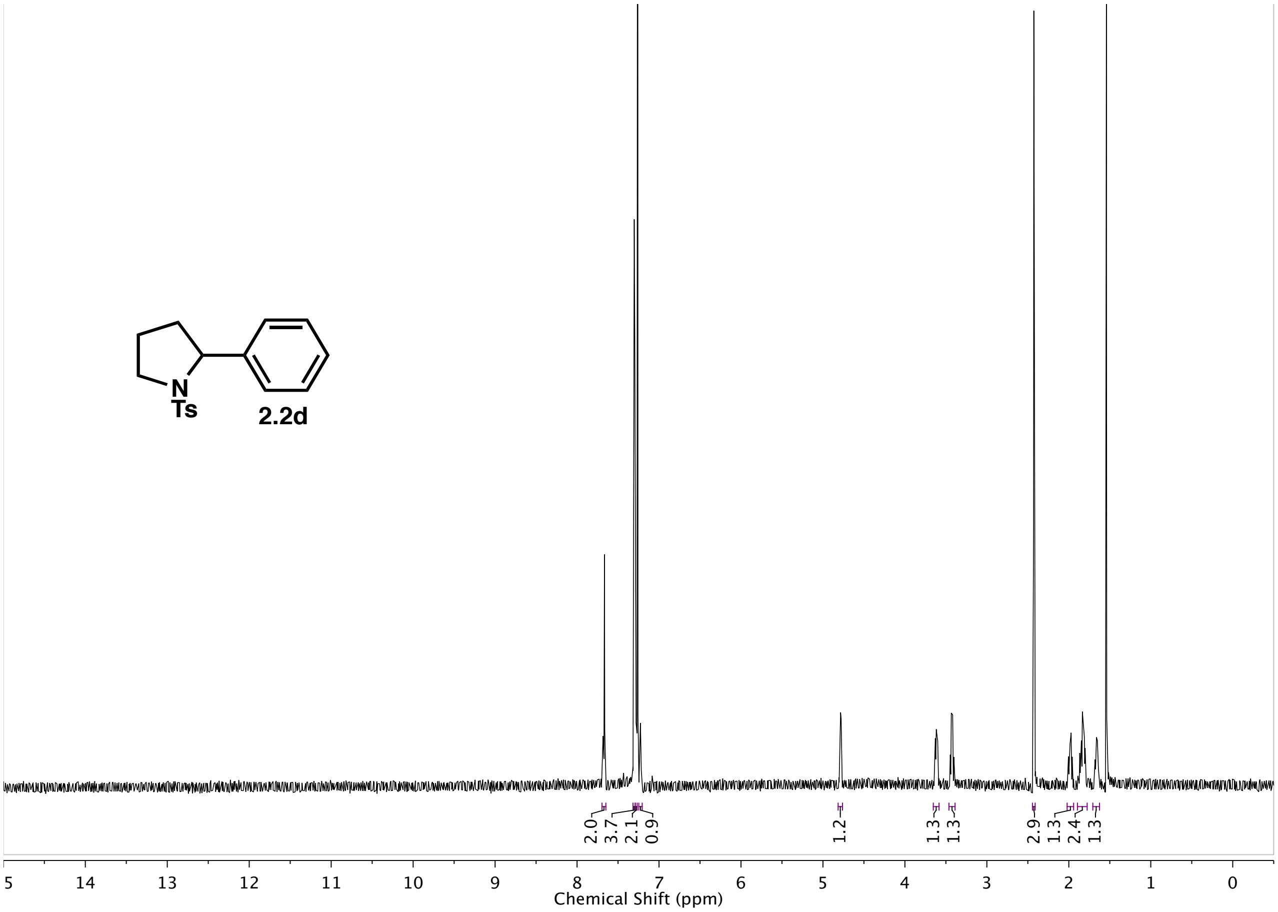
N
Ts
2.2d
2.0
3.7
2.1
0.9
1.2
1.3
1.3
2.9
1.3
2.4
1.3
5
14
13
12
11
10
9
8
7
6
5
4
3
2
1
0
Chemical Shift (ppm)

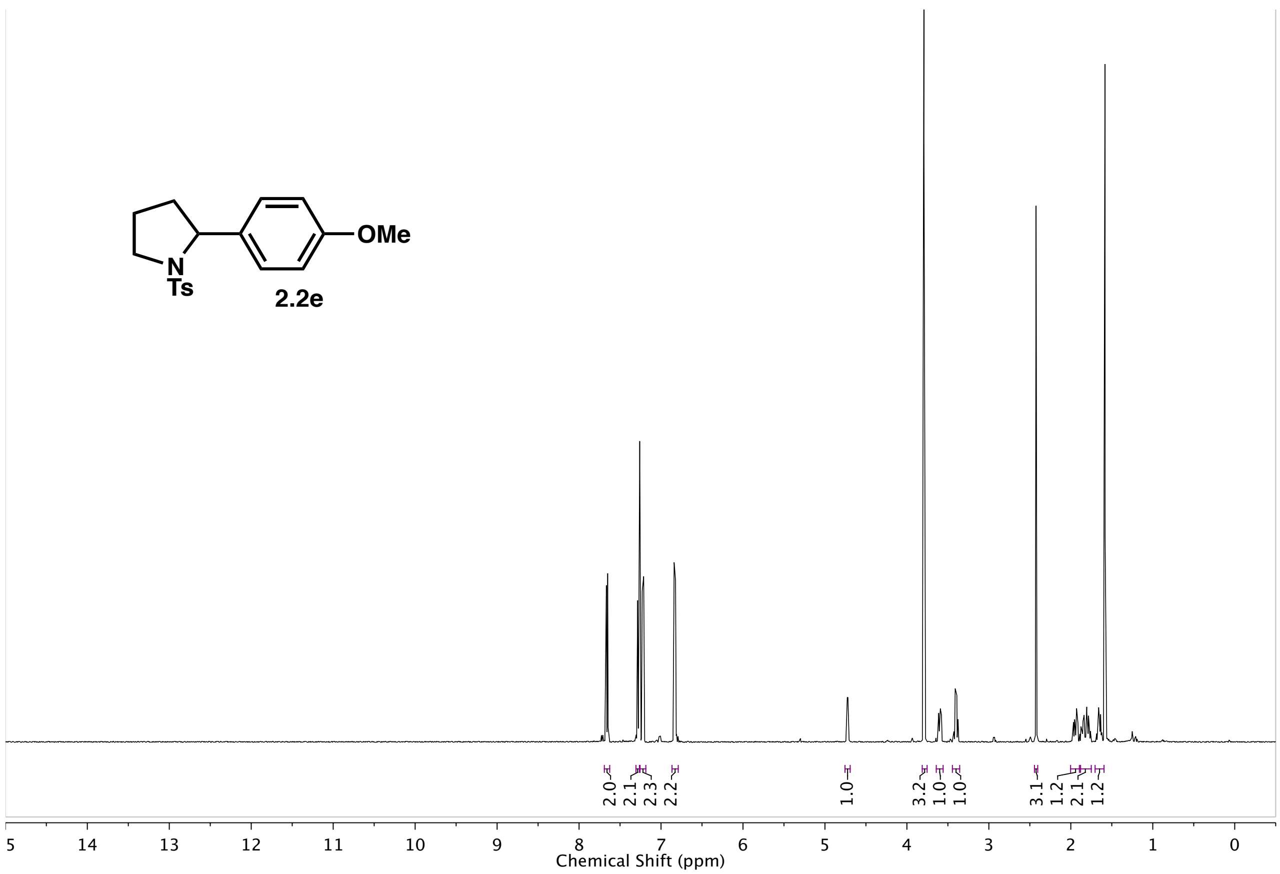
OMe
N
Ts
2.2e
2.0
2.1
2.3
2.2
1.0
3.2
1.0
1.0
3.1
1.2
2.1
1.2
5
14
13
12
11
10
9
8
7
6
5
4
3
2
1
0
Chemical Shift (ppm)

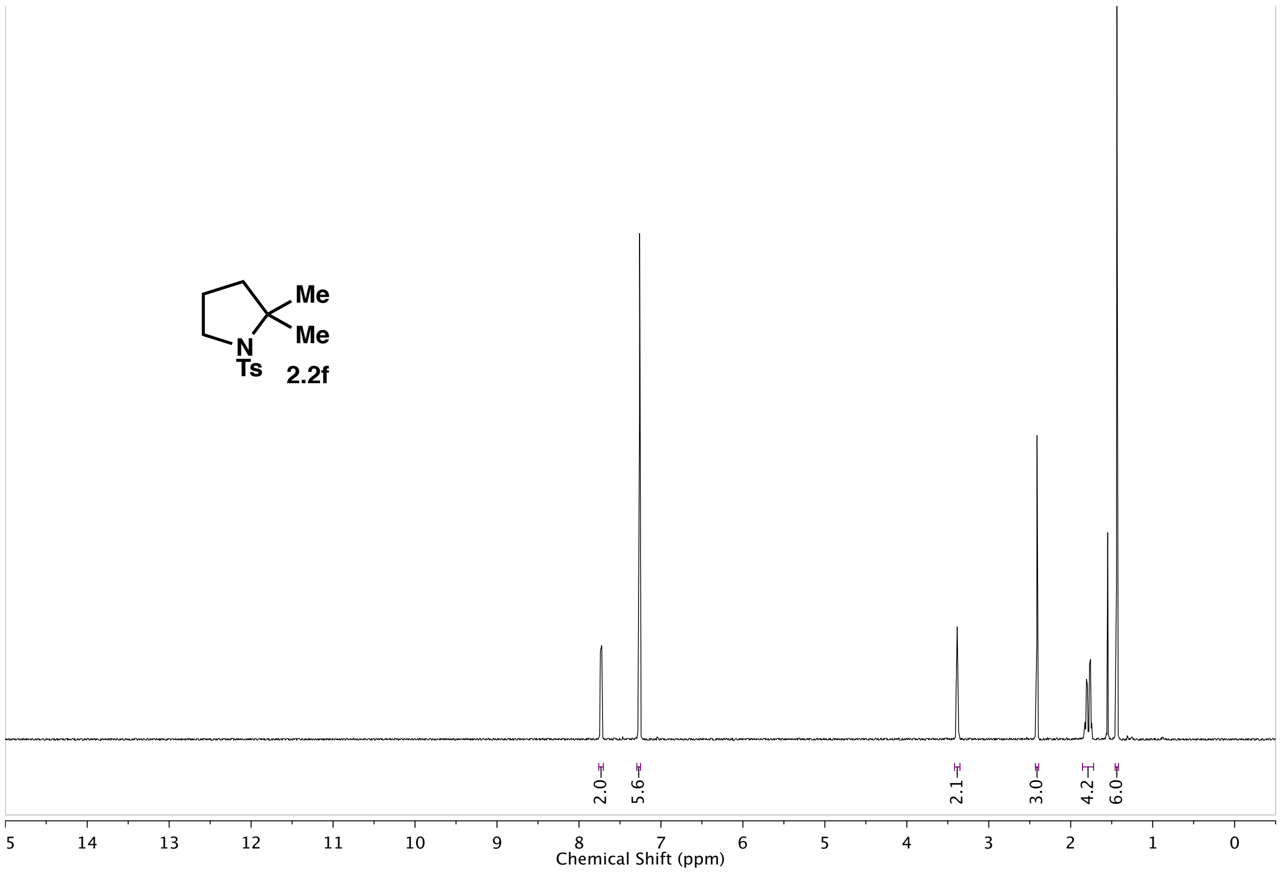
Me
Me
N
Ts
2.2f
2.0
5.6
2.1
3.0
4.2
6.0
5
14
13
12
11
10
9
8
7
6
5
4
3
2
1
0
Chemical Shift (ppm)

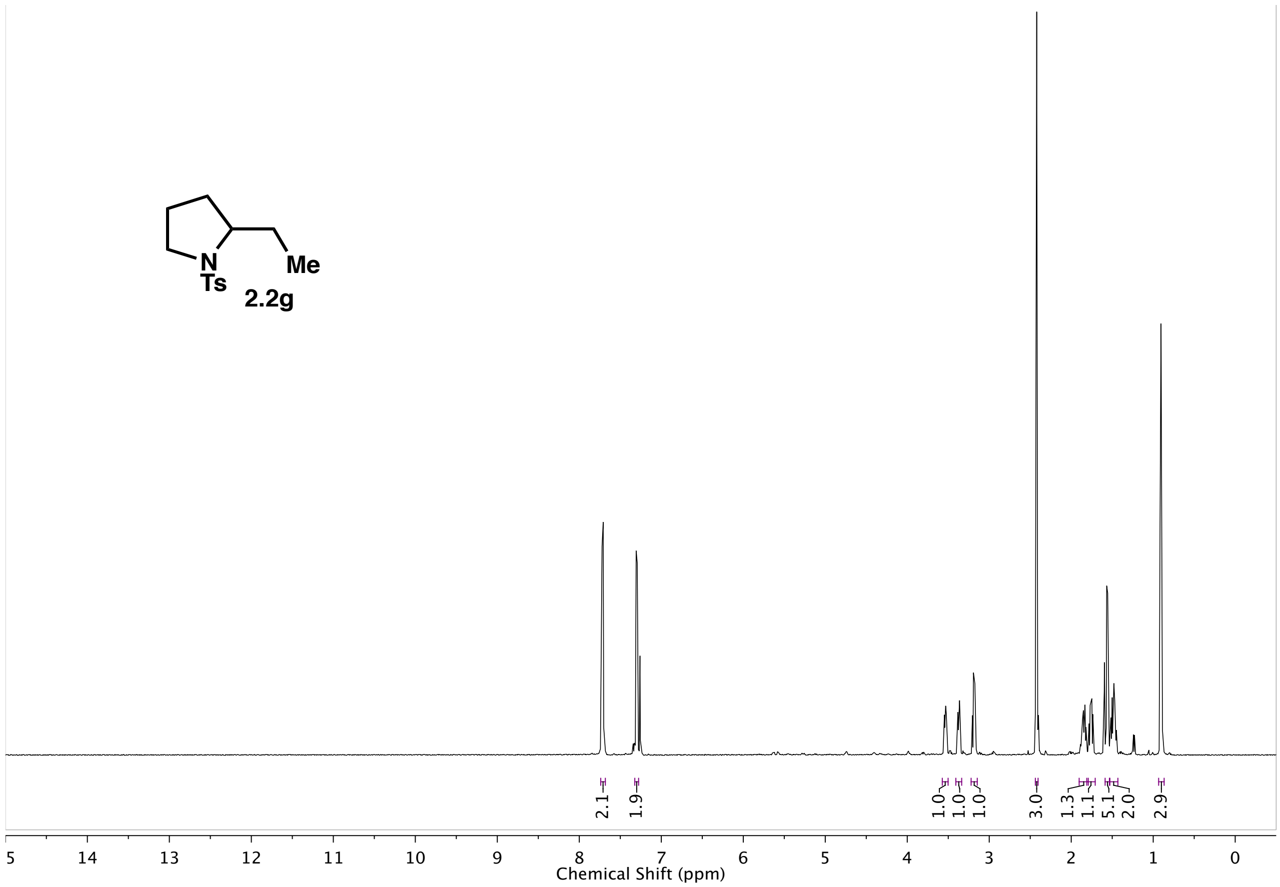
N
Ts
Me
2.2g
2.1
1.9
1.0
1.0
1.0
3.0
1.3
1.1
5.1
2.0
2.9
5
14
13
12
11
10
9
8
7
6
5
4
3
2
1
0
Chemical Shift (ppm)

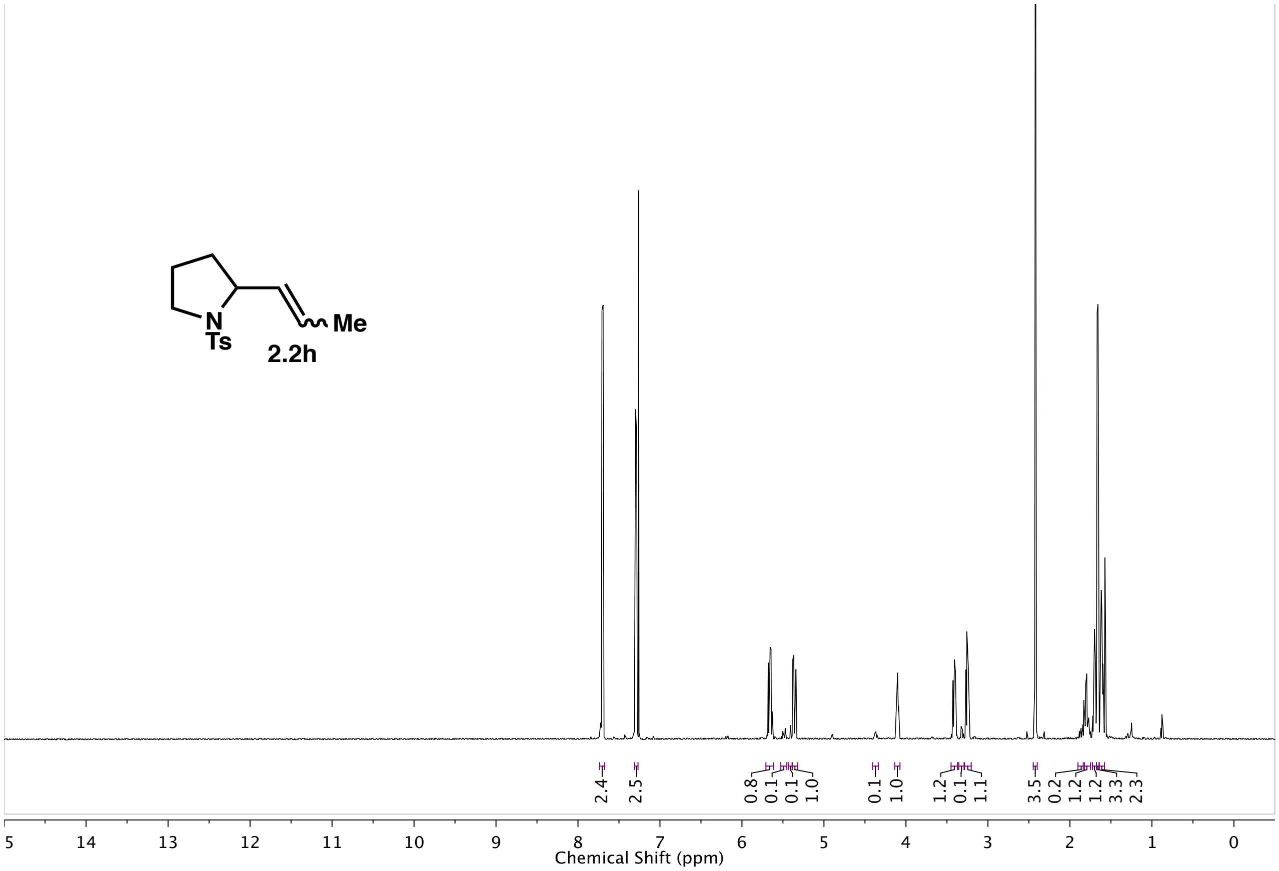
N
Ts
Me
2.2h
2.4
2.5
0.8
0.1
0.1
1.0
0.1
1.0
1.2
0.1
1.1
3.5
0.2
1.2
1.2
3.3
2.3
5
14
13
12
11
10
9
8
7
6
5
4
3
2
1
0
Chemical Shift (ppm)

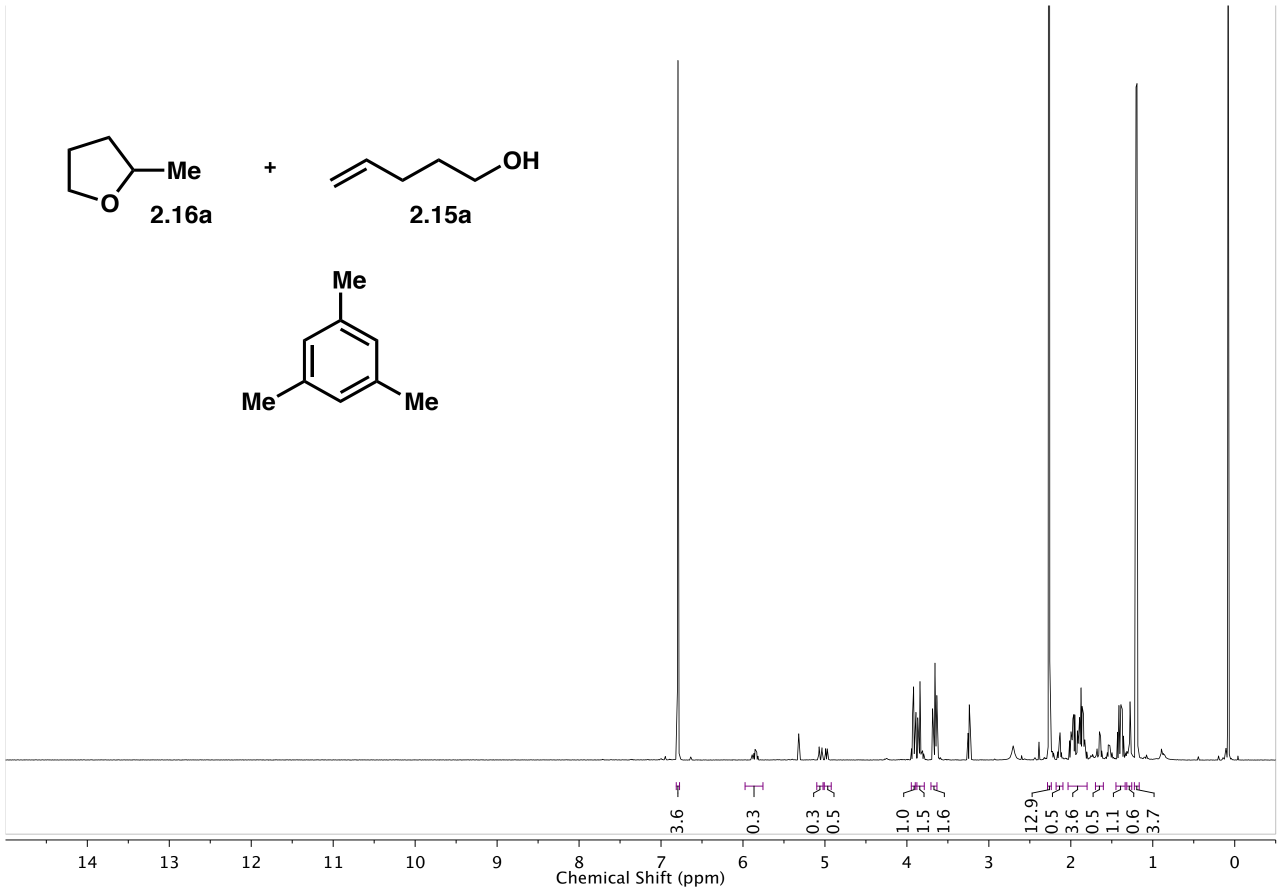
Me
O
2.16a
+
OH
2.15a
Me
Me
Me
3.6
0.3
0.3
0.5
1.0
1.5
1.6
12.9
0.5
3.6
0.5
1.1
0.6
3.7
14
13
12
11
10
9
8
7
6
5
4
3
2
1
0
Chemical Shift (ppm)

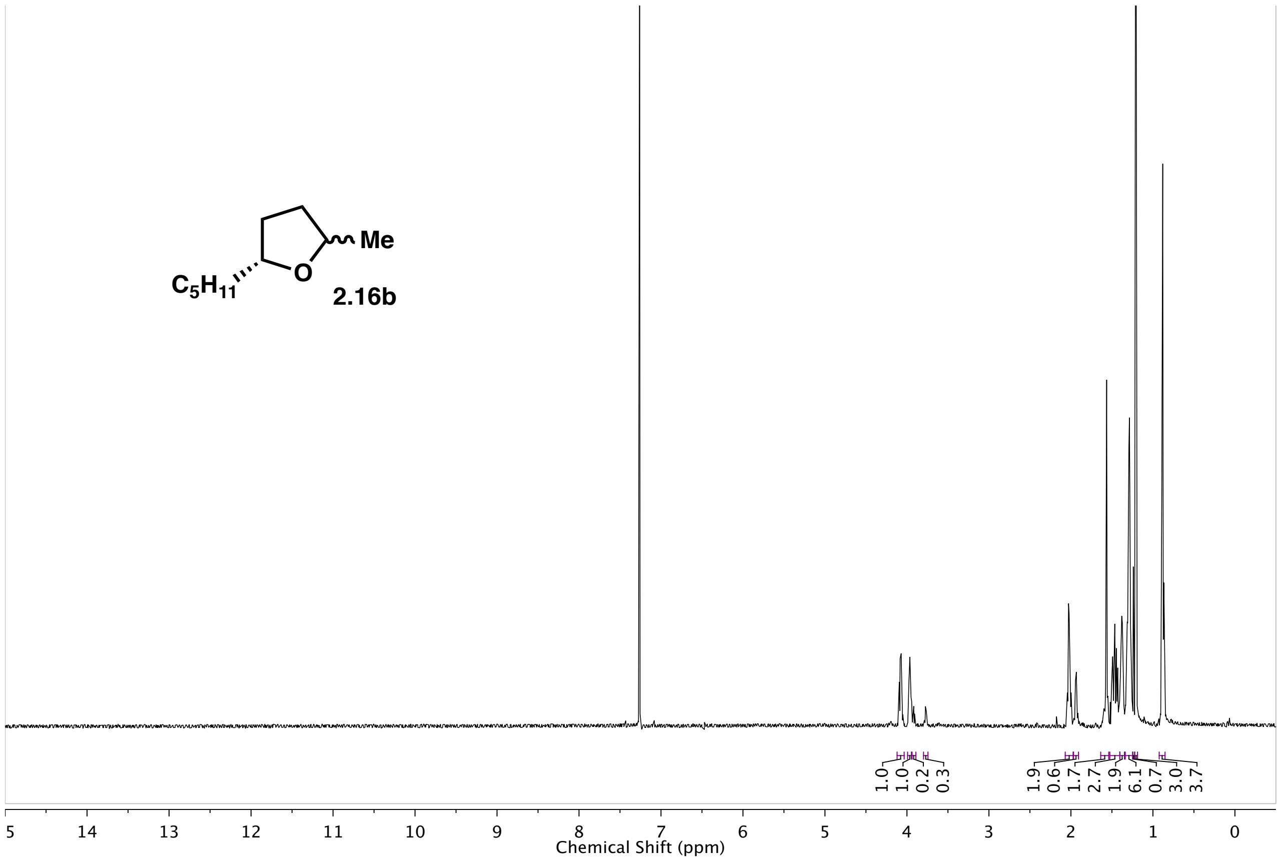
Me
O
C5H11
2.16b
1.0
1.0
0.2
0.3
1.9
0.6
1.7
2.7
1.9
6.1
0.7
3.0
3.7
5
14
13
12
11
10
9
8
7
6
5
4
3
2
1
0
Chemical Shift (ppm)

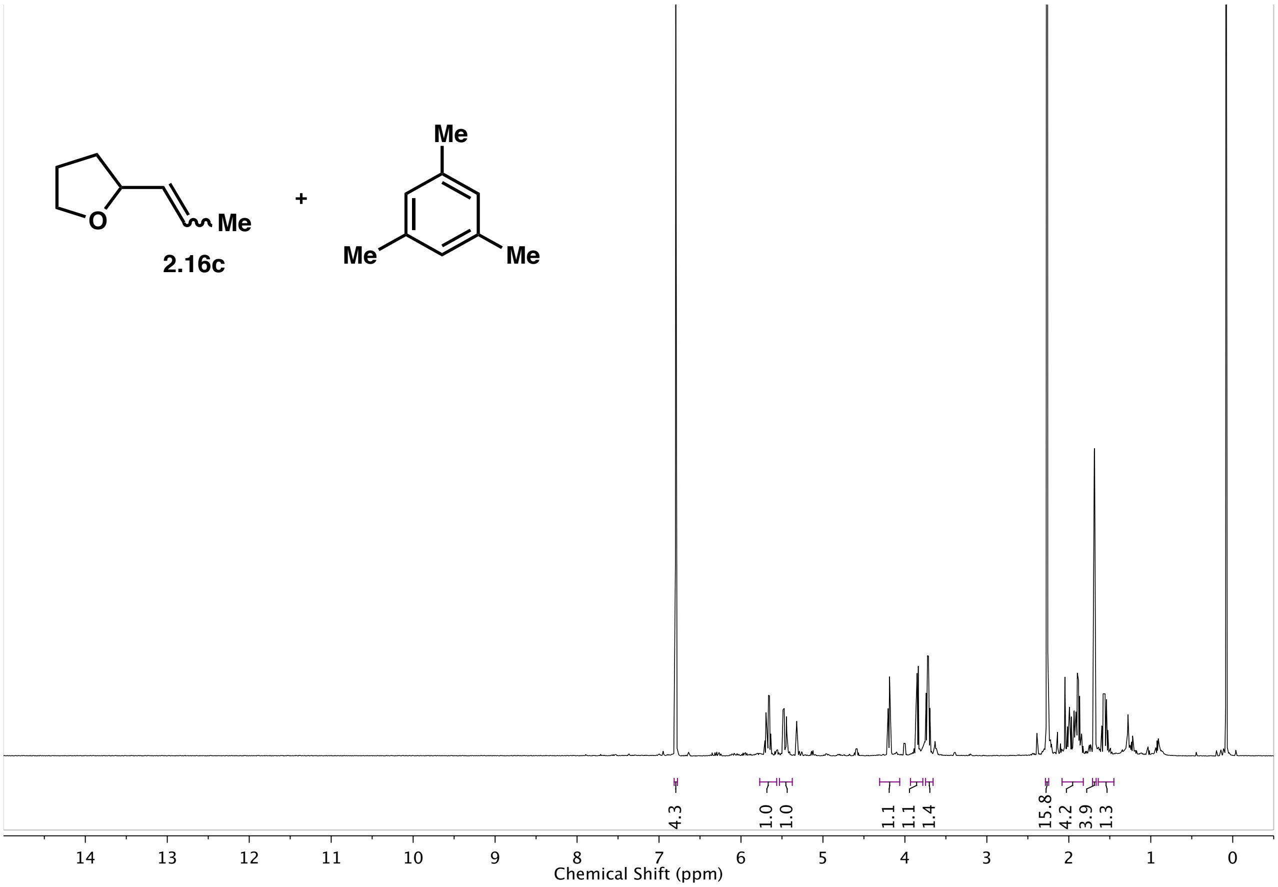
Me
Me
Me
+
2.16c
4.3
1.0
1.0
1.1
1.1
1.4
15.8
4.2
3.9
1.3
14
13
12
11
10
9
8
7
6
5
4
3
2
1
0
Chemical Shift (ppm)

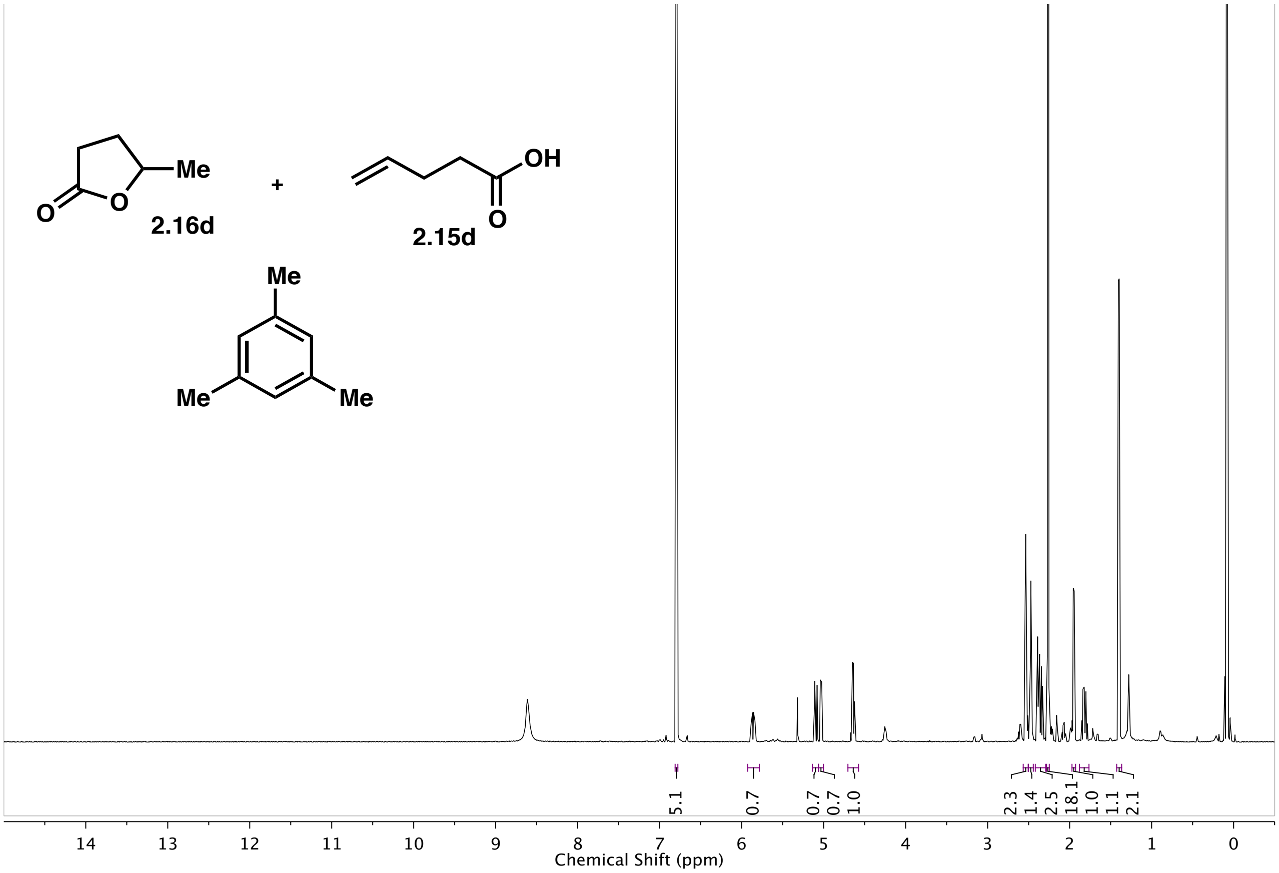
Me
O
O
2.16d
+
OH
O
2.15d
Me
Me
Me
5.1
0.7
0.7
0.7
1.0
2.3
1.4
2.5
18.1
1.0
1.1
2.1
14
13
12
11
10
9
8
7
6
5
4
3
2
1
0
Chemical Shift (ppm)

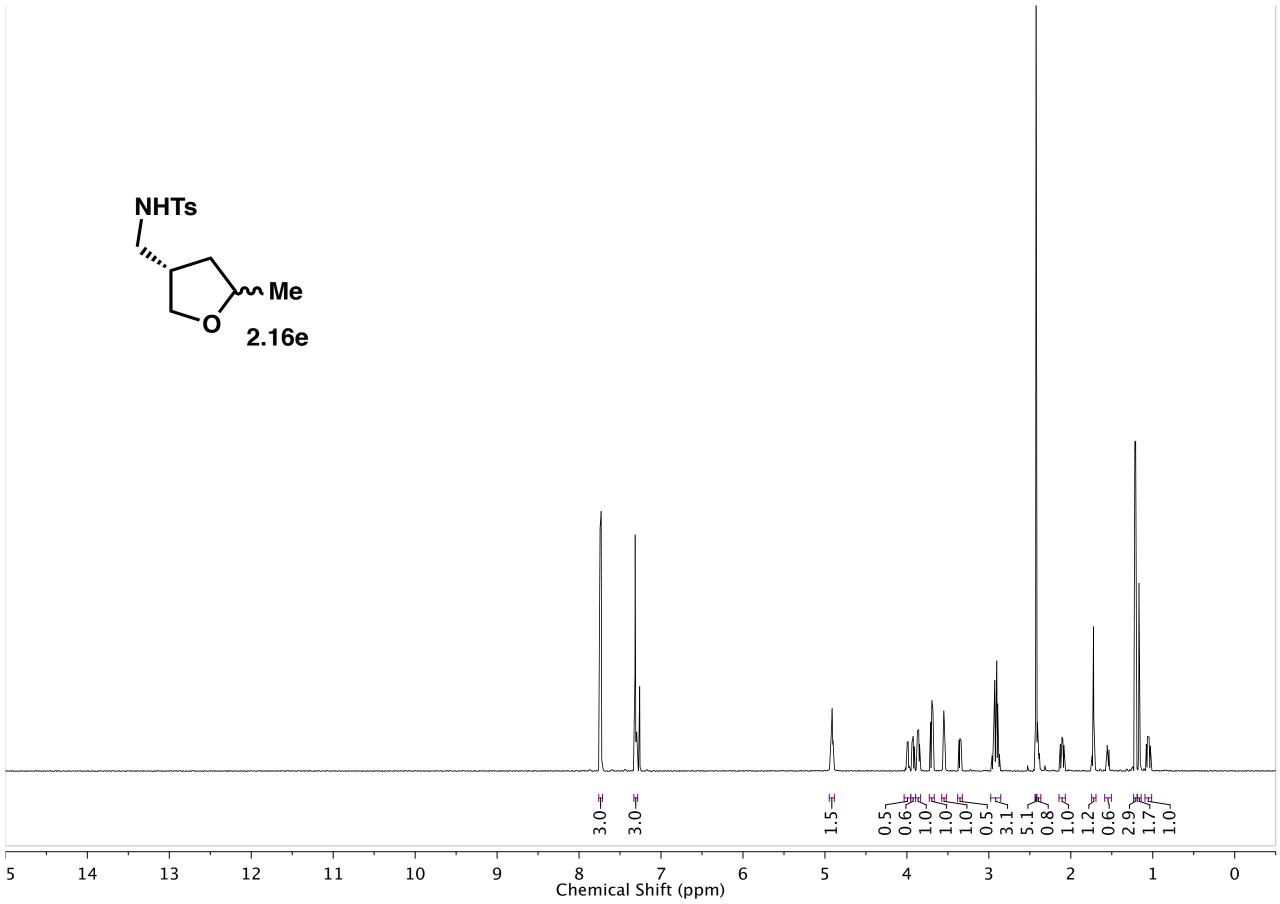
NHTs
Me
O
2.16e
3.0
3.0
1.5
0.5
0.6
1.0
1.0
1.0
0.5
3.1
5.1
0.8
1.0
1.2
0.6
2.9
1.7
1.0
5
14
13
12
11
10
9
8
7
6
5
4
3
2
1
0
Chemical Shift (ppm)

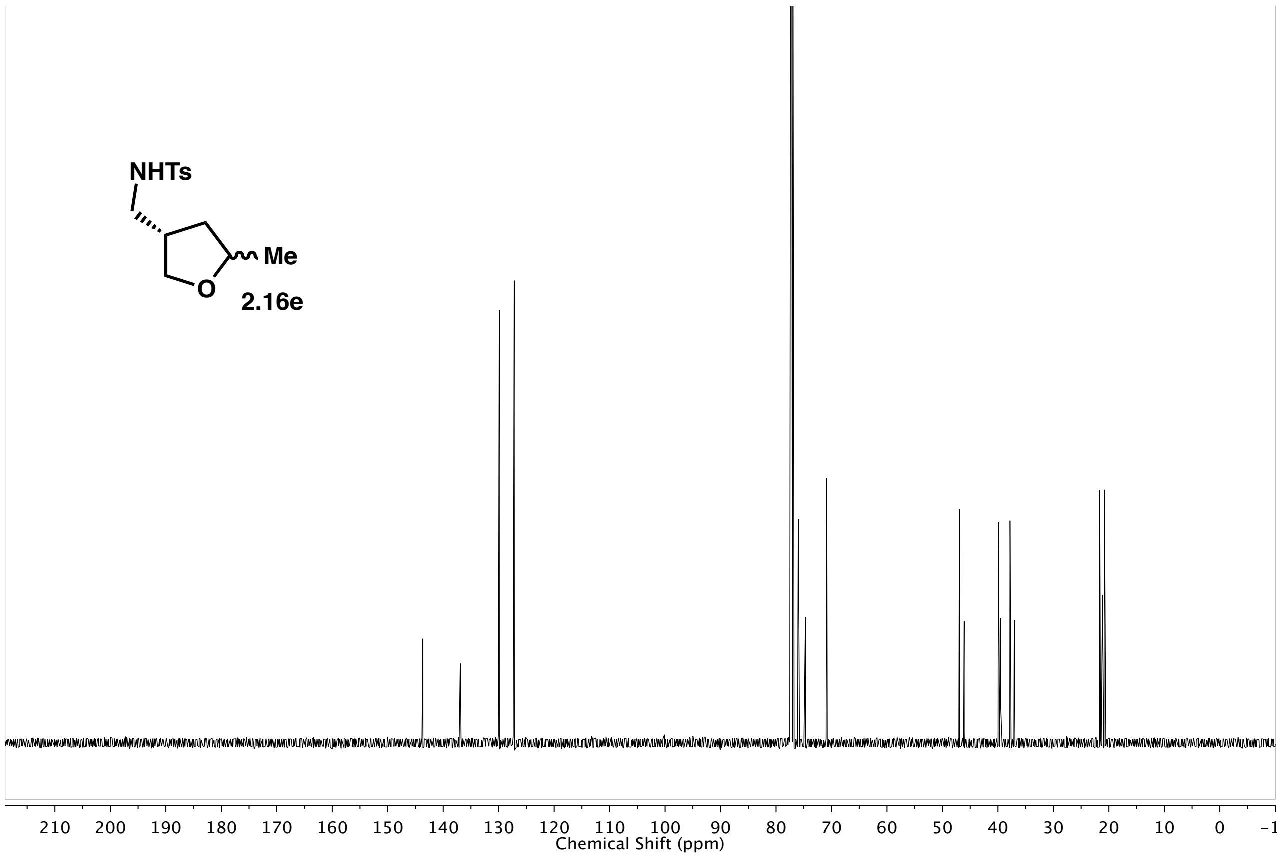
NHTs
Me
O
2.16e
210
200
190
180
170
160
150
140
130
120
110
100
90
80
70
60
50
40
30
20
10
0
–1
Chemical Shift (ppm)

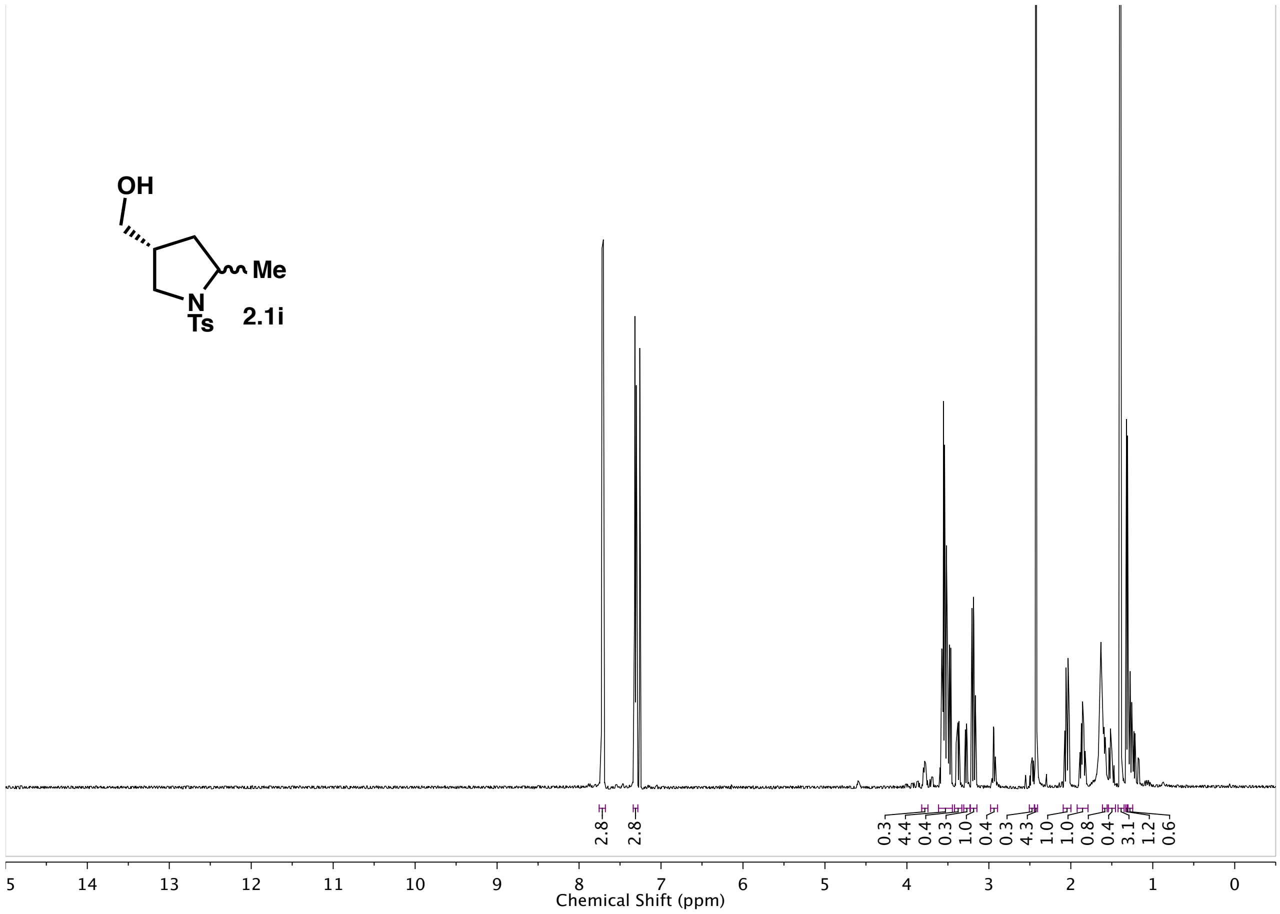
OH
Me
N
Ts
2.1i
2.8
2.8
0.3
4.4
0.4
0.3
1.0
0.4
0.3
4.3
1.0
1.0
0.8
0.4
3.1
1.2
0.6
5
14
13
12
11
10
9
8
7
6
5
4
3
2
1
0
Chemical Shift (ppm)

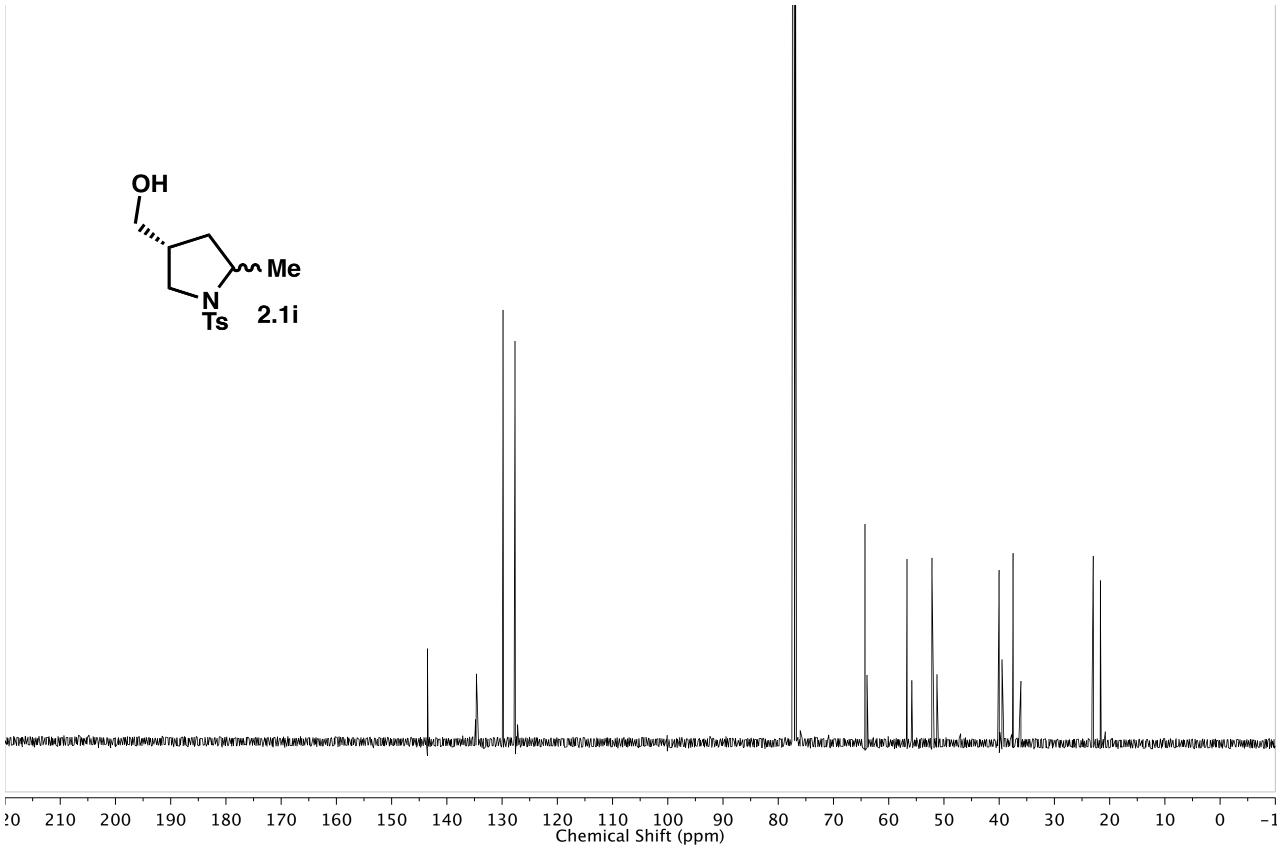
OH
Me
N
Ts
2.1i
20
210
200
190
180
170
160
150
140
130
120
110
100
90
80
70
60
50
40
30
20
10
0
−1
Chemical Shift (ppm)

Chapter 3: Initial Strategies for the Synthesis of Phomactin Natural Products

3.1: Structural Overview of the Phomactin Terpenoids

The phomactin natural products are a small but intriguing class of terpenoids.[1] They have been known since 1991 when Sato and coworkers initially isolated phomactin A (**3.1**) from a *Phoma* species of marine fungus (Figure 1).[2] This particular fungus grows on the backs of the snow crab *Chinoecetes opilioi* off the coast of Japan. The same group continued to investigate this *Phoma* species and proceeded to isolate many more phomactin natural products including phomactin B2 (**3.2**), phomactin D (**3.3**), phomactin G (**3.4**), and phomactin F (**3.5**).[3] To date, there have been 21 distinct phomactin natural products that have been isolated and disclosed by various groups.[4]

Figure 1: Representative phomactin natural products

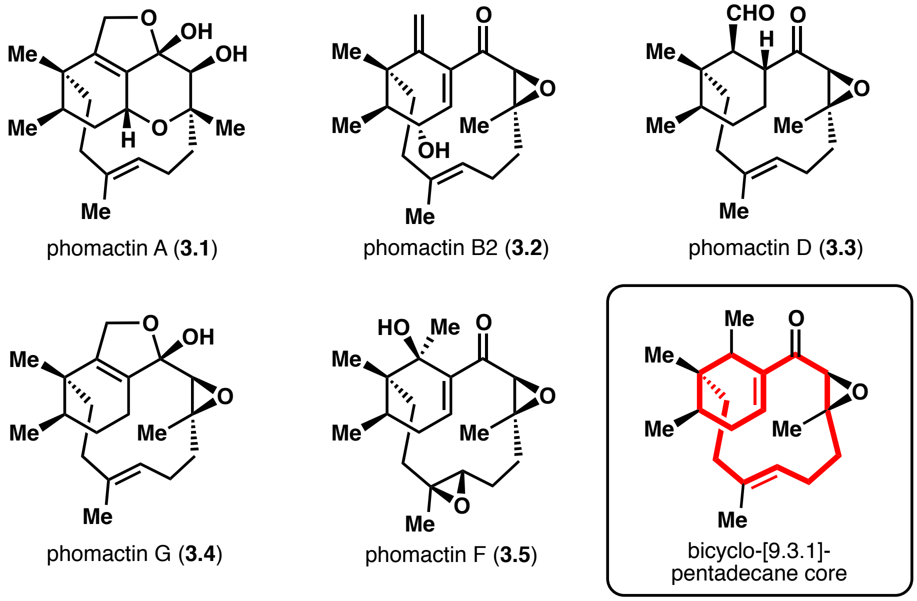
phomactin A (**3.1**)
phomactin B2 (**3.2**)
phomactin D (**3.3**)
phomactin G (**3.4**)
phomactin F (**3.5**)
bicyclo-[9.3.1]-pentadecane core

The phomactin terpenoids are characterized by their interesting structural topology – namely, a bicyclo[9.3.1]pentadecane core that comprises their carbocyclic framework (see Figure 1). As a result, each natural product contains a densely functionalized cyclohexyl ring, bridged by a macrocyclic "strap". The 12-membered macrocycle is a defining characteristic of the phomactins as well as a unique synthetic challenge. Phomactin A is arguably the most structurally complex member of the phomactin family. It contains an oxadecalin system embedded in its core structure as well as a highly sensitive hydrated furan motif, also present in phomactin G.

Biosynthetically, it is believed that the phomactin natural products all arise from a common biosynthetic precursor, phomacta-1(14),3,7-triene (**3.9**, Scheme 1).[5] This species originates from geranylgeranyl diphosphate, which initially cyclizes to give the cembrane carbocation (**3.6**). A subsequent transannular cyclization gives the verticillenyl carbocation (**3.7**). Interestingly, the verticillenyl carbocation is also an intermediate in taxane biosynthesis, a related class of terpenoids. However, to deliver the phomactin skeleton from **3.7**, a 1,2-hydride shift followed by 1,2 methyl shift must take place to give carbocation **3.8**. A final 1,2 hydride shift and loss of proton yields phomacta-1(14),3,7-triene. From this common carbocyclic framework, a series of enzymatic oxidations occur to give the various phomactin natural products.

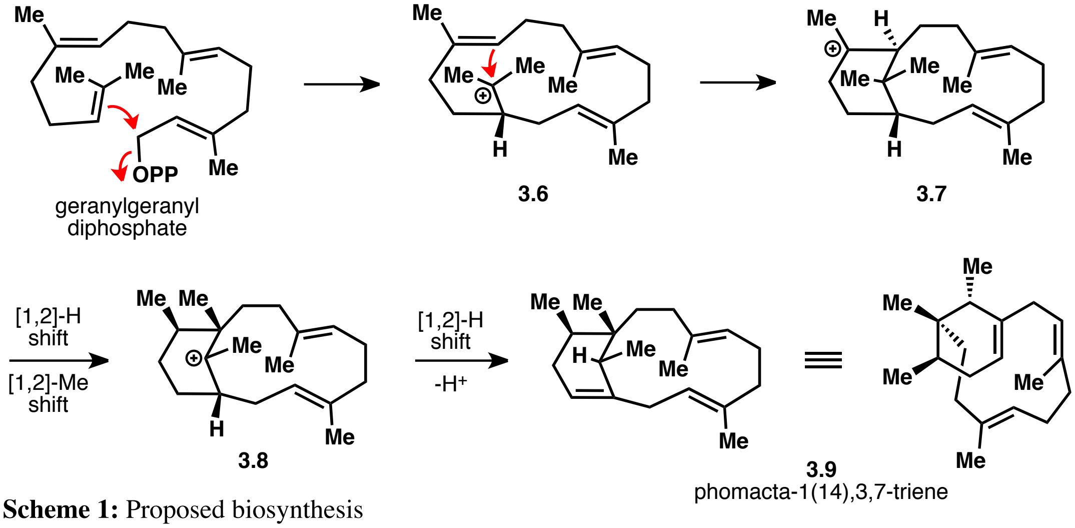

Scheme 1: Proposed biosynthesis

3.2: Platelet Activating Factor

Phomactin A was originally discovered by Sato and coworkers as a result of their program to identify new fungal metabolites that display platelet activating factor (PAF) antagonism. PAF (**3.10**, Figure 2) is a potent phospholipid agonist responsible for mediating many critical cellular activities such as inflammation, chemotaxis, immune responses, and platelet aggregation.[6] Being responsible for so many important processes, it's not surprising that PAF levels are highly regulated by the cell. However, inhibiting the binding of PAF to its receptor could have great therapeutic potential for many disease areas such as stroke, sepsis, cancer, cardiac rehabilitation, and many others. Currently, PAF antagonists are being used for the treatment of allergies, taking advantage of PAF's role in the immune-inflammatory response.[7]

Figure 2: Structure of platelet activating factor

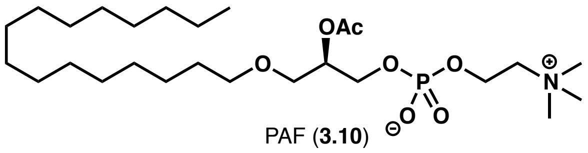

The PAF receptor (PAFR) is a rhodopsin-like G-protein coupled receptor, consisting of 7 transmembrane α-helixes. G-protein coupled receptors are notoriously difficult to crystallize and the human PAFR is no exception. In the absence of a protein crystal structure, structural information must be deduced through homology studies with bovine rhodopsin. Combining these with molecular dynamics and docking studies with PAF (ligand) and ginkgolide B (antagonist), the mode of action of PAFR has been postulated (Figure 3).[8] In the unbound, *apo*-protein state, transmembrane helix VI is kinked with an internal angle of 145°. Binding to PAF induces a structural change in helix VI, opening it up to an internal angle of 175°. This physical change results in downstream signal transduction. However, when a PAF antagonist such as ginkgolide B (GB) is added, helix VI becomes locked in its kincked state, thus inactivating the protein. However, it is unknown how the phomactin natural products bind to PAFR and whether they exhibit the same mode of action as other antagonists. Even though the study of PAF and PAFR remains a fast-growing research area, much remains unknown, especially with respect to the application of PAF antagonists to alter disease states.

Figure 3: PAFR mode of action for ligand binding (PAF) and antagonist (ginkgolide B) (Fig. from ref. 8)

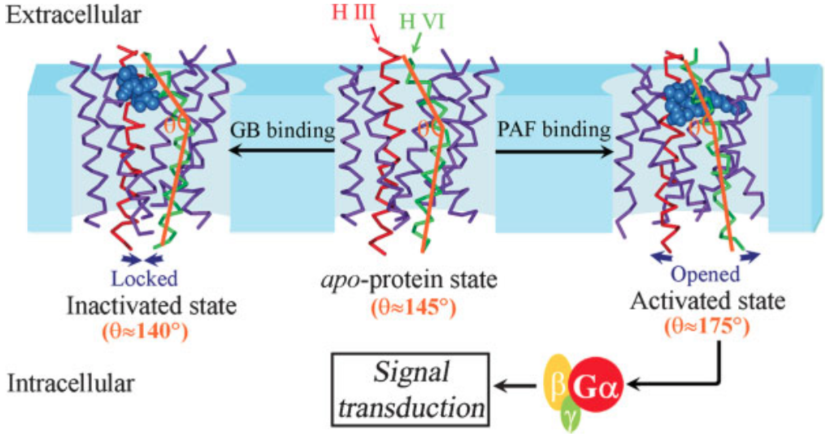

Recently, PAF antagonists have been gaining traction as a means of improving cancer therapies. It has been found that the PAFR is over-expressed in cancer cells after they've been treated with chemotherapeutic agents or gamma radiation.[9] Additionally, these therapies induce the generation of PAF and oxidized PAF-like phospholipids. It has been postulated that the interaction of PAFR with these PAFR-ligands produces anti-apoptotic factors, protects tumor cells, and promotes rapid growth following radiation or chemotherapy. In essence, cancer cells use the PAF signaling pathway as a means of protection as well as repopulation following a cancer treatment. To this end, PAF antagonists have been investigated as a means of slowing down cancer repopulation following treatment with chemo or radiation therapy.[10] The Jancar group has documented this effect in mice when a PAF antagonist (WEB2086) was used in combination with cisplatin (Figure 4). As shown in the graph, tumor size steadily increased when no treatments were administered (control). If the mice were treated with additional rounds of cisplatin, tumor growth slowed, but repopulation still occurred. This same effect was noticed when cancer cells were treated with WEB2086. Importantly, when a combination of cisplatin and WEB2086 was given to the mice, tumor growth was completely arrested. Thus, combination therapies with PAF antagonists seem to enhance the effectiveness of current cancer therapies and might lead to simple and valuable cancer treatments in the future.

Figure 4: PAF antagonist WEB2086 enhances cisplatin effectiveness (Fig. from ref. 10)

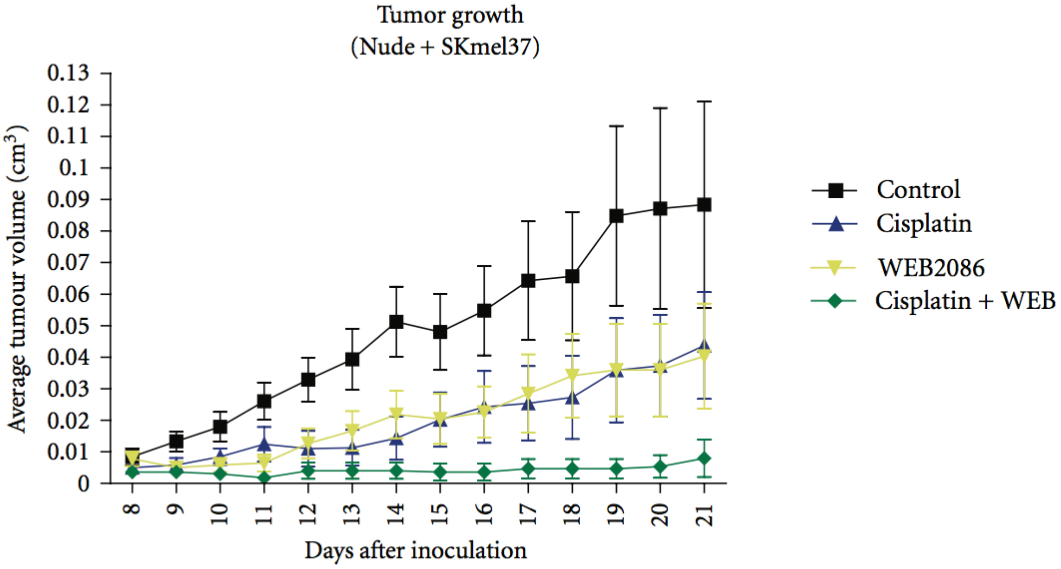

Because of the potential utility of the phomactin scaffold in designing improved PAF antagonists, the structure activity relationships (SAR) of several phomactin natural products have been studied. Phomactin A displays moderate inhibition of PAF binding to its receptor (IC_{50} = 2.3 μM) while phomactin D displays the best and lowest inhibitory concentration (IC_{50} = 0.12 μM). Several groups have explored analogues of phomactin A, G, and D, but the Sato group has reported the most potent ones to date, all modified from phomactin D (Figure 5).[11] They found that although reducing phomactin D to alcohol **3.11** led to a loss of activity, appending a (methylcarbonyl)oxy group to give compound **3.12** resulted in a much lower inhibitory concentration (IC_{50} = 0.026 μM). Finally, reduction of the ketone group in **3.12** to the corresponding alcohol (**3.13**) led to further improvement in inhibition (IC_{50} = 0.013 μM).

Figure 5: Select SAR studies by Sato and coworkers (IC_{50} values in parentheses)

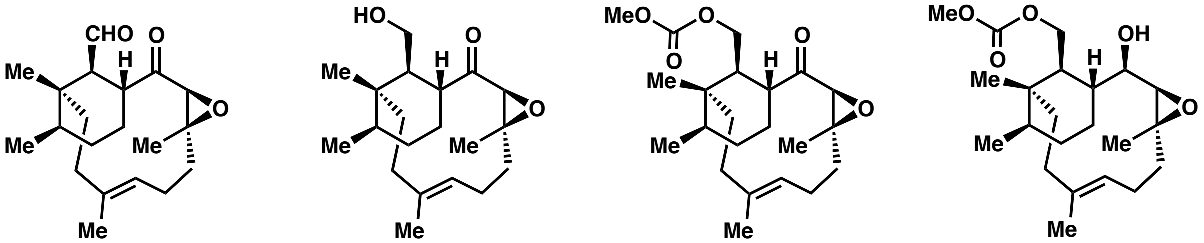

phomactin D (0.12 μM)

3.11 (1.3 μM)

3.12 (0.026 μM)

3.13 (0.013 μM)

3.3: Previous Phomactin Total Syntheses

Possessing PAF antagonist activity as well as intriguing architecture, the phomacin natural products have garnered much attention from the synthetic community. To date, there have been 6 total syntheses of these natural products – three syntheses of phomactin A and one synthesis each of phomactin B2, phomactin D, and phomactin G. Yet in the 25 years since phomactin A was first isolated, there have been over 20 distinct strategies for the construction of either the common bicyclo[9.3.1]pentadecane core or the reduced furanochroman system unique to phomactin A, highlighting the synthetic challenge inherent in these molecules.

The first total synthesis of any phomactin natural product was achieved by Yamada and co-workers in 1996 (Scheme 2).[12] They accessed (+)-phomactin D in 32 steps starting with a formal [4+2] reaction between cyclohexenone and chiral Michael acceptor **3.14**. Upon ozonolytic cleavage of [2.2.2] bicycle **3.15**, 19 more steps were necessary to transform the initial product **3.16** into the desired functionalized cyclohexyl aldehyde **3.17**. An appropriate vinyl lithium derived from vinyl iodide **3.18** (5 steps from 4-pentyn-1-ol) was added to aldehyde **3.17** to give allylic alcohol **3.19**. In preparation for macrocyclization, the allylic alcohol was protected as the BOM ether, the TBS group was cleaved, and the resultant alcohol was converted to allylic chloride **3.20**. Cyclization was induced with KHMDS, effecting a deprotonation alpha to the sulfone group followed by intramolecular displacement. Reductive removal of the sulfone and BOM cleavage with sodium and ammonia yielded macrocycle **3.21** in 38% over two steps. The synthesis was completed following directed epoxidation and global oxidation to yield (+)-phomactin D in 32 steps (longest linear sequence).

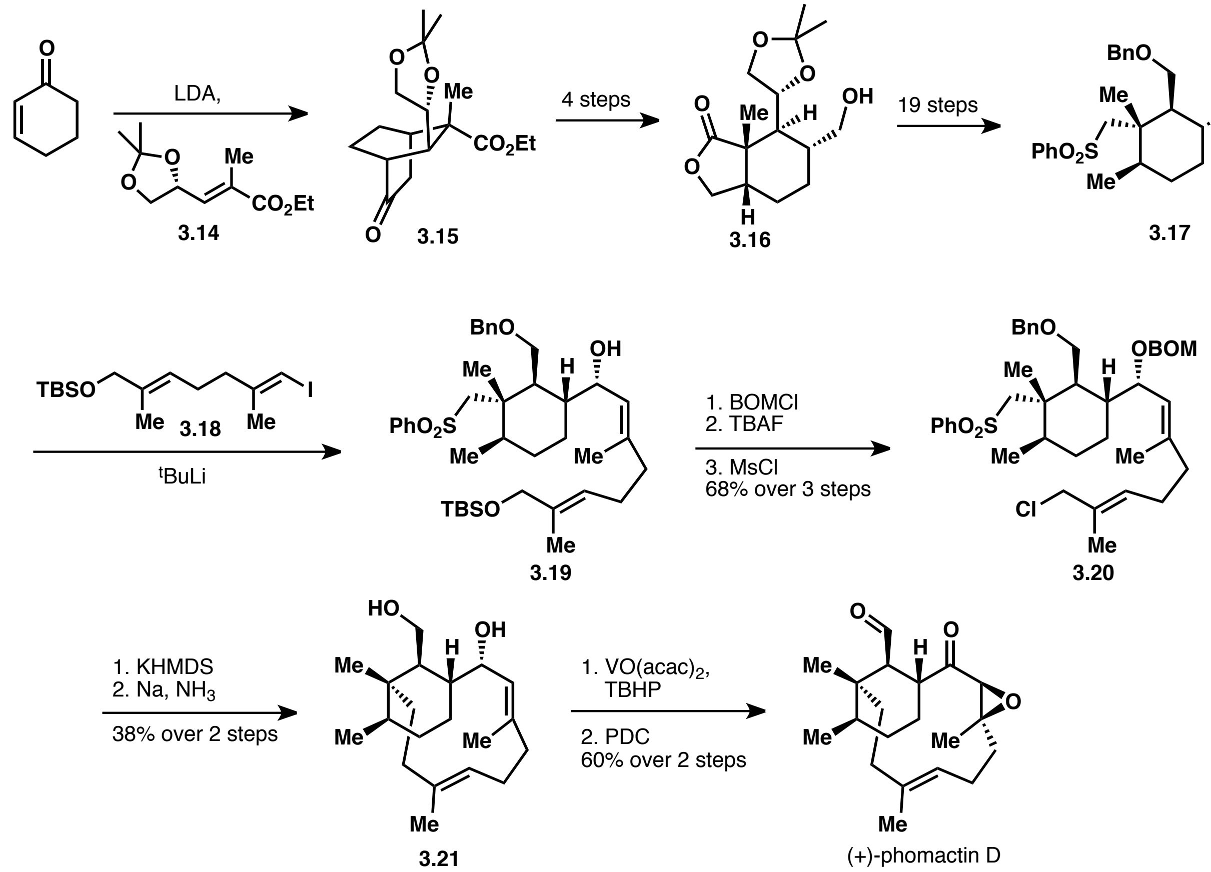

Scheme 2: Yamada's asymmetric synthesis of phomactin D

Although Yamada's strategy was lengthy and required many functional group manipulations, it set a precedent for phomactin synthesis by forming the functionalized cyclohexyl system and the linear "strap" portion separately, then bringing them together to forge the macrocycle late-stage. This has proven to be a good strategy and one that many others have also explored.

The first total synthesis of phomactin A was published by Pattenden and coworkers in 2002 (Scheme 3).[13] Initial dioxin formation from 5-methyl-1,3-cyclohexanedione and 1,3,5-trioxane afforded dioxane **3.22**. Double alkylation, first with methyl iodide, then with alkyl iodide **3.23** (6 step synthesis), afforded compound **3.24** and set the vicinal C6 and C7 stereocenters. Direct addition into the ketone with $LiCH_2OPMB$ followed by dioxane hydrolysis produced compound **3.25**. At this stage, the Pattenden group recognized that direct reduction of the ketone moiety resulted in the undesired diastereomer at the C8a position. Thus, this stereocenter was set by reduction to the undesired diastereomer followed by inversion through displacement of the corresponding chloride with *p*-methoxybenzyl alcohol. Finally, oxidation gave aldehyde **3.26**. This compound was the substrate for a Nozaki-Hiyama-Kishi macrocyclization, providing secondary allylic alcohol **3.27** as a single diastereomer in 36% yield.

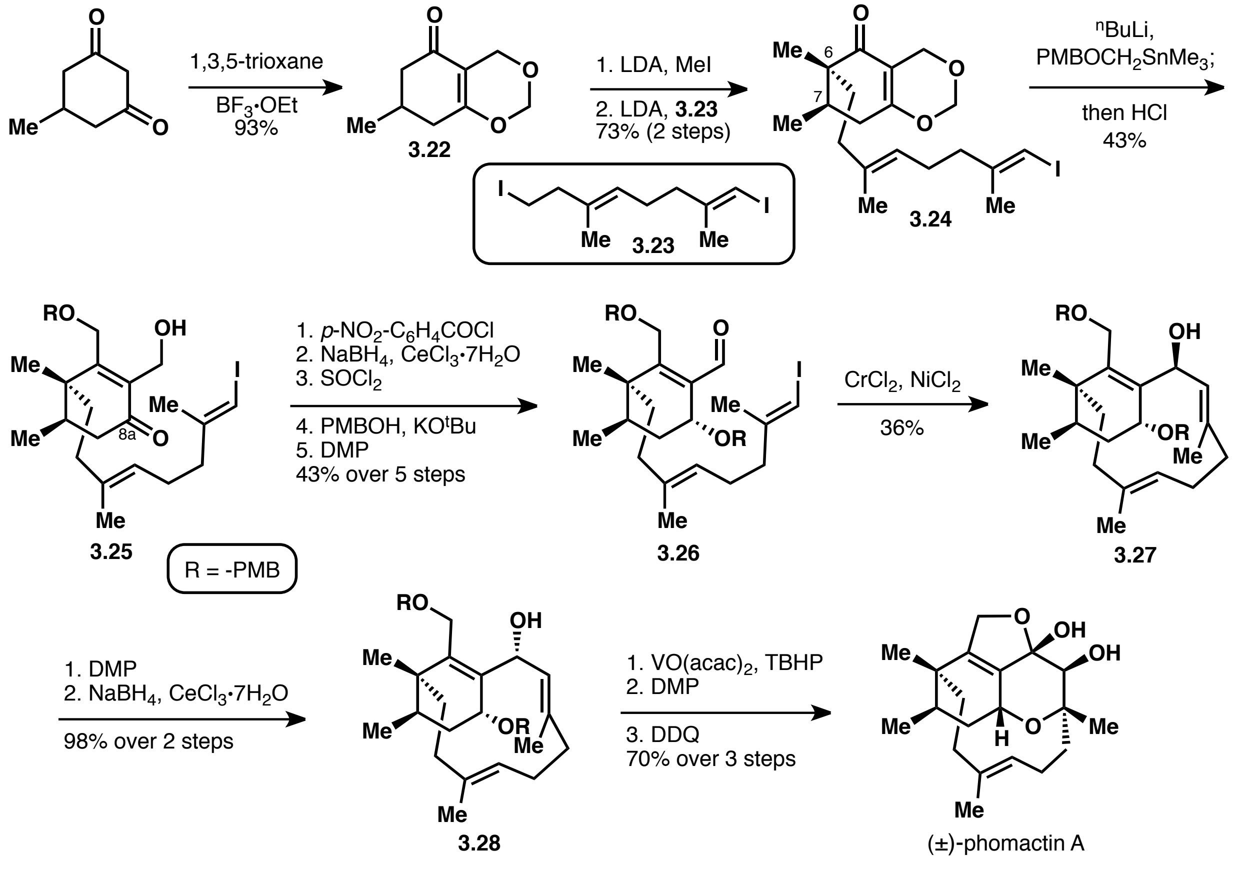

Me
1,3,5-trioxane
BF3•OEt
93%
3.22
1. LDA, MeI
2. LDA, 3.23
73% (2 steps)
3.23
Me
6
7
3.24
nBuLi,
PMBOCH2SnMe3;
then HCl
43%
RO
OH
8a
3.25
R = -PMB
1. p-NO2-C6H4COCl
2. NaBH4, CeCl3•7H2O
3. SOCl2
4. PMBOH, KOtBu
5. DMP
43% over 5 steps
3.26
CrCl2, NiCl2
36%
3.27
1. DMP
2. NaBH4, CeCl3•7H2O
98% over 2 steps
3.28
1. VO(acac)2, TBHP
2. DMP
3. DDQ
70% over 3 steps
(±)-phomactin A

Scheme 3: Pattenden's racemic synthesis of phomactin A

Counterintuitively, when this β-allylic alcohol (**3.27**) was subjected to directed epoxidation with $VO(acac)_2$, the undesired α-epoxide diastereomer was obtained. Using NMR analysis along with molecular mechanics predictions, the authors rationalized that the preferred conformation for β-allylic alcohol **3.27** was such that the trisubstituted double bond adjacent to the hydroxyl group presented one face to the outside of the macrocycle and epoxidation from this face led to the undesired α-epoxide (Figure 6). However, when the epimeric α-allylic alcohol (**3.28**) was modeled, the opposite face of the double bond was exposed, predicting that the desired β-epoxide should be obtained. In practice, oxidation of β-allylic alcohol **3.27** followed by reduction inverted the stereochemistry to give α-allylic alcohol **3.28** (see Scheme 3). Epoxidation with VO(acac)$_2$ delivered the desired β-epoxide, albeit with a substantial amount of undesired bis-epoxidation. Finally, oxidation and global deprotection resulted in a spontaneous cyclization to afford (±)-phomactin A.

Figure 6: Allylic alcohol stereochemistry affects macrocycle conformation

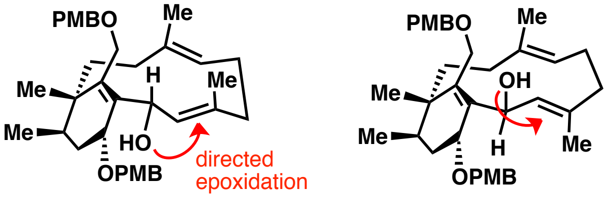

3.27
β-epimer

3.28
α-epimer

Although racemic, this synthesis provided the natural product in a sequence of 19 steps (longest linear sequence) or 14 steps from 5-methyl-1,3-cyclohexanedione (synthesis of iodide **3.23** not included). To date, this is the shortest synthesis of any phomactin natural product. Additionally, Pattenden and coworkers were able to modify their synthesis to access phomactin G (see Figure 1 for structure) in the same number of steps, in this case effecting a deoxygenation of a late-stage intermediate.[14] Through their studies, they highlighted the challenge of setting the correct stereochemistry of the hydroxyl group at C8a via ketone reduction. Additionally, the necessity of the α-epimer (**3.28**) to direct a diastereoselective late-stage epoxidation was rationalized. Directed epoxidation is a common strategy employed by many teams because this epoxide moiety (or derivative) is ubiquitous in the phomactin natural products.

Shortly after the Pattenden synthesis was reported, the first asymmetric synthesis of (+)-phomactin A was reported by Halcomb in 2003 (Scheme 4).[15] Their synthesis commenced with elaboration of chiral pool compound (+)-pulegone to cyclohexenone **3.29** in 6 steps. Addition of LiCH$_2$OMOM to the ketone group followed by Babler-Dauben oxidative transposition afforded enone **3.30**. Introduction of a functional handle at the α position was challenging, requiring 7 steps to construct α-bromo enone **3.31**. Similarly to Pattenden's route, direct reduction of the ketone resulted in the undesired diastereomer at C8a, thus requiring a Mitsunobu reaction to invert the stereochemistry to give functionalized cyclohexenyl bromide **3.32**. Treatment of this vinyl bromide with tert-butyl lithium generated the vinyl lithium species which was added to aldehyde **3.33** (prepared in 12 steps from geraniol) to afford compound **3.34** following oxidation with Dess-Martin periodinane. A 5-step sequence of deprotection and re-protection afforded reduced furanochroman **3.35**, the substrate for the key *B*-alkyl Suzuki macrocyclization. Thus, treatment with 9-BBN accomplished a hydroboration across the terminal double bond; subsequent treatment with Pd(dppf)Cl$_2$ and triphenylarsine forged the macrocyclic ring. Finally, global deprotection with tetrabutylammonium fluoride afforded (+)-phomactin A in a sequence of 27 steps (longest linear sequence).

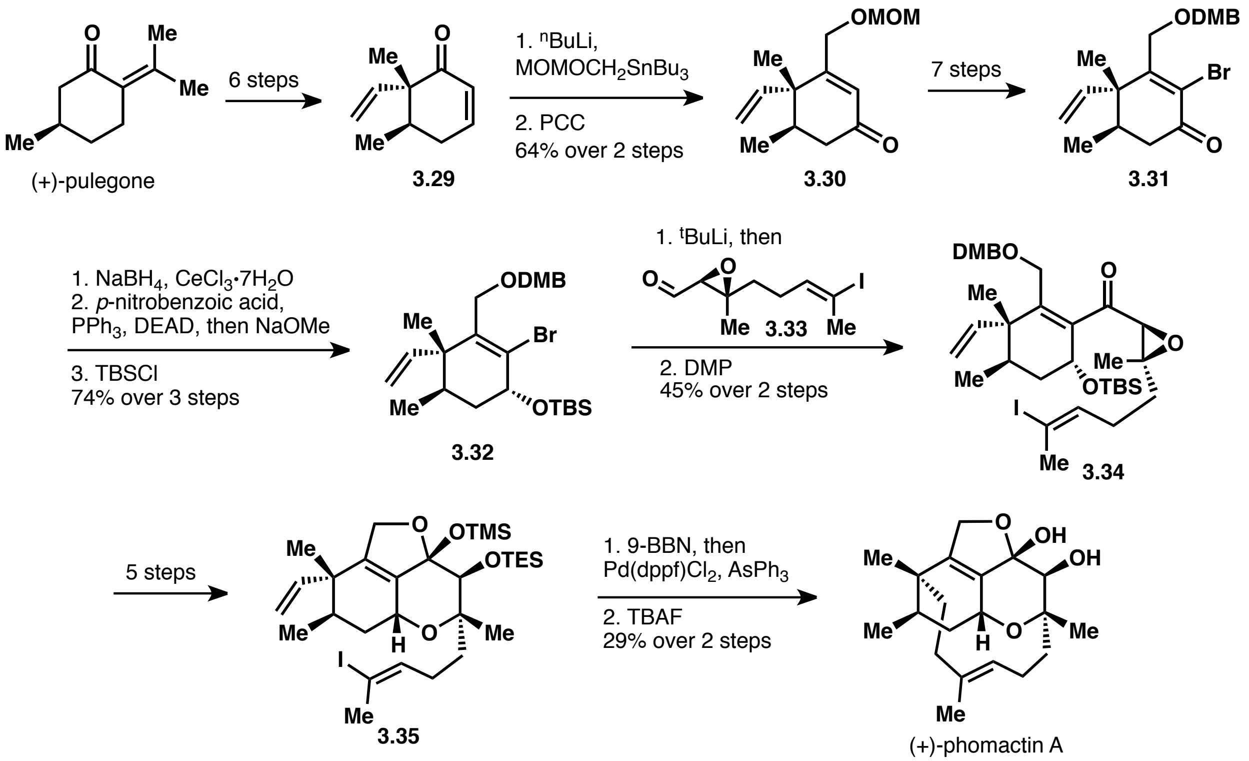
(+)-pulegone
6 steps
3.29
1. ⁿBuLi, MOMOCH₂SnBu₃
2. PCC
64% over 2 steps
3.30
7 steps
3.31
1. NaBH₄, CeCl₃·7H₂O
2. p-nitrobenzoic acid, PPh₃, DEAD, then NaOMe
3. TBSCl
74% over 3 steps
3.32
1. ᵗBuLi, then
3.33
2. DMP
45% over 2 steps
3.34
5 steps
3.35
1. 9-BBN, then Pd(dppf)Cl₂, AsPh₃
2. TBAF
29% over 2 steps
(+)-phomactin A

Scheme 4: Halcomb's asymmetric synthesis of phomactin A

In the sole synthesis of phomactin B2, Wulff and coworkers employed a chromium-mediated cyclohexadienone annulation of **3.36** to simultaneously construct the cyclohexyl ring and the macrocycle (Scheme 5).[16] This occurred with high diastereoselectivity to yield cyclohexadienone **3.37** in 60% yield. Fourteen more steps were required to convert this compound into (±)-phomactin B2.

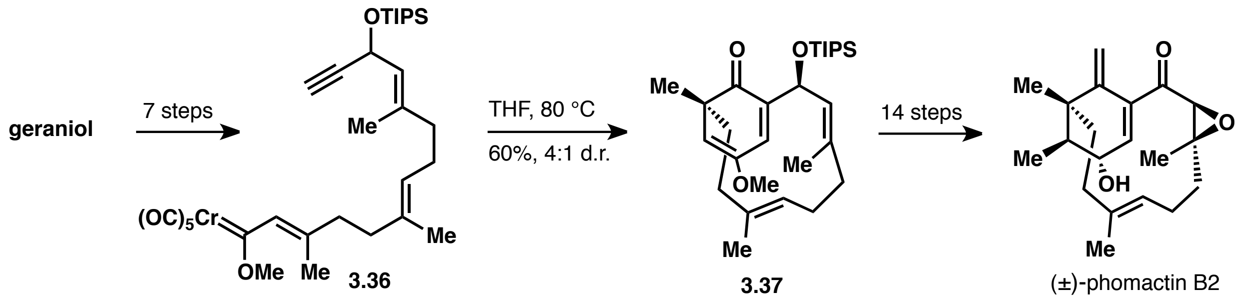
geraniol
7 steps
3.36
THF, 80 °C
60%, 4:1 d.r.
3.37
14 steps
(±)-phomactin B2

Scheme 5: Wulff's synthesis of phomactin B2

The most recent synthesis of phomactin A was accomplished by Hsung and coworkers in 2009 (Scheme 6).[17] Their key step relied on an intramolecular formal *oxa*-[3+3] of compound **3.38** to simultaneously construct the oxadecalin core and the macrocycle. This reaction was plagued with the formation of constitutional isomers, resulting in a low yield of desired compound **3.39**. Additionally, this scaffold proved challenging to work with and required an additional 25 steps for elaboration into phomactin A.

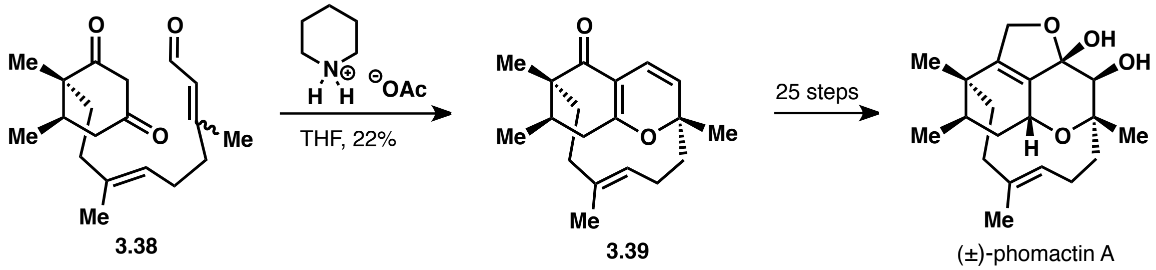

Scheme 6: Hsung's synthesis of phomactin A

In the 25 years since phomactin A was first isolated, many beautiful strategies have been developed to build these interesting structures. But we recognized that there was still a lot of room for improvement in these syntheses, a sentiment that was highlighted in a recent review on the phomactins: "Still, a truly efficient, enantioselective synthesis that provides access to multiple family members has yet to be developed, which underscores the difficulty of the [phomactin] problem."[1] We thought we could solve this problem by utilizing a strategy built around C–C activation of a carvone-derived cyclobutanol.

3.4: Cyclobutanol C–C Activation

The cleavage of a carbon-carbon sigma bond through the interaction with a transition metal is a challenging and underdeveloped process in organic synthesis. An interaction of a stable, non-polar C–C sigma bond with a transition metal is generally unfavorable, but direct oxidative insertion into a C–C bond is feasible, specifically if significant ring strain is relieved or if assisted by a chelating group (Scheme 7).[18] Another method for achieving C–C activation is through β-carbon elimination. This process can be thought of as the reverse reaction of a migratory insertion into a double bond, or alternatively, the carbon analogue of the more common β-hydride elimination. The β-carbon elimination step is usually driven by the formation of a strong C–O pi bond and the relief of ring strain is often employed to enable facile reactions.[19]

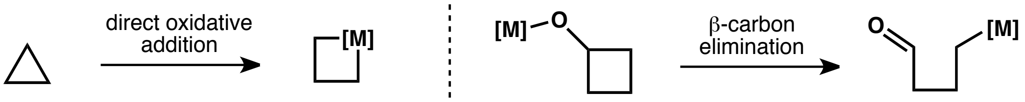

Scheme 7: Common pathways for C–C activation

In regards to β-carbon eliminations of cyclobutanols, several metals including palladium(II), nickel(II), and rhodium(I) have been shown to effectively catalyze this process. Even though several metals are effective catalysts, the identity of the metal is important as each metal can accomplish complementary reactivity (such as migratory insertion or transmetalation) before or after the β-carbon elimination process. With rhodium catalysis, the labs of Murakami and Cramer have produced seminal work highlighting the synthetic utility of these processes. Murakami and coworkers published the first report of rhodium-catalyzed cyclobutanol ring opening in 2004 (Scheme 8).[20] They showed that following direct addition of an aryl boronic ester into cyclobutanone **3.40**, rhodium can effect a β-carbon elimination to afford the ring-opened ketone **3.42**. Interestingly, if deuterated water was added to the reaction, deuterium incorporation was observed at the alpha position and not at the gamma position of **3.44**, indicating a rhodium migration prior to protodemetalation (e.g. **3.42** to **3.43**), possibly through successive β-hydride elimination/re-insertion or direct C–H activation.

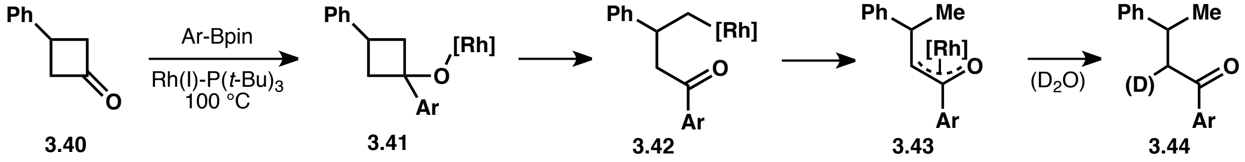

Scheme 8: Murakami's rhodium-catalyzed cyclobutanol opening

Recently in the Sarpong group, we've built upon past research on cyclobutanol ring opening and shown the utility of oxygenated pinene derivatives **3.46** and **3.47** as substrates. These cyclobutanols can be obtained in 2 steps from readily available and inexpensive *S*-(+)-carvone following a modification of a procedure reported by Bermejo and coworkers (Scheme 9).[21] In this procedure, carvone was subjected to *meta*-chloroperoxybenzoic acid to give epoxide **3.45** as a 1:1 mixture of diastereomers. Treatment with in situ generated Cp_2TiCl produced diastereomeric cyclobutanols **3.46** and **3.47**, presumably through transition states such as **TS1** and **TS2**. We found that switching the solvent to a 1:1 mixture of dioxane and diethyl ether gave consistently higher yields of the minor (and desired) diastereomer **3.46**. Even though conditions for utilizing catalytic titanium have been developed for reductive epoxide opening,[22] attempts to use sub-stoichiometric titanium in this cyclobutanol formation have been unsuccessful.

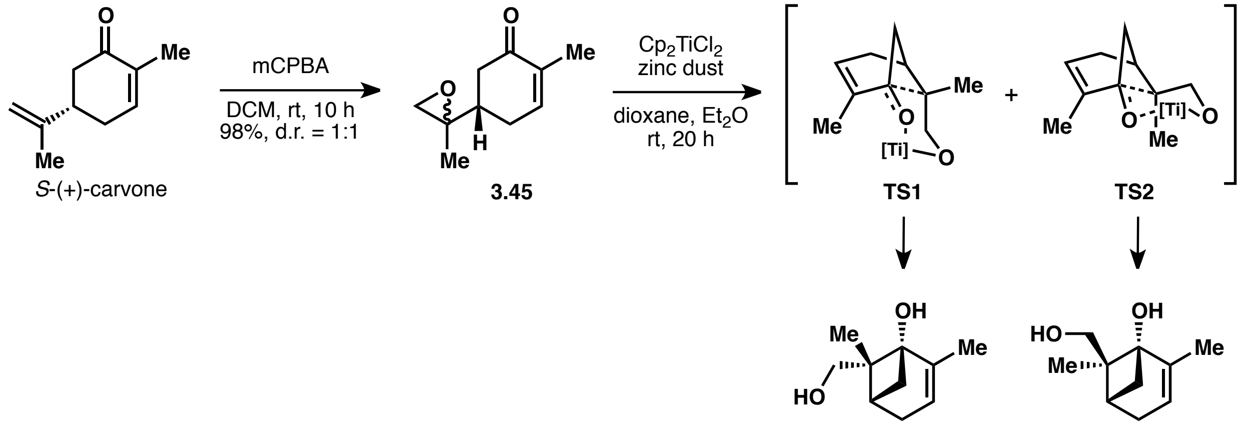

Scheme 9: Carvone-derived cyclobutanol synthesis

The Sarpong group has shown that subjecting cyclobutanol **3.46** to $[Rh(cod)OH]_2$ results in clean conversion to cyclohexenone **3.52** (Scheme 10).[23] Mechanistically, a ligand exchange first occurs to give rhodium alkoxide **3.48**. This initiates β-carbon elimination to give alkyl rhodium **3.49**. Importantly, this step is selective for breaking the C1–C2 bond over the C1–C4 bond, thus placing the rhodium center on the sterically and electronically favorable primary carbon. The C1–C2 bond is actually stronger than the C1–C4 bond as shown by the bond lengths of the X-ray crystal structure (C1–C2 = 1.535 Å, C1–C4 = 1.589 Å).[23] When bond rearrangement of **3.46** is induced by other means, (e.g., an electrophile interacting with the carbon-carbon double bond) the weaker C1–C4 bond is cleaved. Transition metals are required to achieve the unique activation of the stronger C1–C2 bond. After alkyl rhodium **3.49** is formed, mechanistic studies suggested that a 1,3-Rh shift occurs to place the metal center at a more thermodynamically stable allylic position (e.g. **3.50**). This is believed to proceed via a C–H activation process as opposed to successive β-hydride elimination/re-insertion (as supported by computational and experimental evidence).[23] Finally, protodemetalation occurs at the α-position of allyl rhodium species **3.50** to give unconjugated enone **3.51**, which can be isolated under the appropriate conditions (short reaction times). Double bond isomerization gives conjugated enone **3.52** as the final product.

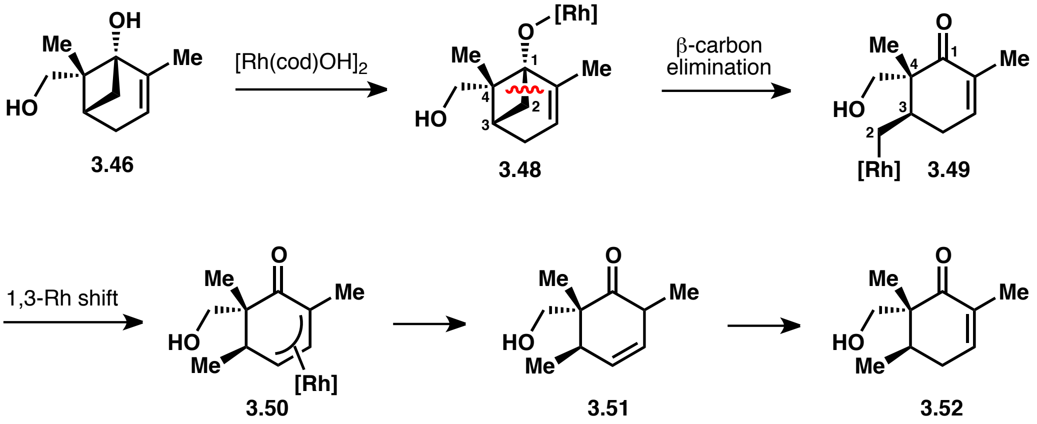
OH
Me
Me
HO
3.46
[Rh(cod)OH]$_2$
[Rh]
O
1
Me
Me
HO
4
2
3
3.48
β-carbon elimination
O
1
Me
4
Me
HO
3
2
[Rh]
3.49
1,3-Rh shift
O
Me
Me
HO
Me
[Rh]
3.50
O
Me
Me
HO
Me
3.51
O
Me
Me
HO
Me
3.52

Scheme 10: Proposed mechanism for rhodium-catalyzed cyclobutanol opening

Utilizing rhodium-catalyzed C–C activation, we have shown that a simple 3-step procedure can transform carvone into a novel enantiopure cyclohexenone scaffold (**3.52**) via rearrangement of the skeletal carbons (Scheme 11). We recognized that this cyclohexenone maps on perfectly to the densely functionalized cyclohexenyl core present in all the phomactin natural products. To demonstrate the utility of C–C activation in total synthesis, we wanted to devise a unified route to transform cyclohexenone **3.52** into complex terpenoid (+)-phomactin A and related natural products.

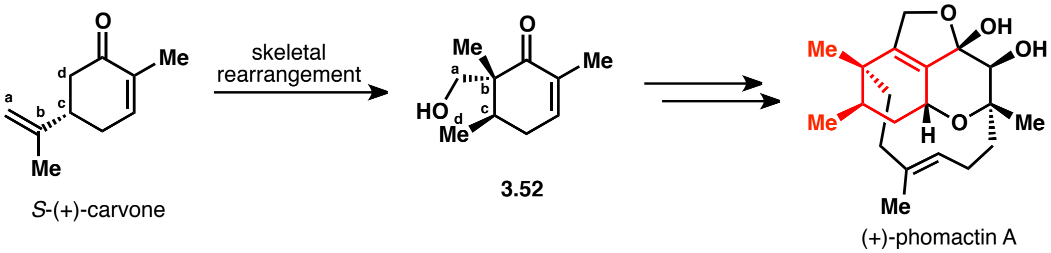
O
Me
d
a
b
c
Me
S-(+)-carvone
skeletal rearrangement
O
Me
a
b
Me
HO
d
c
Me
3.52
O
OH
OH
Me
Me
O
H
Me
Me
(+)-phomactin A

Scheme 11: Inspiration to demonstrate the utility of C–C activation in total synthesis

3.5: Initial Strategy: Ketone-Directed C–H Functionalization

To construct any of the phomactin terpenoids, we recognized that it would be essential to achieve a fragment coupling – joining the cyclohexenyl portion with the linear "strap" portion – in order to construct the macrocyclic framework (Scheme 12). In order to do this efficiently, we aspired to perform a C–H functionalization of the allylic methyl position to directly forge the requisite C–C bond. We envisioned capitalizing on the neighboring ketone group (or derivative thereof) of compounds **3.53** or **3.54** to direct the C–H metalation event, with vinyl halide or vinyl boronic ester **3.55** as the other coupling partner.

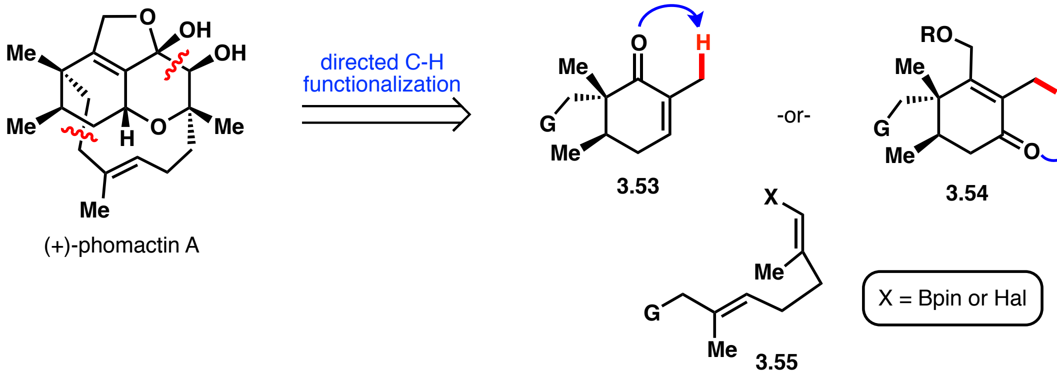

OH
OH
Me
Me
Me
H
O
O
Me
(+)-phomactin A
directed C-H functionalization
O
H
Me
G
Me
3.53
-or-
RO
Me
H
G
Me
O
3.54
X
Me
G
Me
3.55
X = Bpin or Hal

Scheme 12: Ketone-directed C─H functionalization approach to phomactin A

We were keenly aware that this type of direct C–C bond formation was unprecedented and warranted further exploration on simple systems before translation to the total synthesis. For C(sp^3)–H functionalization, ketone-derived directing groups have been utilized for forging carbon-heteroatom bonds such as the acetoxylation chemistry pioneered by the Sanford group (Scheme 13A)[24] or the amidation chemistry developed by Chang and coworkers (Scheme 13B).[25] At the time, ketone-derived directing groups had never been utilized for the direct formation of a carbon-carbon bond through C(sp^3)–H functionalization.

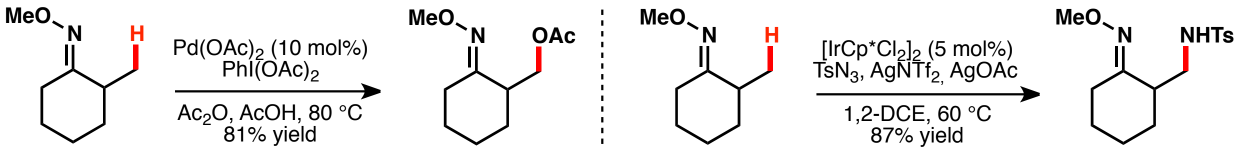
A) Sanford (2004)

B) Chang (2014)

MeO
N
H
Pd(OAc)2 (10 mol%)
PhI(OAc)2
Ac2O, AcOH, 80 °C
81% yield
MeO
N
OAc
MeO
N
H
[IrCp*Cl2]2 (5 mol%)
TsN3, AgNTf2, AgOAc
1,2-DCE, 60 °C
87% yield
MeO
N
NHTs

Scheme 13: Oxime-directed functionalization to forge carbon-heteroatom bonds

The vast majority of reactions that form C(sp^3)–carbon bonds utilize carboxylic acid derivatives as directing groups (Figure 7). Many of the weakly coordinating directing groups such as carboxylic acids (**3.56**), hydroxamic acid ethers (**3.57**) and *N*-aryl amides (**3.58**) have been popularized by Jin-Quan Yu's group.[26] Additionally, strongly coordinating bi-dentate directing groups such as 8-aminoquinolines (**3.59**) have been utilized by Daugulis[27] and others to forge new C–C bonds through C(sp^3)–H functionalization.

Figure 7: Carboxylic acid-derived directing groups for C─C bond formation

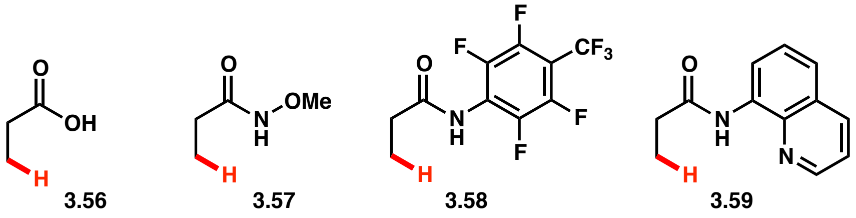

O
OH
H
3.56
O
N
OMe
H
H
3.57
F
F
CF3
O
N
H
F
F
H
3.58
O
N
H
N
H
3.59

We recognized a clear gap in the C(sp^3)–H functionalization literature and sought to develop a direct method to construct C–C bonds by utilizing ketone-derived directing groups. Initially, since methyl oxime ethers have shown productive reactivity in C–H functionalization, we decided to explore this directing group in the context of carvone (Scheme 14). Carvone oxime **3.60** and phenylboronic pinacol ester were subjected to palladium catalyzed coupling conditions that employed a mono-*N*-protected amino acid ligand and silver carbonate as an oxidant.[28] To our delight, the desired product **3.61** was obtained in 25% yield along with 25% of oxidative Heck product **3.62** and 20% returned starting material. We knew that removal of the disubstituted double bond would not allow for Heck-type chemistry, so hydrogenated derivative **3.63** was prepared. Surprisingly, we observed almost no reactivity with this substrate, forming the desired product **3.64** in about 2% yield. Primarily starting material was recovered.

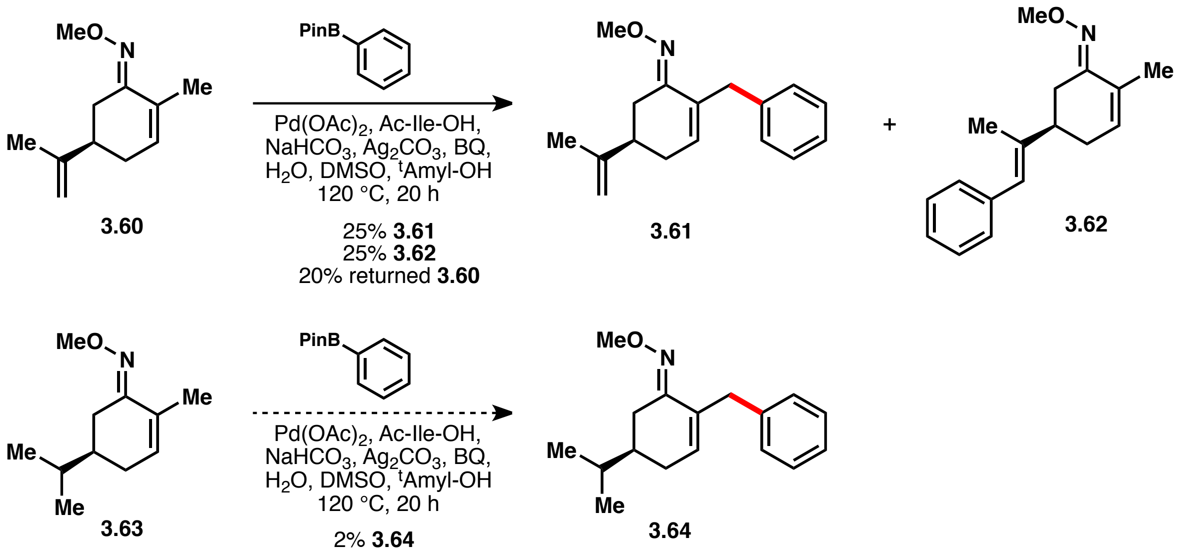

Scheme 14: Carboxylic acid-derived directing groups for C–C bond formation

This drastic drop in reactivity was surprising since the isopropenyl/isopropyl group is situated far away from the site of reactivity. We wondered whether the pi system could be serving as a ligand for palladium, but when we modeled the system, we couldn't find a reasonable conformation that placed this double bond close enough to the allylic methyl group to support intramolecular chelation. Intermolecular ligation was ruled out because running the reaction on a mixture of compounds **3.60** and **3.63** only resulted in products **3.61** and **3.62** with still no formation of hydrogenated product **3.64**. Nonetheless, we were intrigued by the possibility that additional coordinating groups could be incorporated and assist in ligating the palladium center during the reaction. To this effect, we synthesized olefinic oxime **3.65** and pyridyl oxime **3.66** to assess the effects of both weakly and strongly coordinating moieties (Scheme 15). Unfortunately, neither of these substrates proceeded to give more than a trace of the desired C–H arylated product.

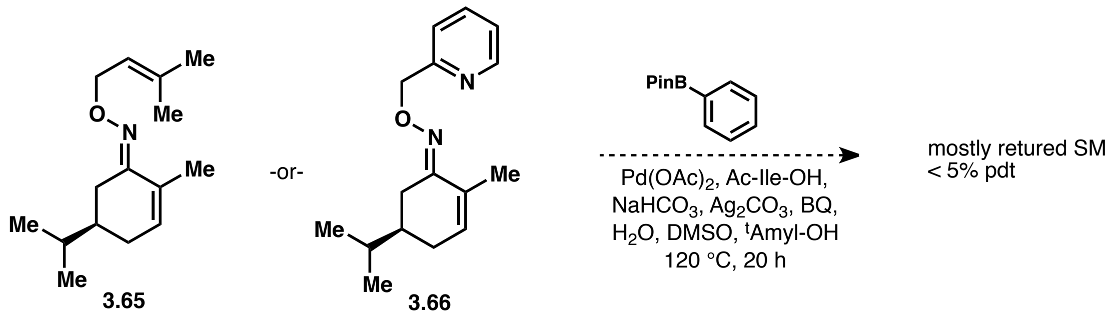
Me
Me
O
N
Me
Me
Me
-or-
N
O
N
Me
Me
Me
PinB
Pd(OAc)2, Ac-Ile-OH,
NaHCO3, Ag2CO3, BQ,
H2O, DMSO, tAmyl-OH
120 °C, 20 h
mostly retured SM
< 5% pdt

3.65 **3.66**

Scheme 15: Incorporating additional chelating groups to the directing group

Revisiting the carboxylic acid derivatives that are commonly utilized in C–H arylation chemistry, we wondered if a critical component was the presence of an acidic proton in the directing group (see Figure 7). This would allow for tautomerization and thus fluctuation between X-type and L-type ligands during the course of the reaction. This acid/base chemistry could also be important for the concerted metalation deprotonation (CMD) step.[29] To incorporate this design element, we synthesized carbamoyl oximes **3.67** and **3.68** that allow for 2-point binding as well as carbamate tautomerization (Scheme 16). At lower temperatures (40 °C), these substrates displayed some promising reactivity, yielding between 5 and 10% of the desired C–H arylation product. However, these carbamoyl compounds were not very stable and fragmented to give an isocyanate and free oxime at higher temperatures.

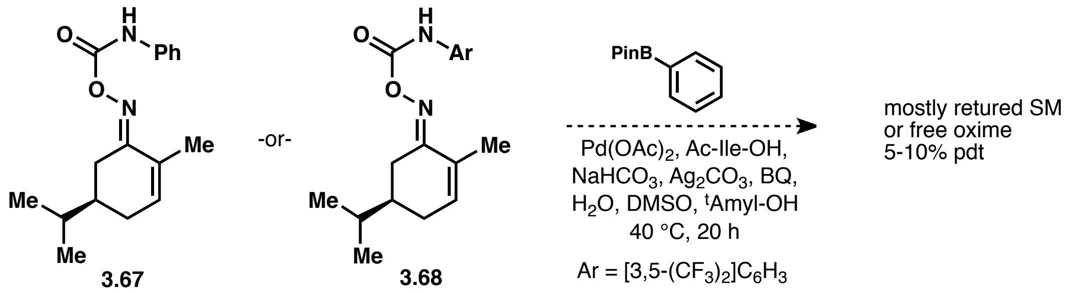
H
O
N
Ph
O
N
Me
Me
Me
-or-
H
O
N
Ar
O
N
Me
Me
Me
PinB
Pd(OAc)2, Ac-Ile-OH,
NaHCO3, Ag2CO3, BQ,
H2O, DMSO, tAmyl-OH
40 °C, 20 h
Ar = [3,5-(CF3)2]C6H3
mostly retured SM
or free oxime
5-10% pdt

3.67 **3.68**

Scheme 16: Carbamoyl-oximes for C–H arylation

Slightly more drastic effects were observed upon a brief solvent screen and oxidant screen utilizing the simple methyl oxime ether directing group. By switching from *t*-amyl alcohol to hexafluoroisopropanol (HFIP), a jump in product yield from 2% to 8% was realized. Additionally, changing the oxidant from silver carbonate to silver acetate increased the yield up to 13% (Table 1, entry 2) although this change in oxidant did not effect the reaction with *t*-amyl alcohol as solvent (entry 1). Leaving out sodium bicarbonate and the amino acid ligand did not result in a drop in yield. As shown in Table 1, further examination indicated that the majority of solvents were incapable of generating the desired C–H arylation product in greater than 2% yield. Although HFIP showed a dramatic increase in product yield, a corresponding drop in recovered starting material was also observed (see entry 2). Using acetic acid as solvent also showed higher levels of reactivity, generating 9% of the desired C–H arylation product along with 23% of the C–H acetoxylation compound (entry 7). This indicated that a slightly acidic solvent was necessary for productive reactivity.

Table 1: Solvent effect on reaction efficiency

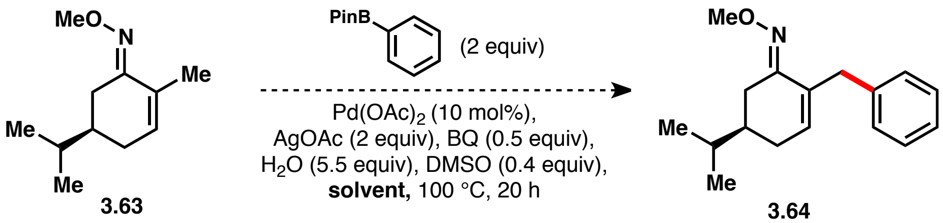
MeO
N
Me
Me
Me
3.63
PinB
(2 equiv)
Pd(OAc)$_2$ (10 mol%),
AgOAc (2 equiv), BQ (0.5 equiv),
H_2O (5.5 equiv), DMSO (0.4 equiv),
solvent, 100 °C, 20 h
MeO
N
Me
Me
3.64

entry	solvent	returned SM*	product yield*
1	*t*-amyl-OH	74%	2%
2	**HFIP**	**27%**	**13%**
3	toluene	76%	<1%
4	dioxane	51%	2%
5	DCE	70%	2%
6	EtOAc	82%	<1%
7	AcOH	19%	9% (23% acetoxylation)

*NMR yields based on CH_2Br_2 as internal standard

While utilizing HFIP as solvent resulted in an increase in product yield, it was concerning that the overall recovery of material was quite low. We wanted to get a better indication of the rate of product formation versus the rate of decomposition, so we varied the reaction duration and quantified the resulting amount of starting material and product (Table 2). We observed that the product had already been formed in maximal yield at just 1 hour (entry 1). As the reaction time increased, the product yield stayed roughly constant while the amount of returned starting material dropped steadily. There were several possibilities for this: (1) The reaction stalled out quickly and the starting material slowly degraded while the product was stable. (2) The product was not stable under the reaction conditions but a steady state of product was maintained because product formation roughly equaled product decomposition after 1 hour. (3) Both reactant and product were subject to decomposition. No matter which pathway was operative, it was clear that harsh reaction conditions were responsible for the overall low yield.

Table 2: Effect of reaction time on efficiency

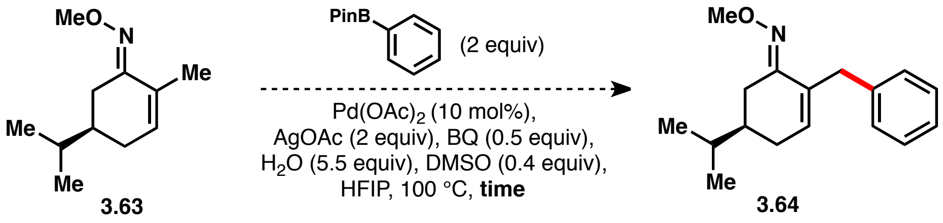
MeO
N
Me
Me
Me
3.63
PinB
(2 equiv)
Pd(OAc)$_2$ (10 mol%),
AgOAc (2 equiv), BQ (0.5 equiv),
H_2O (5.5 equiv), DMSO (0.4 equiv),
HFIP, 100 °C, **time**
MeO
N
Me
Me
3.64

entry	reaction time	returned SM*	product yield*
1	1 hour	42%	15%
2	2 hours	45%	16%
3	4 hours	26%	14%
4	8 hours	37%	14%
5	20 hours	27%	13%
6	40 h, 120 °C	2%	3%

*NMR yields based on CH_2Br_2 as internal standard

We next wanted to see if high reaction temperatures were required to achieve the desired reactivity. Interestingly, we found that the C–H arylation product forms at all the temperatures surveyed, even room temperature (Table 3, entry 4). Notably, the mass recovery was much better at lower temperatures, although some decomposition still occurred.

Table 3: Temperature effects on reaction efficiency

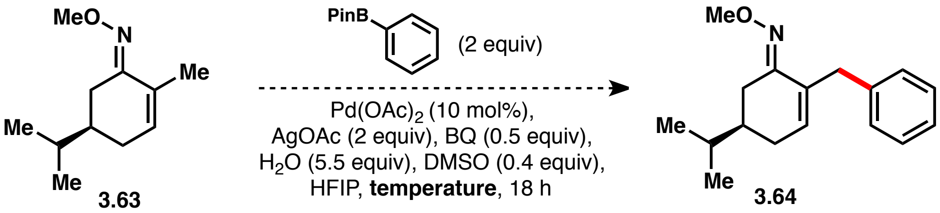
MeO
N
Me
Me
Me
3.63
PinB
(2 equiv)
Pd(OAc)$_2$ (10 mol%),
AgOAc (2 equiv), BQ (0.5 equiv),
H_2O (5.5 equiv), DMSO (0.4 equiv),
HFIP, **temperature**, 18 h
MeO
N
Me
Me
3.64

entry	temperature	returned SM*	product yield*
1	100 °C	27%	13%
2	70 °C	44%	14%
3	50 °C	37%	16%
4	room temp	59%	10%

*NMR yields based on CH_2Br_2 as internal standard

Having evaluated the solvent and temperature for this reaction, we set out to systematically evaluate the other reaction parameters (palladium catalysts, ligands, bases, benzoquinone equivalents, oxime ether derivatives, and aryl coupling partners) to improve room temperature reactivity (Table 4). Unfortunately, after exhaustive screening, we were never able to improve the product yield above 16% (for a detailed list of optimization conditions and results, see Section 3.9). Additionally, we recognized that our retrosynthetic plan for phomactin A required a more challenging C(sp^3)–H vinylation instead of a C(sp^3)–H arylation. Because of these considerations, we abandoned our investigation into direct C–C bond-forming processes.

Table 4: Summary of optimization conditions

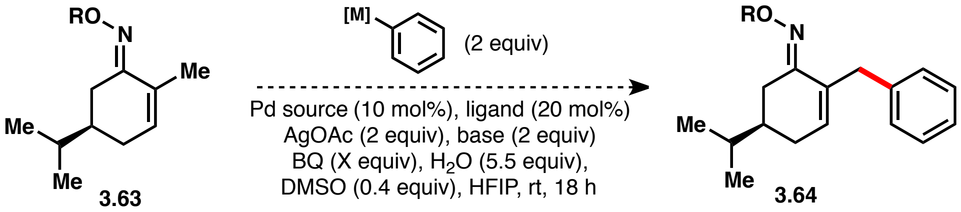
RO
N
Me
Me
Me
3.63
[M]
(2 equiv)
Pd source (10 mol%), ligand (20 mol%)
AgOAc (2 equiv), base (2 equiv)
BQ (X equiv), H_2O (5.5 equiv),
DMSO (0.4 equiv), HFIP, rt, 18 h
RO
N
Me
Me
3.64

Pd source	ligand	base	BQ equiv	oxime R	coupling partner
Pd(OAc)$_2$	Ac-Ile-OH	Cs_2CO_3	0	Me	Ph-BPin
$PdCl_2$	Boc-Ile-OH	K_2CO_3	0.2	H	Ph-B(OH)$_2$
$PdCl_2$(MeCN)$_2$	2-picoline	CsOAc	0.5	Ac	K$^+$ Ph-BF$_3^-$
Pd(TFA)$_2$	quinoline	K_2HPO_4	1	*t*-Bu	Ph-SnMe$_3$
Pd(OPiv)$_2$	pyridine	CsF			
Pd(OAc)$_2$·sulfoxide	IPr				
[PdCl(allyl)]$_2$	SIMes-HBF$_4$				

Nonetheless, we were pleased to find that known methods for C(sp^3)–H acetoxylation were successful at functionalizing the desired methyl group, gaining access to allylic acetate **3.69** (Scheme 17).[24] From this functionalized compound, we thought that pi-allyl cross coupling methodologies should be amenable to accessing various arylated or vinylated species. Diana Wang, an undergraduate working in the Sarpong lab, was able to optimize this type of reaction to effect a pi-allyl Suzuki coupling, affording skipped diene **3.70** in good yield. This overall sequence demonstrated that a 2-step vinylation sequence could be amenable to the phomactin synthesis in lieu of a direct vinylation protocol.

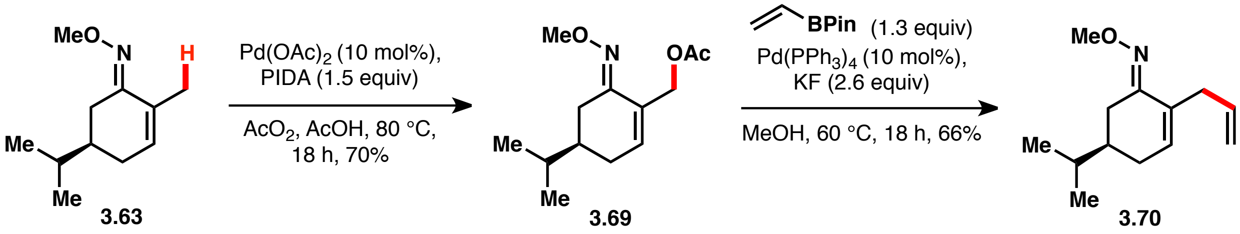

MeO
N
H
Me
Me
3.63
Pd(OAc)2 (10 mol%),
PIDA (1.5 equiv)
AcO2, AcOH, 80 °C,
18 h, 70%
OAc
3.69
BPin (1.3 equiv)
Pd(PPh3)4 (10 mol%),
KF (2.6 equiv)
MeOH, 60 °C, 18 h, 66%
3.70

Scheme 17: An alternative 2-step vinylation sequence

Additionally, after we moved on from our studies on C(sp^3)–H arylation directed by ketone derivatives, two papers were published showcasing this type of transformation. In the first report, Xia and coworkers demonstrated that iridium could catalyze a direct C–H arylation utilizing aryl iodonium salts as the coupling partners (Scheme 18A).[30] In the second report, Yu and coworkers showed that palladium can be a viable catalyst, utilizing glycine to form a transient imine directing group in situ (Scheme 18B).[31] These reports along with our ability to effect a 2-step acetoxylation/coupling sequence assured us that a ketone-directed C(sp^3)–H functionalization was reasonable to propose in our retrosynthetic analysis (see Scheme 12 and Scheme 19).

A) Xia and Shi (2015)

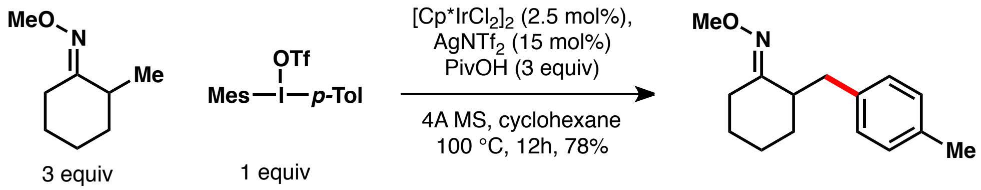

MeO
N
Me
3 equiv
OTf
Mes—I—p-Tol
1 equiv
[Cp*IrCl2]2 (2.5 mol%),
AgNTf2 (15 mol%)
PivOH (3 equiv)
4A MS, cyclohexane
100 °C, 12h, 78%
MeO
N
Me

B) Yu (2016)

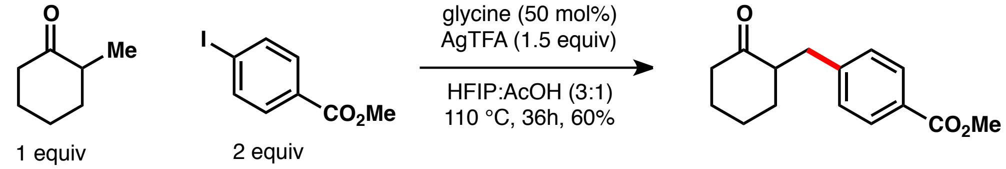

O
Me
1 equiv
I
CO2Me
2 equiv
Pd(OAc)2 (10 mol%)
glycine (50 mol%)
AgTFA (1.5 equiv)
HFIP:AcOH (3:1)
110 °C, 36h, 60%
O
CO2Me

Scheme 18: Recent advances in C–C bond formation from ketone-derived directing groups

3.6: Initial Strategy: "Traceless" Bond Construction

As shown by Yamada, Pattenden, Halcomb, and others, an effective synthesis of the phomactin natural products often relies on efficient fragment coupling and subsequent macrocyclization (see Section 3.3). We were confident in our abilities to forge the key C3a–C3 bond via C–H functionalization and subsequent intramolecular coupling (e.g., from **3.71**, Scheme 19). However, we were less certain how to construct the key C1'–C2' bond (highlighted in red, **3.72**). This required the formation of a new C(sp^3)–C(sp^3) bond, so the application of cross-coupling methodologies would be challenging. Most methods for constructing these types of bonds rely on neighboring functional groups to impart reactivity to the two reacting partners. Commonly, an electron-withdrawing group is appended to enable deprotonation and generation of a good nucleophile. However, after the reaction has taken place, the electron-withdrawing group needs to be removed unless it is present in the target molecule. To avoid this type of functional group manipulation, we sought to employ a "traceless" coupling reaction that was recently reported by Thomson and coworkers.[32] This would enable the construction of the desired C(sp^3)–C(sp^3) bond starting from aldehyde **3.73** and hydrazine **3.74**, yielding coupled product **3.72** without any trace of the aldehyde or hydrazine functional groups. Aldehyde **3.73** could arise from carvone-derived cyclobutanol **3.46** through the C–C activation chemistry that we've developed.

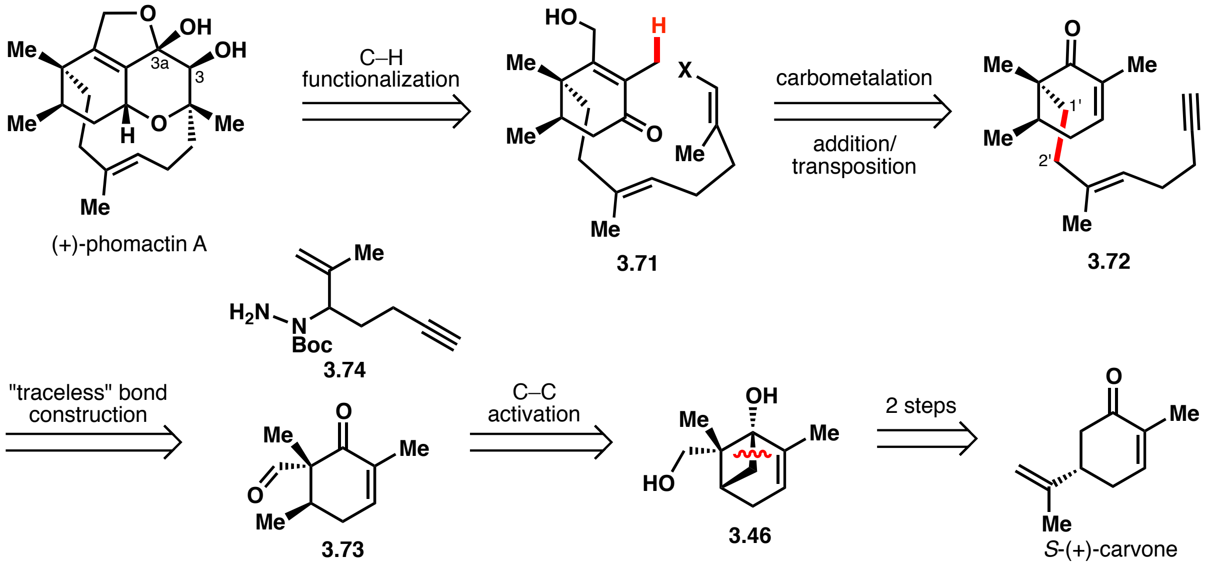

Scheme 19: Retrosynthesis featuring C–H functionalization and "traceless" bond construction as key steps

In the "traceless" bond formation reaction that Thomson and coworkers developed, an aldehyde (such as **3.75**) and an allylic hydrazine (such as **3.76**) are first condensed to form hydrazone **3.77** (Scheme 20). Upon heating in the presence of the strong acid triflimide, a [3,3]-sigmatropic rearrangement takes place to give putative intermediate **3.79**. Acid-catalyzed loss of the Boc group (CO_2 and ethylene) followed by loss of nitrogen gives the final product **3.81**. This product is devoid of any functionality that can be traced back to an aldehyde or a hydrazine moiety. Additionally, this reaction forges a new bond between two unfunctionalized sp^3-carbon atoms while also forming a stereodefined double bond. On these simple substrates, the *E* diastereomer is favored, presumably due to the *iso*-butyl group sitting pseudo-equatorial in the chair-like transition state of the [3,3]-sigmatropic rearrangement.

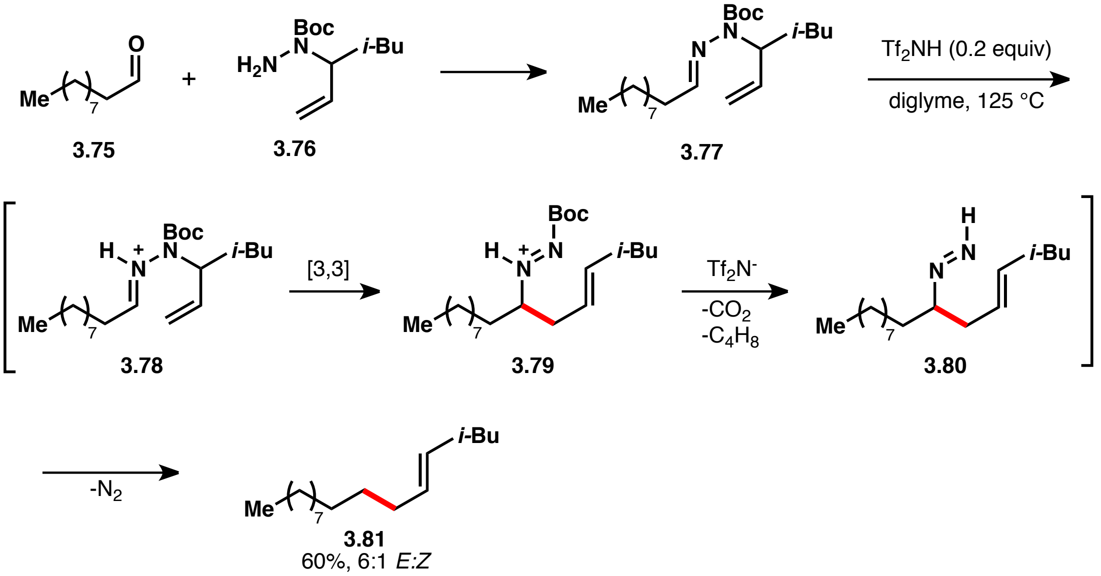

Scheme 20: Thomson's "traceless" bond construction between an aldehyde and a hydrazine

To apply this strategy toward a synthesis of the phomactin terpenoids, we first carried out the synthesis of hydrazine **3.83** (Scheme 21). Starting from 4-pentyn-1-ol, Swern oxidation followed by addition of in situ generated isopropenylmagnesium bromide delivered allylic alcohol **3.82**. Mitsunobu reaction with *tert*-butyl-4,5,6,7-tetrachloro-1,3-dioxoisoindolin-2-ylcarbamate followed by phthalimide cleavage with ethylene diamine afforded desired hydrazine **3.83**. The aldehyde partner **3.84** was readily accessible from carvone-derived cyclobutanol **3.46** by rhodium-catalyzed C–C bond cleavage followed by DMP oxidation. Heating the aldehyde and hydrazine together afforded condensation product **3.85** in 76% yield. Unfortunately, heating this hydrazone in the presence of triflimide did not result in desired product **3.86**. Instead, starting material was isolated after heating at 125 °C for 2 hours; increasing the temperature to 150 °C only resulted in decomposition of the hydrazone. It is likely that this system is too sterically demanding for this reaction to proceed. We had attempted to form a trisubstituted double bond whereas the Thomson communication only reported the synthesis of disubstituted double bonds. Additionally, the aldehyde component (**3.84**) is very sterically encumbered. In the published substrate scope, alpha-branched aldehydes were never used, so aldehydes with alpha-quaternary centers are probably prohibitively bulky. Due to this steric hindrance, the transition state for the [3,3]-sigmatropic rearrangement may be too high in energy to access before decomposition of the starting material occurs.

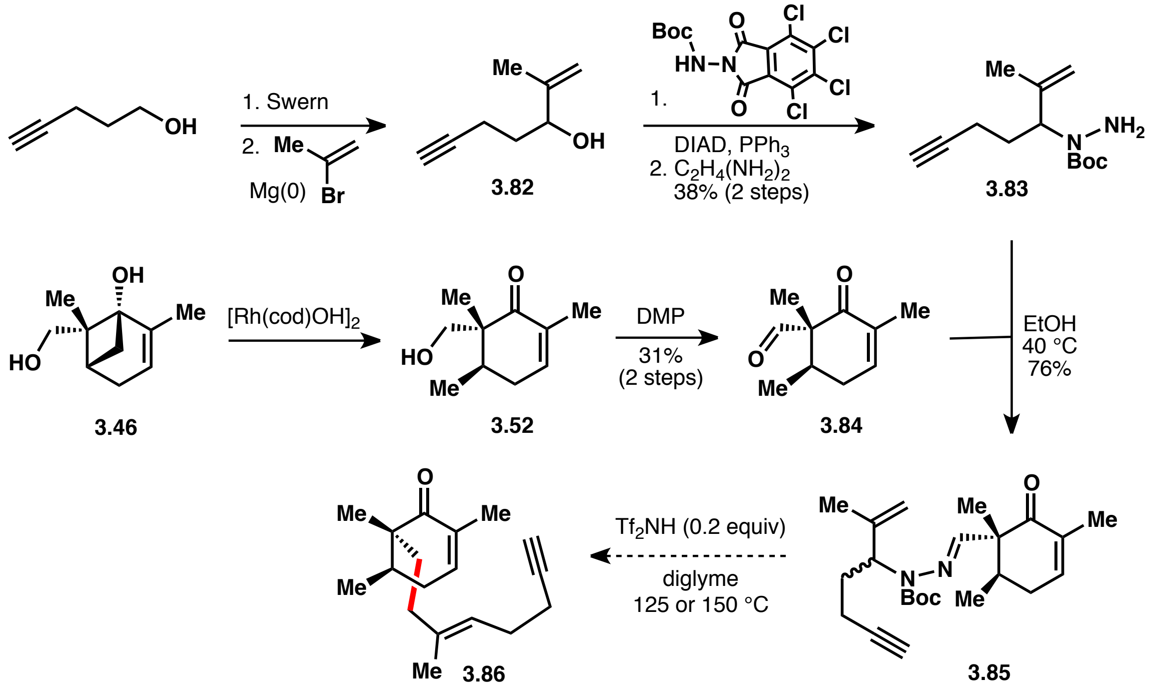
1. Swern
2. Me Br
Mg(0)
OH
Me
3.82
1. Boc HN–N O Cl Cl Cl Cl O
DIAD, PPh$_3$
2. $C_2H_4(NH_2)_2$
38% (2 steps)
Me
N NH$_2$
Boc
3.83
OH
Me
Me
HO
3.46
$[Rh(cod)OH]_2$
O
Me
Me
HO
Me
3.52
DMP
31%
(2 steps)
O
Me
Me
O
Me
3.84
EtOH
40 °C
76%
O
Me
Me
Me
Me
3.86
Tf$_2$NH (0.2 equiv)
diglyme
125 or 150 °C
Me
Me
O
Me
N–N
Boc
Me
3.85

Scheme 21: Synthesis of hydrazone **3.85** and attempted "traceless" bond construction

3.7: Conclusion

The phomactin natural products are fascinating due to their structural topology as well as their ability to inhibit the activity of platelet activating factor. We believe that employing a carvone-derived cyclobutanol in conjuncture with C–C activation methodologies will provide efficient access to a wide range of these natural products. This is enabled by our ability to quickly access a densely functionalized enantiopure cyclohexenone scaffold. Investigations into fragment coupling indicated that a C–H functionalization approach could be successful, most likely through a 2-step sequence since optimization of the direct C–C bond forming process proved challenging. To form the other bond necessary for the macrocycle, a “traceless” bond construction between an aldehyde and a hydrazine was investigated. Unfortunately, this ideal disconnection was not successful on the requisite sterically demanding substrates. A new approach that overcomes these hurdles will be discussed in Chapter 4.

3.8: Experimental Contributors

Diana Wang (undergraduate, Sarpong lab) optimized the pi-allyl Suzuki coupling reaction in the 2-step vinylation protocol (Scheme 17). The rhodium-catalyzed C–C activation chemistry of cyclobutanol **3.46** (Scheme 10) was previously published by Ahmad Masarwa (postdoc, Sarpong group) and Manuel Weber (postdoc, Sarpong group). The remainder of the work presented in this chapter was conducted by Paul R. Leger.

3.9: Experimental Methods

All reactions were run in flame-dried round-bottom flasks or vials under a nitrogen atmosphere. Reactions were monitored by thin layer chromatography (TLC) on Silicycle Siliaplate™ glass backed TLC plates (250 μm thickness, 60 Å porosity, F- 254 indicator) and visualized using UV irradiation and *para*-anisaldehyde stain. For heated reactions, the temperature was monitored using an IKA® temperature control. Dry acetonitrile, diethyl ether, tetrahydrofuran (THF), triethylamine (TEA), benzene, toluene, and methanol were obtained by passing these previously degassed solvents through activated alumina columns. Dichloromethane (DCM) was distilled over calcium hydride before use. Volatile solvents were removed under reduced pressure on a rotary evaporator. All flash chromatography was conducted using Sorbent Technologies 60 Å, 230x400 mesh silica gel (40-63 μm). ^{1}H NMR and ^{13}C NMR spectra were acquired using Bruker 300, 400, 500, and 600 MHz (75, 100, 125, and 150 MHz for ^{13}C NMR) spectrometers in $CDCl_3$. Chemical shifts are measured relative to the shift of the residual solvent (^{1}H NMR - $CDCl_3$ $\delta = 7.26$; ^{13}C NMR $CDCl_3$ $\delta = 77.16$). NMR data are reported as follows: chemical shift (multiplicity, coupling constant, integration). Splitting is reported with the following symbols: s = singlet, bs = broad singlet, d = doublet, t = triplet, q = quartet, m = multiplet. IR spectra were acquired on a Bruker Alpha FTIR (neat) unless otherwise specified. Spectra are reported in frequency of absorption in cm^{-1}. Only selected resonances are reported. High-resolution mass spectra (HRMS) were performed by the mass spectral facility at the University of California, Berkeley.

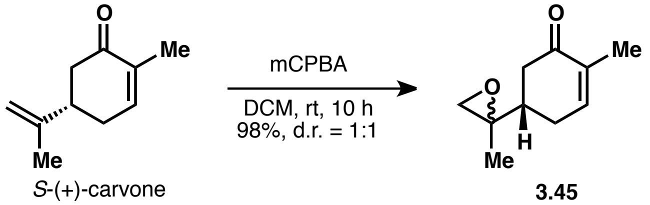

Epoxy carvone **3.45**

A 2 L flask was charged with *S*-(+)-carvone (30 mL, 192 mmol) and DCM (1 L) and cooled to 0 °C. Then, 3-chloroperoxybenzoic acid (51.6 g, 230 mmol) was added portionwise (over the course of 15 min), after which the reaction was allowed to warm to room temperature and stir for 15 h. The reaction was filtered over Celite. $Na_2S_2O_3$ (500 mL) was added to the filtrate and stirred for 1 h. The layers were separated and to the organic layer was added $NaHCO_3$ (500 mL) and stirred for 1 h. The organic layer was then dried over magnesium sulfate, filtered, and concentrated to yield epoxy carvone **3.45** (31.9 g, 99%, 1:1 d.r.) as a colorless oil. The spectral data are consistent with those reported in the literature.[33] ^{1}H NMR (600 MHz, $CDCl_3$) δ 6.72 (t, *J* = 6.7 Hz, 2H), 2.68 (dd, *J* = 21.7, 4.6 Hz, 2H), 2.63-2.51 (m, 4H), 2.40 (td, *J* = 18.0, 12.5, 6.3 Hz, 2H), 2.29-2.12 (m, 5H), 2.06 (ddd, *J* = 14.5, 9.7, 4.7 Hz, 1H), 1.76 (s, 6H), 1.31 (d, *J* = 10.0 Hz, 6H).

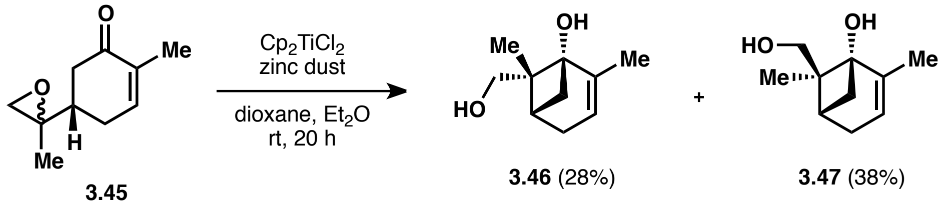

Cyclobutanol **3.46**

A 1 L flask was charged with Cp_2TiCl_2 (16.5 g, 66.2 mmol) and zinc dust (13.0 g, 199 mmol), equipped with an addition funnel, and filled with an inert nitrogen atmosphere. A mixture of diethyl ether (100 mL, nitrogen sparged) and dioxane (100 mL, nitrogen sparged) was added to the flask and the heterogeneous mixture was stirred for 1.5 h, after which the color of the mixture had turned a deep green color. Meanwhile, the addition funnel was charged with epoxy carvone **3.45** (5.00 g, 30.1 mmol), diethyl ether (100 mL), and dioxane (100 mL) and this solution was sparged with nitrogen for 30 min. Then, the epoxy carvone solution was allowed to slowly drop into the deep green reaction mixture over the course of 2 h and the reaction was allowed to stir an additional 18 h. The reaction was quenched with NaH_2PO_4 (200 mL), brine (50 mL), and ethyl acetate (150 mL) and poured into a 2 L Erlenmeyer flask. This was allowed to stir open to air for 4 h where upon the mixture turned a bright orange color. The solids were removed by filter paper vacuum filtration. Brine (200 mL) was added to the filtrate, the layers were separated, and the aqueous layer was extracted with ethyl acetate (2 x 200 mL). The combined organic layers were dried over magnesium sulfate, filtered, concentrated, and purified by column chromatography (SiO_2, 25% to 60% EtOAc/ hexane) to yield cyclobutanol **3.46** (1.40 g, 28%) as a pale yellow solid along with the undesired diastereomeric product (1.90 g, 38%). The spectral data are consistent with those reported in the literature.[21] ^{1}H NMR (500 MHz, $CDCl_3$) δ 5.28 (tt, *J* = 3.0, 1.6 Hz, 1H), 3.75 (d, *J* = 10.3 Hz, 1H), 3.41 (d, *J* = 10.3 Hz, 1H), 2.27 (dd, *J* = 8.3, 6.8 Hz, 1H), 2.21-2.12 (m, 2H), 2.07 (dq, *J* = 18.4, 2.7 Hz, 1H), 1.85 (bs, 1H), 1.81 (q, *J* = 2.1 Hz, 3H), 1.63 (d, *J* = 8.3 Hz, 1H), 1.35 (s, 3H).

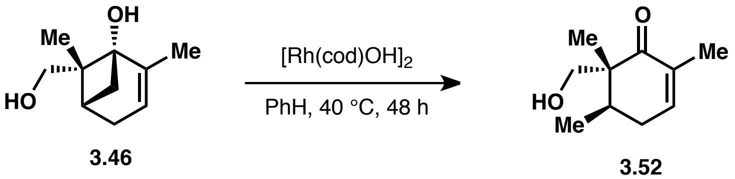

Cyclohexenone **3.52**

In the glovebox, a 25 mL Schlenk flask was charged with cyclobutanol **3.46** (89 mg, 0.53 mmol), $[Rh(OH)cod]_2$ (24 mg, 0.053 mmol), and benzene-d_6 (5.3 mL). This flask was sealed and heated to 40 °C for 48 h. The mixture was then filtered through a plug of Celite with diethyl ether, concentrated, and purified by column chromatography (SiO_2, 15% Et_2O/ pentane) to yield enone **3.52** (45 mg, 51%) as a colorless oil. The spectral data are consistent with those reported in the literature.[23] ^{1}H NMR (500 MHz, $CDCl_3$) δ 6.67 (ddt, *J* = 5.5, 2.5, 1.5 Hz, 1H), 3.87 (dd, *J* = 11.5, 5.8 Hz, 1H), 3.52 (dd, *J* = 11.5, 5.6 Hz, 1H), 2.60 (t, *J* = 7.0 Hz, 1H), 2.40-2.10 (m, 3H), 1.76 (dt, *J* = 2.7, 1.4 Hz, 3H), 0.97 (d, *J* = 6.7 Hz, 3H), 0.93 (s, 3H).

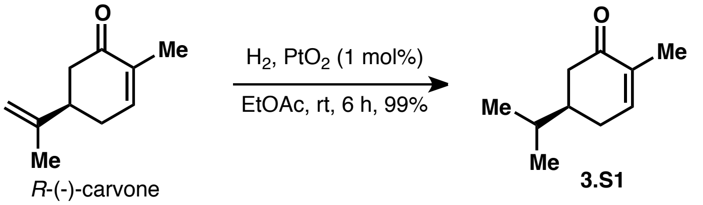
O
Me
H$_2$, PtO$_2$ (1 mol%)
EtOAc, rt, 6 h, 99%
Me
R-(-)-carvone
O
Me
Me
Me
3.S1

Carvotanacetone (**3.S1**)

A solution of *R*-(-)-carvone (10 mL, 63.9 mmol) in ethyl acetate (35 mL) was added to a flask containing PtO_2 (140 mg, 0.64 mmol). The flask was sealed and filled with hydrogen gas (balloon, 1 atm) and stirred until the reaction was completed as shown by LCMS (between 3-9 hours). The reaction was then filtered over a pad of Celite and concentrated to yield carvotanacetone (**3.S1**, 9.63 g, 99%) as a colorless oil. The spectral data are consistent with those reported in the literature.[34] ^1H NMR (600 MHz, $CDCl_3$) δ 6.74 (d, *J* = 6.1 Hz, 1H), 2.53 (dd, *J* = 16.0, 3.5 Hz, 1H), 2.35 (dt, *J* = 18.6, 5.3 Hz, 1H), 2.15-2.02 (m, 2H), 1.84 (ddt, *J* = 19.9, 10.4, 4.4 Hz, 1H), 1.76 (s, 3H), 1.56 (h, *J* = 6.8 Hz, 1H), 0.91 (d, *J* = 7.0 Hz, 6H).

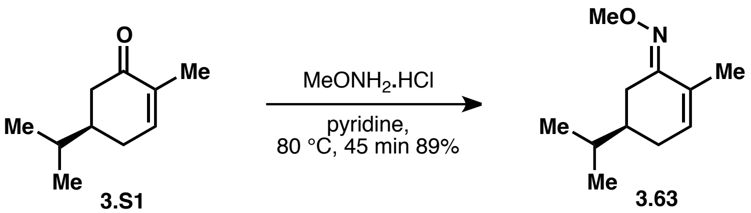
O
Me
Me
Me
3.S1
MeONH$_2$.HCl
pyridine,
80 °C, 45 min 89%
MeO
N
Me
Me
Me
3.63

Oxime methyl ether **3.63**

A 50 mL flask was charged with carvotanacetone (**3.S1**, 4.00 g, 26.3 mmol), pyridine (11 mL), and *O*-methylhydroxylamine hydrochloride (2.63 g, 31.5 mmol) and heated to 80 °C for 45 min. The mixture was then diluted with EtOAc (60 mL) and washed with 20% aqueous AcOH (5 x 50 mL) followed by aqueous $NaHCO_3$ (3 x 50 mL). The organic layer was then dried over magnesium sulfate, filtered, and concentrated to yield oxime methyl ether **3.63** (4.24 g, 89%) as a colorless oil. The spectral data are consistent with those reported in the literature.[25] ^1H NMR (600 MHz, $CDCl_3$) δ 5.98 (dt, *J* = 5.9, 1.5 Hz, 1H), 3.90 (s, 3H), 3.08 (ddd, *J* = 16.5, 4.2, 1.7 Hz, 1H), 2.17 (dt, *J* = 16.3, 5.4 Hz, 1H), 1.86 (ddt, *J* = 14.7, 6.2, 2.7 Hz, 1H), 1.82 (s, 3H), 1.77 (dd, *J* = 16.6, 12.8 Hz, 1H), 1.54 (dq, *J* = 13.1, 6.6 Hz, 1H), 1.48 (dtd, *J* = 15.8, 8.4, 2.4 Hz, 1H), 0.91 (dd, *J* = 12.0, 6.7 Hz, 6H).

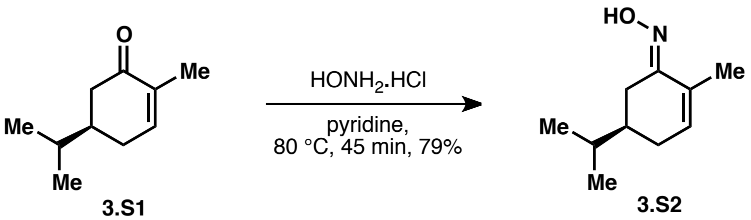
O
Me
Me
Me
3.S1
HONH$_2$.HCl
pyridine,
80 °C, 45 min, 79%
HO
N
Me
Me
Me
3.S2

Oxime **3.S2**

A 50 mL flask was charged with carvotanacetone (**3.S1**, 3.00 g, 19.7 mmol), pyridine (9 mL), and hydroxylamine hydrochloride (1.85 g, 26.6 mmol) and heated to 80 °C for 45 min. The mixture was then diluted with EtOAc (50 mL) and washed with 20% aqueous AcOH (5 x 40 mL) followed by aqueous $NaHCO_3$ (3 x 40 mL). The organic layer was then dried over magnesium sulfate, filtered, and concentrated to yield oxime **3.S2** (2.59 g, 79%) as a colorless oil. The spectral data are consistent with those reported in the literature.[35] ^{1}H NMR (600 MHz, $CDCl_3$) δ 6.03 (d, *J* = 6.3 Hz, 1H), 3.19 (dd, *J* = 16.5, 3.8 Hz, 1H), 2.20 (dt, *J* = 17.5, 5.5 Hz, 1H), 1.93-1.80 (m, 2H), 1.83 (s, 3 H), 1.60-1.47 (m, 2H), 0.93 (dd, *J* = 14.1, 6.6 Hz, 6H).

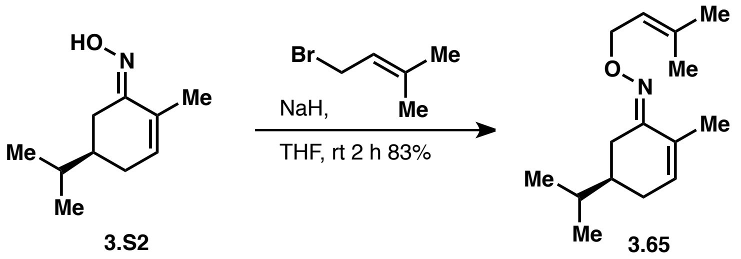

Olefinic oxime **3.65**

A 25 mL flask was charged with oxime **3.S2** (254 mg, 1.51 mmol), THF (6 mL), and sodium hydride (73 mg, 60wt%, 1.81 mmol) and stirred for 30 min. Then 3,3-dimethylallyl bromide (0.21 mL, 1.81 mmol) was added and stirred for 2 h. The solution was then quenched with NH_4Cl (6 mL), extracted with EtOAc (3 x 6 mL), dried over magnesium sulfate, filtered, concentrated, and purified by column chromatography (SiO_2, 5% EtOAc/ hexane) to yield olefin oxime **3.65** (374 mg, 83%) as a colorless oil. ^{1}H NMR (400 MHz, $CDCl_3$) δ 5.96 (d, *J* = 5.2 Hz, 1H), 5.46 (td, *J* = 8.0, 1.9 Hz, 1H), 4.60 (d, *J* = 6.8 Hz, 2H), 3.09 (dd, *J* = 17.7, 3.7 Hz, 1H), 2.15 (dt, *J* = 18.3, 5.5 Hz, 1H), 1.90 – 1.79 (m, 5H), 1.77 (s, 3H), 1.73 (s, 3H), 1.62 – 1.42 (m, 2H), 0.91 (dd, *J* = 10.1, 6.6 Hz, 6H); ^{13}C NMR (101 MHz, $CDCl_3$) δ 156.68, 137.40, 132.61, 130.81, 120.73, 70.75, 39.68, 32.28, 28.65, 26.90, 26.05, 20.07, 19.67, 18.34, 17.79; IR (neat) 2958, 2928, 2873, 1447, 1370, 1004 cm^{-1}; HRMS (ESI) calculated for $[C_{15}H_{26}NO]^+$ $[M+H]^+$: *m/z* 236.2009, found 236.2007.

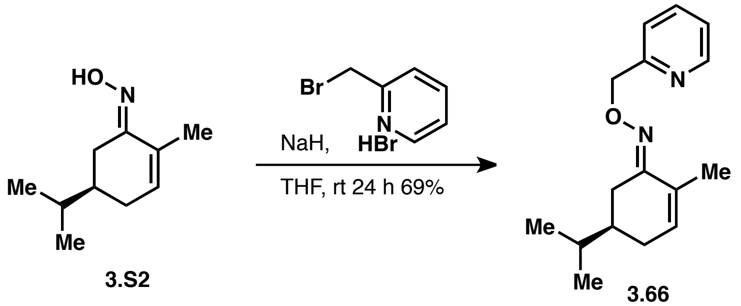

Pyridyl oxime **3.66**

A 25 mL flask was charged with oxime **3.S2** (300 mg, 1.79 mmol), THF (7 mL), and sodium hydride (103 mg, 60wt%, 2.58 mmol) and stirred for 30 min. Then 2-(bromomethyl)pyridine hydrobromide (543 mg, 2.15 mmol) was added and stirred for 24 h. The solution was then quenched with NH_4Cl (7 mL), extracted with EtOAc (3 x 7 mL), dried over magnesium sulfate, filtered, concentrated, and purified by column chromatography (SiO_2, 10% to 20 % EtOAc/ hexane) to yield pyridyl oxime **3.66** (320 mg, 69%) as a pale yellow oil. ^{1}H NMR (400 MHz, $CDCl_3$) δ 8.56 (dd, *J* = 5.0, 1.5 Hz, 1H), 7.67 (td, *J* = 7.7, 1.8 Hz, 1H), 7.37 (d,

J = 7.8 Hz, 1H), 7.18 (dd, J = 7.5, 4.9 Hz, 1H), 5.99 (dt, J = 6.2, 1.7 Hz, 1H), 5.26 (s, 2H), 3.20 (dd, J = 17.0, 3.1 Hz, 1H), 2.18 (dt, J = 17.4, 5.2 Hz, 1H), 1.94 – 1.80 (m, 2H), 1.77 (s, 3H), 1.62 – 1.45 (m, 2H), 0.92 (dd, J = 10.0, 6.5 Hz, 6H); ^{13}C NMR (101 MHz, $CDCl_3$) δ 159.01, 157.58, 149.11, 136.56, 133.27, 130.60, 122.34, 121.83, 76.56, 39.63, 32.25, 28.69, 26.99, 20.05, 19.71, 17.72; IR (neat) 2957, 2925, 2872, 1434, 1097 cm^{-1}; HRMS (ESI) calculated for $[C_{16}H_{23}N_2O]^+$ $[M+H]^+$: *m/z* 259.1805, found 259.1801.

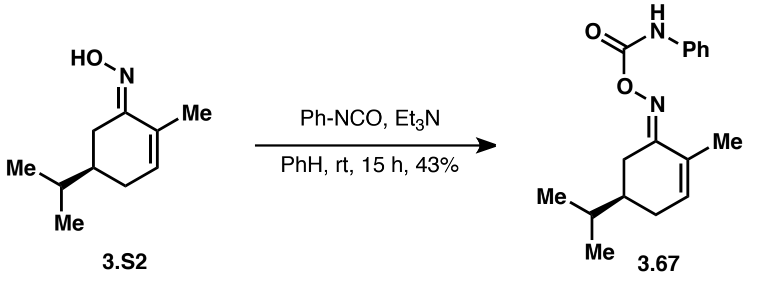

Phenyl carbamoyl oxime **3.67**

A 50 mL flask was charged with oxime **3.S2** (250 mg, 1.49 mmol), benzene (25 mL) and triethylamine (0.021 mL, 0.15 mmol). Phenyl isocyanate (0.32 mL, 2.99 mmol) was then added and the reaction was stirred for 15 h. The solution was concentrated and purified by column chromatography (SiO_2, 10% EtOAc/ hexane) to yield phenyl carbamoyl oxime **3.67** (185 mg, 43%) as a white powder. ^{1}H NMR (600 MHz, $CDCl_3$) δ 8.46 (s, 1H), 7.50 (d, J = 8.0 Hz, 2H), 7.34 (t, J = 7.7 Hz, 2H), 7.12 (t, J = 7.4 Hz, 1H), 6.30 (d, J = 6.0 Hz, 1H), 3.29 (dd, J = 17.0, 3.4 Hz, 1H), 2.27 (dt, J = 18.8, 5.4 Hz, 1H), 2.03 (dd, J = 17.1, 12.4 Hz, 1H), 1.96 (d, J = 11.4 Hz, 1H), 1.93 (s, 3H), 1.59 (tq, J = 10.4, 5.8, 5.1 Hz, 2H), 0.94 (dd, J = 13.3, 6.2 Hz, 6H); ^{13}C NMR (151 MHz, $CDCl_3$) δ 161.54, 152.68, 139.01, 137.24, 129.20, 129.13, 124.25, 119.74, 39.44, 32.03, 28.78, 28.00, 19.86, 19.58, 17.62; IR (neat) 3359, 2958, 2873, 1750, 1727, 1600, 1517, 1465, 1195 cm^{-1}; HRMS (ESI) calculated for $[C_{17}H_{23}N_2O_2]^+$ $[M+H]^+$: *m/z* 287.1754, found 287.1756. m.p. = 130.5-132.0 °C.

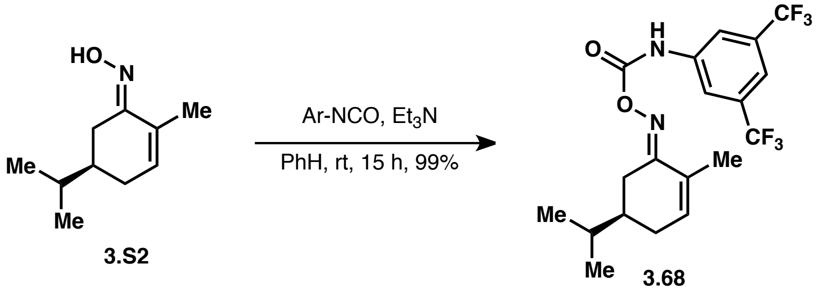

3,5-bis(CF_3)phenyl carbamoyl oxime **3.68**

A 100 mL flask was charged with oxime **3.S2** (500 mg, 2.99 mmol), benzene (30 mL) and triethylamine (0.042 mL, 0.30 mmol). 3,5-bis(trifluoromethyl)phenyl isocyanate (0.62 mL, 3.59 mmol) was then added and the reaction was stirred for 15 h. The solution was concentrated and purified by column chromatography (SiO_2, 1% MeOH/ DCM) to yield 3,5-bis(CF_3)phenyl carbamoyl oxime **3.68** (1.26 g, 99%) as a white powder. ^{1}H NMR (600 MHz, $CDCl_3$) δ 8.77 (s, 1H), 7.99 (s, 2H), 7.61 (s, 1H), 6.36 (d, J = 6.0 Hz, 1H), 3.25 (dd, J = 17.0, 3.0 Hz, 1H), 2.29 (dt,

J = 18.5, 5.3 Hz, 1H), 2.04 (dd, J = 16.9, 12.7 Hz, 1H), 1.97 (dd, J = 10.6, 2.4 Hz, 1H), 1.95 (s, 3H), 1.58 (tt, J = 12.3, 6.5 Hz, 2H), 0.92 (dd, J = 10.0, 6.2 Hz, 6H); ^{13}C NMR (151 MHz, $CDCl_3$) δ 162.72, 152.44, 140.11, 138.88, 132.67 (q, J = 34.1 Hz), 128.80, 125.90, 124.09, 122.28, 119.38, 117.63, 39.43, 32.01, 28.79, 28.14, 19.83, 19.52, 17.67; IR (neat) 3342, 2964, 2877, 1721, 1566, 1275, 1172, 1129 cm^{-1}; HRMS (ESI) calculated for $[C_{19}H_{21}N_2O_2F_6]^+$ $[M+H]^+$: *m/z* 423.1502, found 423.1499. m.p. = 132.0-133.0 °C.

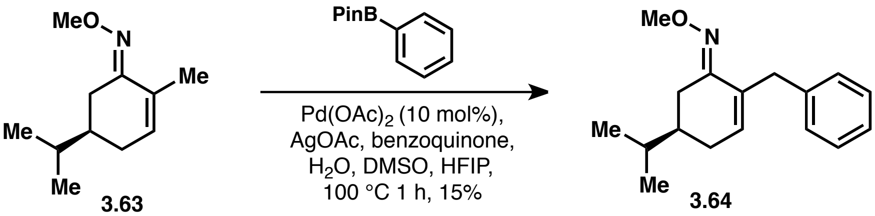

Arylated product **3.64**

A small microwave vial was charged with methyl oxime ether **3.63** (36.3 mg, 0.20 mmol), phenylboronic pinacol ester (81.6 mg, 0.40 mmol), palladium acetate (4.5 mg, 0.02 mmol), silver acetate (66.8 mg, 0.40 mmol), and 1,4-benzoquinone (10.8 mg, 0.10 mmol). The vial was sealed and backfilled with nitrogen. Then, hexafluoroisopropanol (1.0 mL), dimethylsulfoxide (5.7 µL, 0.08 mmol), and water (20 µL, 1.1 mmol) were added successively via syringe. The heterogeneous mixture was heated at 100 °C for 1 h. Upon cooling, ethyl acetate (2 mL) was added and the mixture was filtered over a silica plug. The crude material was analyzed by NMR with a known concentration of dibromomethane in $CDCl_3$. The crude material can be purified by column chromatography (SiO_2, 5% EtOAc/ hexane) to yield phenylated product **3.64** (7.7 mg, 15%) as a colorless oil. ^{1}H NMR (600 MHz, $CDCl_3$) δ 7.26 (t, J = 7.4 Hz, 2H), 7.22 (d, J = 7.2 Hz, 2H), 7.18 (tt, J = 7.2, 1.3 Hz, 1H), 5.83 (dd, J = 6.4, 2.3 Hz, 1H), 3.89 (s, 3H), 3.57 (q, J = 15.3 Hz, 2H), 3.08 (ddd, J = 16.6, 4.1, 1.7 Hz, 1H), 2.17 (dt, J = 17.8, 5.5 Hz, 1H), 1.85 (ddq, J = 17.9, 11.2, 2.4 Hz, 1H), 1.78 (dd, J = 16.6, 12.8 Hz, 1H), 1.53 (q, J = 7.0, 6.4 Hz, 1H), 1.48 (dtd, J = 14.1, 9.9, 2.9 Hz, 1H), 0.90 (dd, J = 12.7, 6.7 Hz, 6H); ^{13}C NMR (151 MHz, $CDCl_3$) δ 155.61, 140.78, 134.51, 133.72, 129.56, 128.15, 125.84, 61.86, 39.43, 36.93, 32.29, 28.87, 26.76, 19.93, 19.76; IR (neat) 2957, 2895, 1051, 907 cm^{-1}; HRMS (ESI) calculated for $[C_{17}H_{24}NO]^+$ $[M+H]^+$: *m/z* 258.1852, found 258.1850.

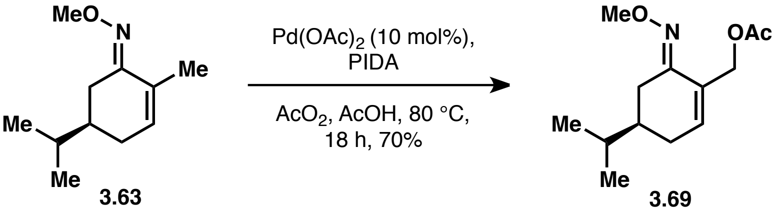

Allylic acetate **3.69**

A 100 mL Schlenk flask was charged with oxime methyl ether **3.63** (1.00 g, 5.52 mmol), (diacetoxyiodo)benzene (2.66 g, 8.27 mmol), $Pd(OAc)_2$ (62 mg, 0.28 mmol), acetic acid (23 mL), and acetic anhydride (23 mL). The flask was sealed and heated at 100 °C for 20 h. Upon cooling, the solution was diluted with hexane (40 mL) and washed with water (2 x 100 mL) then $NaHCO_3$ (2 x 50 mL) then brine (1 x 50 mL). The organics were dried over magnesium sulfate, filtered, concentrated, and purified by column chromatography (SiO_2, 5% EtOAc/ hexane) to yield allylic acetate **3.69** (734 mg, 56%) as yellow oil. ^{1}H NMR (400 MHz, $CDCl_3$) δ 6.24 (dd, *J* = 6.4, 2.4 Hz, 1H), 4.79 (s, 2H), 3.87 (s, 3H), 3.08 (ddd, *J* = 16.5, 3.9, 1.7 Hz, 1H), 2.26 (dt, *J* = 18.0, 5.0 Hz, 1H), 2.09 (s, 3H), 1.90 (ddq, *J* = 17.9, 10.8, 2.4 Hz, 1H), 1.78 (dd, *J* = 16.6, 12.6 Hz, 1H), 1.60 – 1.45 (m, 2H), 0.91 (t, *J* = 6.3 Hz, 6H); ^{13}C NMR (101 MHz, $CDCl_3$) δ 170.96, 154.12, 134.13, 129.66, 62.65, 62.01, 39.10, 32.19, 28.54, 26.29, 21.20, 19.85, 19.72; IR (neat) 2960, 2874, 1744, 1227, 1051 cm^{-1}; HRMS (ESI) calculated for $[C_{13}H_{22}NO_3]^+$ $[M+H]^+$: *m/z* 240.1594, found 240.1592.

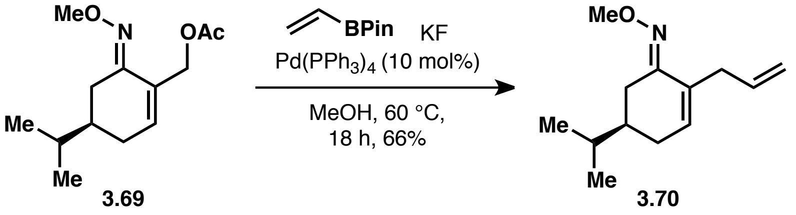

Skipped diene **3.70**

A small microwave vial was charged with allylic acetate **3.69** (47.9 mg, 0.20 mmol), tetrakis(triphenylphosphine)palladium (23.1 mg, 0.02 mmol), and methanol (1.0 mL) and stirred for 10 min. Then, vinylboronic pinacol ester (45 µL, 0.26 mmol) and potassium fluoride (30 mg, 0.52 mmol) were added, the vessel was sealed under nitrogen, and heated to 60 °C for 16 h. Upon cooling, brine (2 mL) was added and the mixture was extracted with diethyl ether (3 x 2 mL). The organics were dried over magnesium sulfate, filtered, concentrated, and purified by column chromatography (SiO_2, 5% EtOAc/ hexane) to yield skipped diene **3.70** (27.3 mg, 66%) as a colorless oil. ^{1}H NMR (400 MHz, $CDCl_3$) δ 5.99 (ddd, *J* = 7.5, 2.6, 1.3 Hz, 1H), 5.93 (ddt, *J* = 16.9, 10.0, 6.8 Hz, 1H), 5.10-4.96 (m, 2H), 3.89 (s, 3H), 3.09 (ddd, *J* = 16.5, 4.1, 1.8 Hz, 1H), 3.03-2.97 (m, 2H), 2.20 (dt, *J* = 17.8, 6.2 Hz, 1H), 1.86 (ddq, *J* = 17.6, 10.9, 2.3 Hz, 1H), 1.77 (dd, *J* = 16.5, 12.7 Hz, 1H), 1.60-1.40 (m, 2H), 0.91 (dd, *J* = 7.8, 6.6 Hz, 6H); ^{13}C NMR (101 MHz, $CDCl_3$) δ 155.60, 137.06, 133.25, 132.75, 115.65, 61.85, 39.47, 35.24, 32.28, 28.84, 26.73, 19.95, 19.76; IR (neat) 2957, 2925, 1464, 1051 cm^{-1}; HRMS (ESI) calculated for $[C_{13}H_{22}NO]^+$ $[M+H]^+$: *m/z* 208.1696, not found.

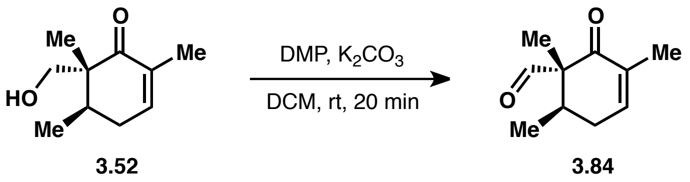

Aldehyde **3.84**

To crude enone **3.52** (89 mg, 0.53 mmol) was added DCM (11 mL), K_2CO_3 (439 mg, 3.17 mmol), and Dess-Martin periodinane (449 mg, 1.06 mmol). This mixture was stirred at room temperature for 20 min. The reaction was quenched with $NaHCO_3$ (4 mL) and Na_2SO_3 (4 mL) and extracted with ethyl acetate (3 x 6 mL). The organic layers were dried over magnesium sulfate, filtered, concentrated, and purified by column chromatography (SiO_2, 20% EtOAc/ hexane) to yield aldehyde **3.84** (27.2 mg, 31% over 2 steps) as a colorless oil. ^1H NMR (500 MHz, $CDCl_3$) δ 9.52 (s, 1H), 6.73 (ddq, *J* = 5.7, 2.9, 1.4 Hz, 1H), 2.63 (dqd, *J* = 9.8, 6.9, 5.0 Hz, 1H), 2.46 (dddd, *J* = 19.4, 6.8, 3.5, 1.6 Hz, 1H), 2.18 (ddq, *J* = 19.3, 9.8, 2.5 Hz, 1H), 1.79 (dt, *J* = 2.7, 1.5 Hz, 3H), 1.15 (s, 3H), 0.90 (d, *J* = 6.9 Hz, 3H); ^{13}C NMR (151 MHz, $CDCl_3$) δ 200.78, 200.31, 144.71, 134.22, 61.06, 32.62, 30.94, 15.91, 15.39, 10.91; IR (neat) 2958, 2927, 2878, 1731, 1657 cm^{-1}; HRMS (ESI) calculated for $[C_{10}H_{15}O_2]^+$ $[M+H]^+$: *m/z* 167.1067, not found.

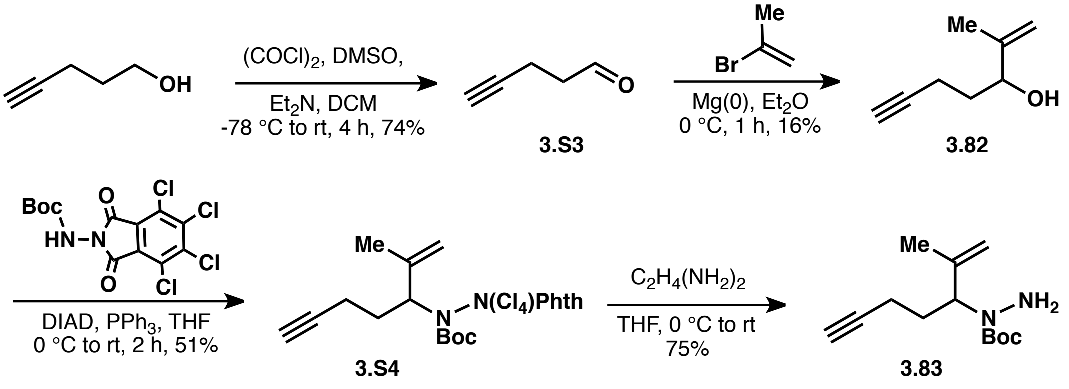

Hydrazine **3.83**

A 250 mL flask was charged with oxalyl chloride (2.7 mL, 32 mmol) and DCM (50 mL) and cooled to -78 °C. A solution of dimethylsulfoxide (4.6 mL, 65 mmol) in DCM (10 mL) was added dropwise (10 min) to the reaction mixture and stirring was continued for 30 min. A solution of 4-pentyn-1-ol (2.5 mL, 27 mmol) in DCM (20 mL) was added dropwise (10 min) to the reaction mixture and stirring was continued for 1 h. Then, triethylamine (22 mL, 161 mmol) was added dropwise (10 min) and the reaction was allowed to warm to room temperature and stir for an additional 3 h. The reaction was quenched with HCl (2 N, 30 mL) and brine (30 mL) and washed with HCl/brine (1:1, 3 x 40 mL). The organics were dried over magnesium sulfate, filtered, and concentrated to yield aldehyde **3.S3** (1.63 g, 74%) as a colorless oil.

A 100 mL flask was charged with magnesium turnings (365 mg, 15 mmol), diethyl ether (4 mL), 2-bromopropene (0.09 mL, 1 mmol), and 1,2-dibromoethane (0.01 mL). The mixture was stirred vigorously until the flask was warm to the touch (5 min). Then, diethyl ether (16 mL) and 2-bromopropene (0.8 mL, 9 mmol) were added and the mixture was stirred for another 30 min. Then, after cooling to 0 °C, a solution of aldehyde **3.S3** (410 mg, 5 mmol) in diethyl ether (3 mL) was added dropwise (10 min) to the mixture and stirred for 1 h at 0 °C. The reaction was quenched with NH_4Cl (20 mL) and extracted with Et_2O (3 x 20 mL). The organics were dried over magnesium sulfate, filtered, and concentrated to yield allylic alcohol **3.82** (98 mg, 16%) as a colorless oil.

A 25 mL flask was charged with triphenylphosphine (132 mg, 0.502 mmol) and THF (2 mL) and cooled to 0 °C. Diisopropyl azodicarboxylate (0.091 mL, 0.464 mmol) was added and stirred for 5 min during which a white precipitate formed. A solution of allylic alcohol **3.82** (48 mg, 0.387 mmol) and *tert*-butyl-4,5,6,7-tetrachloro-1,3-dioxoisoindolin-2-ylcarbamate (155 mg, 0.287 mmol) in THF (2 mL) was added to the mixture. After warming to room temperature, the reaction was allowed to stir for 2 h. The mixture was concentrated and purified by column chromatography (SiO_2, 5% EtOAc/ hexane) to yield protected hydrazine **3.S4** (100.3 mg, 51%) as a white solid.

A 10 mL flask was charged with protected hydrazine **3.S4** (100 mg, 0.197 mmol) and THF (1 mL) and cooled to 0 °C. Ethylene diamine (0.026 mL, 0.40 mmol) was added and the mixture was allowed to warm to room temperature and stir for 24 h. The white precipitate was removed by filtration over Celite with Et_2O. The filtrate was concentrated and purified by column chromatography (SiO_2, 20% EtOAc/ hexane) to yield hydrazine **3.83** (35.0 mg, 75%) as a colorless oil. ^{1}H NMR (500 MHz, $CDCl_3$) δ 4.91 (s, 1H), 4.82 (s, 1H), 4.50 (dd, *J* = 10.3, 4.4 Hz, 1H), 3.62 (bs, 2H), 2.17 (tt, *J* = 7.4, 3.7 Hz, 2H), 2.06 (ddt, *J* = 13.2, 10.4, 6.5 Hz, 1H), 1.94 (t, *J* = 2.6 Hz, 1H), 1.83 (dtd, *J* = 14.3, 7.3, 4.3 Hz, 1H), 1.69 (s, 3H), 1.46 (s, 9H); ^{13}C NMR (101 MHz, $CDCl_3$) δ 157.48, 144.07, 112.29, 84.12, 80.74, 68.48, 60.15, 28.48, 28.29, 21.02, 15.91; IR (neat) 3313, 2974, 2933, 1687, 1390, 1367, 1169 cm^{-1}; HRMS (ESI) calculated for $[C_{13}H_{23}N_2O_2]^+$ $[M+H]^+$: *m/z* 239.1754, not found.

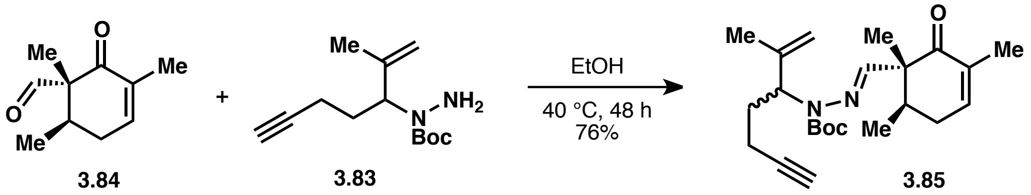

Hydrazone **3.85**

A 4 mL vial was charged with aldehyde **3.84** (11.2 mg, 0.0671 mmol), hydrazine **3.83** (16.0 mg, 0.0671 mmol), and ethanol (0.4 mL), sealed, and heated to 40 °C for 48 h. The solution was concentrated and purified by column chromatography (SiO_2, 5% to 20% EtOAc/ hexane) to yield hydrazone **3.85** (19.6 mg, 76%) as a pale yellow oil. $[\alpha]_D^{22}$ (*c* 0.0098, $CHCl_3$) = −53.2; ^{1}H NMR (500 MHz, $CDCl_3$) δ 8.11 (s, 1H), 6.61-6.52 (m, 1H), 4.83 (dd, *J* = 6.9, 3.1 Hz, 2H), 4.76 (td, *J* = 10.4, 9.4, 4.7 Hz, 1H), 2.48 (dqd, *J* = 18.9, 4.7, 2.3 Hz, 1H), 2.37 (tt, *J* = 7.1, 4.9 Hz, 1H), 2.24-2.02 (m, 4H), 1.94 (q, *J* = 2.4 Hz, 1H), 1.91-1.80 (m, 1H), 1.76 (dq, *J* = 7.3, 1.9 Hz, 3H), 1.70 (s, 3H), 1.47 (d, *J* = 2.4 Hz, 9H), 1.14 (d, *J* = 2.2 Hz, 3H), 0.96 (dd, *J* = 6.9, 3.5 Hz, 3H); ^{13}C NMR (126 MHz, $CDCl_3$) δ 201.66, 201.60, 159.13, 158.31, 153.47, 153.42, 144.88, 144.82, 142.46 (x2), 134.24, 134.23, 112.16, 112.03, 84.19 (x2), 81.24, 81.20, 68.65 (x2), 61.89 (x2), 54.39, 54.37, 36.18, 36.15, 31.60 (x2), 29.61, 29.33, 28.47 (x2), 20.43, 20.38, 16.42 (x2), 15.60, 15.57, 15.46 (x2), 14.76, 14.66; IR (neat) 3309, 2976, 2924, 1693, 1668, 1154 cm^{-1}; HRMS (ESI) calculated for $[C_{23}H_{34}N_2O_3Na]^+$ $[M+Na]^+$: *m/z* 409.2462, found 409.2458.

Supplementary tables for C–H arylation optimization conditions

Supplementary Table 1: Screen of palladium sources

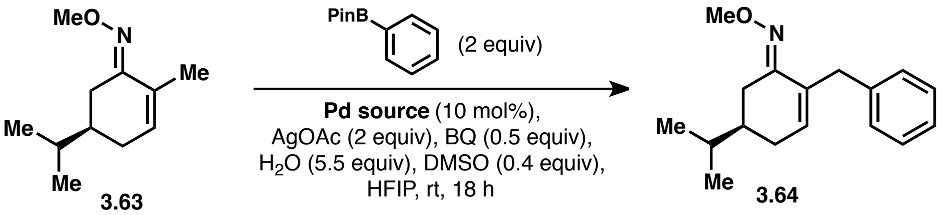

MeO
N
Me
Me
Me
3.63
PinB
(2 equiv)
Pd source (10 mol%),
AgOAc (2 equiv), BQ (0.5 equiv),
H_2O (5.5 equiv), DMSO (0.4 equiv),
HFIP, rt, 18 h
MeO
N
Me
Me
3.64

entry	Pd source	returned SM*	product yield*
1	$Pd(OAc)_2$	59%	10%
2	$PdCl_2$	83%	1%
3	$PdCl_2(MeCN)_2$	67%	3%
4	$Pd(TFA)_2$	58%	8%
5	$Pd(OPiv)_2$	56%	9%
6	$Pd(OAc)_2$·sulfoxide	59%	4%
7	$[PdCl(allyl)]_2$	65%	4%

*NMR yields based on CH_2Br_2 as internal standard

Supplementary Table 2: Screen of added ligands

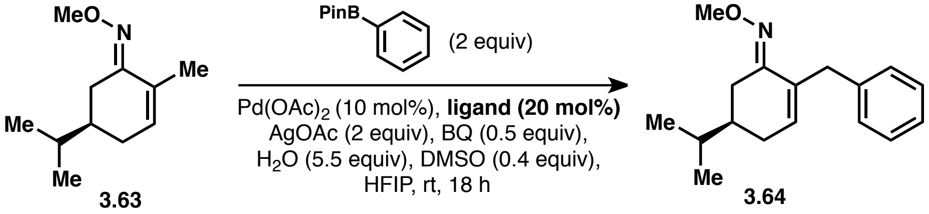

MeO
N
Me
Me
Me
3.63
PinB
(2 equiv)
$Pd(OAc)_2$ (10 mol%), **ligand (20 mol%)**
AgOAc (2 equiv), BQ (0.5 equiv),
H_2O (5.5 equiv), DMSO (0.4 equiv),
HFIP, rt, 18 h
MeO
N
Me
Me
3.64

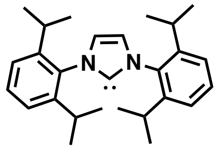

IPr

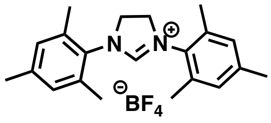

SIMes-HBF$_4$

entry	ligand	returned SM*	product yield*
1	none	59%	10%
2	2-picoline	68%	7%
3	quinoline	70%	3%
4	pyridine	55%	1%
5	IPr	59%	9%
6	SIMes-HBF_4	64%	8%
7			

*NMR yields based on CH_2Br_2 as internal standard

Supplementary Table 3: Screen of added bases

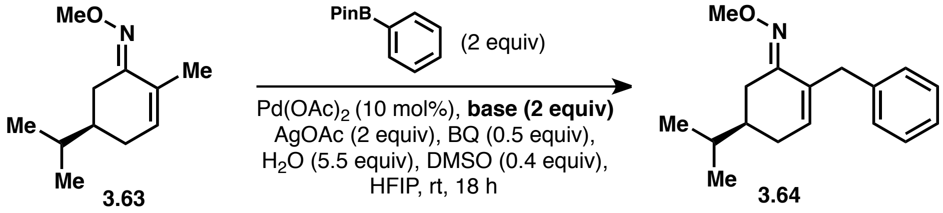
MeO
N
Me
Me
Me
3.63
PinB
(2 equiv)
Pd(OAc)$_2$ (10 mol%), **base (2 equiv)**
AgOAc (2 equiv), BQ (0.5 equiv),
H_2O (5.5 equiv), DMSO (0.4 equiv),
HFIP, rt, 18 h
MeO
N
Me
Me
3.64

entry	base	returned SM*	product yield*
1	none	59%	10%
2	Cs_2CO_3	65%	8%
3	K_2CO_3	67%	8%
4	CsOAc	63%	10%
5	K_2HPO_4	79%	6%
6	CsF	66%	9%

*NMR yields based on CH_2Br_2 as internal standard

Supplementary Table 4: Screen of benzoquinone equivalents

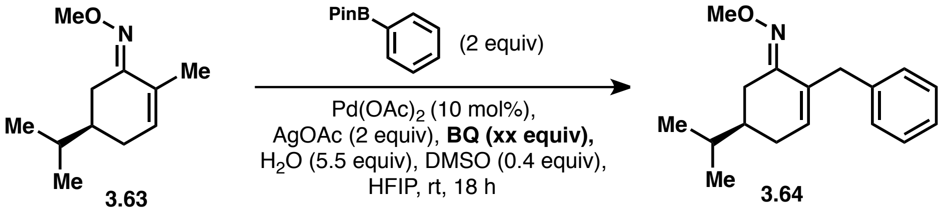
MeO
N
Me
Me
Me
3.63
PinB
(2 equiv)
Pd(OAc)$_2$ (10 mol%),
AgOAc (2 equiv), **BQ (xx equiv),**
H_2O (5.5 equiv), DMSO (0.4 equiv),
HFIP, rt, 18 h
MeO
N
Me
Me
3.64

entry	BQ equiv	returned SM*	product yield*
1	0	63%	2%
2	0.2	61%	7%
3	0.5	59%	10%
4	1	66%	9%

*NMR yields based on CH_2Br_2 as internal standard

Supplementary Table 5: Screen of oxime ether derivatives

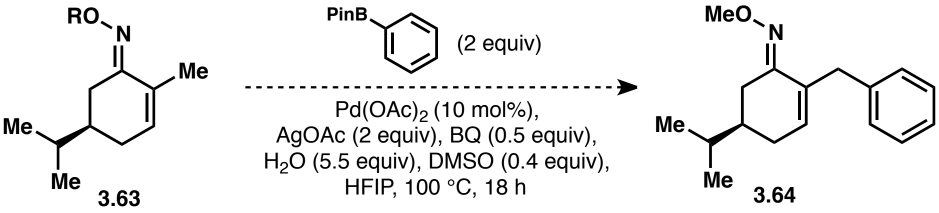

$Pd(OAc)_2$ (10 mol%), AgOAc (2 equiv), BQ (0.5 equiv), H_2O (5.5 equiv), DMSO (0.4 equiv), HFIP, 100 °C, 18 h

entry	oxime R	returned SM*	product yield*
1	Me	27%	13%
2	^{t}Bu	28%	4%
3	Ac	47% **3.S5**	0%

*NMR yields based on CH_2Br_2 as internal standard

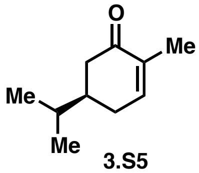

3.S5

3.10 References and Notes

[1] Ciesielski, J.; Frontier, A. *Org. Prep. Proced. Int.* **2014**, *46*, 214-251.

[2] Sugano, M.; Sato, A.; Iijima, Y.; Oshima, T.; Furuya, K.; Kuwano, H.; Hata, T.; Hanzawa, H. *J. Am. Chem. Soc.* **1991,** *113,* 5463-5464.

[3] [a] Sugano, M.; Sato, A.; Iijima, Y.; Furuya, K.; Haruyama, H.; Yoda, K.; Hata, T. *J. Org. Chem.* **1994,** *59,* 564-569. [b] Sugano, M.; Sato, A.; Iijima, Y.; Furuya, K.; Kuwano, H.; Hata, T. *J. Antibiot.* **1995**, *48*, 1188-1190.

[4] [a] Chu, M.; Patel, M. G.; Gullo, V. P.; Truumees, I.; Puar, M. S.; McPhail, A. T. *J. Org. Chem.*, **1992**, *57*, 5817-5818. [b] Koyama, K.; Ishino, M.; Takatori, K.; Sugita, T.; Kinoshita, K.; Takahashi, K. *Tetrahedron Lett.* **2004**, *45*, 6947-6948. [c] Ishino, M.; Kiyomichi, N.; Takatori, K.; Sugita, T.; Shiro, M.; Kinoshita, K.; Takahashi, K.; Koyama, K. *Tetrahedron* **2010**, *66*, 2594-2597. [d] Ishino, M.; Kinoshita, K.; Takahashi, K.; Sugita, T.; Shiro, M.; Hasegawa K.; Koyama, K. *Tetrahedron* **2012**, *68*, 8572-8576. [e] Ishino, M.; Kamauchi, H.; Takatori, K.; Kinoshita, K.; Sugita, T.; Koyama, K. *Tetrahedron* **2016**, *57*, 4341-4344.

[5] Tokiwano, T.; Fukushi, E.; Endo, T.; Oikawa, H. *Chem. Commun.* **2004**, 1324-1325.

[6] Prescott, S. M.; Zimmerman, G. A.; Stafforini, D. M.; McIntyre, T. M. *Annu. Rev. Biochem.* **2000,** *69,* 419-445.

[7] [a] Merlos, M.; Giral, M.; Balsa, D.; Ferrando, R.; Queralt, M.; Puigdemont, A.; Garcia-Rafanell, J.; Forn, J. *J. Pharmacol. Expt. Ther.* **1997**, *208*, 114-121. [b] Kasperska-Zajac, A.; Brzoza, Z.; Rogala, B. *Recent Pat. Inflamm. Allergy Drug Discov.* **2008**, *2*, 72-76.

[8] Gui, C.; Zhu, W.; Chen, G.; Luo, X.; Liew, O. W.; Puah, C. M.; Chen K.; Jiang, H. *Proteins: Struct., Func., Bioinf.* **2007**, *67*, 41-52.

[9] Jancar, S.; Chammas, R. *Curr. Drug Targets* **2014,** *15,* 982-987.

[10] Onuchic, A. C.; Machado, C. M. L.; Saito, R. F.; Rios, F. J.; Jancar, S.; Chammas, R. *Mediators Inflamm.* **2012,** Article ID 175408.

[11] Sugano, M.; Sato, M.; Saito, K.; Takaishi, S.; Matsushita, Y.; Iijima, Y. *J. Med. Chem.* **1996**, *39*, 5281-5284.

[12] Miyaoka, H.; Saka, Y.; Miura, S.; Yamada, Y. *Tetrahedron Lett.* **1996,** *37,* 7107-7110.

[13] [a] Goldring, W. P. D.; Pattenden, G. *Chem Commun.* **2002,** 1736-1737. [b] Foote, K. M.; Hayes, C. J.; John, M. P.; Pattenden, G. *Org. Biomol. Chem.* **2003,** *1,* 3917-3948. [c] Diaper, C. M.; Goldring, W. P. D.; Pattenden, G. *Org. Biomol. Chem.* **2003,** *1,* 3949-3956.

[14] Goldring, W. P. D.; Pattenden, G. *Org. Biomol. Chem.* **2004,** *2,* 466-473.

[15] Mohr, P. J.; Halcomb, R. L. *J. Am. Chem. Soc.* **2003,** *125,* 1712-1713.

[16] Huang, J.; Wu, C.; Wulff, W. D. *J. Am. Chem. Soc.* **2007**, *129*, 13366-13367.

[17] [a] Tang, Y.; Cole, K. P.; Buchanan, G. S.; Li, G.; Hsung, R. P. *Org. Lett.* **2009**, *11*, 1591-1594. [b] Buchanan, G. S.; Cole, K. P.; Li, G.; Tang, Y.; You, L.-F.; Hsung, R. P. *Tetrahedron* **2011**, *67*, 10105-10118. [c] Buchanan, G. S.; Cole, K. P.; Tang, Y.; Hsung, R. P. *J. Org. Chem.* **2011**, *76*, 7027-7039.

[18] Souillart, L.; Cramer, N. *Chem. Rev.* **2015**, *115*, 9410-9464.

[19] [a] Murakami, M.; Makino, M.; Ashida, S.; Matsuda, T. *Bull. Chem. Soc. Jpn.* **2006**, *79*, 1315-1321. [b] Cramer, N.; Seiser, T. *Synlett* **2011**, *4*, 449-460.

[20] Matsuda, T.; Makino, M.; Murakami, M. *Org. Lett.* **2004**, *6*, 1257-1259.

[21] Bermejo, F. A.; Mateos, A. F.; Escribano, A. E.; Lago, R. M.; Buron, L. M.; Lopez, M. R.; Gonzalez, R. R. *Tetrahedron* **2006**, *62*, 8933-8942.

[22] [a] Gansäuer, A.; Pierobon, M.; Bluhm, H. *Angew. Chem. Int. Ed.* **1998**, *37*, 101-103. [b] Gansäuer, A.; Bluhm, H.; Pierobon, M. *J. Am. Chem. Soc.* **1998**, *120*, 12849-12859.

[23] Masarwa, A.; Weber, M.; Sarpong. R. *J. Am. Chem. Soc.* **2015**, *137*, 6327-6334.

[24] Desai, L. V.; Hull, K. L.; Sanford, M. S. *J. Am. Chem. Soc.* **2004,** *126,* 9542-9543.

[25] Kang, T.; Kim, Y.; Lee, D.; Wang, Z.; Chang, S. *J. Am. Chem. Soc.* **2014,** *136,* 4141-4144.

[26] Chen, X.; Engle, K. M.; Wang, D.-H.; Yu, J.-Q. *Angew. Chem. Int. Ed.* **2009**, *48*, 5094-5115.

[27] Zaitsev, V. G.; Shabashov, D.; Daugulis, O. *J. Am. Chem. Soc.* **2005,** *127,* 13154-13155.

[28] [a] Engle, K. M.; Yu, J.-Q. *J. Org. Chem.* **2013,** *78*, 8927-8955. [b] Chan, K. S. L.; Wasa, M.; Chu, L.; Laforteza, B. N.; Miura, M.; Yu, J.-Q. *Nat. Chem.* **2014**, *6*, 146-150.

[29] Lapointe D.; Fagnou, K. *Chem. Lett.* **2010**, *39*, 1118-1126.

[30] Gao, P.; Guo, W.; Xue, J.; Zhao, Y.; Yuan, Y.; Xia, Y.; Shi, Z. *J. Am. Chem. Soc.* **2015**, *137*, 12231-12240.

[31] Zhang, F.-L.; Hong, K.; Li, T.-J.; Park, H.; Yu, J.-Q. *Science* **2016**, *351*, 252-256.

[32] [a] Mundal, D. A.; Avetta, C. T.; Thomson, R. J. *Nature Chem.* **2010**, *2*, 294-297. [b] Gutierrez, O.; Strick, B. F.; Thomson, R. J.; Tantillo, D. J. *Chem. Sci.* **2013**, *4*, 3997-4003.

[33] [a] Kenji, M.; Yasuhiro, I. *Liebigs Ann. Chem.* **1988**, *1*, 93-95. [b] Nishimura, H.; Hiramoto, S.; Mizutani, J.; Noma, Y.; Furusaki, A.; Matsumoto, T. *Agric. Biol. Chem.* **1983**, *47*, 2697-2699.

[34] [a] Deslongchamps, P. et al. *Can. J. Chem.* **1990**, *68*, 127-152. [b] Kannan, N.; Rangaswamy, M. J.; Kemapaiah, B. B. *J. Chem. Sci.* **2015**, *127*, 1405-1410.

[35] Singaram et al. *Indian J. Chem.* **1977**, *15*, 908.

Appendix 3: Spectra Relevant to Chapter 3

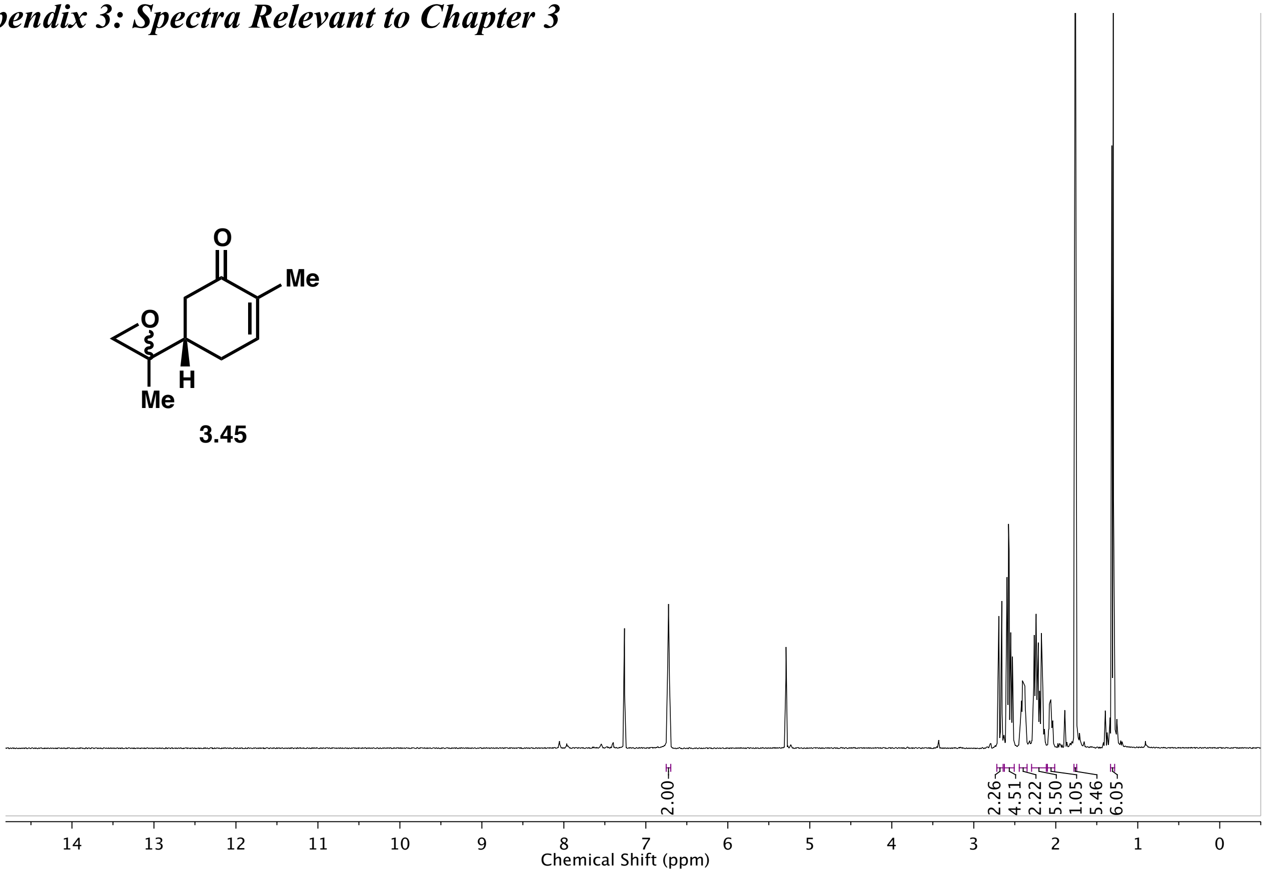

3.45

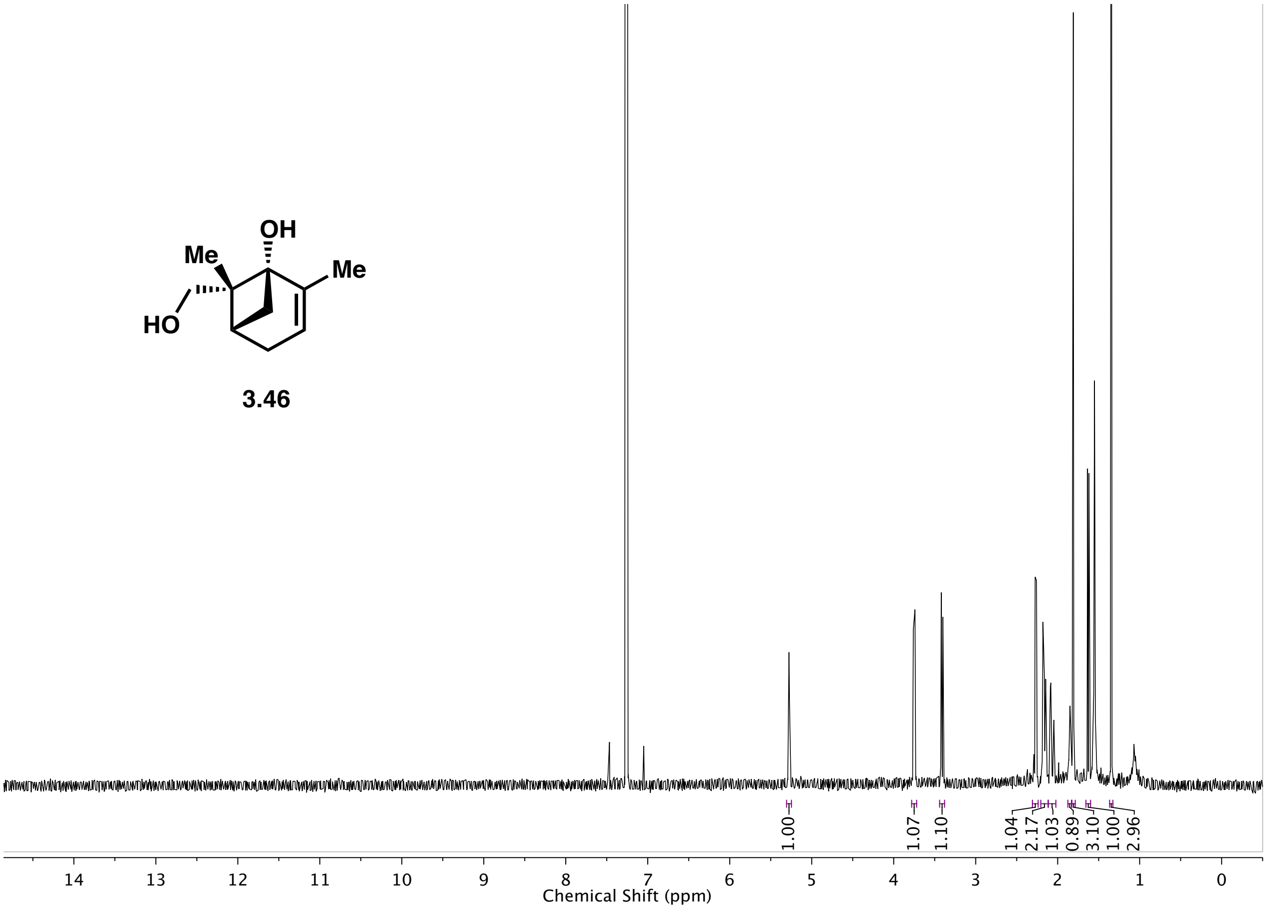

3.46

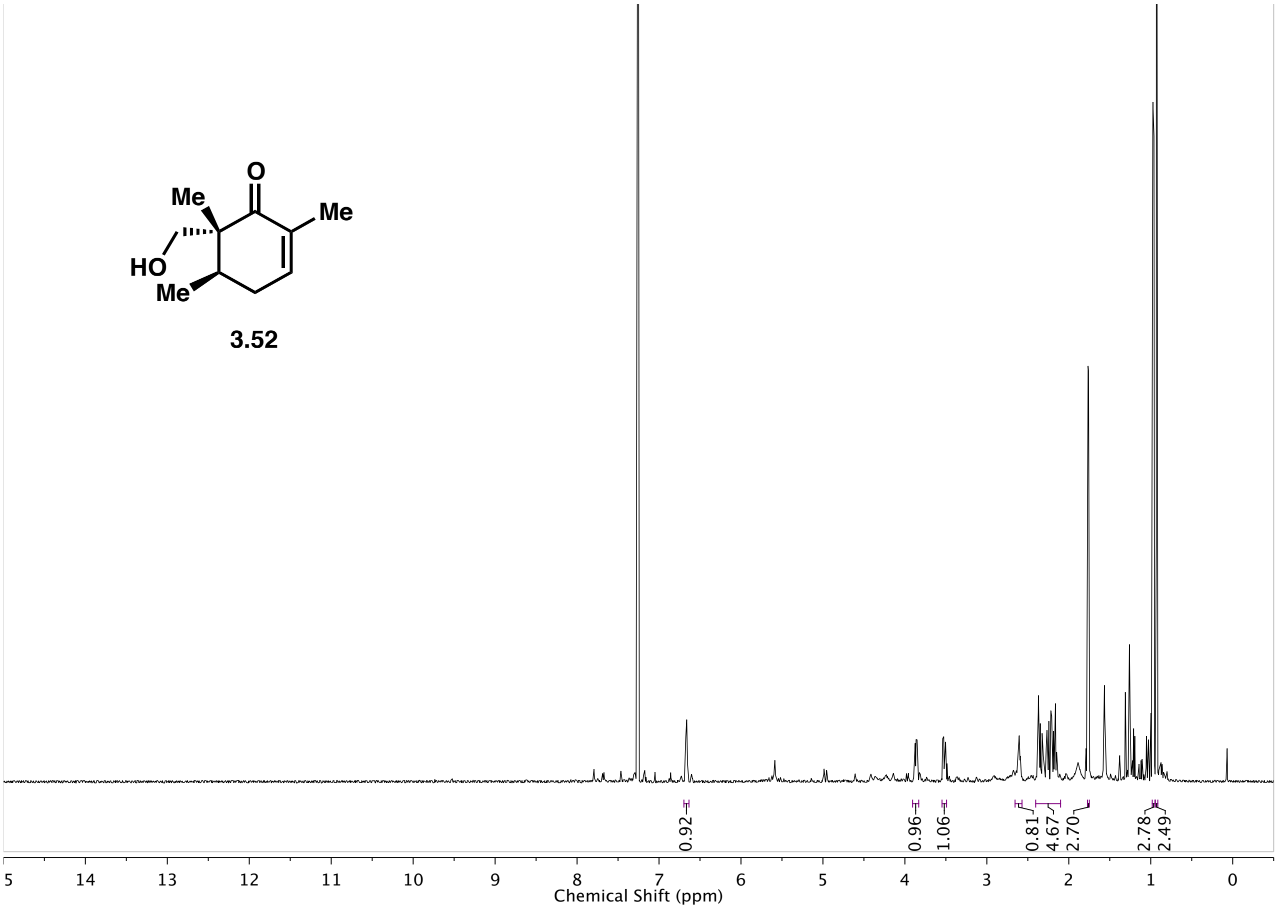
O
Me
Me
HO
Me
0.92
0.96
1.06
0.81
4.67
2.70
2.78
2.49
5
14
13
12
11
10
9
8
7
6
5
4
3
2
1
0
Chemical Shift (ppm)

3.52

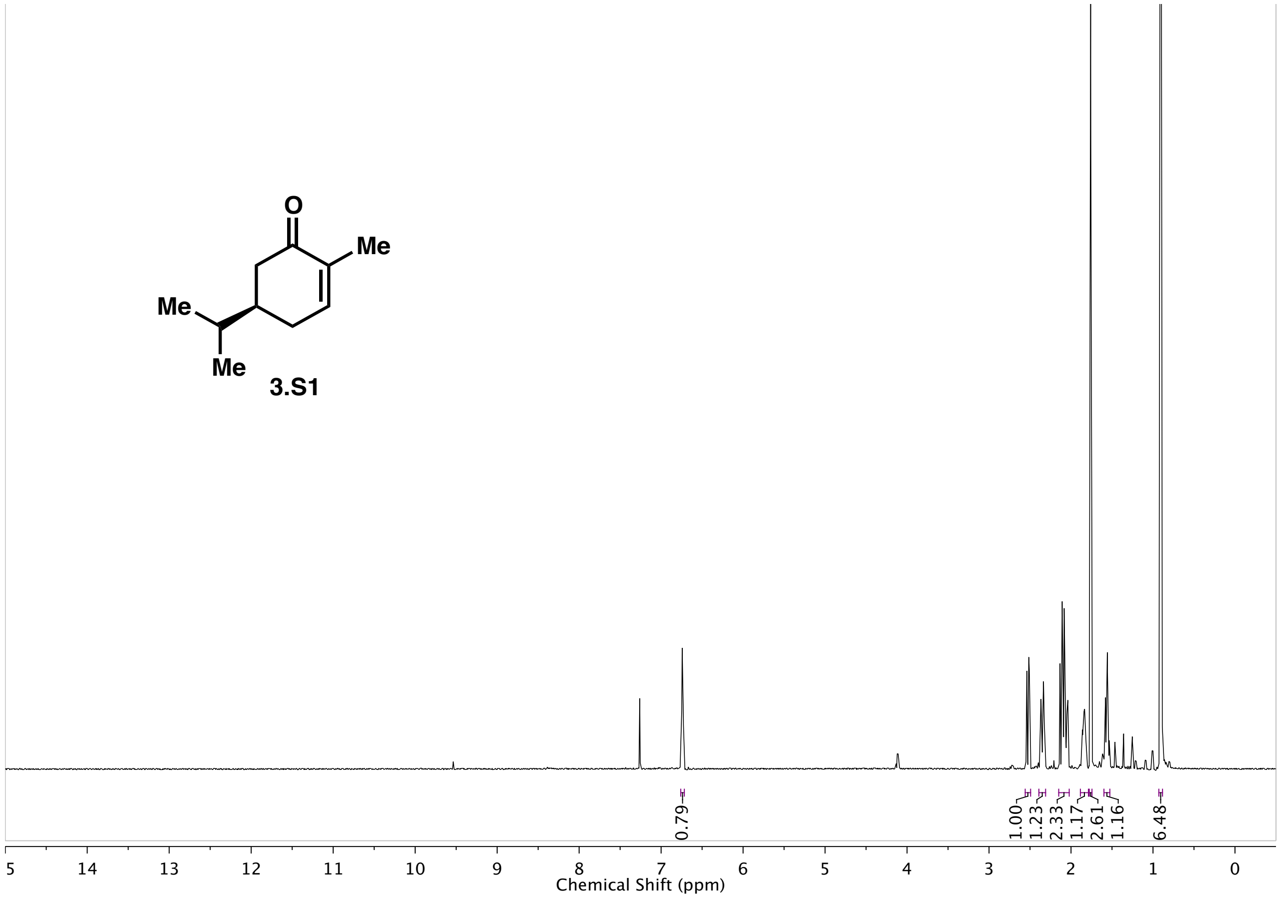
O
Me
Me
Me
0.79
1.00
1.23
2.33
1.17
2.61
1.16
6.48
5
14
13
12
11
10
9
8
7
6
5
4
3
2
1
0
Chemical Shift (ppm)

3.S1

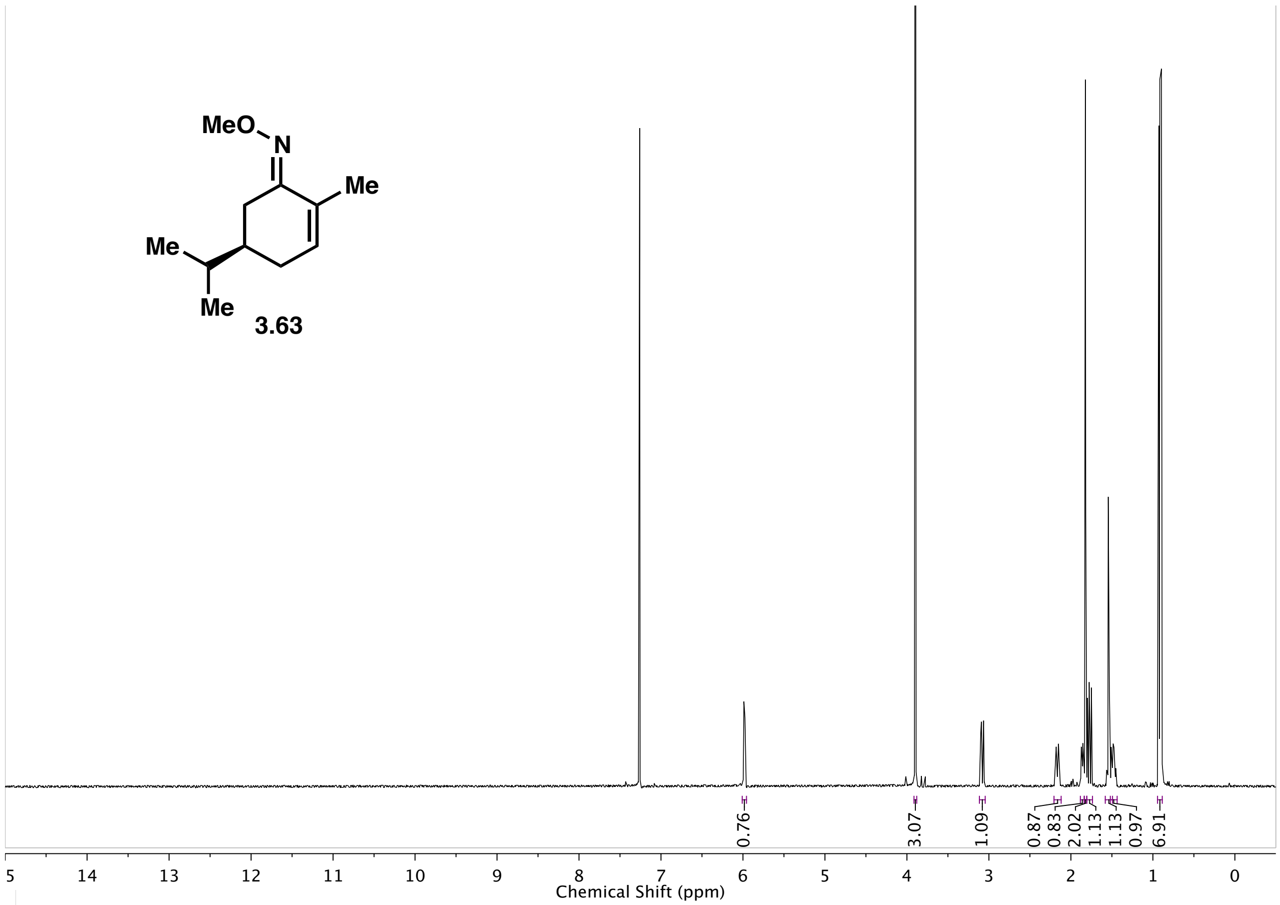
MeO
N
Me
Me
Me
3.63
0.76
3.07
1.09
0.87
0.83
2.02
1.13
1.13
0.97
6.91
5
14
13
12
11
10
9
8
7
6
5
4
3
2
1
0
Chemical Shift (ppm)

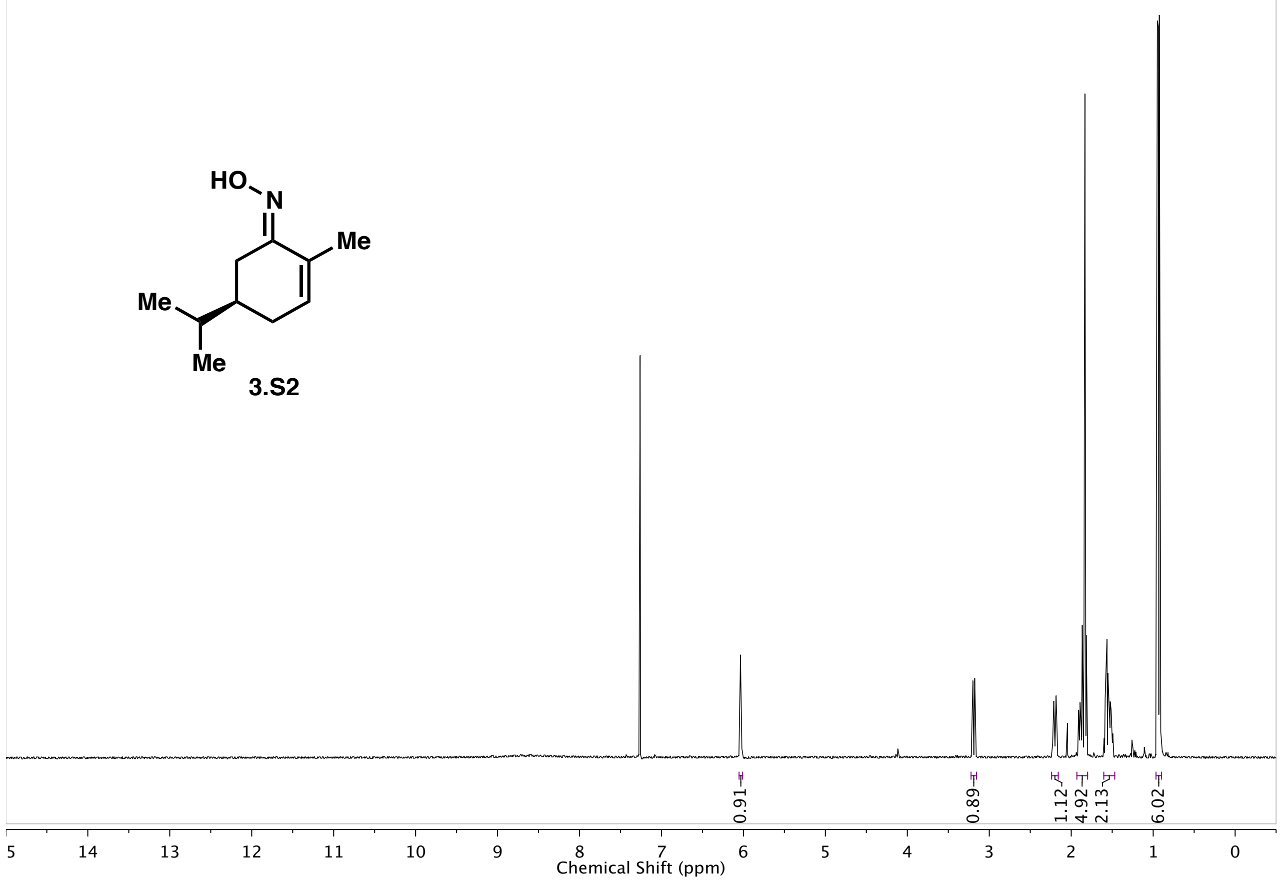
HO
N
Me
Me
Me
3.S2
0.91
0.89
1.12
4.92
2.13
6.02
5
14
13
12
11
10
9
8
7
6
5
4
3
2
1
0
Chemical Shift (ppm)

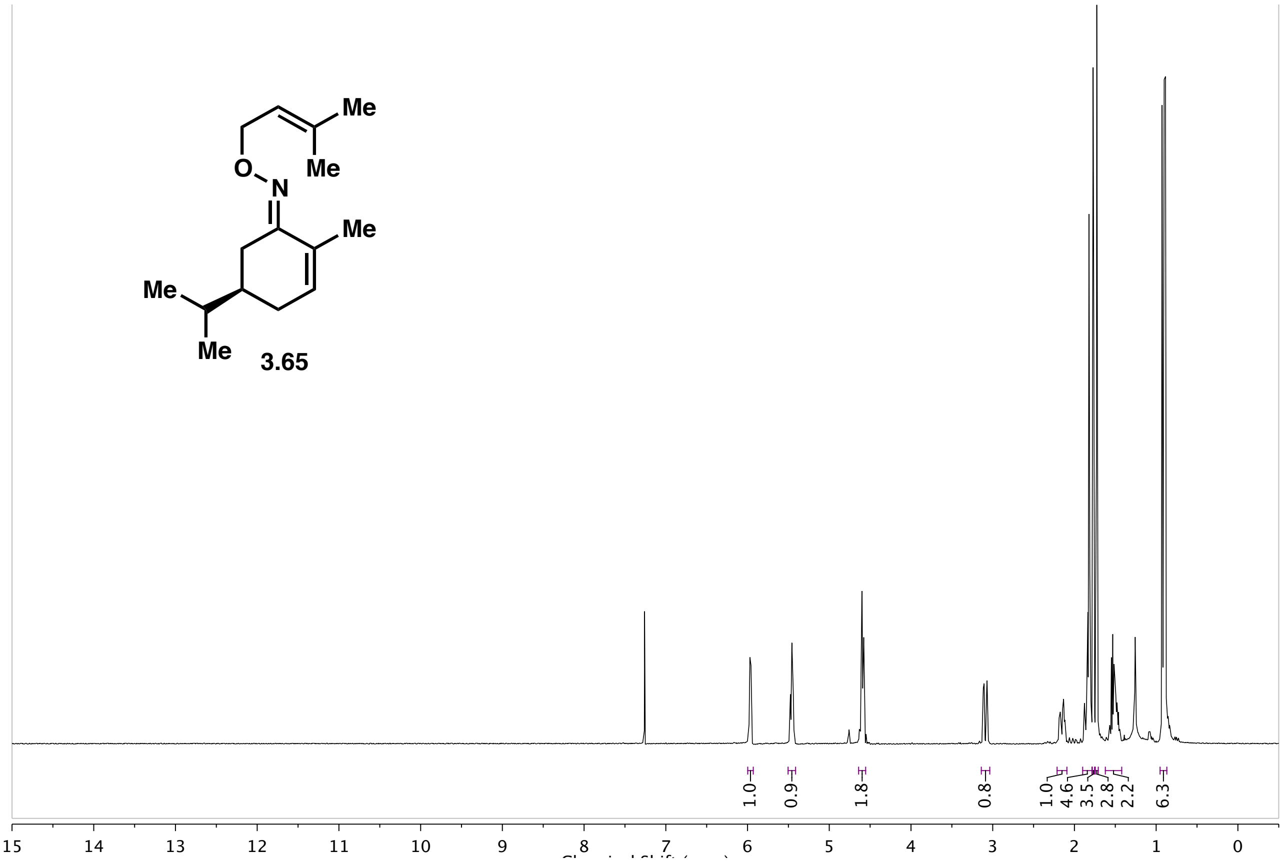
Me
Me
O
N
Me
Me
Me
3.65
1.0
0.9
1.8
0.8
1.0
4.6
3.5
2.8
2.2
6.3
15
14
13
12
11
10
9
8
7
6
5
4
3
2
1
0

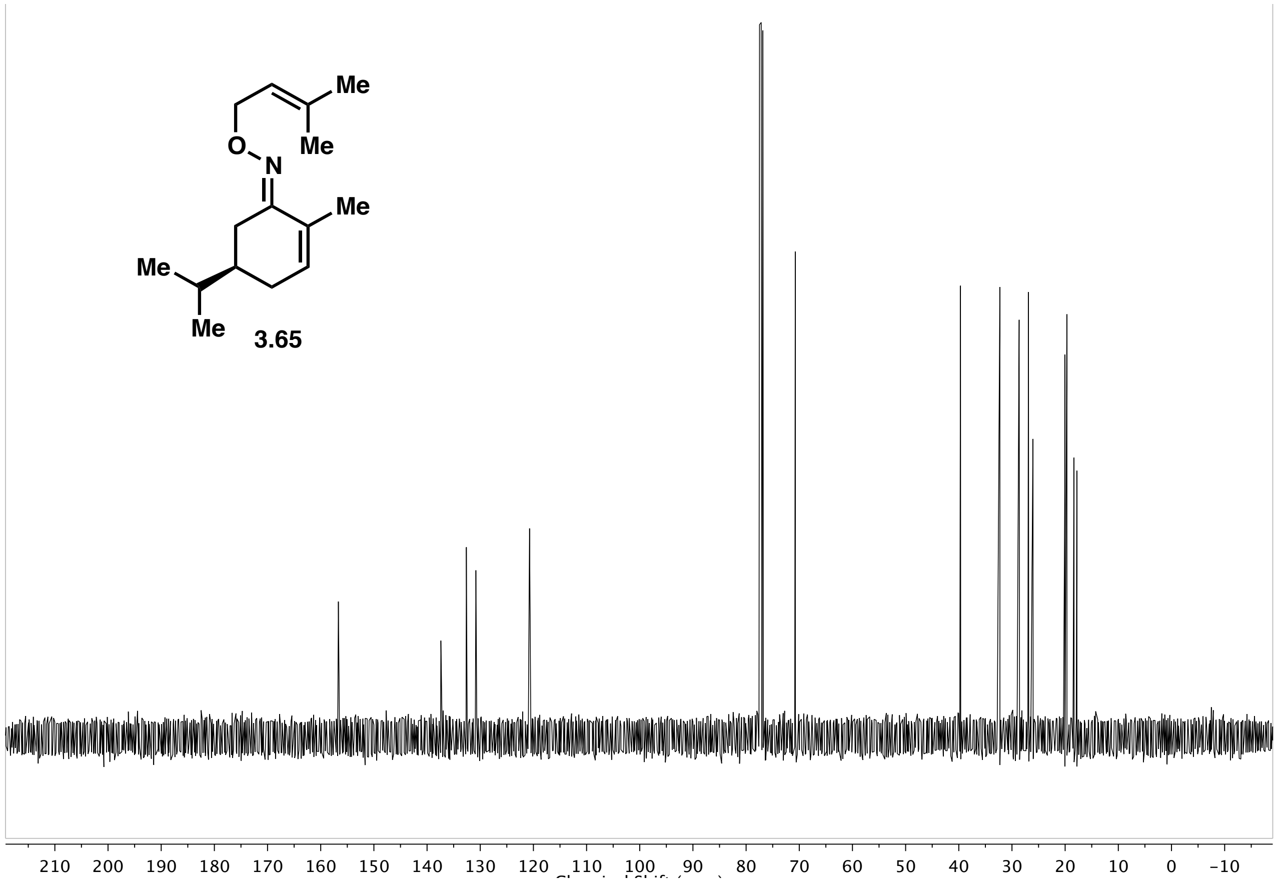
Me
Me
O
N
Me
Me
Me
3.65
210
200
190
180
170
160
150
140
130
120
110
100
90
80
70
60
50
40
30
20
10
0
−10

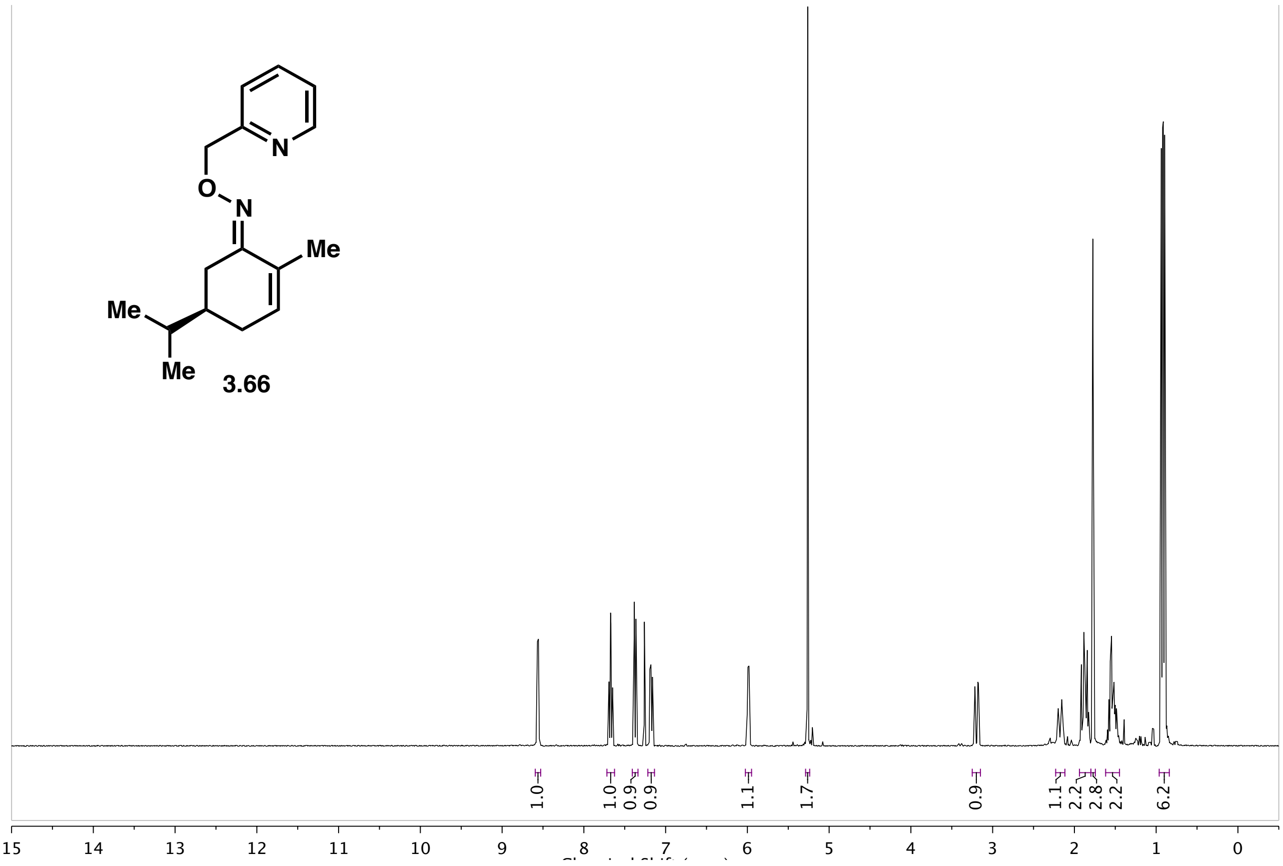

N
O
N
Me
Me
Me
3.66
1.0
1.0
0.9
0.9
1.1
1.7
0.9
1.1
2.2
2.8
2.2
6.2
15
14
13
12
11
10
9
8
7
6
5
4
3
2
1
0

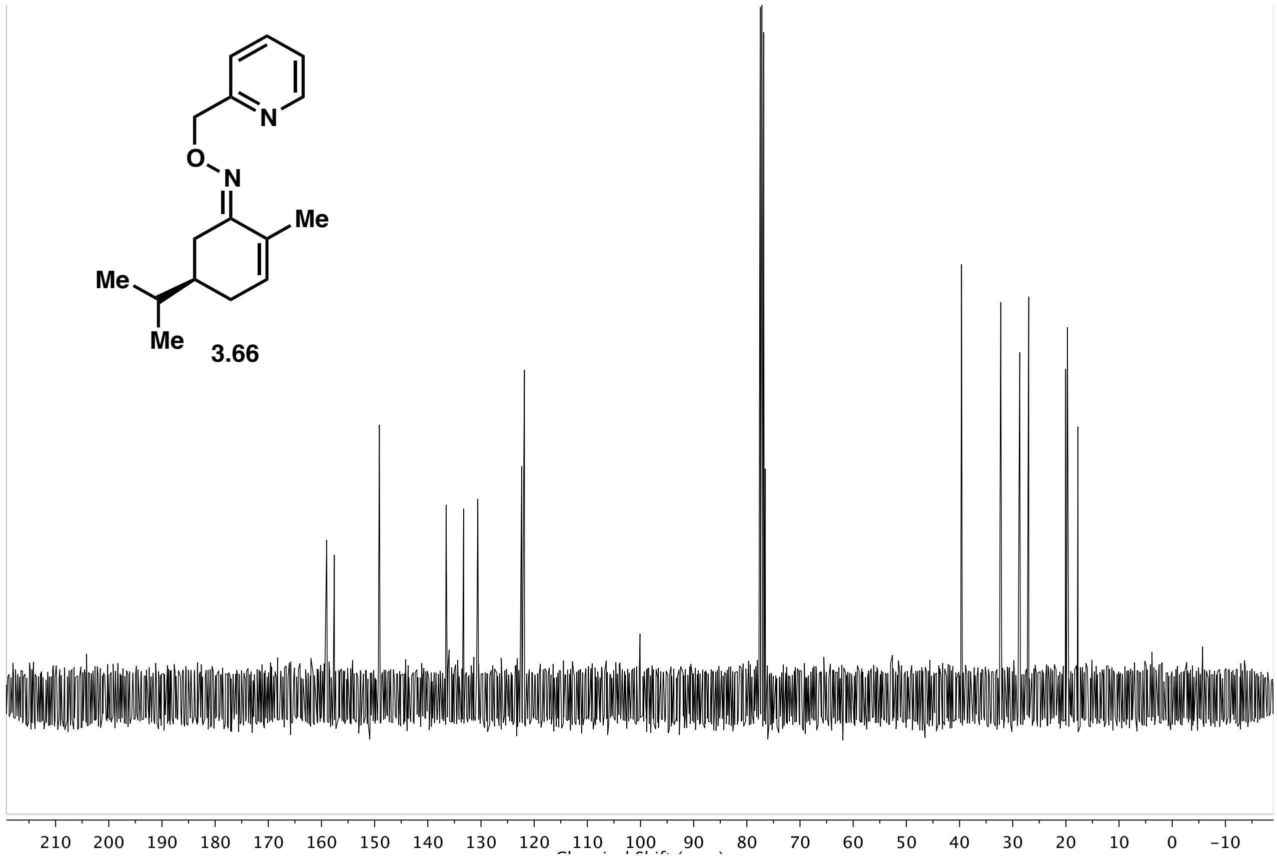

N
O
N
Me
Me
Me
3.66
210
200
190
180
170
160
150
140
130
120
110
100
90
80
70
60
50
40
30
20
10
0
−10

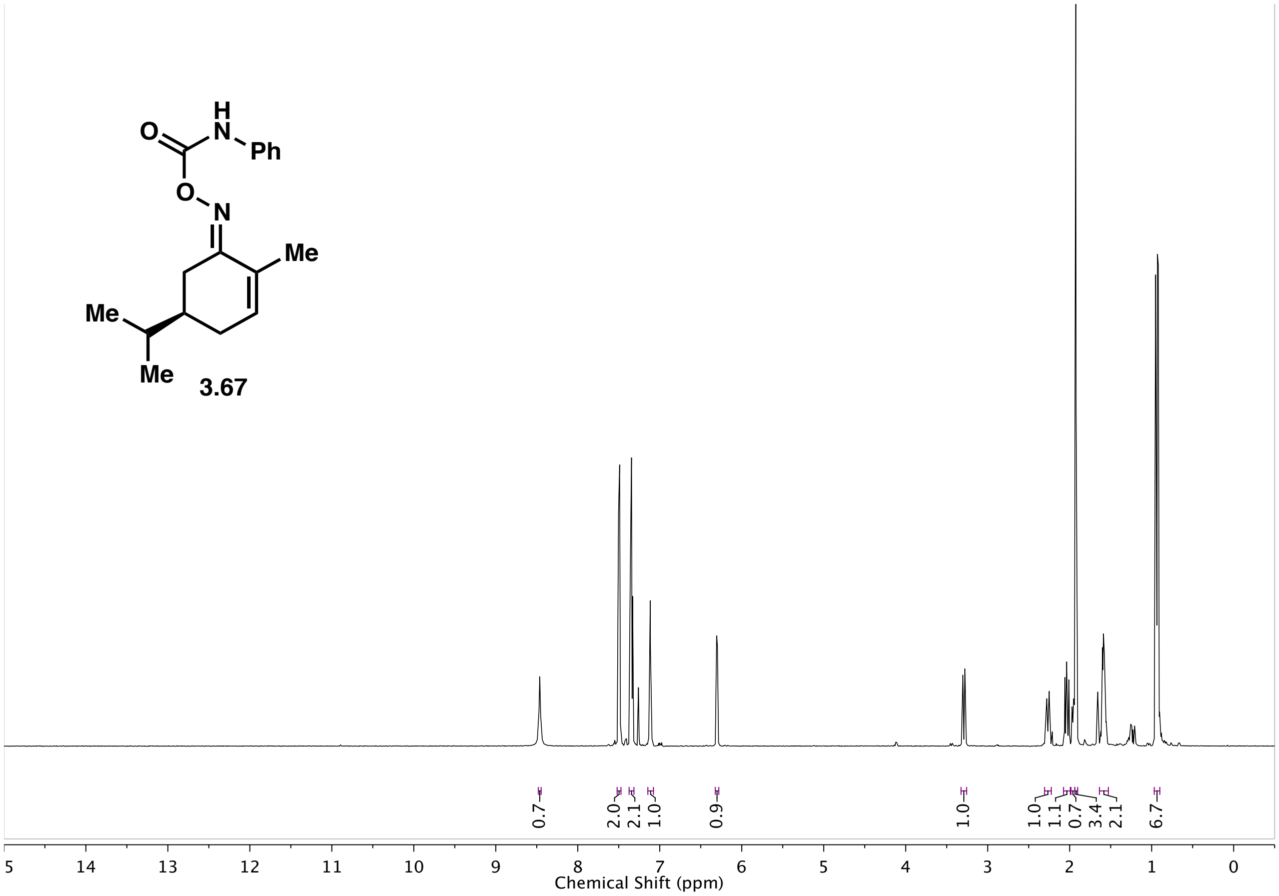

O
H
N
Ph
O
N
Me
Me
Me
3.67
0.7
2.0
2.1
1.0
0.9
1.0
1.0
1.1
0.7
3.4
2.1
6.7
5
14
13
12
11
10
9
8
7
6
5
4
3
2
1
0
Chemical Shift (ppm)

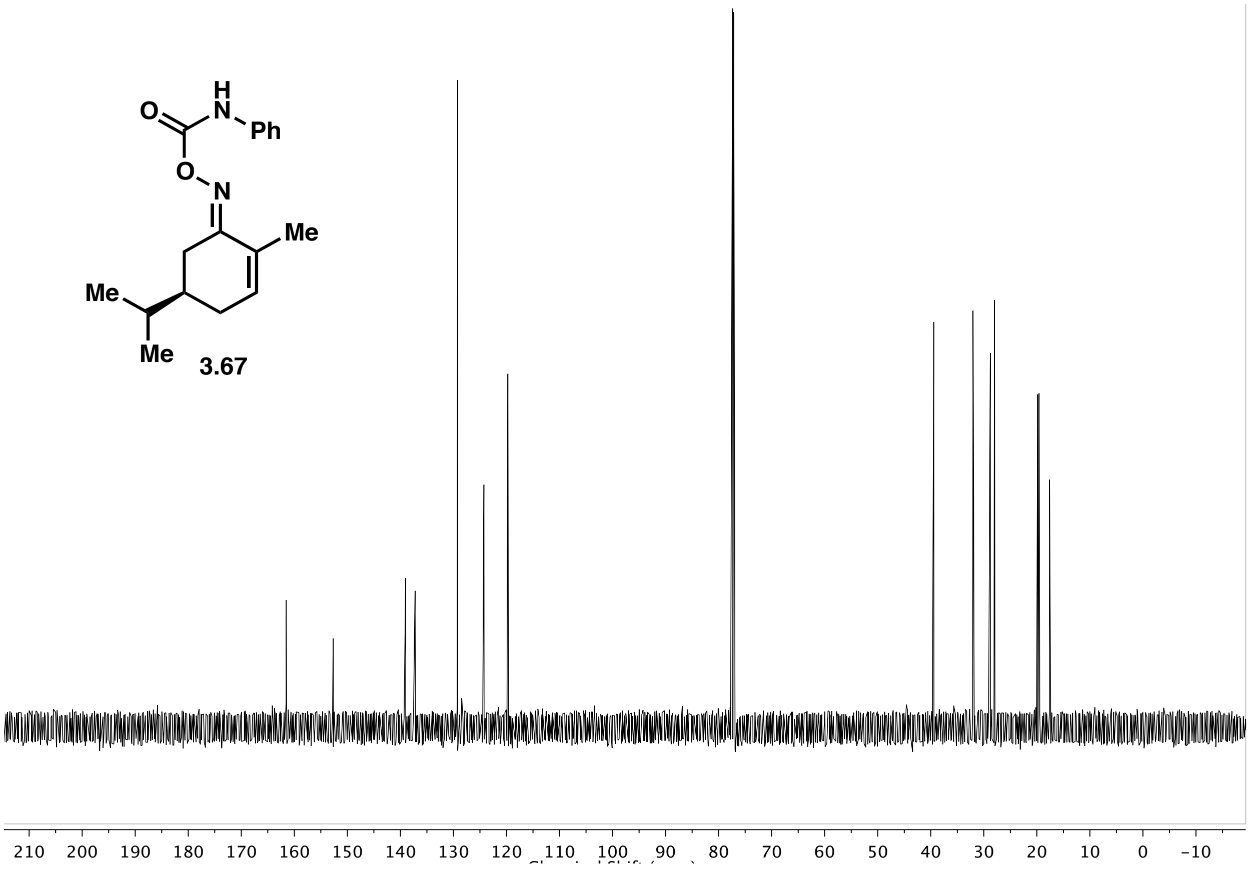

O
H
N
Ph
O
N
Me
Me
Me
3.67
210
200
190
180
170
160
150
140
130
120
110
100
90
80
70
60
50
40
30
20
10
0
−10

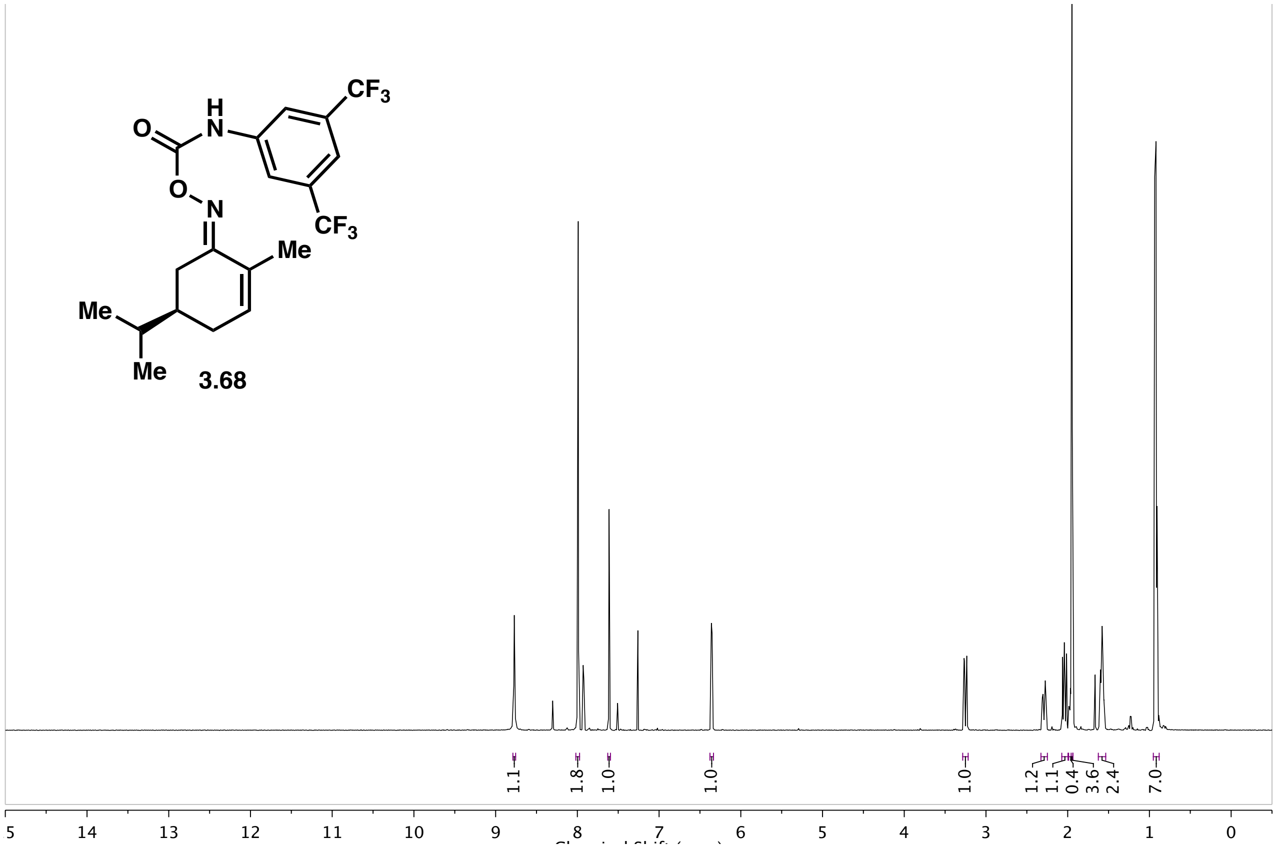

H
N
O
O
N
CF3
CF3
Me
Me
Me
3.68
1.1
1.8
1.0
1.0
1.0
1.2
1.1
0.4
3.6
2.4
7.0
5
14
13
12
11
10
9
8
7
6
5
4
3
2
1
0

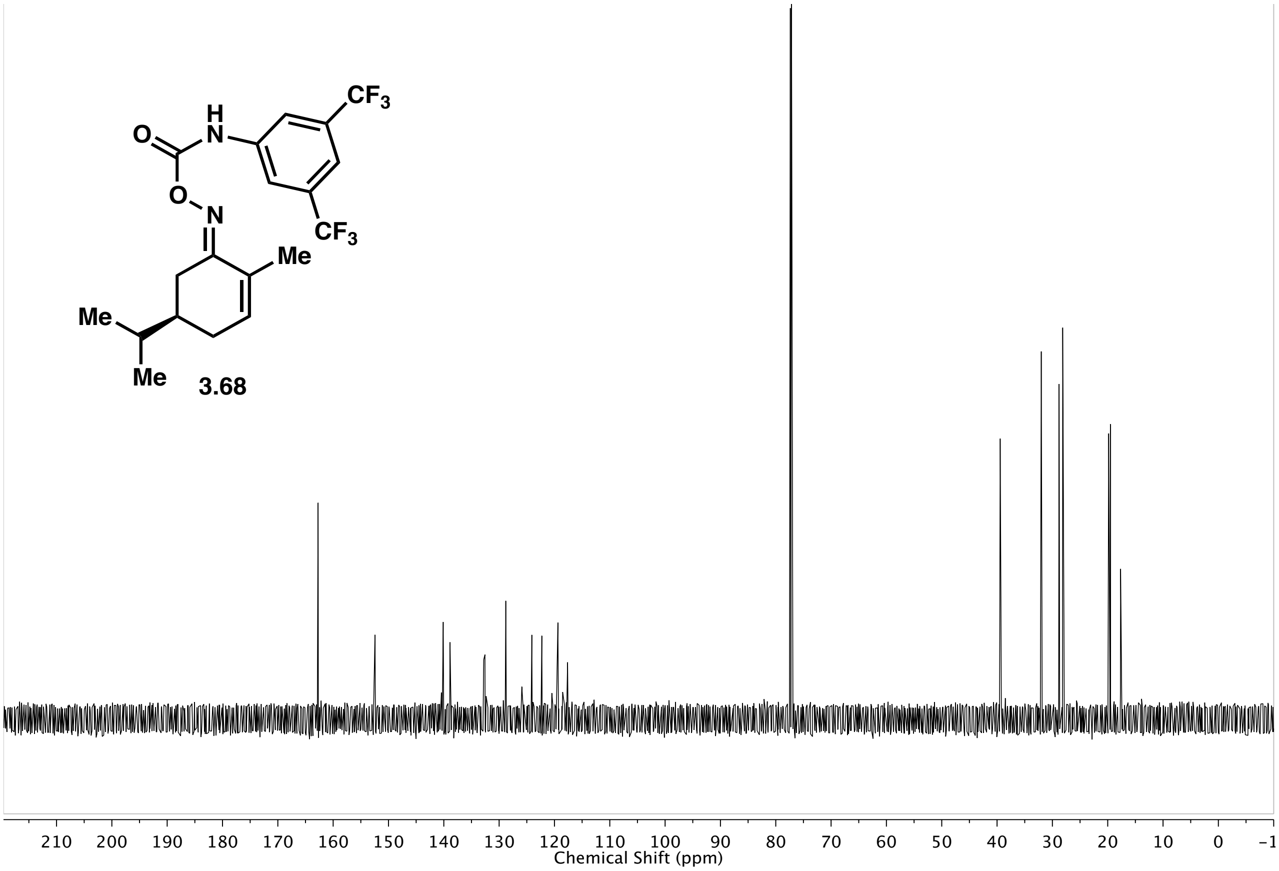

H
N
O
O
N
CF3
CF3
Me
Me
Me
3.68
210
200
190
180
170
160
150
140
130
120
110
100
90
80
70
60
50
40
30
20
10
0
–1
Chemical Shift (ppm)

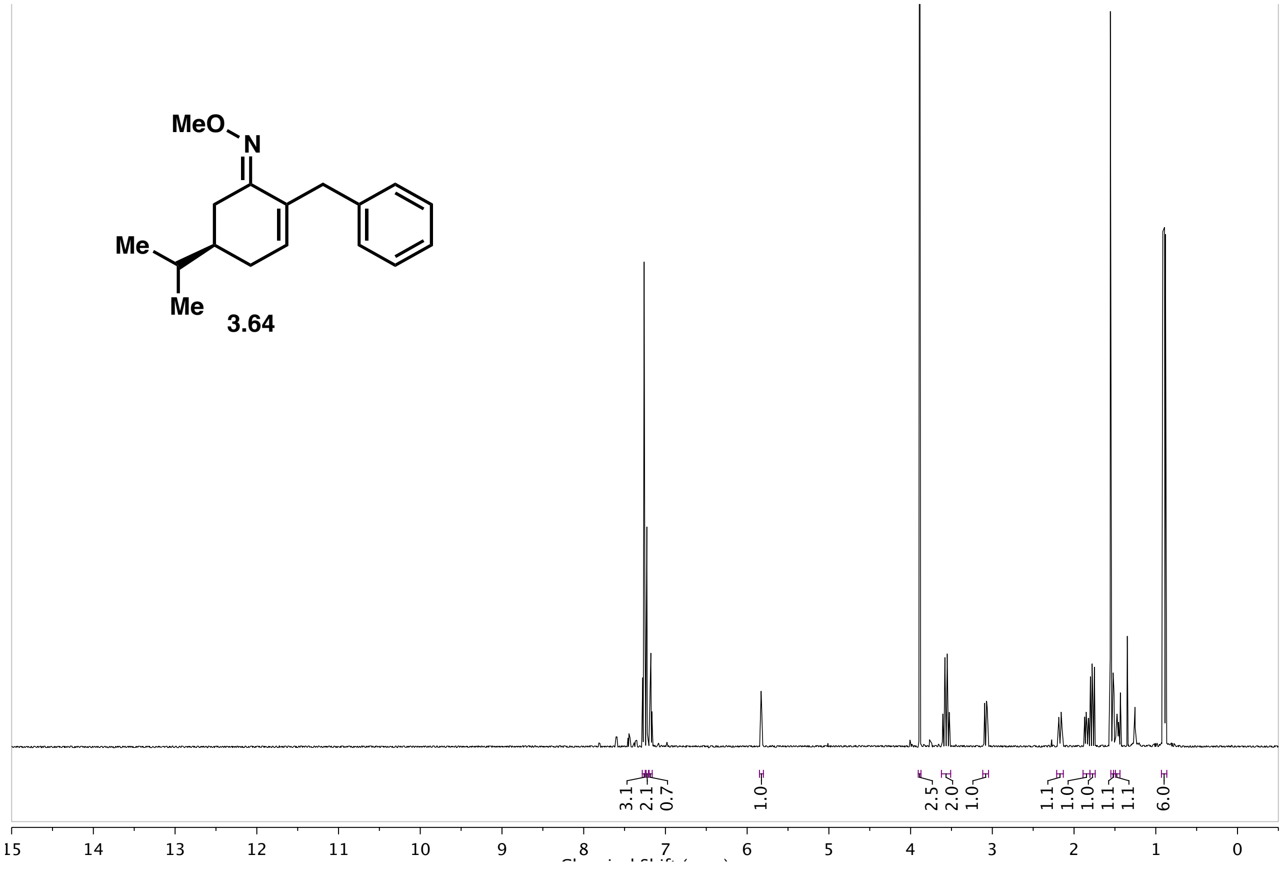
MeO
N
Me
Me
3.64
3.1
2.1
0.7
1.0
2.5
2.0
1.0
1.1
1.0
1.0
1.1
1.1
6.0
15
14
13
12
11
10
9
8
7
6
5
4
3
2
1
0

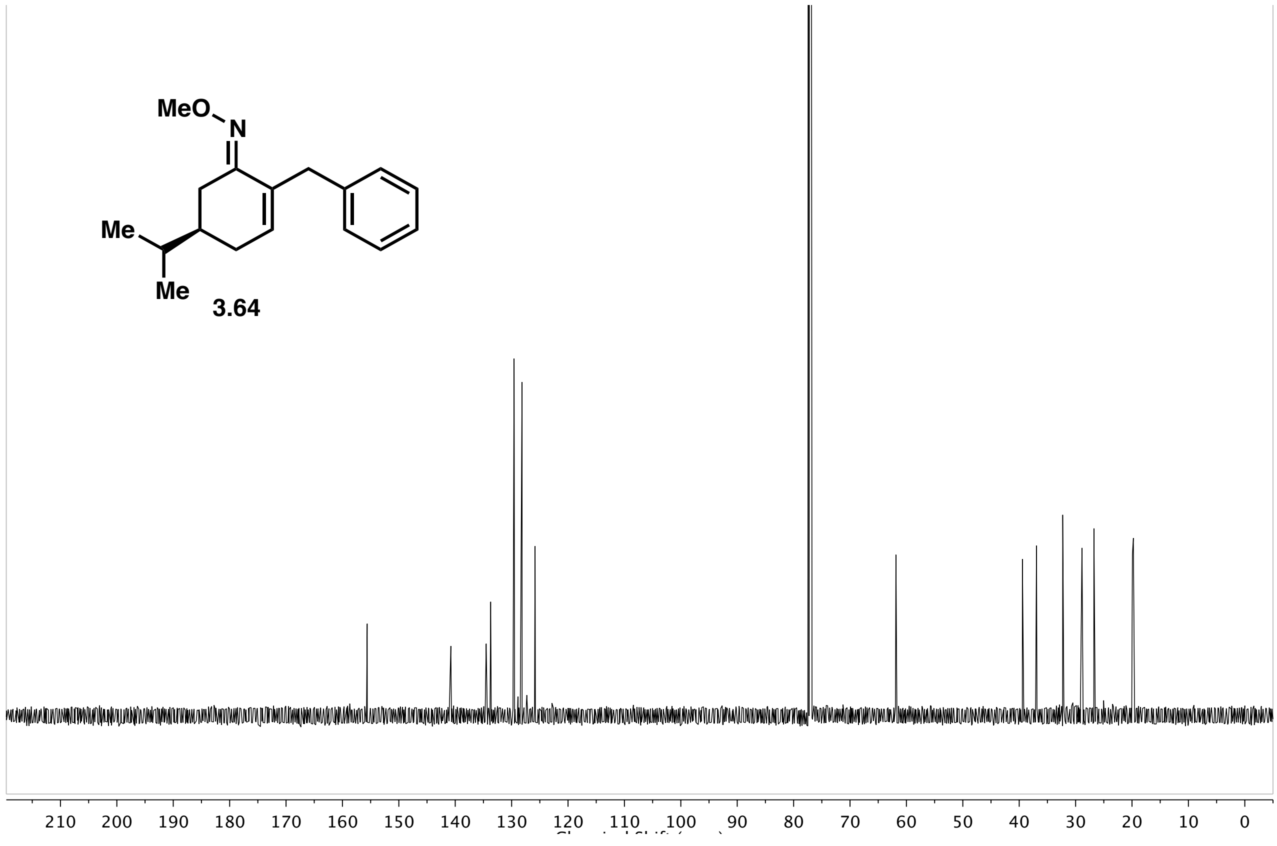
MeO
N
Me
Me
3.64
210
200
190
180
170
160
150
140
130
120
110
100
90
80
70
60
50
40
30
20
10
0

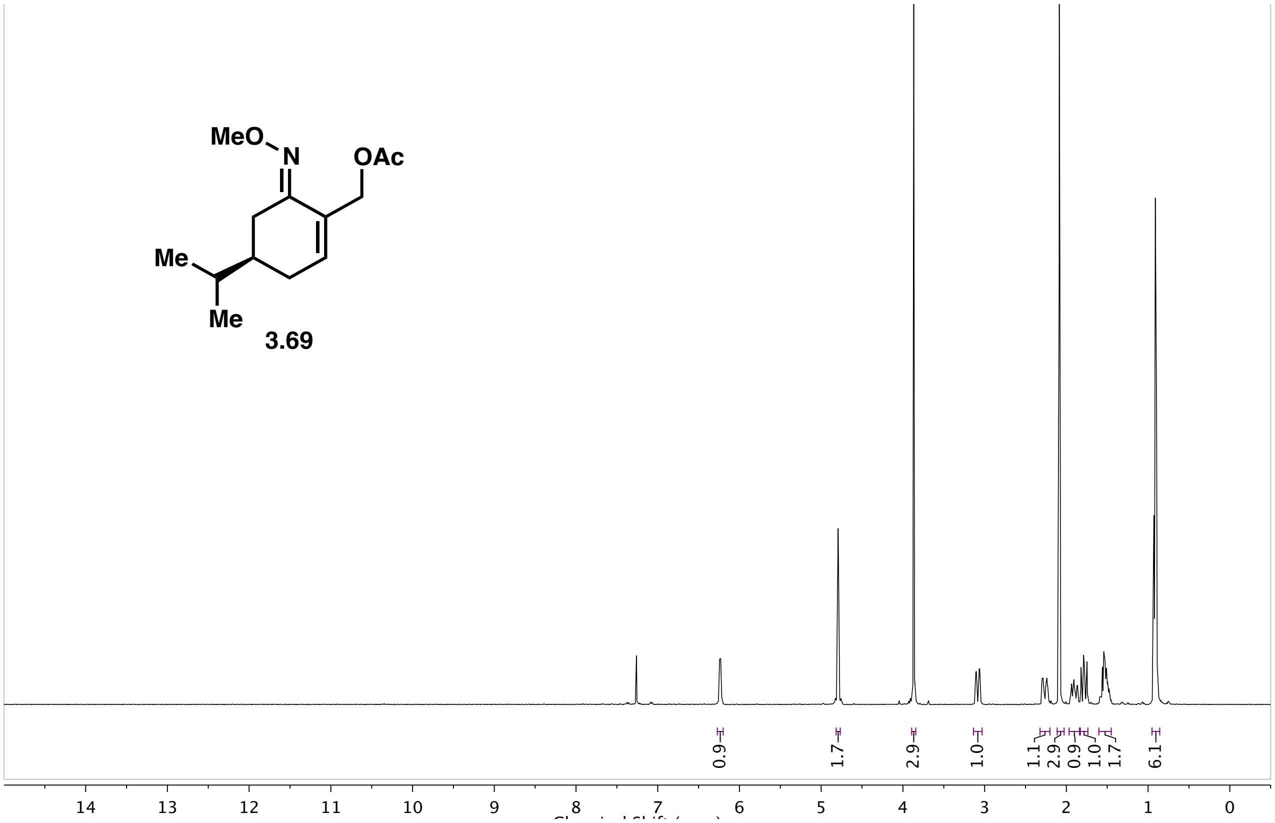
MeO
N
OAc
Me
Me
3.69
0.9
1.7
2.9
1.0
1.1
2.9
0.9
1.0
1.7
6.1
14
13
12
11
10
9
8
7
6
5
4
3
2
1
0
Chemical Shift (ppm)

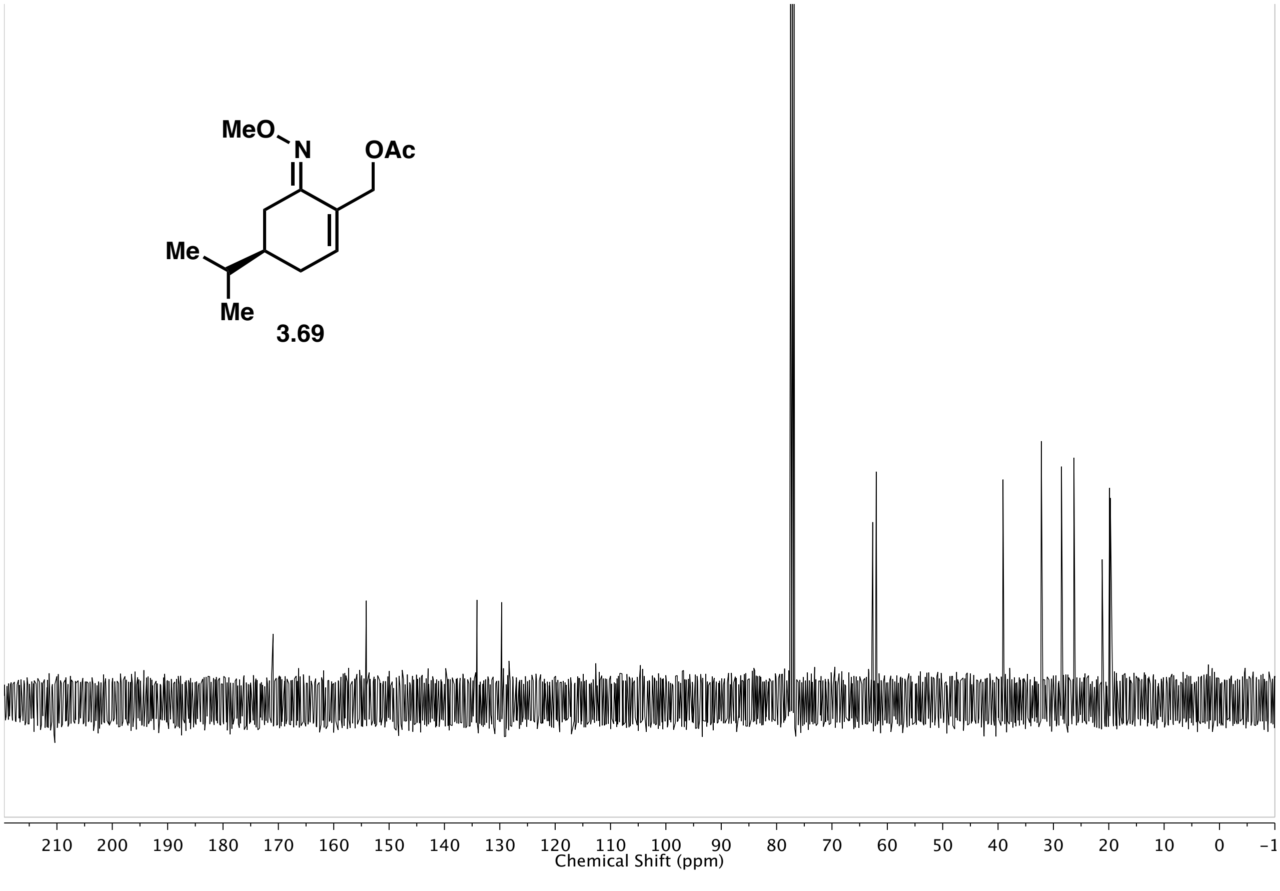
MeO
N
OAc
Me
Me
3.69
210
200
190
180
170
160
150
140
130
120
110
100
90
80
70
60
50
40
30
20
10
0
–1
Chemical Shift (ppm)

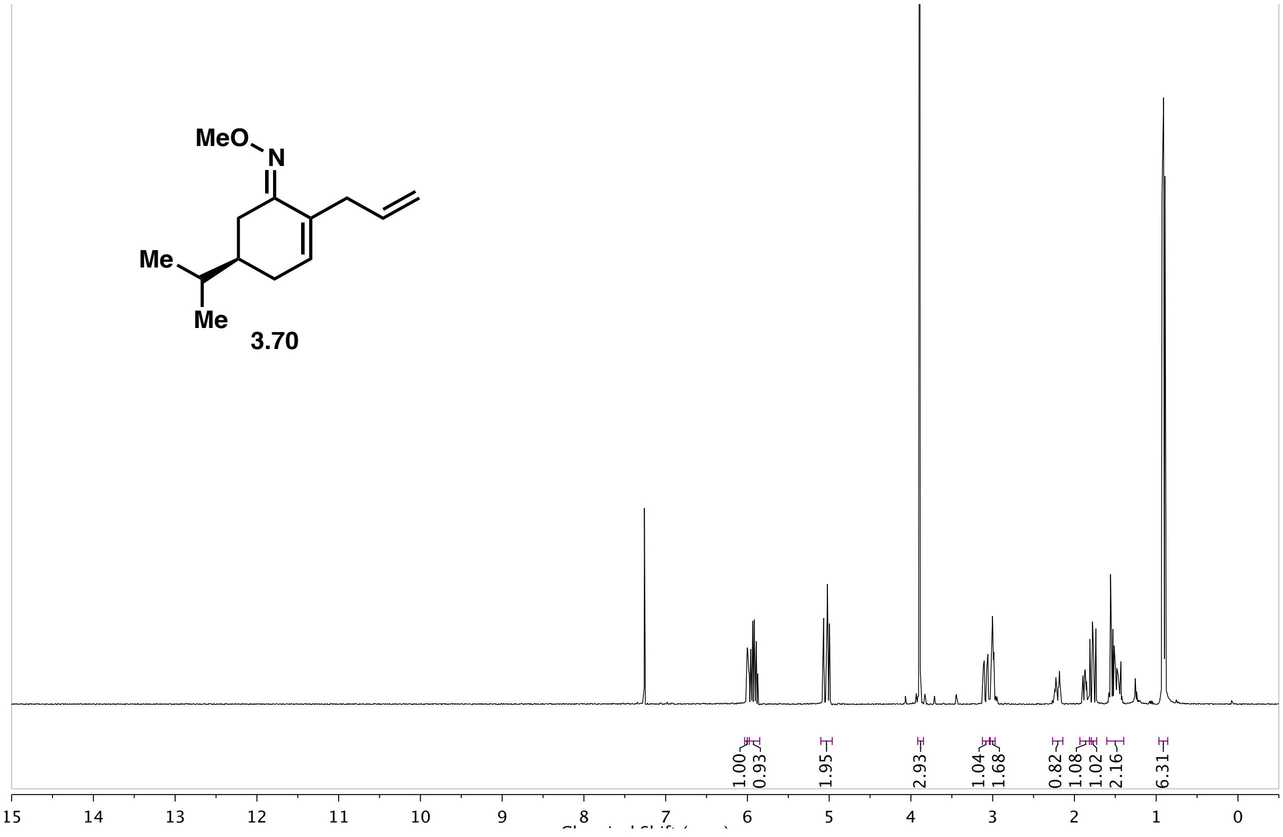
MeO
N
Me
Me
3.70
1.00
0.93
1.95
2.93
1.04
1.68
0.82
1.08
1.02
2.16
6.31
15
14
13
12
11
10
9
8
7
6
5
4
3
2
1
0

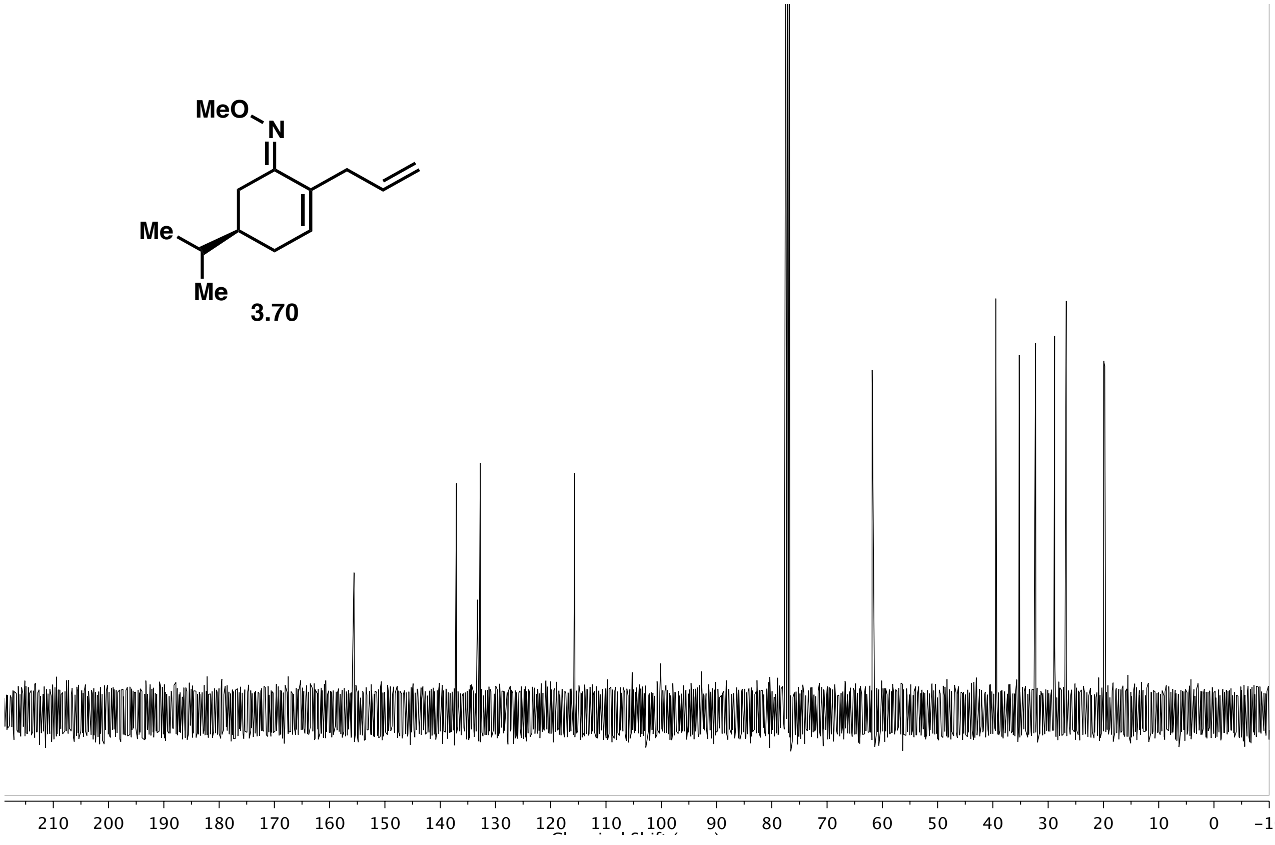
MeO
N
Me
Me
3.70
210
200
190
180
170
160
150
140
130
120
110
100
90
80
70
60
50
40
30
20
10
0
−10

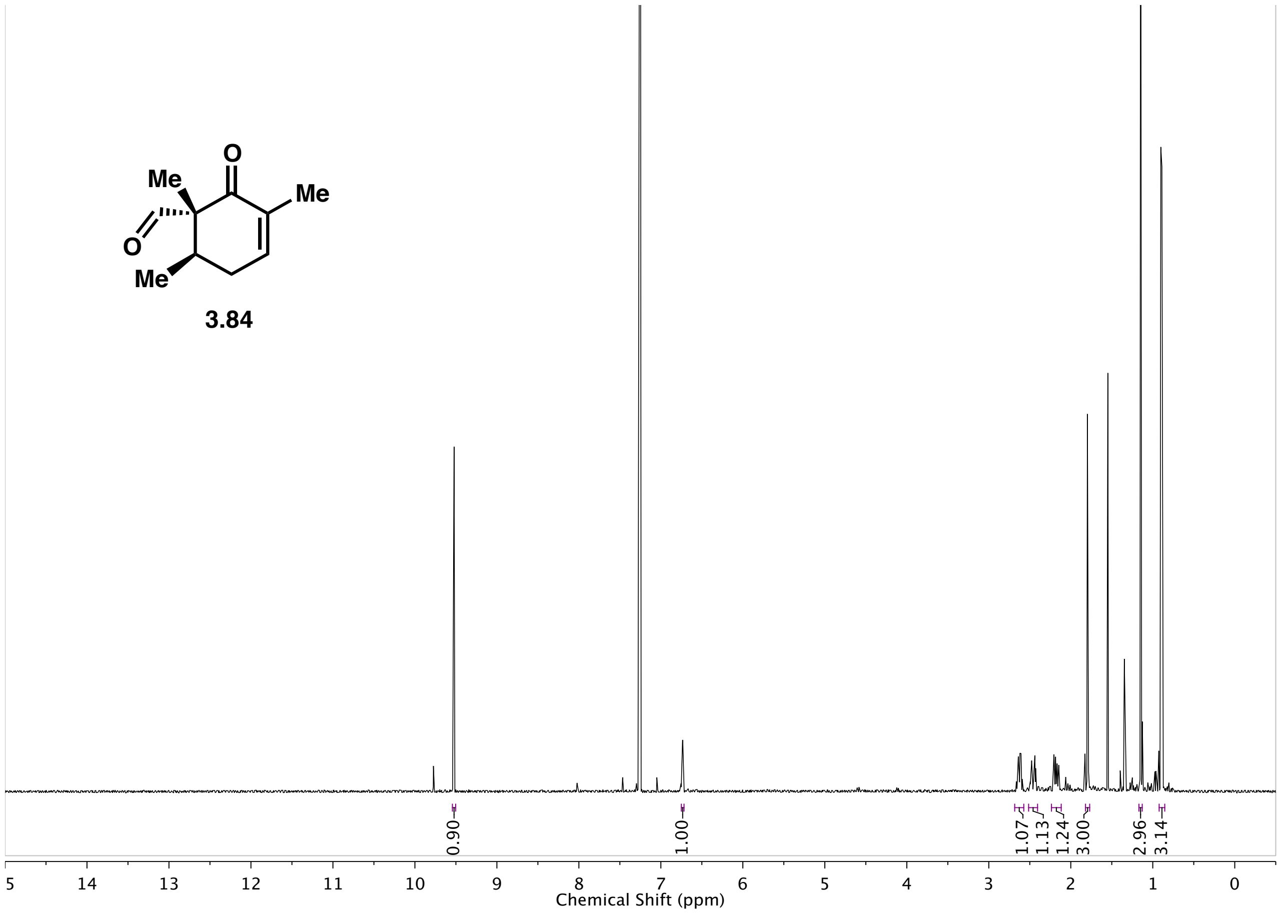

Me
O
Me
O
Me
3.84
0.90
1.00
1.07
1.13
1.24
3.00
2.96
3.14
5
14
13
12
11
10
9
8
7
6
5
4
3
2
1
0
Chemical Shift (ppm)

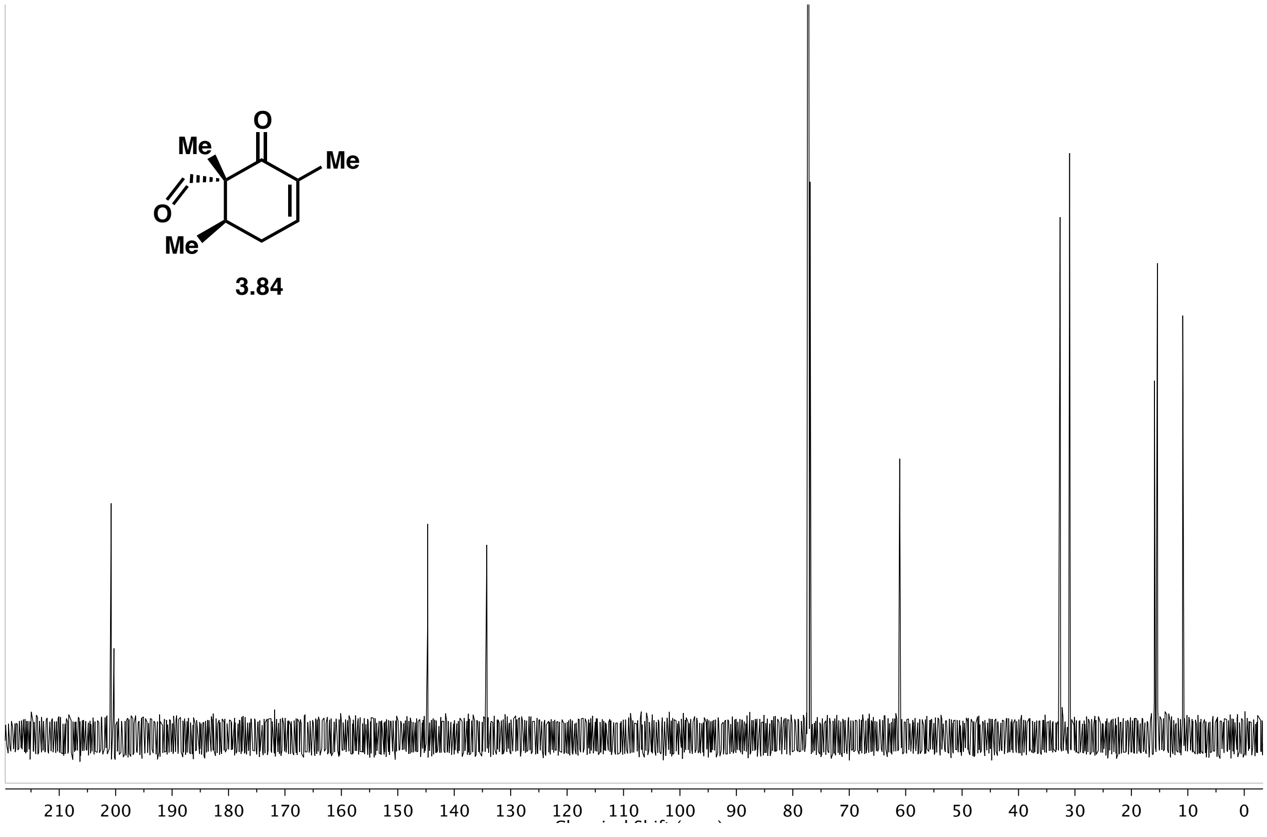

Me
O
Me
O
Me
3.84
210
200
190
180
170
160
150
140
130
120
110
100
90
80
70
60
50
40
30
20
10
0

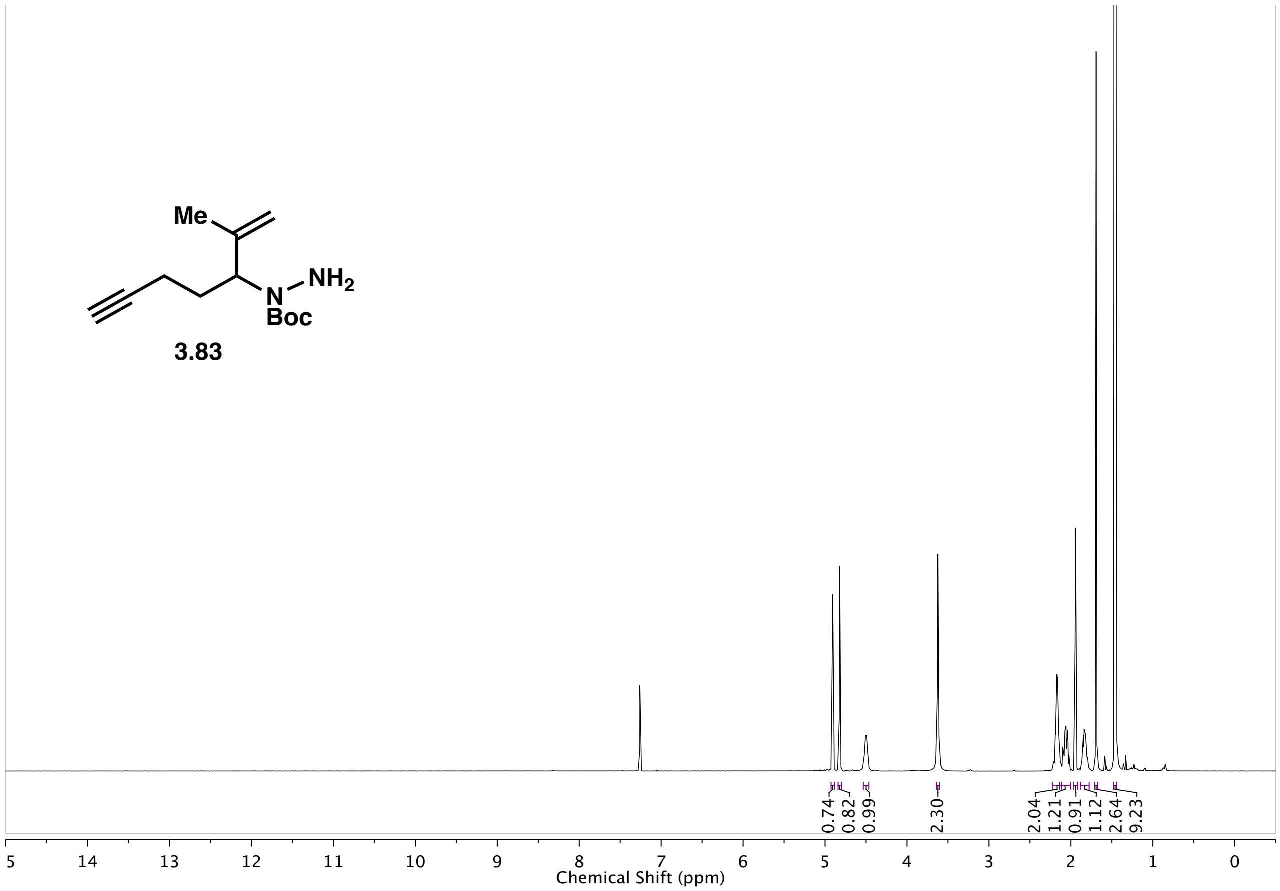
3.83

Me
NH$_2$
N
Boc
0.74
0.82
0.99
2.30
2.04
1.21
0.91
1.12
2.64
9.23
5
14
13
12
11
10
9
8
7
6
5
4
3
2
1
0
Chemical Shift (ppm)

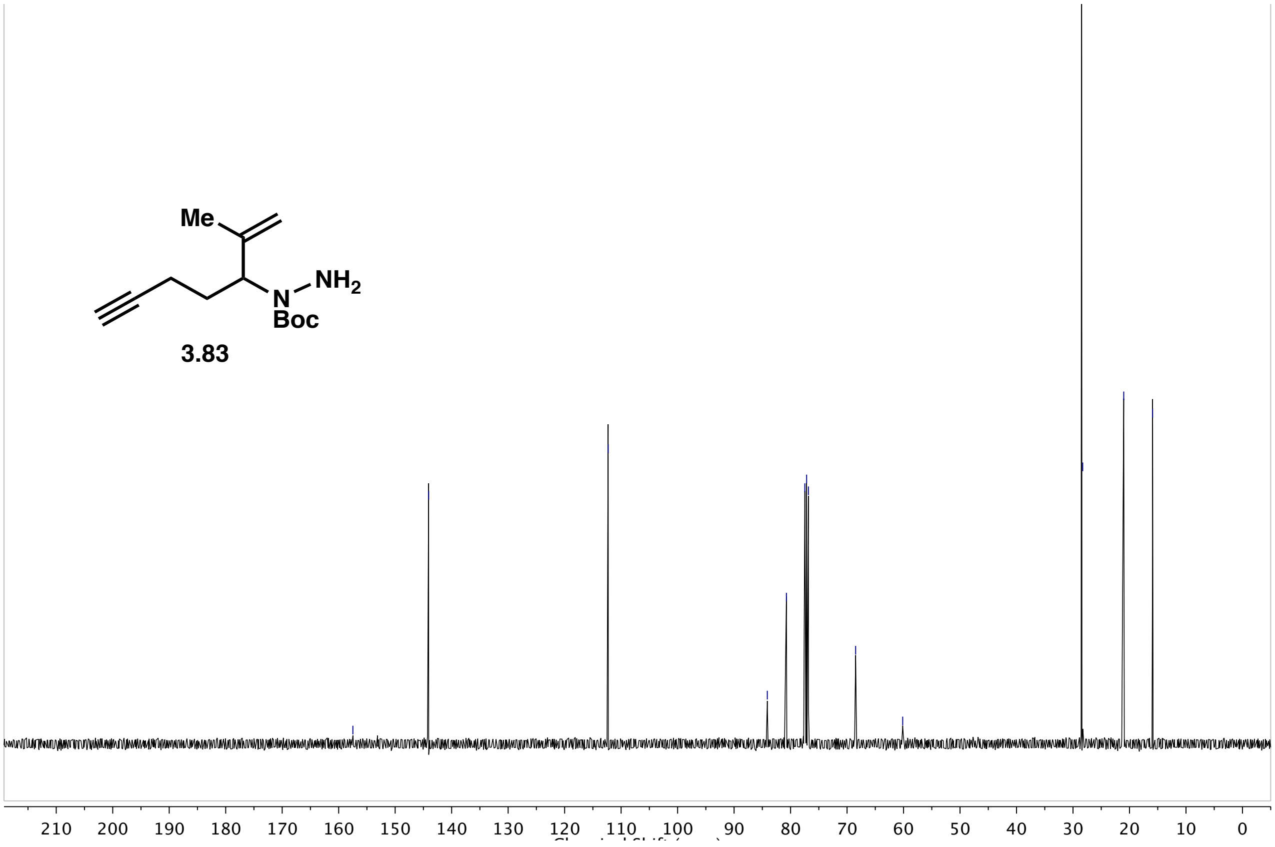
3.83

Me
NH$_2$
N
Boc
210
200
190
180
170
160
150
140
130
120
110
100
90
80
70
60
50
40
30
20
10
0

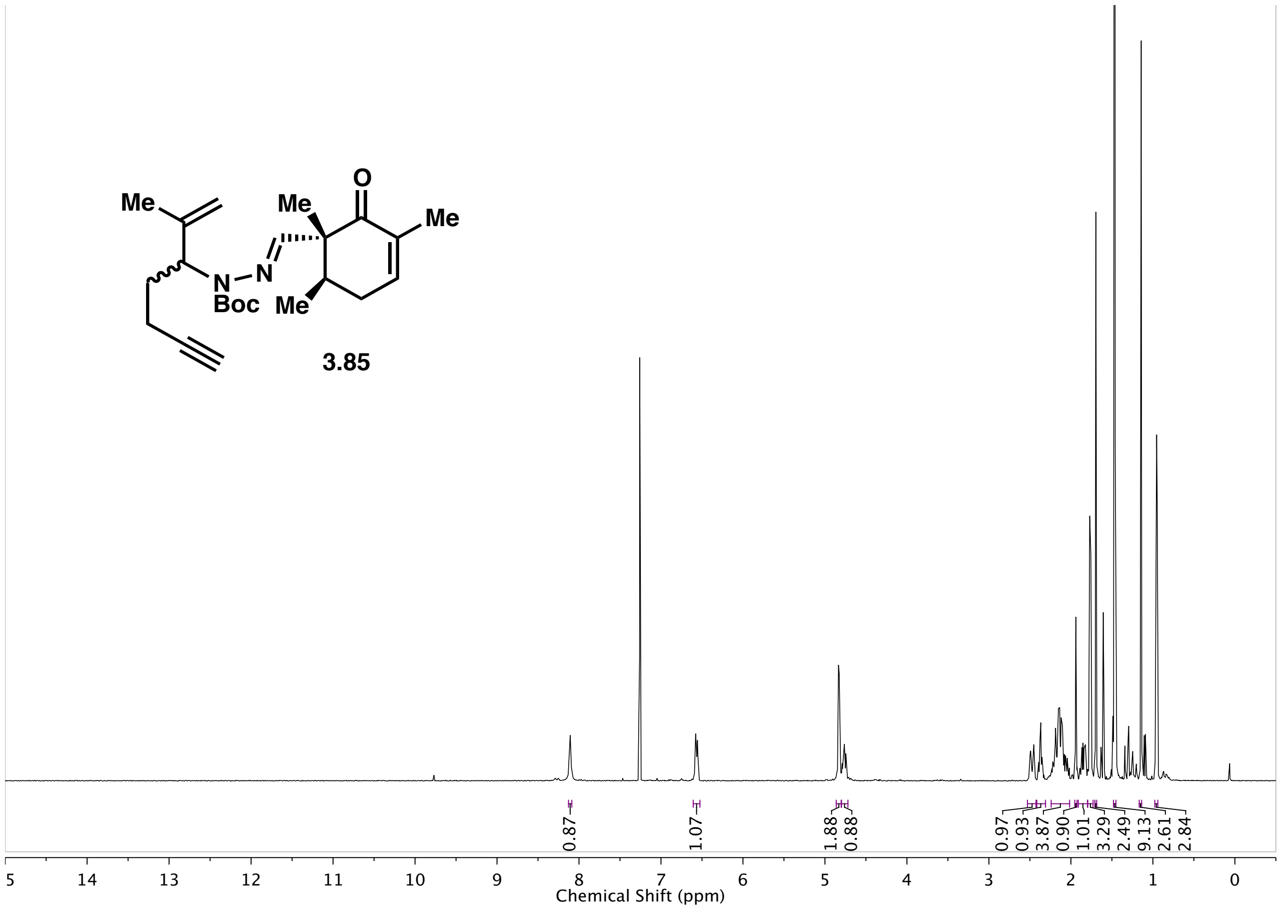

Me
O
Me
Me
N
N
Boc
Me
3.85
0.87
1.07
1.88
0.88
0.97
0.93
3.87
0.90
1.01
3.29
2.49
9.13
2.61
2.84
5
14
13
12
11
10
9
8
7
6
5
4
3
2
1
0
Chemical Shift (ppm)

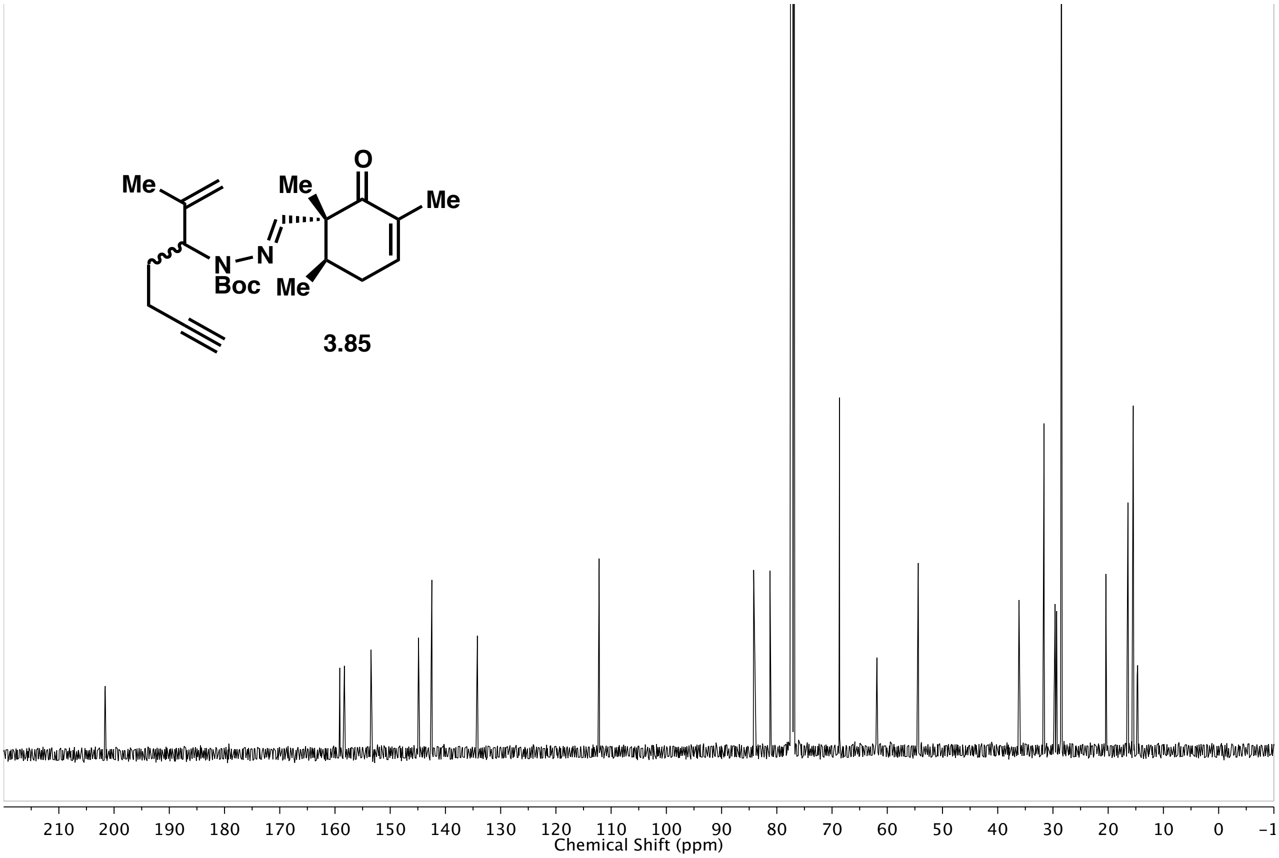

Me
O
Me
Me
N
N
Boc
Me
3.85
210
200
190
180
170
160
150
140
130
120
110
100
90
80
70
60
50
40
30
20
10
0
–1
Chemical Shift (ppm)

Chapter 4: Exploiting Cyclobutanol Reactivity Toward the Total Synthesis of Phomactin Natural Products

4.1: Macrocyclization Considerations

We learned several things about the phomactin architecture from our studies outlined in Chapter 3. First, we showed it was possible to construct the C(sp^3)–C(sp^2) bond (between C3 and C3a, Scheme 1) using a 2-step functionalization/coupling procedure. However, formation of the C(sp^3)–C(sp^3) bond (between C1' and C2') was more challenging. A new strategy would be required to effectively forge this sterically encumbered bond. This reaction would need to be very robust, especially if utilized to form the macrocyclic ring.

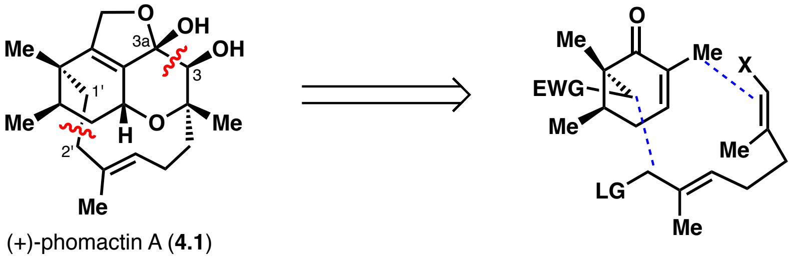

Scheme 1: Key retrosynthetic disconnections

Looking through the phomactin literature, we recognized that the macrocyclization reaction was often low yielding, although it varied greatly depending on the substrate. Perhaps unsurprisingly, forming a 12-membered bridging macrocycle containing two *E* olefins is a challenging process. There is a large entropic penalty for an ordered transition state as well as a low population of reactive conformations. However, it appears that the conformation of the cyclohexyl ring can play a large role in facilitating or impeding this reaction. In particular, the hybridization at C8b appears to be a major factor in achieving an effective macrocyclization (Scheme 2). The cyclization reactions reported by Maleczka[1] and Pattenden[2] nicely demonstrate this effect. Both groups developed a Nozaki-Hiyama-Kishi (NHK) intramolecular coupling reaction to close the 12-membered ring, but Maleczka reported a 60% yield of macrocycle **4.3** whereas Pattenden reported only a 38% yield of macrocycle **4.5**. Although there are a few small variances in these substrates, we believe that the key distinction is that the Maleczka substrate (**4.2**) contains an sp^3 hybridized carbon at C8b whereas the Pattenden substrate (**4.4**) contains an sp^2 hybridized carbon.

When there are no sp^2 carbons in the cyclohexane ring, the scaffold can sit in a chair conformation, placing both the C6 and C8b substituents in an equatorial position (see Scheme 2). This conformation angles the two reacting pieces down and toward each other, acting as a template for cyclization. When the C8b position is sp^2 hybridized, the reactive substituent is forced out and away from the C6 chain. In order to compensate for this, the cyclohexyl ring must undergo a pseudo-chair flip to place the C6 substituent in a pseudo-axial position, allowing for an appropriate cyclization conformation. We believe that this additional barrier results in diminished yields as demonstrated by the Pattenden substrate (**4.4**).

A) Maleczka

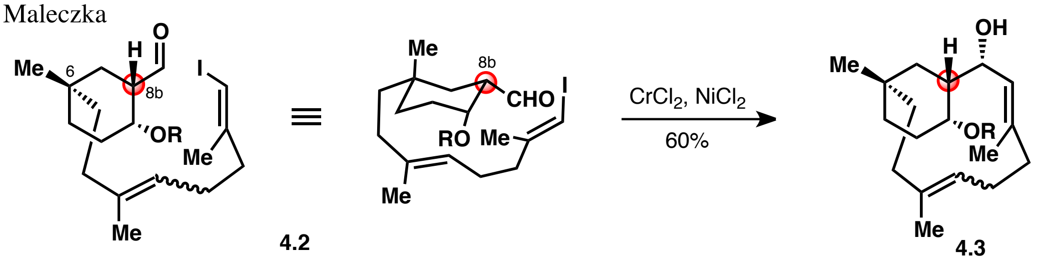

Me
6
H
O
8b
I
'OR
Me
Me
4.2
≡
Me
8b
CHO
I
RO Me
Me
CrCl2, NiCl2
60%
OH
Me
H
'OR
Me
Me
4.3

B) Pattenden

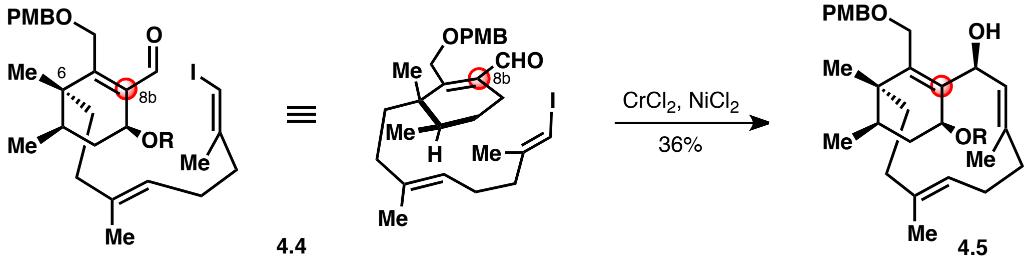

PMBO
O
Me
6
8b
I
Me
OR
Me
Me
4.4
≡
OPMB
CHO
Me
8b
I
Me
H
Me
Me
CrCl2, NiCl2
36%
PMBO
OH
Me
Me
OR
Me
Me
4.5

Scheme 2: NHK macrocyclizations with different carbon hybridization at C8b

Although it is hard to directly compare macrocyclization substrates, the C8b hybridization trend seems to hold – sp^3 hybridization often results in good yields whereas sp^2 hybridization results in low or moderate yields. Another macrocyclization example with sp^2 hybridization at C8b was reported by Rawal (Scheme 3A).[3] Treatment of aldehyde **4.6** with sodium bis(trimethylsilyl)amide (NaHMDS) accomplished a 1,2-addition of the acetylide into the aldehyde group in a modest 46% yield. While the Thomas group utilized a distinctly different substrate and reaction, they showed that an anionic macrocyclization was possible on sulfone **4.8**, bearing an sp^3 hybridized carbon at C8b, in a good 72–85% yield (Scheme 3B).[4] Although the macrocyclization is more efficient with an sp^3-hybridized carbon at C8b, many synthetic routes strive to include sp^2 hybridization since all the phomactin natural products (except phomactin D, see Section 3.1) contain an sp^2-hybridized carbon at C8b. It is not ideal to saturate the double bond to achieve macrocyclization reactivity and later revert back to sp^2 hybridization.

A) Rawal

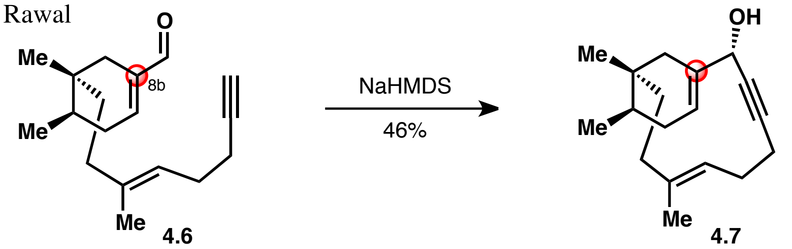

O
Me
8b
Me
Me
4.6
NaHMDS
46%
OH
Me
Me
Me
4.7

B) Thomas

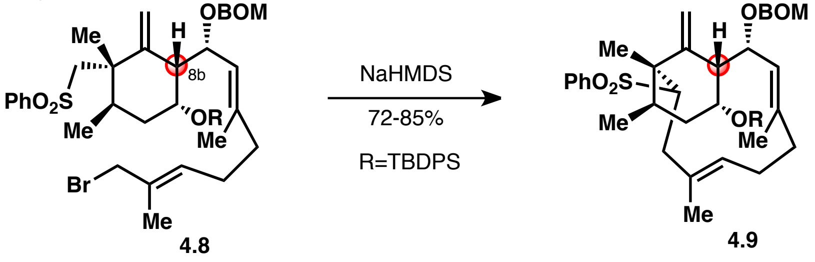

OBOM
Me
H
8b
PhO2S
Me
'OR
Me
Br
Me
4.8
NaHMDS
72-85%
R=TBDPS
OBOM
Me
H
PhO2S
Me
'OR
Me
Me
4.9

Scheme 3: Anionic macrocyclizations with different carbon hybridization at C8b

We recognized that Thomas' macrocyclization disconnection (via sulfone alkylation) provided the requisite C(sp^3)–C(sp^3) bond construction necessary for our total synthesis. But while this reaction worked well on their system (i.e., **4.8**), we were concerned that sp^2 hybridization at C8b would result in a poor yield for our proposed macrocyclization substrate **4.10** (Scheme 4). It is clear by looking at **4.10** in a conformational view that the methylene sulfone and the linear "strap" are projecting straight out from the cyclohexyl core and pointing away from each other – the least ideal scenario for cyclization. We wanted to develop a strategy for biasing this substrate toward cyclization, without conceding to a lengthy rehybridization strategy of the C8b position. We recognized that the cyclohexenone core of **4.10** originated from the selective fragmentation of a cyclobutanol-containing bicycle (see Section 3.4) and that this [3.1.1]bicycle could serve as a suitable scaffold for a templated cyclization.[5] If we kept the cyclobutanol intact until much later in the synthesis, the macrocyclization could be performed on sulfone **4.12**. By embedding the rigid bicyclo[3.1.1]heptane structure into the molecule, some of the entropic cost would be "pre-paid" and the methylene sulfone would be locked in a pseudo-axial position. We anticipated this uniquely rigid [3.1.1]bicyclic scaffold would help to pre-organize the reactive partners and aid in the entropically-challenging cyclization.

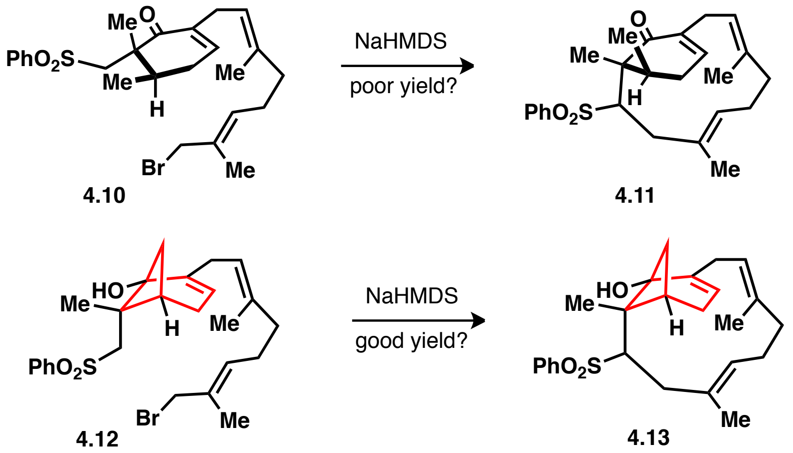

Scheme 4: [3.1.1]bicycle template hypothesis for improving macrocyclization

4.2: Revised Strategy Exploiting the Properties Inherent in Cyclobutanols

Bringing together everything that we've learned from previous studies as well as heeding the precedent for macrocyclization, we revised our retrosynthesis as shown in Scheme 5. We envision disassembling many of the unique C–O bonds present in (+)-phomactin A to bring us back to diol **4.14**. Strategically, this would also allow for late-stage diversification from a common carbocyclic core to access a wide variety of phomactin natural products. Additionally, strong precedent exists for forming many of these particular C–O bonds. A 1,2 addition followed by allylic transposition would allow us to access diol **4.14** from enone **4.15**. Intramolecular sulfone alkylation of cyclobutanol **4.12** will serve to close the macrocycle, exploiting the rigid scaffold of the bicyclo[3.1.1] system to aid in the cyclization. Additionally, selective activation and cleavage of the strained C–C bond inherent in the cyclobutanol will establish the *syn* vicinal methyl groups in enone **4.15**. The linear segment (**4.17**) will be coupled onto cyclobutanol **4.16**, which can be accessed from readily-available chiral pool compound (*S*)-carvone in 2 steps (see Section 3.4).

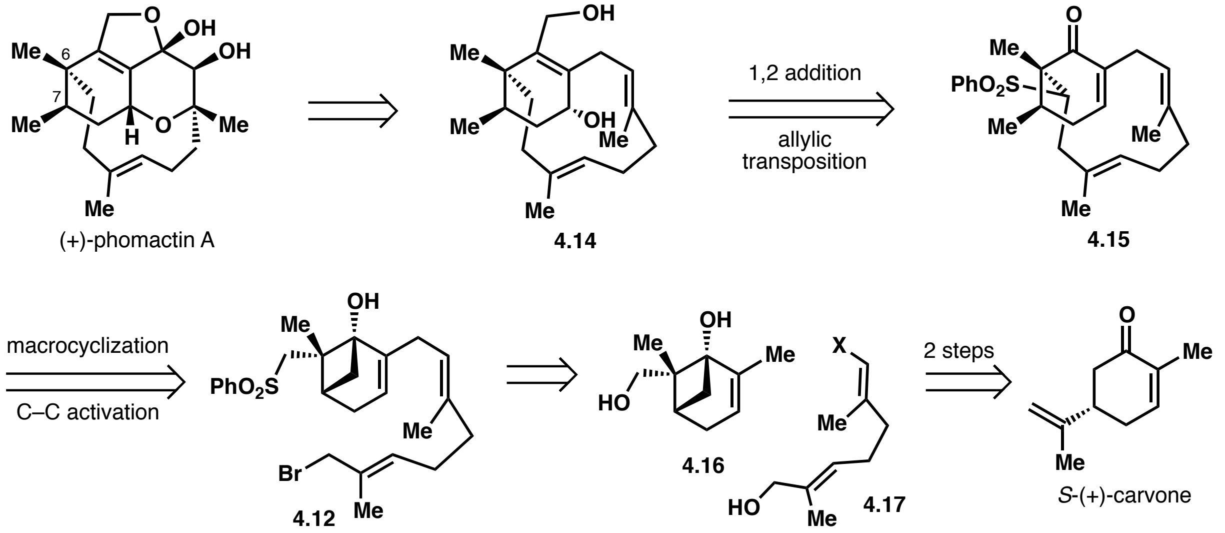

Scheme 5: Retrosynthetic analysis with late-stage fragmentation of the cyclobutanol moiety

Our strategy is notable for our decision to keep the cyclobutanol moiety imbedded in the synthetic intermediates throughout the first half of the synthesis. There are many benefits to this strategy. As already discussed, we believed that the rigid [3.1.1] bicycle will aid in the challenging macrocyclization reaction. Additionally, this cyclobutanol is stereochemically rich and includes the all-carbon quaternary center present in the natural products. We planned to take advantage of this stereochemistry and the inherent strain in the system to selectively open the cyclobutanol and set the *syn* vicinal methyl groups at C6 and C7 (see Scheme 5 for numbering). We also hope to utilize the cyclobutanol hydroxyl group as a directing group for C–H functionalization (see Section 4.3).

However, compounds with strained ring systems are often subject to undesired reactivity pathways that we need to avoid. First, we have seen that the double bond can be quite reactive toward electrophiles such as oxidants or acids (Scheme 6A). This initiates a rearrangement, resulting in formation of [2.2.1]bicycle **4.19**. Additionally, if compound **4.18** contains a good leaving group (X), a Grob-type fragmentation can occur (especially under basic conditions) to give carvone-type structures such as **4.20** (Scheme 6B).

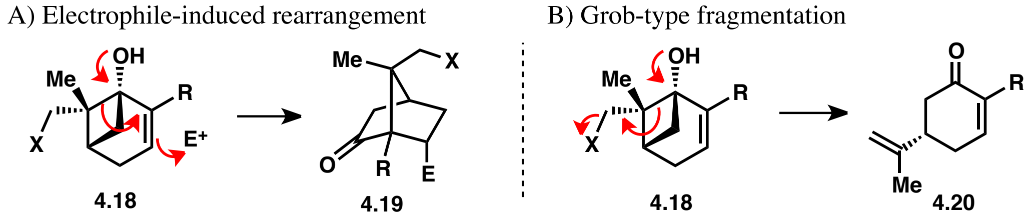
A) Electrophile-induced rearrangement

B) Grob-type fragmentation

Scheme 6: Undesired reactivity pathways for cyclobutanol-containing compounds

4.3: Attempts at Utilizing C–H Silylation for Fragment Coupling

Key to our synthetic strategy is the intermolecular coupling between the unfunctionalized allylic methyl group of **4.16** and a linear fragment **4.17** (see Scheme 5). Previously, we showed that oxime ethers can serve as directing groups for C(sp^3)–H functionalization (see Section 3.5). However, this is not ideal since utilizing the oxime ether would require two additional steps (i.e., the construction and removal of the directing group). We were excited by the opportunity to explore C(sp^3)–H functionalization directed by a hydroxyl group since the cyclobutanol-containing molecules contain this native directing group. We planned to follow precedent from the Hartwig lab where they've shown that iridium can catalyze the C(sp^3)–H dehydrogenative silylation of (hydrido)silyl ether **4.21** to form oxasilolane **4.22** in excellent yield (Scheme 7).[6] The authors report that tertiary alcohols or structurally rigid secondary alcohols are required for this reaction to proceed efficiently. This is ideal for our system as we are dealing with a structurally rigid tertiary alcohol.

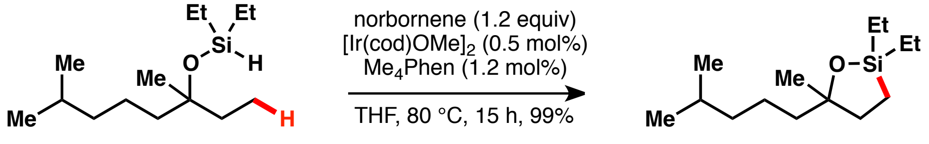

4.21 **4.22**

Scheme 7: Dehydrogenative C–H silylation reported by Hartwig and coworkers

We were pleased to find that application of this methodology to our system was successful without modification of the reaction conditions. This 2-step, 1-pot procedure involves initial silylation of the tertiary alcohol followed by the dehydrogenative C–H silylation to give oxasilolane **4.24** in 80% yield (Scheme 8). Importantly, this reaction is completely chemoselective toward functionalization at the allylic methyl position over the alkyl methyl position. This could arise from the slight activating ability of the neighboring π-system, but it's likely that the dihedral angle between the alkyl methyl group and the silyloxy group is too great to achieve a productive conformation. This is in contrast to the dihedral angle between the allylic methyl group and the silyloxy group which is quite close to 0°.

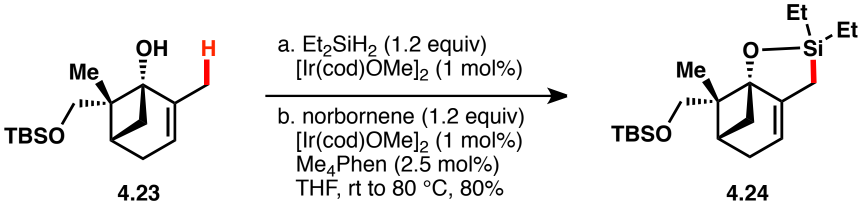
OH
H
Me
TBSO
a. Et$_2$SiH$_2$ (1.2 equiv)
[Ir(cod)OMe]$_2$ (1 mol%)
b. norbornene (1.2 equiv)
[Ir(cod)OMe]$_2$ (1 mol%)
Me$_4$Phen (2.5 mol%)
THF, rt to 80 °C, 80%
Et
Et
O—Si
Me
TBSO

4.23 **4.24**

Scheme 8: Dehydrogenative C–H silylation on cyclobutanol substrate

Having successfully functionalized the desired allylic carbon, we sought to append the vinyl fragment via a cross-coupling reaction. Ideally, we hoped to utilize the carbon-silicon bond of oxasilolane **4.24** as a functional handle for Hiyama-type coupling. This would provide the most direct route for vinylation. Initially, we attempted to couple oxasilolane **4.24** with a simple vinyl bromide, 1-bromo-2-methyl-1-propene, with skipped diene **4.25** as the desired product (Scheme 9). Interestingly, this was not the observed product when this reaction was conducted under palladium catalysis. Instead, cyclohexenone **4.26** was formed as the sole product, presumably through subsequent C–C cleavage and cross-coupling. Nucleophilic silane activation is often necessary for Hiyama couplings, but with a strained polycyclic system such as **4.24**, the 'ate' complex could exist in equilibrium with the open form, alkoxide **4.27**. Palladium (II) can engage this alkoxide and initiate a β-carbon elimination to give alkyl-palladium species **4.29**. Reductive elimination results in the observed product (**4.26**). Palladium-mediated C–C activation and cross-coupling is a known process, dating back to studies conducted by Uemura and coworkers in 1999 on the arylation of cyclobutanols.[7] In fact, the Sarpong lab has recently expanded the scope of this reaction and shown that carvone-derived cyclobutanols are ideal substrates for palladium-catalyzed C–C bond cleavage/coupling reactions to access enantiopure natural product-like scaffolds.[8]

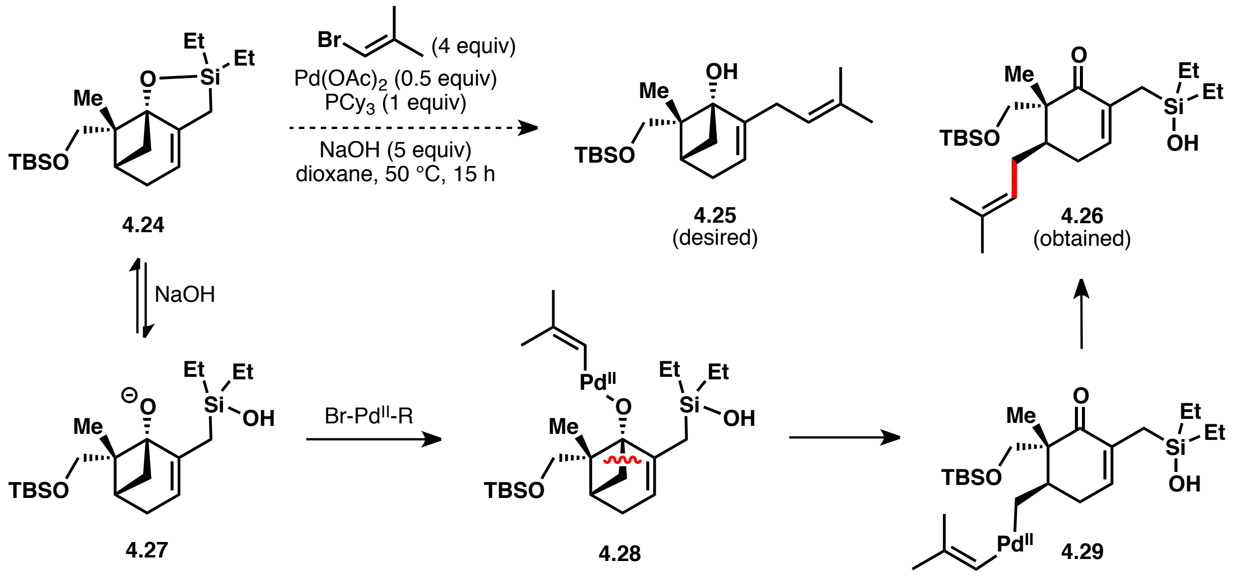
Et
Et
O
Si
Me
TBSO
4.24
Br
(4 equiv)
Pd(OAc)$_2$ (0.5 equiv)
PCy$_3$ (1 equiv)
NaOH (5 equiv)
dioxane, 50 °C, 15 h
OH
Me
TBSO
4.25
(desired)
O
Me
Et
Et
Si
OH
TBSO
4.26
(obtained)
NaOH
Et
Et
Si
OH
O
Me
TBSO
4.27
Br-Pd^{II}-R
Pd^{II}
O
Et
Et
Si
OH
Me
TBSO
4.28
O
Me
Et
Et
Si
OH
TBSO
Pd^{II}
4.29

Scheme 9: Palladium-mediated C–C activation followed by cross coupling

Unfortunately, the observed reactivity was not productive for the synthesis of phomactin A or any phomactin natural product. It appeared that the use of palladium for a Hiyama coupling would only result in C–C cleavage products, so we next sought to explore this reactivity with rhodium catalysis instead (Table 1). Utilizing $[Rh(cod)OH]_2$, the desired cyclohexenone **4.30** was obtained in 32% yield along with two other side products, probably resulting from β-hydride elimination instead of protodemetalation of the alkyl rhodium species (entry 1). Adding ligands to this reaction either had no effect (PCy_3, entry 2), increased the amount of side products (S-BINAP, entry 3), or completely shut down the reaction (1,3-bis(2,6-diisopropylphenyl)imidazol-2-ylidene, entry 4). Varying the rhodium pre-catalyst affected product ratios slightly, but none proved to be better than the original $[Rh(cod)OH]_2$ (entries 5,6).

Table 1: Rhodium-mediated C–C activation of oxasilolane **4.24**

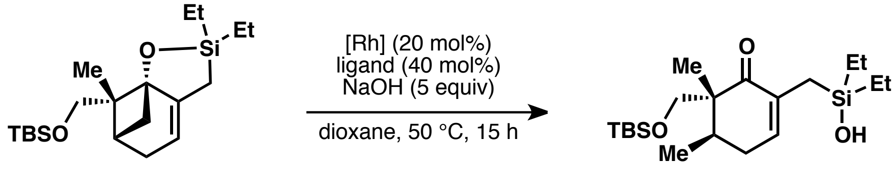

4.24 → **4.30**

entry	[Rh] species	ligand	outcome
1	$[Rh(cod)OH]_2$	none	32% **4.30**, 2 side products
2	$[Rh(cod)OH]_2$	PCy_3	similar to entry 1
3	$[Rh(cod)OH]_2$	S-BINAP	**4.30** is minor product
4	$[Rh(cod)OH]_2$	IPr	mostly SM
5	$[Rh(nbd)Cl]_2$	none	**4.30** is minor product
6	$[Rh(cod)_2]BF_4$	none	similar to entry 1, 25% **4.30**

With allylic silanol **4.30** in hand, we continued our investigations into vinylation reactions by looking at Hiyama-Denmark couplings.[9] The Denmark lab has shown that silanols are privileged class of silicon-containing coupling partners because they can be activated simply by deprotonation. The resulting silanolate can then serve as a nucleophilic activating agent, forming an 'ate' complex with a second substrate molecule (although not always necessary). Additionally, the silanolate can bind to the palladium catalyst, forming a discrete Si–O–Pd linkage and thus accelerating the intramolecular transmetalation step.[10] Although aryl and alkenyl silanols are most commonly used in this reaction, there have also been some examples of successful allylic silanol couplings.[11] Unfortunately, when standard conditions were explored using $KOSiMe_3$ as the activator, no reactivity was observed (Table 2, entry 1). Utilizing sodium hydride to pre-form the silanolate prior to the coupling reaction also did not produce any reaction, even at 100 °C (entries 2 and 3). When the activator was switched to fluoride, instead of the coupled product, only compounds resulting from protodesilylation (i.e., **4.32** and **4.33**) were observed (entries 4 and 5).

Table 2: Attempted Hiyama-Denmark coupling of silanol **4.30**

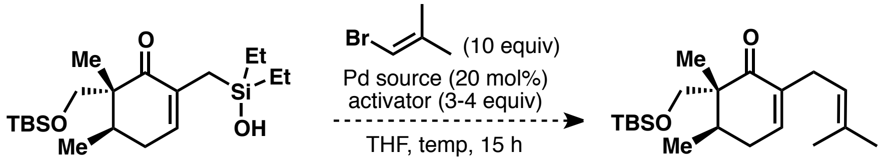

4.30 → **4.31**

entry	Pd source	activator	temp	outcome
1	$Pd(dba)_2$	$KOSiMe_3$	50 °C	SM
2	$Pd(P^tBu_3)_2$	NaH	rt	SM
3	$Pd(OAc)_2$, PCy_3	NaH	100 °C	SM
4	$[Pd(allyl)Cl]_2$	TASF	50 °C	**4.32**
5	$Pd(PPh_3)_4$	TASF	50 °C	**4.32**:**4.33** (1:1)

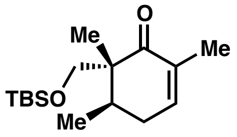

4.32

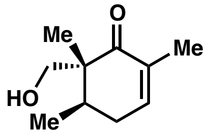

4.33

Ultimately, utilizing the carbon-silicon functional handle for cross-coupling turned out to be fruitless. Additionally, we hoped to keep the cyclobutanol intact until a later stage in the synthesis in order to investigate conformational effects on the macrocyclization, so we turned our attention to π-allyl cross-couplings with cyclobutanol-containing allylic acetates.

4.4: The π-allyl Stille Reaction for Fragment Coupling and Macrocyclization Findings

Since direct coupling from silyl-containing compounds had been unsuccessful, we decided to switch course to investigate π-allyl cross-couplings with allylic electrophiles. Tamao-Fleming oxidation of oxasilolane **4.24** yielded diol **4.34**, which could be selectively acetylated to give allylic acetate **4.35** (Scheme 10A). We hoped to utilize this allylic acetate moiety in a π-allyl cross-coupling reaction. However, with the goal of designing an efficient synthesis of the phomactin natural products, we wanted to minimize the use of protecting groups. So instead of capping primary alcohol **4.16** as the TBS ether, we hoped that early installation of the sulfide group would serve to provide a handle for macrocyclization later in the synthetic route. Conversion of primary alcohol **4.16** to phenyl sulfide **4.36** occurred smoothly in 80% yield (Scheme 10B). We could utilize this compound in the Hartwig silylation chemistry to afford oxasilolane **4.37**, however, this sulfur-containing compound was not amenable to Tamao-Fleming oxidation and only led to a mixture containing decomposition products.

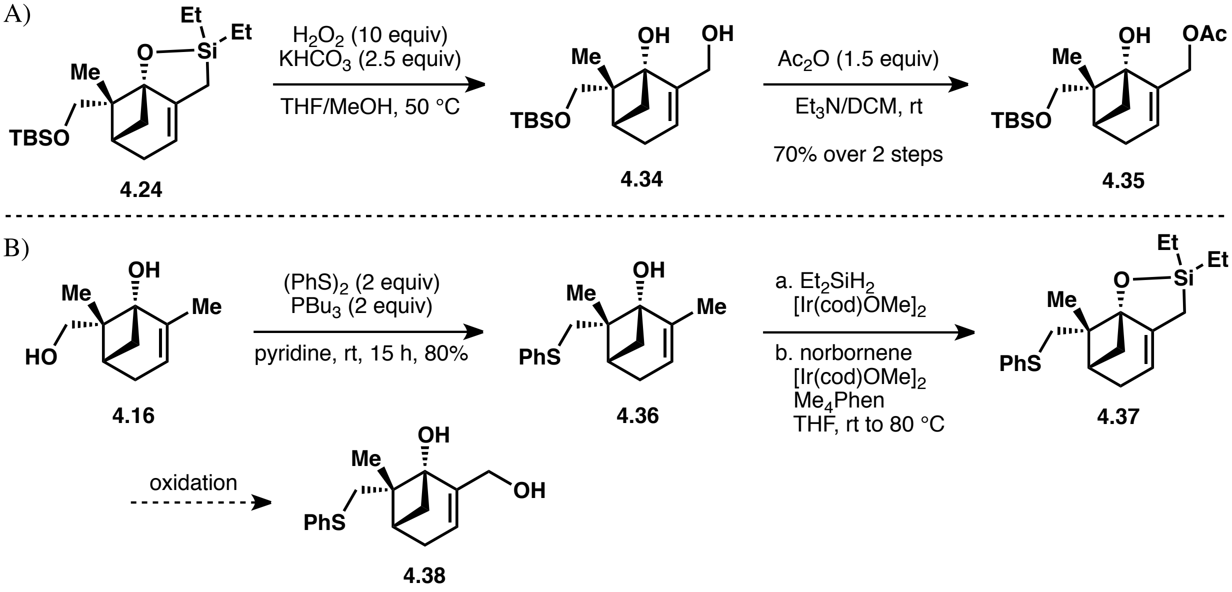
A)
Et
Et
O
Si
Me
TBSO
4.24
H_2O_2 (10 equiv)
$KHCO_3$ (2.5 equiv)
THF/MeOH, 50 °C
OH
OH
Me
TBSO
4.34
Ac_2O (1.5 equiv)
Et_3N/DCM, rt
70% over 2 steps
OH
OAc
Me
TBSO
4.35
B)
OH
Me
Me
HO
4.16
$(PhS)_2$ (2 equiv)
PBu_3 (2 equiv)
pyridine, rt, 15 h, 80%
OH
Me
Me
PhS
4.36
a. Et_2SiH_2
$[Ir(cod)OMe]_2$
b. norbornene
$[Ir(cod)OMe]_2$
Me_4Phen
THF, rt to 80 °C
Et
Et
O
Si
Me
PhS
4.37
oxidation
OH
Me
PhS
OH
4.38

Scheme 10: Tamao-Fleming oxidation, pre-installation of sulfide

Not wanting to abandon the pre-installation of the sulfide group, we sought to investigate other methods for C–H functionalization that took advantage of the allylic nature of the methyl position. We were pleased to find that selenium dioxide was capable of effecting this type of oxidation to give allylic alcohol **4.38** as the major product along with aldehyde **4.39** and enone **4.40** (Scheme 11). The aldehyde product was synthetically useful, but we were never able to optimize away from the rearranged enone product. Optimization of the reaction conditions allowed for 52% yield of desired diol **4.38** which could be selectively acetylated to yield allylic acetate **4.41**.

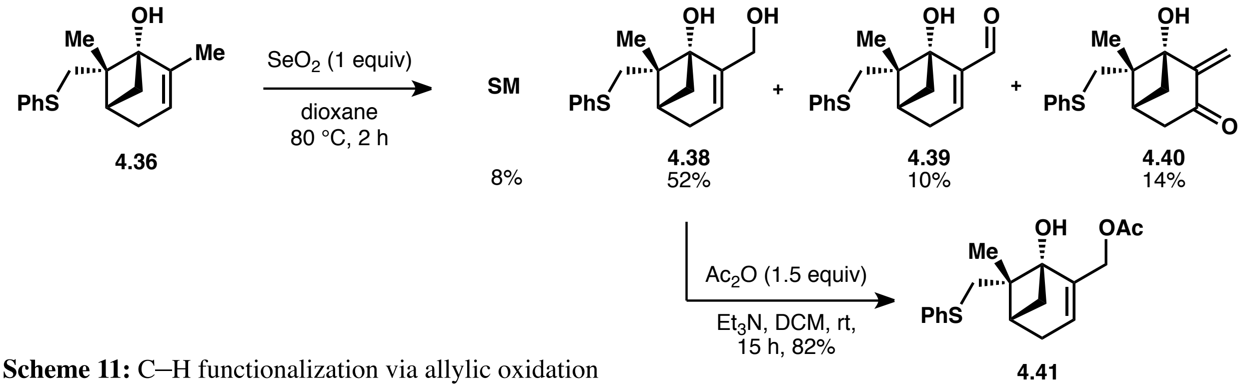

OH
Me
Me
PhS
4.36
SeO2 (1 equiv)
dioxane
80 °C, 2 h
SM
8%
OH
OH
Me
PhS
4.38
52%
+
OH
O
Me
PhS
4.39
10%
+
OH
Me
PhS
O
4.40
14%
Ac2O (1.5 equiv)
Et3N, DCM, rt,
15 h, 82%
OH
OAc
Me
PhS
4.41

Scheme 11: C–H functionalization via allylic oxidation

Allylic acetate **4.41** could serve as an electrophile in a cross coupling reaction. Preparation of the vinyl nucleophile followed a similar course to the fragment prepared by Yamada and coworkers in their synthesis of phomactin D.[12] Starting from 4-pentyn-1-ol, Swern oxidation followed by Wittig olefination yielded enoate **4.42** (Scheme 12). Reduction of the ester group was accomplished with lithium aluminum hydride to give alcohol **4.43**. Zirconium-catalyzed carboalumination of the triple bond followed by trapping with iodine afforded vinyl iodide **4.44**.[13] The free alcohol was critical for this step as any protected variant of compound **4.43** resulted in very low reactivity. The desired vinyl stannane **4.45** was realized via lithium halogen exchange followed by trapping with tributyltin chloride. Formation of the vinyl lithium species was necessary because trapping the vinyl aluminum species with tributyltin chloride was unsuccessful. Additionally, direct carbostannylation of alkyne **4.43** was never effective.[14] We also attempted direct π-allyl coupling with the vinyl zinc species derived from carboalumination/transmetallation of alkyne **4.43** to no avail.[15]

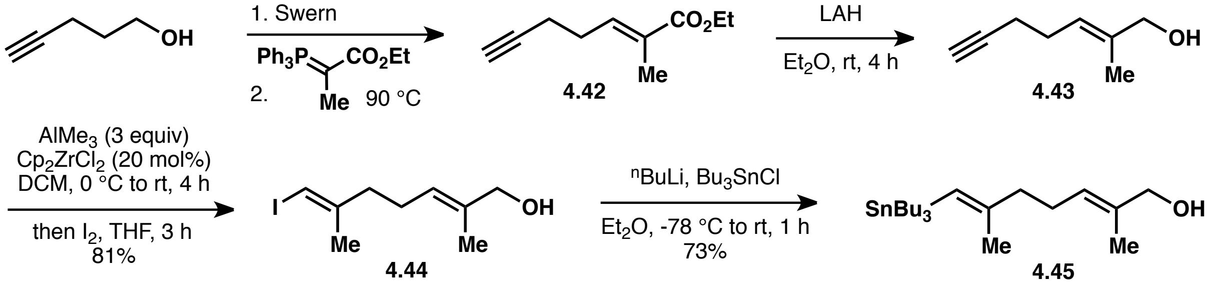

OH
1. Swern
2. Ph3P=C(Me)CO2Et 90 °C
CO2Et
Me
4.42
LAH
Et2O, rt, 4 h
OH
Me
4.43
AlMe3 (3 equiv)
Cp2ZrCl2 (20 mol%)
DCM, 0 °C to rt, 4 h
then I2, THF, 3 h
81%
I
Me
Me
OH
4.44
nBuLi, Bu3SnCl
Et2O, -78 °C to rt, 1 h
73%
SnBu3
Me
Me
OH
4.45

Scheme 12: Synthesis of vinyl stannane **4.45**

With both coupling partners in hand, the π-allyl Stille reaction was attempted to give coupled product **4.46** (Table 3).[16] Known conditions utilizing cesium fluoride and copper iodide as additives only returned the starting acetate (**4.41**) and the product of protodestannylation (**4.47**, entry 1).[17] Employing modified Fürstner conditions with copper (I) diphenylphosphinate (CuDPP) gave a similar result (entry 2)[18] as did conditions developed by Stoltz and Corey using lithium chloride and copper chloride as additives (entry 3).[19] These results indicated that the allylic acetate was unreactive toward oxidative addition, that the sulfide moiety was poisoning the catalyst, or that the vinyl stannane was too reactive and rapidly underwent protodestannylation. Initial screening of palladium sources and different allylic electrophiles (i.e., carbonates and chlorides) did not improve reactivity, so we turned to investigating vinyl stannane reactivity. Copper salts are commonly added to Stille reactions to facilitate transmetalation with the vinyl stannane. We hypothesized that the copper salts could be facilitating protodestannylation, thus destroying the coupling partner. Initially, switching from $Pd(PPh_3)_4$ to $Pd_2(dba)_3$ and lowering the temperature to 40 °C seemed to slow down the protodestannylation (entry 4), but removal of the copper salts finally resulted in productive formation of product **4.46** (entry 5).[20] This indicated that the addition of copper resulted in an overly reactive vinyl nucleophile, whose reactivity was unmatched with the less reactive allylic acetate partner. Additionally, this demonstrated that the sulfide group was compatible with this palladium-catalyzed process. The main side product in this reaction was compound **4.48**, resulting from a Grob-type fragmentation of the coupled product. With these conditions, we found that the PMB protecting group was unnecessary as the free hydroxyl group on vinyl stannane **4.45** was tolerated (entry 6). Many parameters were optimized in this reaction, but the key factor proved to be concentration. Increasing the concentration to 0.1 M (relative to **4.41**) resulted in an increase in yield to 44% (entry 7) while an even more concentrated reaction mixture (0.2 M) resulted in 62% yield (entry 8). It was not possible to suppress the formation of Grob-product **4.48** which formed in about 20% yield under these optimized conditions. Notably, the undesired "branched" product (coupling at the more substituted end of the π-allyl system) was never observed in this reaction.

Table 3: Pi-allyl Stille cross-coupling

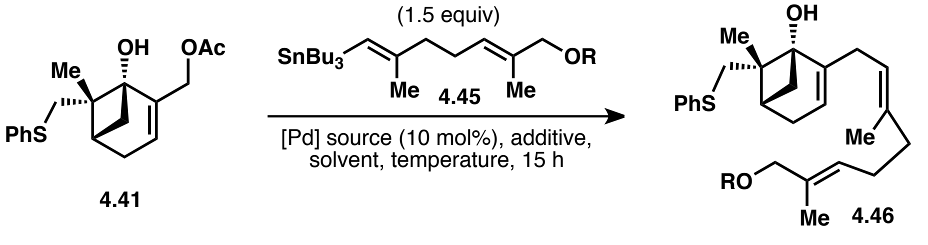

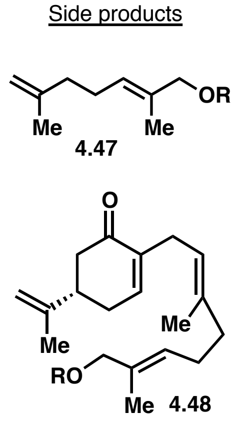

entry	R	[Pd] source	additive (equiv)	solvent (M)	temp	outcome (%yield)
1	PMB	$Pd(PPh_3)_4$	CsF (2), CuI (2)	DMF (0.05)	60 °C	**4.41** + **4.47**
2	PMB	$Pd(PPh_3)_4$	CuDPP (3)	DMF (0.05)	60 °C	**4.41** + **4.47**
3	PMB	$Pd(PPh_3)_4$	LiCl (6), CuCl (5)	DMSO (0.05)	60 °C	**4.41**+ **4.47**
4	PMB	$Pd_2(dba)_3$	LiCl (6), CuCl (5)	NMP (0.05)	40 °C	**4.41** + **4.45** + **4.47**
5	PMB	$Pd_2(dba)_3$	LiCl (6)	NMP (0.05)	40 °C	**4.46** (37%) + **4.48**
6	H	$Pd_2(dba)_3$	LiCl (6)	NMP (0.05)	40 °C	**4.46** (18%) + **4.48**
7	H	$Pd_2(dba)_3$	LiCl (6)	NMP (0.1)	40 °C	**4.46** (44%) + **4.48**
8	H	$Pd_2(dba)_3$	LiCl (6)	NMP (0.2)	40 °C	**4.46** (62%) + **4.48**

In order to advance compound **4.46** to the macrocyclization, we had to oxidize the phenyl sulfide group to the corresponding sulfone. At first inspection, this seemed like an easy transformation, but we were well aware of the propensity of the endocyclic double bond to engage electrophilic oxidants and promote rearrangement to a [2.2.1]bicycle (see Scheme 6). We examined many different oxidants on simplified sulfide **4.36** in order to find conditions that would avoid any rearrangement to compound **4.50** (Scheme 13). Some oxidants such as oxone provided good yields of the sulfoxide product, but resulted in substantial rearrangement to **4.50** upon attempt to further oxidize to the sulfone. We found the best oxidant for the formation of sulfone **4.49** to be a combination of ammonium heptamolybdate and hydrogen peroxide. This resulted in 85% of desired sulfone **4.49** and only 10% of rearranged product **4.50**. However, these optimized conditions did not translate well to coupled product **4.46**, resulting in yields around 30-40% of sulfone **4.51**. Unlike with the simplified system, this reaction resulted in a complex mixture and no clear side products could be identified.

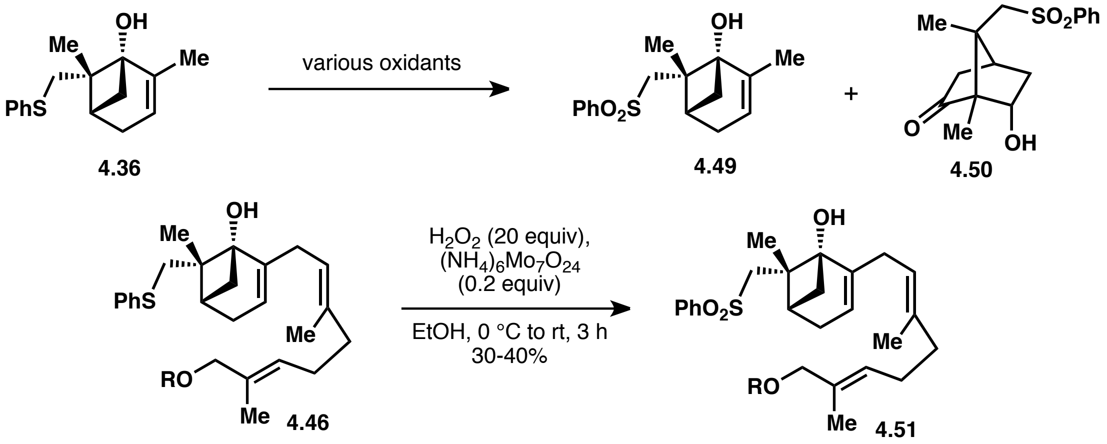

Scheme 13: Sulfide to sulfone oxidation

With sulfide oxidation resulting in low yields, installation of the sulfone moiety prior to π-allyl Stille coupling was explored. We had already shown that phenyl sulfone **4.49** could be obtained in 85% yield from sulfide **4.36** (Scheme 13), although some rearrangement still took place in this reaction. Since the nucleophilicity of the endocyclic double bond initiates the side reaction, we wondered whether the nucleophilicity could be suppressed by utilizing the inductively electron-withdrawing acetate group. Exposure of allylic acetate **4.41** to ammonium heptamolybdate and hydrogen peroxide resulted in clean oxidation to sulfone **4.52** without any trace of the [2.2.1]bicycle, thus validating this hypothesis.

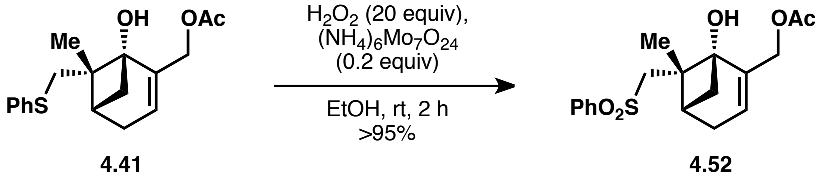

Scheme 14: Acetate group shuts down side reaction in sulfide oxidation

Sulfone-containing allylic acetate **4.52a** was subjected to the optimized Stille coupling conditions (Table 4, entry 1). This substrate gave similar results as the sulfide-containing allylic acetate **4.41**, except for a slightly lower yield of desired compound **4.51a** (55%) and a slightly higher yield of Grob fragmentation product **4.48** (25%). This change is a reflection of the slight increase in leaving group ability of the sulfone versus the sulfide. Grob fragmentation can be tempered if the tertiary hydroxy group of **4.52** is capped as the TMS ether (entry 2). This protection improved the yield of the desired compound to 61%, but fragmentation still occurred, indicating that deprotonation is not necessary to initiate this process. When the hydroxyl group was converted to the corresponding acetate (**4.52b**), Grob fragmentation was completely suppressed due to the electron-withdrawing carbonyl unit (entry 3). The product yield was increased to 77%.

Table 4: Pi-allyl Stille cross-coupling with sulfone-containing compounds

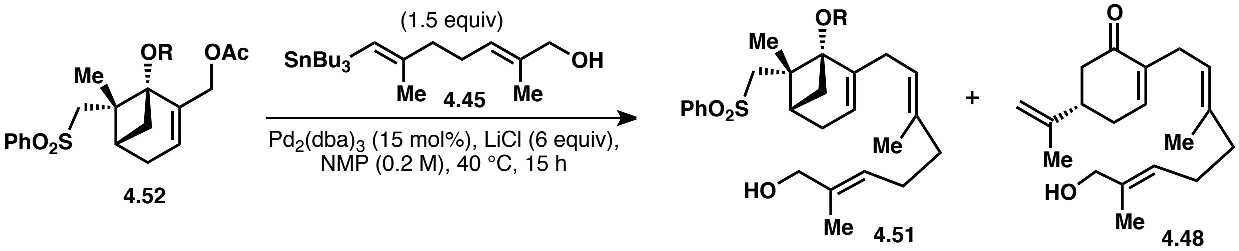

entry	R identity	4.51 yield	4.48 yield
1	H (**4.52a**)	55%	25%
2	TMS (**4.52c**)	61%	10%
3	Ac (**4.52b**)	77%	0%

To investigate the macrocyclization, conversion of primary alcohol **4.51** to the corresponding alkyl bromide **4.12** had to occur (Scheme 15). This was accomplished via a 2-step, 1-pot procedure involving mesylation followed by displacement with lithium bromide. From this compound, we expected that treatment with a strong base would deprotonate α to the sulfone and effect an intramolecular displacement to form the macrocycle. However, with compound **4.12a** (R=H), exposure to strong base deprotonated the acidic hydroxyl proton and resulted in rapid Grob fragmentation to yield compound **4.53**. This was somewhat expected since we knew Grob fragmentation was a competing pathway in these strained systems. Next, we sought to utilize compound **4.12b** capped as the acetate (R=Ac) for the macrocyclization. However, the acetate moiety has acidic α-protons and will spontaneously fragment to form ketene and the alkoxide under these conditions. As shown previously, the alkoxide rapidly fragments to form compound **4.53**.

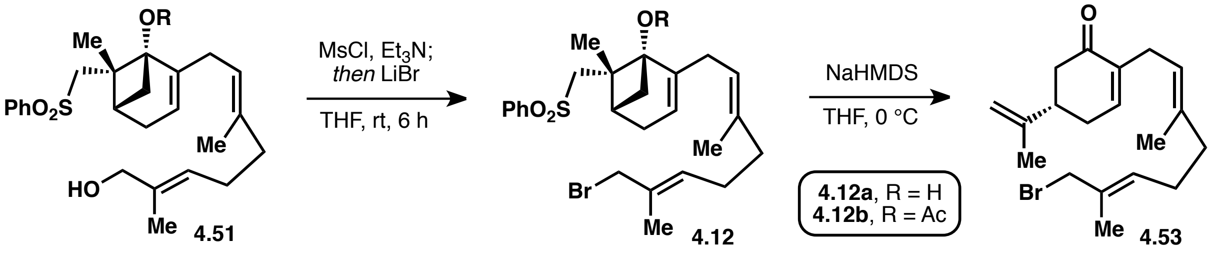

Scheme 15: Early macrocylization attempts resulted in Grob fragmentation

We were hopeful that the TMS protecting group would be better suited for the strongly basic conditions required for cyclization (Scheme 16). Conversion of the primary hydroxyl group to alkyl bromide **4.12c** was accomplished as before. We were excited to see that upon exposure to sodium bis(trimethylsilyl)amide, macrocycle **4.54** was obtained cleanly in 75% yield. No trace of Grob fragmentation was detected in this reaction. This result is the highest yielding macrocyclization on a substrate containing an sp^2 center at C8b. This validated our synthetic strategy of keeping the [3.1.1]bicycle intact throughout this first part of the synthesis in order to serve as a rigid scaffold for a templated macrocyclization. The TMS group could be readily cleaved under the action of an acidic Amberlyst resin and methanol. Acidic conditions were required because basic fluoride conditions led to Grob fragmentation.

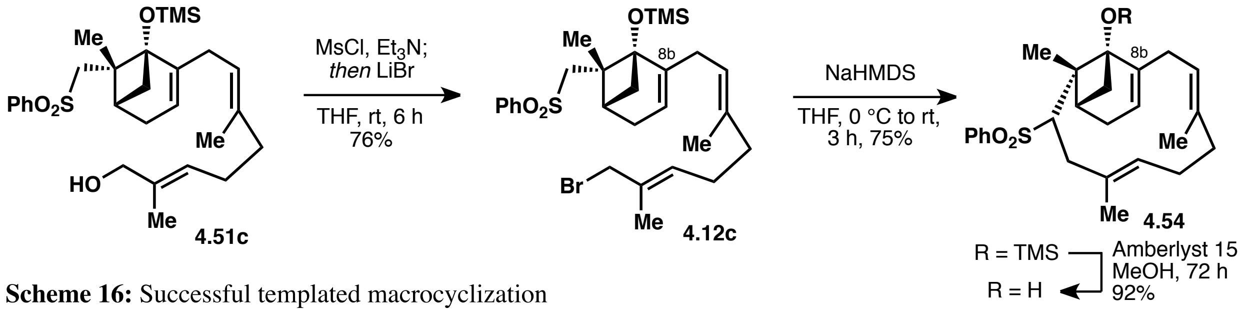

Scheme 16: Successful templated macrocyclization

4.5: Divergent Reactivity in the Rhodium-Catalyzed C–C Activation

The rigid [3.1.1]bicycle had served its purpose admirably in allowing the rapid construction of the carbocyclic framework present in the phomactin natural products. Now with the macrocycle intact, it was time to investigate the selective opening of the cyclobutanol. As shown previously, rhodium(I) catalysts are effective at achieving the desired C–C activation/protodemetalation on simple substrates. However, we were concerned about the complexity of cyclobutanol **4.55**. It was uncertain how the additional strain present in the macrocycle would affect the selectivity of the C–C bond cleavage or whether Grob fragmentation would predominate. We were also concerned about the presence of several double bonds in the substrate that could sequester rhodium or participate in unwanted side reactions. As far as we were aware, a substrate with this level of complexity had never been examined in the context of C–C activation.

We initiated our investigations by heating cyclobutanol **4.55** with $[Rh(cod)OH]_2$ to 40 °C in deuterated benzene so that the reaction could be monitored by NMR (Scheme 17). Although the desired product, cyclohexenone **4.15**, was not observed under these reaction conditions, we were excited to see the formation of unconjugated enone **4.56** as the major product after 6 hours. By observing this compound, we were assured that the rhodium catalyst was capable of effecting the desired C–C bond cleavage process on this complex substrate. The formation of unconjugated enone **4.56** was not surprising since similar double bond isomerizations have been observed in simple substrates (see Section 3.4).[21] In order to corroborate the proposed mechanism for this reaction, we added a small amount of D_2O in order to observe where deuterium would be incorporated in the product. When conducting this reaction, we observed 0% deuterium incorporation at the new methyl position and 90% deuterium incorporation at the position α to the ketone. This supports our proposed mechanism where alkyl-rhodium species **4.57** is first formed after rhodium initiates a β-carbon elimination. If protodemetalation took place at this intermediate, then we would expect substantial deuterium incorporation here. Since only hydrogen is observed, we suspect that this hydrogen atom is being transferred from another part of the molecule, likely, by a 1,3-Rh shift to give allylic rhodium species **4.58**. It is this species that undergoes protodemetalation at the α position to give product ***4.56-D*** with substantial deuterium incorporation.

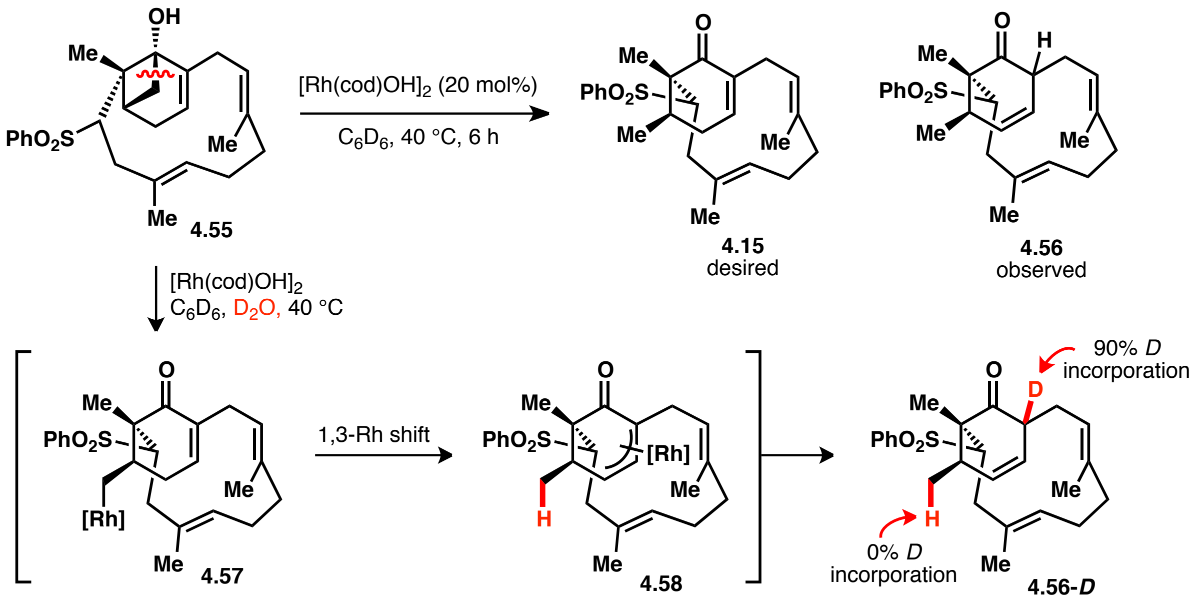
OH
Me
PhO2S
Me
Me
4.55
[Rh(cod)OH]2 (20 mol%)
C6D6, 40 °C, 6 h
O
Me
PhO2S
Me
Me
Me
4.15
desired
O
H
Me
PhO2S
Me
Me
Me
4.56
observed
[Rh(cod)OH]2
C6D6, D2O, 40 °C
O
Me
PhO2S
[Rh]
Me
Me
4.57
1,3-Rh shift
O
Me
PhO2S
[Rh]
H
Me
Me
4.58
90% D
incorporation
O
D
Me
PhO2S
H
0% D
incorporation
Me
Me
4.56-D

Scheme 17: Mechanistic information for the formation of unconjugated enone **4.56**

While we were confident that unconjugated enone **4.56** was forming in the reaction mixture, we were never able to isolate it. Upon exposure to air, unconjugated enone **4.56** oxidizes to give a 1:1 mixture of hydroxy enone **4.59** and enedione **4.60** (Scheme 18). This process, which generates oxidation at C8, was rapid on silica and other chromatographic supports (see Scheme 21 for mechanistic hypothesis).

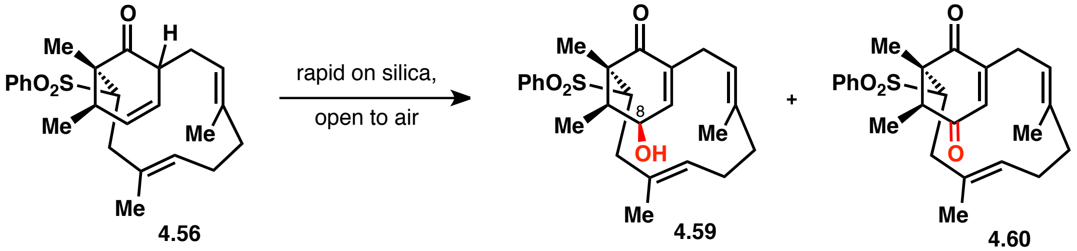
O
H
Me
PhO2S
Me
Me
Me
4.56
rapid on silica,
open to air
O
Me
PhO2S
Me
8
OH
Me
Me
4.59
+
O
Me
PhO2S
Me
O
Me
Me
4.60

Scheme 18: Formation of oxidation compounds upon attempted isolation of **4.56**

This oxidation process is not without precedent. Even within the C–C activation literature, Cramer and coworkers have reported a similar process when unconjugated enone **4.62** was generated (Scheme 19).[22] They report that subjecting allenyl cyclobutanol **4.61** to rhodium catalysis in the presence of a chiral phosphine ligand results in enantioselective C–C bond cleavage and insertion to give unconjugated enone **4.62**. However, this compound rapidly oxidizes to peroxy species **4.63** in the presence of air. Unconjugated enone could be isolated if purified in the presence of a radical inhibitor (although this procedure was never successful in our attempts to purify **4.56**). The Cramer group recognized that the addition of Cs_2CO_3 to their reaction conditions could promote double bond isomerization to directly give enone **4.64** in 99% yield.

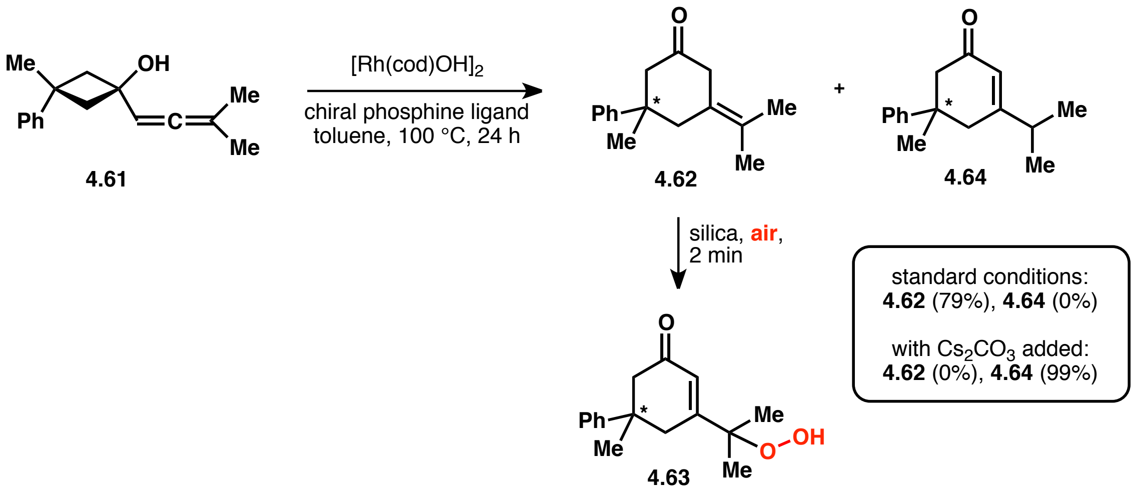

Scheme 19: Oxidation of unconjugated enones as shown by Cramer and coworkers

As described before in our system, heating cyclobutanol **4.55** at 40 °C with [Rh(cod)OH]$_2$ resulted in unconjugated enone **4.56** (Table X, entry 1). The addition of phosphine ligands such as *S*-BINAP did not aid the reaction and only resulted in a mixture of unidentifiable compounds (entry 2). We hoped that increasing the reaction temperature and duration could facilitate olefin isomerization into conjugation, but instead all we observed was a 1:1 mixture of oxidation products **4.59** and **4.60** (entry 3). These compounds originate from oxidation of unconjugated enone **4.56** from either trace oxygen dissolved in the solvent or from another substrate molecule acting as a sacrificial oxidant. Following precedent from the Cramer lab, Cs$_2$CO$_3$ was added in order to facilitate olefin isomerization and out-compete the oxidation process. However, this did not work as intended and only oxidation products **4.59** and **4.60** were formed (entry 4). To remove all oxygen from the system, rigorously degassed benzene was utilized (freeze-pump-thaw method for degassing). While this precaution seemed to diminish the amount of oxidation compounds that were formed, decomposition was also noted and no other products were detected in the reaction mixture (entry 5). We were pleased to find that in conjunction with Cs$_2$CO$_3$, increasing the temperature to 100 °C was an effective method for olefin isomerization. This procedure was able to generate conjugated enone **4.15** in 56% yield (entry 6). Continuing to optimize this reaction, methanol was found to be a far superior solvent, resulting in a superior 86% yield of the desired product (entry 7). Finally, lowering the rhodium dimer loading to 10 mol% did not have a deleterious effect on the reaction outcome (entry 8).

Table 5: C–C activation optimization to achieve cyclohexenone **4.15**

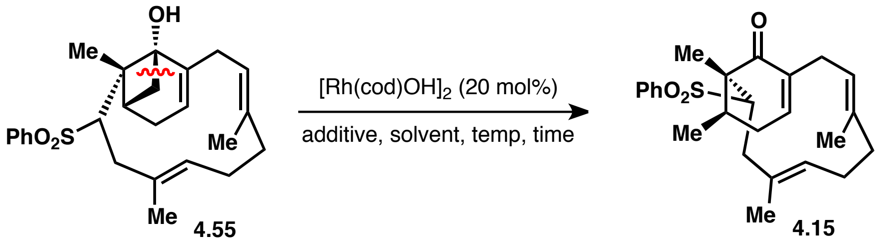
OH
Me
PhO$_2$S
Me
Me
4.55
[Rh(cod)OH]$_2$ (20 mol%)
additive, solvent, temp, time
O
Me
PhO$_2$S
Me
Me
Me
4.15

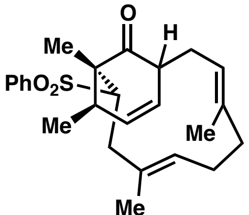
O
H
Me
PhO$_2$S
Me
Me
Me

4.56

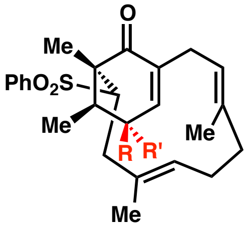
O
Me
PhO$_2$S
Me
R R'
Me
Me

4.59, R: -OH, R': -H
4.60, R,R': =O

entry	additive	solvent	temp	time	result
1	none	C_6D_6	40 °C	6 h	**4.56**
2	*S*-BINAP	C_6D_6	40 °C	6 h	multiple unknown pdts
3	none	C_6D_6	60 °C	18 h	**4.59,4.60** (1:1)
4	Cs_2CO_3	C_6D_6	40 °C	8 h	**4.59,4.60** (3:2)
5	Cs_2CO_3	C_6D_6 (degassed)	40 °C	8 h	**4.59,4.60**, decomp
6	Cs_2CO_3	PhMe	100 °C	2 h	**4.15** (56% yield)
7	none	MeOH	60 °C	18 h	**4.15** (86% yield)
8*	**none**	**MeOH**	**60 °C**	**18 h**	**4.15 (89% yield)**

*Reaction run with 10 mol% $[Rh(cod)OH]_2$

Switching the solvent from benzene to methanol allowed for clean conversion to cyclohexenone **4.15**. This could result from a more facile olefin isomerization or from a change in mechanism – for example, effecting protodemetalation prior to the 1,3-rhodium shift (see Section 4.6, Scheme 30 for an example). By conducting this reaction in deuterated methanol, we observed quantitative formation of unconjugated enone **4.56-*D*** with deuterium incorporation α to the ketone, indicating that the 1,3-rhodium shift occurs similarly to when the reaction was run in benzene (Scheme 20). Extended heating revealed the formation of cyclohexenone **4.15-*D*** with deuteration now at the γ position. From this information, we believe that methanol enables the reaction to be run at lower temperatures (compared to 100 °C in toluene) because the protic solvent facilitates olefin isomerization by increasing the enolic content of ketone **4.56** and by acting as a proton shuttle for tautomerization.

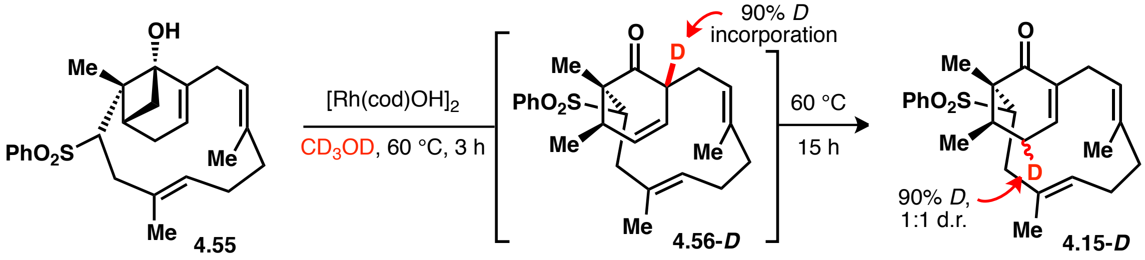
OH
Me
PhO$_2$S
Me
Me
4.55
[Rh(cod)OH]$_2$
CD$_3$OD, 60 °C, 3 h
90% *D* incorporation
O
D
Me
PhO$_2$S
Me
Me
Me
4.56-*D*
60 °C
15 h
O
Me
PhO$_2$S
Me
Me
D
90% *D*, 1:1 d.r.
Me
4.15-*D*

Scheme 20: Mechanistic information with CD_3OD as solvent

Although the formation of oxidation compounds **4.59** and **4.60** was frustrating during reaction optimization, we recognized that this facile oxidation could be beneficial since many of the phomactin natural products contain oxidation at C8, usually at the alcohol oxidation state (Figure 1). In our previous experiments, we found conditions that produce a mixture of compounds with alcohol and ketone oxidation states at C8 (~50% total yield). If conditions could be developed to selectively obtain the hydroxy enone **4.59**, then a divergent synthesis of many phomactin natural products (including phomactin B1 and phomactin I) could be achieved.

Figure 1: Phomactin natural products containing oxidation at the C8 position

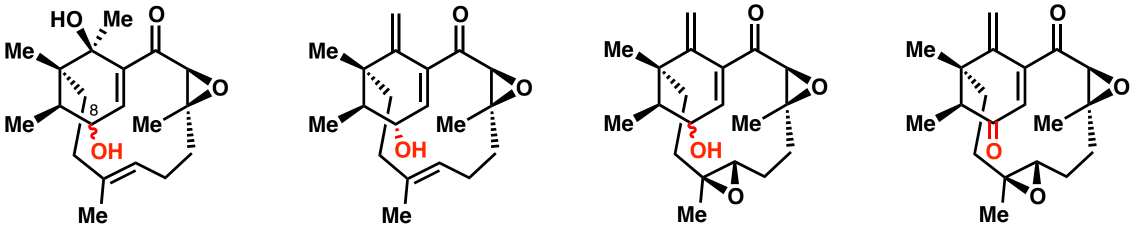

phomactin B (α-OH)
phomactin B1 (β-OH)

phomactin B2

phomactin I (β-OH)
epi-phomactin I (α-OH)

phomactin K

In order to optimize the oxidation reaction, a better understanding of the reaction mechanism was required (Scheme 21). We knew that air oxidation of unconjugated enone **4.56** led to a mixture of hydroxy enone **4.59** and enedione **4.60** and that hydroxy enone **4.59** was a stable compound and would not spontaneously oxidize to enedione **4.60**. Therefore, we hypothesized that both oxidation compounds might arise from the same peroxy species **4.67**. Utilizing conformational searching and molecular modeling, we observed that the α-proton of ketone **4.56** sits pseudo-axial, thus providing good overlap between the C–H σ-bond and both the C–O π* orbital and C–C π* orbital. This weakens the C–H bond and presumably allows for facile hydrogen atom abstraction. If this occurs, allylic radical **4.65** would result, with the major resonance form being allylic radical **4.66**. Radical combination with triplet oxygen would result in allylic peroxy species **4.67**.[23] This intermediate could either undergo in situ reduction to yield hydroxy enone **4.59** or rearrange to give enedione **4.60**.

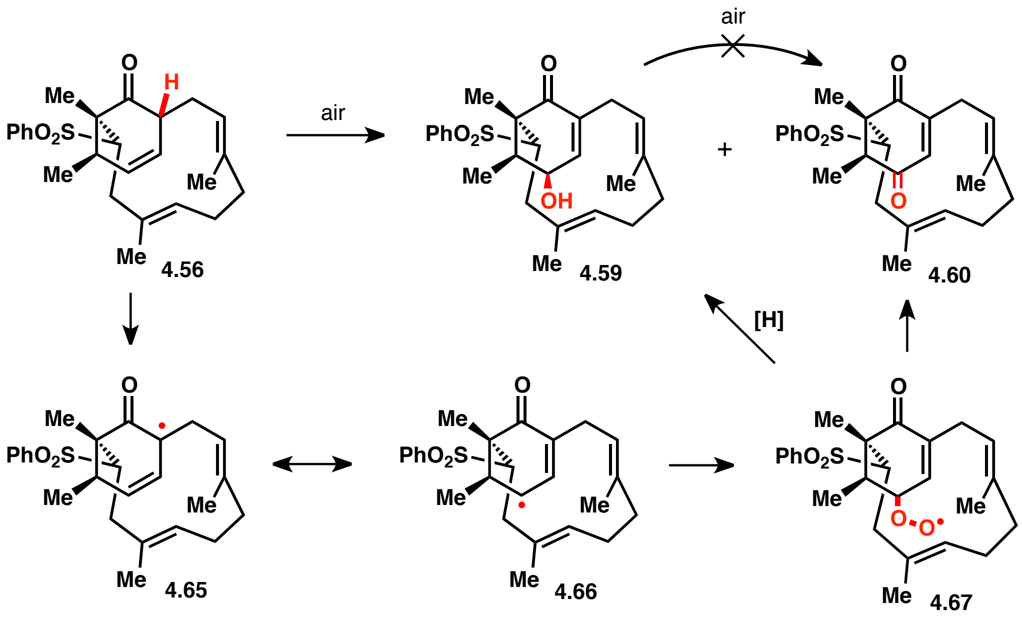

Scheme 21: Mechanistic hypothesis for the formation of oxidation products

To selectively obtain hydroxy enone **4.59**, we hypothesized that a suitable reductant could be added to unconjugated enone **4.56** during air oxidation. This would serve to reduce any peroxy species (such as **4.67**) directly to hydroxy enone **4.59** and not allow for rearrangement to enedione **4.60**. Putting this idea to practice, we first generated unconjugated enone **4.56** with previously reported conditions ([Rh(cod)OH]$_2$ in benzene, 40 °C, 6 hours). Upon opening the reaction flask to expose the mixture to air, the reductant and some silica were immediately added (Scheme 22). Although several reductants did not work (e.g., P(OPh)$_3$ gave no reaction and P(OMe)$_3$ gave conjugated enone **4.15**), dimethyl sulfide proved to be suitable for this process and yielded hydroxy enone **4.59** as the main product in 47% yield (along with 12% of conjugated cyclohexenone **4.15**).

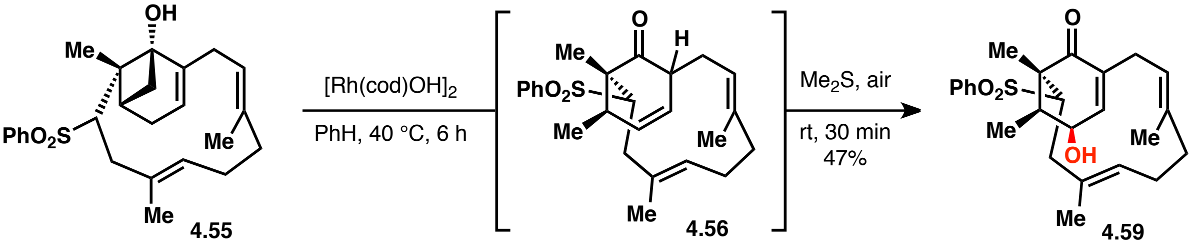
OH
Me
PhO2S
Me
Me
4.55
[Rh(cod)OH]2
PhH, 40 °C, 6 h
O
H
Me
PhO2S
Me
Me
Me
4.56
Me2S, air
rt, 30 min
47%
O
Me
PhO2S
Me
OH
Me
Me
4.59

Scheme 22: Selective formation of hydroxy enone **4.59**

We have developed a divergent set of conditions that enable the conversion of cyclobutanol **4.55** into cyclohexenone **4.15** or its hydroxylated variant, **4.59** (Scheme 23). These compounds could allow access to many phomactin natural products including phomactin A and phomactin B1. One challenge that remained was the selective oxygenation at the doubly allylic C3a position. All of the phomactin terpenoids possess a ketone oxidation level at this carbon.

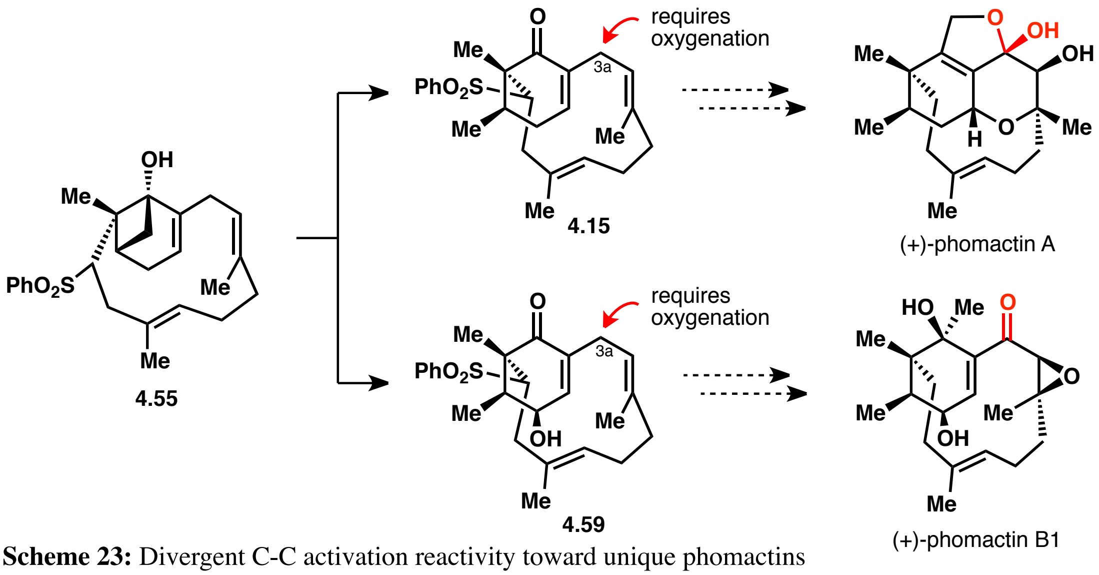
OH
Me
PhO2S
Me
Me
4.55
O
Me
PhO2S
Me
3a
requires oxygenation
Me
Me
4.15
O
OH
Me
OH
Me
H
O
Me
Me
(+)-phomactin A
O
Me
PhO2S
Me
3a
requires oxygenation
OH
Me
Me
4.59
HO
Me
O
Me
Me
O
Me
OH
Me
(+)-phomactin B1

Scheme 23: Divergent C-C activation reactivity toward unique phomactins

Even though there are seven allylic positions on compound **4.15**, we hypothesized C3a would be the most activated due to its doubly allylic nature. A wide array of allylic oxidation technologies were surveyed to allow access to either alcohol **4.68** or ketone **4.69** (Scheme 24).[24] However, after numerous attempts, we were unable to access either of the desired products (see

Section 4.10 for a detailed list of conditions and results). We recognized that the two π systems flanking C3a cannot be completely coplanar, resulting in less activation than would be anticipated from a doubly allylic position. However, one set of radical-generating conditions using benzoyl peroxide was effective at abstracting an appropriate hydrogen atom at C3a. But upon recombination with NCS, the resulting chlorine atom was placed at the tertiary position along with isomerization of the double bond to give chloride **4.71**. This isomerization might be driven by the formation of a tertiary radical and moving the double bond into conjugation, although full conjugative stabilization is not possible due to conformational restraints. Therefore, we hoped an $\mathrm{S_N}2$’ reaction could be feasible in order to establish the appropriate oxygenation at C3a, but all attempts at utilizing tertiary allylic chloride **4.71** in productive reactions resulted in decomposition to a mixture of products.

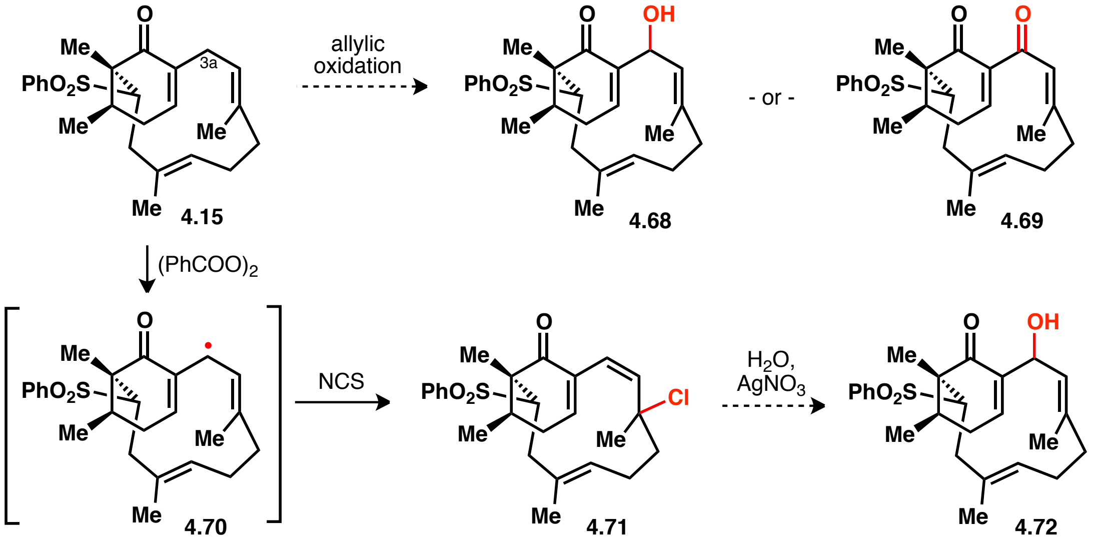

Scheme 24: Difficulty of selective allylic oxidation

4.6: Revised Fragment Coupling – Aldehyde Addition

Late-stage oxygenation at C3a had proven to be challenging. Therefore, we sought to revise our synthesis to install the necessary oxidation at an earlier stage. This would not be too difficult, as we had previously installed oxygenation at this position in the form of an allylic acetate (**4.52c,** Scheme 25). This served as a functional handle for π-allyl Stille cross-coupling, but replaced the C–O bond with a C–C bond. We hoped to revise this coupling strategy and start with a higher level of oxidation, namely, aldehyde **4.73**. By accomplishing a 1,2-addition with the vinyl lithium species derived from vinyl iodide **4.74**, oxygenation would be retained at C3a. This goal was realized by a postdoctoral researcher in our lab, Dr. Stanley Chang. He demonstrated that bis-allylic alcohol **4.75** could be synthesized in 68% yield as a 5:1 mixture of diastereomers. Luckily, the major diastereomer should possess the proper stereochemistry for late-stage directed epoxidation.

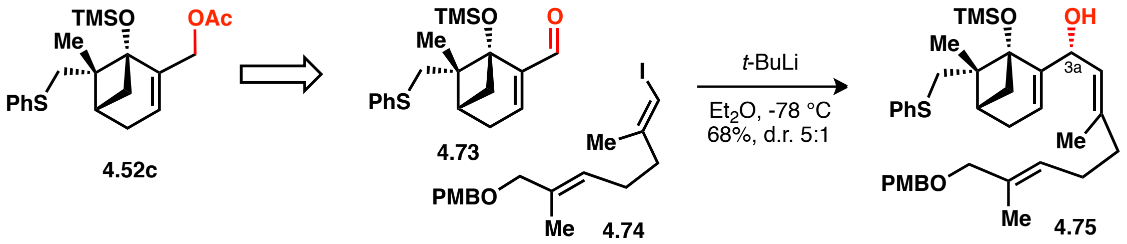

Scheme 25: 1,2-addition to aldehyde **4.73** to retain C3a oxidation

A rationalization for the observed stereochemical preference of 1,2-addition is not immediately obvious. We propose that the *s*-trans enal conformer (as depicted in **4.73**, Scheme 26) should be the reactive conformer because it provides a relatively unencumbered line of attack. The *s*-cis configuration would result in the nucleophile attacking through the bulky trimethylsilyl (TMS) group. With the *s*-trans conformation in mind, we propose that the TMS group shields the top face from attack, resulting in selective addition from the bottom and yielding major diastereomer **4.75**. The TMS group prefers to orient upwards because of the substituents at the neighboring quaternary carbon – the axial methylene phenyl sulfide occupies the bottom face of the molecule.

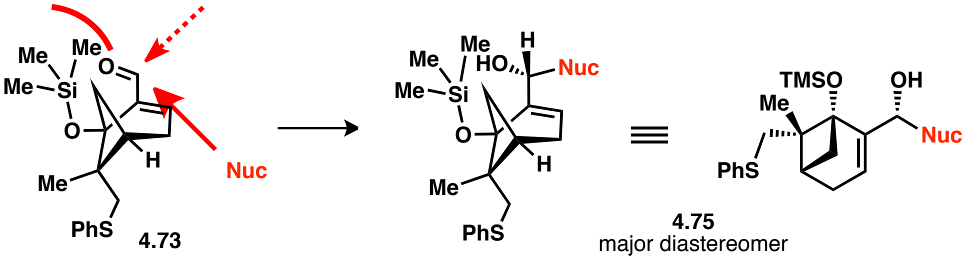

Scheme 26: Rationalization for diastereoselectivity in 1,2-addition

From coupled product **4.75**, Dr. Chang was able to construct the macrocycle through a sulfone alkylation protocol, similarly to the previous route (see Section 4.4). Protection of bis-allylic alcohol **4.75** as the TBS ether followed by sulfide oxidation with ammonium orthomolybdate and hydrogen peroxide yielded sulfone **4.76** (Scheme 27). Cleavage of the *para*-methoxybenzyl group with 2,3-dichloro-5,6-dicyanobenzoquinone (DDQ) and subsequent bromination of the resultant hydroxyl group gave rise to allylic bromide **4.77**. This compound was subjected to sodium bis(trimethylsilyl)amide to effect the intramolecular alkylation, providing macrocycle **4.78** in an excellent 91% yield. This macrocyclization reaction is even higher yielding than that described previously with substrate **4.12c** (see Scheme 16), possibly arising from the Thorpe-Ingold-like effect by the additional sterically-encumbering OTBS group. The efficiency of this macrocyclization provides additional support for our [3.1.1]bicyclic scaffold cyclization strategy.

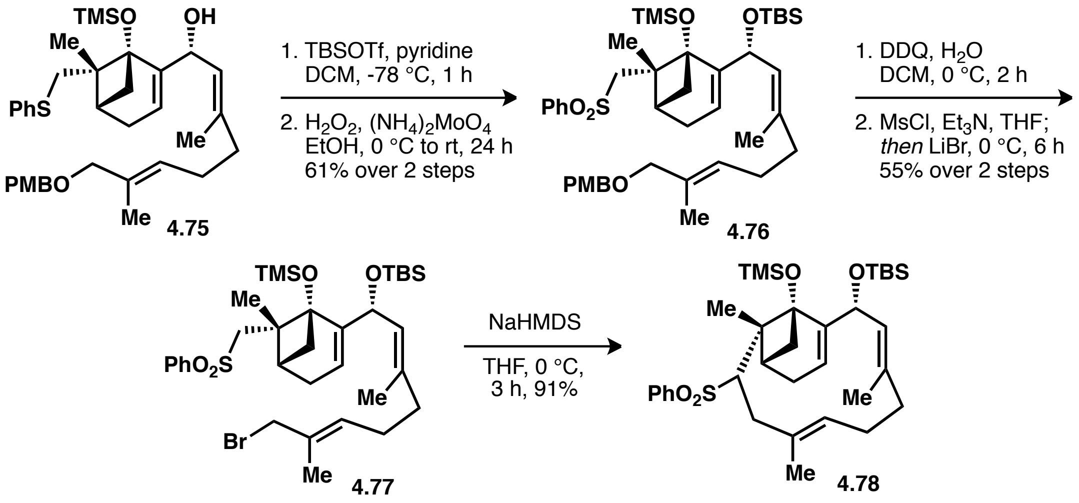
TMSO
OH
Me
PhS
Me
PMBO
Me
4.75
1. TBSOTf, pyridine
DCM, -78 °C, 1 h
2. H_2O_2, $(NH_4)_2MoO_4$
EtOH, 0 °C to rt, 24 h
61% over 2 steps
TMSO
OTBS
Me
PhO_2S
Me
PMBO
Me
4.76
1. DDQ, H_2O
DCM, 0 °C, 2 h
2. MsCl, Et_3N, THF;
then LiBr, 0 °C, 6 h
55% over 2 steps
TMSO
OTBS
Me
PhO_2S
Me
Br
Me
4.77
NaHMDS
THF, 0 °C,
3 h, 91%
TMSO
OTBS
Me
PhO_2S
Me
Me
4.78

Scheme 27: Elaboration of the coupled product to the macrocycle

Removal of the TMS group was not as straightforward as before. Unsurprisingly, treatment with basic fluoride conditions served to remove the TMS group from compound **4.78**, but also initiated a Grob fragmentation to give enone **4.79** (Scheme 28). Previously, we utilized acidic conditions to avoid this problem, but with the addition of the bis-allylic –OTBS group, ionization occurred under acidic conditions, leading to isomerized diene **4.80**.

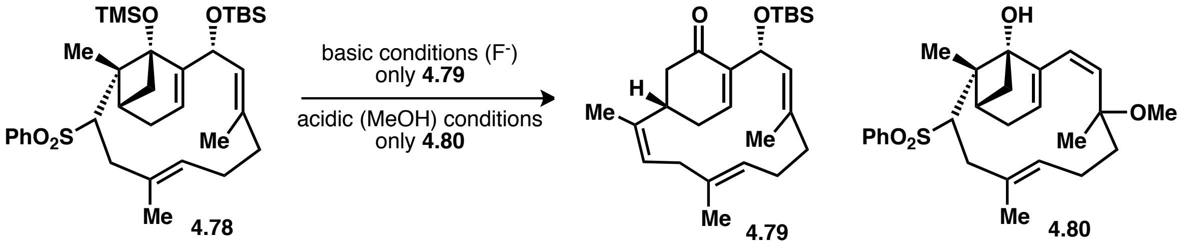
TMSO
OTBS
Me
PhO_2S
Me
Me
4.78
basic conditions (F^-)
only 4.79
acidic (MeOH) conditions
only 4.80
O
OTBS
H
Me
Me
Me
4.79
OH
Me
OMe
PhO_2S
Me
Me
4.80

Scheme 28: Challenges with TMS ether cleavage

We could circumvent this reactivity challenge by utilizing tris(dimethylamino)-sulfonium difluorotrimethylsilicate (TASF) buffered with acetic acid. Under these conditions, neither Grob fragmentation nor –OTBS ionization occurred, although it was difficult to achieve perfect selectivity for the cleavage of a single silyl group (Scheme 29). Utilizing 2 equivalents of TASF, 25 equivalents of acetic acid, and stirring at room temperature for 3 days afforded good conversion to cyclobutanol **4.81** (60% yield) along with some diol **4.82** (36% yield). This selectivity could be modulated by increasing the TASF equivalents and the reaction temperature. This resulted in 26% yield of cyclobutanol **4.81** and 68% yield of diol **4.82**.

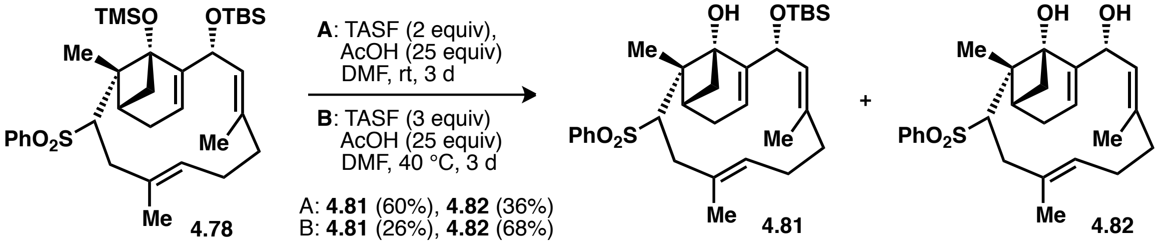
TMSO
OTBS
Me
PhO_2S
Me
Me
4.78
A: TASF (2 equiv),
AcOH (25 equiv)
DMF, rt, 3 d
B: TASF (3 equiv)
AcOH (25 equiv)
DMF, 40 °C, 3 d
A: 4.81 (60%), 4.82 (36%)
B: 4.81 (26%), 4.82 (68%)
OH
OTBS
Me
PhO_2S
Me
Me
4.81
+
OH
OH
Me
PhO_2S
Me
Me
4.82

Scheme 29: Successful silyl group cleavage with TASF buffered with AcOH

With cyclobutanol **4.81** in hand, we turned to investigating the C–C activation reaction, uncertain if the additional TBS ether would affect the desired reactivity. Upon subjecting cyclobutanol **4.81** to [Rh(cod)OH]$_2$ in benzene at 60 °C, we were disheartened to observe the formation of triene **4.84** as the major product (Scheme 30). Presumably, β-carbon elimination and 1,3-Rh shift occur as expected to give allyl rhodium species **4.83**, but instead of protodemetalation, β-silyloxy elimination occurs rapidly to give triene **4.84**. Luckily, once again methanol proved to be a superior solvent for the desired transformation. Simply switching benzene for methanol produced cyclohexenone **4.86** in a 46% yield. A screen of other protic solvents did not result in yields above 46%. Interestingly, in direct contrast to the previous route (see Scheme 20), deuterium incorporation was observed at the newly formed methyl position and not at the γ position of enone ***4.86-D***. This observation implies that alkyl rhodium species **4.85** undergoes protodemetalation instead of a 1,3-Rh shift in the presence of methanol. This could be due to the additional steric bulk of the TBS ether moiety that sits in close proximity to the position where the rhodium complex would migrate, thus suppressing the 1,3-Rh shift. Protodemetalation, accelerated by the protic solvent, outcompetes the rhodium shift and the product of β-silyloxy elimination is not observed.

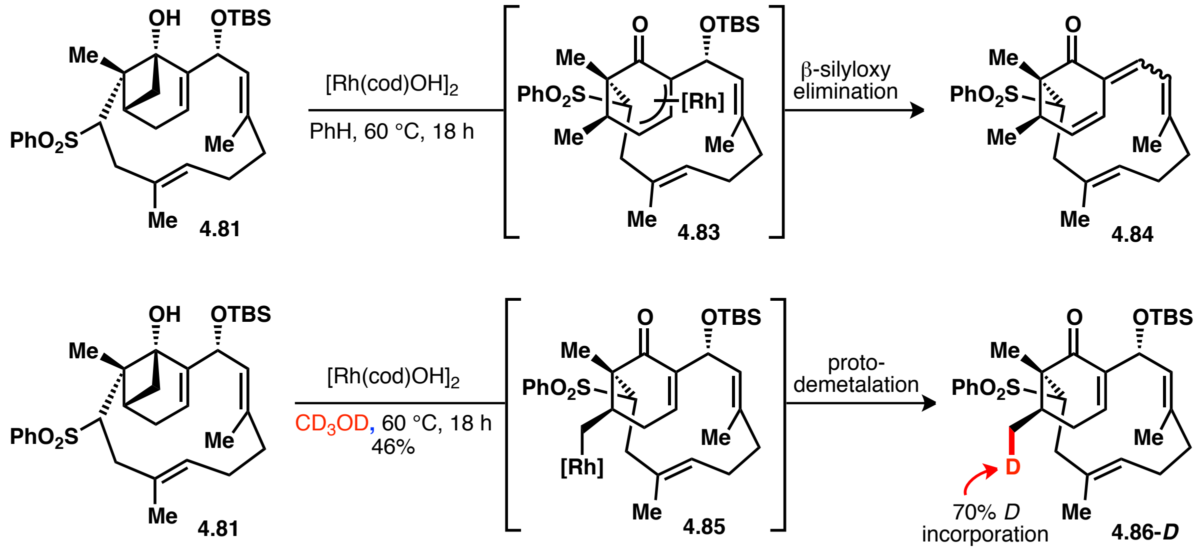
OH
OTBS
Me
PhO2S
Me
Me
4.81
[Rh(cod)OH]2
PhH, 60 °C, 18 h
O
OTBS
Me
PhO2S
Me
[Rh]
Me
Me
4.83
β-silyloxy elimination
O
Me
PhO2S
Me
Me
Me
4.84
OH
OTBS
Me
PhO2S
Me
Me
4.81
[Rh(cod)OH]2
CD3OD, 60 °C, 18 h
46%
O
OTBS
Me
PhO2S
[Rh]
Me
Me
4.85
proto-demetalation
O
OTBS
Me
PhO2S
D
Me
70% D incorporation
Me
4.86-D

Scheme 30: Solvent effects on rhodium-catalyzed C–C activation

Additionally, diol **4.82** was amenable to the rhodium-catalyzed C–C bond cleavage process, producing cyclohexenone **4.87** in 49% yield (Scheme 31).

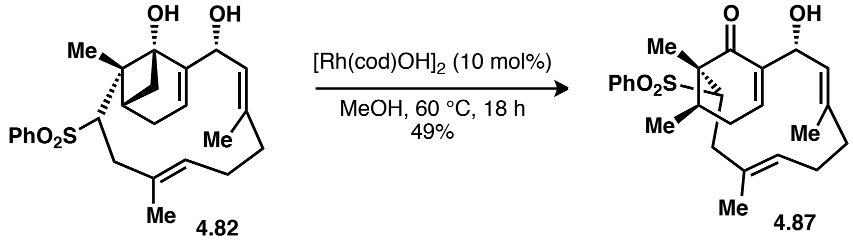
OH
OH
Me
PhO2S
Me
Me
4.82
[Rh(cod)OH]2 (10 mol%)
MeOH, 60 °C, 18 h
49%
O
OH
Me
PhO2S
Me
Me
Me
4.87

Scheme 31: C–C activation with diol **4.82**

4.7: Late-stage Functionalization and Challenges

In order to elaborate these late-stage compounds to any of the phomactin natural products, several functional group manipulations had to occur. We were confident that most would be trivial (such as alcohol oxidation and epoxidation) given the literature precedent. We demonstrated that directed epoxidation was indeed viable by converting allylic alcohol **4.87** to the desired diastereomer of epoxide **4.88** (Scheme 32).

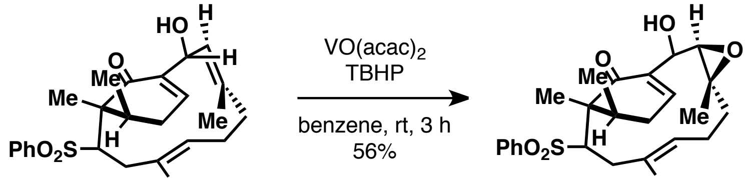

4.87 **4.88**

Scheme 32: Directed epoxidation with VO(acac)$_2$

The two challenging operations that had to be completed were the removal of the sulfone moiety and the addition of a one-carbon unit into the carbonyl group. We first sought to investigate reductive cleavage of the sulfone group, although we recognized that the presence of a readily reduced enone moiety could be problematic. Conditions employing sodium/mercury amalgam or magnesium metal in ethanol did not provide any reactivity while samarium iodide only resulted in 1,4-reduction of the enone system. The only conditions that were found to cleave the alkyl sulfone moiety from **4.87** were Birch-type conditions involving sodium, ammonia, and isopropanol (Scheme 33). As expected, one of the products formed was diol **4.89**, the product of sulfone cleavage and global reduction. However, this product was formed only in 20% yield. The major component of the reaction mixture was unstable and hard to purify, but we eventually determined it to be cyclopropanol **4.90**, formed from carbanion addition into the carbonyl group. Heating the crude mixture of compounds **4.89** and **4.90** with sodium methoxide induced cyclopropanol cleavage to form enone **4.91** (diol **4.89** was unaffected in this second step). In a way, the fortuitously formed cyclopropanol serves as an in situ "protecting group" for the enone moiety, preventing further reduction under the harsh dissolving metal conditions. After successful removal of the sulfone group, the cyclopropanol can be opened to reinstate the enone system. The corresponding TBS ether-containing sulfone **4.86** was also amenable to this reductive cleavage/cyclopropanol rearrangement protocol.

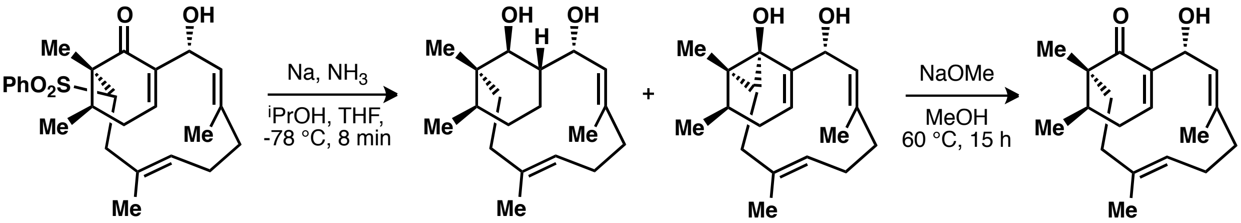

4.87 **4.89** (20%) **4.90** (60%) **4.91**

Scheme 33: Reductive cleavage of the sulfone group, rearrangment of resultant cyclopropanol

Reduced compound **4.92** could serve as a useful intermediate toward the synthesis of phomactin D (Scheme 34). If the free hydroxyl group can be converted to a xanthate or other radical precursor, then generation of the secondary carbon radical and trapping with *tert*-butyl isocyanide would generate a cyano group or a formyl group upon reduction and hydrolysis.[25] A few attempts at converting secondary alcohol **4.92** into xanthate **4.93** were investigated, but only starting material was recovered. The secondary hydroxyl group appears to be quite sterically congested, so more forcing conditions might be necessary.

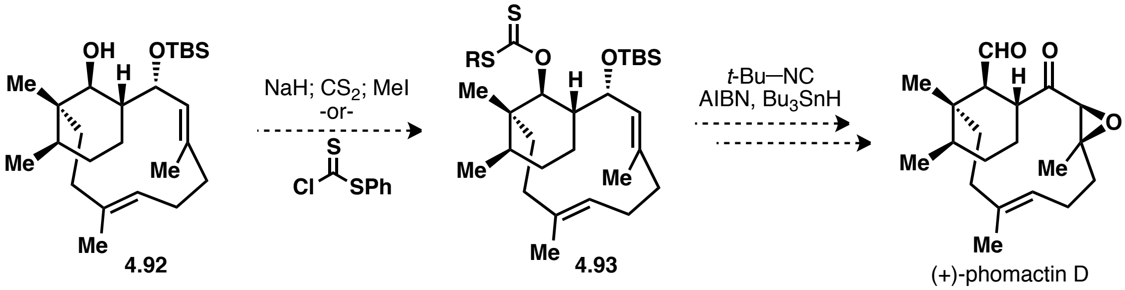

Scheme 34: Plans to elaborate reduced compound **4.92** to phomactin D via radical formylation

To construct the phomactin natural products, the remaining task was to conduct a 1,2-addition of a one-carbon nucleophile into enone **4.91**. Although seemingly trivial, this proved to be a major challenge. Several nucleophiles resulted in no reaction, and even methyl lithium provided only 1,4-addition product **4.94** (Scheme 35). We knew that the carbonyl group of enone **4.91** was sterically hindered, being next to a quaternary center. Molecular modeling and conformational searching provided an explanation for why direct addition was so challenging.[26] The macrocyclic "strap" sits directly underneath the cyclohexenone ring system, completely blocking the approach of any nucleophile from this face. Moreover, the presence of the macrocyclic ring confines the cyclohexenone in the conformation shown below, locking the β-methyl group in an axial position. This severely obstructs the Bürgi-Dunitz approach of a nucleophile from the top face.

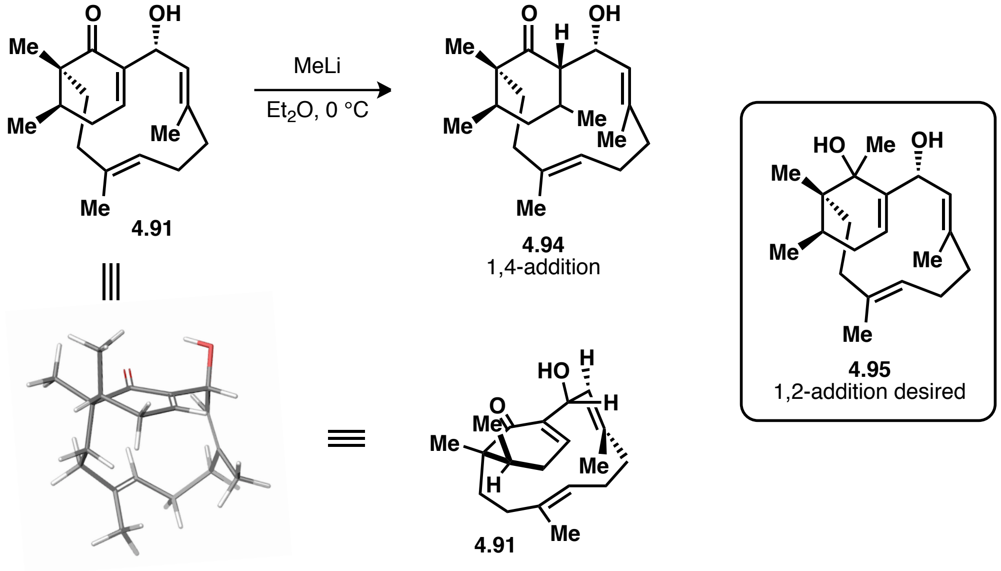

Scheme 35: Methyl lithium reactivity with enone **4.91** and conformational analysis

We investigated a wide variety of conditions to accomplish the 1,2-addition of a methyl nucleophile to provide alcohol **4.96** (Scheme 36). Conditions included the addition of lanthanide salt additives[27] or the generation of magnesiate or aluminate species. Unfortunately, these did not provide the desired 1,2-adduct. We next screened a range of methylenation conditions to give diene **4.97**. Standard Wittig conditions only returned starting material as did utilization of the Nysted reagent.[28] The Lombardo reagent[29] or its derivatives[30] gave a complex mixture of products, most of which were derived from an ionization/elimination of the bis-allylic hydroxyl group. In fact, we have been unsuccessful at adding any intermolecular nucleophile into enone **4.87** or **4.91**, even cyanide or hydroxylamine.

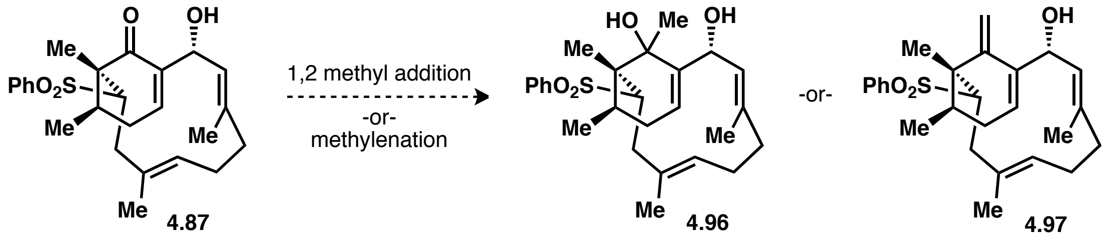

Scheme 36: Targeted 1,2-addition or methylenation

We recognized that unfavorable steric effects were resulting in a lack of reactivity at the carbonyl moiety. Similar issues arose in the Hsung group's synthesis of phomactin A and careful conformational modifications had to be considered.[31] We sought to lessen the steric congestion in our system by eliminating the axial β-methyl group. To do this, we reconsidered the cyclobutanol opening step. Instead of utilizing rhodium, we hypothesized that palladium could accomplish the C–C activation step to afford alkyl palladium species **4.98** (Scheme 37). Subsequent β-hydride elimination would produce exomethylene **4.99**.[32] By turning the methyl group into a methylene, the top face of the cyclohexenone would be open for nucleophilic addition. Unfortunately, although this palladium-catalyzed reaction worked on simplified substrates, we were never able to access the desired exomethylene compound (**4.99**); only complex mixtures of decomposition products were obtained.

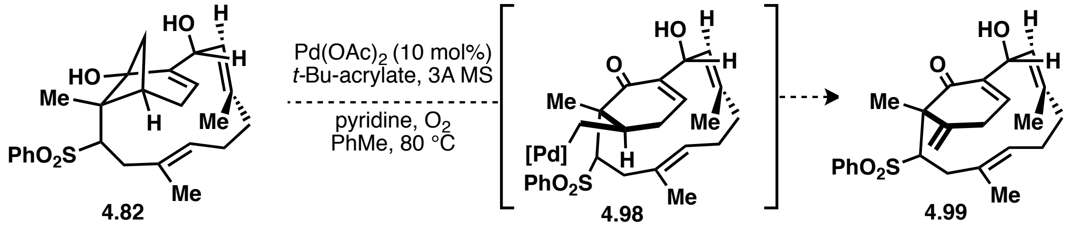

Scheme 37: Attempted palladium-catalyzed C–C bond cleavage/hydride elimination

Being unable to lessen the steric congestion, we next sought to utilize the hydroxyl group for a tethered intramolecular delivery of a carbon nucleophile. By examining the conformational model (see Scheme 35), it appeared that the hydroxyl group was ideally situated to direct addition into the carbonyl from the top face and away from the steric hindrance of the axial methyl group. We first synthesized compounds that would enable the generation of a stabilized carbanion – ester **4.100** and phosphonate **4.101** (Scheme 38). However, treating either of these compounds with a strong base resulted in complete decomposition, even at –78 °C.

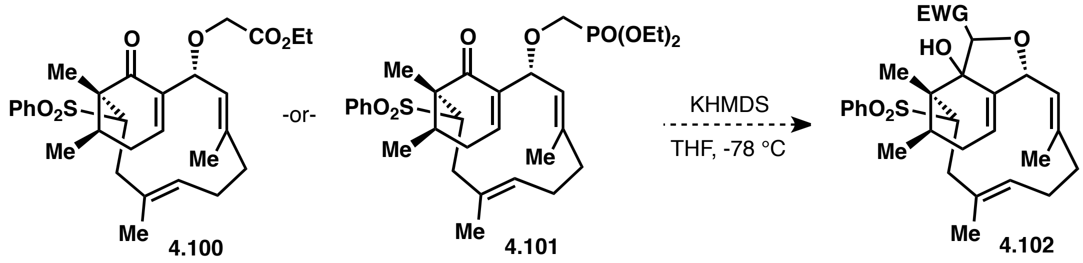

Scheme 38: Attempted stabilized-carbanion intramolecular delivery

The (bromomethyl)dimethylsilyl ether tether has been extensively studied for radical cyclizations with olefins.[33] It has been less thoroughly studied with respect to anionic additions into ketones, but several examples have been reported.[34] Nonetheless, we synthesized (bromomethyl)dimethylsilyl ether **4.103** from alcohol **4.91** to examine its reactivity (Scheme 39). Exposure to *tert*-butyl lithium primarily led to protodebromination while treatment with samarium iodide mostly led to 1,4-reduction of the enone system. Although the desired product **4.105** was not formed, it was encouraging to see the product of protodebromination as this indicated that the carbanion was being formed under the action of *tert*-butyl lithium. We thought that we could bias the substrate towards cyclization if we incorporated larger R groups onto the silyl tether. These bulky groups should prefer to orient away from the cyclohexenone, thus placing the reactive carbanion in close proximity to the carbonyl group. Unfortunately, subjecting (iodomethyl)diisopropylsilyl ether **4.104** to *tert*-butyl lithium only resulted in protodeiodination and not the desired product **4.105.** Although this strategy has not yet proved effective, we believe that additional tuning of the silyl R groups as well as the halide identity could provide a successful route to incorporate the final carbon atom into the phomactin skeleton.

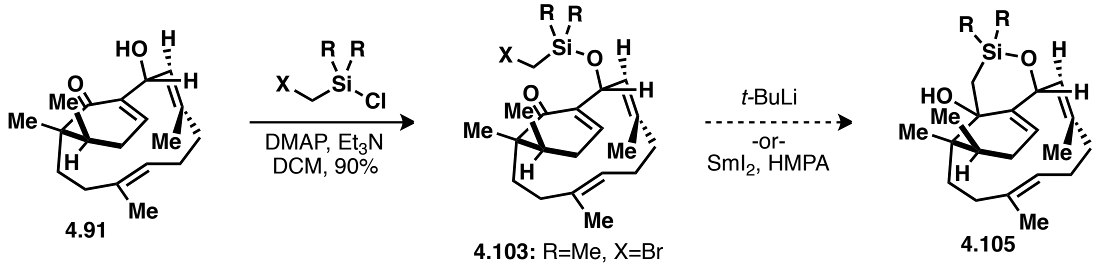

Scheme 39: Proposed silyl-tethered nucleophilic delivery

If we are successful with the addition of the silyl-tethered carbanion, different functionalizations of the carbon-silicon bond will provide ideal late-stage diversification for the total synthesis of several phomactin natural products (Scheme 40). Peterson elimination would provide diene **4.107** which would be a single oxidation away from newly isolated phomactin **4.108**. Alternatively, cleavage of the Si–O bond and oxidation could provide silane **4.109**. Tamao-Fleming oxidation followed by tandem allylic transposition/epoxide opening[35] would provide (+)-phomactin A. This and other strategies are currently ongoing in the Sarpong lab.

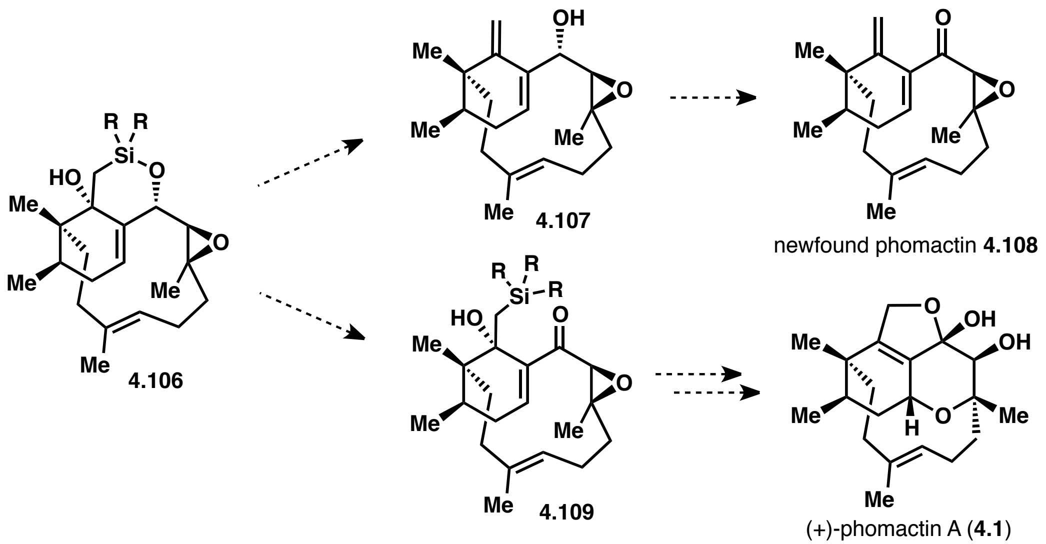

Scheme 40: Versatility of silyl tether for divergent synthesis

4.8: Conclusion and Outlook

We have designed an enantiospecific synthesis of the phomactin skeleton, showcasing the reactivity of cyclobutanol-containing molecules. Fine-tuning the electronics of these structures was critical to avoid unwanted rearrangements or fragmentations. We demonstrated the effectiveness of a hydroxyl-directed C–H silylation as well as a selenium dioxide-mediated allylic oxidation for selective functionalization early on in the synthesis. Both π-allyl Stille coupling and 1,2-addition were effective methods for joining the cyclohexyl and linear fragments together – the aldehyde addition method proving superior due to the additional level of oxidation. Aided by the rigid [3.1.1]bicyclic framework, macrocyclization proved to be facile, providing excellent yields with two distinct substrates.

We demonstrated the utility of rhodium-catalyzed C–C activation methodologies in a complex molecule setting in order to selectively open the cyclobutanol and establish the C6 and C7 *syn* methyl groups. We showed mechanistically that the products of these reactions can depend on subtle changes to the substrate as well as the solvent. Finally, sulfone removal was accomplished under Birch-type conditions. Cyclopropanol formation and rearrangement protected the enone system from over-reduction. This resulting compound required the 1,2-addition of a methyl nucleophile to access a range of phomactin natural products. Although seemingly trivial, this proved to be a major challenge – one for which an elegant solution has not yet been discovered. Continued investigations, along with an alternative strategy to install the problematic methyl group at an earlier stage in the synthesis, are well underway.

4.9: Experimental Contributors

Stanley Chang (postdoc, Sarpong group) was responsible for developing the aldehyde addition route and was the first to conduct all the chemistry presented in Section 4.6. The remainder of the work presented in this chapter was conducted by Paul R. Leger.

4.10: Experimental Methods

All reactions were run in flame-dried round-bottom flasks or vials under a nitrogen atmosphere. Reactions were monitored by thin layer chromatography (TLC) on Silicycle Siliaplate^{TM} glass backed TLC plates (250 µm thickness, 60 Å porosity, F- 254 indicator) and visualized using UV irradiation and *para*-anisaldehyde stain. For heated reactions, the temperature was monitored using an IKA® temperature control. Dry acetonitrile, diethyl ether, tetrahydrofuran (THF), triethylamine (TEA), benzene, toluene, and methanol were obtained by passing these previously degassed solvents through activated alumina columns. Dichloromethane (DCM) was distilled over calcium hydride before use. Volatile solvents were removed under reduced pressure on a rotary evaporator. All flash chromatography was conducted using Sorbent Technologies 60 Å, 230x400 mesh silica gel (40-63 µm). ^{1}H NMR and ^{13}C NMR spectra were acquired using Bruker 300, 400, 500, and 600 MHz (75, 100, 125, and 150 MHz for ^{13}C NMR) spectrometers in $CDCl_3$. Chemical shifts are measured relative to the shift of the residual solvent (^{1}H NMR - $CDCl_3$ $\delta = 7.26$, C_6D $\delta = 7.16$, MeOD $\delta = 3.31$; ^{13}C NMR $CDCl_3$ $\delta = 77.16$, C_6D $\delta = 128.06$, MeOD $\delta = 49.00$). NMR data are reported as follows: chemical shift (multiplicity, coupling constant, integration). Splitting is reported with the following symbols: s = singlet, bs = broad singlet, d = doublet, t = triplet, q = quartet, m = multiplet. IR spectra were acquired on a Bruker Alpha FTIR (neat) unless otherwise specified. Spectra are reported in frequency of absorption in cm^{-1}. Only selected resonances are reported. High-resolution mass spectra (HRMS) were performed by the mass spectral facility at the University of California, Berkeley.

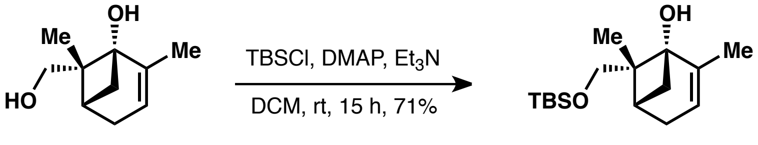

4.16 **4.23**

TBS ether **4.23**

A 25 mL flask was charged with diol[36] **4.16** (197 mg, 1.17 mmol), DCM (5 mL), triethylamine (0.49 mL, 3.51 mmol), 4-(dimethylamino)pyridine (14 mg, 0.12 mmol), and *tert*-butyldimethylsilyl chloride (212 mg, 1.41 mmol). The solution was stirred for 15 h, then diluted with DCM (10 mL) and washed with HCl (1 N, 3 x 10 mL) and brine (1 x 10 mL). The organics were dried over magnesium sulfate, filtered, concentrated, and purified by column chromatography (SiO_2, 10% EtOAc/ hexane) to yield TBS ether **4.23** (234 mg, 71%) as a colorless oil. $[\alpha]_D^{22}$ (*c* 0.0074, $CHCl_3$) = −26.5; ^{1}H NMR (500 MHz, $CDCl_3$) δ 5.23 (t, *J* = 1.7 Hz, 1H), 3.70 (d, *J* = 9.1 Hz, 1H), 3.26 (d, *J* = 9.1 Hz, 1H), 2.27 (dd, *J* = 8.5, 6.8 Hz, 1H), 2.18 – 2.08 (m, 2H), 2.04 (dq, *J* = 18.2, 2.4, 2.4 Hz, 1H), 1.78 (d, *J* = 2.1 Hz, 3H), 1.57 (d, *J* = 8.2 Hz, 1H), 1.29 (s, 3H), 0.87 (s, 9H), 0.01 (d, *J* = 5.3 Hz, 6H); ^{13}C NMR (126 MHz, $CDCl_3$) δ 146.33, 116.94, 65.97, 46.09, 38.84, 34.63, 31.11, 26.07, 18.35, 17.64, 17.53, -5.44, -5.49; IR (neat) 3459, 2928, 2856, 1471, 1070, 864, 772 cm^{-1}; HRMS (EI) calculated for $[C_{16}H_{30}O_2Si]^+$ $[M]^+$: *m/z* 282.2015, found 282.2012.

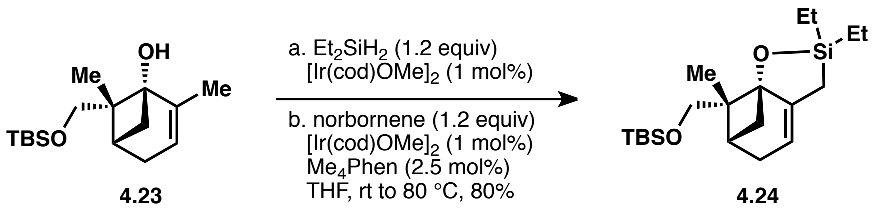
OH
Me
Me
TBSO
4.23
a. Et2SiH2 (1.2 equiv)
[Ir(cod)OMe]2 (1 mol%)
b. norbornene (1.2 equiv)
[Ir(cod)OMe]2 (1 mol%)
Me4Phen (2.5 mol%)
THF, rt to 80 °C, 80%
Et
Et
O
Si
Me
TBSO
4.24

Oxasilolane **4.24**

In the glovebox, a 4 mL vial was charged with TBS ether **4.23** (62.5 mg, 0.221 mmol), $[Ir(cod)OMe]_2$ (1.5 mg, 0.0022 mmol), THF (0.5 mL) and then diethylsilane (0.035 mL, 0.266 mmol). The yellow solution was allowed to stir in the glovebox for 12 h during which time hydrogen evolution was obvious. The solution was then concentrated and subjected to reduced pressure for several hours to remove all traces of excess diethylsilane. This material was then taken back into the glovebox where the vial was charged with $[Ir(cod)OMe]_2$ (1.5 mg, 0.0022 mmol), 3,4,7,8-tetramethyl-1,10-phenanthroline (1.3 mg, 0.0055 mmol), norbornene (25 mg, 0.265 mmol), and THF (0.5 mL). The solution was allowed to stir in the glovebox for 2 h during which time the solution turned a dark brown color. The vial was then sealed, brought out of the glovebox, and heated to 80 °C for 18 h. After cooling, the reaction was concentrated to yield oxasilolane **4.24** (65 mg, 80%). This material was used crude for the Tamao-Flemming oxidation to **4.34** or it can be filtered over a small pad of silica (5% EtOAc/ hexane) for subsequent palladium or rhodium chemistry. $[\alpha]_D^{22}$ (*c* 0.0156, $CHCl_3$) = +14.4; ^1H NMR (500 MHz, $CDCl_3$) δ 5.39 (h, *J* = 2.4 Hz, 1H), 3.55 (d, *J* = 9.7 Hz, 1H), 3.30 (d, *J* = 9.7 Hz, 1H), 2.40 (t, *J* = 7.5 Hz, 1H), 2.15 (p, *J* = 2.9 Hz, 2H), 2.10 (dp, *J* = 5.3, 2.6 Hz, 1H), 1.65 (dq, *J* = 18.6, 2.6 Hz, 1H), 1.49 (dq, *J* = 18.7, 3.5 Hz, 1H), 1.44 (d, *J* = 8.0 Hz, 1H), 1.28 (s, 3H), 0.94 (q, *J* = 8.0 Hz, 6H), 0.87 (s, 9H), 0.70-0.55 (m, 4H), 0.00 (s, 6H); ^{13}C NMR (126 MHz, $CDCl_3$) δ 146.40, 118.10, 84.76, 64.79, 47.72, 39.51, 33.59, 31.38, 26.09, 18.52, 16.93, 12.09, 6.68, 6.61, 6.58, 6.47, -5.29, -5.32; IR (neat) 2955, 2877, 1462, 1077 cm^{-1}; HRMS (ESI) calculated for $[C_{20}H_{39}O_2Si_2]^+$ $[M+H]^+$: *m/z* 367.2483, found 367.2485.

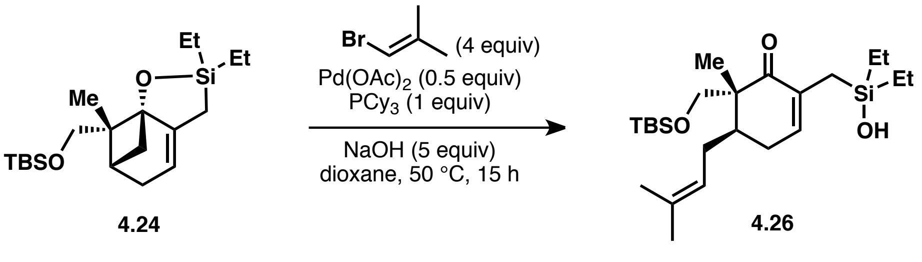
Et
Et
O
Si
Me
TBSO
4.24
Br
(4 equiv)
Pd(OAc)2 (0.5 equiv)
PCy3 (1 equiv)
NaOH (5 equiv)
dioxane, 50 °C, 15 h
O
Me
Et
Et
Si
OH
TBSO
4.26

Cyclohexenone **4.26**

A 4 mL vial was charged with oxasilolane **4.24** (25 mg, 0.068 mmol), $Pd(OAc)_2$ (4.6 mg, 0.021 mmol), tricyclohexylphosphine (11.5 mg, 0.041 mmol), 1-bromo-2-methylpropene (0.028 mL, 0.27 mmol), dioxane (0.7 mL) and NaOH (4 M, 0.085 mL, 0.34 mmol). The mixture was stirred at for 30 min, then heated to 50 °C and stirred for 15 h. The mixture was filtered through a short silica plug (EtOAc), concentrated, and purified by column chromatography (SiO_2, 2% to 5% EtOAc/ hexane) to yield cyclohexenone **4.26** (10.3 mg, 34%) as a colorless oil. $[\alpha]_D^{22}$ (*c* 0.0069, $CHCl_3$) = −0.3; ^1H NMR (500 MHz, $CDCl_3$) δ 6.53 (dd, *J* = 5.7, 2.7 Hz, 1H), 5.10 (t, *J* = 7.5 Hz, 1H), 4.11 (d, *J* = 9.7 Hz, 1H), 3.41 (d, *J* = 9.6 Hz, 1H), 2.99 (s, 1H), 2.46-2.31 (m, 2H), 2.13 (dq, J = 13.5, 3.4 Hz, 1H), 2.04 (dd, J = 19.2, 10.0 Hz, 1H), 1.94-1.81 (m, 4H), 1.71 (s, 3H), 1.68 (dd, J = 13.7, 2.2 Hz, 1H), 1.61 (s, 3H), 1.46 (ddd, J = 17.6, 12.2, 8.2 Hz, 1H), 0.93 (q, J = 7.8 Hz, 6H), 0.85 (s, 9H), 0.52 (dtd, J = 16.1, 8.0, 2.5 Hz, 4H), 0.03 (d, J = 4.8 Hz, 6H); ^{13}C NMR (126 MHz, $CDCl_3$) ? 205.01, 142.77, 136.18, 133.11, 122.71, 64.56, 51.10, 37.15, 30.41, 28.00, 27.63, 26.02, 25.97, 19.71, 18.35, 18.05, 14.35, 6.76, 6.14, 6.04, -5.43, -5.55; IR (neat) 2927, 2875, 1656, 1102, 836 cm^{-1}; HRMS (ESI) calculated for $[C_{24}H_{47}O_3Si_2]^+$ $[M+H]^+$: *m/z* 439.3058, found 439.3063.

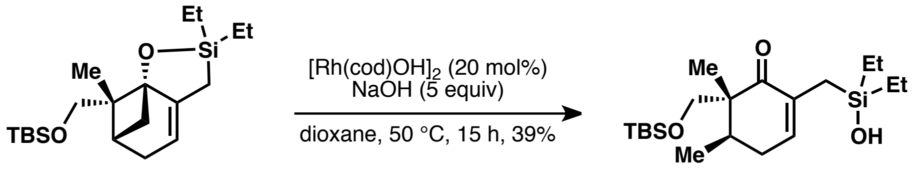
Et
Et
O
Si
Me
TBSO
[Rh(cod)OH]2 (20 mol%)
NaOH (5 equiv)
dioxane, 50 °C, 15 h, 39%
Me
O
Et
Si
Et
TBSO
Me
OH

4.24 **4.30**

Silanol **4.30**

A 4 mL vial was charged with oxasilolane **4.24** (10 mg, 0.027 mmol), $[Rh(cod)OH]_2$ (2.5 mg, 0.0055 mmol), dioxane (0.4 mL, degassed) and NaOH (4 M, 0.034 mL, 0.14 mmol). The mixture was heated to 50 °C and stirred for 15 h. The mixture was filtered through a short silica plug (EtOAc), concentrated, and purified by column chromatography (SiO_2, 2% to 5% EtOAc/hexane) to yield silanol **4.30** (3.9 mg, 39%) as a colorless oil. $[\alpha]_D^{22}$ (c 0.0031, $CHCl_3$) = −7.8; ^{1}H NMR (500 MHz, $CDCl_3$) δ 6.54 (dd, J = 5.8, 2.7 Hz, 1H), 4.08 (d, J = 9.6 Hz, 1H), 3.33 (d, J = 9.6 Hz, 1H), 2.95 (s, 1H), 2.54 (dtd, J = 11.3, 7.1, 6.7, 2.6 Hz, 1H), 2.31 (dt, J = 19.2, 5.4 Hz, 1H), 2.14 (ddt, J = 19.5, 10.8, 2.8, 2.4 Hz, 1H), 1.70 (d, J = 13.8 Hz, 1H), 1.59 (d, J = 12.2 Hz, 1H), 0.96-0.90 (m, 9H), 0.85 (s, 9H), 0.80 (s, 3H), 0.58-0.48 (m, 4H), 0.03 (d, J = 6.5 Hz, 6H); ^{13}C NMR (126 MHz, $CDCl_3$) δ 205.17, 142.53, 136.20, 76.91, 64.58, 50.87, 31.69, 31.38, 25.95, 19.76, 18.36, 15.00, 13.60, 6.76, 6.75, 6.16, 6.08, -5.39, -5.60; IR (neat) 2954, 2876, 1659, 1093, 836 cm^{-1}; HRMS (ESI) calculated for $[C_{20}H_{40}O_3Si_2Na]^+$ $[M+Na]^+$: *m/z* 407.2408, found 407.2408.

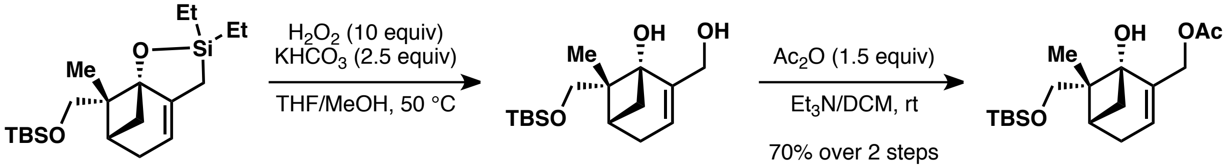
Et
Et
O
Si
Me
TBSO
H2O2 (10 equiv)
KHCO3 (2.5 equiv)
THF/MeOH, 50 °C
OH
OH
Me
TBSO
Ac2O (1.5 equiv)
Et3N/DCM, rt
70% over 2 steps
OH
OAc
Me
TBSO

4.24 **4.34** **4.35**

Allylic acetate **4.35**

To a vial of crude oxasilolane **4.24** (65 mg, 0.18 mmol) was added THF (0.5 mL), methanol (0.5 mL), $KHCO_3$ (45 mg, 0.45 mmol), and hydrogen peroxide (0.2 mL, 30%, 1.8 mmol). This vial was sealed and heated to 50 °C for 18 h. The orange mixture was quenched with Na_2SO_3 (1 mL) and extracted with EtOAc (3 x 1 mL). The organics were dried over magnesium sulfate, filtered, and concentrated to yield diol **4.34**. This crude material was dissolved in DCM (0.5 mL). Triethylamine (0.1 mL) and acetic anhydride (0.026 mL, 0.27 mmol) were added to the solution and stirred for 18 h. The reaction mixture was diluted with

EtOAc, filtered through a silica plug (EtOAc), concentrated, and purified by column chromatography (SiO_2, 10% to 20% EtOAc/ hexane) to yield allylic acetate **4.35** (34.2 mg, 70% over 2 steps). $[\alpha]_D^{22}$ (*c* 0.0166, $CHCl_3$) = −14.7; ^1H NMR (500 MHz, $CDCl_3$) δ 5.62 (d, *J* = 2.9 Hz, 1H), 4.71 (d, *J* = 12.9 Hz, 1H), 4.65 (d, *J* = 12.9 Hz, 1H), 3.46 (d, *J* = 9.5 Hz, 1H), 3.36 (d, *J* = 9.4 Hz, 1H), 2.40 (s, 1H), 2.33 (t, *J* = 8.2, 6.9 Hz, 1H), 2.25-2.12 (m, 3H), 2.06 (s, 3H), 1.58 (d, *J* = 8.4 Hz, 1H), 1.29 (s, 3H), 0.87 (d, *J* = 0.2 Hz, 9H), 0.00 (d, *J* = 2.7 Hz, 6H); ^{13}C NMR (126 MHz, $CDCl_3$) δ 171.19, 144.17, 123.50, 76.91, 65.27, 63.52, 46.42, 39.02, 33.92, 30.99, 26.05, 21.29, 18.39, 17.14, -5.39, -5.43; IR (neat) 2928, 2855, 1741, 1250, 1076 cm^{-1}; HRMS (ESI) calculated for $[C_{18}H_{31}O_4Si]^-$ $[M-H]^-$: *m/z* 339.1997, found 339.1999.

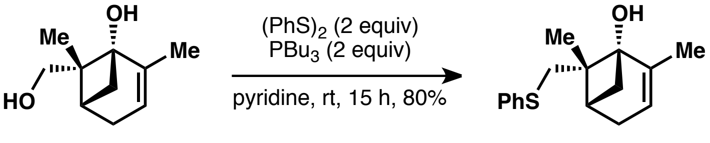

4.16 **4.36**

Phenyl sulfide **4.36**

To a round bottomed flask containing diol **4.16** (1.57 g, 9.35 mmol) and diphenyl disulfide (4.08 g, 18.7 mmol) in pyridine (18.5 mL) was added tri-*n*-butylphosphine (4.70 mL, 18.8 mmol). The resulting mixture was stirred for 20 h at room temperature, and was treated with EtOAc (50 mL) and H_2O (20 mL). The phases were separated, and the organic phase was washed with 1M HCl (3 x 25 mL), saturated aqueous solution of $NaHCO_3$ (2 x 25 mL), then brine (50 mL). The organic phase was dried over $MgSO_4$, and concentrated *in vacuo* to provide a dark brown oil. The crude product was purified by flash chromatography (SiO_2, 10% to 30% EtOAc/ hexanes) to provide phenyl sulfide **4.36** (1.96 g, 80%) as a light yellow oil. $[\alpha]_D^{22}$ (*c* 1.18, $CHCl_3$) = −14.6; ^1H NMR (600 MHz, $CDCl_3$): δ 7.30 (d, *J* = 7.6 Hz, 2H), 7.25 (t, *J* = 7.9 Hz, 2H), 7.14 (t, *J* = 7.6 Hz, 1H), 5.27 (br s, 1H), 3.16 (d, *J* = 11.1 Hz, 1H), 2.92 (d, *J* = 11.1 Hz, 1H), 2.27 (dd, *J* = 8.1, 7.2 Hz, 1H), 2.22 (m, 1H), 2.18-2.15 (m, 2H), 1.98 (br s, 1H), 1.80 (s, 3H), 1.61 (d, *J* = 8.3 Hz, 1H), 1.37 (s, 3H); ^{13}C NMR (151 MHz, $CDCl_3$): δ 145.7, 138.0, 129.0, 129.0, 125.8, 117.9, 78.6, 45.8, 39.4, 38.9, 35.9, 31.1, 19.0, 17.5; IR (ATR): 3454, 2934, 2881, 2835, 1583, 1480, 1438, 1231, 1157, 736, 689 cm^{-1}; HRMS (EI) calculated for $[C_{16}H_{20}OS]^+$ $[M]^+$: *m/z* 260.1235, found 260.1233.

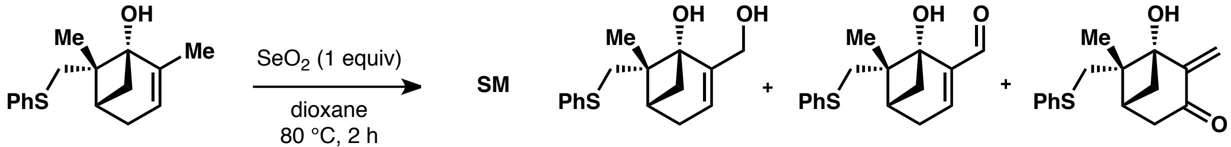

4.36 8% **4.38** 52% **4.39** 10% **4.40** 14%

Allylic alcohol **4.38**

To a round bottomed flask containing phenyl sulfide **4.36** (1.96 g, 7.51 mmol) in 1,4-dioxane (38.0 mL) was added selenium dioxide (0.833 g, 7.51 mmol). The resulting mixture was heated at 80 °C in an oil bath for 2 h. Upon cooling the mixture to room temperature, the mixture was diluted with EtOAc (40 mL), H_2O (40 mL), then separated. The aqueous phase was

extracted with EtOAc (3 x 40 mL). The combined organic phases were washed with brine (50 mL), dried over magnesium sulfate, concentrated, and purified by column chromatography (SiO_2, 20% to 70% EtOAc/ hexane) to provide allylic alcohol **4.38** (1.08 g, 52%) as a yellow oil. $[\alpha]_D^{22}$ (*c* 0.84, $CHCl_3$) = −16; ^1H NMR (600 MHz, $CDCl_3$): δ 7.31-7.24 (m, 4H), 7.19-7.14 (m, 1H), 5.52 (s, 1H), 4.32 (t, *J* = 9.9 Hz, 1H), 4.21 (dd, *J* = 12.2, 3.2 Hz, 1H), 3.30 (s, 1H), 3.10 (d, *J* = 10.9 Hz, 1H), 2.92 (d, *J* = 10.9 Hz, 1H), 2.37 (dd, *J* = 8.5, 6.7 Hz, 1H), 2.31 (dd, *J* = 8.3, 4.0 Hz, 1H), 2.27-2.21 (m, 2H), 1.66 (d, *J* = 8.7 Hz, 1H), 1.42 (s, 3H); ^{13}C NMR (151 MHz, $CDCl_3$): δ 147.9, 137.4, 129.1, 128.9, 126.0, 121.0, 78.8, 64.1, 45.6, 38.9, 38.9, 35.3, 30.9, 18.6; IR (neat): 3382, 2935, 2886, 1438, 1235, 738 cm^{-1}; HRMS (ESI) calculated for $[C_{16}H_{19}O_2S]^+$ $[M+H]^+$: *m/z* 275.1100, not found.
Data for aldehyde **4.39** is found further below in this section.

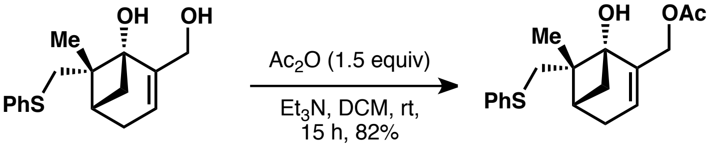

4.38 **4.41**

Allylic acetate **4.41**

To a flask containing allylic alcohol **4.38** (1.10 g, 3.98 mmol) and dichloromethane (40 mL) was added triethylamine (2.2 mL, 15.9 mmol) and acetic anhydride (0.56 mL, 5.97 mmol). The resulting mixture was stirred for 12 h at room temperature, then diluted with hexane (40 mL) and ethyl acetate (40 mL) and filtered through a silica plug. The filtrate was concentrated and purified by column chromatography (SiO_2, 10% to 30% EtOAc/ hexane) to yield allylic acetate **4.41** (1.04 g, 82%) as a yellow oil. $[\alpha]_D^{22}$ (*c* 0.010, $CHCl_3$) = −1.1; ^1H NMR (600 MHz, $CDCl_3$): δ 7.30-7.22 (m, 4H), 7.15 (tt, *J* = 7.7, 1.5 Hz, 1H), 5.72 (q, *J* = 2.8 Hz, 1H), 4.70 (s, 2H), 3.00 (d, *J* = 11.2 Hz, 1H), 2.92 (d, *J* = 11.2 Hz, 1H), 2.80 (bs, 1H), 2.37 (dd, *J* = 8.6, 6.8 Hz, 1H), 2.28-2.22 (m, 3H), 2.02 (s, 3H), 1.61 (d, *J* = 8.5 Hz, 1H), 1.40 (s, 3H); ^{13}C NMR (151 MHz, $CDCl_3$) δ 171.25, 144.02, 137.91, 128.89, 128.74, 125.70, 124.89, 78.11, 63.48, 45.53, 38.86, 38.63, 35.04, 31.02, 21.18, 18.69; IR (neat): 3460, 2942, 1738, 1246 cm^{-1}; HRMS (ESI) calculated for $[C_{18}H_{22}O_3SNa]^+$ $[M+Na]^+$: *m/z* 341.1182, found 341.1182.

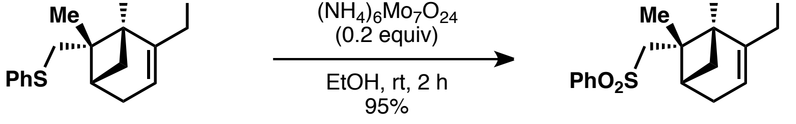

4.41 **4.52**

Sulfone **4.52**

A flask containing allylic acetate **4.41** (1.03 g, 3.23 mmol), ammonium heptamolybdate (0.81 g, 0.65 mmol), and ethanol (32 mL) was cooled to 0 °C. To this mixture was added hydrogen peroxide (4.4 mL, 50%, 65 mmol) dropwise over the course of 5 min. The mixture was allowed to warm to room temperature and stir for an additional 3 h. After removal of most of the ethanol under reduced pressure, water (50 mL) was added and the mixture was extracted with diethyl ether (3 x 50 mL). The combined organics were dried over magnesium sulfate, concentrated, and filtered to yield sulfone **4.52** as a colorless oil (1.08 g, 95%). $[\alpha]_D^{22}$ (*c* 0.0003, $CHCl_3$) = −15; ^{1}H NMR (500 MHz, $CDCl_3$): δ 7.89 (d, *J* = 7.5 Hz, 2H), 7.65 (t, *J* = 7.4 Hz, 1H), 7.56 (t, *J* = 7.7 Hz, 2H), 5.53 (s, 1H), 4.91 (d, *J* = 13.9 Hz, 1H), 4.83 (d, *J* = 14.0 Hz, 1H), 3.50 (bs, 1H), 3.49 (d, *J* = 14.4 Hz, 1H), 3.03 (d, *J* = 13.8 Hz, 1H), 2.52 (dd, *J* = 8.8, 6.7 Hz, 1H), 2.31-2.22 (m, 2H), 2.10 (s, 3H), 2.03 (dt, *J* = 19.5, 2.9 Hz, 1H), 1.72 (d, *J* = 8.8 Hz, 1H), 1.60 (s, 3H); ^{13}C NMR (126 MHz, $CDCl_3$) δ 171.09, 145.79, 141.36, 133.76, 129.48, 127.55, 120.78, 77.24, 62.93, 59.70, 43.19, 37.92, 36.23, 30.75, 21.23, 18.65; IR (neat): 3486, 2942, 1737, 1305, 1146 cm^{-1}; HRMS (ESI) calculated for $[C_{18}H_{22}O_5SNa]^+$ $[M+Na]^+$: *m/z* 373.1080, found 373.1081.

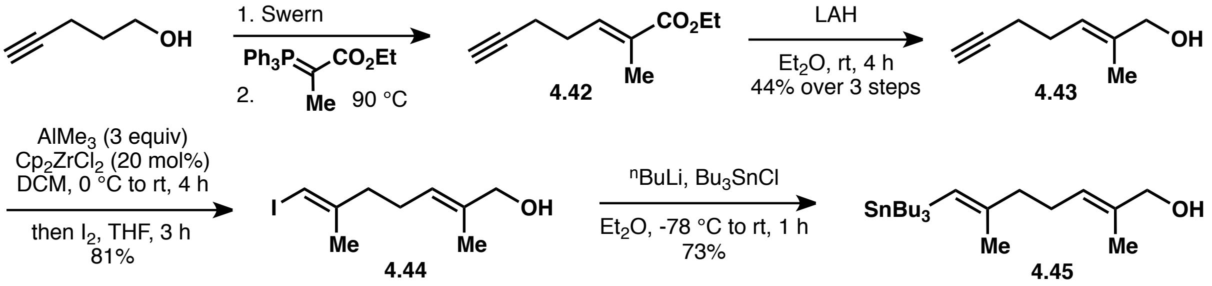

Vinyl stannane **4.45**

A 250 mL flask was charged with oxalyl chloride (2.7 mL, 32 mmol) and DCM (50 mL) and cooled to -78 °C. A solution of dimethylsulfoxide (4.6 mL, 65 mmol) in DCM (10 mL) was added dropwise (10 min) to the reaction mixture and stirring was continued for 30 min. A solution of 4-pentyn-1-ol (2.5 mL, 27 mmol) in DCM (20 mL) was added dropwise (10 min) to the reaction mixture and stirring was continued for 1 h. Then, triethylamine (22 mL, 161 mmol) was added dropwise (10 min) and the reaction was allowed to warm to room temperature and stir for an additional 3 h. The reaction was quenched with HCl (2 N, 30 mL) and brine (30 mL) and washed with HCl/brine (1:1, 3 x 40 mL). The organics were dried over magnesium sulfate, filtered, and concentrated to yield aldehyde **4.S1** (1.63 g, 74%) as a colorless oil.

A 250 mL Schlenk flask was charged with aldehyde **4.S1** (1.63 g, 19.8 mmol), (carbethoxyethylidene)triphenylphosphorane (10.1 g, 27.8 mmol), and toluene (100 mL), sealed, and heated to 90 °C. After 12 h, the mixture was cooled to room temperature, filtered through a silica plug (20% EtOAc/ hexane) and concentrated to yield enoate **4.42** as a colorless oil. This material was carried on without further purification.

A 250 mL flask was charged with lithium aluminum hydride (1.49 g, 39.4 mmol) and diethyl ether (40 mL) and cooled to 0 °C. A solution of enoate **4.42** (19.8 mmol) in diethyl ether (10 mL) was added dropwise (5 min). Upon warming to room temperature, the mixture was allowed to stir for 4 h. The reaction was then cooled to 0 °C and quenched by the slow addition of water (1.5 mL), then sodium hydroxide (15% aq, 1.5 mL), then water (4.5 mL). After stirring at room temperature for 1 h, magnesium sulfate was added. The mixture was filtered over a Celite plug and concentrated to yield alcohol **4.43** (1.48 g, 60% over 2 steps) as a colorless oil.

A 50 mL flask was charged with zirconocene dichloride (88 mg, 0.30 mmol) and dichloromethane (6 mL) and cooled to 0 °C. Trimethylaluminum (2.25 mL, 2 M toluene, 4.50 mmol) was added slowly (3 min) and the mixture was allowed to stir for an additional 10 min.

Then, a solution of alcohol **4.43** (186 mg, 1.50 mmol) in dichloromethane (1.5 mL) was added to the yellow reaction mixture. After stirring for 10 min at 0 °C, the mixture was allowed to warm to room temperature and stir for an additional 4 h. Then, after cooling to 0 °C, a solution of iodine (761 mg, 3.0 mmol) in THF (3 mL) was added slowly (5 min). The mixture was allowed to warm to room temperature and stir for 3 h. After cooling to 0 °C, the reaction was quenched by the addition of a saturated solution of K_2CO_3 (0.5 mL). After stirring for 1 h, Rochelle's salt solution was added and the mixture was extracted with ethyl acetate (3 x 15 mL). The organics were dried over magnesium sulfate, filtered, concentrated, and purified by column chromatography (SiO_2, 10% to 25% EtOAc/ hexane) to yield vinyl iodide **4.44** (324 mg, 81%) as a colorless oil.

A 50 mL flask was charged with vinyl iodide **4.44** (560 mg, 2.10 mmol) and diethyl ether (10 mL) and cooled to -78 °C. n-Butyllithium (1.9 mL, 2.5 M hexane, 4.6 mmol) was added dropwise (3 min) and the mixture was allowed to stir for 30 min. Tributyltin chloride (1.7 mL, 6.3 mmol) was then added. The ice bath was allowed to expire, letting the reaction stir at -78 °C for 1 h, slowly warming to room temperature over 1 h, and then stir at room temperature for an additional 12 h. The reaction was quenched by the addition of NH_4Cl (10 mL). After diluting with diethyl ether (10 mL), the organics were vigorously washed with KF (1 M, 3 x 15 mL). The organics were then filtered through a silica plug (w/ diethyl ether), concentrated, and purified by filtration over a second silica plug (w/ 30% EtOAc/ hexane) to yield vinyl stannane **4.45** (658 mg, 78%) as a colorless oil. ^1H NMR (500 MHz, $CDCl_3$): δ 5.45 (s, 1H), 5.41 (t, J = 6.5, 5.3 Hz, 1H), 4.00 (d, J = 6.1 Hz, 2H), 2.18 (s, 3H), 1.81-1.71 (m, 4H), 1.68 (s, 3H), 1.55-1.42 (m, 6H), 1.30 (h, J = 7.3 Hz, 6H), 1.21 (t, J = 6.2 Hz, 1H), 0.89 (t, J = 7.1 Hz, 15H); ^{13}C NMR (151 MHz, $CDCl_3$) δ 154.51, 134.92, 126.27, 122.00, 69.20, 41.67, 29.37, 27.45, 26.56, 24.70, 13.84, 13.83, 10.20; IR (neat): 3320, 2923, 2853, 1456, 1043 cm^{-1}; HRMS (ESI) calculated for $[C_{21}H_{43}OSn]^+$ $[M+H]^+$: *m/z* 431.2330, not found.

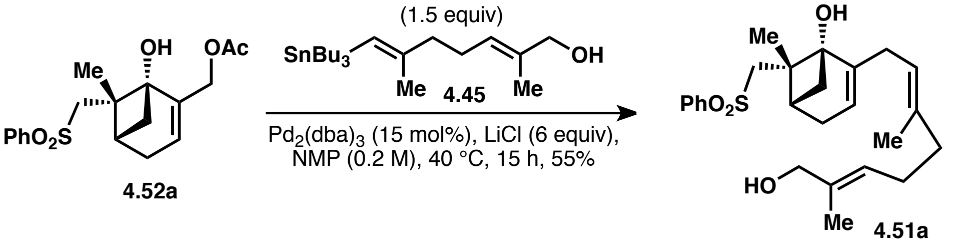

Coupled product **4.51a**

A 10 mL Schlenk tube was charged with allylic acetate **4.52a** (81 mg, 0.231 mmol), vinyl stannane **4.45** (200 mg, 0.462 mmol), tris(dibenzylideneacetone)dipalladium (32 mg, 0.035 mmol), lithium chloride (59 mg, 1.39 mmol), and *N*-methyl-2-pyrrolidone (1.1 mL). The tube was sealed and heated to 40 °C for 15 h. Upon cooling, water (5 mL) was added and the mixture was extracted with diethyl ether (3 x 5 mL). The organics were dried over magnesium sulfate, filtered, concentrated, and purified by column chromatography (SiO_2, 35% to 50% EtOAc/ hexane) to yield coupled product **4.51a** (54.8 mg, 55%) as a light yellow oil. $[\alpha]_D^{22}$ (*c* 0.0038, $CHCl_3$) = +5.5; ^1H NMR (600 MHz, $CDCl_3$): δ 7.84 (d, J = 7.1 Hz, 2H), 7.64 (t, J = 7.4 Hz, 1H), 7.55 (t, J = 7.7 Hz, 2H), 5.38 (tq, J = 6.8, 1.2 Hz, 1H), 5.24 (tq, J = 7.2, 1.2 Hz, 1H), 5.20 (q, J = 2.4 Hz, 1H), 3.98 (d, J = 5.1 Hz, 2H), 3.57 (d, J = 13.9 Hz, 1H), 3.37 (s, 1H), 3.10-3.01 (m, 2H), 2.95 (dd, J = 17.1, 6.9 Hz, 1H), 2.48 (dd, J = 8.7, 6.6 Hz, 1H), 2.24-2.16 (m, 4H), 2.11 (t, J = 8.1

Hz, 2H), 1.96 (dq, *J* = 16.3, 2.9 Hz, 1H), 1.73 (t, *J* = 6.2 Hz, 1H), 1.67 (s, 3H), 1.64 (s, 3H), 1.56 (s, 3H); ^{13}C NMR (151 MHz, $CDCl_3$) δ 150.37, 141.80, 136.47, 135.19, 133.64, 129.45, 127.43, 125.89, 122.18, 116.42, 77.87, 69.11, 60.02, 43.20, 39.44, 37.94, 36.56, 31.04, 29.60, 25.98, 18.86, 16.04, 13.88; IR (neat): 3465, 2924, 2853, 1145 cm^{-1}; HRMS (ESI) calculated for $[C_{25}H_{34}O_4SNa]^+$ $[M+H]^+$: *m/z* 453.2070, found 453.2071.

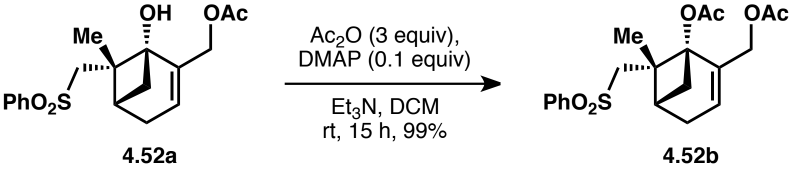

Bis-acetate **4.52b**

A 4 mL vial was charged with sulfone **4.52a** (23.5 mg, 0.0671 mmol), triethylamine (0.1 mL), 4-dimethylaminopyridine (0.9 mg, 0.0067 mmol), and dichloromethane (0.4 mL). Then, acetic anhydride (0.019 mL, 0.201 mmol) was added and the reaction was allowed to stir for 15 h. The mixture was passed through a silica plug (washing with 50% EtOAc/ hexane), concentrated, and purified by column chromatography to yield bis-acetate **4.52b** (26.0 mg, 99%) as a colorless oil. $[\alpha]_D^{22}$ (*c* 0.0077, $CHCl_3$) = +15; ^{1}H NMR (500 MHz, $CDCl_3$): δ 7.89 (d, *J* = 7.5 Hz, 2H), 7.63 (t, *J* = 7.4 Hz, 1H), 7.56 (t, *J* = 7.6 Hz, 2H), 5.74 (q, *J* = 2.0 Hz, 1H), 4.45 (dd, *J* = 17.0, 13.5 Hz, 2H), 3.44 (dd, *J* = 22.1, 14.6 Hz, 2H), 2.70 (dq, *J* = 7.1, 2.6 Hz, 1H), 2.66-2.54 (m, 2H), 2.39 (dt, *J* = 19.2, 2.7 Hz, 1H), 2.03 (s, 3H), 1.99 (d, *J* = 7.8 Hz, 1H), 1.97 (s, 3H), 1.54 (s, 3H); ^{13}C NMR (151 MHz, $CDCl_3$) δ 170.46, 170.35, 142.06, 141.23, 133.45, 129.34, 127.38, 125.12, 83.68, 62.84, 59.91, 44.22, 38.66, 36.66, 31.80, 20.94, 20.91, 18.59; IR (neat): 2948, 1735, 1240 cm^{-1}; HRMS (ESI) calculated for $[C_{20}H_{24}O_6SNa]^+$ $[M+H]^+$: *m/z* 415.1186, found 415.1185.

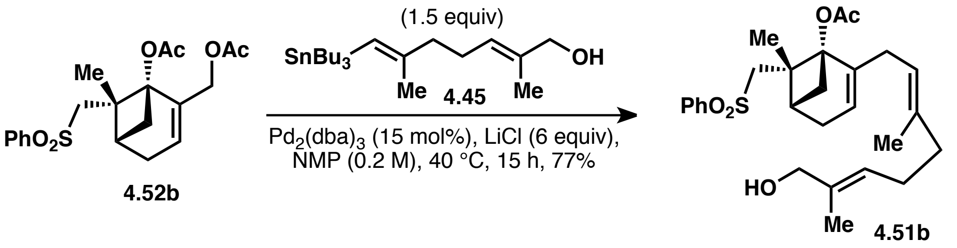
OAc
OAc
Me
PhO2S
4.52b
(1.5 equiv)
SnBu3
OH
Me
4.45
Me
Pd2(dba)3 (15 mol%), LiCl (6 equiv),
NMP (0.2 M), 40 °C, 15 h, 77%
OAc
Me
PhO2S
Me
HO
Me
4.51b

Coupled product **4.51b**

A 4 mL vial was charged with bis-acetate **4.52b** (26.0 mg, 0.0662 mmol), vinyl stannane **4.45** (42.7 mg, 0.0994 mmol), tris(dibenzylideneacetone)dipalladium (9.1 mg, 0.0099 mmol), lithium chloride (16.9 mg, 0.397 mmol), and *N*-methyl-2-pyrrolidone (0.3 mL). The vial was sealed and heated to 40 °C for 15 h. Upon cooling, water (1 mL) was added and the mixture was extracted with diethyl ether (3 x 1 mL). The organics were dried over magnesium sulfate, filtered, concentrated, and purified by column chromatography (SiO_2, 30% to 40% EtOAc/ hexane) to yield coupled product **4.51b** (24.2 mg, 77%) as a light yellow oil. $[\alpha]_D^{22}$ (*c* 0.0117, $CHCl_3$) = −5.9; ^{1}H NMR (500 MHz, $CDCl_3$): δ 7.87 (d, *J* = 7.7 Hz, 2H), 7.61 (t, *J* = 7.4 Hz, 1H), 7.53 (t, *J* = 7.6 Hz, 2H), 5.34 (t, *J* = 7.1 Hz, 1H), 5.28 (s, 1H), 5.06 (t, *J* = 7.2 Hz, 1H), 3.96 (s, 2H), 3.48 (q, *J* = 14.5 Hz, 2H), 2.66-2.43 (m, 5H), 2.29 (d, *J* = 18.4 Hz, 1H), 2.08 (q, *J* = 7.3 Hz, 2H), 2.03 (s, 3H), 1.99 (t, *J* = 7.5 Hz, 2H), 1.92 (d, *J* = 9.0 Hz, 1H), 1.63 (s, 3H), 1.49 (s, 3H), 1.45 (s, 3H); ^{13}C NMR (151 MHz, $CDCl_3$) δ 170.50, 145.29, 142.23, 136.91, 134.98, 133.35, 129.29, 127.42, 125.68, 120.81, 118.94, 84.96, 68.86, 60.04, 44.17, 39.24, 38.63, 36.90, 31.85, 29.29, 26.08, 21.04, 18.71, 15.92, 13.80; IR (neat): 3506, 2928, 1733, 1146 cm^{-1}; HRMS (ESI) calculated for $[C_{27}H_{36}O_5SNa]^+$ $[M+Na]^+$: *m/z* 495.2176, found 495.2175.

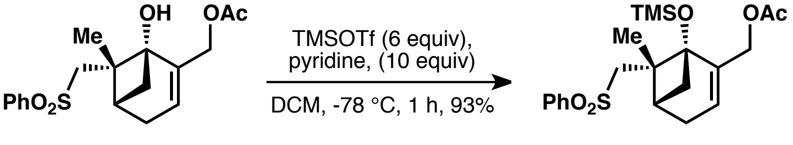

4.52a **4.52c**

TMS ether **4.52c**

A 100 mL flask was charged with sulfone **4.52a** (734 mg, 2.09 mmol) and dichloromethane (21 mL) and cooled to -78 °C. Pyridine (1.7 mL, 20.9 mmol) was added and then trimethylsilyl trifluoromethanesulfonate (2.3 mL, 12.6 mmol) was added dropwise (3 min). The solution was allowed to stir at -78 °C for 1 h. After this time, the reaction mixture was treated with triethylamine (5.0 mL) and methanol (5.0 mL). Upon warming to room temperature, the mixture was diluted with H_2O (30 mL), EtOAc (30 mL), and hexanes (30 mL), and extracted with EtOAc (3 x 30 mL). The organics were dried over magnesium sulfate, filtered, concentrated, and purified by column chromatography (SiO_2, 20% to 30% EtOAc/ hexane) to yield TMS ether **4.52c** (819 mg, 93%) as a colorless oil. $[\alpha]_D^{22}$ (*c* 0.010, $CHCl_3$) = +16.6; ^{1}H NMR (500 MHz, $CDCl_3$): δ 7.88 (d, *J* = 7.7 Hz, 2H), 7.63 (t, *J* = 7.4 Hz, 1H), 7.55 (t, *J* = 7.7 Hz, 2H), 5.63 (d, *J* = 2.9 Hz, 1H), 4.50 (d, *J* = 13.5 Hz, 1H), 4.40 (d, *J* = 13.3 Hz, 1H), 3.40 (d, *J* = 14.4 Hz, 1H), 3.06 (d, *J* = 14.4 Hz, 1H), 2.59 (t, *J* = 7.8 Hz, 1H), 2.54 (dd, *J* = 6.2, 3.5 Hz, 1H), 2.44 (dt, *J* = 19.0, 2.5 Hz, 1H), 2.31 (dt, *J* = 19.1, 2.6 Hz, 1H), 1.97 (s, 3H), 1.74 (d, *J* = 8.3 Hz, 1H), 1.50 (s, 3H), 0.12 (s, 9H); ^{13}C NMR (126 MHz, $CDCl_3$) δ 170.64, 144.53, 142.10, 133.45, 129.34, 127.51, 123.27, 80.27, 63.17, 59.72, 44.68, 39.93, 35.68, 31.72, 21.13, 18.76, 1.82; IR (neat): 2957, 1736, 1223 cm^{-1}; HRMS (ESI) calculated for $[C_{21}H_{30}O_5SSiNa]^+$ $[M+H]^+$: *m/z* 445.1475, found 445.1474.

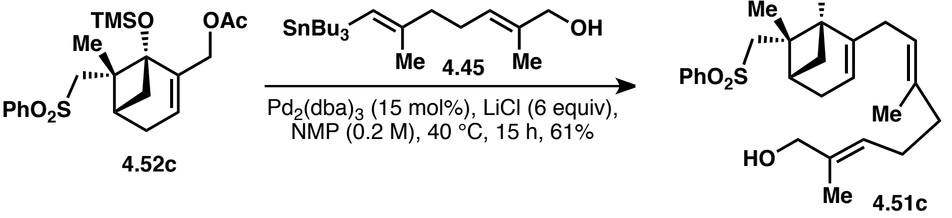
TMSO
OAc
Me
PhO2S
(1.5 equiv)
SnBu3
OH
Me
Me
4.45
Pd2(dba)3 (15 mol%), LiCl (6 equiv),
NMP (0.2 M), 40 °C, 15 h, 61%
OTMS
Me
PhO2S
Me
HO
Me

4.52c **4.51c**

Coupled product **4.51c**

A 25 mL Schlenk flask was charged with allylic acetate **4.52c** (220 mg, 0.521 mmol), vinyl stannane **4.45** (335 mg, 0.781 mmol), tris(dibenzylideneacetone)dipalladium (72 mg, 0.078 mmol), lithium chloride (132 mg, 3.12 mmol), and *N*-methyl-2-pyrrolidone (2.6 mL). The flask was sealed and heated to 40 °C for 15 h. Upon cooling, water (10 mL) was added and the mixture was extracted with diethyl ether (3 x 10 mL). The organics were dried over magnesium sulfate, filtered, concentrated, and purified by column chromatography (SiO$_2$, 15% to 30% EtOAc/ hexane) to yield coupled product **4.51c** (160 mg, 61%) as a light yellow oil. $[\alpha]_D^{22}$ (*c* 0.0101, CHCl$_3$) = +17.6; ^{1}H NMR (600 MHz, CDCl$_3$): δ 7.86 (d, *J* = 7.8 Hz, 2H), 7.61 (t, *J* = 7.5 Hz, 1H), 7.53 (t, *J* = 7.6 Hz, 2H), 5.36 (t, *J* = 6.9 Hz, 1H), 5.21 (s, 1H), 5.12 (t, *J* = 7.4 Hz, 1H), 4.06-3.96 (m, 2H), 3.43 (d, *J* = 14.4 Hz, 1H), 2.99 (d, *J* = 14.4 Hz, 1H), 2.66 (dd, *J* = 17.4, 7.5 Hz, 1H), 2.60-2.47 (m, 3H), 2.36 (dt, *J* = 17.7, 2.2 Hz, 1H), 2.23 (dt, *J* = 18.6, 2.9 Hz, 1H), 2.06 (hept, *J* = 9.3, 8.2 Hz, 2H), 1.94 (t, *J* = 6.9 Hz, 2H), 1.70 (d, *J* = 8.1 Hz, 1H), 1.66 (s, 3H), 1.60 (bs, 1H), 1.47 (s, 3H), 1.41 (s, 3H), 0.13 (s, 9H); ^{13}C NMR (126 MHz, CDCl$_3$) δ 148.93, 142.17, 136.25, 134.94, 133.28, 129.22, 127.41, 125.81, 121.42, 117.48, 80.97, 68.89, 59.97, 44.44, 39.86, 39.21, 35.86, 31.80, 30.02, 26.04, 18.75, 15.85, 13.81, 1.86; IR (neat): 3480, 2934, 1144, 735 cm^{-1}; HRMS (ESI) calculated for $[C_{28}H_{43}O_4SSi]^+$ $[M+H]^+$: *m/z* 502.2573, not found.

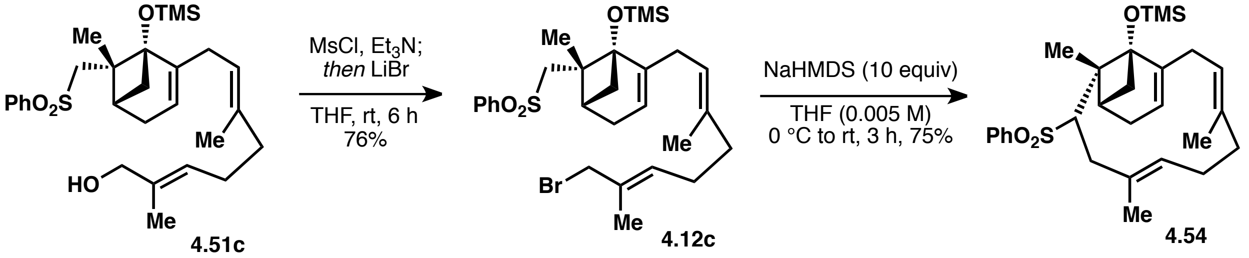

Macrocycle **4.54**

To a flask containing allyl alcohol **4.51c** (35.1 mg, 0.070 mmol), tetrahydrofuran (2 mL), and triethylamine (0.039 mL, 0.28 mmol) was added methanesulfonyl chloride (0.010 mL, 0.14 mmol). The resulting mixture was stirred for 2 h. Then, a solution of lithium bromide (61 mg, 0.70 mmol) in tetrahydrofuran (1 mL) was added dropwise (2 min). The reaction was allowed to stir an additional 4 h. Water (3 mL) was added and the mixture was extracted with diethyl ether (3 x 5 mL). The combined organic phases were dried over magnesium sulfate, filtered, concentrated, and purified over a quick silica plug (washing with 20% EtOAc/ hexane + 1% triethylamine) to give allyl bromide **4.12c** (30.1 mg, 76%) as a colorless oil.

To a round bottomed flask containing allyl bromide **4.12c** (30.1 mg, 0.053 mmol) in tetrahydrofuran (11 mL) at 0 °C was dropwise added a solution of sodium bis(trimethylsilyl)amide (2.0 M solution in tetrahydrofuran, 0.27 mL, 0.53 mmol) over 10 min. The resulting mixture was stirred for 1 h at 0 °C, then gradually warmed to room temperature (30 min) and stirred for an additional 1 h. After this time, the reaction was treated with a saturated aqueous solution of NH$_4$Cl (1 mL), EtOAc (5 mL), and H$_2$O (5 mL). The phases were separated, and the aqueous phase was extracted with EtOAc (3 x 5 mL). The combined organic phases were dried over magnesium sulfate, filtered, concentrated, and purified by column chromatography (SiO$_2$, 10% EtOAc/ hexanes) to yield macrocycle **4.54** (19.3 mg, 75%) as a colorless oil. $[\alpha]_D^{22}$ (*c* 0.0018, CHCl$_3$) = −5.7; ^{1}H NMR (500 MHz, CDCl$_3$): δ 7.78 (dt, *J* = 8.6, 1.7 Hz, 2H), 7.53 (tt, *J* = 7.5, 1.9 Hz, 1H), 7.45 (tt, *J* = 7.7, 1.7 Hz, 2H), 5.38 (d, *J* = 2.7 Hz, 1H), 4.78 (ddd, *J* = 10.5, 5.9, 1.7 Hz, 1H), 4.20 (td, *J* = 10.0, 8.1, 2.0 Hz, 1H), 3.95 (dd, *J* = 7.0, 1.9 Hz, 1H), 2.84-2.75 (m, 2H), 2.72 (dq, *J* = 7.6, 2.6 Hz, 1H), 2.69-2.57 (m, 2H), 2.56 (dd, *J* = 8.2, 6.9 Hz, 1H), 2.44 (d, *J* = 19.0 Hz, 1H), 2.27 (dq, *J* = 18.6, 3.1 Hz, 1H), 1.90 (qd, *J* = 8.1, 6.7, 2.9 Hz, 2H), 1.75 (dt, *J* = 11.9, 5.9 Hz, 1H), 1.69 (d, *J* = 8.2 Hz, 1H), 1.67-1.58 (m, 1H), 1.54 (s, 3H), 1.49 (s, 3H), 1.14 (s, 3H), 0.16 (s, 9H); ^{13}C NMR (126 MHz, $CDCl_3$) δ 150.04, 141.24, 133.16, 131.75, 129.62, 128.86, 128.76, 125.66, 122.33, 119.34, 82.83, 62.25, 48.64, 41.32, 38.79, 38.44, 34.66, 32.19, 31.81, 23.78, 16.88, 16.64, 15.36, 2.09; IR (neat): 2953, 2921, 2851, 1143 cm^{-1}; HRMS (ESI) calculated for $[C_{28}H_{40}O_3SSiNa]^+$ $[M+H]^+$: *m/z* 507.2360, found 507.2365.

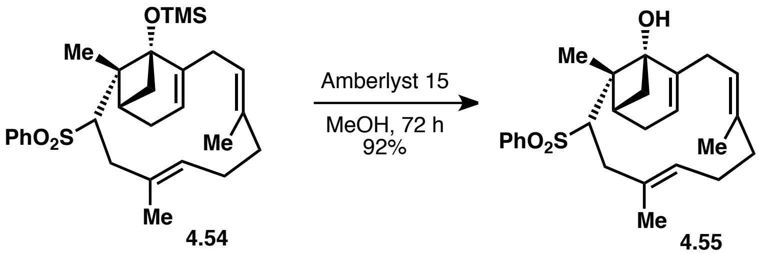

Cyclobutanol **4.55**

A 4 mL vial was charged with macrocycle **4.54** (36 mg, 0.074 mmol), methanol (0.8 mL), and Amberlyst 15 beads (36 mg). The mixture was allowed to stir at room temperature for 72 h. The methanol solution was then decanted away from the beads and concentrated. This crude material was purified by column chromatography (SiO_2, 20% to 30% EtOAc/ hexanes) to yield cyclobutanol **4.55** (28.2 mg, 92%) as a white solid. $[\alpha]_D^{22}$ (*c* 0.0037, $CHCl_3$) = +16.9; ^{1}H NMR (500 MHz, $CDCl_3$): δ 7.88 (d, *J* = 7.9 Hz, 2H), 7.62 (t, *J* = 7.4 Hz, 1H), 7.55 (t, *J* = 7.6 Hz, 2H), 5.41 (dd, *J* = 4.1, 2.1 Hz, 1H), 4.77-4.67 (m, 2H), 3.69 (dd, *J* = 6.0, 2.7 Hz, 1H), 3.17 (tt, *J* = 12.4, 1.8 Hz, 1H), 2.90 (dq, *J* = 18.9, 2.2 Hz, 1H), 2.76 (dt, *J* = 5.1, 2.7 Hz, 1H), 2.67-2.43 (m, 5H), 2.30 (dq, *J* = 19.1, 3.4 Hz, 1H), 2.20-2.06 (m, 2H), 1.94 (d, *J* = 15.7 Hz, 1H), 1.82 (td, *J* = 11.6, 6.1 Hz, 1H), 1.63 (d, *J* = 2.9 Hz, 3H), 1.58 (s, 3H), 0.82 (s, 3H); ^{13}C NMR (126 MHz, $CDCl_3$) δ 146.68, 140.38, 133.44, 132.44, 131.21, 129.21, 128.84, 126.91, 125.91, 120.16, 81.77, 62.32, 47.39, 40.67, 37.67, 35.93, 35.85, 32.46, 31.92, 24.56, 17.27, 15.93, 14.89; IR (neat): 3498, 2923, 2852, 1447, 1141 cm^{-1}; HRMS (EI) calculated for $[C_{25}H_{32}O_3S]^+$ $[M]^+$: *m/z* 412.2072, found 412.2065; mp = 61-70 °C.

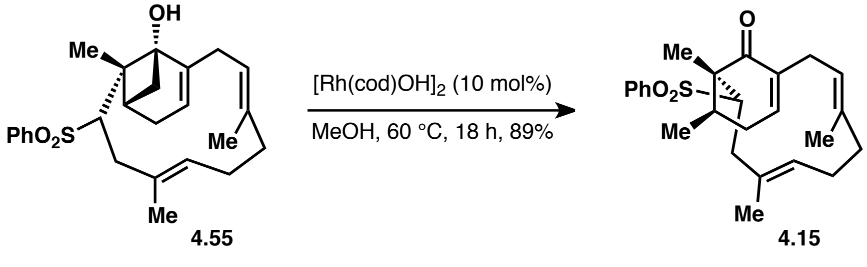

Cyclohexenone **4.15**

In the glovebox, a 4 mL vial was charged with cyclobutanol **4.55** (12.3 mg, 0.0298 mmol), $[Rh(cod)OH]_2$ (1.4 mg, 0.0030 mmol), and methanol (0.6 mL). The vial was sealed, brought out of the glovebox, and heated to 60 °C for 18 h. Upon cooling to room temperature, the mixture was concentrated and purified by column chromatography (SiO_2, 10% to 20% EtOAc/ hexanes) to yield cyclohexenone **4.15** (11.0 mg, 89%) as a white solid. $[\alpha]_D^{22}$ (*c* 0.0070, $CHCl_3$) = +23.6; ^{1}H NMR (500 MHz, $CDCl_3$): δ 7.88 (d, *J* = 7.5 Hz, 2H), 7.61 (t, *J* = 7.4 Hz,

1H), 7.52 (t, *J* = 7.7 Hz, 2H), 6.49 (dq, *J* = 4.8, 1.5 Hz, 1H), 5.03 (t, *J* = 8.1 Hz, 1H), 4.50 (t, *J* = 7.0 Hz, 1H), 3.71 (t, *J* = 4.0 Hz, 1H), 3.44 (qd, *J* = 7.2, 5.2 Hz, 1H), 3.18 (ddt, *J* = 20.1, 4.9, 2.5 Hz, 1H), 3.05 (ddd, *J* = 13.5, 7.7, 2.3 Hz, 1H), 2.53 (dd, *J* = 13.5, 8.6 Hz, 1H), 2.47 (d, *J* = 3.1 Hz, 1H), 2.36 (dd, *J* = 17.6, 4.7 Hz, 1H), 2.19 (ddt, *J* = 20.1, 5.8, 1.9 Hz, 1H), 2.01-1.80 (m, 4H), 1.46 (s, 3H), 1.39 (s, 3H), 0.96 (d, *J* = 7.1 Hz, 3H), 0.79 (s, 3H); ^{13}C NMR (126 MHz, $CDCl_3$) δ 199.56, 140.42, 140.13, 138.36, 134.08, 133.79, 129.28, 129.15, 128.46, 126.17, 123.78, 61.49, 54.12, 37.97, 36.69, 35.09, 31.58, 31.10, 24.53, 16.49, 16.17, 15.03, 14.52; IR (neat): 2917, 2851, 1670, 1303, 1146 cm^{-1}; HRMS (ESI) calculated for $[C_{25}H_{32}O_3SNa]^+$ $[M+Na]^+$: *m/z* 435.1964, found 435.1969; mp = 145-147 °C.

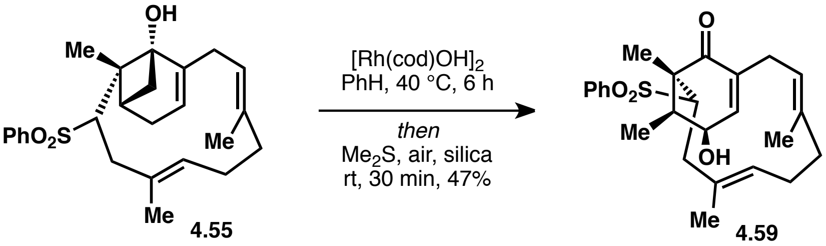

Hydroxy enone **4.59**

In the glovebox, a 4 mL vial was charged with cyclobutanol **4.55** (7.4 mg, 0.018 mmol), $[Rh(cod)OH]_2$ (1.6 mg, 0.0036 mmol), and benzene (0.4 mL). The vial was sealed, brought out of the glovebox, and heated to 40 °C for 6 h. Upon cooling to room temperature, the vial was opened and immediately added dimethyl sulfide (0.013 mL, 0.18 mmol) and dry silica gel (50 mg). This mixture was allowed to stir, open to air, for 30 min. The mixture was then filtered, concentrated, and purified by column chromatography (SiO_2, 20% to 50% EtOAc/ hexanes) to yield hydroxy enone **4.59** (3.6 mg, 47%) as a white solid. Cyclohexenone **4.15** was also isolated (0.9 mg, 12%). $[\alpha]_D^{22}$ (*c* 0.0006, $CHCl_3$) = +53; ^{1}H NMR (500 MHz, $CDCl_3$): δ 7.89 (d, *J* = 7.7 Hz, 2H), 7.59 (t, *J* = 7.4 Hz, 1H), 7.50 (t, *J* = 7.7 Hz, 2H), 6.50 (dt, *J* = 5.5, 1.8 Hz, 1H), 5.00 (t, *J* = 8.2 Hz, 1H), 4.87 (dd, *J* = 5.3, 2.9 Hz, 1H), 4.50 (t, *J* = 8.2 Hz, 1H), 4.41 (dq, *J* = 5.0, 1.1 Hz, 1H), 3.75 (qt, *J* = 7.4, 1.8 Hz, 1H), 3.51 (s, 1H), 3.06 (dd, *J* = 13.5, 7.6 Hz, 1H), 2.59 (dd, *J* = 13.6, 8.7 Hz, 1H), 2.46 (d, *J* = 17.8 Hz, 1H), 2.35 (dd, *J* = 17.9, 5.4 Hz, 1H), 2.00-1.77 (m, 4H), 1.49 (s, 3H), 1.46 (s, 3H), 0.94 (d, *J* = 7.2 Hz, 3H), 0.70 (s, 3H); ^{13}C NMR (101 MHz, $CDCl_3$) δ 199.46, 139.82, 138.87, 137.60, 134.92, 133.74, 129.21, 129.12, 129.10, 126.03, 122.78, 71.35, 62.07, 52.70, 41.28, 38.01, 35.31, 31.07, 24.70, 17.96, 16.66, 15.27, 14.52; IR (neat): 3422, 2926, 2853, 1707, 1678, 1447, 1286, 1142 cm^{-1}; HRMS (EI) calculated for $[C_{25}H_{32}O_3S]^+$ $[M]^+$: *m/z* 428.2021, found 428.2021; mp = 72-75 °C.

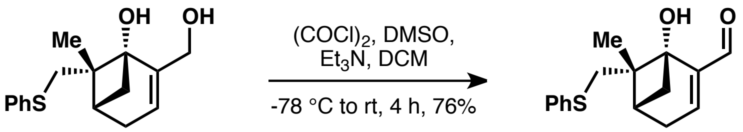

4.38 **4.39**

Aldehyde **4.39**

To a round bottomed flask containing oxalyl chloride (0.200 mL, 2.33 mmol) in dichloromethane (5.80 mL) at −78 °C was added a solution of dimethylsulfoxide (0.340 mL, 4.79 mmol) in dichloromethane (2.0 mL) over 3 min. The resulting mixture was stirred for 30 min at −78 °C, and was dropwise added a solution of allylic alcohol **4.38** (0.546 g, 1.98 mmol) over 10 min. After stirring the mixture for an additional 1 h, triethylamine (1.65 mL, 11.8 mmol) was added and the suspension warmed to room temperature. After 2 h, the suspension as diluted with H_2O (10 mL), dichloromethane (10 mL), and the phases were separated. The aqueous phase was extracted with dichloromethane (3 x 10 mL). The combined organic phases were washed with brine (10 mL), dried over magnesium sulfate, filtered, concentrated, and purified by column chromatography (SiO_2, 10% to 60% EtOAc/ hexane) to provide aldehyde **4.39** (0.412 g, 76%) as a light yellow oil. $[\alpha]_D^{22}$ (*c* 0.82, $CHCl_3$) = +85; ^{1}H NMR (600 MHz, $CDCl_3$): δ 9.45 (s, 1H), 7.28-7.23 (m, 4H), 7.16 (m, 1H), 6.73 (q, *J* = 2.6 Hz, 1H), 5.92 (s, 1H), 2.85 (d, *J* = 11.2 Hz, 1H), 2.82 (d, *J* = 11.2 Hz, 1H), 2.58 (ddd, *J* = 21.3, 2.7, 2.7 Hz, 1H), 2.53 (ddd, *J* = 21.3, 2.7, 2.7 Hz, 1H), 2.48 (dd, *J* = 9.0, 7.2 Hz, 1H), 2.24 (dd, *J* = 6.7, 2.4 Hz, 1H), 1.59 (d, *J* = 9.0 Hz, 1H), 1.45 (s, 3H); ^{13}C NMR (151 MHz, $CDCl_3$): δ 194.1, 150.7, 147.2, 137.7, 129.1, 129.0, 126.0, 79.1, 46.5, 39.1, 39.0, 33.5, 33.0, 18.4; IR (neat): 3423, 2956, 1656, 1243, 741 cm^{-1}; HRMS (ESI) calculated for $[C_{16}H_{21}O_2S]^+$ $[M+H]^+$: *m/z* 277.1257, not found.

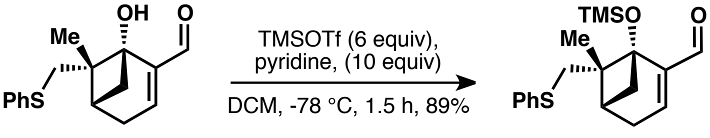

4.39 **4.73**

TMS ether **4.73**

To a round bottomed flask containing aldehyde **4.39** (1.24 g, 4.53 mmol) in dichloromethane (45.0 mL) at −78 °C was added pyridine (3.60 mL, 44.5 mmol) followed by dropwise addition of trimethylsilyl trifluoromethanesulfonate (4.90 mL, 27.1 mmol) over 5 min. The resulting mixture was stirred at −78 °C for 1.5 h, and after this time was treated with triethylamine (5.0 mL) and methanol (5.0 mL). Upon warming to room temperature, the mixture was diluted with H_2O (30 mL), EtOAc (30 mL), hexanes (30 mL). After separation of the phases, the organic phase was washed with 5% aqueous solution of citric acid (3 x 25 mL), and brine (30 mL). The organic phase was dried ($MgSO_4$), filtered, and concentrated *in vacuo*. The crude product was purified by column chromatography (SiO_2, 5% to 20% EtOAc/ hexanes) to provide TMS ether **4.73** (1.40 g, 89%) as a yellow-orange solid. $[\alpha]_D^{22}$ (*c* 1.23, $CHCl_3$) = +45.6; ^{1}H NMR (600 MHz, $CDCl_3$): δ 9.63 (s, 1H), 7.28-7.21 (m, 4H), 7.14 (m, 1H), 6.69 (q, *J* = 2.7 Hz, 1H), 2.88 (d, *J* = 11.4 Hz, 1H), 2.85 (d, *J* = 11.4 Hz, 1H), 2.57 (dd, *J* = 8.4, 7.4 Hz, 1H), 2.47 (ddd, *J* = 20.9, 2.8, 2.8 Hz, 1H), 2.40 (ddd, *J* = 20.9, 2.8, 2.8 Hz, 1H), 2.30 (m, 1H), 1.63 (d, *J* = 8.8 Hz, 1H), 1.39 (s, 3H), −0.2 (s, 9H); ^{13}C NMR (151 MHz, $CDCl_3$): δ 190.3, 148.2, 140.3, 137.7, 129.3, 128.9, 125.9, 79.3, 46.1, 39.1, 38.8, 34.7, 32.0, 19.0, 1.7; IR (neat): 3436, 2957, 1657, 1245, 741 cm^{-1}; HRMS (EI) calculated for $[C_{19}H_{26}O_2SSi]^+$ $[M]^+$: *m/z* 346.1423, found 346.1421; mp = 49-51 °C.

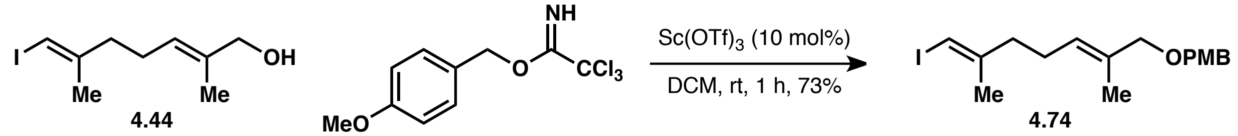

Vinyl iodide **4.74**

A 250 mL flask was charged with alcohol **4.44** (1.49 g, 5.60 mmol), 4-methoxybenzyl-2,2,2-trichloroacetimidate (2.37 g, 8.40 mmol), and toluene (55 mL). The solution was cooled to 0 °C, then a solution of $Sc(OTf)_3$ (138 mg, 0.280 mmol) in acetonitrile (1.5 mL) was added dropwise (5 min). This mixture was stirred for 40 min at 0 °C. $NaHCO_3$ (40 mL) was added and the mixture was extracted with diethyl ether (3 x 30 mL). The organics were dried over magnesium sulfate, filtered, concentrated, and purified by column chromatography (SiO_2, 30% to 90 % DCM/ hexane) to give vinyl iodide **4.74** (1.57 g, 73%) as a pale yellow oil. ^1H NMR (400 MHz, $CDCl_3$): δ 7.28-7.23 (m, 2H), 6.88 (d, J = 8.7 Hz, 2H), 5.89 (br s, 1H), 5.36 (t, J = 6.5 Hz, 1H), 4.37 (s, 2H), 3.86 (s, 2H), 3.81 (s, 3H), 2.30-2.15 (m, 4H), 1.84 (s, 3H), 1.66 (s, 3H); ^{13}C NMR (100 MHz, $CDCl_3$): δ 159.2, 147.7, 133.3, 130.8, 129.5, 126.7, 113.9, 75.9, 75.1, 71.3, 55.4, 39.2, 26.1, 24.0, 14.1; IR (neat): 2911, 2849, 1612, 1511, 1244, 818 cm^{-1}; HRMS (EI) calculated for $[C_{17}H_{23}O_2I]^+$ $[M]^+$: m/z 386.0743, found 386.0739.

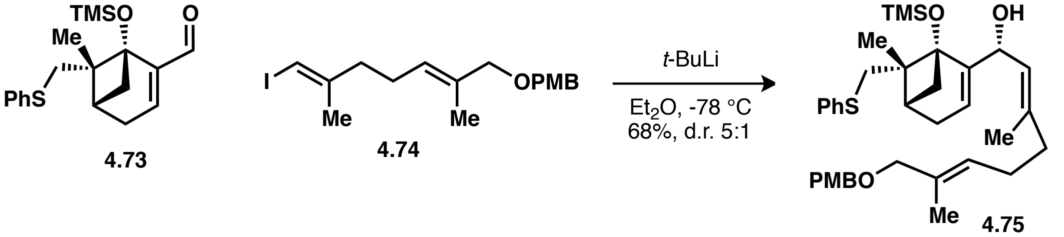

Bis-allylic alcohol **4.75**

To a round bottomed flask containing vinyl iodide **4.74** (1.38 g, 3.57 mmol) in diethyl ether (15 mL) at -78 °C was dropwise added a solution of *tert*-butyllithium (1.55 M in hexanes, 4.6 mL, 7.15 mmol) over 5 min. The resulting mixture was stirred for 15 min, and was then added a solution of silyl ether **4.73** (0.95 g, 2.75 mmol) in diethyl ether (16.5 mL) over 10 min. After stirring the suspension for 4 h, the reaction was treated with a saturated aqueous solution of NH_4Cl (15 mL) then warmed to room temperature. The mixture was diluted with EtOAc (50 mL), H_2O (15 mL), and the phases were separated. The aqueous phase was extracted with EtOAc (3 x 40 mL). The combined organic phases were washed with brine (40 mL), dried ($MgSO_4$), filtered, and concentrated *in vacuo*. The crude mixture was purified by column chromatography (SiO_2, 10% to 30% EtOAc/ hexanes) to provide bis-allylic alcohol **4.75** (935 mg, 56% major product) as a light yellow oil (also isolated was 195 mg, 12% of the minor diastereomer). $[\alpha]_D^{22}$ (c 0.98, $CHCl_3$) = + 26; ^1H NMR (400 MHz, C_6D_6): δ 7.32 (d, J = 7.6 Hz, 2H), 7.28 (d, J = 8.4 Hz, 2H), 7.02 (t, J = 7.6 Hz, 2H), 6.90 (t, J = 7.3 Hz, 1H), 6.82 (d, J = 8.4 Hz, 2H), 5.53 (d, J = 7.9 Hz, 1H), 5.50-5.42 (m, 2H), 5.11 (t, J = 6.8 Hz, 1H), 4.37 (s, 2H), 3.85 (s, 2H), 3.32 (s, 3H), 3.29 (d, J = 11.3 Hz, 1H), 2.98 (d, J = 11.3 Hz, 1H), 2.29 (t, J = 7.7 Hz, 1H), 2.25-2.12 (m, 3H), 2.12-1.95 (m, 5H), 1.67 (s, 3H), 1.64 (s, 3H), 1.57 (d, J = 8.3 Hz, 1H), 1.38 (s, 3H), 0.20 (s, 9H); ^{13}C NMR (101 MHz, C_6D_6): δ 159.7, 152.0, 139.3, 136.2, 133.2, 131.4, 129.5, 129.1, 128.7, 127.4, 125.5, 119.4, 114.1, 81.4, 76.1, 71.5, 68.4, 54.8, 46.8, 40.0, 39.7, 38.7, 25.3, 30.8, 26.4, 19.9, 16.8, 14.2, 2.4; IR (neat): 2953, 2934, 1612, 1512, 1248, 840 cm^{-1}; HRMS (ESI) calculated for $[C_{36}H_{49}O_3SSi]^+$ $[M\text{-}OH^-]^+$: *m/z* 589.3166, found 589.3170.

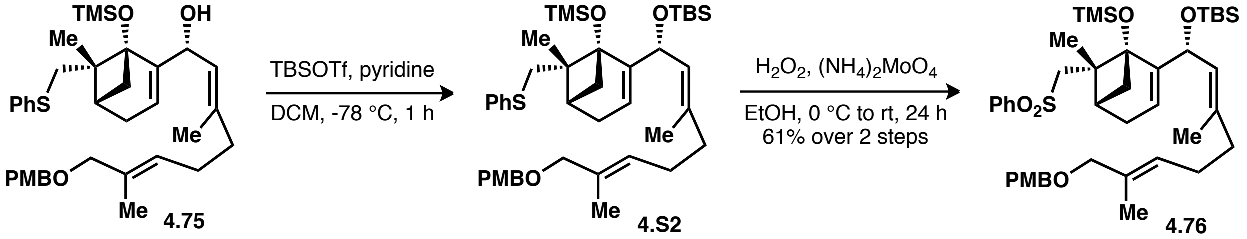

Sulfone **4.76**

A 50 mL flask was charged with alcohol **4.75** (930 mg, 1.53 mmol), dichloromethane (15 mL) and pyridine (0.62 mL, 7.66 mmol) and cooled to -78 °C. *tert*-Butyldimethylsilyl trifluoromethanesulfonate (1.06 mL, 4.60 mmol) was added dropwise (3 min) and the reaction was allowed to stir for 1.5 h. Methanol (2 mL) and triethylamine (2 mL) were added and the mixture was warmed to room temperature. Water (15 mL), hexane (10 mL), and ethyl acetate (10 mL) were added, then the mixture was washed with citric acid (2 x 20 mL) and brine (1 x 20 mL). The organics were dried over magnesium sulfate, filtered, and concentrated to yield silyl ether **4.S2**. The material was carried on without further purification.

A 500 mL flask was charged with silyl ether **4.S2** (1.53 mmol), ethanol (150 mL), and ammonium ortho-molybdate (450 mg, 2.29 mmol) and cooled to 0 °C. Hydrogen peroxide (3.5 mL, 30%, 31 mmol) was added dropwise (5 min). After stirring for 1 h, the reaction was allowed to warm to room temperature and stir an additional 15 h. Then, another portion of ammonium ortho-molybdate (300 mg, 1.53 mmol) and hydrogen peroxide (3.5 mL, 31 mmol) were added and stirring was continued for 15 h. After partial evaporation of the ethanol, water (200 mL) was added and the mixture was extracted with diethyl ether (3 x 100 mL). The organics were dried over magnesium sulfate, filtered, concentrated, and purified by column chromatography (SiO_2, 20% EtOAc/ hexanes with 1% triethyl amine) to provide sulfone **4.76** (701 mg, 61%) as a colorless oil. $[\alpha]_D^{22}$ (*c* 1.15, $CHCl_3$) = +17.4; ^1H NMR (600 MHz, C_6D_6): δ 7.87 (d, *J* = 7.3 Hz, 2H), 7.30 (d, *J* = 8.4 Hz, 2H), 6.99-6.92 (m, 3H), 6.83 (d, *J* = 8.4 Hz, 2H), 5.80 (br s, 1H), 5.34 (t, *J* = 6.7 Hz, 1H), 5.09 (d, *J* = 7.7 Hz, 1H), 4.98 (d, *J* = 7.7 Hz, 1H), 4.40 (s, 2H), 3.89 (s, 2H), 3.58 (d, *J* = 14.1 Hz, 1H), 3.32 (s, 3H), 2.91 (d, *J* = 14.1 Hz, 1H), 2.78 (d, *J* = 18.2 Hz, 1H), 2.66 (dd, *J* = 7.1, 2.8 Hz, 1H), 2.37 (t, *J* = 7.7 Hz, 1H), 2.29 (dq, *J* = 18.5, 3.0, 2.7 Hz, 1H), 1.95-1.86 (m, 2H), 1.73 (s, 3H), 1.70-1.61 (m, 1H), 1.64 (s, 3H), 1.60 (d, *J* = 8.3 Hz, 1H), 1.51 (s, 3H), 0.99 (s, 9H), 0.14 (s, 9H), 0.11 (s, 3H), 0.11 (s, 3H); ^{13}C NMR (151 MHz, C_6D_6): δ 159.8, 152.1, 135.7, 133.1, 132.8, 131.4, 129.5, 129.2, 128.3, 127.5, 127.1, 117.5, 114.1, 81.4, 76.1, 71.7, 68.1, 61.0, 54.8, 45.3, 40.5, 39.8, 36.3, 31.9, 26.1, 19.3, 18.5, 17.4, 14.1, 2.2, −4.1, −4.5; IR (neat): 2954, 2854, 1613, 1513, 1307, 1250, 1148, 837 cm^{-1}; HRMS (ESI) calculated for $[C_{42}H_{64}O_6SSi_2Na]^+$ $[M+Na]^+$: *m/z* 775.3854, found 775.3864.

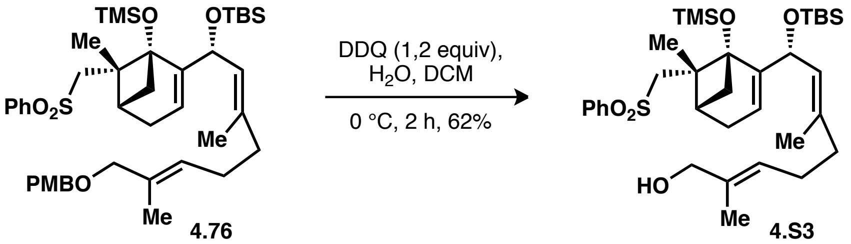
TMSO
OTBS
Me
PhO$_2$S
Me
PMBO
Me
4.76
DDQ (1,2 equiv),
H$_2$O, DCM
0 °C, 2 h, 62%
TMSO
OTBS
Me
PhO$_2$S
Me
HO
Me
4.S3

Alcohol **4.S3**

To round bottomed flask containing PMB ether **4.76** (302 mg, 0.401 mmol) in dichloromethane (8.0 mL) at 0 °C was added H_2O (0.45 mL) followed by DDQ (106 mg, 0.467 mmol) over 3 min. The resulting green suspension was stirred for 2 h, after which time the orange-yellow suspension was treated with H_2O (10 mL), dichloromethane (10 mL), and EtOAc (5 mL). The phases were separated, and the aqueous phase was extracted with 10:1 dichloromethane/EtOAc (3 x 11 mL). The combined organic phases were washed with a saturated aqueous solution of $NaHCO_3$ (15 mL), brine (15 mL), and dried ($MgSO_4$). The crude suspension was filtered, and concentrated. The crude product was purified by column chromatography (SiO_2, 10% to 50% EtOAc + 0.1% Et_3N in hexanes) to provide alcohol **4.S3** (157 mg, 62%) as a colorless oil. $[\alpha]_D^{22}$ (*c* 1.05, $CHCl_3$) = +21.3; ^1H NMR (400 MHz, C_6D_6): δ 7.87 (m, 2H), 7.02-6.92 (m, 3H), 5.78 (br s, 1H), 5.30 (app t, *J* = 6.8 Hz, 1H), 5.11 (d, *J* = 7.7 Hz, 1H), 4.97 (d, *J* = 7.7 Hz, 1H), 3.93 (br s, 2H), 3.56 (d, *J* = 14.2 Hz, 1H), 2.98 (d, *J* = 14.2 Hz, 1H), 2.70 (dt, *J* = 18.3, 3.1, 2.7 Hz, 1H), 2.63 (dd, *J* = 6.8, 2.4 Hz, 1H), 2.37 (d, *J* = 7.9, 7.9 Hz, 1H), 2.27 (dq, *J* = 18.4, 2.9 Hz, 1H), 1.99-1.83 (m, 2H), 1.70 (s, 3H), 1.71-1.63 (m, 2H), 1.59 (d, *J* = 8.4 Hz, 1H), 1.56 (s, 3H), 1.47 (s, 3H), 0.98 (s, 9H), 0.14 (s, 9H), 0.10 (s, 3H), 0.10 (s, 3H); ^{13}C NMR (101 MHz, C_6D_6): δ 152.2, 143.3, 135.9, 132.9, 129.2, 128.6, 128.4, 127.5, 124.6, 117.2, 81.4, 68.6, 68.2, 60.8, 45.2, 40.4, 39.6, 36.2, 31.8, 26.1, 25.6, 19.2, 18.5, 17.4, 13.8, 2.2, −4.2, −4.6; IR (neat): 3542, 2954, 2928, 2855, 1306, 1252, 1176, 915, 690 cm^{-1}; HRMS (ESI) calculated for $[C_{34}H_{56}O_5SSi_2Na]^+$ $[M+Na]^+$: *m/z* 655.3279, found 655.3288.

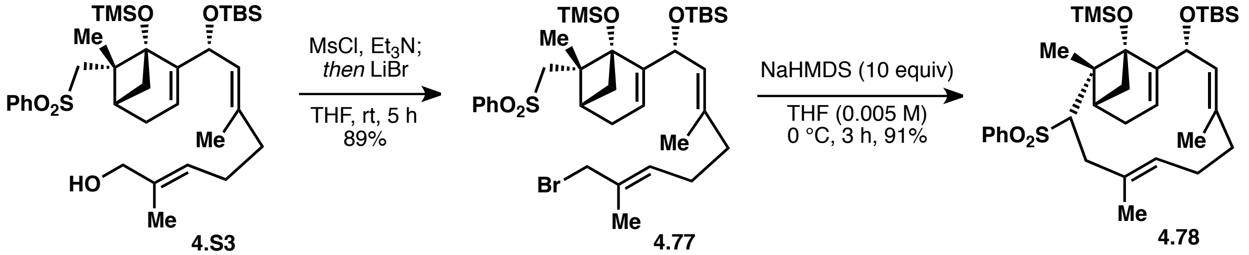
TMSO
OTBS
Me
PhO$_2$S
Me
HO
Me
4.S3
MsCl, Et$_3$N;
then LiBr
THF, rt, 5 h
89%
TMSO
OTBS
Me
PhO$_2$S
Me
Br
Me
4.77
NaHMDS (10 equiv)
THF (0.005 M)
0 °C, 3 h, 91%
TMSO
OTBS
Me
PhO$_2$S
Me
Me
4.78

Macrocycle **4.78**

To a round bottomed flask containing allyl alcohol **4.S3** (57.2 mg, 90.4 μmol) in tetrahydrofuran (3.0 mL) at 0 °C was added triethylamine (0.060 mL, 0.43 mmol) followed by methanesulfonyl chloride (0.020 mL, 0.26 mmol). The resulting mixture was stirred for 80 min at 0 °C, and was dropwise added a solution of lithium bromide (39.2 mg, 0.451 mmol) solution in tetrahydrofuran (0.40 mL). Following an additional 3 h at 0 °C, the reaction was treated with H_2O (3 mL), EtOAc (5 mL), hexanes (5 mL), and the phases were separated. The aqueous phase was extracted with 1:1 EtOAc/hexanes (3 x 5 mL). The combined organic phases were washed with brine (2 mL), dried ($MgSO_4$), filtered, and concentrated. The crude product was filtered through a silica gel pipette plug, and rinsed with 1:1 EtOAc/hexanes (15 mL). Upon concentration, crude allyl bromide **4.77** was used in the next step without further purification.

To a round bottomed flask containing crude allyl bromide **4.77** in tetrahydrofuran (6.2 mL) at 0 °C was dropwise added a solution of sodium bis(trimethylsilyl)amide (2.0 M solution in tetrahydrofuran, 0.18 mL, 0.36 mmol) over 4 min. The resulting yellow mixture was stirred for 2.5 h in an ice-water bath. After this time, the reaction was treated with a saturated aqueous solution of NH_4Cl (0.5 mL), EtOAc (5 mL), and H_2O (5 mL). The phases were separated, and the aqueous phase was extracted with EtOAc (3 x 5 mL). The combined organic phases were washed with brine (5 mL), dried ($MgSO_4$), filtered, and concentrated *in vacuo*. Purification of the crude product by column chromatography (SiO_2, 10% to 20% EtOAc/ hexanes) provided macrocycle **4.78** (45.7 mg, 82% over 2 steps) as a colorless oil. $[\alpha]_D^{22}$ (*c* 0.76, $CHCl_3$) = +22; ^1H NMR (600 MHz, C_6D_6): δ 7.87 (m, 2H), 6.94-6.87 (m, 3H), 5.95 (d, *J* = 2.9 Hz, 1H), 5.01 (d, *J* = 8.5 Hz, 1H), 4.93 (d, *J* = 8.5 Hz, 1H), 4.29 (t, *J* = 7.4 Hz, 1H), 4.02 (dd, *J* = 6.2, 2.6 Hz, 1H), 3.30 (ddd, *J* = 19.0, 2.5 Hz, 1H), 2.94 (dq, *J* = 5.8, 2.8 Hz, 1H), 2.88 (dd, *J* = 18.2, 6.2 Hz, 1H), 2.54 (d, *J* = 18.2 Hz, 1H), 2.45 (dd, *J* = 8.1, 7.2 Hz, 1H), 2.37 (ddd, *J* = 19.0, 3.0, 3.0 Hz, 1H), 1.92-1.77 (m, 3H), 1.75 (s, 3H), 1.68 (d, *J* = 8.2 Hz, 1H), 1.67-1.62 (m, 1H), 1.52 (d, *J* = 1.2 Hz, 3H), 1.09 (s, 3H), 1.02 (s, 9H), 0.17 (s, 9H), 0.16 (s, 3H), 0.15 (s, 3H); ^{13}C NMR (151 MHz, C_6D_6): δ 153.8, 142.4, 132.7, 132.5, 131.2, 130.1, 129.1, 128.8, 123.2, 120.6, 83.1, 66.9, 63.3, 49.3, 42.2, 39.2, 38.8, 36.0, 32.2, 26.0, 23.9, 18.5, 17.4, 17.0, 16.2, 2.3, −3.5, −4.1; IR (neat): 2954, 2927, 2855, 1304, 1252, 1171, 1026, 835 cm^{-1}; HRMS (EI) calculated for $[C_{34}H_{54}O_4SSi_2]^+$ $[M]^+$: *m/z* 614.3281, found 614.3265.

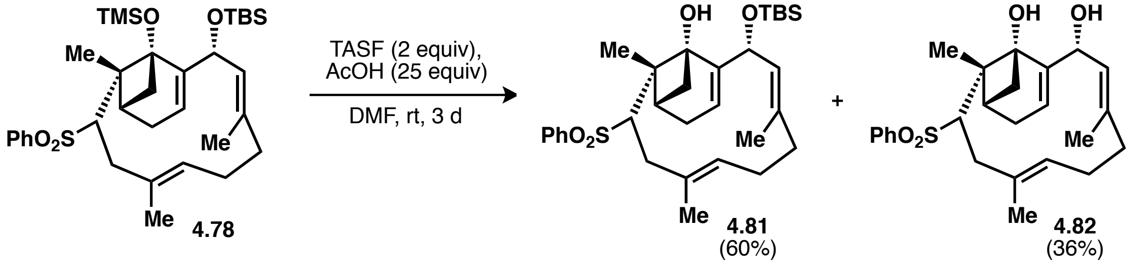

Alcohol **4.81** and diol **4.82**

To round bottomed flask with macrocycle **4.78** (39.6 mg, 64.4 μmol) in *N*,*N*-dimethylformamide (2.6 mL) at 0 °C was added glacial acetic acid (0.075 mL, 1.3 mmol), followed by tris(dimethylamino)sulfonium difluorotrimethylsilicate (37.2 mg, 0.135 mmol) in *N*,*N*-dimethylformamide (0.40 mL). The resulting mixture was stirred for 67 h, and was then treated with pH 7 buffer (1 mL), EtOAc (5 mL), H_2O (5 mL). The phases were separated, and the aqueous phase was extracted with EtOAc (3 x 5 mL). The combined organic phases were washed with brine (5 mL), dried ($MgSO_4$), filtered, and concentrated. The crude products were purified by column chromatography (SiO_2, 10% to 80% EtOAc in hexanes) to provide alcohol **4.81** (21.1 mg, 60%) as a colorless oil and diol **4.82** (9.9 mg, 20%) as an off-white solid.

Data for alcohol **4.81**:
$[\alpha]_D^{22}$ (*c* 0.945, $CHCl_3$) = +14.1; ^1H NMR (400 MHz, C_6D_6): δ 7.84 (dt, *J* = 7.1, 1.9 Hz, 2H), 6.90 (tt, *J* = 7.2, 1.4 Hz, 1H), 6.88-6.84 (m, 2H), 6.07 (dq, *J* = 4.3, 2.1 Hz, 1H), 5.21 (dq, *J* =

10.1, 2.1 Hz, 1H), 4.76 (d, *J* = 10.0 Hz, 1H), 4.47 (dd, *J* = 10.3, 4.1 Hz, 1H), 3.76 (dd, *J* = 6.9, 1.3 Hz, 1H), 3.37 (dq, *J* = 19.0, 2.1 Hz, 1H), 3.06 (dq, *J* = 5.4, 2.5 Hz, 1H), 2.71 (d, *J* = 15.9 Hz, 1H), 2.64 (dd, *J* = 15.9, 7.1 Hz, 1H), 2.52 (dd, *J* = 8.4, 6.7 Hz, 1H), 2.42 (dq, *J* = 19.1, 3.5 Hz, 1H), 1.96 (m, 1H), 1.93 (s, 3H), 1.92 (m, 1H), 1.68 (d, *J* = 8.4 Hz, 1H), 1.62 (m, 1H), 1.59 (s, 3H), 1.50 (m, 1H), 0.97 (s, 9H), 0.68 (s, 3H), 0.09 (s, 3H), 0.08 (s, 3H); ^{13}C NMR (101 MHz, C_6D_6): δ 150.0, 141.3, 132.8, 132.8, 132.2, 130.6, 129.0, 127.0, 118.1, 81.3, 67.3, 62.7, 47.4, 41.1, 38.4, 36.9, 35.3, 32.2, 26.2, 24.6, 18.6, 18.4, 16.4, 14.8, −4.3, −4.6; IR (neat): 3522, 2954, 2931, 2855, 1446, 1303, 1141, 1069, 835 cm^{-1}; HRMS (EI) calculated for $[C_{30}H_{43}O_4SSi]^+$ $[M-Me^-]^+$: *m/z* 527.2651, found 527.2657.

Data for diol **4.82**:
$[\alpha]_D^{22}$ (*c* 0.0035, $CHCl_3$) = −16.1; ^{1}H NMR (500 MHz, $CDCl_3$): δ 7.88 (d, *J* = 7.6 Hz, 2H), 7.64 (t, *J* = 7.4 Hz, 1H), 7.57 (t, *J* = 7.6 Hz, 2H), 5.79 (h, *J* = 2.3 Hz, 1H), 5.10 (dq, *J* = 10.5, 1.7 Hz, 1H), 4.74 (dd, *J* = 10.7, 3.6 Hz, 1H), 4.65 (d, *J* = 10.3 Hz, 1H), 3.56 (dd, *J* = 6.2, 2.6 Hz, 1H), 3.02 (dq, *J* = 19.1, 2.4 Hz, 1H), 2.80 (dq, *J* = 5.5, 2.8 Hz, 1H), 2.59 – 2.47 (m, 3H), 2.39 (dq, *J* = 19.1, 3.5 Hz, 1H), 2.33 – 2.14 (m, 2H), 2.08 (s, 1H), 2.01 – 1.94 (m, 1H), 1.88 (ddd, *J* = 15.3, 10.0, 4.9 Hz, 1H), 1.68 (d, *J* = 8.4 Hz, 1H), 1.67 (s, 3H), 1.63 (s, 3H), 0.76 (s, 3H); ^{13}C NMR (126 MHz, $CDCl_3$) δ 148.97, 140.09, 136.15, 133.59, 132.49, 129.34, 128.84, 128.33, 127.25, 117.29, 80.83, 65.94, 62.44, 46.88, 40.32, 37.71, 36.29, 35.12, 31.65, 24.46, 18.36, 15.98, 14.81; IR (neat): 3487, 2956, 2924, 2853, 1446, 1140 cm^{-1}; HRMS (ESI) calculated for $[C_{25}H_{33}O_4S]^+$ $[M+H]^+$: *m/z* 429.2094, not found.

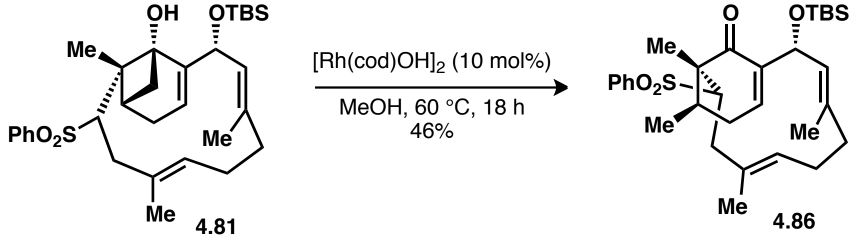

Cyclohexenone **4.86**

In the glovebox, a 4 mL vial was charged with cyclobutanol **4.81** (32 mg, 0.059 mmol), $[Rh(cod)OH]_2$ (2.7 mg, 0.0059 mmol), and methanol (1.2 mL). The vial was sealed, brought out of the glovebox, and heated to 60 °C for 18 h. Upon cooling to room temperature, the mixture was concentrated and purified by column chromatography (SiO_2, 10% EtOAc/ hexanes) to yield cyclohexenone **4.86** (14.7 mg, 46%) as a colorless oil. $[\alpha]_D^{22}$ (*c* 0.47, $CHCl_3$) = +45.3; ^{1}H NMR (500 MHz, $CDCl_3$): δ 7.91 (d, *J* = 7.3 Hz, 2H), 7.63 (t, *J* = 7.5 Hz, 1H), 7.55 (t, *J* = 7.6 Hz, 2H), 6.96 (dd, *J* = 6.3, 2.0 Hz, 1H), 5.18 (dd, *J* = 9.4, 2.0 Hz, 1H), 4.61 (t, *J* = 6.7 Hz, 1H), 4.47 (d, *J* = 9.4 Hz, 1H), 3.56 (dd, *J* = 5.4, 3.0 Hz, 1H), 3.49 (qt, *J* = 6.8, 5.1, 1.8 Hz, 1H), 3.23 (ddt, *J* = 20.1, 4.7, 2.3 Hz, 1H), 2.52–2.47 (m, 2H), 2.30 (ddt, *J* = 20.2, 6.0, 1.5 Hz, 1H), 2.03–1.83 (m, 3H), 1.64 (s, 3H), 1.40 (s, 3H), 0.95 (d, *J* = 7.0 Hz, 3H), 0.87 (s, 9H), 0.85 (d, *J* = 7.7 Hz, 1H), 0.66 (s, 3H), 0.01 (s, 6H); ^{13}C NMR (126 MHz, $CDCl_3$) δ 198.25, 141.05, 140.13, 139.92, 134.57, 133.88, 129.98, 129.35, 129.30, 127.84, 127.78, 66.21, 61.96, 53.90, 36.83, 36.68, 36.05, 31.47, 26.04, 24.24, 18.40, 17.00, 16.30, 16.27, 13.83, -4.39, -4.78; IR (neat): 2953, 2928, 2854, 1673, 1447, 1305, 1147, 1084, 835 cm^{-1}; HRMS (EI) calculated for $[C_{31}H_{46}O_4SSi]^+$ $[M]^+$: *m/z* 542.2886, found 542.2879.

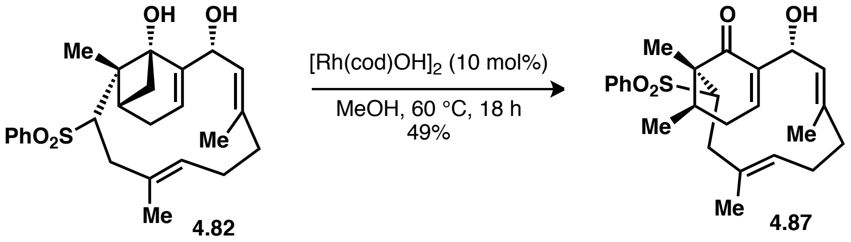

Cyclohexenone **4.87**

In the glovebox, a 4 mL vial was charged with cyclobutanol **4.82** (32 mg, 0.075 mmol), $[Rh(cod)OH]_2$ (3.4 mg, 0.0075 mmol), and methanol (1.5 mL). The vial was sealed, brought out of the glovebox, and heated to 60 °C for 18 h. Upon cooling to room temperature, the mixture was concentrated and purified by column chromatography (SiO_2, 20% to 50% EtOAc/ hexanes) to yield cyclohexenone **4.87** (15.6 mg, 49%) as a white foam. ^1H NMR (500 MHz, $CDCl_3$) δ 7.92 (d, *J* = 7.7 Hz, 2H), 7.64 (t, *J* = 7.4 Hz, 1H), 7.56 (t, *J* = 7.6 Hz, 2H), 6.98 (d, *J* = 6.0 Hz, 1H), 5.27 (d, *J* = 9.7 Hz, 1H), 4.59 (t, *J* = 6.6 Hz, 1H), 4.47 (d, *J* = 9.7 Hz, 1H), 3.56 (dd, *J* = 5.8, 2.6 Hz, 1H), 3.50 (p, *J* = 6.8 Hz, 1H), 3.22 (dd, *J* = 20.2, 4.8 Hz, 1H), 2.56–2.44 (m, 2H), 2.33 (dd, *J* = 20.3, 6.1 Hz, 1H), 2.06–1.87 (m, 4H), 1.69 (s, 3H), 1.59 (d, *J* = 3.8 Hz, 1H), 1.39 (s, 3H), 0.97 (d, *J* = 7.1 Hz, 3H), 0.67 (s, 3H); ^{13}C NMR (126 MHz, $CDCl_3$) δ 198.20, 140.15, 140.07, 139.32, 137.65, 133.94, 130.02, 129.39, 129.33, 127.98, 126.93, 65.39, 61.98, 53.82, 36.65, 36.47, 36.06, 31.36, 24.21, 17.18, 16.32, 16.28, 13.81; IR (neat): 3503, 2923, 2852, 1670, 1302, 1144 cm^{-1}; HRMS (EI) calculated for $[C_{25}H_{32}O_4S]^+$ $[M]^+$: *m/z* 428.2021, found 428.2022.

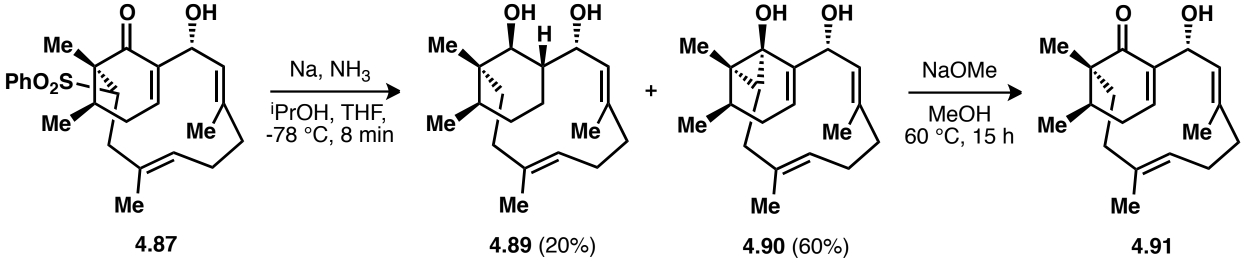

De-sulfonylated enone **4.91** and diol **4.89**

A 10 mL Schlenk tube was evacuated and filled with argon. Ammonia (1.0 mL) was condensed into the tube at -78 °C. Then, a solution of sulfone **4.87** (13 mg, 0.30 mmol) in tetrahydrofuran (0.5 mL) and isopropanol (0.2 mL) was added to the liquid ammonia. Tetrahydrofuran (0.3 mL) was used to wash down the sides of the tube. This solution was stirred at -78 °C for 2 min. Then, sodium (2 small balls, ~50 mg) was added. The mixture was stirred vigorously (to break up the sodium) for 8 min. Then, solid ammonium chloride (0.5 g) and diethyl ether (1 mL) were added and the flask was allowed to warm to room temperature to evaporate the ammonia. Water (2 mL) was then added and the mixture was extracted with diethyl ether (3 x 1 mL). The organics were dried over magnesium sulfate, filtered, and concentrated to yield a crude mixture of diol **4.89** and cyclopropanol **4.90** (1:4 ratio).

A 4 mL vial was charged with the crude mixture of **4.89** and **4.90**, methanol (0.3 mL), and sodium methoxide (0.3 mL, 0.5 M MeOH, 0.15 mmol). The vial was sealed and heated to 60

°C for 12 h. Upon cooling to room temperature, ammonium chloride (0.3 mL) and water (0.5 mL) were added and the mixture was extracted with diethyl ether (3 x 1 mL). The organics were dried over magnesium sulfate, filtered, concentrated, and purified by column chromatography (SiO_2, 20% to 50% EtOAc/ hexane) to yield enone **4.91** (2.3 mg, 26%) as a white foam and diol **4.89** (1.6 mg, 18%) as a colorless oil.

Data for enone **4.91**
$[\alpha]_D^{22}$ (*c* 0.0015, $CHCl_3$) = +182; ^{1}H NMR (600 MHz, $CDCl_3$) δ 6.92 (dt, *J* = 6.3, 1.8 Hz, 1H), 5.39 (d, *J* = 9.5 Hz, 1H), 4.63–4.58 (m, 2H), 2.43–2.05 (m, 7H), 1.98–1.86 (m, 3H), 1.73 (s, 3H), 1.62 (s, 3H), 1.44 (bs, 1H), 1.36 (dd, *J* = 14.7, 7.6 Hz, 1H), 0.92 (d, *J* = 6.4 Hz, 3H), 0.85 (s, 3H); ^{13}C NMR (126 MHz, $CDCl_3$) δ 202.13, 141.59, 138.11, 137.99, 135.75, 128.25, 124.13, 65.78, 48.04, 39.49, 34.53, 33.09, 31.11, 30.50, 25.97, 19.02, 16.01, 15.52, 14.72; IR (neat): 3369, 2956, 2919, 2852, 1666, 1367 cm^{-1}; HRMS (EI) calculated for $[C_{19}H_{28}O_2]^+$ $[M]^+$: *m/z* 288.2089, found 288.2083.

Data for diol **4.89**
$[\alpha]_D^{22}$ (*c* 0.0013, $CHCl_3$) = +68.3; ^{1}H NMR (600 MHz, $CDCl_3$) δ 5.24 (d, *J* = 10.5 Hz, 1H), 1.62 – 1.53 (m, 1H), 5.08 (d, *J* = 11.7 Hz, 1H), 4.76 (dd, *J* = 10.5, 5.0 Hz, 1H), 3.99 (dd, *J* = 10.8, 6.8 Hz, 1H), 2.46 (dtd, *J* = 15.1, 12.2, 11.7, 3.8 Hz, 1H), 2.32 – 2.23 (m, 2H), 2.17 (td, *J* = 12.6, 4.1 Hz, 1H), 2.04 (d, *J* = 12.9 Hz, 1H), 1.92 (dd, *J* = 10.9, 2.7 Hz, 1H), 1.82 (tt, *J* = 16.5, 4.9 Hz, 2H), 1.70 (s, 3H), 1.68 (d, *J* = 1.3 Hz, 3H), 1.43 (dq, *J* = 13.4, 3.3 Hz, 1H), 1.28 – 1.16 (m, 3H), 1.08 (qd, *J* = 14.2, 13.3, 3.9 Hz, 1H), 0.92 – 0.82 (m, 1H), 0.81 (d, *J* = 6.8 Hz, 3H), 0.68 (s, 3H); ^{13}C NMR (126 MHz, $CDCl_3$) δ 139.17, 136.97, 128.18, 124.96, 74.55, 69.41, 43.00, 42.30, 41.04, 34.74, 34.57, 29.28, 29.00, 25.77, 22.72, 16.10, 15.41, 15.24, 14.35; IR (neat): 3224, 2960, 2923, 2855, 1445, 1038 cm^{-1}; HRMS (EI) calculated for $[C_{19}H_{32}O_2]^+$ $[M]^+$: *m/z* 292.2402, found 292.2407.

Supplementary Table 1: Allylic oxidation conditions screened on **4.15**

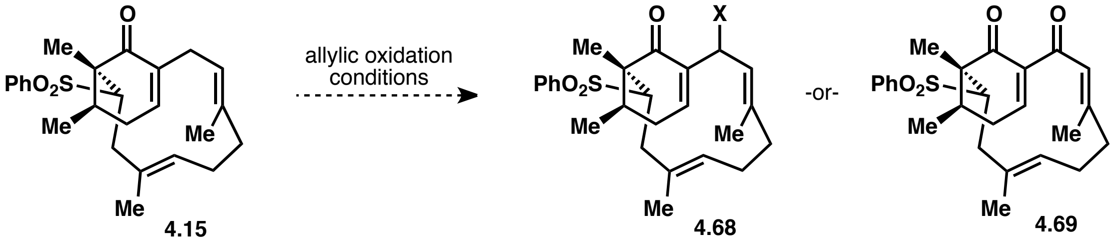

O
Me
PhO_2S
Me
Me
Me
4.15
allylic oxidation
conditions
O
X
Me
PhO_2S
Me
Me
Me
4.68
-or-
O
O
Me
PhO_2S
Me
Me
Me
4.69

entry	conditions	result
1	$Mn(OAc)_3$, TBHP, 3A MS, EtOAc, rt, 24 h	SM -> degradation
2	NBS, $(PhCOO)_2$, CCl_4, rt or 80 °C, 1 h	degradation
3	O_2, AIBN, MeCN, 60 °C, 1.5 h	degradation
4	Cr(V) complex **4.S5**, MnO_2, 15-crown-5, $PhCF_3$, 60 °C, 20 h	no rxn @ rt, slow degradation @ 60 °C
5	phenylglyoxylic acid, TBHP, TBAI, PhH, 80 °C, 15 h	SM
6	SeO_2, dioxane, rt or 80 °C, 2 h	degradation @ rt or 80 °C
7	$Pd(OH)_2/C$, TBHP, K_2CO_3, DCM, rt, 20 h	SM + **4.S4**
8	mCPBA, DCM, rt, 30 min	**4.S4**, quant, 4:1 d.r.
9	NCS, $(PhCOO)_2$, CCl_4, 80 °C, 1 h	one major comp **4.71**; minor comp **4.S4** (?)
10	TEMPO, $(PhCOO)_2$, CCl_4, 80 °C, 18 h	SM, degradation
11	$Rh_2(cap)_4$, TBHP, K_2CO_3, DCM, 40 °C, 4 h	SM + **4.71** (Cl incorporation from DCM?!?)
12	$Rh_2(cap)_4$, TBHP, K_2CO_3, EtOAc, 40 °C, 6 h	SM, degradation
13	CAN, silica, H_2O, DCM, rt, 5 min	SM + several new comps
14	IBX, DMSO, 80 °C, 18 h	SM, degradation
15	I_2O_5, H_2O, THF, rt or 60 °C, 1 h	no rxn @ rt, messy but new comps @ 60 °C
16	$Co(OAc)_2$, AcOOH, AcOH, rt or 60 °C, 15 h	SM

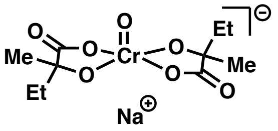

O
O
Me
O
Cr
O
O
Et
Et
Me
O
O
O
$Na^{\oplus}$
$\ominus$

Cr(V) complex **4.S5**

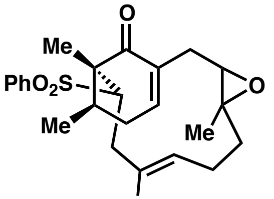

O
Me
PhO_2S
Me
O
Me
Me

4.S4

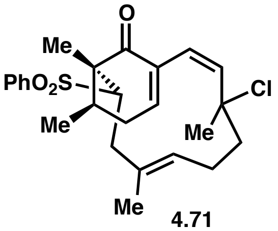

O
Me
PhO_2S
Cl
Me
Me
Me

4.71

4.11 References and Notes

[1] Mi, B.; Maleczka, R. E. *Org. Lett.* **2001,** *3,* 1491-1494.

[2] Goldring, W. P. D.; Pattenden, G. *Chem Commun.* **2002,** 1736-1737.

[3] Houghton, T. J.; Choi, S.; Rawal, V. H. *Org. Lett.* **2001,** *3,* 3615-3617.

[4] [a] Blackburn, T. J.; Helliwell, M.; Kilner, M. J.; Lee, A. T. L.; Thomas, E. J. *Tetrahedron Lett.* **2009,** *50,* 3550-3554. [b] Blackburn, T. J.; Kilner, M. J.; Thomas, E. J. *Tetrahedron* **2015**, *71*, 7293-7309.

[5] Martí-Centelles, V.; Pandey, M. D.; Burguete, M. I.; Luis, S. V. *Chem. Rev.* **2015,** *115,* 8736-8834. .

[6] [a] Simmons, E. M.; Hartwig, J. F. *Nature* **2012,** *483,* 70-73. [b] Li, B.; Driess, M.; Hartwig, J. F. *J. Am. Chem. Soc.* **2014**, *136*, 6586-6589.

[7] Nishimura, T.; Uemura, S. *J. Am. Chem. Soc.* **1999**, *121*, 11010-11011.

[8] Weber, M.; Owens, K.; Masarwa, A.; Sarpong, R. *Org. Lett.* **2015**, *17,* 5432-5435.

[9] Denmark, S. E.; Ambrosi, A. *Org. Process Res. Dev.* **2015,** *19,* 982-994.

[10] [a] Tymonko, S. A.; Smith, R. C.; Ambrosi, A.; Denmark, S. E. *J. Am. Chem. Soc.* **2015**, *137*, 6192-6199. [b] Tymonko, S. A.; Smith, R. C.; Ambrosi, A.; Ober, M. H.; Wang, H.; Denmark, S. E. *J. Am. Chem. Soc.* **2015**, *137*, 6200-6218.

[11] [a] Denmark, S. E.; Werner, N. S. *J. Am Chem. Soc.* **2008**, *130*, 16382-16393. [b] Denmark, S. E.; Werner, N. S. *J. Am Chem. Soc.* **2010**, *132*, 3612-3620.

[12] Miyaoka, H.; Saka, Y.; Miura, S.; Yamada, Y. *Tetrahedron Lett.* **1996,** *37,* 7107-7110.

[13] [a] Van Horn, D. E.; Negishi, E. *J. Am. Chem. Soc.* **1978**, *100*, 2252-2254. [b] Negishi, E.; Kondakov, D. Y. *Chem. Soc. Rev.* **1996**, *25*, 417-426.

[14] Lipshutz, B. H.; Ellsworth, E. L.; Dimock, S. H.; Reuter, D. C. *Tetrahedron Lett.* **1989**, *30*, 2065-2068.

[15] Negishi, E. Okukado, N.; King, A. O. Van Horn, D. E.; Spiegel, B. I. *J. Am. Chem. Soc.* **1978**, *100*, 2254-2256.

[16] Del Valle, L.; Stille, J. K.; Hegedus, L. S. *J. Org. Chem.* **1990**, *55*, 3019-3023.

[17] Mee, S. P. H.; Lee, V.; Baldwin, J. E. *Angew. Chem. Int. Ed.* **2004**, *43*, 1132-1136.

[18] Fürstner, A.; Funel, J.-A.; Tremblay, M.; Bouchez, L. C.; Nevado, C.; Waser, M.; Ackerstaff, J.; Stimson, C. C. *Chem. Commun.* **2008**, 2873-2875.

[19] Han, X.; Stoltz, B. M.; Corey, E. J. *J. Am. Chem. Soc.* **1999**, *121*, 7600-7605.

[20] Vanderwal, C. D.; Vosburg, D. A.; Weiler, S.; Sorensen, E. J. *J. Am. Chem. Soc.* **2003,** *125,* 5393-5407.

[21] Masarwa, A.; Weber, M.; Sarpong. R. *J. Am. Chem. Soc.* **2015**, *137*, 6327-6334.

[22] [a] Seiser, T.; Cramer, N. *Angew. Chem. Int. Ed.* **2008,** *47,* 9294-9297. [b] Seiser, T.; Cramer, N. *Chem. Eur. J.* **2010,** *16,* 3383-3391.

[23] Beckwith, A. L. J.; Davies, A. G.; Davison, I. G. E.; Maccoll, A.; Mruzek, M. H. *J. Chem. Soc. Perkin Trans. II* **1989**, 815-824.

[24] Nakamura, A.; Nakada, M. *Synthesis* **2013**, *45*, 1421-1451.

[25] Stork, G.; Sher, P. M. *J. Am. Chem. Soc.* **1983**, *105*, 6765-6766.

[26] Monte Carlo conformational searches (OPLS_2005).

[27] Krasovskiy, A.; Kopp, F.; Knochel, P. *Angew. Chem. Int. Ed.* **2006**, *45*, 497-500.

[28] Nysted, L. N., *Chem. Abstr.,* **1975**, *83,* 10406q.

[29] [a] Lombardo, L., *Tetrahedron Lett.,* **1982**, *23*, 4293-4296. [b] Lombardo, L., *Org. Synth. Coll*, **1993**, *31*, 386.

[30] Yan, T.-H.; Tsai, C.-C.; Chien, C.-T.; Cho, C.-C.; Huang, P.-C. *Org. Lett.* **2004**, *6*, 4961-4963.

[31] Buchanan, G. S.; Cole, K. P.; Tang, Y.; Hsung, R. P. *J. Org. Chem.* **2011**, *76*, 7027-7039.

[32] Nishimura, T.; Uemura, S. *J. Am. Chem. Soc.* **1999**, *121*, 11010-11011.

[33] [a] Nishiyama, H.; Kitajima, T.; Matsumoto, M.; Itoh, K. *J. Org. Chem.* **1984**, *49*, 2298-2300. [b] Stork, G.; Kahn, M. *J. Am. Chem. Soc.* **1985**, *107*, 500.

[34] [a] Park, H. S.; Lee, I. S.; Kwon, D. W.; Kim, Y. H. *Chem. Commun.* **1998**, 2745-2746. [b] Iwamoto, M.; Miyano, M.; Utsugi, M.; Kawada, H.; Nakada, M. *Tetrahedron Lett.* **2004**, *45*, 8647-8451. [c] Gu, Q.; Zheng, Y.-H.; Li, Y.-C. *Synthesis* **2006**, *6*, 975-978.

[35] Xie, Y.; Floreancig, P. *Angew. Chem. Int. Ed.* **2013**, *52*, 625-628.

[36] For the synthesis of diol **4.16** see Section 3.9.

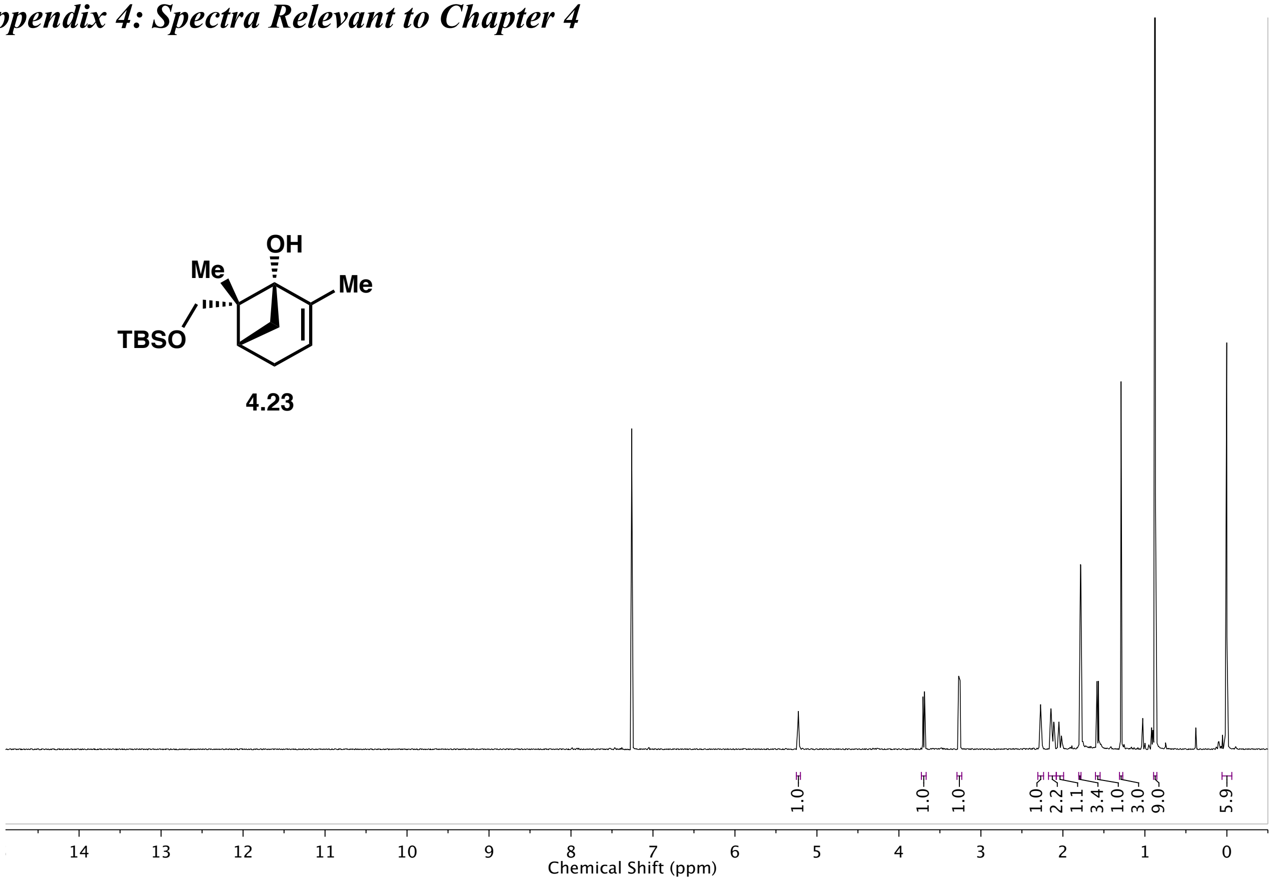
OH
Me
Me
TBSO
4.23
1.0
1.0
1.0
1.0
2.2
1.1
3.4
1.0
3.0
9.0
5.9
14
13
12
11
10
9
8
7
6
5
4
3
2
1
0
Chemical Shift (ppm)

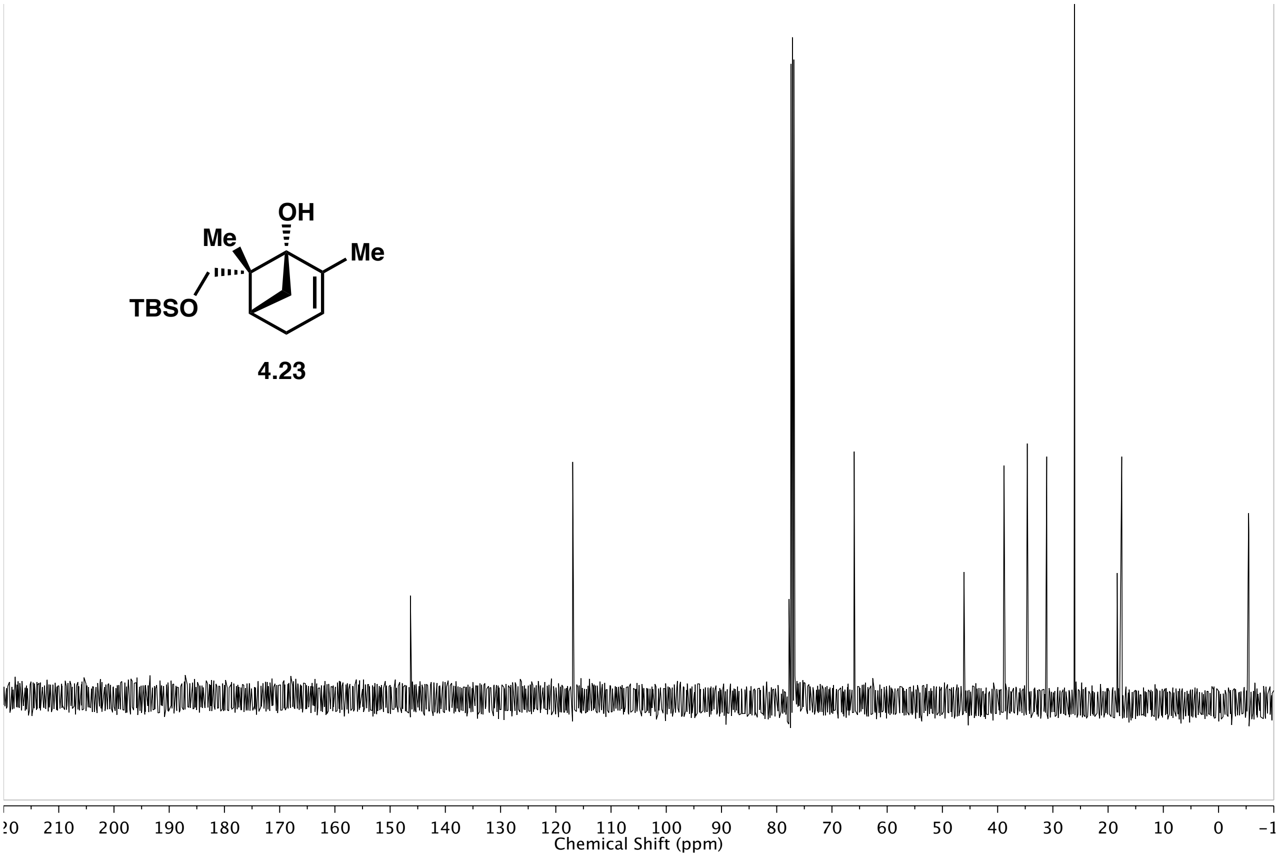
OH
Me
Me
TBSO
4.23
20
210
200
190
180
170
160
150
140
130
120
110
100
90
80
70
60
50
40
30
20
10
0
−1
Chemical Shift (ppm)

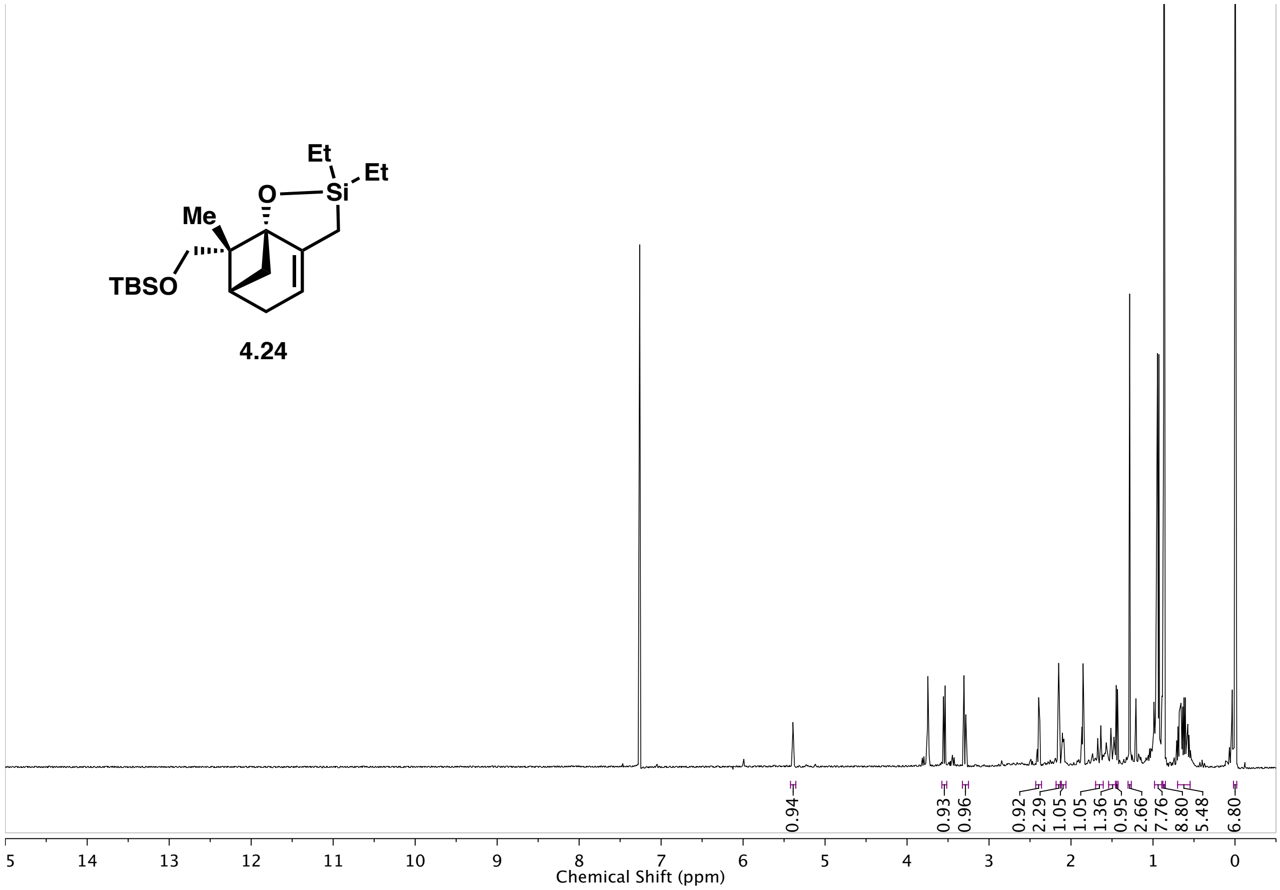
Et
Et
O
Si
Me
TBSO
4.24
0.94
0.93
0.96
0.92
2.29
1.05
1.05
1.36
0.95
2.66
7.76
8.80
5.48
6.80
5
14
13
12
11
10
9
8
7
6
5
4
3
2
1
0
Chemical Shift (ppm)

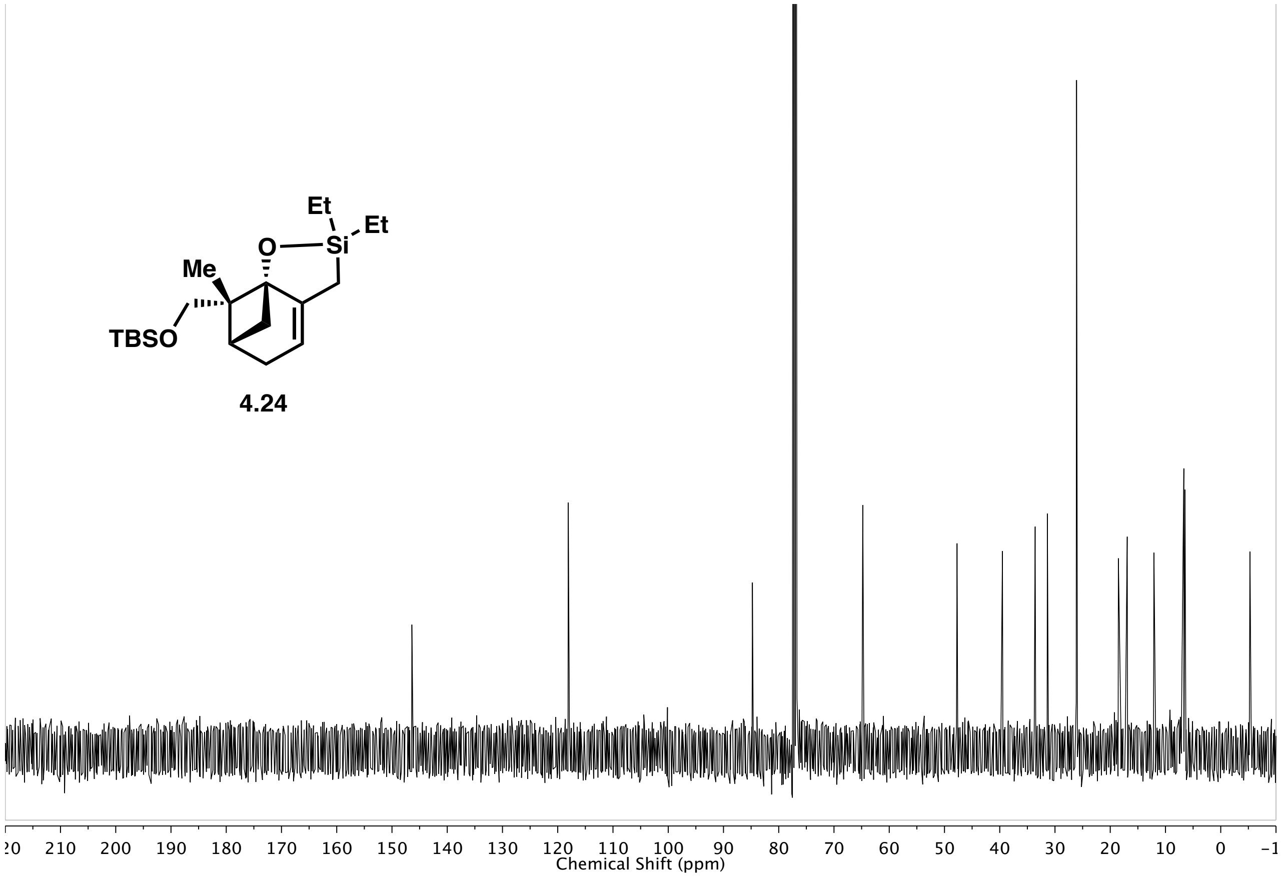
Et
Et
O
Si
Me
TBSO
4.24
20
210
200
190
180
170
160
150
140
130
120
110
100
90
80
70
60
50
40
30
20
10
0
–1
Chemical Shift (ppm)

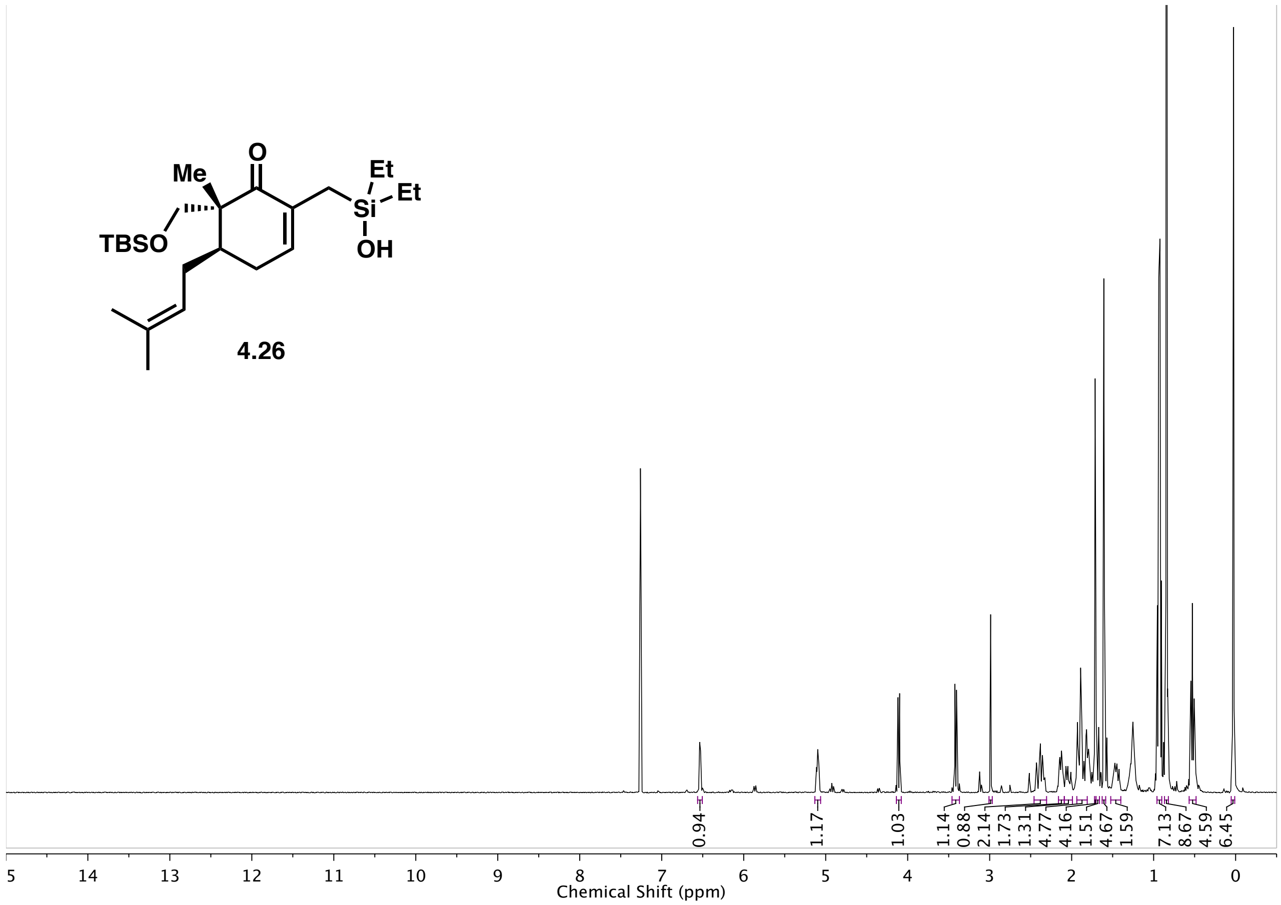
Me
O
Et
Et
Si
OH
TBSO
0.94
1.17
1.03
1.14
0.88
2.14
1.73
1.31
4.77
4.16
1.51
4.67
1.59
7.13
8.67
4.59
6.45
5 14 13 12 11 10 9 8 7 6 5 4 3 2 1 0
Chemical Shift (ppm)

4.26

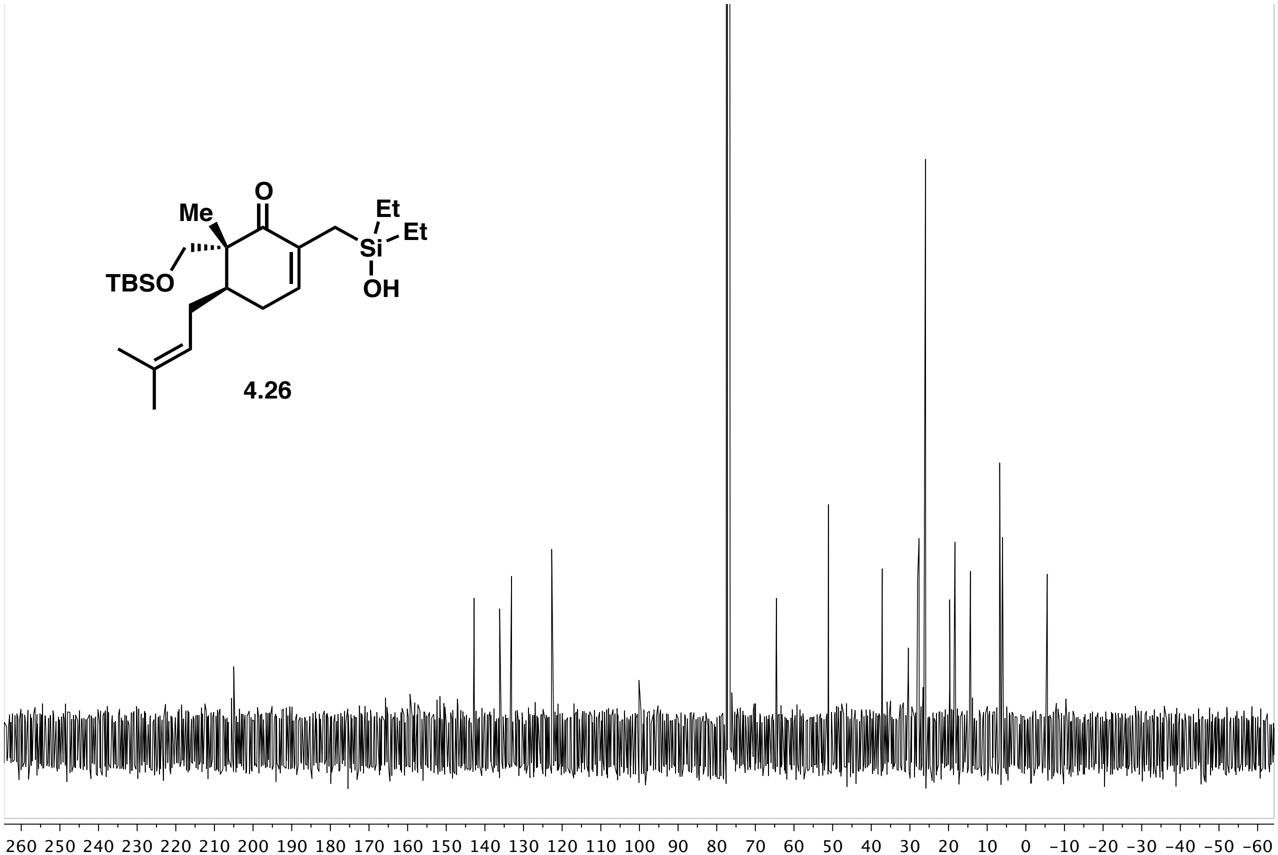
Me
O
Et
Et
Si
OH
TBSO
260 250 240 230 220 210 200 190 180 170 160 150 140 130 120 110 100 90 80 70 60 50 40 30 20 10 0 −10 −20 −30 −40 −50 −60
Chemical Shift (ppm)

4.26

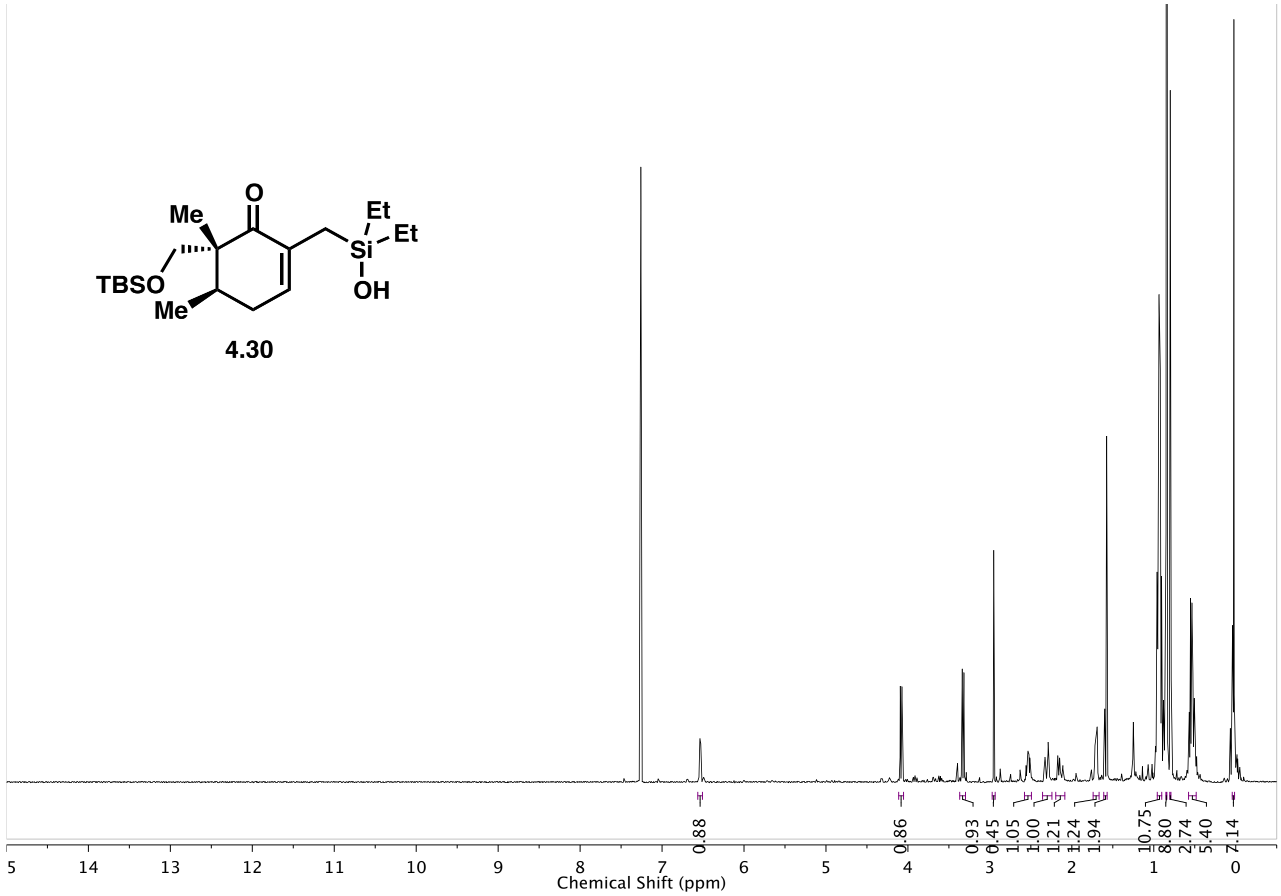
O
Me
Et
Et
Si
OH
TBSO
Me
4.30
0.88
0.86
0.93
0.45
1.05
1.00
1.21
1.24
1.94
10.75
8.80
2.74
5.40
7.14
5
14
13
12
11
10
9
8
7
6
5
4
3
2
1
0
Chemical Shift (ppm)

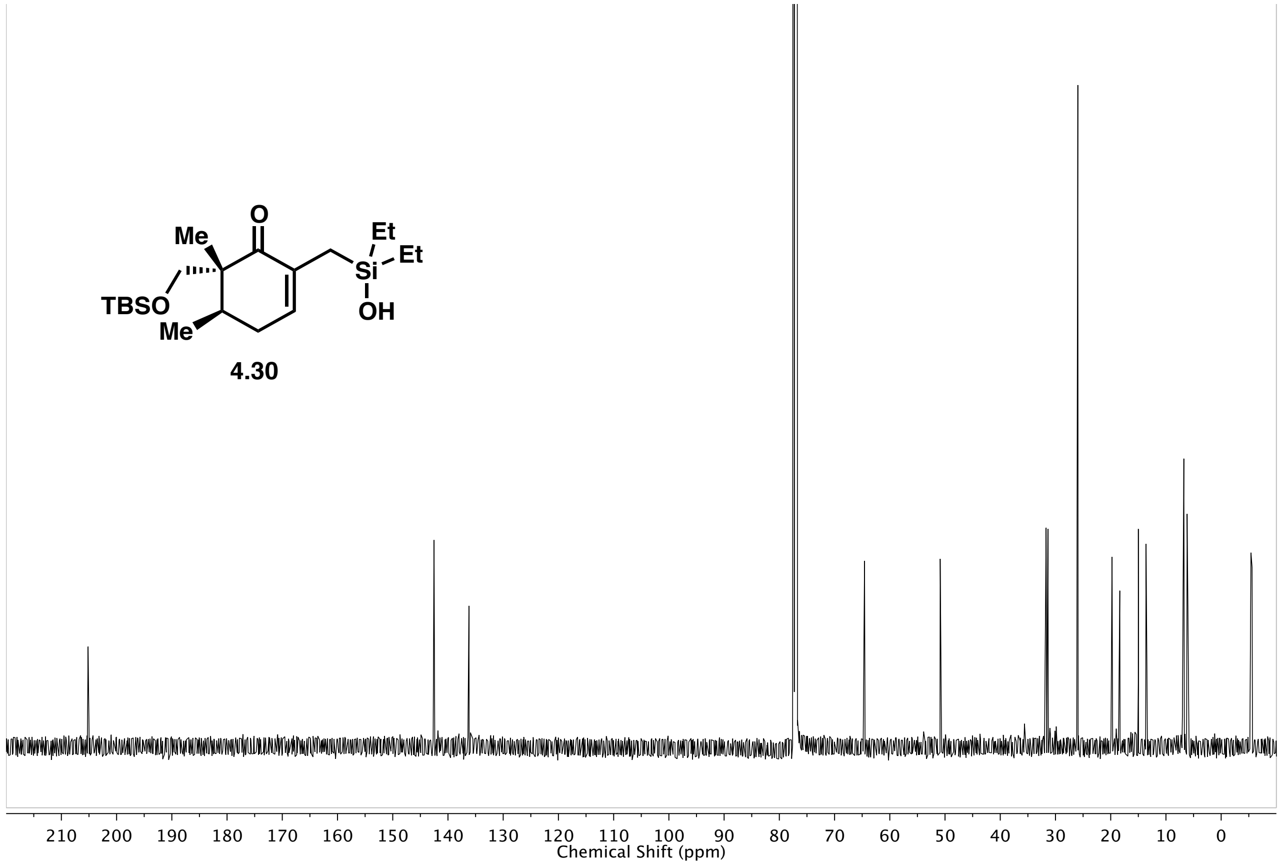
O
Me
Et
Et
Si
OH
TBSO
Me
4.30
210
200
190
180
170
160
150
140
130
120
110
100
90
80
70
60
50
40
30
20
10
0
Chemical Shift (ppm)

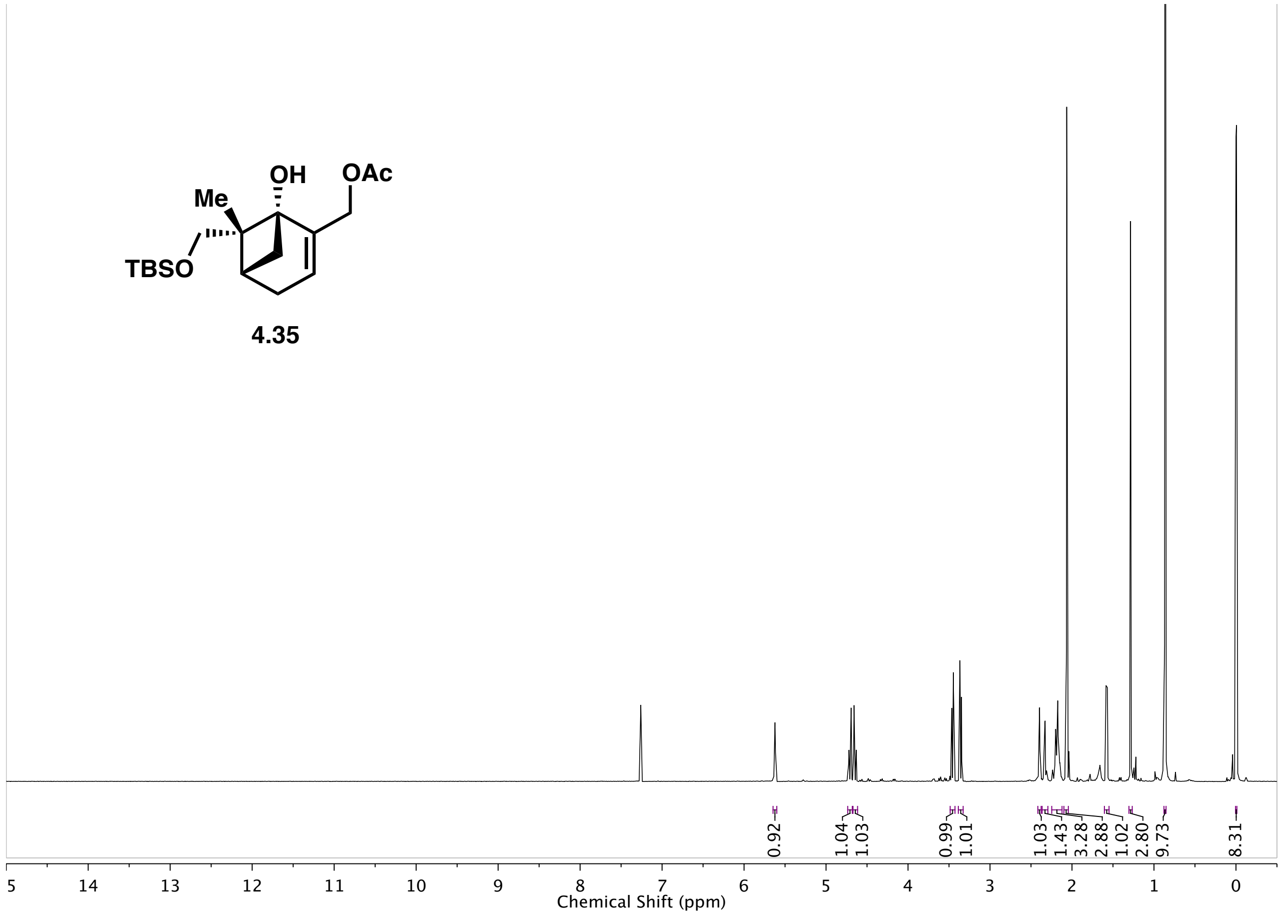
OH
OAc
Me
TBSO
4.35
0.92
1.04
1.03
0.99
1.01
1.03
1.43
3.28
2.88
1.02
2.80
9.73
8.31
5
14
13
12
11
10
9
8
7
6
5
4
3
2
1
0
Chemical Shift (ppm)

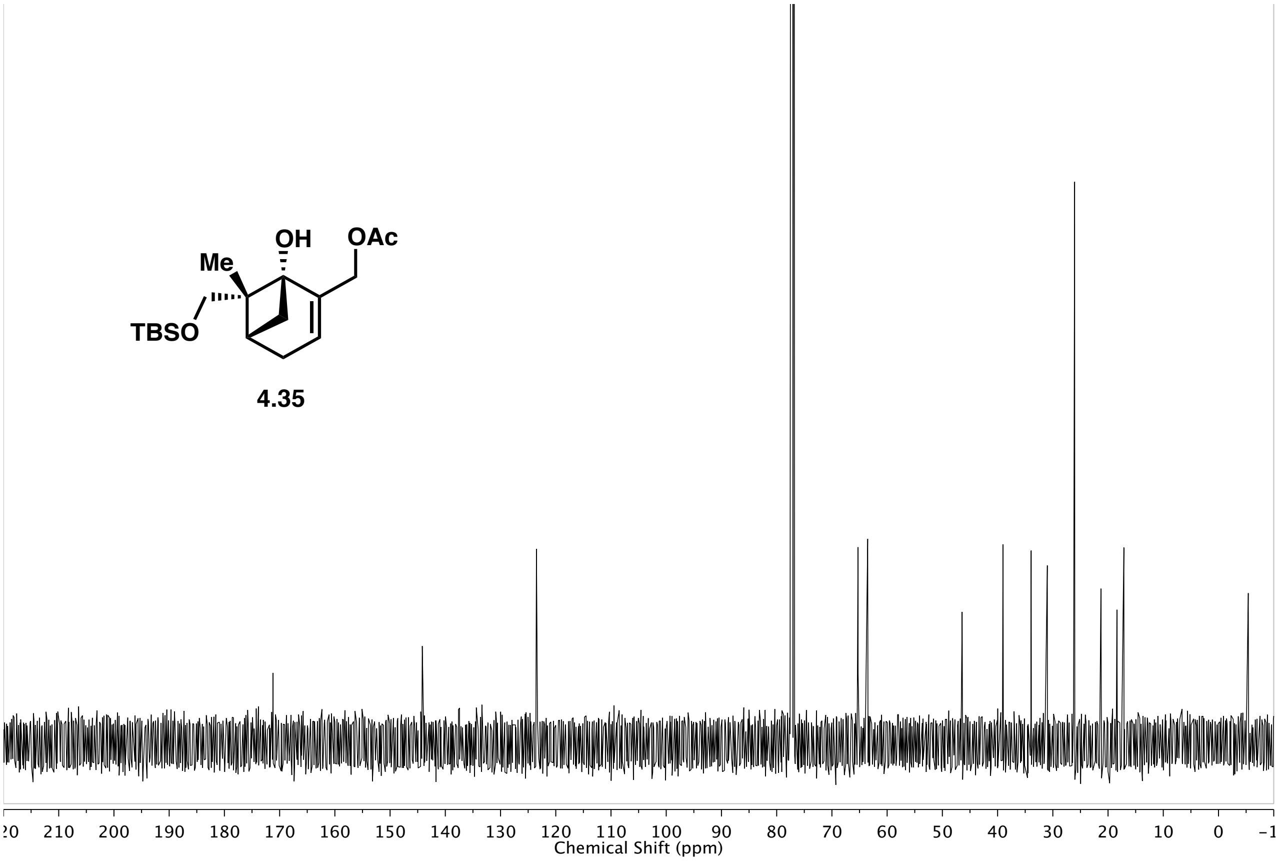
OH
OAc
Me
TBSO
4.35
210
200
190
180
170
160
150
140
130
120
110
100
90
80
70
60
50
40
30
20
10
0
–1
Chemical Shift (ppm)

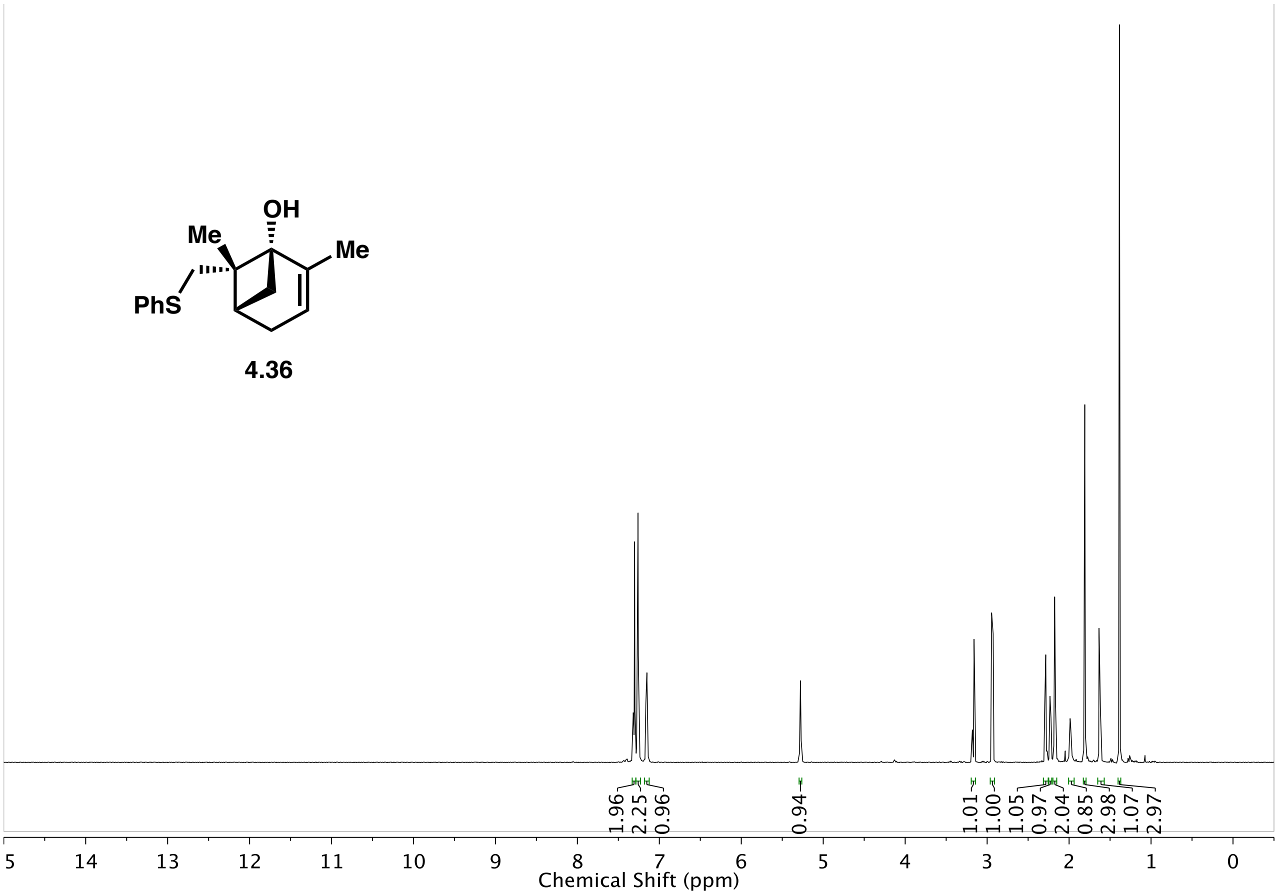

OH
Me
Me
PhS
4.36
1.96
2.25
0.96
0.94
1.01
1.00
1.05
0.97
2.04
0.85
2.98
1.07
2.97
5
14
13
12
11
10
9
8
7
6
5
4
3
2
1
0
Chemical Shift (ppm)

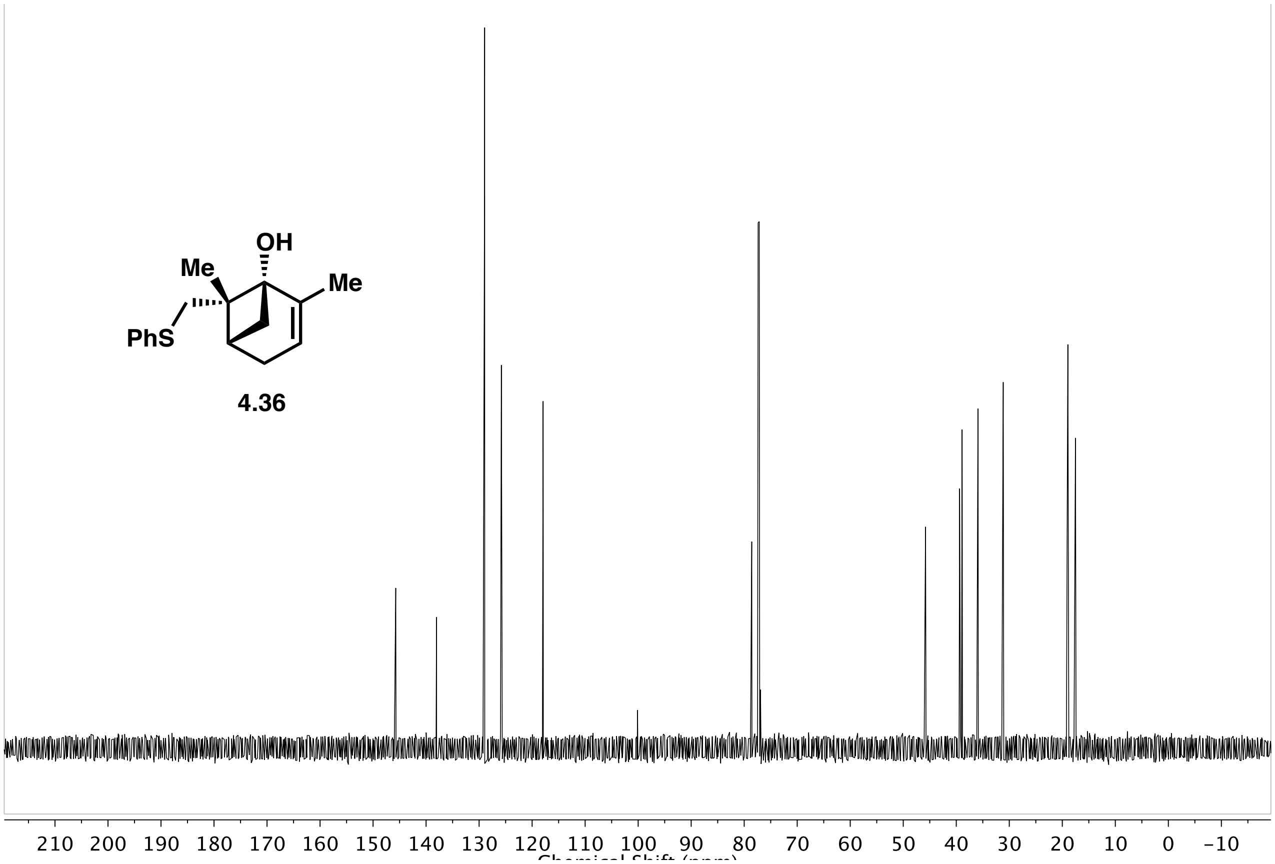

OH
Me
Me
PhS
4.36
210
200
190
180
170
160
150
140
130
120
110
100
90
80
70
60
50
40
30
20
10
0
−10

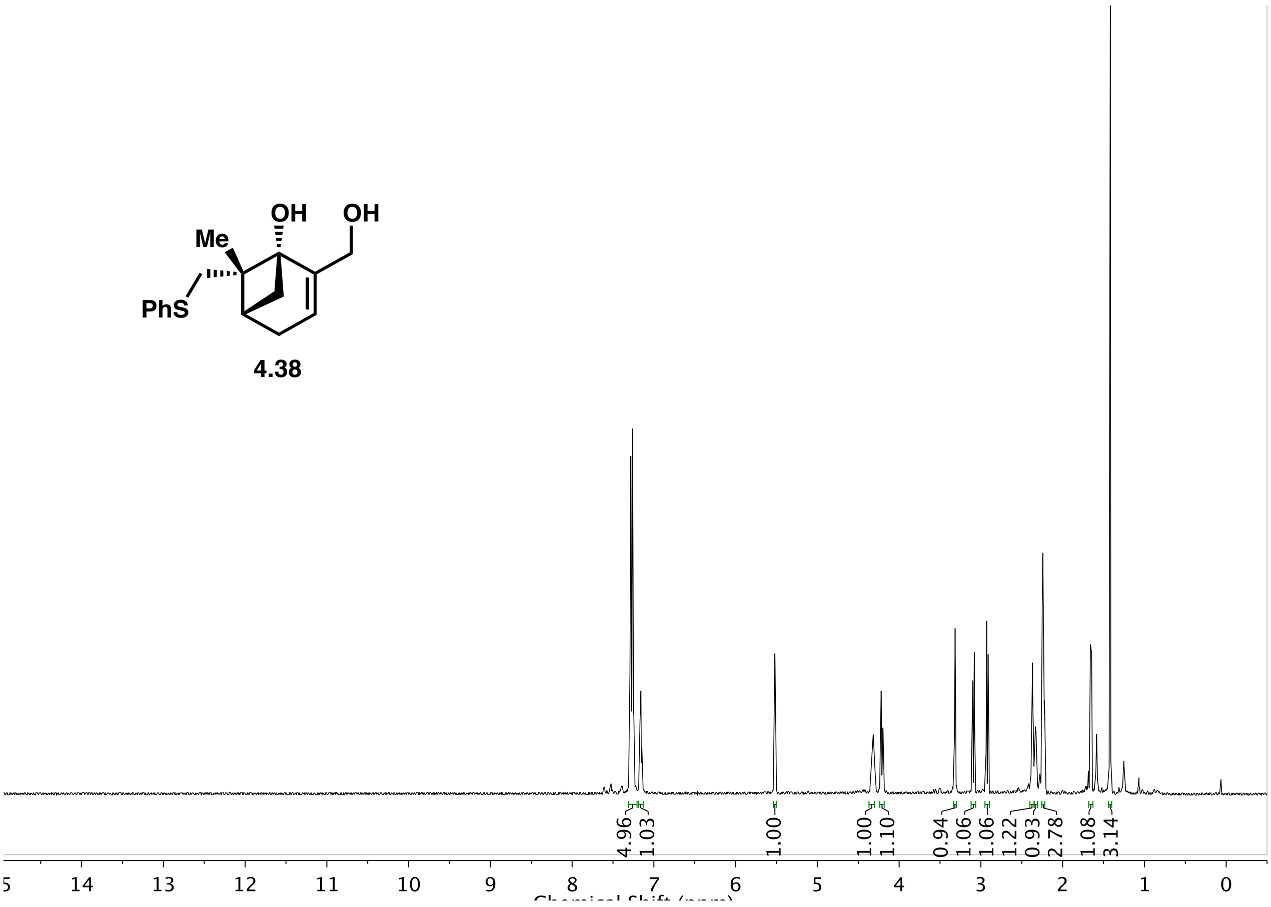
OH
OH
Me
PhS
4.96
1.03
1.00
1.00
1.10
0.94
1.06
1.06
1.22
0.93
2.78
1.08
3.14
14
13
12
11
10
9
8
7
6
5
4
3
2
1
0
Chemical Shift (ppm)

4.38

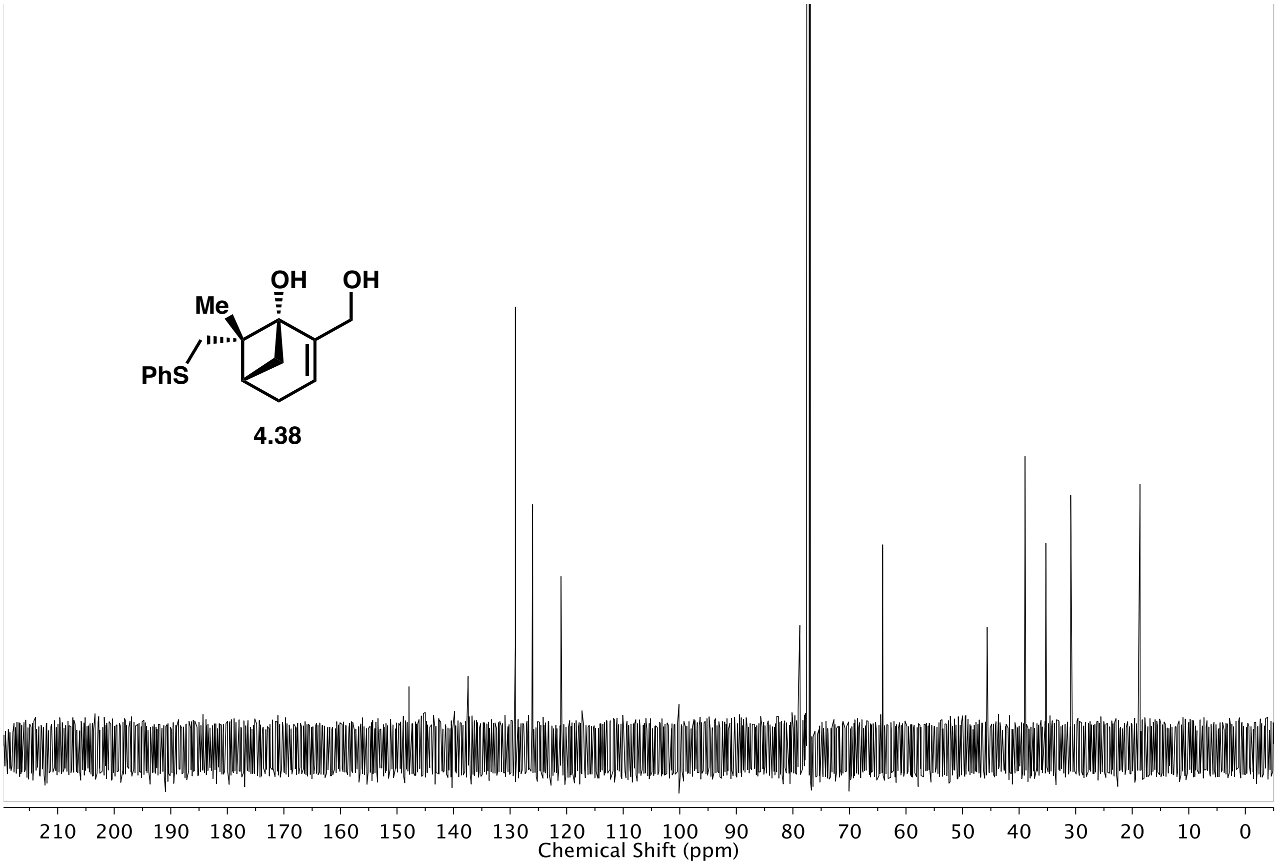
OH
OH
Me
PhS
210
200
190
180
170
160
150
140
130
120
110
100
90
80
70
60
50
40
30
20
10
0
Chemical Shift (ppm)

4.38

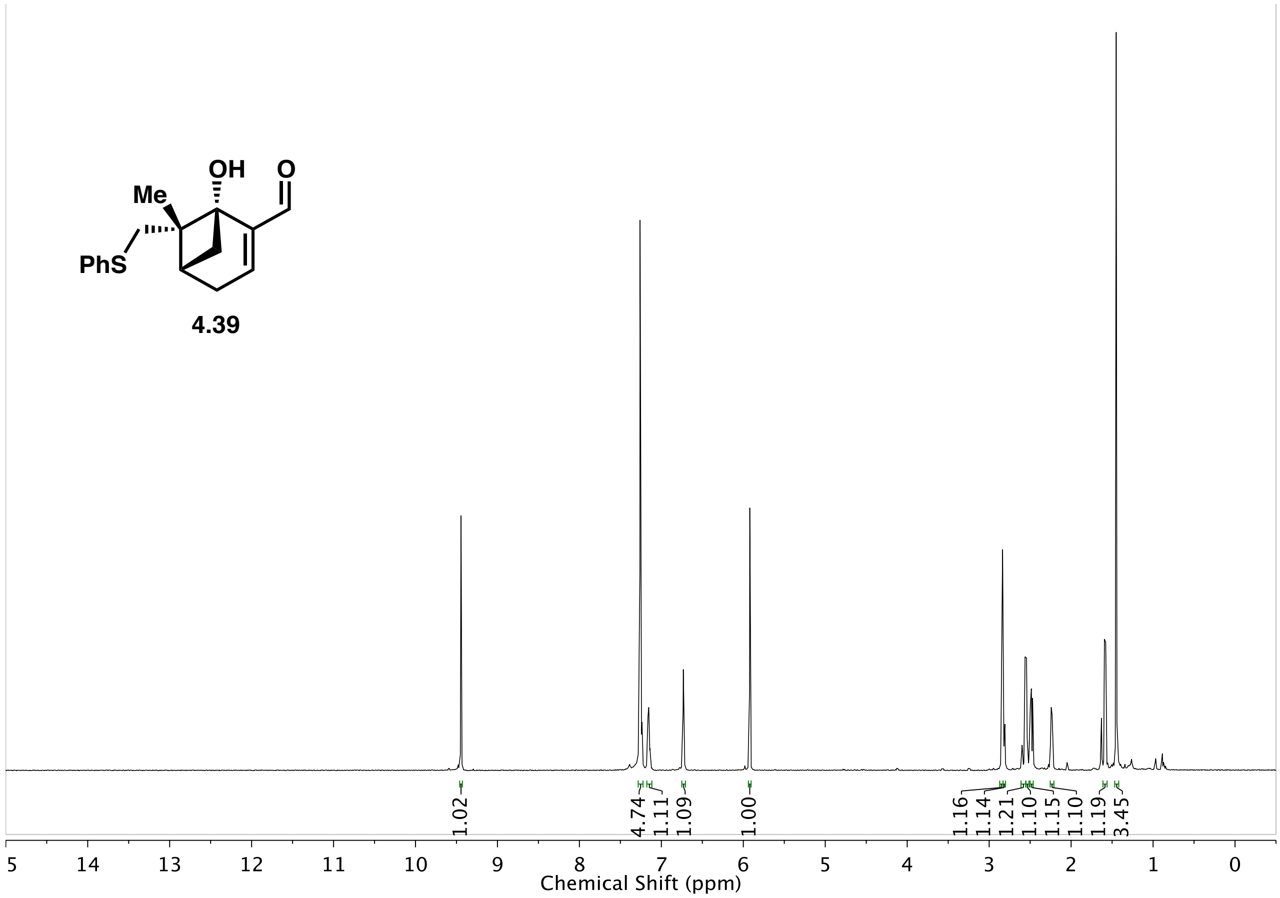

OH
O
Me
PhS
4.39
1.02
4.74
1.11
1.09
1.00
1.16
1.14
1.21
1.10
1.15
1.10
1.19
3.45
5 14 13 12 11 10 9 8 7 6 5 4 3 2 1 0
Chemical Shift (ppm)

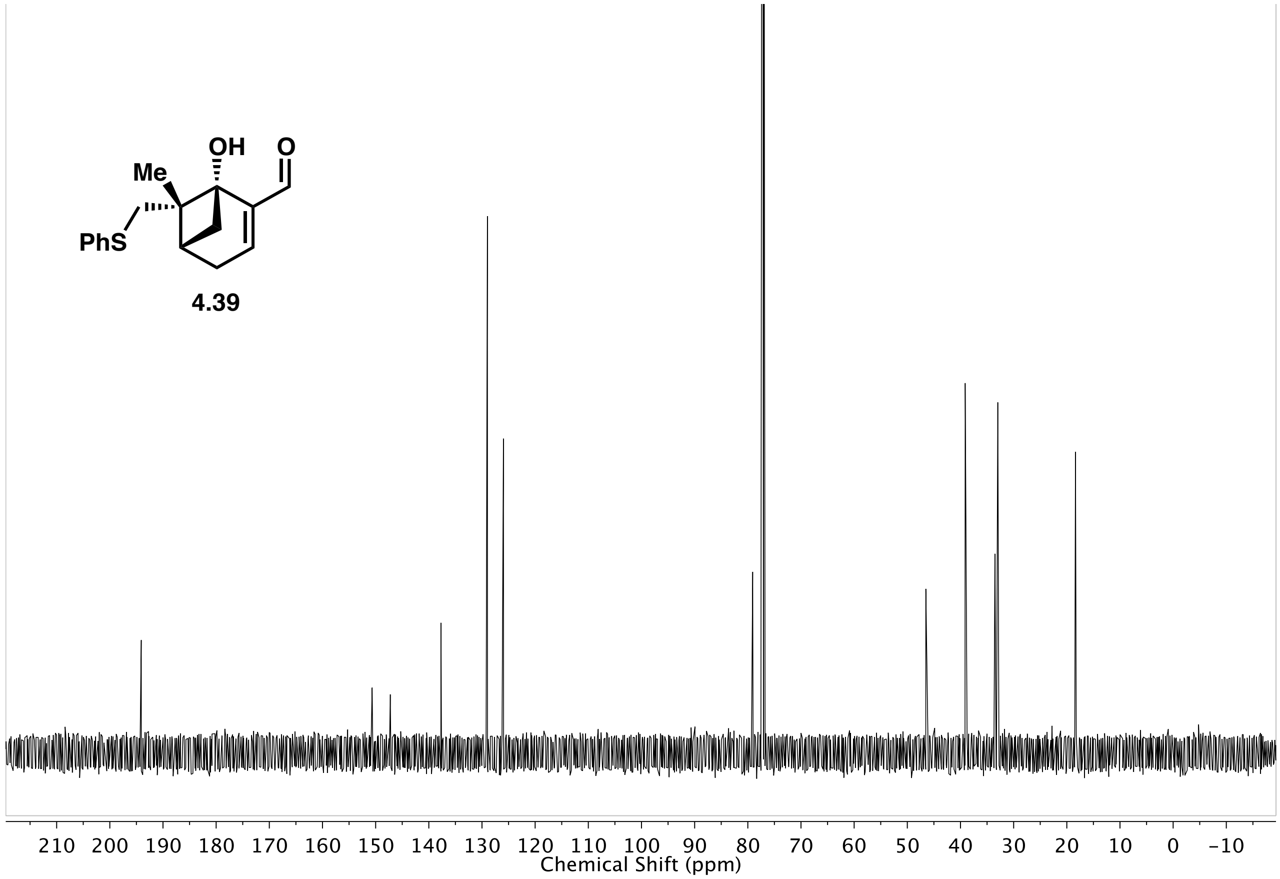

OH
O
Me
PhS
4.39
210 200 190 180 170 160 150 140 130 120 110 100 90 80 70 60 50 40 30 20 10 0 −10
Chemical Shift (ppm)

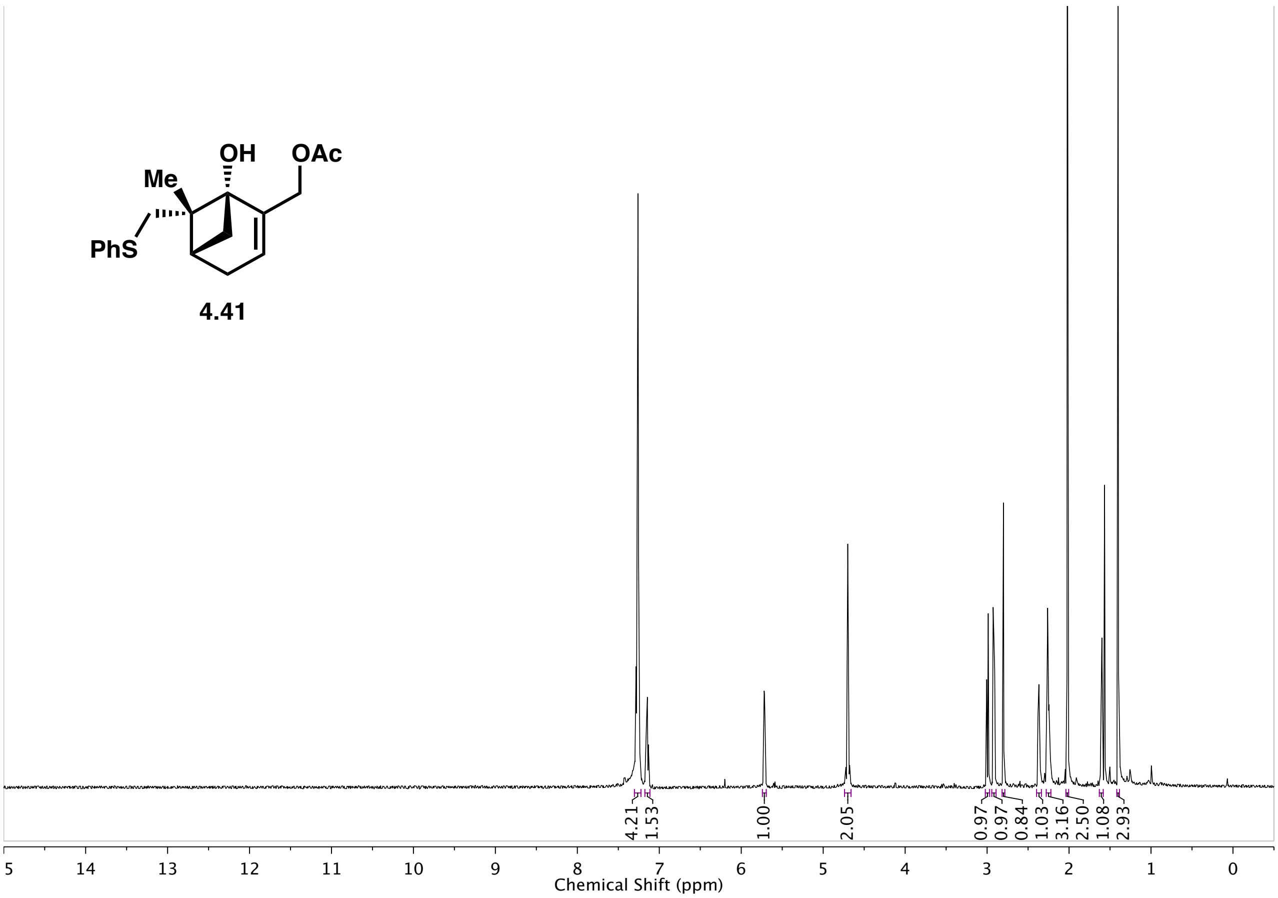
OH
OAc
Me
PhS
4.21
1.53
1.00
2.05
0.97
0.97
0.84
1.03
3.16
2.50
1.08
2.93
5
14
13
12
11
10
9
8
7
6
5
4
3
2
1
0
Chemical Shift (ppm)

4.41

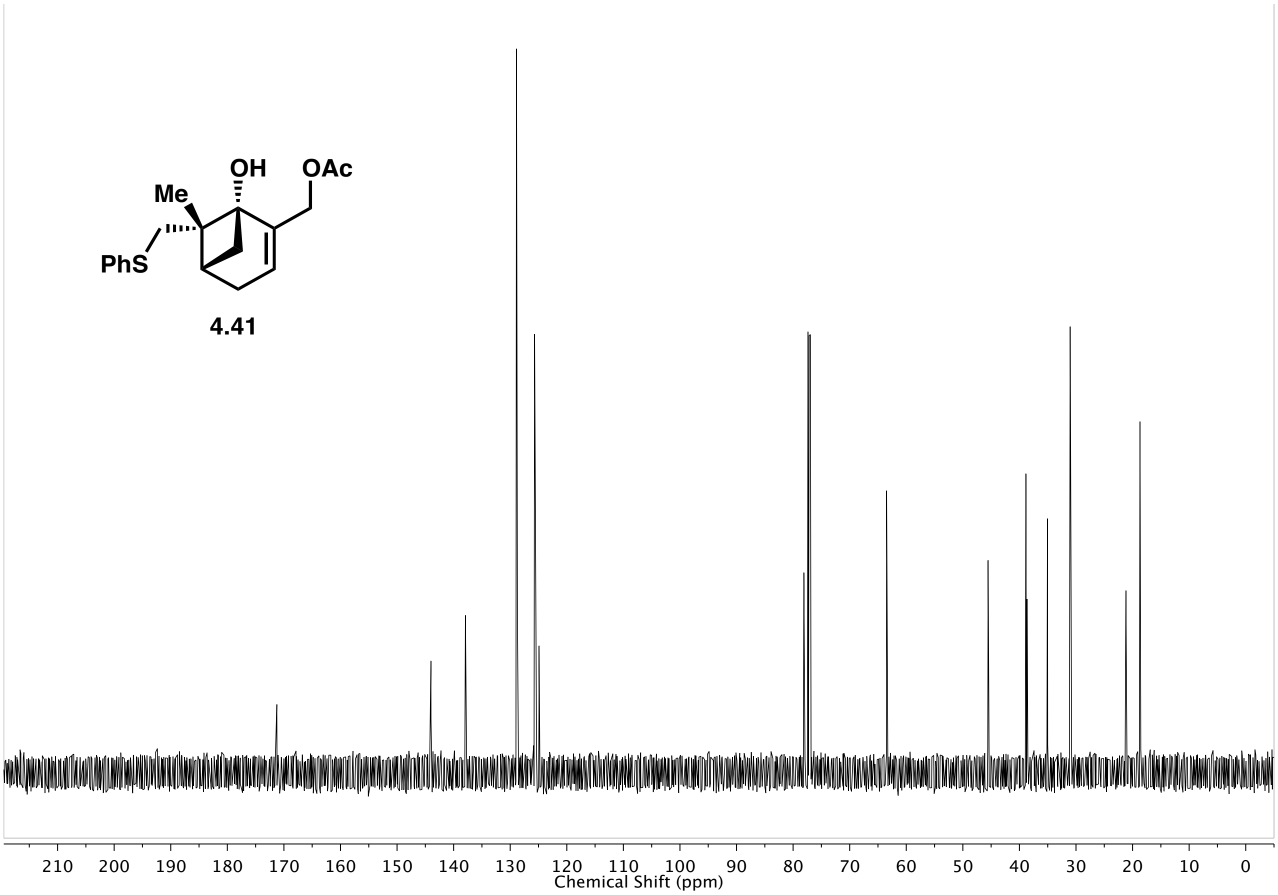
OH
OAc
Me
PhS
210
200
190
180
170
160
150
140
130
120
110
100
90
80
70
60
50
40
30
20
10
0
Chemical Shift (ppm)

4.41

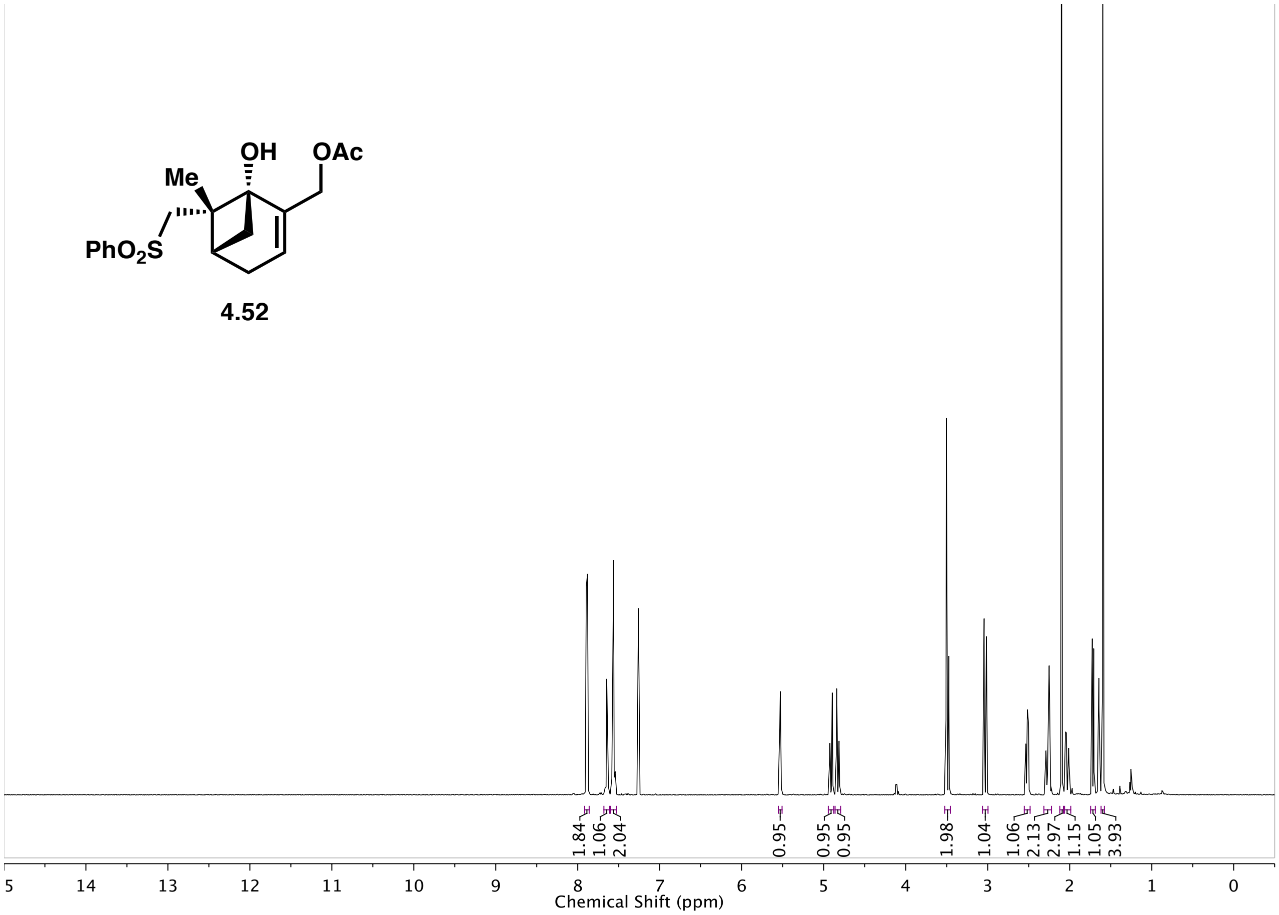
OH
OAc
Me
PhO2S
4.52
1.84
1.06
2.04
0.95
0.95
0.95
1.98
1.04
1.06
2.13
2.97
1.15
1.05
3.93
5
14
13
12
11
10
9
8
7
6
5
4
3
2
1
0
Chemical Shift (ppm)

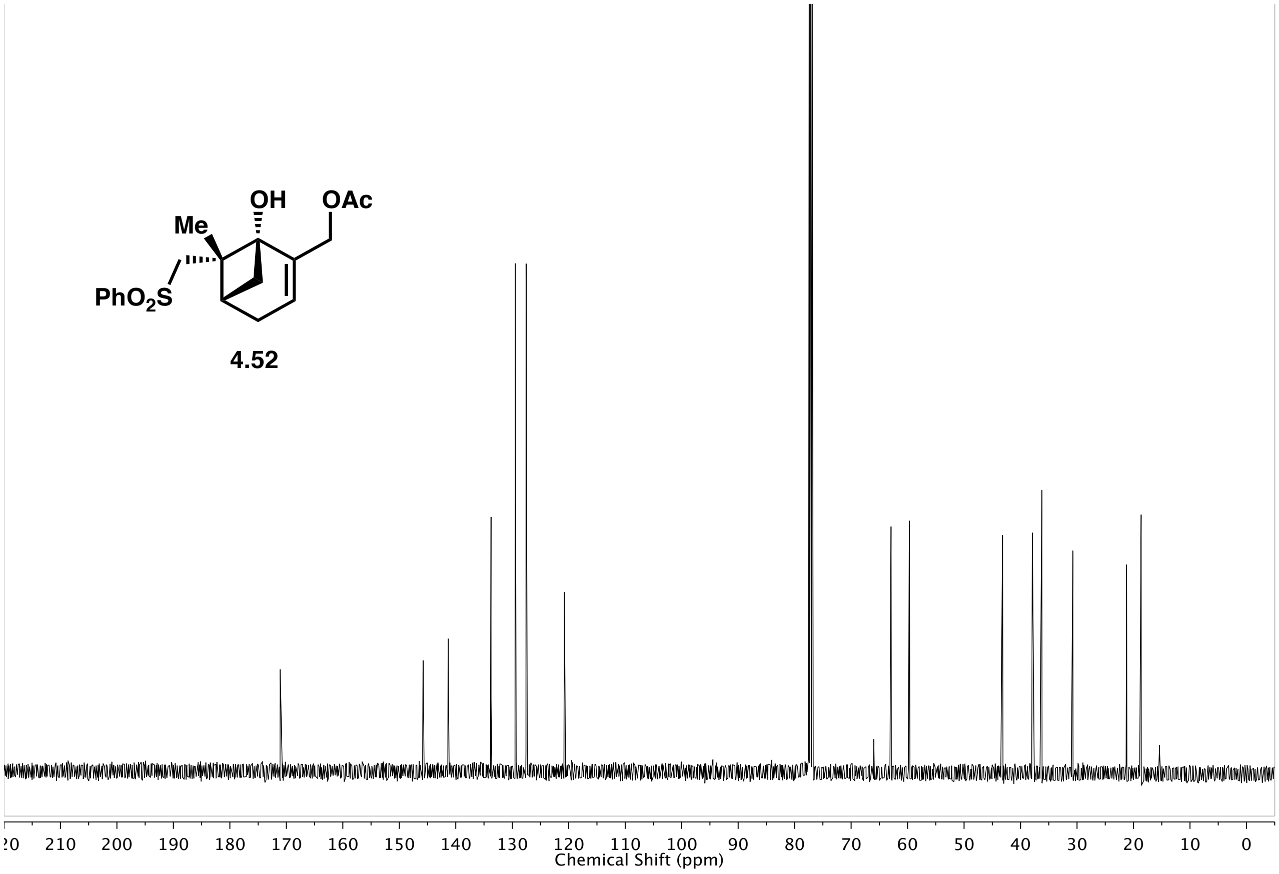
OH
OAc
Me
PhO2S
4.52
20
210
200
190
180
170
160
150
140
130
120
110
100
90
80
70
60
50
40
30
20
10
0
Chemical Shift (ppm)

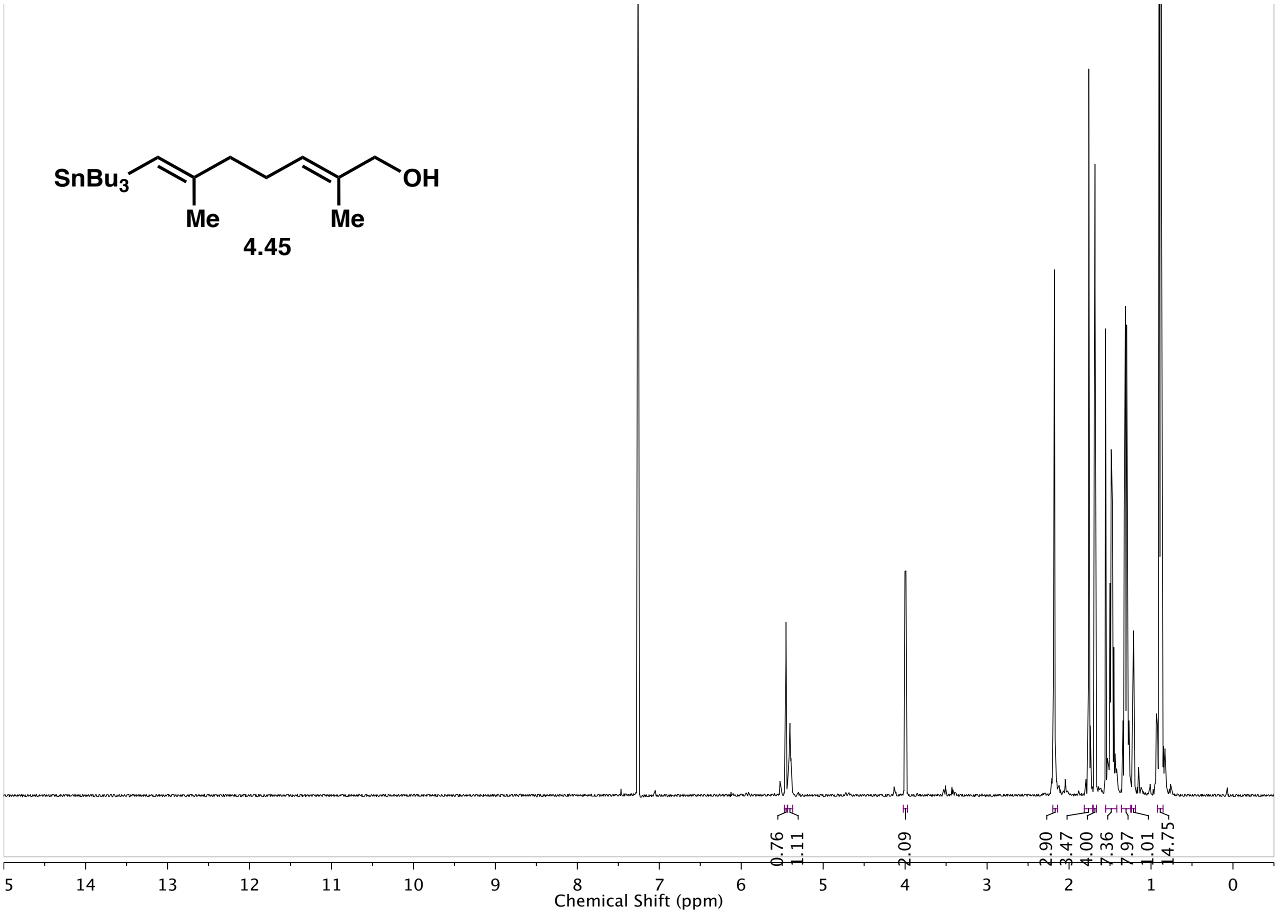
SnBu$_3$
OH
Me
Me
4.45
0.76
1.11
2.09
2.90
3.47
4.00
7.36
7.97
1.01
14.75
5
14
13
12
11
10
9
8
7
6
5
4
3
2
1
0
Chemical Shift (ppm)

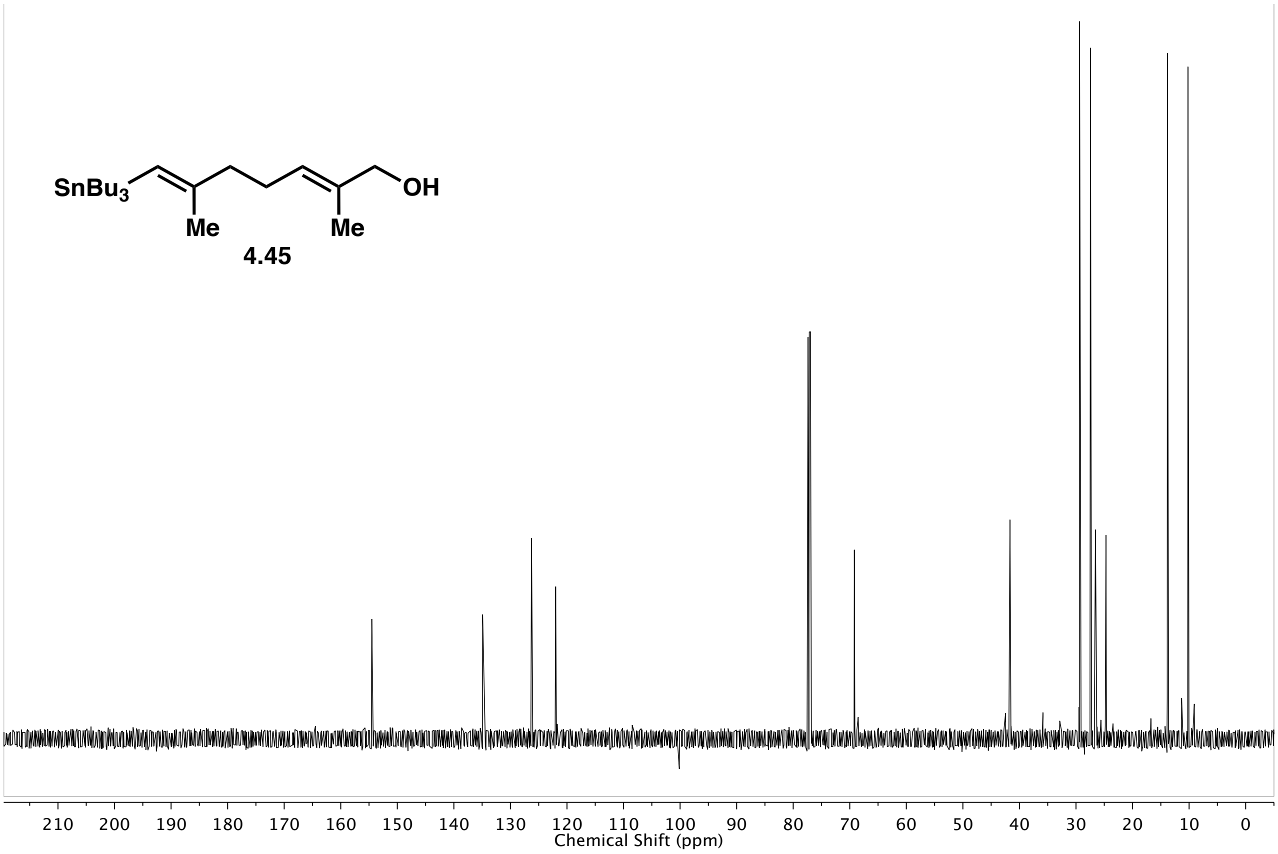
SnBu$_3$
OH
Me
Me
4.45
210
200
190
180
170
160
150
140
130
120
110
100
90
80
70
60
50
40
30
20
10
0
Chemical Shift (ppm)

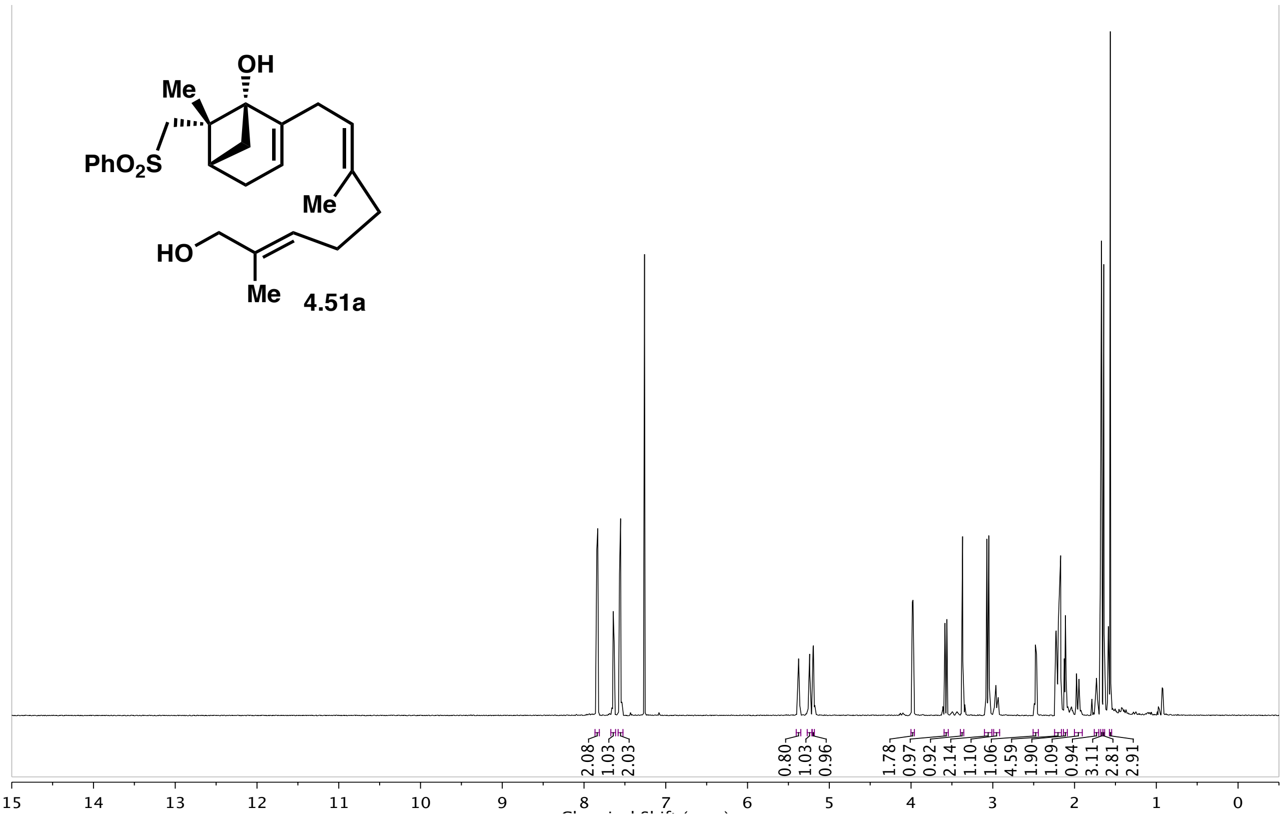
OH
Me
PhO2S
Me
HO
Me
4.51a
2.08
1.03
2.03
0.80
1.03
0.96
1.78
0.97
0.92
2.14
1.10
1.06
4.59
1.90
1.09
0.94
3.11
2.81
2.91
15
14
13
12
11
10
9
8
7
6
5
4
3
2
1
0

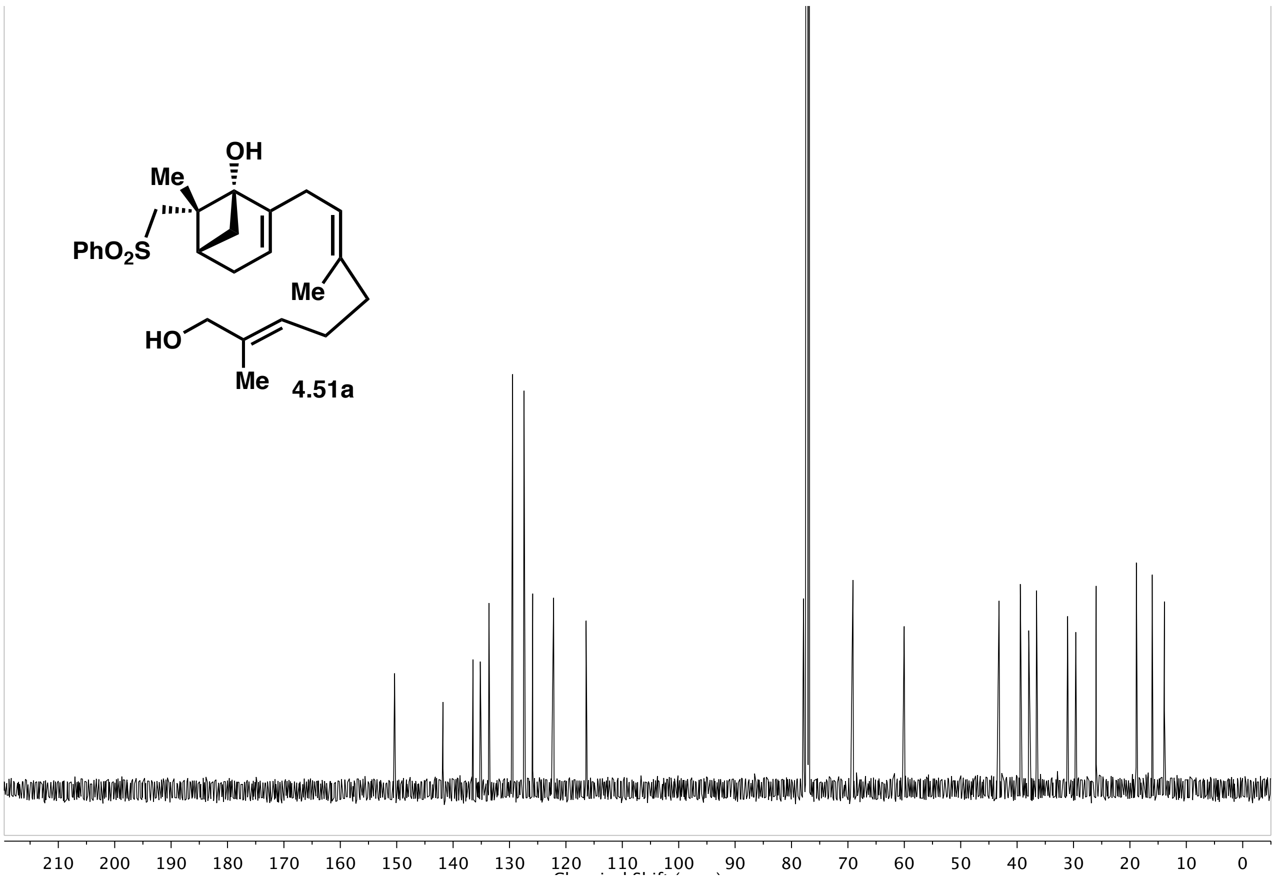
OH
Me
PhO2S
Me
HO
Me
4.51a
210
200
190
180
170
160
150
140
130
120
110
100
90
80
70
60
50
40
30
20
10
0

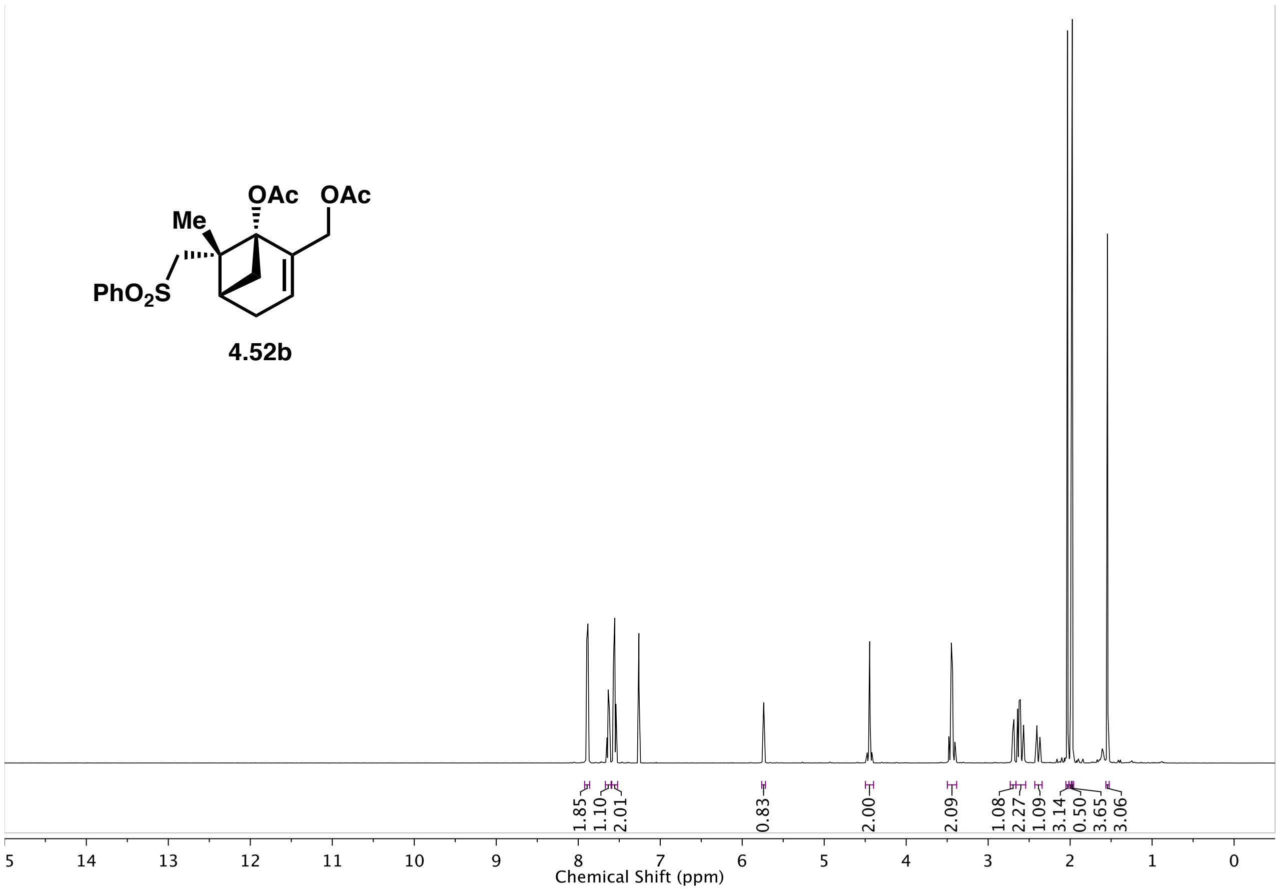
OAc
OAc
Me
PhO₂S
4.52b
1.85
1.10
2.01
0.83
2.00
2.09
1.08
2.27
1.09
3.14
0.50
3.65
3.06
5
14
13
12
11
10
9
8
7
6
5
4
3
2
1
0
Chemical Shift (ppm)

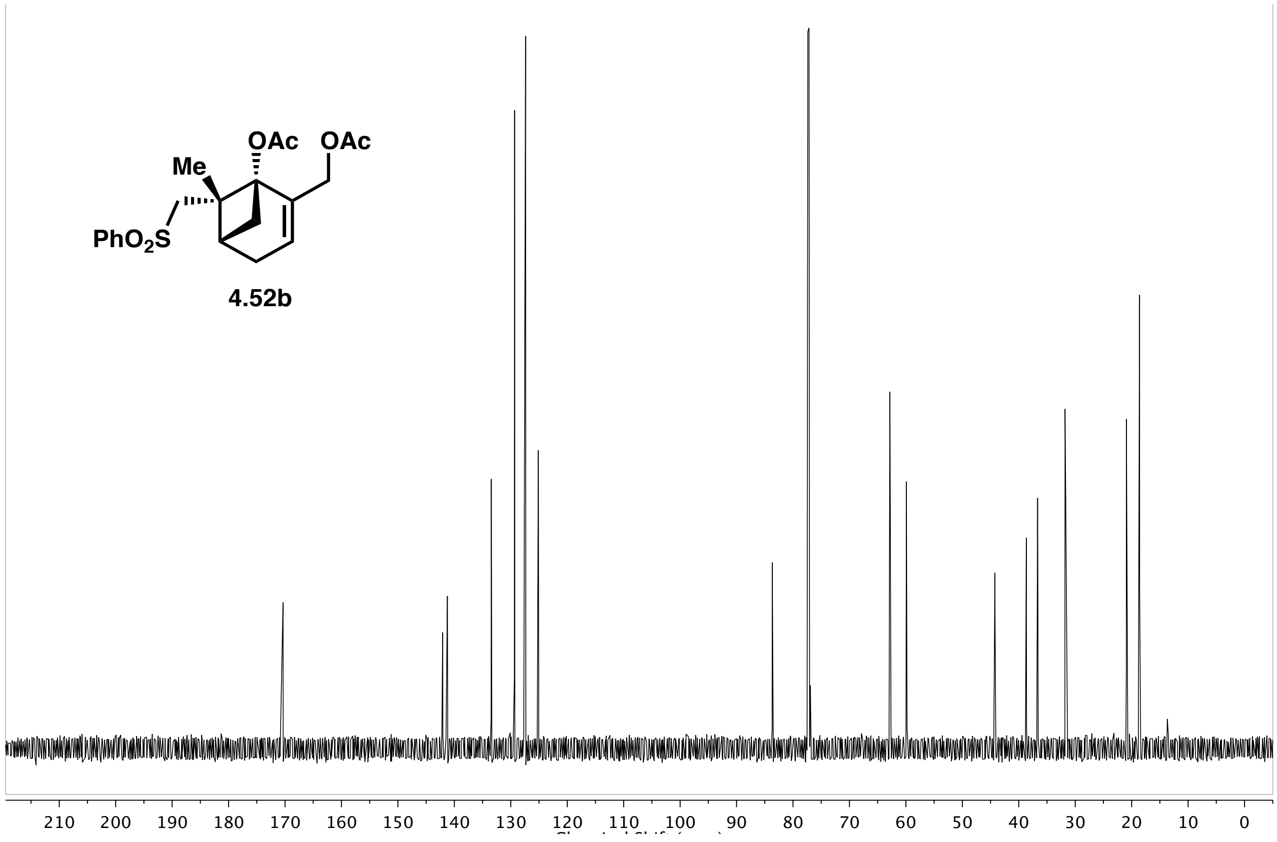
OAc
OAc
Me
PhO₂S
4.52b
210
200
190
180
170
160
150
140
130
120
110
100
90
80
70
60
50
40
30
20
10
0

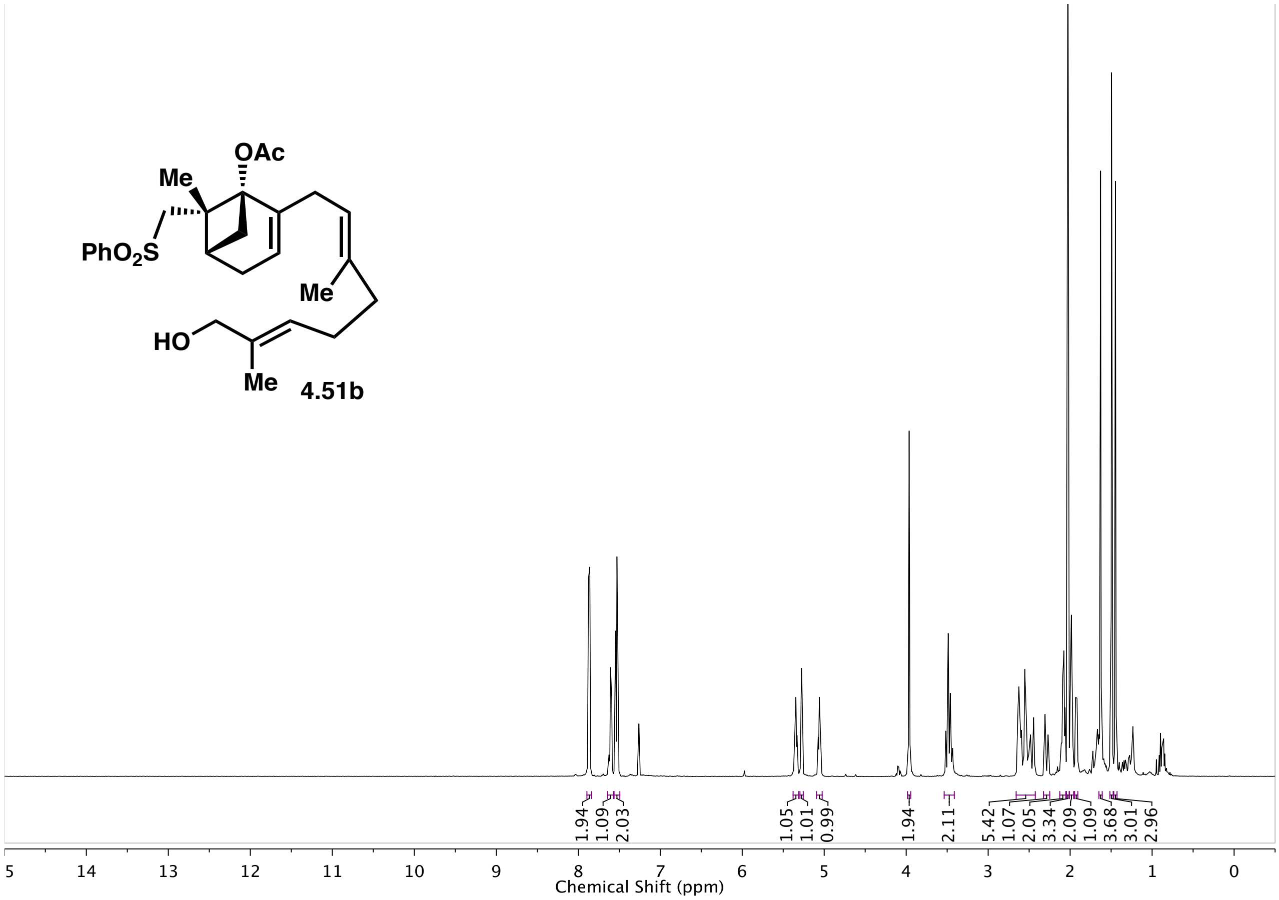
OAc
Me
PhO2S
Me
HO
Me
4.51b
1.94
1.09
2.03
1.05
1.01
0.99
1.94
2.11
5.42
1.07
2.05
3.34
2.09
1.09
3.68
3.01
2.96
5
14
13
12
11
10
9
8
7
6
5
4
3
2
1
0
Chemical Shift (ppm)

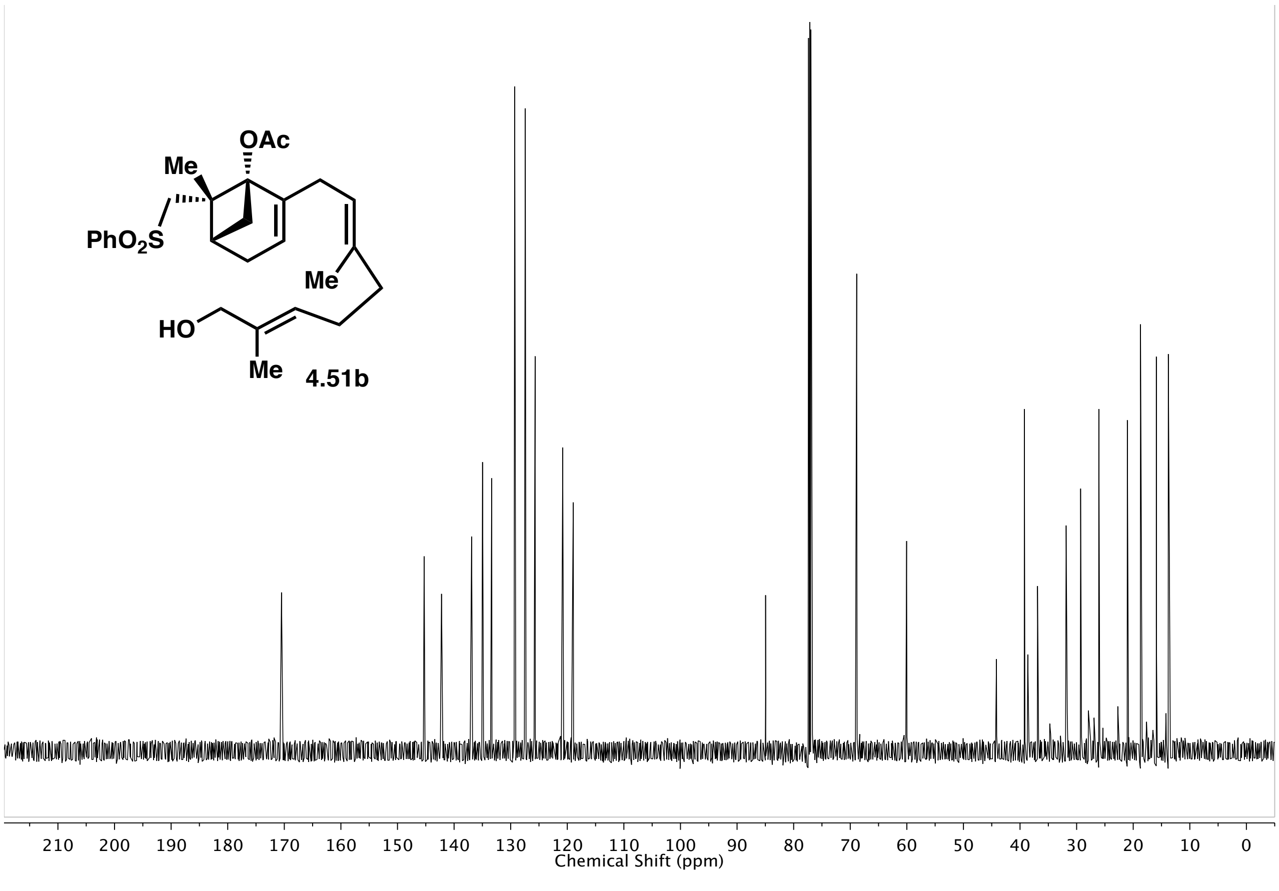
OAc
Me
PhO2S
Me
HO
Me
4.51b
210
200
190
180
170
160
150
140
130
120
110
100
90
80
70
60
50
40
30
20
10
0
Chemical Shift (ppm)

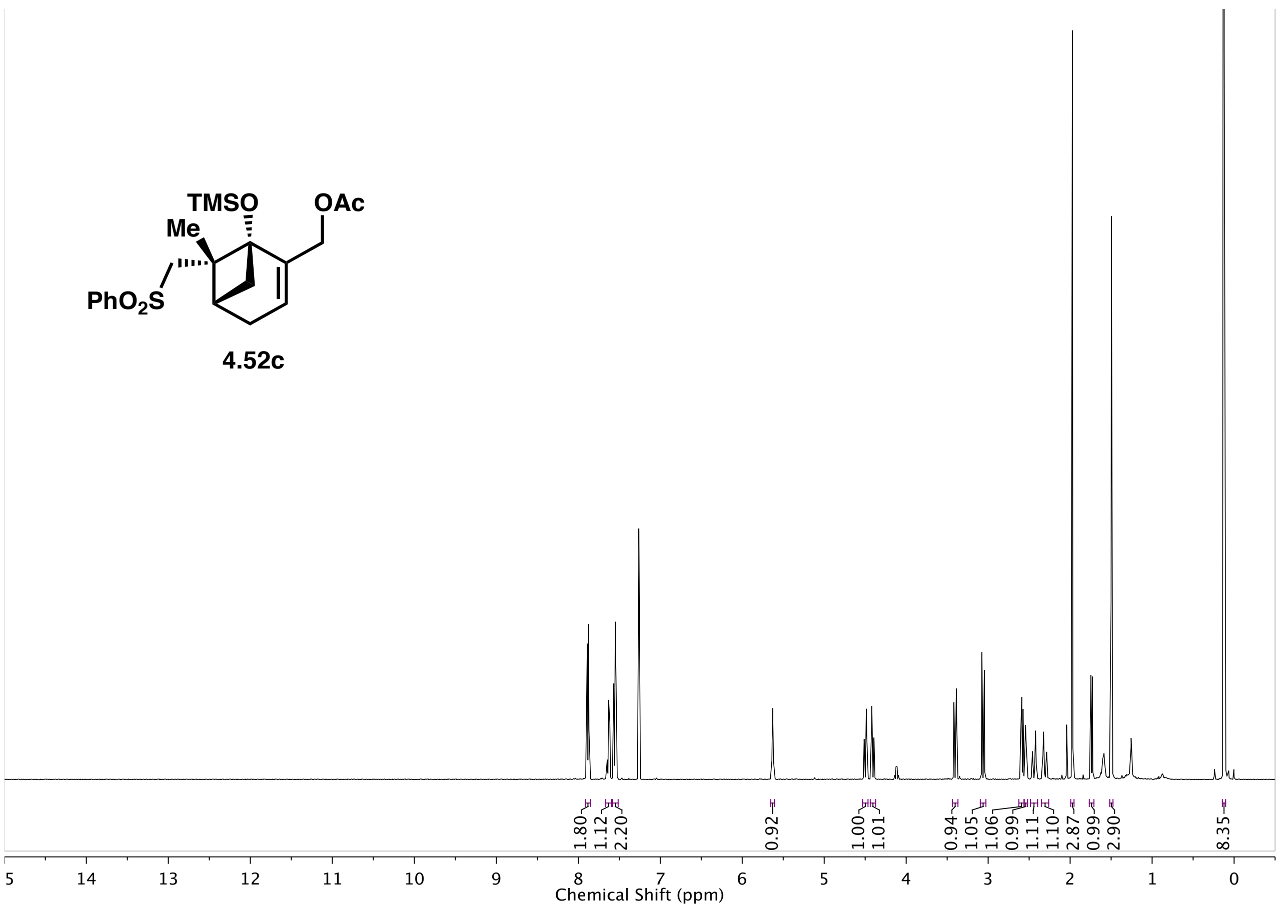
TMSO
OAc
Me
PhO$_2$S
1.80
1.12
2.20
0.92
1.00
1.01
0.94
1.05
1.06
0.99
1.11
1.10
2.87
0.99
2.90
8.35
15 14 13 12 11 10 9 8 7 6 5 4 3 2 1 0
Chemical Shift (ppm)

4.52c

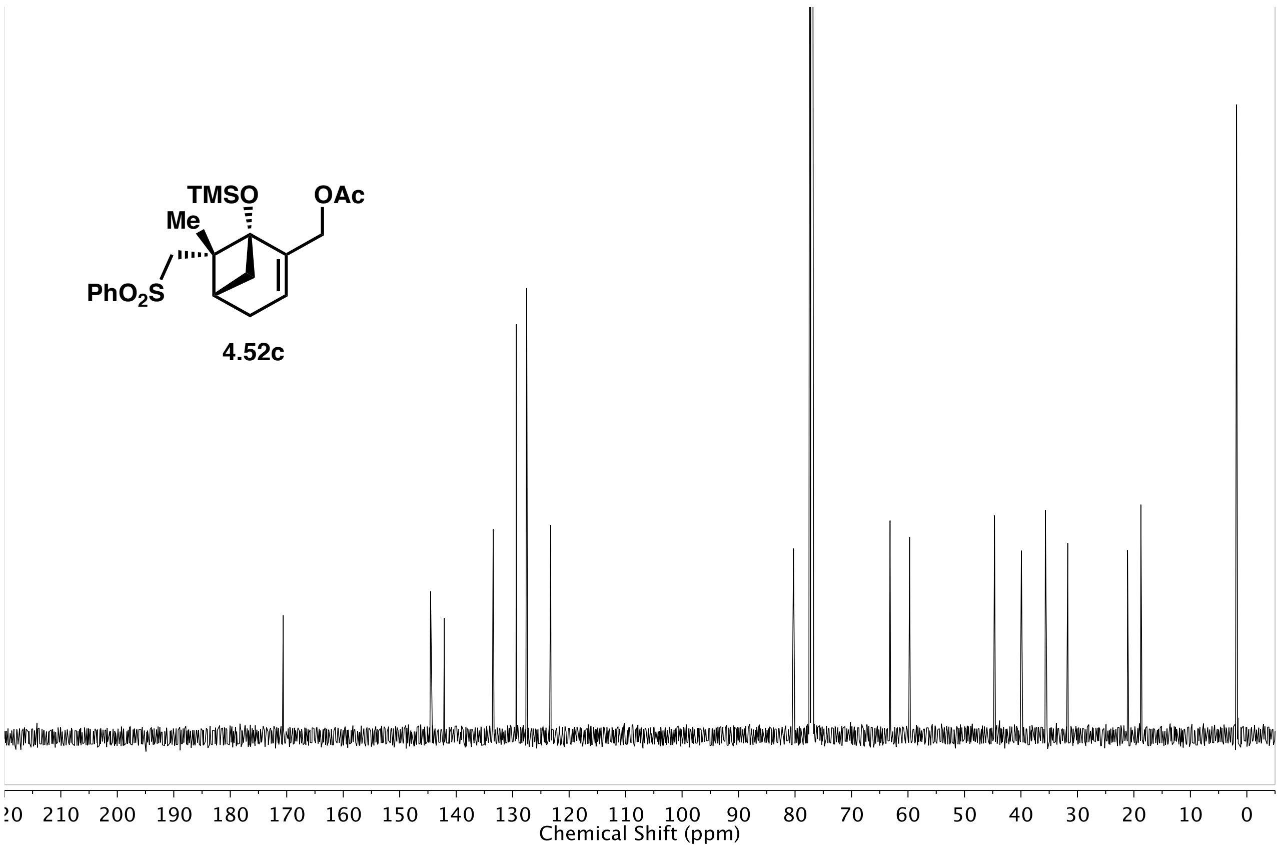
TMSO
OAc
Me
PhO$_2$S
220 210 200 190 180 170 160 150 140 130 120 110 100 90 80 70 60 50 40 30 20 10 0
Chemical Shift (ppm)

4.52c

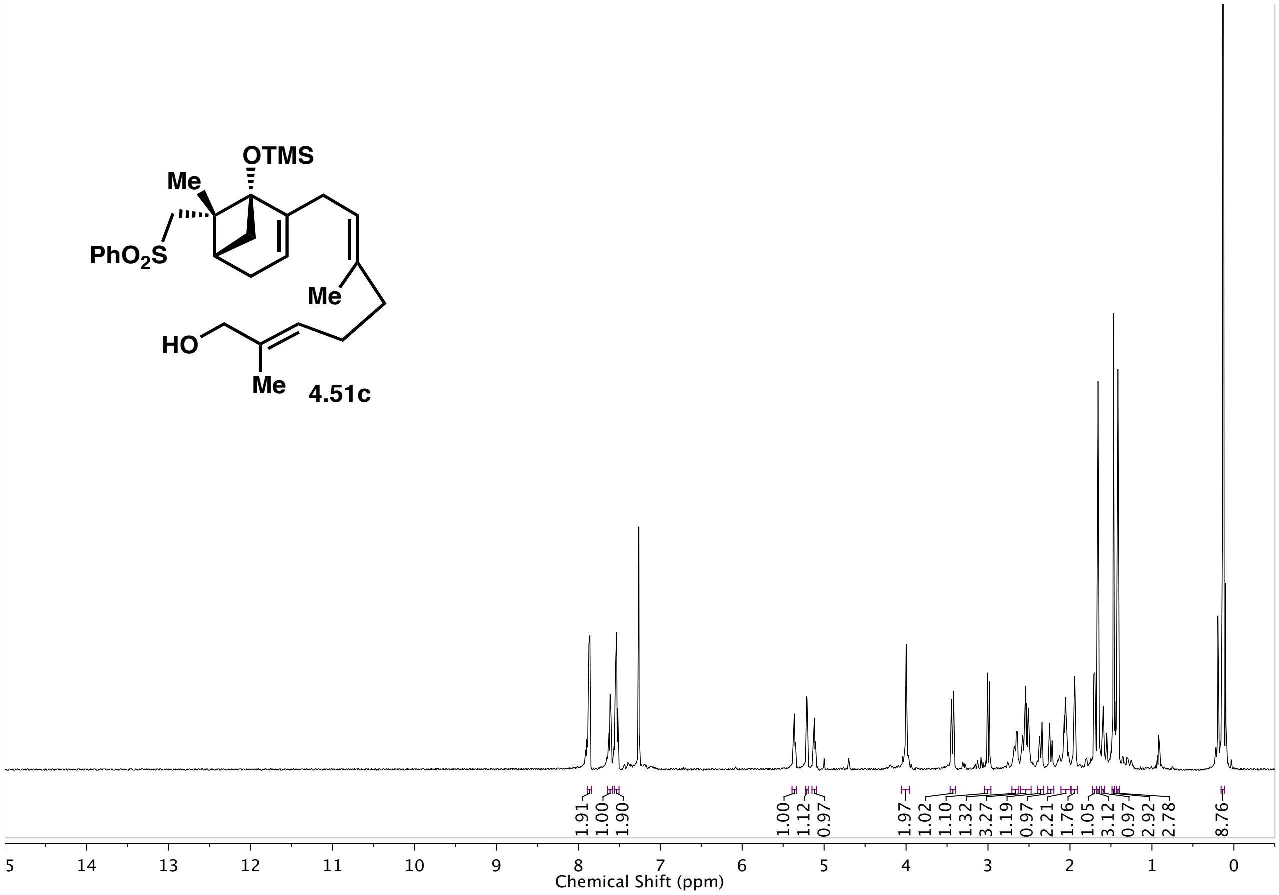
OTMS
Me
PhO2S
Me
HO
Me
4.51c
1.91
1.00
1.90
1.00
1.12
0.97
1.97
1.02
1.10
1.32
3.27
1.19
0.97
2.21
1.76
1.05
3.12
0.97
2.92
2.78
8.76
5
14
13
12
11
10
9
8
7
6
5
4
3
2
1
0
Chemical Shift (ppm)

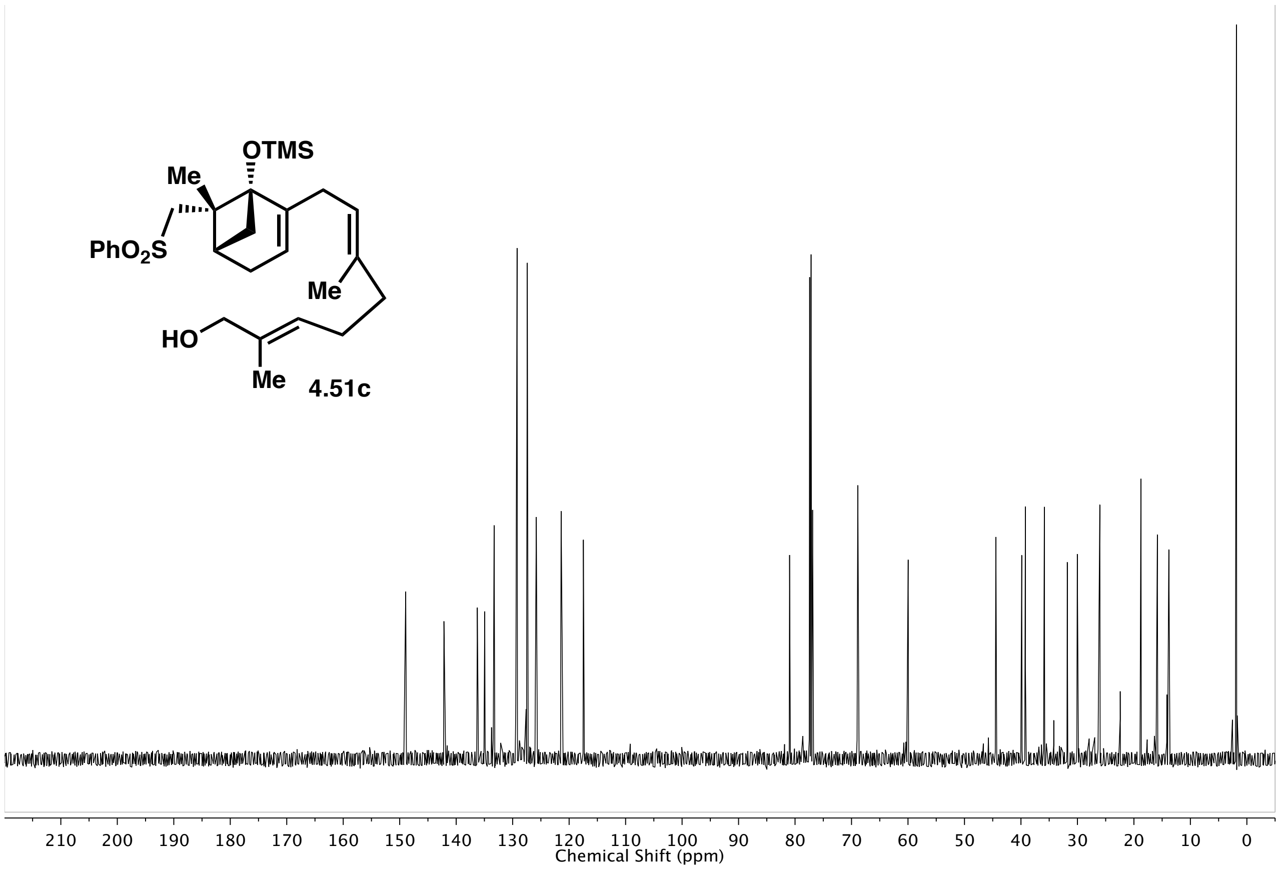
OTMS
Me
PhO2S
Me
HO
Me
4.51c
210
200
190
180
170
160
150
140
130
120
110
100
90
80
70
60
50
40
30
20
10
0
Chemical Shift (ppm)

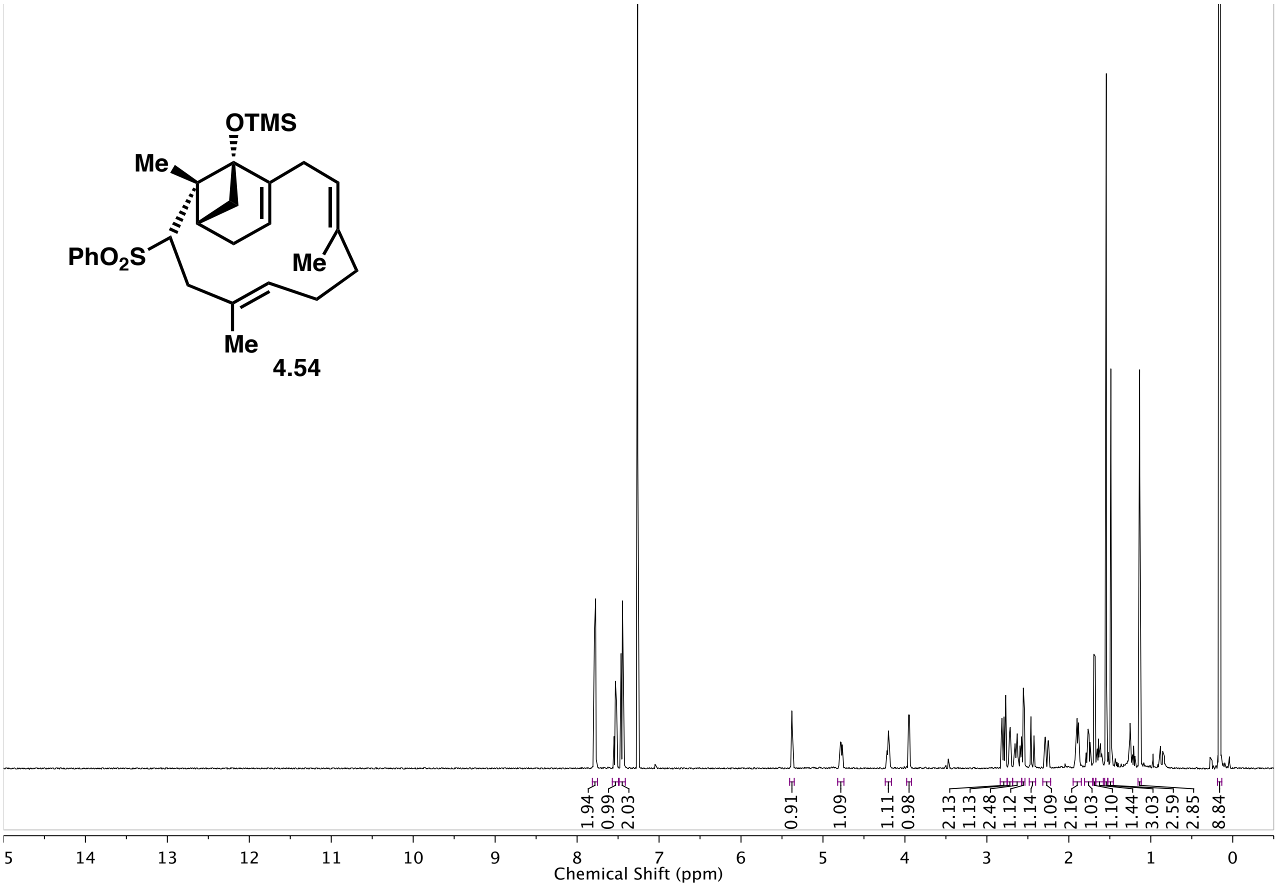
OTMS
Me
PhO2S
Me
Me
4.54
1.94
0.99
2.03
0.91
1.09
1.11
0.98
2.13
1.13
2.48
1.12
1.14
1.09
2.16
1.03
1.10
1.44
3.03
2.59
2.85
8.84
5
14
13
12
11
10
9
8
7
6
5
4
3
2
1
0
Chemical Shift (ppm)

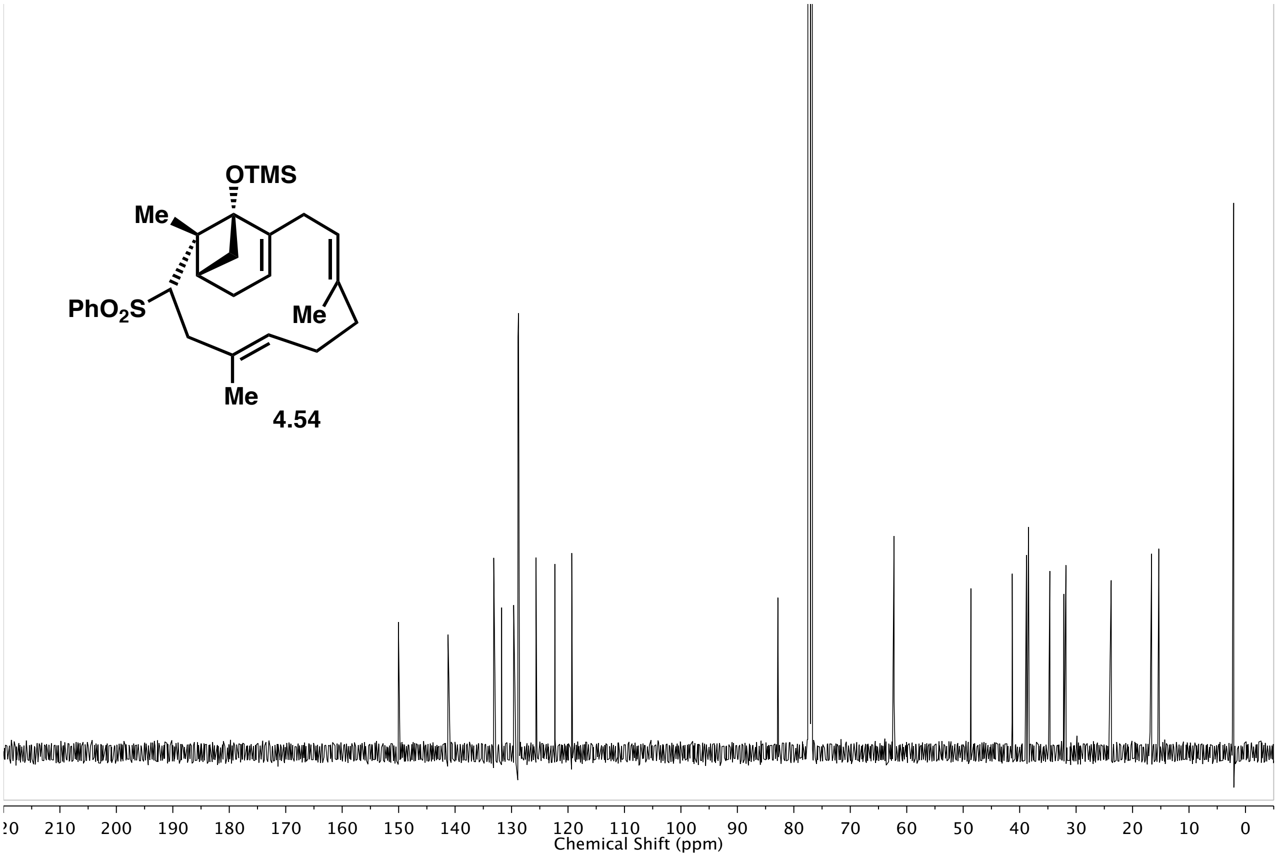
OTMS
Me
PhO2S
Me
Me
4.54
20
210
200
190
180
170
160
150
140
130
120
110
100
90
80
70
60
50
40
30
20
10
0
Chemical Shift (ppm)

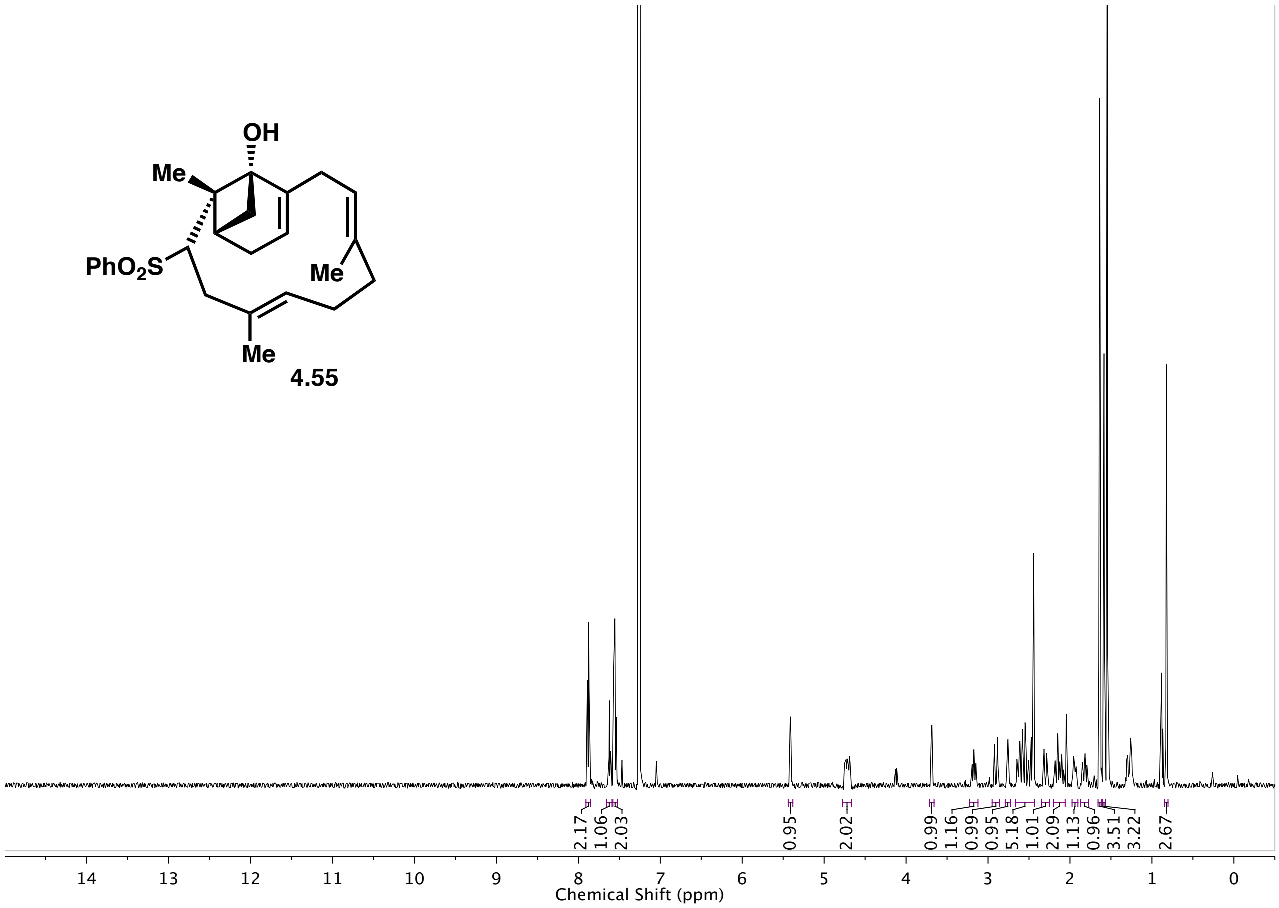
OH
Me
PhO$_2$S
Me
Me
4.55
2.17
1.06
2.03
0.95
2.02
0.99
1.16
0.99
0.95
5.18
1.01
2.09
1.13
0.96
3.51
3.22
2.67
14
13
12
11
10
9
8
7
6
5
4
3
2
1
0
Chemical Shift (ppm)

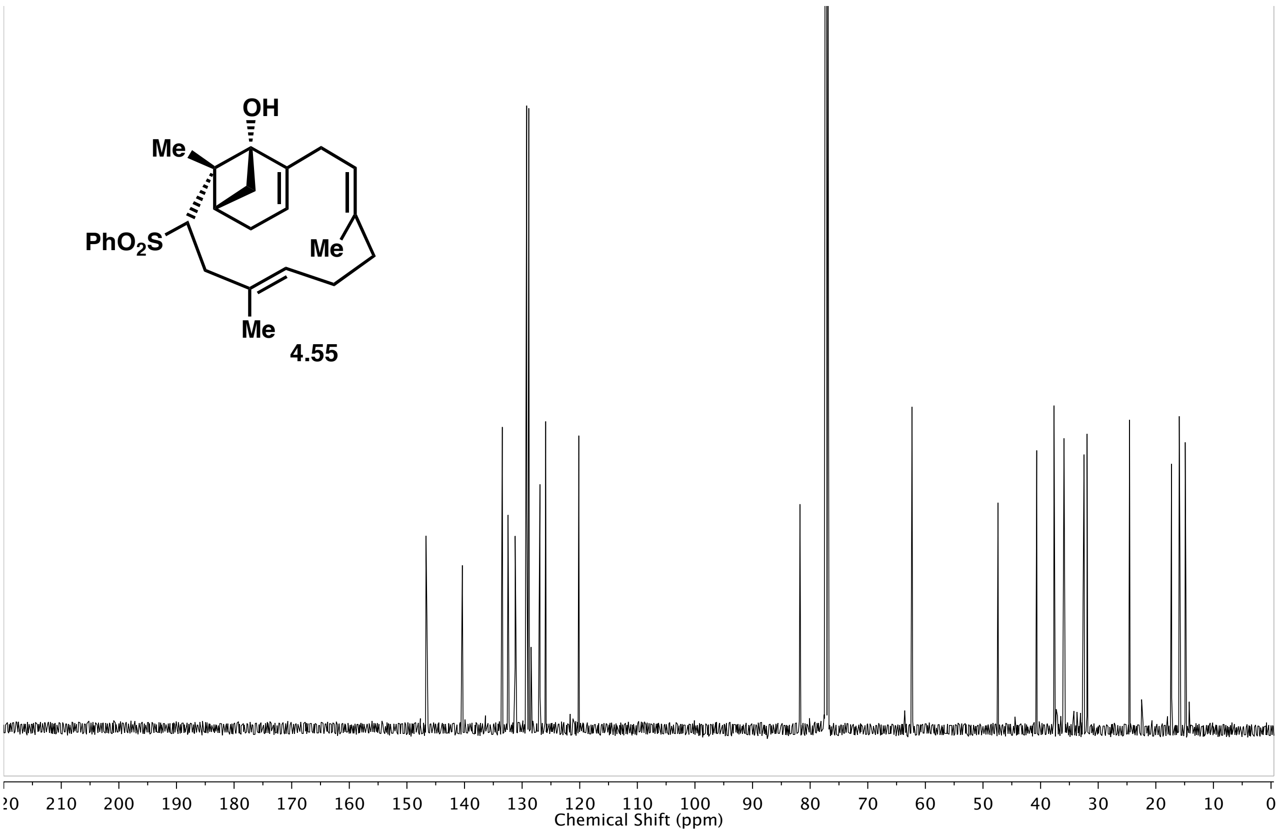
OH
Me
PhO$_2$S
Me
Me
4.55
20
210
200
190
180
170
160
150
140
130
120
110
100
90
80
70
60
50
40
30
20
10
0
Chemical Shift (ppm)

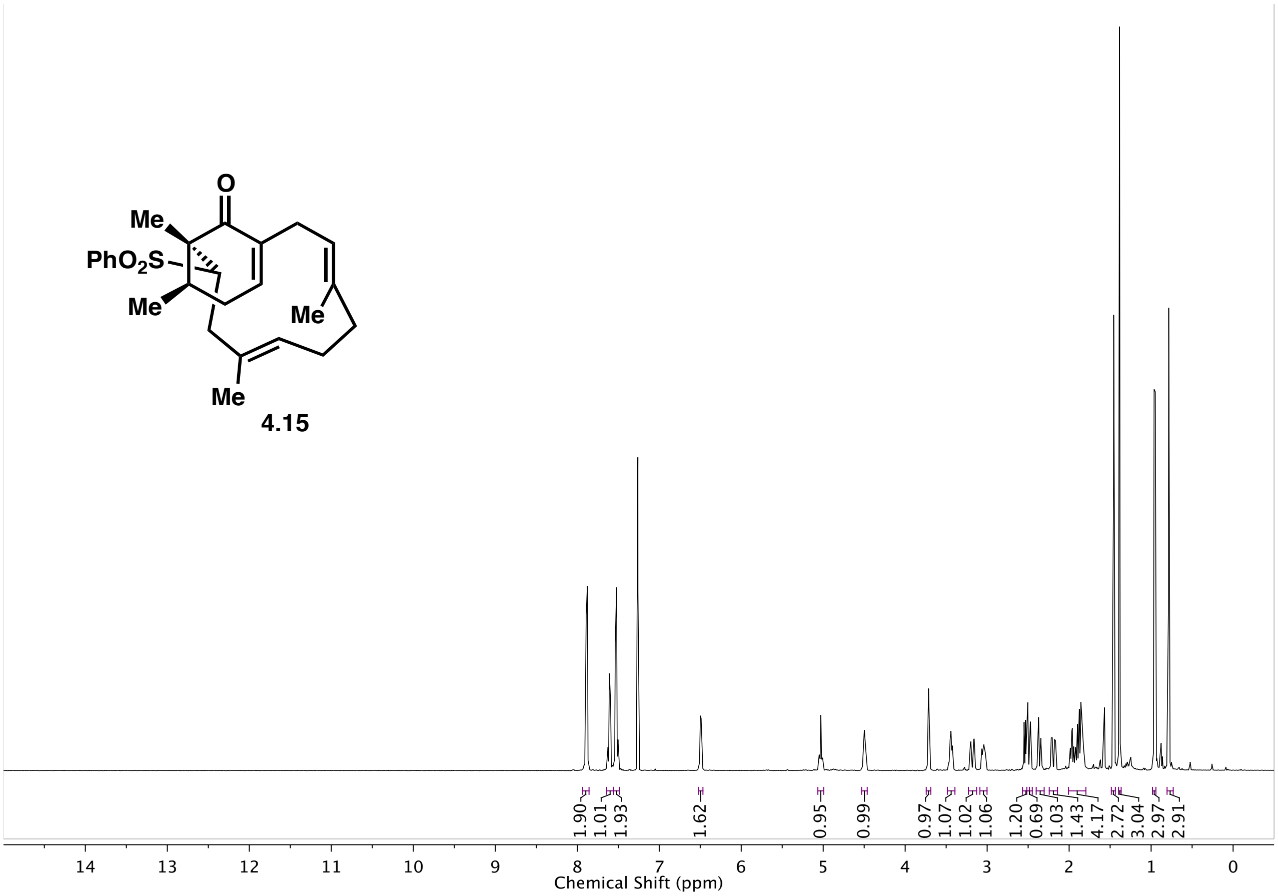
O
Me
PhO$_2$S
Me
Me
Me
4.15
1.90
1.01
1.93
1.62
0.95
0.99
0.97
1.07
1.02
1.06
1.20
0.69
1.03
1.43
4.17
2.72
3.04
2.97
2.91
14 13 12 11 10 9 8 7 6 5 4 3 2 1 0
Chemical Shift (ppm)

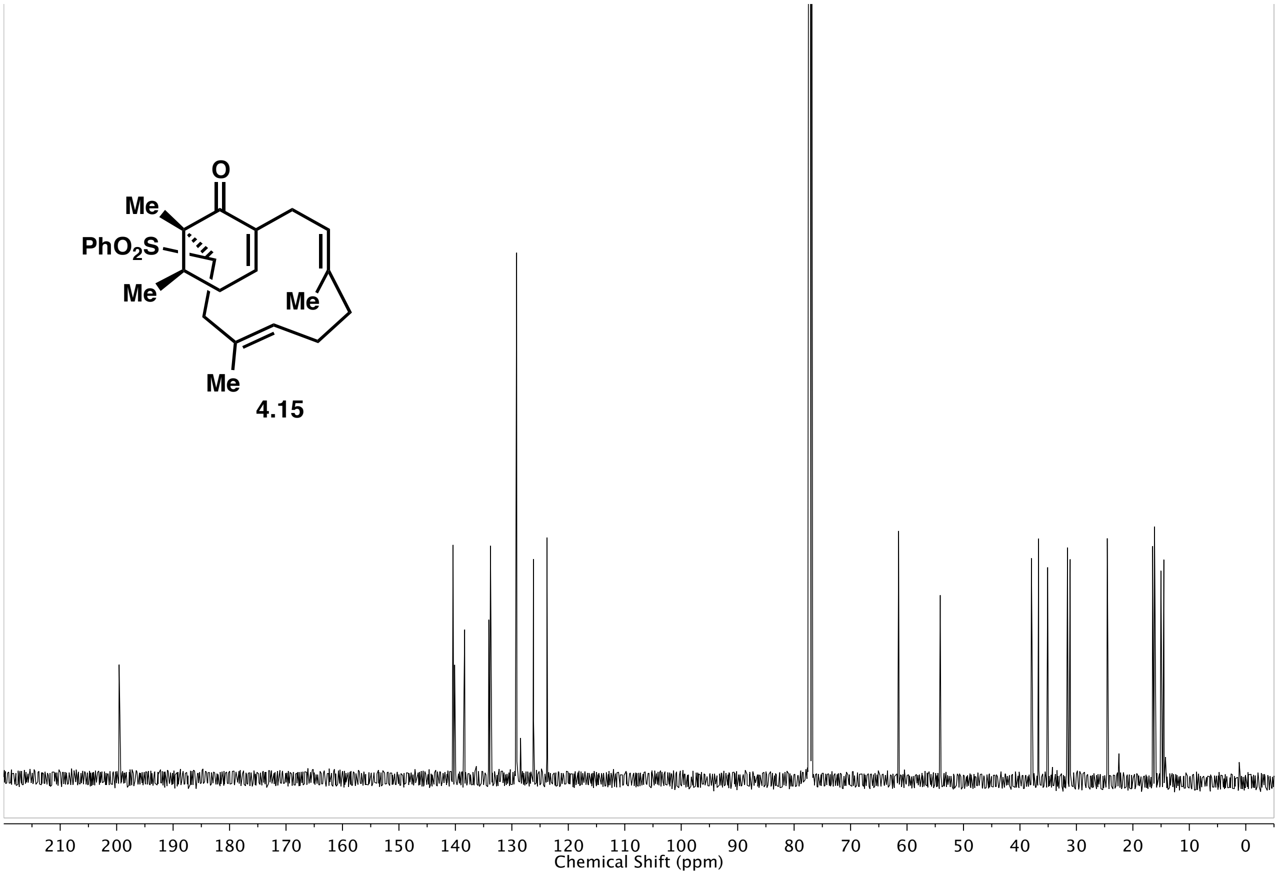
O
Me
PhO$_2$S
Me
Me
Me
4.15
210 200 190 180 170 160 150 140 130 120 110 100 90 80 70 60 50 40 30 20 10 0
Chemical Shift (ppm)

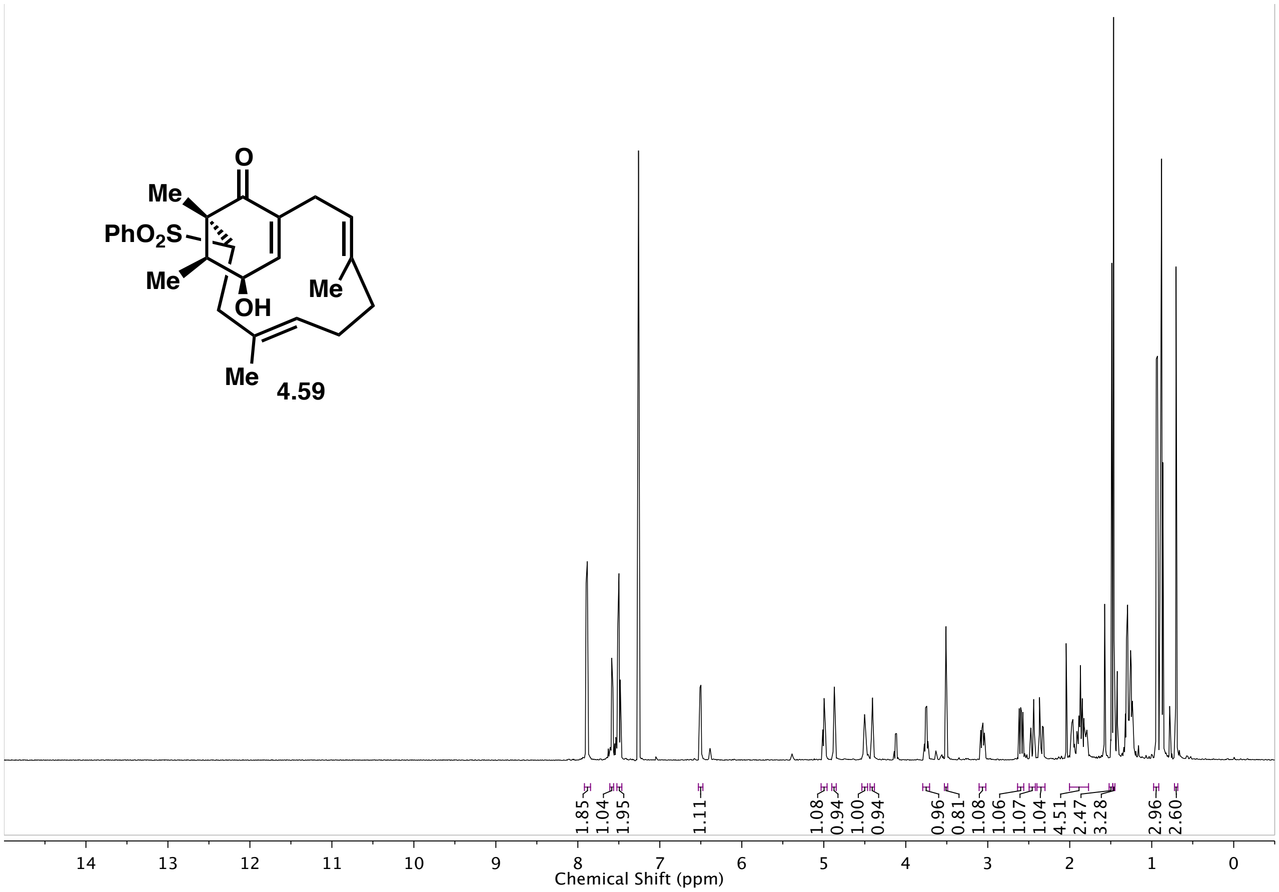
4.59
O
Me
PhO2S
Me
OH
Me
Me
1.85
1.04
1.95
1.11
1.08
0.94
1.00
0.94
0.96
0.81
1.08
1.06
1.07
1.04
4.51
2.47
3.28
2.96
2.60
14
13
12
11
10
9
8
7
6
5
4
3
2
1
0
Chemical Shift (ppm)

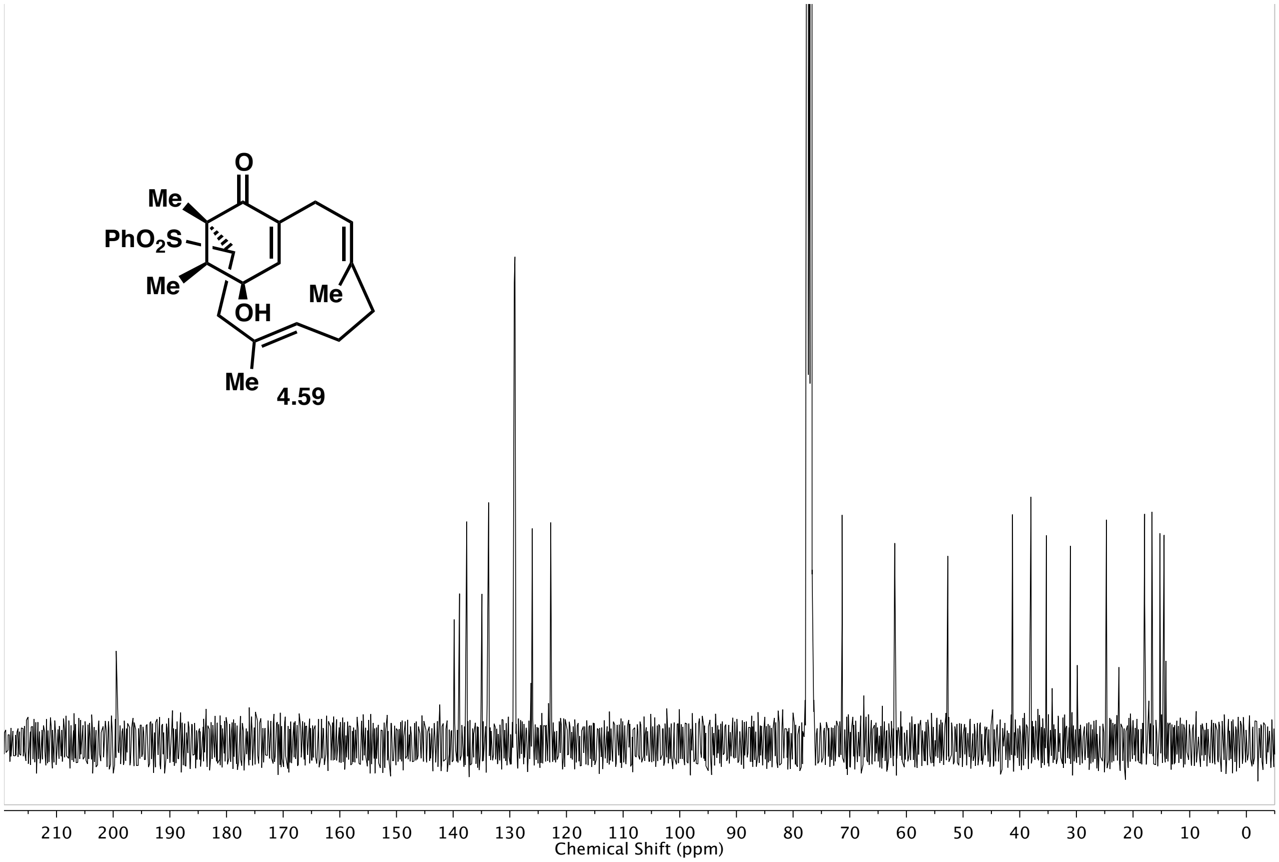
4.59
O
Me
PhO2S
Me
OH
Me
Me
210
200
190
180
170
160
150
140
130
120
110
100
90
80
70
60
50
40
30
20
10
0
Chemical Shift (ppm)

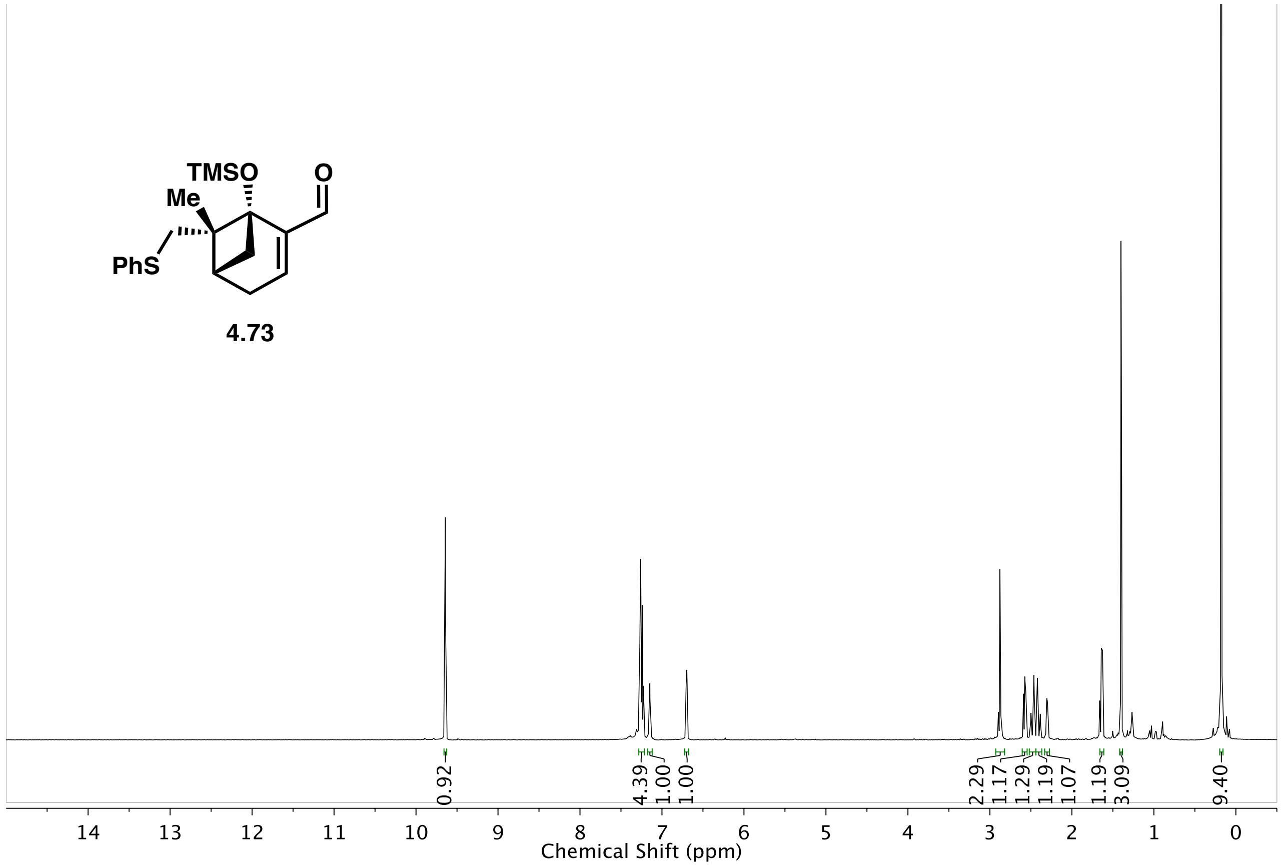
4.73
TMSO
O
Me
PhS
0.92
4.39
1.00
1.00
2.29
1.17
1.29
1.19
1.07
1.19
3.09
9.40
14
13
12
11
10
9
8
7
6
5
4
3
2
1
0
Chemical Shift (ppm)

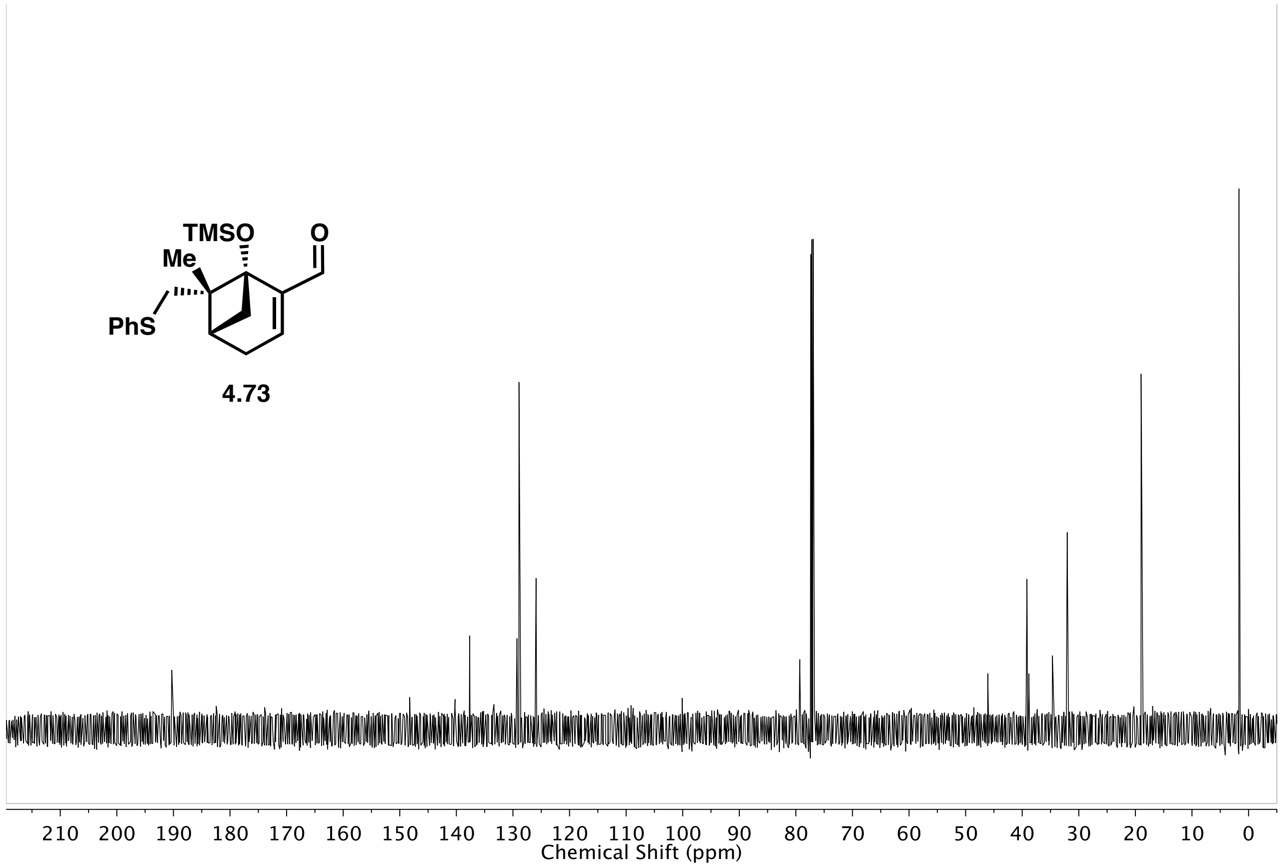
4.73
TMSO
O
Me
PhS
210
200
190
180
170
160
150
140
130
120
110
100
90
80
70
60
50
40
30
20
10
0
Chemical Shift (ppm)

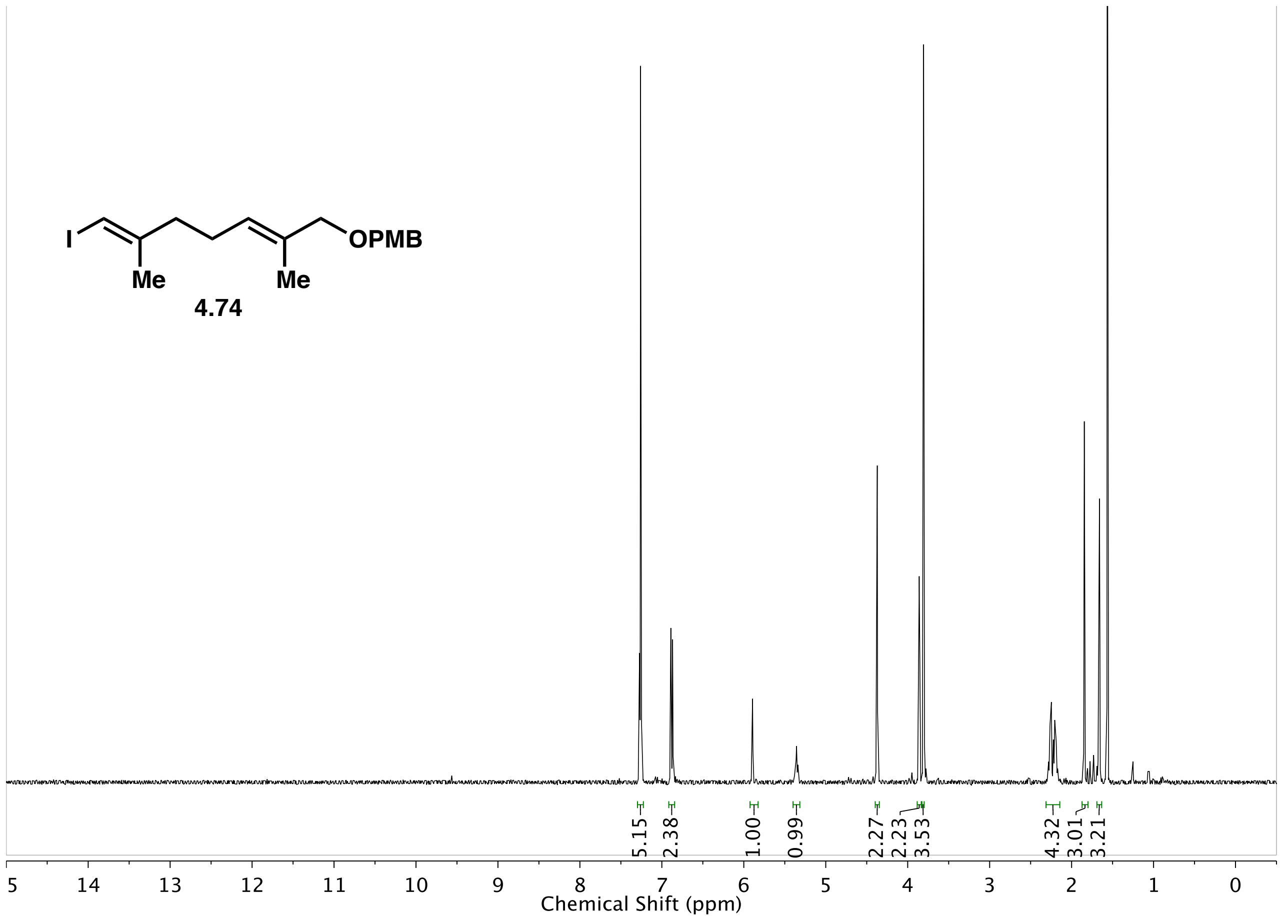
I
OPMB
Me
Me
4.74
5.15
2.38
1.00
0.99
2.27
2.23
3.53
4.32
3.01
3.21
5
14
13
12
11
10
9
8
7
6
5
4
3
2
1
0
Chemical Shift (ppm)

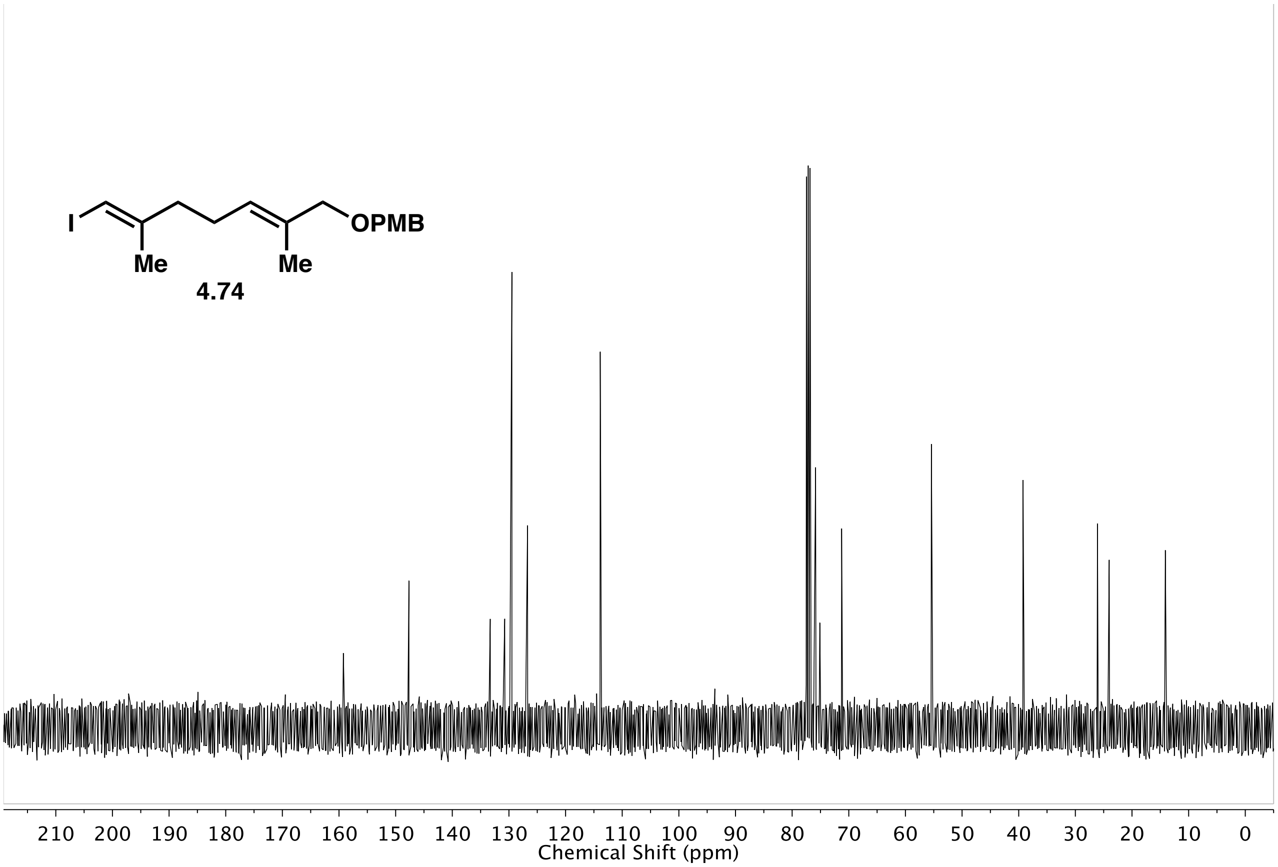
I
OPMB
Me
Me
4.74
210
200
190
180
170
160
150
140
130
120
110
100
90
80
70
60
50
40
30
20
10
0
Chemical Shift (ppm)

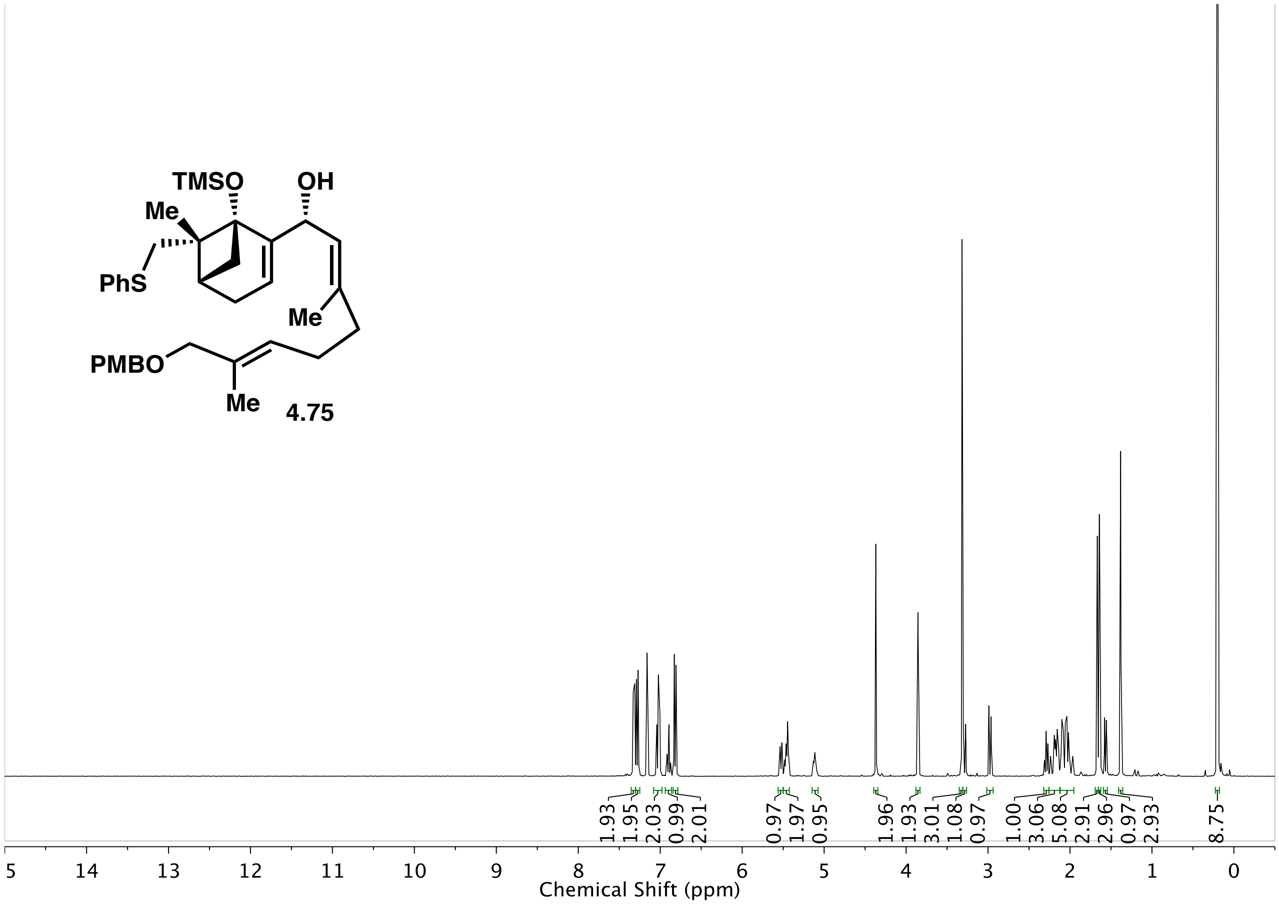
TMSO
OH
Me
PhS
Me
PMBO
Me
4.75
1.93
1.95
2.03
0.99
2.01
0.97
1.97
0.95
1.96
1.93
3.01
1.08
0.97
1.00
3.06
5.08
2.91
2.96
0.97
2.93
8.75
5
14
13
12
11
10
9
8
7
6
5
4
3
2
1
0
Chemical Shift (ppm)

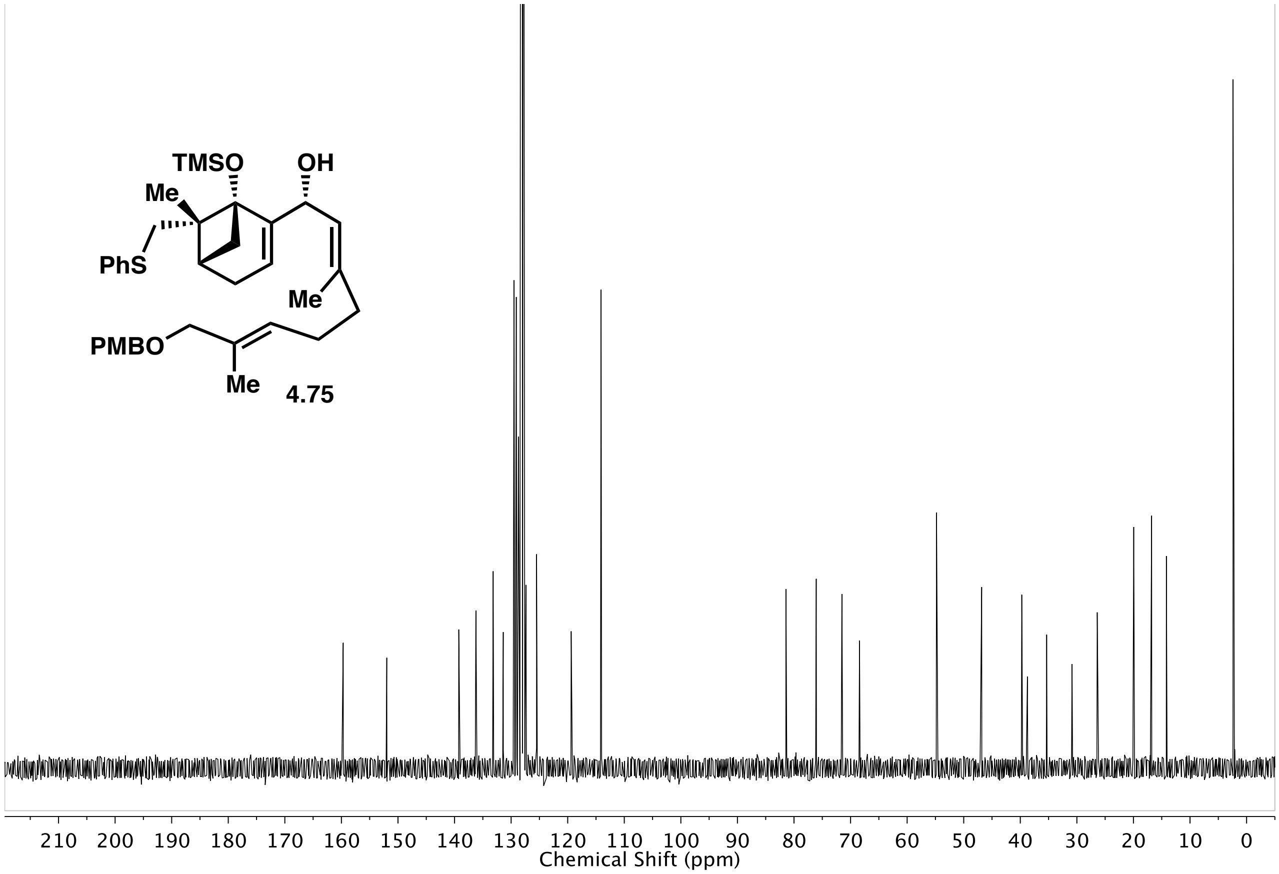
TMSO
OH
Me
PhS
Me
PMBO
Me
4.75
210
200
190
180
170
160
150
140
130
120
110
100
90
80
70
60
50
40
30
20
10
0
Chemical Shift (ppm)

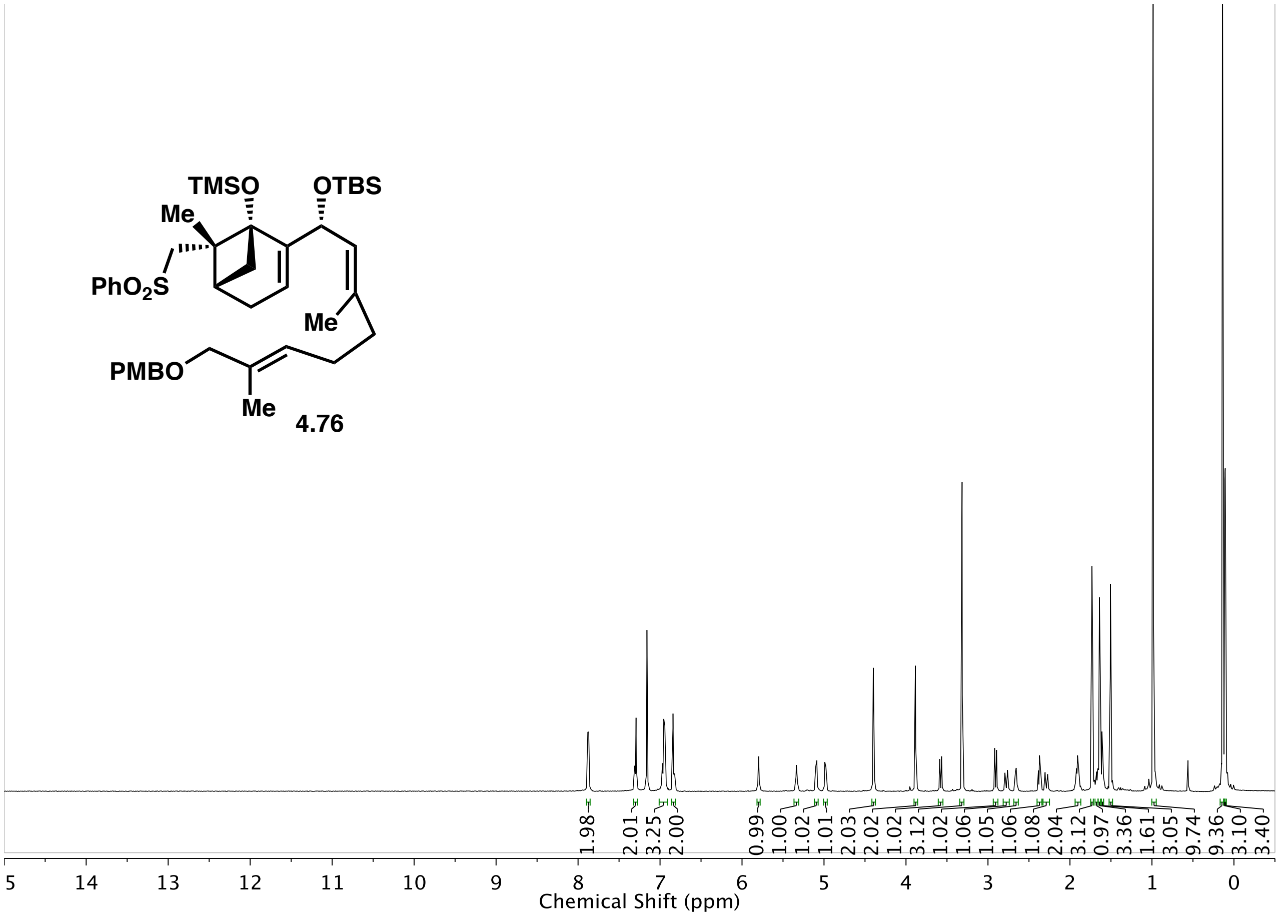
TMSO
OTBS
Me
PhO₂S
Me
PMBO
Me
1.98
2.01
3.25
2.00
0.99
1.00
1.02
1.01
2.03
2.02
1.02
3.12
1.02
1.06
1.05
1.06
1.08
2.04
3.12
0.97
3.36
1.61
3.05
9.74
9.36
3.10
3.40
5
14
13
12
11
10
9
8
7
6
5
4
3
2
1
0
Chemical Shift (ppm)

4.76

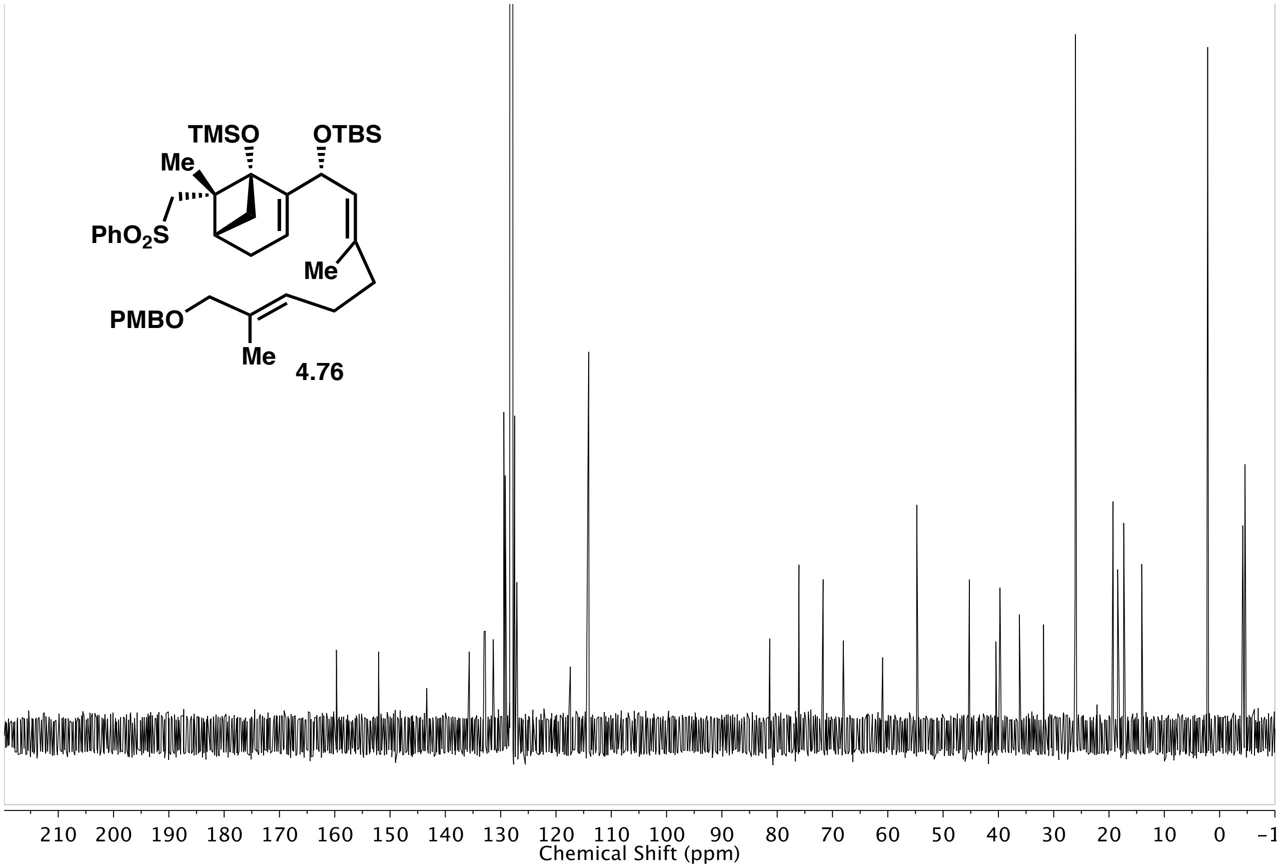
TMSO
OTBS
Me
PhO₂S
Me
PMBO
Me
210
200
190
180
170
160
150
140
130
120
110
100
90
80
70
60
50
40
30
20
10
0
–1
Chemical Shift (ppm)

4.76

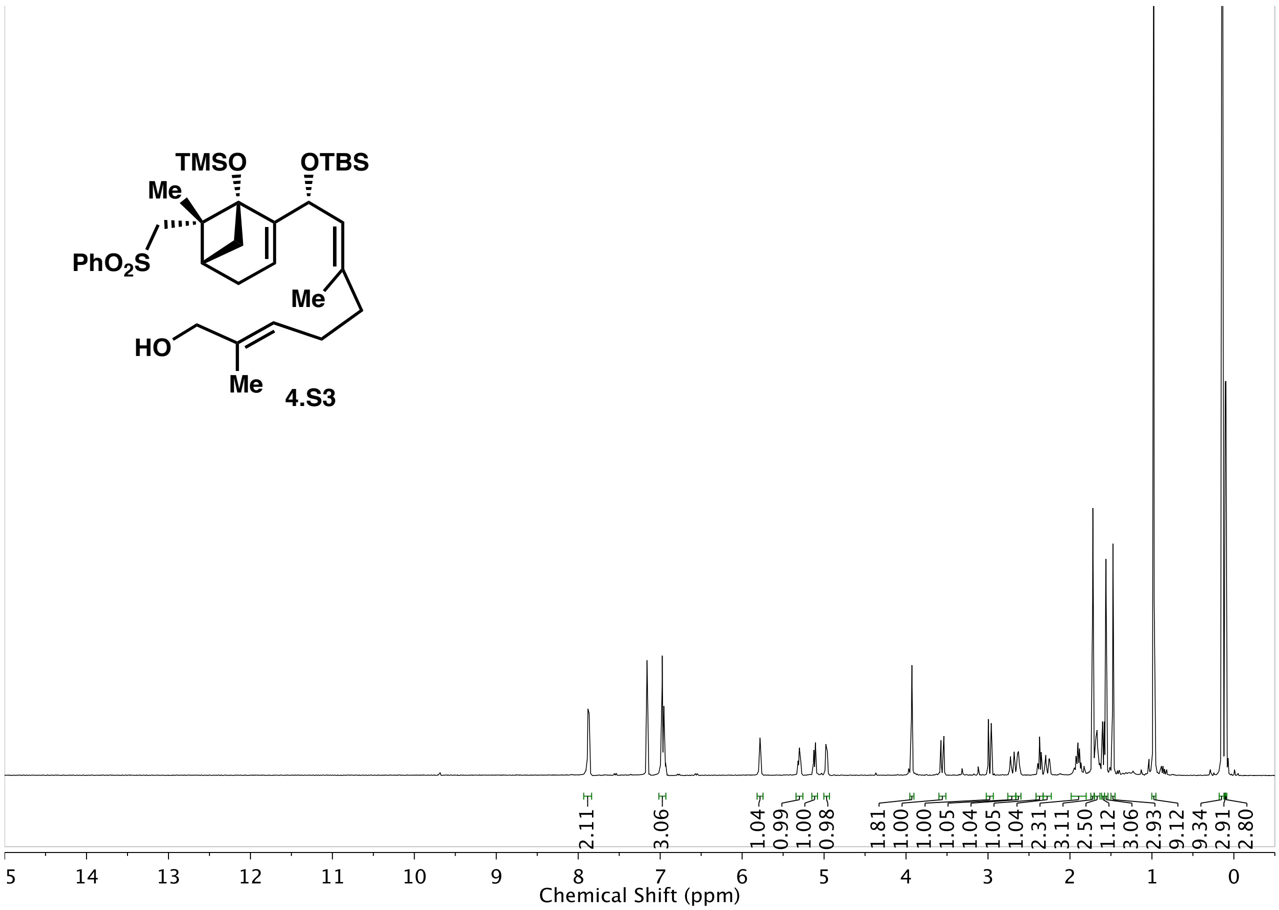
TMSO
OTBS
Me
PhO2S
Me
HO
Me
4.S3
2.11
3.06
1.04
0.99
1.00
0.98
1.81
1.00
1.00
1.05
1.04
1.05
1.04
2.31
3.11
2.50
1.12
3.06
2.93
9.12
9.34
2.91
2.80
15 14 13 12 11 10 9 8 7 6 5 4 3 2 1 0
Chemical Shift (ppm)

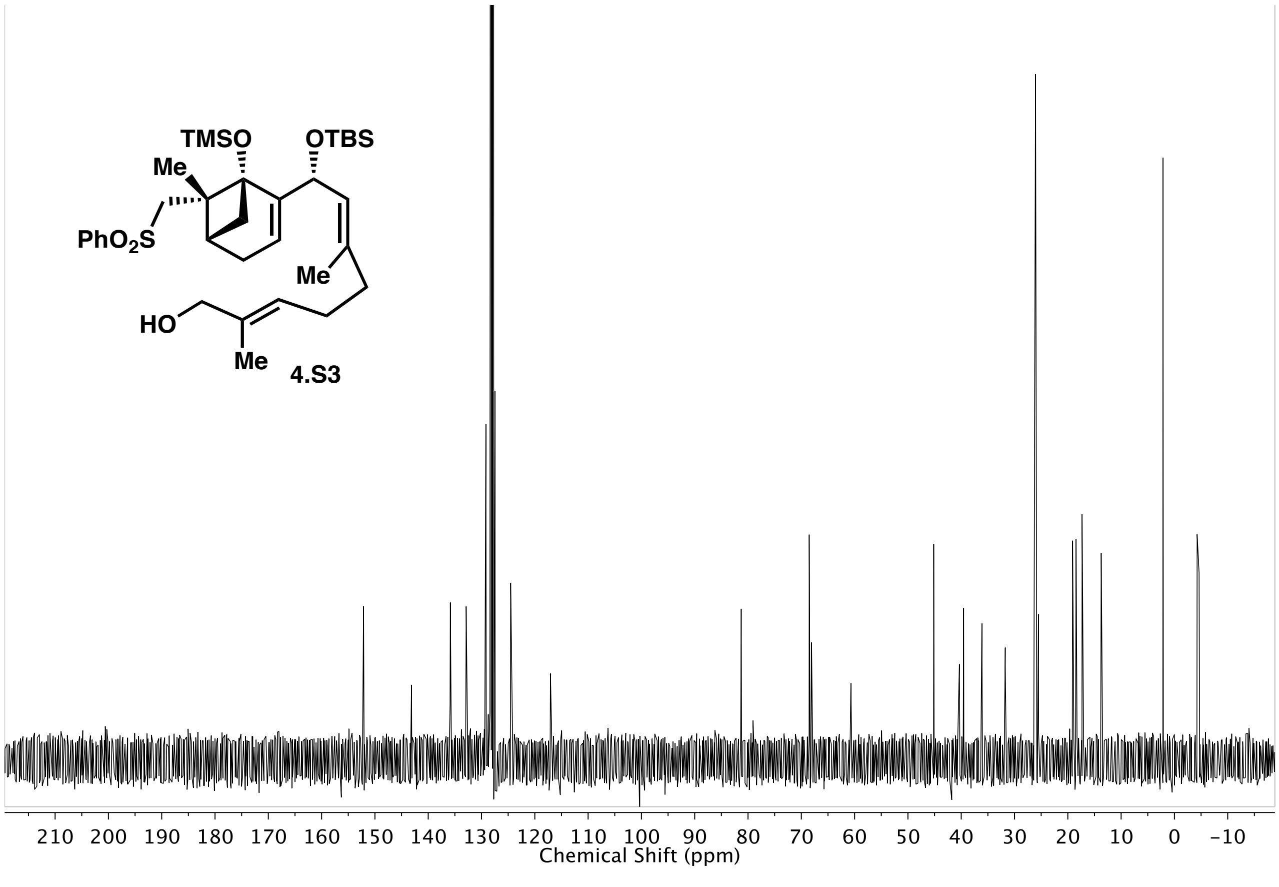
TMSO
OTBS
Me
PhO2S
Me
HO
Me
4.S3
210 200 190 180 170 160 150 140 130 120 110 100 90 80 70 60 50 40 30 20 10 0 −10
Chemical Shift (ppm)

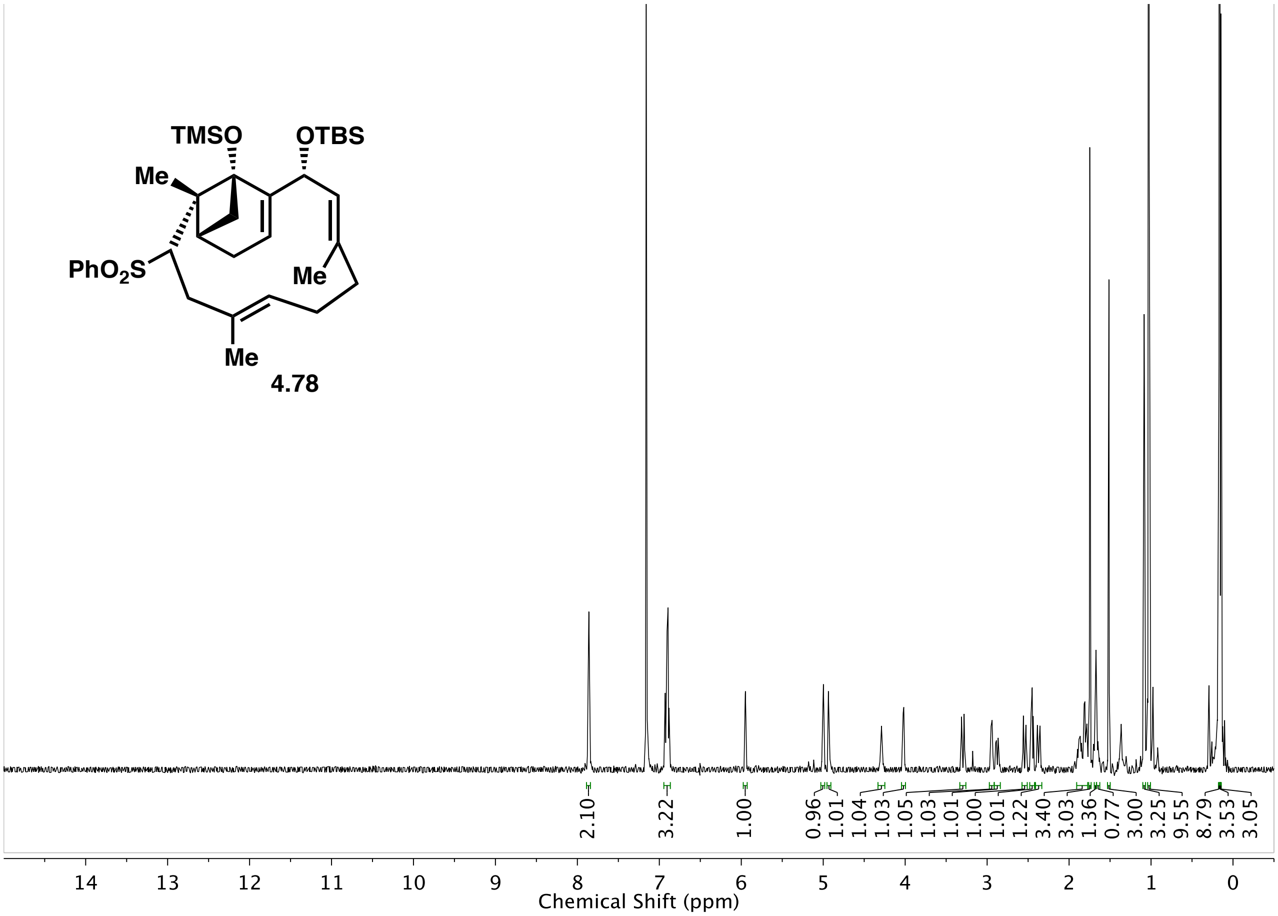
TMSO
OTBS
Me
PhO2S
Me
Me
4.78
2.10
3.22
1.00
0.96
1.01
1.04
1.03
1.05
1.03
1.01
1.00
1.01
1.22
3.40
3.03
1.36
0.77
3.00
3.25
9.55
8.79
3.53
3.05
14
13
12
11
10
9
8
7
6
5
4
3
2
1
0
Chemical Shift (ppm)

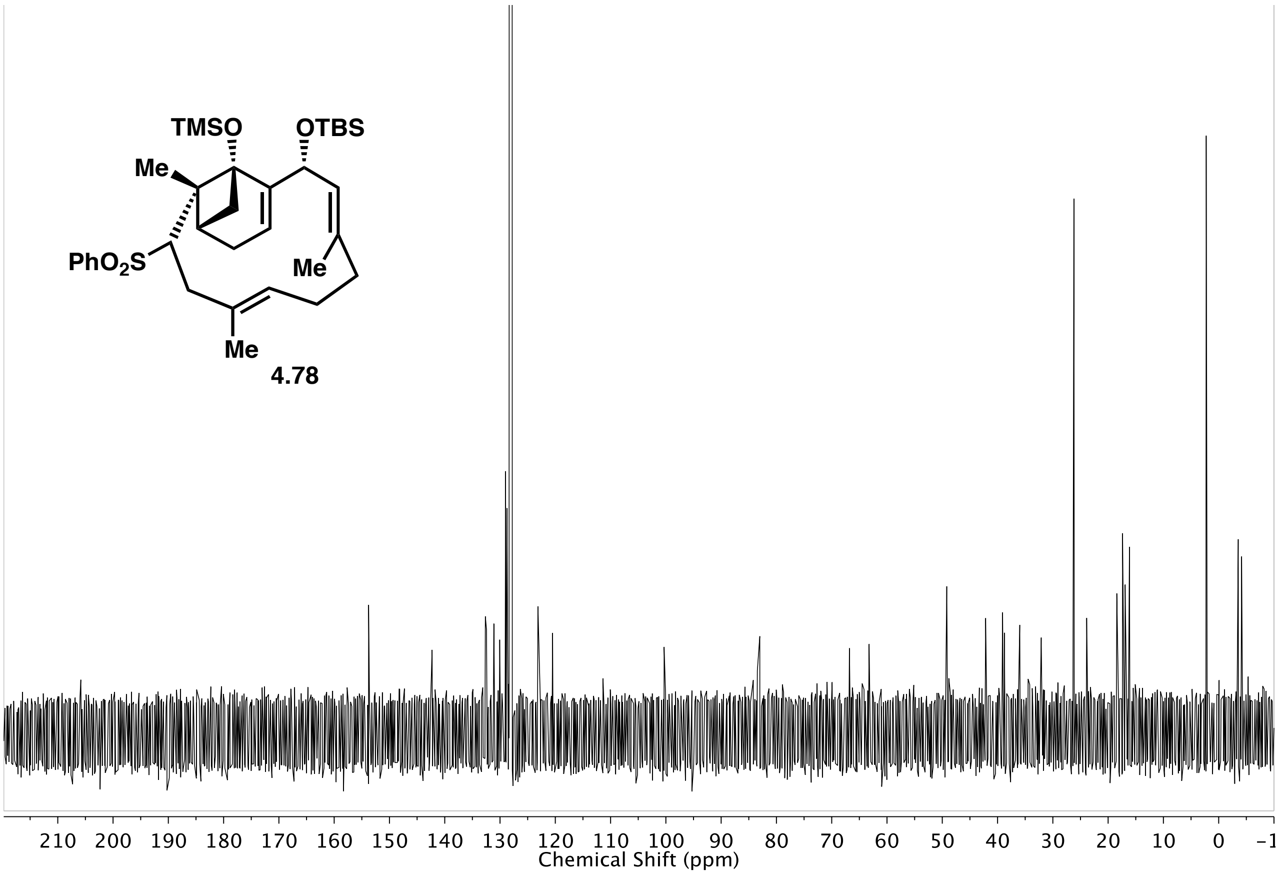
TMSO
OTBS
Me
PhO2S
Me
Me
4.78
210
200
190
180
170
160
150
140
130
120
110
100
90
80
70
60
50
40
30
20
10
0
–1
Chemical Shift (ppm)

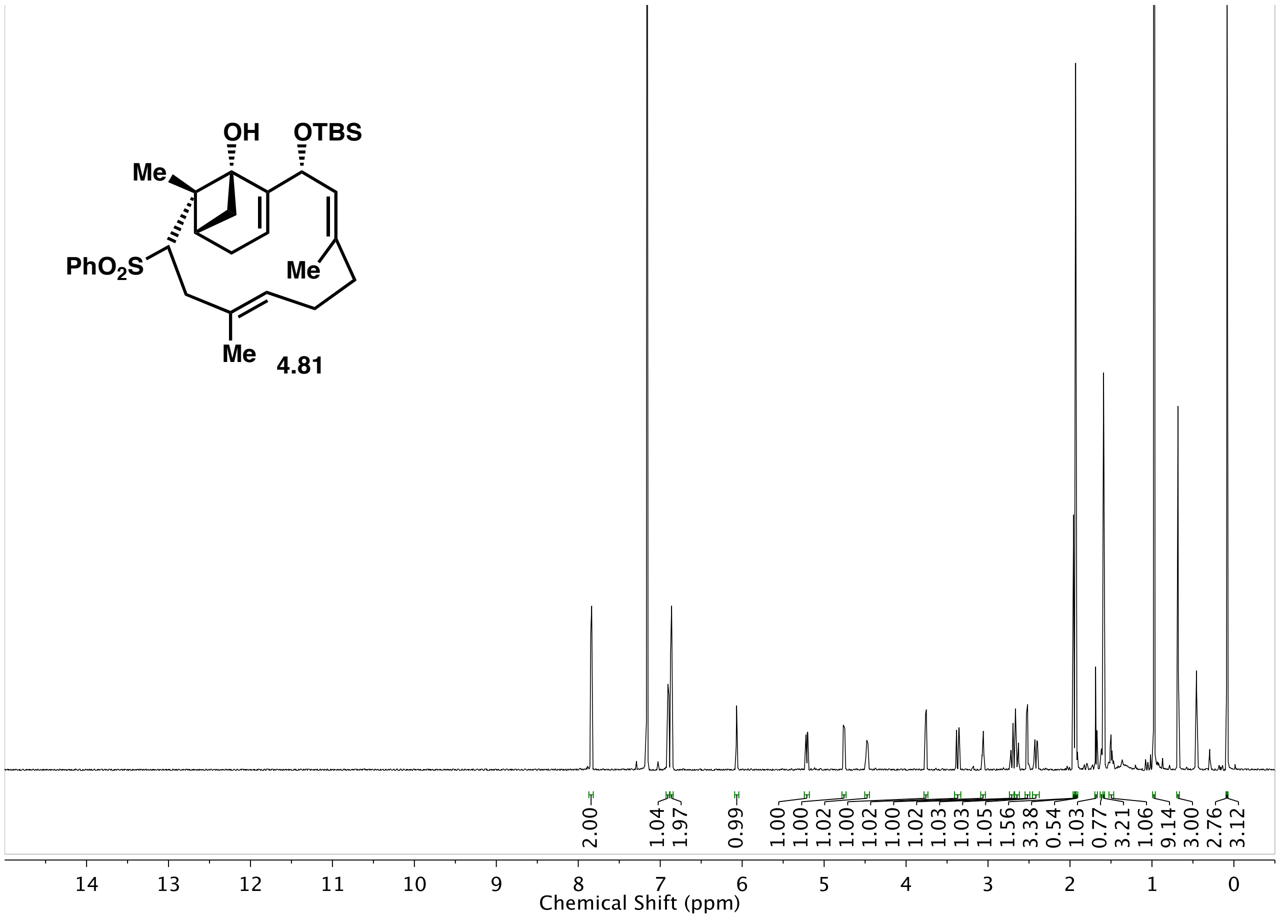
OH
OTBS
Me
PhO2S
Me
Me
4.81
2.00
1.04
1.97
0.99
1.00
1.00
1.02
1.00
1.02
1.00
1.02
1.03
1.03
1.05
1.56
3.38
0.54
1.03
0.77
3.21
1.06
9.14
3.00
2.76
3.12
14 13 12 11 10 9 8 7 6 5 4 3 2 1 0
Chemical Shift (ppm)

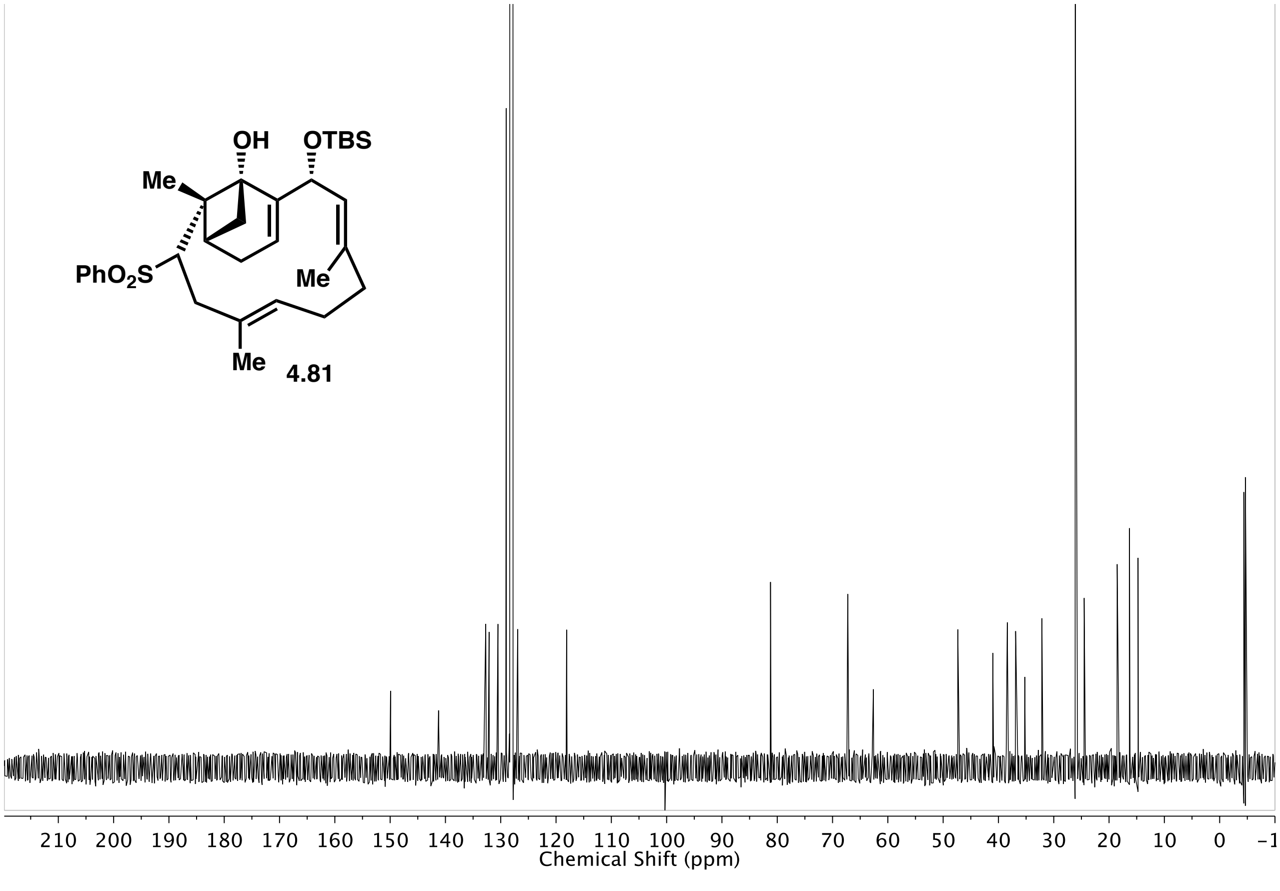
OH
OTBS
Me
PhO2S
Me
Me
4.81
210 200 190 180 170 160 150 140 130 120 110 100 90 80 70 60 50 40 30 20 10 0 −1
Chemical Shift (ppm)

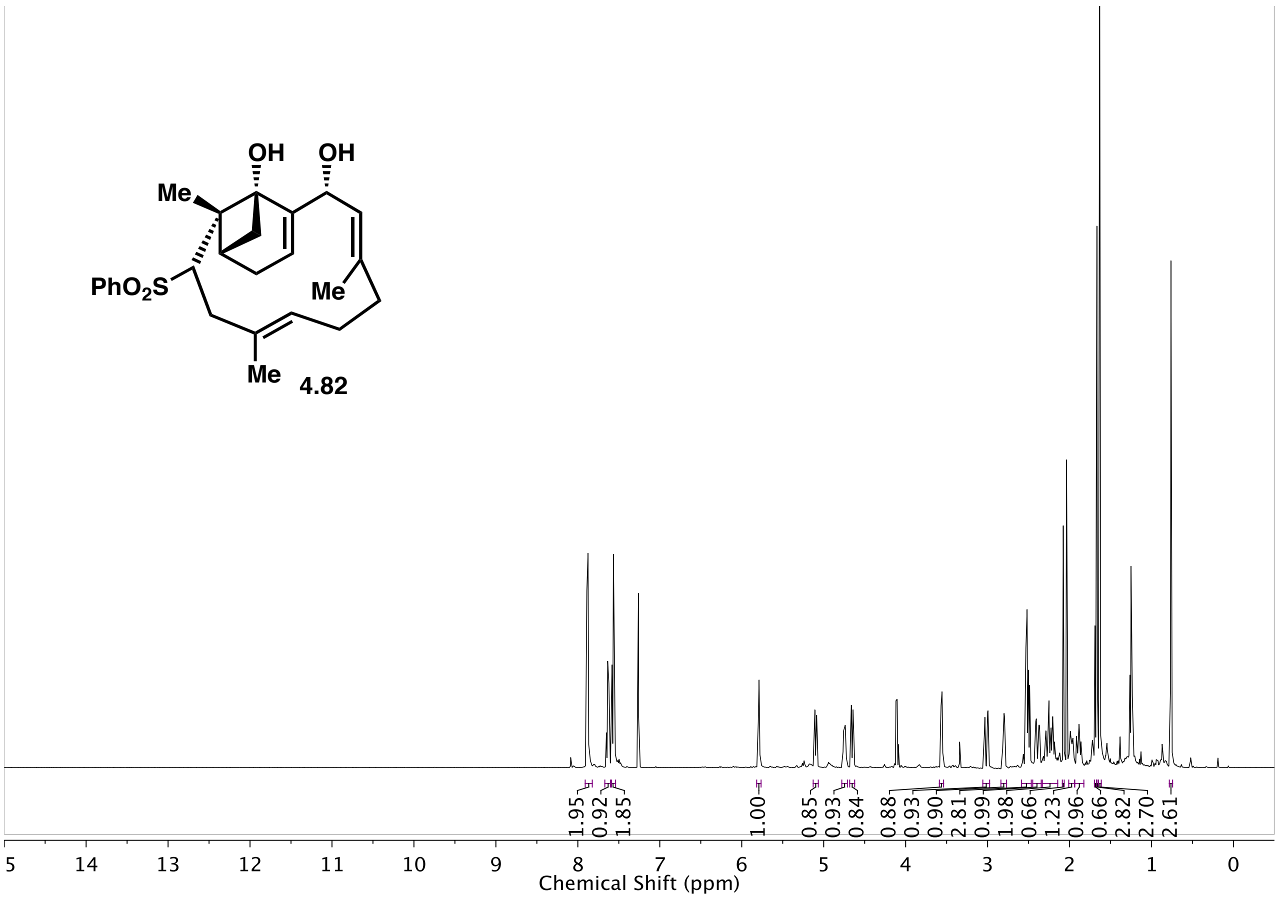
OH
OH
Me
PhO2S
Me
Me
4.82
1.95
0.92
1.85
1.00
0.85
0.93
0.84
0.88
0.93
0.90
2.81
0.99
1.98
0.66
1.23
0.96
0.66
2.82
2.70
2.61
5
14
13
12
11
10
9
8
7
6
5
4
3
2
1
0
Chemical Shift (ppm)

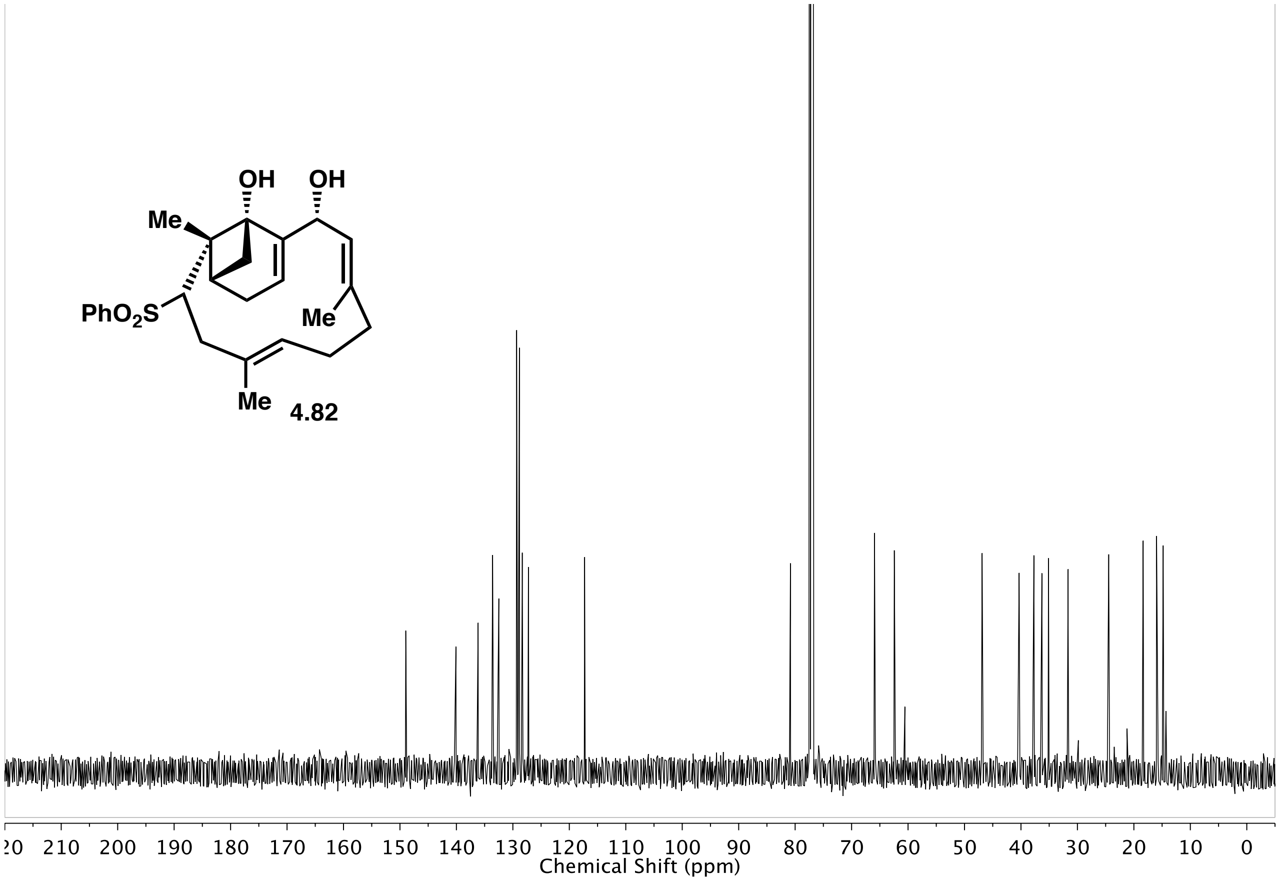
OH
OH
Me
PhO2S
Me
Me
4.82
20
210
200
190
180
170
160
150
140
130
120
110
100
90
80
70
60
50
40
30
20
10
0
Chemical Shift (ppm)

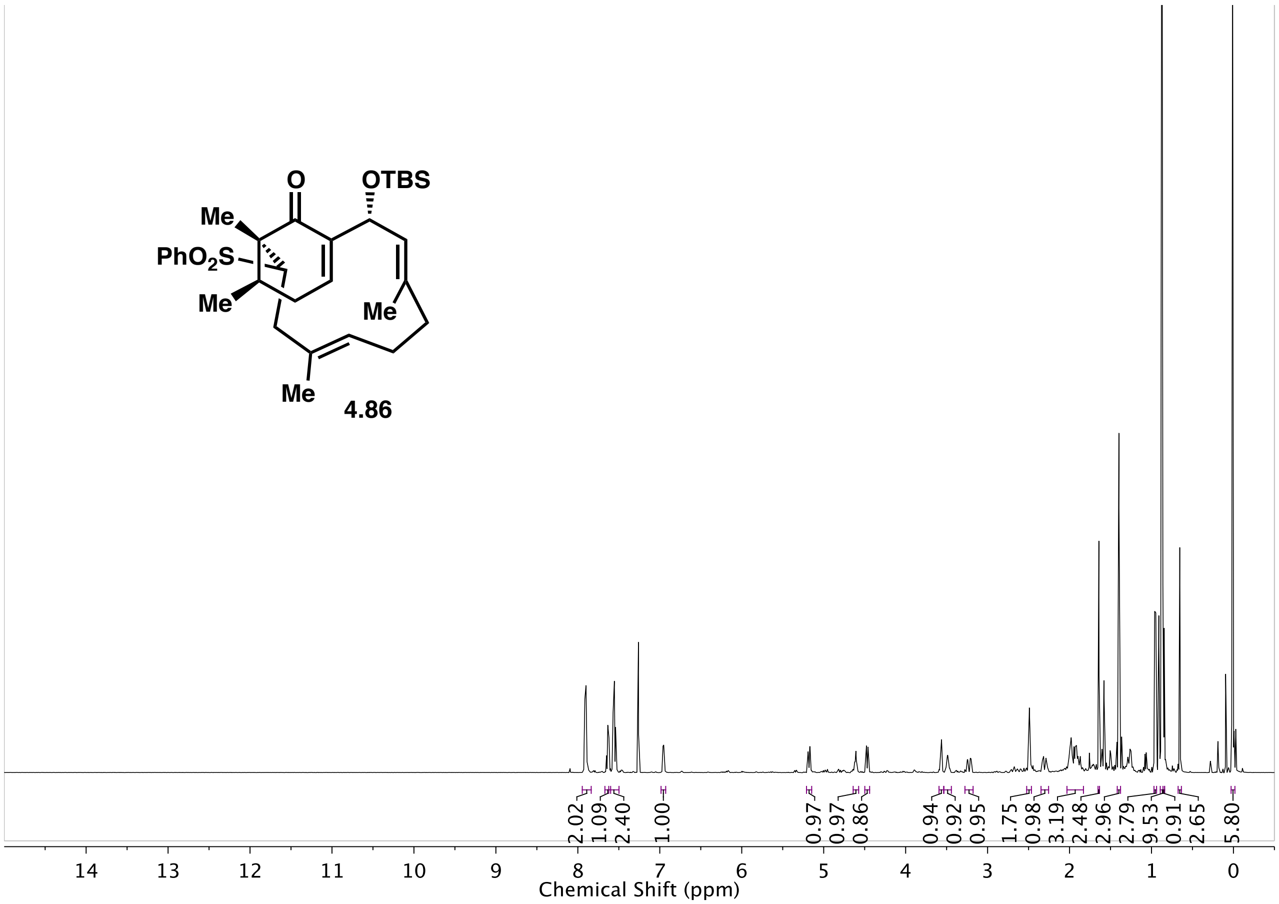
O
OTBS
Me
PhO2S
Me
Me
Me
2.02
1.09
2.40
1.00
0.97
0.97
0.86
0.94
0.92
0.95
1.75
0.98
3.19
2.48
2.96
2.79
9.53
0.91
2.65
5.80
14
13
12
11
10
9
8
7
6
5
4
3
2
1
0
Chemical Shift (ppm)

4.86

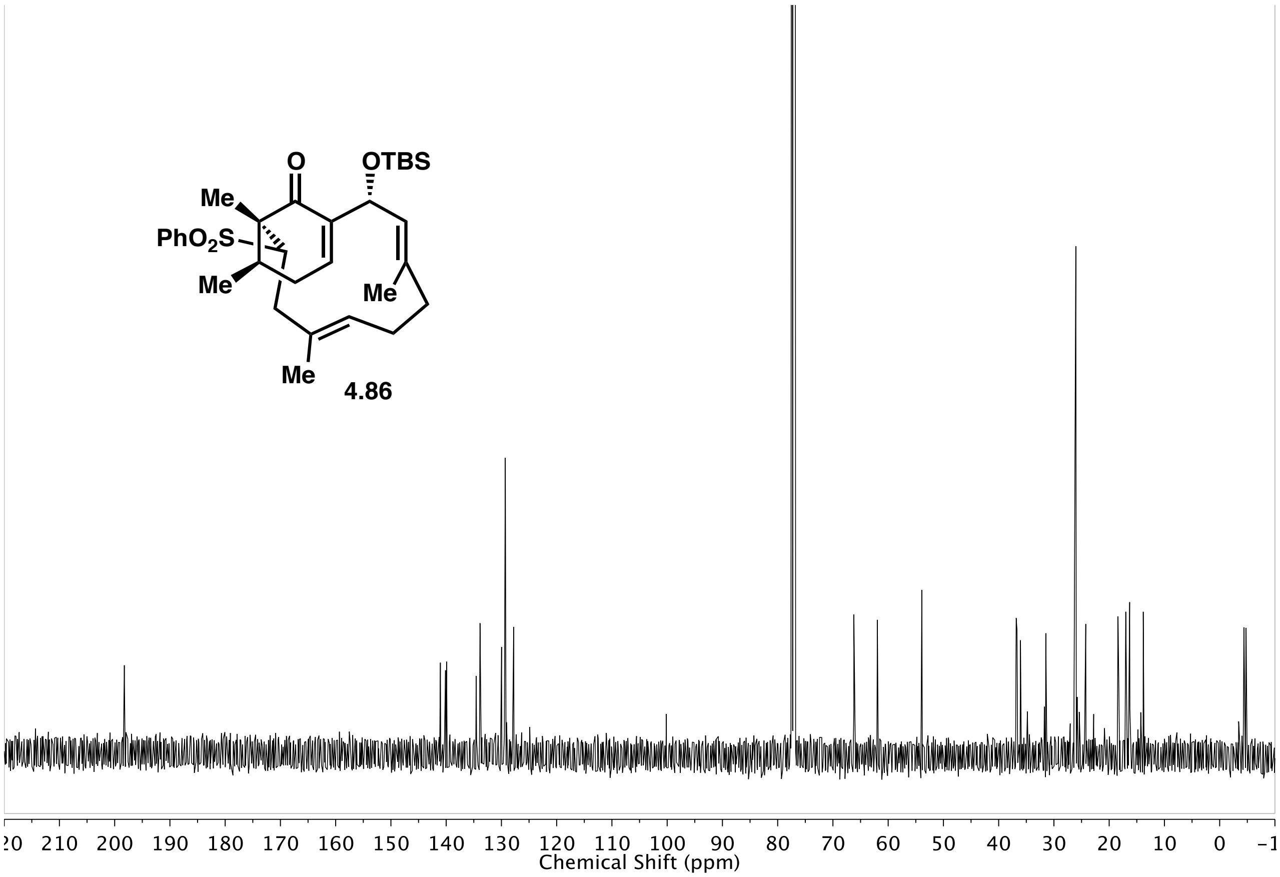
O
OTBS
Me
PhO2S
Me
Me
Me
20
210
200
190
180
170
160
150
140
130
120
110
100
90
80
70
60
50
40
30
20
10
0
–1
Chemical Shift (ppm)

4.86

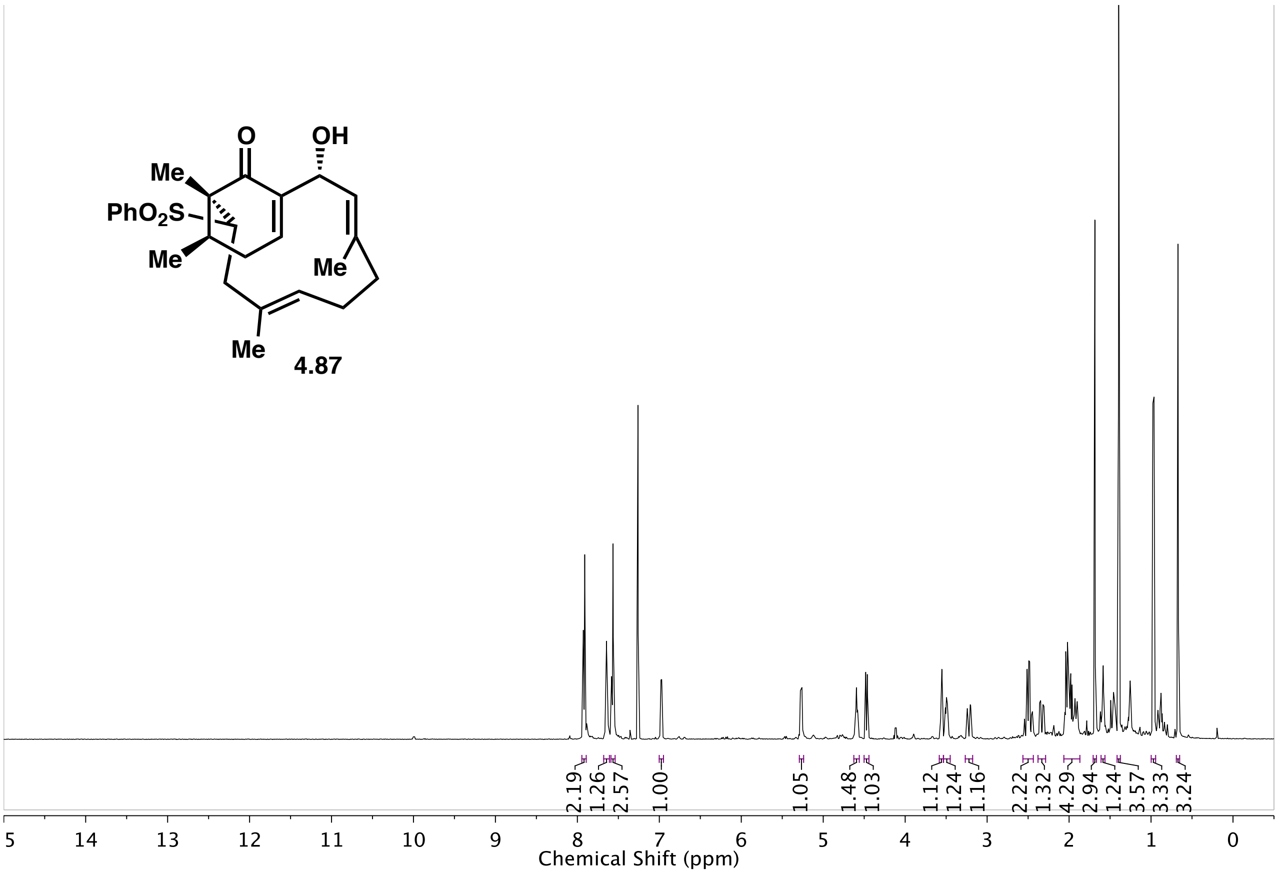
O
OH
Me
PhO2S
Me
Me
Me
4.87
2.19
1.26
2.57
1.00
1.05
1.48
1.03
1.12
1.24
1.16
2.22
1.32
4.29
2.94
1.24
3.57
3.33
3.24
5
14
13
12
11
10
9
8
7
6
5
4
3
2
1
0
Chemical Shift (ppm)

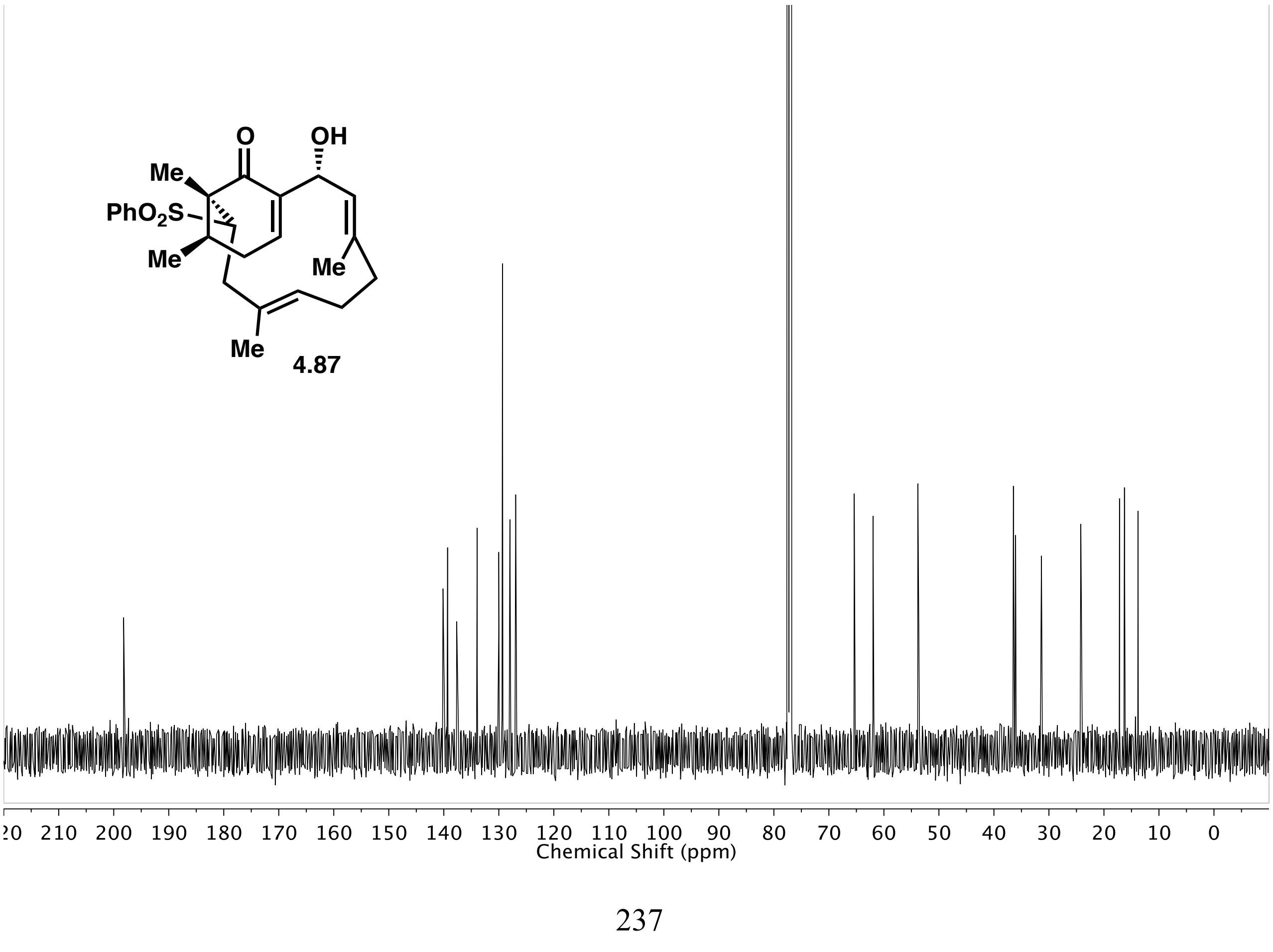
O
OH
Me
PhO2S
Me
Me
Me
4.87
20
210
200
190
180
170
160
150
140
130
120
110
100
90
80
70
60
50
40
30
20
10
0
Chemical Shift (ppm)

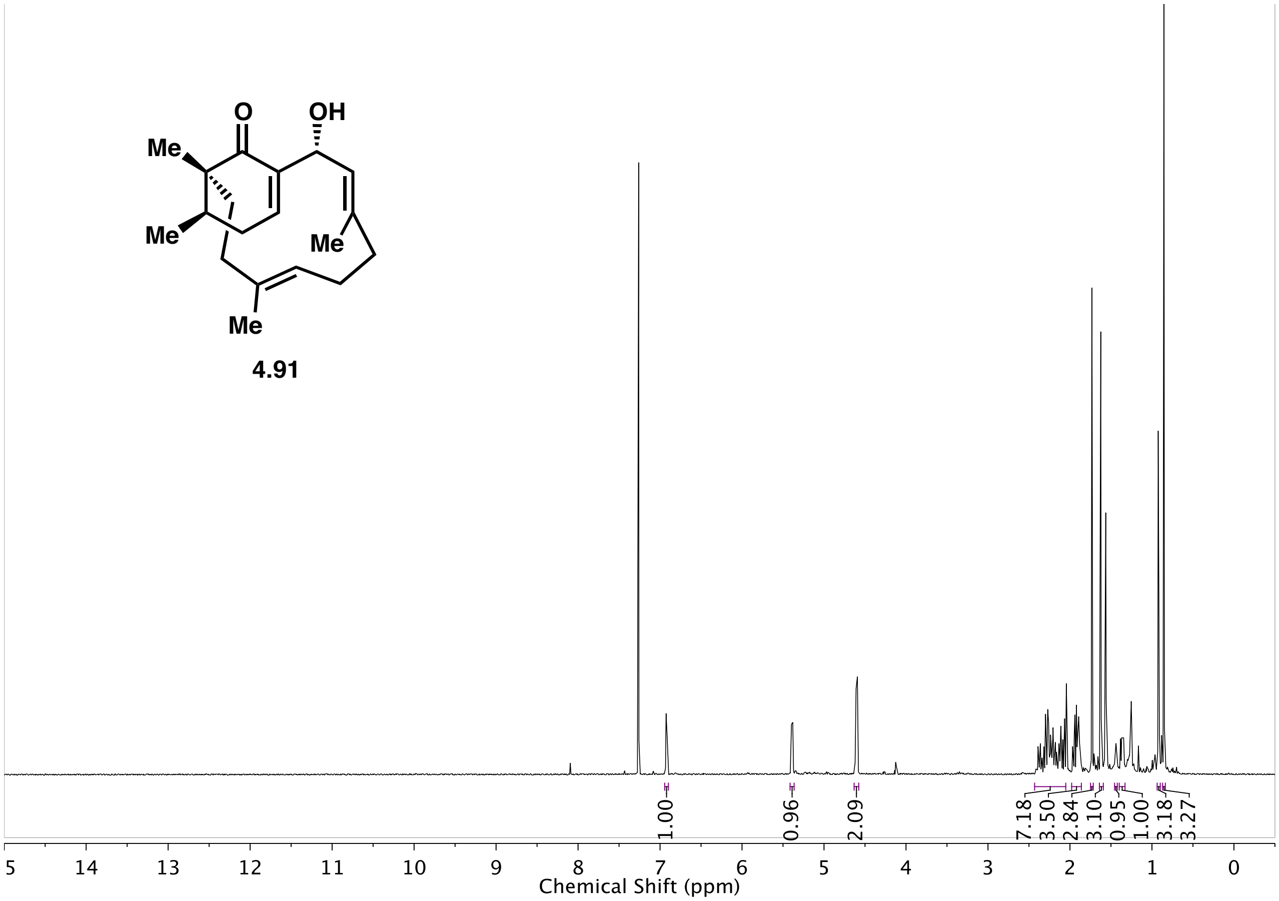
O
OH
Me
Me
Me
Me
4.91
1.00
0.96
2.09
7.18
3.50
2.84
3.10
0.95
1.00
3.18
3.27
5
14
13
12
11
10
9
8
7
6
5
4
3
2
1
0
Chemical Shift (ppm)

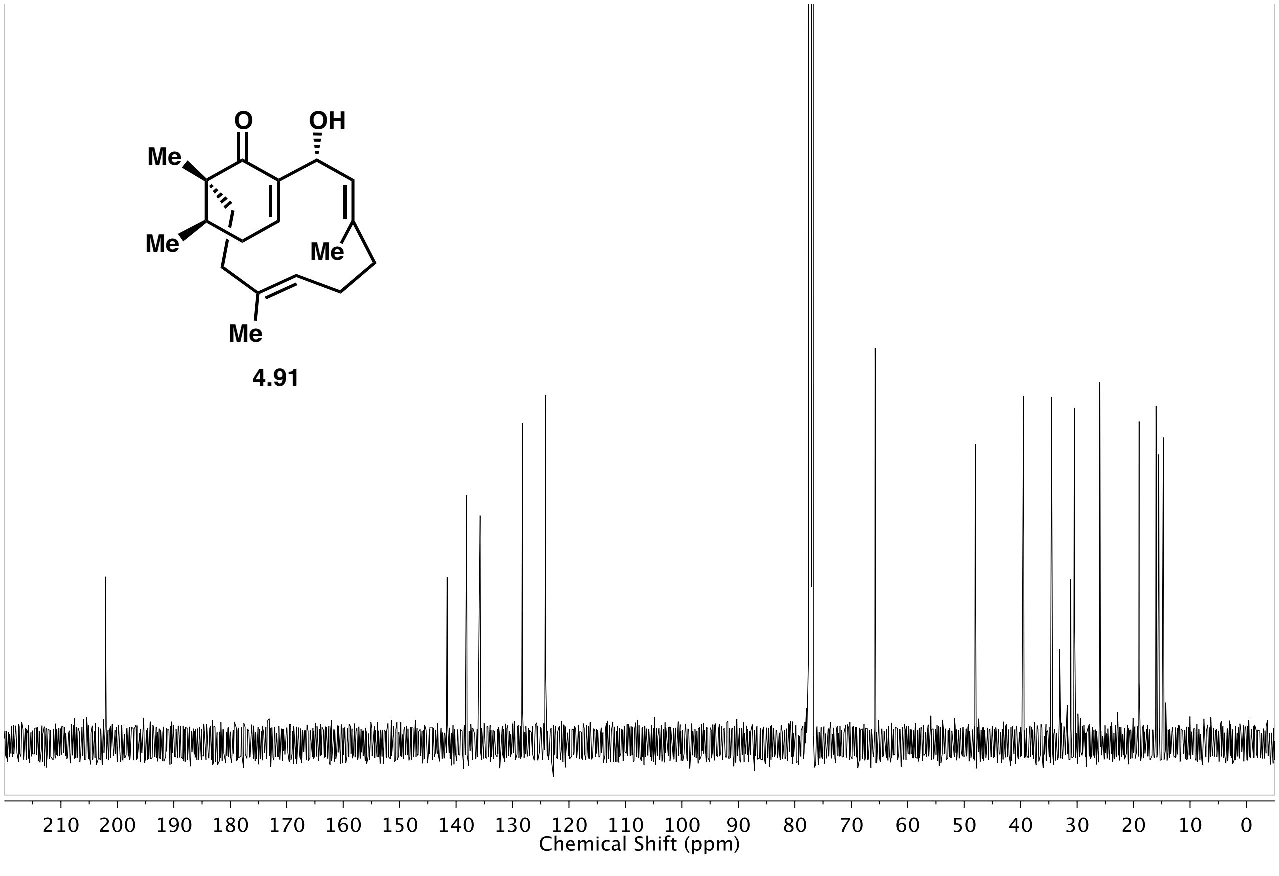
O
OH
Me
Me
Me
Me
4.91
210
200
190
180
170
160
150
140
130
120
110
100
90
80
70
60
50
40
30
20
10
0
Chemical Shift (ppm)

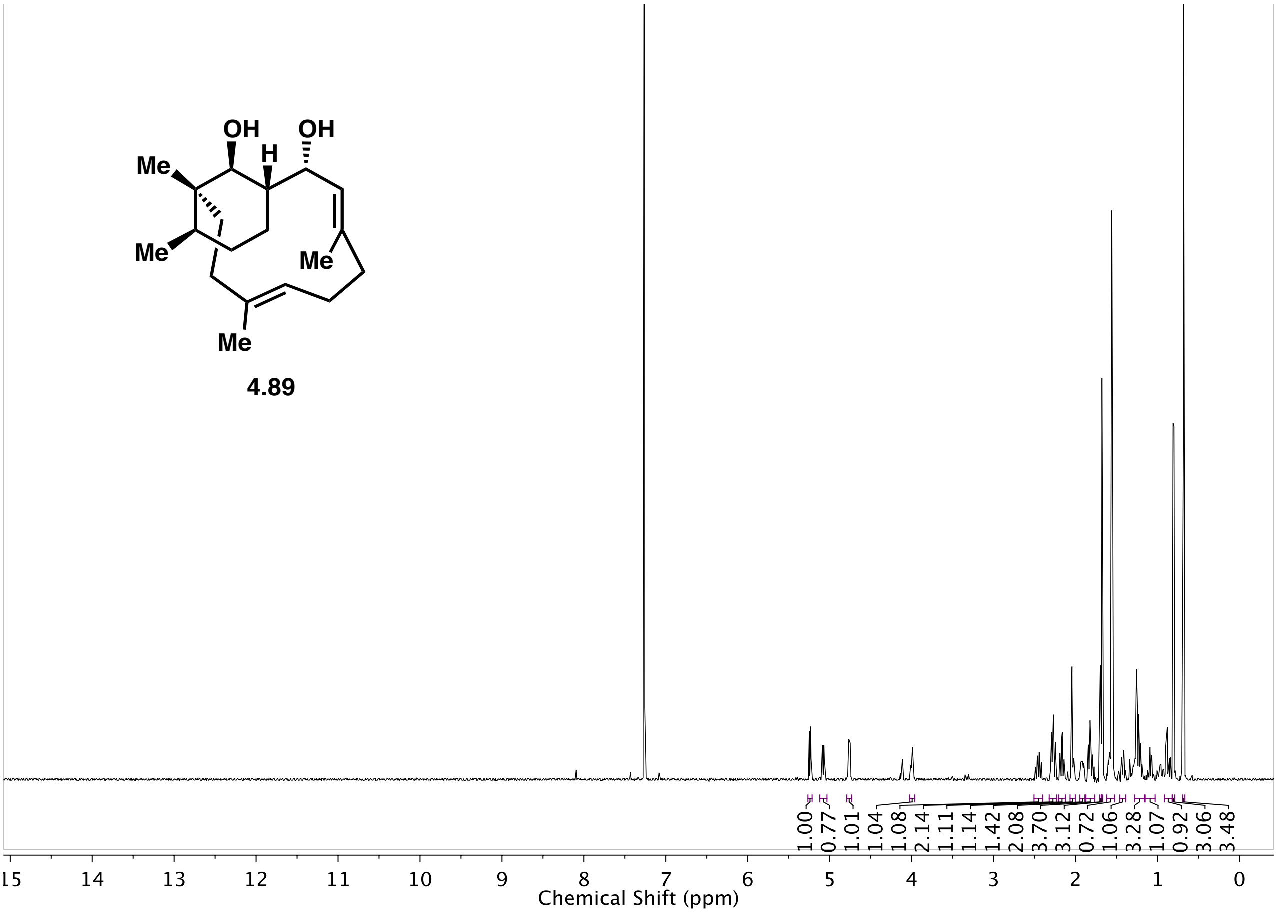
OH
OH
H
Me
Me
Me
Me
4.89
1.00
0.77
1.01
1.04
1.08
2.14
1.11
1.14
1.42
2.08
3.70
3.12
0.72
1.06
3.28
1.07
0.92
3.06
3.48
15
14
13
12
11
10
9
8
7
6
5
4
3
2
1
0
Chemical Shift (ppm)

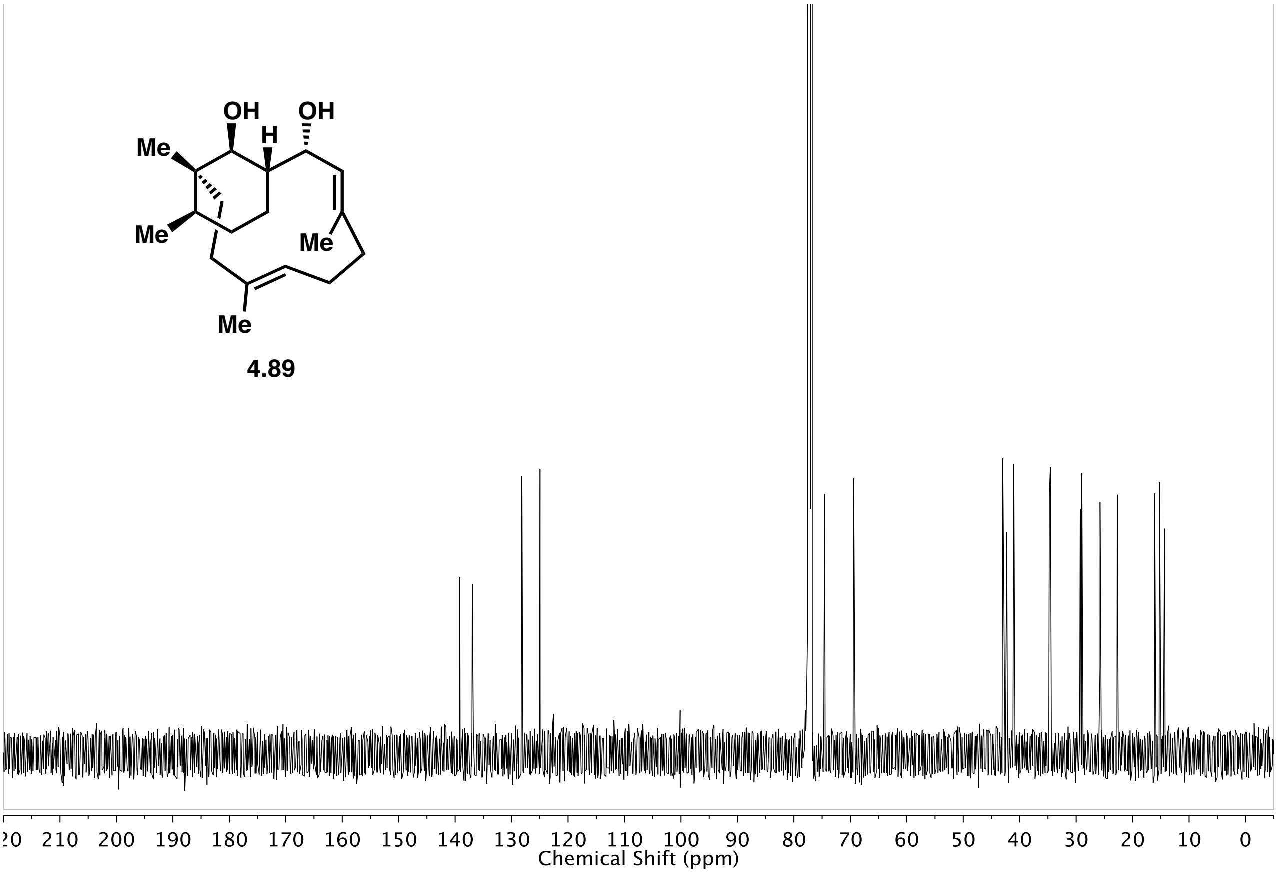
OH
OH
H
Me
Me
Me
Me
4.89
220
210
200
190
180
170
160
150
140
130
120
110
100
90
80
70
60
50
40
30
20
10
0
Chemical Shift (ppm)